Shri Gajanan Shikshan Sanstha's

SHRI SANT GAJANAN MAHARAJ COLLEGE OF ENGINEERING
SHEGAON – 444203, DIST. BULDHANA (MAHARASHTRA STATE), INDIA

"Recognized by A.I.C.T.E., New Delhi" Affiliated to Sant Gadge Baba Amravati University, Amravati
"Approved by the D.T.E., M.S. Mumbai"

| Ph   +918669638081/82 | Email.   principal@ssgmce.ac.in, |
| Website- www.ssgmce.ac.in | registrar@ssgmce.ac.in |

CRITERION III - RESEARCH, INNOVATIONS AND EXTENSION

Key Indicator 3.3 - Research Publications and Awards

Metric No	Assessment Indicators	Evidences
3.3.2	Number of research papers per teachers in the Journals notified on UGC website during the year	List of research papers
		Copy of paper/Certificate

PRINCIPAL
Shri Sant Gajanan Maharaj
College of Engineering, Shegaon.

Shri Gajanan Shikshan Sanstha's

SHRI SANT GAJANAN MAHARAJ COLLEGE OF ENGINEERING
SHEGAON – 444203, DIST. BULDHANA (MAHARASHTRA STATE),
INDIA

"Recognized by A.I.C.T.E., New Delhi" Affiliated to Sant Gadge Baba Amravati University, Amravati
"Approved by the D.T.E., M.S. Mumbai"

Ph   +918669638081/82   Email.   principal@ssgmce.ac.in,
Website- www.ssgmce.ac.in   registrar@ssgmce.ac.in

List of Research Papers

SN	Title of paper	Name of the author/s	Department of the teacher
1	A Hilbert Transform Based Approach for Classification of Complex Power Quality Disturbances	Sneha Khodke, Ravishankar Kankale, Dr Sudhir Paraskar	Electrical Engineering
2	, "A Hilbert Transform Based Approach for Classification of Power Quality Disturbances",	Sneha Khodke, Ravishankar Kankale, Dr Sudhir Paraskar and Dr. Saurabh Jadhao	Electrical Engineering
3	"Battery State of Charge Estimation Methods – A Critical Review"	P.R.Dhabe Dr Sudhir Paraskar and Dr. Saurabh Jadhao	Electrical Engineering
4	"Comparative Analysis Of Various Methodologies For Voltage Swell And Sag Detection In Online And Offline Conditions "	G. N. Bonde, Dr. S. R. Paraskar, V. S. Karale, R. Z. Fulare, Dr. S. S. Jadhao	Electrical Engineering
5	"Hilbert Transform Based Approach for Detection and Classification of Power Quality Disturbances",	Ravishankar S. Kankale, Dr. S. R. Paraskar, Dr. S. S. Jadhao,	Electrical Engineering
6	Analysis of Neuro Fuzzy based STATCOM and SSSC	R.K.Mankar Dr.Anjali U. Jawadekar	Electrical Engineering
7	PCA and ANN Based Induction Motor Fault Classification	Mukesh R. Chavan Anjali U. Jawadekar	Electrical Engineering
8	SOBI-ANN Based Induction Motor Fault Classification	Mukesh R. Chavan Anjali U. Jawadekar Danton Diego Ferreira	Electrical Engineering
9	Analyzing Polar Decoding Approaches: A Comparative Study	S. P. Badar and K. Khanchandani,	Electronics and Telecommunication Engineering
10	Statistical Analysis of Retinal Image Processing Techniques from an Empirical Perspective	Rupesh Mundhada, Dr D.D. Nawgaje	Electronics and Tel comm

Shri Gajanan Shikshan Sanstha's

SHRI SANT GAJANAN MAHARAJ COLLEGE OF ENGINEERING
SHEGAON – 444203, DIST. BULDHANA (MAHARASHTRA STATE), INDIA

"Recognized by A.I.C.T.E., New Delhi" Affiliated to Sant Gadge Baba Amravati University, Amravati
"Approved by the D.T.E., M.S. Mumbai"

Ph   +918669638081/82   Email. principal@ssgmce.ac.in,
Website- www.ssgmce.ac.in   registrar@ssgmce.ac.in

11	U-Net-based gannet sine cosine algorithm enabled lesion segmentation and deep CNN for diabetic retinopathy classification	Rupesh Mundhada, Dr D.D. Nawgaje	Electronics and Tel comm
12	A survey on Motion Artifact Correction in Magnetic Resonance Imaging for Improved Diagnostics	Manish N. Tibdewal	Electronics and Telecommunication Engineering
13	Performance Analysis of Un-doped and Doped Titania (TiO2) as an Electron Transport Layer (ETL) for Perovskite Solar Cells	Neerja Dharmale, Aadhityan A , Ashutosh Srivastava and Saurabh Chaudhury	Electronics and Telecommunication Engineering
14	Evaluating the Effect of Metal, Nonmetal, and Co-doping on Brookite TiO2	Neerja Dharmale.rupesh Mahamune,Modugu Krishnaiah ,Jayant Kumar Kar	Electronics and Telecommunication Engineering
15	A powerful method for interactive content-based image retrieval by variable compressed convolutional info neural networks	Vishwanath S. Mahalle, Narendra M. Kandoi, Santosh B. Patil	Electronics and Telecommunication Engineering
16	Denoising of motion artifacted MRI scans using conditional generative adversarial network	Vijay Tripathi, Manish N.Tibdewal	Electronics and Telecommunication Engineering
17	A survey on Motion Artifact Correction in Magnetic Resonance Imaging for Improved Diagnostics	Vijay Tripathi, Manish N.Tibdewal	Electronics and Telecommunication Engineering
18	Enhancing thermal efficiency of cookware through fin implantation: experimental analysis and numerical validation	Prof.S.P. Joshi	Mechanical Engineering
19	CFD Analysis and Validation of Axial Compressor Rotor Blade	Prof. S.Q.Syed	Mechanical Engineering
20	Design and Development modified seed sowing machine	Prof. N. B Borkar, Prof. C. V. Patil	Mechanical Engineering
21	Review on design and fabrication of solar panel cleaning mechanism	Dr. Nilesh Khandare	Mechanical Engineering

Shri Gajanan Shikshan Sanstha's

SHRI SANT GAJANAN MAHARAJ COLLEGE OF ENGINEERING
SHEGAON – 444203, DIST. BULDHANA (MAHARASHTRA STATE),
INDIA

"Recognized by A.I.C.T.E., New Delhi" Affiliated to Sant Gadge Baba Amravati University, Amravati
"Approved by the D.T.E., M.S. Mumbai"

Ph +918669638081/82   Email. principal@ssgmce.ac.in,
Website- www.ssgmce.ac.in   registrar@ssgmce.ac.in

22	Review on Sanitary Waste Management with the Help of Incinerator	Prof. K. V. Chandan	Mechanical Engineering
23	Performance analysis of photovoltaic panel using machine learning method	Prof. G. S. Wahile, Dr. S. P Trikal	Mechanical Engineering
24	A Novel Approach to Fake News Detection Using Generative AI	Dr. Jaikumar M. Patil	Computer Science and Engineering
25	Studies on the Use of Various Noise Strategiesfor Perturbing Data in Privacy-Preserving Data Mining	Dr. Jaikumar M. Patil	Computer Science and Engineering
26	Mobile Cum Web BasedVoting System for Rural Areas in India	Prof. C. M. Mankar	Computer Science and Engineering
27	An Enhanced Query Optimization Implemented in Hadoop using Bio-Inspired Algorithm with HDFS Technique	Prof. V. S. Mahalle	Computer Science and Engineering
28	A powerful method for interactive content - based image retrieval by variable compressed convolutional infoneural networks	Prof. V. S. Mahalle, Narendra M.Kandoi, Santosh B. Patil	Computer Science and Engineering
29	Efficient Content Based Image Retrieval System Based on Early and Late Fusion Technique	Prof. V. S. Mahalle, Narendra M.Kandoi, Santosh B. Patil	Computer Science and Engineering
30	Detection of Insects and Pests in Agriculture Field using MobileNet	Prof. V. S. Mahalle	Computer Science and Engineering
31	Stock Market Prediction Module Using Ann & Swarm Intelligence	Dr.Pankaj K. Bharne	Computer Science and Engineering
32	Enhancing Educational Experiences: A Personalized Course Recommendation System Employing Machine Learning Algorithms	Kshitij Mahurpwar, Tushar Nimbolkar, Aryan Shah, Faizan Raza, A. S. Manekar	Information Technology

Shri Gajanan Shikshan Sanstha's

SHRI SANT GAJANAN MAHARAJ COLLEGE OF ENGINEERING
SHEGAON – 444203, DIST. BULDHANA (MAHARASHTRA STATE), INDIA

"Recognized by A.I.C.T.E., New Delhi" Affiliated to Sant Gadge Baba Amravati University, Amravati
"Approved by the D.T.E., M.S. Mumbai"

Ph   +918669638081/82

Website- www.ssgmce.ac.in

Email.   principal@ssgmce.ac.in,
registrar@ssgmce.ac.in

33	Exploring an Immersive AR/VR Pedagogical Approach: Experiential Learning for Autism Spectrum Disorder (ASD) Education	Amitkumar Manekar, Vedant Gade, Rutuja Unhale, Harshit Manker, Riya Dhole	Information Technology
34	Bespoke Academic Guidance: Machine Learning for Course Recommendations	Dr. A. S. Manekar, Tushar K. Nimbolkar, Kshitij Mahurpwar, Mohd. Faizan Raza, Aryan Shah	Information Technology
35	Improving Autism Education: An Innovative Immersion AR/VR Pedagogical Method Using Experiential Learning	Riya Dhole,Vedant Gade, Rutuja Unhale, Harshit Manker, Amit Manekar	Information Technology
36	Agile Database Maintenance: ChatGPT-Enabled EOL Data Verification and Updates	Gauri Borle, Juee Gore, Riya Dangra, Amit Manekar	Information Technology
37	Enhancing Database Maintenance: Leveraging ChatGPT for Real-Time Verification and Updates of End-of-Life (EOL) Data	Gauri Borle, Juee Gore, Riya Dangra, Amit Manekar	Information Technology
38	Food Recommendation System Based on Geographical Location - DineLocate	Harshit Dharmik, Karan Motwani, Khushbu Pareek, Shraddha Tikar, M. Faizan I. Khandwani	Information Technology
39	A Survey of Student Education Platform	Sanket Gode, Prajwal Gawande, Vaishnavi Dabhade, Saurabh Wankhade, M. Faizan I. Khandwani	Information Technology
40	A Survey of Various Recommendation Systems	Harshit Dharmik, Karan Motwani, Khushbu Pareek, Shraddha Tikar, Faizan Khandwani	Information Technology
41	Analysis of Fruit Identification and Nutritional Assessment	Dr Sagar D Padiya, Saurabh S Yengade, Riya R Chikankar, Payal G Chavhan, Prashant G Dandage	Information Technology
42	Android Application for Activity Based Nutritional Needs	Anushka Narkhede, Mandar Nashikkar, Sanjana Daberao, Rohan Gaykwad, Mrs. P. P. Bute	Information Technology

Shri Gajanan Shikshan Sanstha's

SHRI SANT GAJANAN MAHARAJ COLLEGE OF ENGINEERING
SHEGAON – 444203, DIST. BULDHANA (MAHARASHTRA STATE), INDIA

"Recognized by A.I.C.T.E., New Delhi" Affiliated to Sant Gadge Baba Amravati University, Amravati
"Approved by the D.T.E., M.S. Mumbai"

Ph   +918669638081/82   Email.   principal@ssgmce.ac.in,
Website- www.ssgmce.ac.in   registrar@ssgmce.ac.in

43	A Survey of Android Application for Activity Based Nutritional Needs	Anushka Narkhede, Mandar Nashikkar, Rohan Gaykwad, Sanjana Daberao, Mrs. P. P. Bute	Information Technology
44	A System for Recommending Food Based on User's Health Preferences	Pratik Diwan, Yash Dahiwale, Deepak Sangale, Sumit Muddalkar	Information Technology
45	Personalized Health-Centric Food Recommendation System	Atharva Urade, Mohan Bhambere, Prathamesh Mahajan, Vaibhav Shirbhate, Sumit Muddalkar	Information Technology
46	A Survey of Integration into 3D Printing for Image Processing using AI ML	Abhay Kadu, Pranav Kaware, Rushikesh Kaldate, Ayush Solav, Mrs. S. N. Khandare	Information Technology
47	Body Part Implant Dashboard for Real-Time Monitoring and Reporting	Riddhi Gadewar, Pranjal Patil, Sakshi Dhakade, Gaurinandan Joshi, S. N. Khandare	Information Technology
48	Integration into 3D Printing for Image Processing using AI ML	S. N. Khandare, Abhay Kadu, Pranav Kaware, Rushikesh Kaldate, Ayush Solav	Information Technology
49	VidMagic: Prompt to Image Clips	Ms. Nayana Ghuikar, Mr. Tejas Moon, Mr. Prasad Bhagat, Mr. Sushant Chafale, Mr. Gaurav Sabe	Information Technology
50	Effective End-of-Life Management of Assets in Organization by Snowflake Integration	Dr J. M. Patil, Prof. N. N. Ghuikar, Surabhi Lahoti, Aditya More, Kunal Chandore	Information Technology
51	Females' Buying Behavior for Cell Phones- An Analytical Study	Priyanka Gajanan Dahi Dr. H. M. Jha "Bidyarthi"	MBA
52	"Balancing Books and Happiness: Understanding Job Satisfaction in Banking Workforce of Akola Region"	Mansi Vilas Bharane Dr. H. M. Jha "Bidyarthi"	MBA
53	Breaking Barriers: Examining Women's Empowerment through Government Initiatives in Khamgaon	Vishakha Vijay Tantak Dr. H. M. Jha "Bidyarthi"	MBA

Shri Gajanan Shikshan Sanstha's

SHRI SANT GAJANAN MAHARAJ COLLEGE OF ENGINEERING

SHEGAON – 444203, DIST. BULDHANA (MAHARASHTRA STATE), INDIA

"Recognized by A.I.C.T.E., New Delhi" Affiliated to Sant Gadge Baba Amravati University, Amravati
"Approved by the D.T.E., M.S. Mumbai"

Ph   +918669638081/82   Email.   principal@ssgmce.ac.in,
Website- www.ssgmce.ac.in   registrar@ssgmce.ac.in

54	Fortifying Financial Frontiers: Safeguarding Online Banking in Chhindwara City	Utkarsha Dhanraj Nitnaware Dr. H. M. Jha "Bidyarthi"	MBA
55	"Harvesting Opportunities through PMMY in Agribusiness - A Study of Pradhan Mantri Mudra Yojana's Contribution to Agricultural Development in Jalgaon Jamod"	Aditya Haridas Sable Dr. H. M. Jha "Bidyarthi"	MBA
56	Bits and Bytes of Change: Examining Digitalization's Impact on Khamgaon's Socio-Economic Fabric	Akshay Arun Jadhao Dr. H. M. Jha "Bidyarthi"	MBA
57	Empirical Study on Stock Surge in First Twenty Years of 21st Century Investigating the Interplay between FDI, FII and Indian Market Dynamics	Gaurav Ajay Varma Dr. H. M. Jha "Bidyarthi"	MBA
58	"Harnessing Sunlight: A Probe into the PM-KUSUM Solar Initiative in Sangrampur Taluka"	Mahesh Ratanlal Girhe Dr. H. M. Jha "Bidyarthi"	MBA
59	Work Life Balance in Information Technology - A study in Yavatmal Region	Anjali Dadubhaiya Rangari Dr. L. B. Deshmukh	MBA
60	Impact of Employee Motivation on Organization Productivity-A Study of Gajanan Industries Khamgaon	Ku.Prachi Narayandas Sureka Dr. L. B. Deshmukh	MBA
61	Competency Mapping and Training & Development	Monika Kishor Ghawat Dr. L. B. Deshmukh	MBA
62	A Study of Navigating the Landscape of Organic Farming: Analysing Challenges and Exploring Opportunities for Sustainability in Buldhana Region	Vaibhav J Ahir Dr. L. B. Deshmukh	MBA
63	The study on work life balance strategies and initiatives amongst working women in Buldana district	Shruti Prakash Auti Dr. L. B. Deshmukh	MBA
64	"Comparative Analysis Of Customer Satisfaction Towards Indian Postal Services And State Bank Of India Services."	Madhuri Vijay Nagalkar Dr. L. B. Deshmukh	MBA

Shri Gajanan Shikshan Sanstha's

SHRI SANT GAJANAN MAHARAJ COLLEGE OF ENGINEERING
SHEGAON – 444203, DIST. BULDHANA (MAHARASHTRA STATE), INDIA

"Recognized by A.I.C.T.E., New Delhi" Affiliated to Sant Gadge Baba Amravati University, Amravati
"Approved by the D.T.E., M.S. Mumbai"

Ph   +918669638081/82   Email.   principal@ssgmce.ac.in,
Website- www.ssgmce.ac.in   registrar@ssgmce.ac.in

65	Analysis of Organized Retailers and their Strategies-A Study of Akola District	ARJUN P. WASATKAR Dr. L. B. Deshmukh	MBA
66	Impact of Digital Marketing on Buying Behavior of Select Product categories in Buldana Region	Sumersing Barwal Dr. L. B. Deshmukh	MBA
67	A Study On Customer Satisfaction Towards Honda Bikes With Special Reference To Apollo Enterprises	Ganesh Arun Mandal Dr. L. B. Deshmukh	MBA
68	A Study on Consumer Buying Behavior for Laptop in Khamgaon Region.	Priya Devidas Mapari Dr. P. M. Kuchar	MBA
69	A Comparative Analysis of Fertilizer Practices in Soybean Farming: Organic vs. Chemical Approaches in Washim region	Shubham D. Rathod Dr. P. M. Kuchar	MBA
70	Involvement of Girls in Sports and Physical Activities: An Assessment of Initiatives from Government and Institutions	Pratiksha Santosh Gawande Dr. P. M. Kuchar	MBA
71	An Evaluation of Pradhan Mantri Awas Yojna In Tiosa Region	Roshan Anil Karale Dr. P. M. Kuchar	MBA
72	Perspective towards Entrepreneurship – A Study of Students with Special Reference to Atmanirbhar Bharat	Rushikesh Subhash Paulzagade Dr. P. M. Kuchar	MBA
73	Effect of training and development on employee retention	Pooja N. Thakare Dr. P. M. Kuchar	MBA
74	Insights into purchase decision and post-purchase behavior of selects bags	Vaishnavi M. Tivhane Dr. P. M. Kuchar	MBA
75	Insights into purchase decision and post-purchase behavior of selects bags	Vaishnvi A. Nimkarde Dr. P. M. Kuchar	MBA
76	"Scanning Inclusive Workplace – A Study of Select Organization"	Vaishnavi Anil Hage Dr. M. A. Dande	MBA
77	A study of brand loyalty in tea powder market.	Vishal gujar Dr. M. A. Dande	MBA

Shri Gajanan Shikshan Sanstha's

SHRI SANT GAJANAN MAHARAJ COLLEGE OF ENGINEERING
SHEGAON – 444203, DIST. BULDHANA (MAHARASHTRA STATE),
INDIA

"Recognized by A.I.C.T.E., New Delhi" Affiliated to Sant Gadge Baba Amravati University, Amravati
"Approved by the D.T.E., M.S. Mumbai"

Ph   +918669638081/82   Email. principal@ssgmce.ac.in,
Website- www.ssgmce.ac.in   registrar@ssgmce.ac.in

78	A Study of Impact of Organizational Culture on Employee Behavior and Performance	Krushna J. Thakur Dr. M. A. Dande	MBA
79	Consumer Buying Behavior- "A Comparative Study Of Select Spices Brands"	Ishan Pavan ShahDr. M. A. Dande	MBA
80	A Study of Emotional Intelligence As An Employability Pre-Requisite	Shrusti S. Purwar Dr. M. A. Dande	MBA
81	A Study on Diffusion of Innovation in Fintech Banking with a special Reference to Khamgaon Region.	Sneha Sunil Wankhede Dr. M. A. Dande	MBA
82	A Study of Market Potential for Spirulina	Pratik Pramod Dhage Dr. M. A. Dande	MBA
83	Empowering Women through Self-Help Groups: An In-depth Study of Socioeconomic Development & Gender Equality	Tanaya Ajay Mate Dr. S. M. Mishra	MBA
84	A Study of Self-Help Groups And Women Empowerment In A Rural Area of The Akola Region	Poonam P. Parchure Dr. S. M. Mishra	MBA
85	Impact of Pradhan Mantri Ujjwala Yojana in Buldhana District	Trupti Sunil Jamode Dr. S. M. Mishra	MBA
86	An Investigation into Factors Affecting Financial Exclusion in Rural Areas.	Vitthal D. Ramekar Dr. S. M. Mishra	MBA
87	Market Potential of Organic Food in Maharashtra Region(Vidharbha)	Shubaham K Gade Dr. S. M. Mishra	MBA
88	"The Study on Analyzing the Impact of Social Media on Consumer Buying Behavior in the Khamgaon Region"	Nagesh Banait Dr. S. M. Mishra	MBA
89	" Study On Inclusive Growth Of Women's Empowerment, Challenges And Opportunities At Padegaon, Chhatrapati Sambhaji Nagar	Sneha B. Gaikwad Dr. S. M. Mishra	MBA
90	Navigating the workplace upheaval and its impact on employee retention and turnover	Vashishtha D. Thakur Dr. S. M. Mishra	MBA

Shri Gajanan Shikshan Sanstha's

SHRI SANT GAJANAN MAHARAJ COLLEGE OF ENGINEERING
SHEGAON – 444203, DIST. BULDHANA (MAHARASHTRA STATE), INDIA

"Recognized by A.I.C.T.E., New Delhi" Affiliated to Sant Gadge Baba Amravati University, Amravati
"Approved by the D.T.E., M.S. Mumbai"

Ph   +918669638081/82
Website- www.ssgmce.ac.in

Email.   principal@ssgmce.ac.in,
registrar@ssgmce.ac.in

91	An In-depth Analysis of Financial Literacy's Influence on Investment Behavior	Siddheshwar Dilip Parihar Dr. S. M. Mishra	MBA
92	A study of factors and levels of satisfaction of employees in banking sector of Buldhana.	Harshali S. Khandagale Dr. W. Z. Suliya	MBA
93	A Study of Work Life and Satisfaction of Employees in Banking Sector in Akola District	Aishwarya Vinayak Tayade Dr. W. Z. Suliya	MBA
94	A Study on Satisfaction and Consumer Behaviour for Amul Milk in Buldana Region	Swapnil Gajanan Ikhare Dr. W. Z. Suliya	MBA
95	A study on impact of social media on recruitment process of applicant's in Buldhana region	Samruddhi Purkar Dr. W. Z. Suliya	MBA
96	A Study on Employee Engagement with Special Reference to Banking Sector	Padmini Madhav Ingole Dr. W. Z. Suliya	MBA
97	A study of market potential analysis of e-bike in Shegaon region.	Harshal Gawai Dr. W. Z. Suliya	MBA
98	A study of work life balance and stress management approach of working women in the Khamgoan region	Pallavi Ravindra sabe Dr. W. Z. Suliya	MBA
99	A study of mechanization of agriculture business in Akola region	Dhanashree S. Deshmukh Dr. W. Z. Suliya	MBA
100	Study of comparative analysis of amazon and flipkart	Vaishnavi Sachin Vaishnav Dr. W. Z. Suliya	MBA
101	"Weather and climate variability impact on farmers financial planning: A longitudinal study in khamgaon region"	Shambala R. Mahokar Prof. V. V. Patil	MBA
102	Navigating the Digital Divide: Challenges Faced by Senior Citizens in Digital Banking Adoption	Shraddha R. Gondchwar Prof. V. V. Patil	MBA
103	"The Influence of Fintech on Investment Patterns of Salaried Individuals"	Kunal Sanjay Bhise Prof. V. V. Patil	MBA

Shri Gajanan Shikshan Sanstha's

**SHRI SANT GAJANAN MAHARAJ COLLEGE OF ENGINEERING
SHEGAON – 444203, DIST. BULDHANA (MAHARASHTRA STATE),
INDIA**

"Recognized by A.I.C.T.E., New Delhi" Affiliated to Sant Gadge Baba Amravati University, Amravati
"Approved by the D.T.E., M.S. Mumbai"

Ph   +918669638081/82   Email.   principal@ssgmce.ac.in,
Website- www.ssgmce.ac.in   registrar@ssgmce.ac.in

104	Role of Online Job Portals in Shaping Candidate's Job Search Behavior	Vaishnavi Manish Hiwrale Prof. V. V. Patil	MBA
105	Employee Engagement Strategies for Enhancing productivity	Revati S Mahalle Prof. V. V. Patil	MBA
106	Channel optimization strategies a catalyst for enhanced supply chain integration and supply chain performance	Arati Gautam Tayade Prof. V. V. Patil	MBA
107	Exploring the Challenges and Opportunities of E-commerce Implementation in Small Businesses: Insights from Shegaon	Vaibhav Tejrao Dali Prof. V. V. Patil	MBA
108	A Study of Stress Management Practices Adopted By College Student	Samrudhi S. Raut Prof. V. V. Patil	MBA
109	Comparative Study of Job Satisfaction of Working Women in Government Jobs and Private Jobs Malkapur	Madhuri Sumare Prof. V. V. Patil	MBA
110	A Study on Factors Influencing Buying Behavior of Graduate and post- Graduate Students towards Laptop Purchase with a Special Reference to Shegaon Region	Pratik Shegokar Dr. B.T. Husain	MBA
111	A study on factors influencing saving and investment decisions of salaried individuals with a special reference to Akola region	Arti Ananda Jamnik Dr. B.T. Husain	MBA
112	"A study on Human Resource Management practices at strategic Business unit in Khamgaon region."	Vaishnavi M. Panchbhai Dr. B.T. Husain	MBA
113	Enhancing Mid-Course Internship Programs: Identifying Challenges and Promoting Collaborative Solutions in Shegaon's Educational Landscape	Akshada Narendra Parchure Dr. B.T. Husain	MBA

Shri Gajanan Shikshan Sanstha's

SHRI SANT GAJANAN MAHARAJ COLLEGE OF ENGINEERING

SHEGAON – 444203, DIST. BULDHANA (MAHARASHTRA STATE),

INDIA

"Recognized by A.I.C.T.E., New Delhi" Affiliated to Sant Gadge Baba Amravati University, Amravati
"Approved by the D.T.E., M.S. Mumbai"

Ph   +918669638081/82   Email.   principal@ssgmce.ac.in,
Website- www.ssgmce.ac.in   registrar@ssgmce.ac.in

114	"A Study Of Consumer Satisfaction In Public Transportation System with A Special Reference To M.S.R.T.C. Khamgaon"	Shivani Sanjay Girjapure Dr. B.T. Husain	MBA
115	Navigating the Accreditation Landscape: Insight from Students in Rural India	Prof. V.V. Patil Dr. M.A. Burghate Dr. O.M. Deshmukh	MBA
116	Rihizopus Keratitis	Dr. B. T. Husain	MBA
117	"Synthesis, Characterization of Gd-doped Ceria Nanocomposites	Dr. Anand S. Tale	Applied Sciences & Humanities
118	Effect of Noble Metal (Ag) doping on Hydrogen Sensitivity of WO3 Thin Film Sensors	Dr. Anand S. Tale	Applied Sciences & Humanities
119	An overview on nanocrystalline perovskite (ABO3): Apotential material for solid state gas sensor and its applications	Dr. Mrs. M. S. Pande	Applied Sciences & Humanities
120	Preparation of zinc doped magnesium ferrite nanoparticles by sol-gel method	Dr. Mrs. M. S. Pande	Applied Sciences & Humanities
121	Role of matrices and its application in Science and Engineering	Dr. Mrs.J. S. Gawande	Applied Sciences & Humanities

PRINCIPAL
Shri Sant Gajanan Maharaj
College of Engineering,Shegaon.

3.3.2 Number of research papers per teachers in the Journals notified on UGC website during the year 2023-24

Sr. No.	Title of paper	Name of the author/s	Department of the Teacher	Name of journal	Year of publication	ISSN number	Link to the recognition in UGC enlistment of the Journal
1	A Hilbert Transform Based Approach for Classification of Complex Power Quality Disturbances	Sneha Khodke, Ravishankar Kankale, Dr Sudhir Paraskar	Electrical Engineering	The Indian Journal of Technical Education	2023	ISSN 0971-3034	http://www.isteonline.in/Datafiles/cms//Special%20Issues//Special%20issue%20July%202023.pdf
2	, "A Hilbert Transform Based Approach for Classification of Power Quality Disturbances",	Sneha Khodke, Ravishankar Kankale, Dr Sudhir Paraskar and Dr. Saurabh Jadhao	Electrical Engineering	International Journal of Innovative Research in Electrical, Electronics, Instrumentation and Control Engineering (IJIREEICE), Vol. 11, Issue 8, August 2023 DOI: 10.17148/IJIREEICE.2023.11801	2023	ISSN Online 2321-2004 ISSN Print 2321-5526	https://ijireeice.com/wp-content/uploads/2023/08/IJIREEICE.2023.11801.pdf
3	"Battery State of Charge Estimation Methods – A Critical Review"	P.R.Dhabe Dr Sudhir Paraskar and Dr. Saurabh Jadhao	Electrical Engineering	International Journal Of Innovative Research In Electrical, Electronics, Instrumentation And Control Engineering Volume 11, Issue 12, December 2023 DOI: 10.17148/IJIREEICE.2023.111201	2023	ISSN (Online) 2321–2004	https://ijireeice.com/wp-content/uploads/2023/12/IJIREEICE.2023.111201.pdf

4	"Comparative Analysis of Various Methodologies For Voltage Swell And Sag Detection In Online And Offline Conditions "	G. N. Bonde, Dr. S. R. Paraskar, V. S. Karale, R. Z. Fulare, Dr. S. S. Jadhao	Electrical Engineering	International Journal of Advanced Research in Science, Communication and Technology (IJARSCT) Volume 4, Issue 5, April 2024 IF 7.53	2024	ISSN (Online) 2581-9429	https://www.ijarsct.co.in/Paper17529.pdf
5	"Hilbert Transform Based Approach for Detection and Classification of Power Quality Disturbances",	Ravishankar S. Kankale, Dr. S. R. Paraskar, Dr. S. S. Jadhao,	Electrical Engineering	Journal of Recent Trends in Electrical Power System, Vol 7, No 2 (2024)	2024	e-ISSN: 2584-2404,	https://ijireeice.com/wp-content/uploads/2023/08/IJIREEICE.2023.11801.pdf
6	Analysis of Neuro Fuzzy based STATCOM and SSSC	R.K.Mankar Dr.Anjali U. Jawadekar	Electrical Engineering	International Journal of Research Publicationsand Revoews Vol 4,No 7, Pp, 89-100,July 2023	2023	ISSN 2582-7421	https://ijrpr.com/uploads/V4ISSUE7/IJRPR15214.pdf
7	PCA and ANN Based Induction Motor Fault Classification	Mukesh R. Chavan Anjali U. Jawadekar	Electrical Engineering	Journal of Advanced Research in Artificial Intelligence & It's Applications, Volume 1 Issue 2 Page 47-56 2024, DOI: https://doi.org/10.5281/zenodo.110447 87	2024	ISSN: 3048-6440	http://hbrppublication.com/OJS/index.php/JARAIIA/issue/view/1113
8	SOBI-ANN Based Induction Motor Fault Classification	Mukesh R. Chavan Anjali U. Jawadekar Danton Diego Ferreira	Electrical Engineering	TTIC, Vol. 7, 2023	2024	ISSN No : 2582-5879	https://tiutic.org/pdf/volume/Vol_7/Vol7_Article_5.pdf

THE INDIAN JOURNAL OF TECHNICAL EDUCATION

INDIAN JOURNAL OF TECHNICAL EDUCATION

A Hilbert Transform Based Approach for Classification of Complex Power Quality Disturbances

Sneha Khodke
M.E Student
Department of Electrical Engineering
SSGMCE, Shegaon

Ravishankar Kankale
Assistant Professor
Department of Electrical Engineering
SSGMCE, Shegaon

Sudhir Paraskar
Associate Professor & HOD
Department of Electrical Engineering
SSGMCE, Shegaon

ABSTRACT

This research work presents a Hilbert Transform-based algorithm for categorizing Multiple and Multistage Power Quality Disturbances (PQDs). The MATLAB software combines a number of mathematical equations to create these power quality issues. These PQDs are produced by implementing a variety of mathematical equations in the MATLAB Environment. The multiple power quality issues considered in this study are voltage sag with harmonics, voltage swell with harmonics and voltage interruption with harmonics. The multistage power quality issues considered in this study are multistage voltage sag, multistage voltage swell, and multistage voltage sag with swell. These PQDs are processed using Hilbert Transform and PQ index curves are obtained from it. The PQ index curve is further used to extract four features namely F1, F2, F3, and F4. The thresholding-based algorithms are developed using the extracted features in order to classify the multiple and multistage PQDs.

KEYWORDS: *Hilbert transform. Power quality index curve, Power quality disturbances*

INTRODUCTION

For electric power providers and their customers, the quality of the electricity is now a crucial concern. The equipment utilised in electrical utilities today is more sensitive to the power quality. These devices have power electronic components, which are delicate to changes in power quality. Therefore, any disturbance in the voltage, current, or frequency of the power signal that may also have an impact on the customer's side is referred to as a power quality issue. We must be able to recognise and categorise the disturbances into distinct sorts in order to identify their sources and causes. PQ disturbances comprise a variety of PQ phenomena, such as transients, interruptions, sags, swells, power frequency changes, long duration variations, and steady state variations, according to IEEE standard 1159-1995 [1]. These Disturbances are the main culprits for power quality degradation. The signal processing techniques such as Fourier Transform (FT), short time Fourier Transform (STFT), wavelet transform (WT), Stockwell's Transform (ST), Hilbert Transform(HT) etc. have been utilized for the feature extraction to detect a particular PQ event available in the voltage signal[2]. Also ST with SVM used for classification of PQD [15]. The artificial intelligence techniques such as Artificial Neural network (ANN), Fuzzy logic, decision rules etc. have been used extensively for the classification of the PQ events [3]. Combination of features of Hilbert transform (HT) and Stockwell transform (ST) to identify the single-stage and multiple (multi-stage) power quality disturbances (PQDs)[4,5]. In [6] smart sensor based on Hilbert transform used for detection, classification, and quantification of PQD. An advance signal processing method that is Hilbert Haung Transform is used to classify the power quality event[7].

POWER QUALITY

As per IEEE power quality is define as "the concept of powering and grounding sensitive electronics

equipment in a manner that is suitable to the operation of that equipment"[8].

A. Voltage Sag: A voltage sag is a fall in the rms value of voltage or current between 0.1 and 0.9 pu at the power frequency over a time of between 0.5 cycle and 1 minute.

B. Voltage Swell: A swell is defined as a rise in rms value of voltage or current between 1.1 and 1.8 pu at the power frequency for duration between 0.5 cycle and 1 minute.

C. Interruptions: When the supply voltage or load current drops to less than 0.1 pu for more than a minute, an interruption occurs.

HILBERT TRANSFORM (HT)

From the input signal, the HT derives the discrete-time analytical signal. Complexity characterises the analytic signal. The imaginary component of which represents the 90° phase shifted version of the original signal, while the real part represents the original signal. The frequency and amplitude of the modified version of the original signal match those of the original signal. A time series' instantaneous features are estimated using the HT.

In HT phase angle of all positive frequency spectral components of the given signals are shifted by -900 and negative frequency spectral components of the given signal are shifted by 900. The resulting function of time is called Hilbert Transform of a signal. The amplitude spectrum of a signal is unchanged only phase spectrum is changed. HT does not bring about a change of domain. The HT $x^\wedge(t)$ of a signal x(t) is obtained by convolving x(t) with $1/(\pi t)$.

METHODOLOGY

An algorithm for the classification of complex PQDs uses the following steps:

1. Generation of complex PQDs using the integral mathematical models of PQDs using MATLAB programming[9]

2. Applying Hilbert transform to the voltage signals with complex PQDs.

A = Hilbert (v)

3. Obtaining the PQ Index Curves using the following command and plotting it.

B=abs (A)

4. Extracting the features F1, F2, F3, and F4 from the PQ index curve.

F1 = median (B)

F2=kurtosis

F3=var (B)

F4=std (B)

5. Developing thresholding-based algorithm using the extracted features for classification of PQDs

GENERATION OF POWER QUALITY DISTURBANCES

In order to provide the necessary power quality disturbance, a collection of parametric equations involving various mathematical functions is used to construct the integral mathematical models of PQDs[10,11]. In this study project, the MATLAB programming is used to perform the mathematical equations presented in table I in order to produce the numerous and multistage power quality disturbances.

SIMULATION RESULTS AND DISCUSSION

Results of Generation of PQDs

The parametric equations are programmed in MATLAB programming to produce the multiple, and multistage PQDs. The parameter A controls the PQDs' amplitudes, while the temporal constants t1 and t2 govern their durations. The greatest value of the instantaneous waveform under three phase is A=326; the RMS value for this value was found to be 400 V.

Figure 1 shows the waveform of voltage sag with harmonics that results from altering the parameters α=0.5, t1=0.3, and t2=0.7. The voltage signal has a sag along with harmonics that lasts for 0.4 seconds. The length of the signal is one second.

Table 1. Mathematical Models of PQDs

PQDs	Equations	Parameters
Voltage sag with harmonics	$x(t) = A (1 - \alpha (u(t-t1) - u(t-t2))) \sin(\omega t) * \alpha 1 \sin(\omega t) + \alpha 3 \sin(3\omega t) + \alpha 5 \sin(5\omega t) + \alpha 7 \sin(7\omega t)$	$0.1 \leq \alpha \leq 0.8$, $T \leq (t2 - t1) \leq 9T$
Voltage swell with harmonics	$x(t) = A (1 + \alpha (u(t-t1) - u(t-t2))) \sin(\omega t) * \alpha 1 \sin(\omega t) + \alpha 3 \sin(3\omega t) + \alpha 5 \sin(5\omega t) + \alpha 7 \sin(7\omega t)$	$0.1 \leq \alpha \leq 0.8$, $T \leq (t2 - t1) \leq 9T$
Voltage interruption with harmonics	$x(t) = A (1 - \alpha (u(t-t1) - u(t-t2))) \sin(\omega t) * \alpha 1 \sin(\omega t) + \alpha 3 \sin(3\omega t) + \alpha 5 \sin(5\omega t) + \alpha 7 \sin(7\omega t)$	$0.1 \leq \alpha \leq 0.8$, $T \leq (t2 - t1) \leq 9T$
Multistage voltage sag	$x(t) = A [(0.5 - \alpha 1 (u(t-t1) - u(t-t2)) + (0.5 - \alpha 2 (u(t-t2) - u(t-t3))] * \sin(\omega t)$	$0.1 \leq \alpha \leq 0.8$, $T \leq (t2 - t1) \leq 9T$
Multistage voltage swell	$x(t) = A [(0.5 + \alpha 1 (u(t-t1) - u(t-t2)) + (0.5 - \alpha 2 (u(t-t2) - u(t-t3))] * \sin(\omega t)$	$0.1 \leq \alpha \leq 0.8$, $T \leq (t2 - t1) \leq 9T$
Multistage voltage sag with swell	$x(t) = A [(0.5 - \alpha 1 (u(t-t1) - u(t-t2)) + (0.5 - \alpha 2 (u(t-t2) - u(t-t3))] * \sin(\omega t)$	$0.9 \leq \alpha \leq 1$, $T \leq (t2 - t1) \leq 9T$
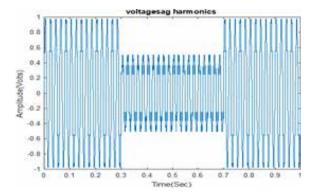
Fig. 1. Waveform of Voltage Sag with Harmonics

Figure 2 shows the waveform of voltage swell with harmonics that results from altering the parameters α=0.5, t1=0.3, and t2=0.7. The voltage signal has a swell along with harmonics that lasts for 0.4 seconds. The length of the signal is one second.
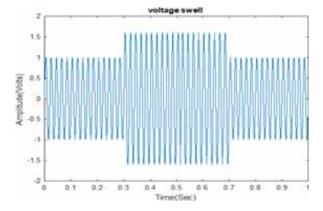
Fig 2. Waveform of Voltage Swell with Harmonics

Figure 3 shows the waveform of voltage interruption with harmonics that results from altering the parameters α=0.5, t1=0.3, and t2=0.7. The voltage signal has a swell along with harmonics that lasts for 0.4 seconds. The length of the signal is one second.
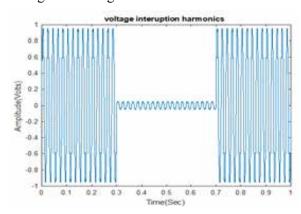
Fig 3. Waveform of Voltage Interruption with Harmonics

Figure 4 shows the waveform of multistage voltage sag that results from altering the parameters α=0.5, t1=0.3, and t2=0.7. The voltage signal has a multistage sag for 0.4 seconds. First stage of sag is obtained between duration 0.3 to 0.5 and second stage is obtained between 0.5 to 0.7 sec. The length of the signal is one second.

Figure 5 shows the waveform of multistage voltage swell that results from altering the parameters α=0.5, t1=0.3, and t2=0.7. The voltage signal has a multistage swell that lasts for 0.4 seconds. First stage of swell is obtained between duration 0.3 to 0.5 and second stage

of swell is obtained between 0.5 to 0.7 sec. The length of the signal is one second.
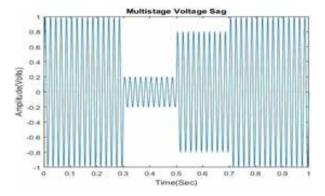
Fig 4. Waveform of Multistage Voltage Sag
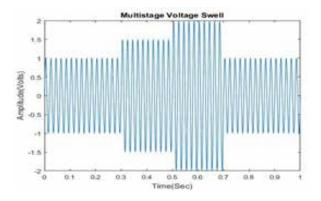
Fig 5. Waveform of Multistage Voltage Swell

Figure 6 shows the waveform of multistage voltage sag with swell that results from altering the parameters α=0.5, t1=0.3, and t2=0.7. The voltage signal has a multistage swell that lasts for 0.4 seconds. In first stage of sag is obtained between duration 0.3 to 0.5 and in second stage swell is obtained between 0.5 to 0.7 sec. The length of the signal is one second.
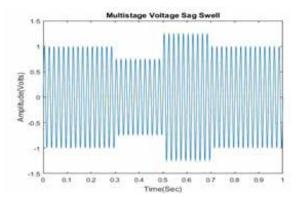
Fig 6. Waveform of Multistage Voltage Sag with Swell

RESULTS OF PQ INDEX CURVES

The voltage signal with harmonic sag that was created by simulating the mathematical equations in MATLAB is being subjected to the Hilbert transform. Calculating the absolute value from Hilbert transform's yields the PQ index curve[12,13]. The waveform of a signal containing a voltage sag harmonic, and a PQ index curve is shown in figure 7. The harmonic voltage sag and reduction in PQ index curve is obtained between 0.3 to 0.7 seconds as shown in figure 7.
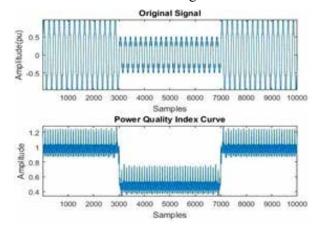
Fig 7 PQ Index Curve for Voltage Sag with Harmonics

The voltage signal with harmonic swell that was created by simulating the mathematical equations in MATLAB is being subjected to the Hilbert transform. Calculating the absolute value from Hilbert transform's yields the PQ index curve. The waveform of a signal containing a voltage swell harmonic, and a PQ index curve is shown in Figure 8. The harmonic voltage swell and increase in PQ index curve is obtained between duration 0.3 to 0.7 seconds as shown in figure 8.
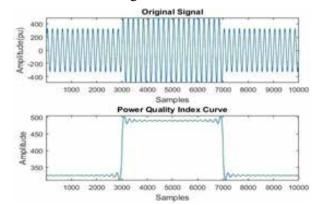
Fig 8 PQ Index Curve for Voltage Swell with Harmonics

The voltage signal with harmonic interruption that was created by simulating the mathematical equations in MATLAB is being subjected to the Hilbert transform. Calculating the absolute value from Hilbert transform's yields the PQ index curve. The waveform of a signal containing a voltage interruption harmonic, and PQ index curve is shown in Figure 9. The harmonic voltage interruption and reduction in PQ index curve is obtained between duration 0.3 to 0.7 seconds as shown in figure 9.
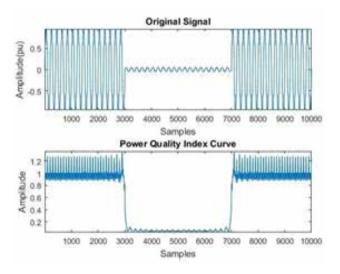
Fig 9 PQ Index Curve for Voltage Interruption with Harmonics

The voltage signal with multistage voltage sag that was created by simulating the mathematical equations in MATLAB is being subjected to the Hilbert transform. Calculating the absolute value from Hilbert transform's yields the PQ index curve. The waveform of a signal containing a multistage voltage sag, and a PQ index curve is shown in figure 10. In first stage the PQ index curve drop from 0.3 to 0.5 seconds again in second stage PQ index curve drop from 0.5 to 0.7 sec.

The voltage signal with multistage voltage swell that was created by simulating the mathematical equations in MATLAB is being subjected to the Hilbert transform. Calculating the absolute value from Hilbert transform's yields the PQ index curve. The waveform of a signal containing a multistage voltage swell and a PQ index curve is shown in Figure 10. In first stage the PQ index curve increase from 0.3 to 0.5 seconds again PQ index curve increase from 0.5 to 0.7 sec.
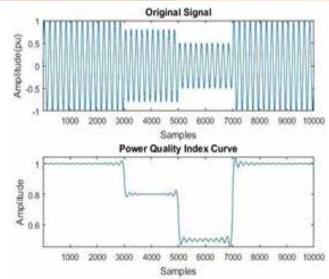
Fig 10 PQ Index Curve for Multistage Voltage Sag
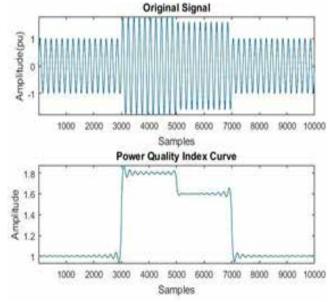
Fig 11 PQ Index Curve for Multistage Voltage Swell

The voltage signal with multistage voltage swell sag that was created by simulating the mathematical equations in MATLAB is being subjected to the Hilbert transform. Calculating the absolute value from Hilbert transform's yields the PQ index curve. The waveform of a signal containing a multistage voltage swell and sag and a PQ index curve is shown in figure 12. In first stage the PQ index curve increase from 0.3 to 0.5 sec again in second stage PQ index curve decrease from 0.5 to 0.7 sec.

Fig 12 PQ Index Curve for Multistage Voltage Sag with Swell

Table 2. Features Extracted from PQ Index Curves

PQ Disturbances	F1	F2	F3	F4
Voltage Sag Harmonics	0.91079	1.68467	0.06897	0.26262
Voltage Swell Harmonics	327.0745	1.18059	6359.913	79.7490
Voltage Interruption Harmonics	0.91101	1.27345	0.22256	0.47177
Multistage Voltage Sag Swell	1.00001	2.56209	0.16833	0.41028
Multistage Voltage Sag	0.99770	2.45786	0.03820	0.19547
Multistage Voltage Swell	1.00444	1.39493	0.12126	0.34822

CLASSIFICATION RESULTS OF PQDS

The values of the features F1, F2, F3, and F4 extracted from PQ Index Curves are shown in Table II. These features are supplied as input to the thresholding-based algorithm, which uses them to classify the different PQDs. The categorization process starts with the attribute F1. The PQDs considered in the first algorithm are voltage sag with harmonics, voltage swell with harmonics and voltage interruption with harmonics. First group consists of voltage swell with harmonics whereas the second group consists of the voltage sag with harmonics and voltage interruption

with harmonics. Figure 6.1 shows the classification of multiple PQDs using the thresholding-based algorithm.
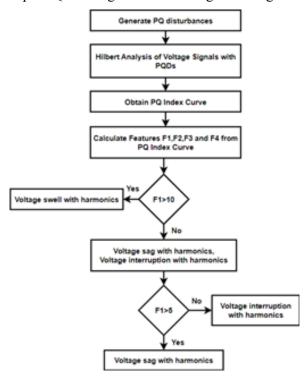
Fig 6.1 Algorithm for Classification of Multiple PQ D
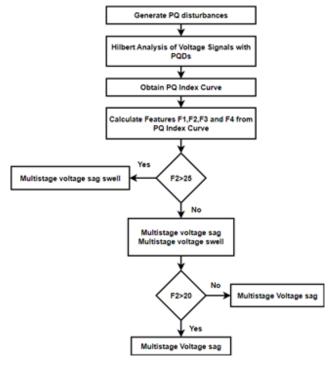
Fig 6.2 Algorithm for Classification of Multistage PQDs

The values of the features F1, F2, F3, and F4 extracted from PQ Index Curves are shown in Table II. These features are supplied as input to the thresholding-based algorithm, which uses them to classify the different PQDs. The categorization process starts with the attribute F2. The PQDs considered in the second algorithm are multistage voltage sag, multistage voltage swell and multistage voltage sag with swell. First group consists of multistage voltage swell with sag whereas the second group consists of the multistage voltage sag and multistage voltage swell. Figure 6.2 shows the classification of multistage PQDs using the thresholding-based algorithm.

CONCLUSION

In this study, an algorithm for classifying multiple and multistage PQ disturbances is presented that makes use of Hilbert transform and a thresholding based algorithm. The main aim of this study is to generate complex PQ disturbances using integral mathematical equations implemented in MATLAB software and classify them accurately. Using the Hilbert Transform, the voltage signals with PQ disturbances derived via mathematical modelling are processed. The features that can be derived from the Hilbert transform are fairly straightforward but very powerful. The Hilbert transform may be calculated quickly, making the suggested method more effective The features extracted from the PQ Index Curve are found to be sufficient to accurately classify the complex PQ disturbances with ease. The thresholding based algorithms classifies both multiple and multistage PQ disturbances. The propsed approach gives satisfactory results. Overall the algorithms developed are less complex. The proposed technique has been found to be successful in classifying the various complex PQ disturbances.

REFERENCES

1. IEEE Standards Board, IEEE Std. 1159-1995, IEEE Recommended Practice for Monitoring Electric Power Quality (New York: IEEE, Inc. June, 1995).

2. R. S. Kankale, S. R. Paraskar, and S. S. Jadhao, "Classification of Power Quality Disturbances in Emerging Power System Using Discrete Wavelet Transform and K-Nearest Neighbor," ECS Transactions, vol. 107, no. 1, pp. 5281–5291, 2022, doi: 10.1149/10701.5281ecst

3. T. Jayasree a, D. Devaraj, R. Sukanesh, "Power quality disturbance classification using Hilbert transform and RBF networks," neurocomputing, volume 73, issues 7–9, 2010, pages 1451- 1456, ISSN 0925-2312

4. Vishakha Pandya, Om Prakash Mahela, Sunil Agarwal, Sunita Choudhary, "Recognition of Power Quality Disturbances Using Hybrid Algorithm Based on Combined Features of Stockwell Transform and Hilbert Transform," 2020 IEEE International Students' Conference on Electrical, Electronics and Computer Science (SCEECS)

5. R. Kaushik, O. P. Mahela, P. K. Bhatt, B. Khan, S. Padmanaban and F. Blaabjerg, "A hybrid algorithm for recognition of power quality disturbances," in IEEE access, vol. 8, pp. 229184-229200, 2020, doi: 10.1109/access.2020.3046425

6. Granados-Lieberman, M. Valtierra-Rodriguez, L. A. Morales- Hernandez, R. J. Romero-Troncoso, and R. A. Osornio-Rios, "A Hilbert transform-based smart sensor for detection, classification, and quantification of power quality disturbances," Sensors (Switzerland), vol. 13, no. 5, pp. 5507–5527, 2013, doi: 10.3390/s130505507.

7. Rahul and M. M. Tripathi, "Hilbert Huang Transform and type-1 Fuzzy based Recognition and Classification of Power Signal Disturbances," pp. 2198–2203.

8. Roger C. Dugan, Mark F. McGranaghan, Surya Santoso, and H. Wayne Beaty, "Electrical power system quality," Second Edition, MscGraw Hill Publication

9. R. H. G. Tan and V. K. Ramachandaramurthy, "Numerical model framework of power quality events," Numerical Journal of Scientific Research Research, Vol. 43, No. 1, pp. 30-47, June 2010.

10. R. S. Kankale, S. R. Paraskar, and S. S. Jadhao, "Implementation of Integral Mathematical Models of Single and Multiple Power Quality Disturbances," vol. 8, no. 6, pp. 330–336, 2021, doi: 10.17148/IARJSET.2021.8657

11. Ms. Rekha Suresh Ghate, A.V. Harkut,, P.R.Jawale,"Review on implementation of integral mathematical model of power quality disturbances," International Journal of Creative Research Thoughts (IJCRT), Vol. 10, June 2022

12. R. Saini, O. P. Mahela and D. Sharma, "Detection and classification of Complex power quality disturbances using Hilbert Transform and rule based decision

tree," 2018 IEEE 8th Power India International Conference (PIICON), 2018, pp. 1-6, doi: 10.1109/poweri.2018.8704427.

13. R. Saini, O. P. Mahela and D. Sharma, "an algorithm based on Hilbert Transform and rule based decision tree classification of power quality disturbances," 2018 IEEE 8th Power India International Conference (PIICON), 2018, pp. 1-6, doi: 10.1109/poweri.2018.8704465.

14. Om Prakash Mahela, Abdul Gafoor Shaik and Neeraj Gupta, "A critical review of detection and classification of power quality events," Renewable and Sustainable Energy Reviews, Vol. 41, pp. 495–505, 201

15. R. S. Kankale, S. R. Paraskar, and S. S. Jadhao,"Classification of Power Quality Disturbances in Emerging Power System using S-transform and Support Vector Machine," 2021 IEEE 2nd International Conference On Electrical Power and Energy Systems (ICEPES), DOI: 10.1109/ICEPES52894.2021.9699673

A Hilbert Transform Based Approach for Classification of Power Quality Disturbances

Sneha Khodke[1], Ravishankar Kankale[2], Dr Sudhir Paraskar[3], Dr. Saurabh Jadhao[4]

PG Student, Department of Electrical Engineering SSGMCE, Shegaon, India[1]

Assistant Professor, Department of Electrical Engineering SSGMCE, Shegaon, India[2]

Professor & Head, Department of Electrical Engineering SSGMCE, Shegaon, India[3]

Associate Professor, Department of Electrical Engineering SSGMCE, Shegaon, India[4]

Abstract: This study proposes an approach for classifying single stage Power Quality Disturbances (PQDs) that is based on the Hilbert Transform. These power quality disturbance signals are produced utilizing the MATLAB environment's simulation models and integral mathematical models of PQDs. Voltage sag, voltage swell, and voltage interruption are the power quality disturbances taken into account in this study. The Power Quality Index (PQI) curve is generated from these signals using the Hilbert transform, and features are then extracted from it. By changing the parameters, multiple instances of power quality disturbances are produced, and a dataset is produced. In order to train and test the Feed Forward Neural Network (FFNN) classifier, the dataset signals are transformed using the Hilbert transform to produce a feature vector. Calculating the efficiency of the proposed algorithm yields the effectiveness of the provided strategy. The single stage power quality disturbances are classified using a thresholding-based method as well.

Keywords: Power Quality Disturbances, Power Quality Index, Hilbert Transform, Feed Forward Neural Network

I INTRODUCTION

Power quality represents an equipment's capacity to use the power being supplied to it as well as the ability of a power grid to efficiently supply power to consumers. Technically speaking, sinusoidal waveform measurement, analysis, and improvement at the rated voltage and frequency constitute power quality.

A power system's efficiency and cost can be significantly impacted by power quality. Therefore, it is crucial to ensure that the system is compatible with the power given to it and that the power it consumes is of the appropriate quality. Consumer awareness of power quality has increased recently, which is why many governments have amended their regulations to require electric utilities to ensure that the power quality is up to design standards. Modern electrical utility equipment is also more susceptible to fluctuations in power quality. Power quality is a problem for utilities, manufacturers, and consumers, and this issue is growing daily.

Disturbances such voltage swell, voltage sag, notch, transients, harmonic distortions, and so on are the main culprits for power quality degradation. Due to the fact that electric motors consume more current while starting than when operating at rated speed. So voltage sag could be caused by an electric motor beginning. A huge capacitor bank being charged up can also increase voltage. Before taking the necessary mitigation measures, such disturbances should first be discovered in a practical distribution network to improve power quality.

II. POWER QUALITY

The term Power Quality is defined in various type, as per IEEE power quality is define as "the concept of powering and grounding sensitive electronics equipment in a manner that is suitable to the operation of that equipment"

IEC (International Electrotechnical Commission) power quality is a set of parameters defining the properties of power supply as delivered to the user in normal operating conditions in terms of continuity of supply and characteristics of voltage (magnitude, frequency, waveform).

[A] Interruption: An interruption occurs when the supply voltage or load current decreases to less than 0.1 pu for a period of time not exceeding 1 min.

[B] Voltage Sag: A sag is decrease in rms value of voltage or current between 0.1 to 0.9 pu at the power frequency for duration from 0.5 cycle to 1 min.

[C] Voltage Swell: A swell is increase in rms value of voltage or current between 1.1 to 1.8 pu at the power frequency for duration from 0.5 cycle to 1 min.

III LITERATURE SURVEY

Rahul Saini et al. (2018) for the classification of power quality disturbances, describe an algorithm based on the Hilbert Transform and Rule base decision tree. In this instance, the power quality index curve is produced after processing the voltage signal using the Hilbert Transform. In order to classify data, features from the Hilbert Transform output are provided as input to the rule-based decision tree. The results of this investigation show that the suggested method is efficient at identifying and categorising complicated power quality issues.

T. Jayasree et al. (2009) the classification of power quality (PQ) disturbances using the Hilbert transform and an artificial neural network (ANN) is presentedIn that the Hilbert transform (HT) is used to obtain the input features for the ANN from the envelope of the disturbance signals. The radial basis function (RBF) neural network receives these information after normalisation. According to the results of this study, the suggested approach is effective, low-sensitive to noise levels, and delivers improved classification accuracy even in noisy environments. Hilbert transform is also calculated more quickly than S-transform and Wavelet transform.

Vishakha Pandya et al. (2020) the combined characteristics of the Stockwell Transform and Hilbert Transform are presented for the detection and categorization of power quality issues. S- and H-transforms are applied to the resulting PQD signal in order to produce the S- and H-indices. To identify PQ disturbances, the ST-index, H-index, and PQ index are displayed and contrasted with reference plots pertaining to pure sine waves. The decision-supported rule uses the peak value of PQ disturbances as an input to effectively classify PQ disturbances. According to the results of this investigation, the proposed method has a high accuracy of better than 99% for both the detection and categorization of PQ disturbances.

R. Kaushik et al (2020) We offer a technique to identify single-stage and multiple (multi-stage) power quality disturbances (PQDs) utilising hybrid characteristics of the Hilbert transform (HT) and the Stockwell transform (ST). For the purpose of identifying PQDs, a power quality index (PI) and temporal location index (TLI), based on features derived from the voltage signal using HT and ST, are proposed. When classifying PQDs using a decision tree with rules, four features taken from the PI and TLI are taken into account. It is discovered that even in the presence of large levels of noise, an algorithm is effective in recognising both single stage and multiple PQD with an efficiency greater than 98%. The algorithm is scalable for use with voltages of all ranges and faster than several reported solution.

David Granados-Lieberman et al (2013) introduces a smart sensor for the identification, categorization, and measurement of PQD. The suggested smart sensor is built using FPGA technology, which offers high online compute performance as well as a cheap, portable, and effective SoC solution. A feed forward neural network (FFNN) classifies the envelope of a PQD while the Hilbert transform (HT) is employed as a detection technique. Last but not least, the indices derived from HT and Parseval's theorem for root mean square voltage (Vrms), peak voltage (Vpeak), crest factor (CF), and total harmonic distortion (THD). This leads to the conclusion that smart sensor results acquired under simulated and actual operating settings demonstrate their accuracy, precision, and immunity to noisy surroundings, making their industrial usefulness clear.demonstrate a hybrid algorithm.

Eyad A. Feilat1a et al (2017) explains a method for quickly identifying and categorising short-lived voltage fluctuations, such as voltage sag, swell, and interruption. The detection method is based on classification using an artificial neural network and envelope generation using the Hilbert transform. The suggested envelope detection-ANN based classifier methodology offers a robust method for the quick and accurate categorization of voltage changes as well as the estimation of the voltage variation's beginning, ending, and length times.

R. S. Kankale et al (2022) explains research on a wavelet and machine learning approach for categorising PQDs in developing power systems. PQDs such voltage sag, swell, and interruptions are produced during the simulation of the new power system utilising a solar PV system and are then processed using a discrete wavelet transform. For the purpose of categorising PQDs, a machine learning-based classifier is created using the features extrapolated from DWT analysis. On a number of PQDs, the suggested approach has been evaluated. The simulation results demonstrate the effectiveness of the suggested technique for PQD classification.

Rahul et al (2018) introduces the Hilbert-Huang transform (HHT) and support vector machine-based hybrid recognition method and classification methodology to improve the accuracy of delivery and ensure effective recognition of power quality events. These power quality events split into intrinsic mode components and empirical mode decomposition Hilbert-Huang transform components. Empirical Mode Decomposition (EMD) is used to execute a decomposition

operation and feature separation for non-stationary power quality disturbances into intrinsic mode functions (IMFs). These factors are crucial in determining the frequency and amplitude of power quality events. Fuzzy rules are created based on these traits, and power quality problems are classified. From this, it is discovered that the suggested method has improved validity and accuracy for monitoring power quality disturbances.

IV METHODOLOGY

The following steps are used in the proposed algorithm for the classification of the single stage PQ disturbances.

- Generate the single stage power quality disturbances using the simulink model and integral mathematical model.
- Apply the Hilbert transform to voltage signal with power quality disturbance using the following command of the MATLAB.
A=Hilbert (v)
- Obtain the power quality index curve values using the following command and plot the curve.
B=abs (A)
- Obtain the features F1, F2, F3 and F4 from the power quality index curve using the following relations
F1=median (B) F2=kurtosis (B) F3=var (B) F4=std (B)
- These features are given as input to the thresholding-based algorithm for classification purpose and all the PQ disturbances are classified effectively.
- A feature vector is created by processing the dataset signals using Hilbert transform in order to train and test the ANN classifier.
- The effectiveness of the proposed approach is obtained by calculating the efficiency of proposed algorithm

V GENERATION OF POWER QUALITY DISTURBANCES

Power quality disturbances are generated by MATLAB Simulated model and integral mathematical equations in MATLAB Software system.

5.1 Generation of PQDs using MATLAB Simulink model

The single stage power quality disturbances such as voltage sag, voltage swell and voltage interruption are generated using MATLAB simulation model. Table I shows the configuration of Simulink models for generation of power quality disturbances.

Table I: Configuration of Simulink model used for generation of PQDs

Components	Parameters
3-Phase Voltage Source	11kV, 400V, 50Hz, 1MVA
3-Phase Programmable Source 11kV, 400V, 50Hz,	11kV, 400V, 50Hz, 1MVA
3-Phase Transformer	3-Phase Transformer 11kV/400V, 50Hz, 1MVA
3-Phase Active Load	500kW, 400V, 50Hz
3-Phase Reactive Load	100kVAR, 400V, 50Hz
Bus1	11 kV
Bus2	0.4 kV
Fault Resistance	1ohm, 1 MVA SC
Breaker Resistance	0.001ohm
Sampling Frequency	10 kHz

A. Generation of Voltage Sag

The voltage sag simulation model in MATLAB is depicted in Figure 2. The model is made up of a feeder representing a three-phase AC voltage source, a three-phase step-down transformer, a three-phase load, and a three-phase fault. Table 2 provides a full setup of each component. A three-phase ground fault is established at the 11 kV bus in order to produce the three-phase balanced voltage sag. A voltage sag is seen at both the 11 kV and 0.4 kV buses for 0.4 sec during the 0.3 second fault initiation and 0.7-second fault clearance. This voltage sag's magnitude can be altered by adjusting the fault resistance.
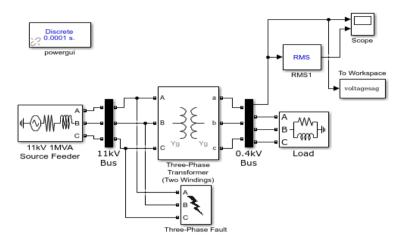
Fig 2. MATLAB Simulink model for Voltage Sag

B. Generation of Voltage Swell

The MATLAB simulation model for voltage swell is shown in Figure 3. A three-phase programmable voltage source that represents a feeder and a three-phase load makes up this model. Table 2 lists every component's precise configuration. Three phase voltage sources with variable amplitudes are used to produce a three-phase balanced voltage swell at 0.4 kV bus. At 0.3 seconds, a voltage swell is initiated and maintained for 0.7 seconds. The size of this voltage swell is adjustable by changing the amplitude in a programmable source.
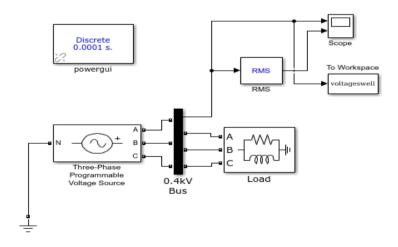
Fig 3 MATLAB Simulink model for Voltage Swell

C. Generation of Voltage Interruption

The MATLAB Simulation model for voltage interruption is displayed in Figure 4. A three-phase circuit breaker, a three-phase step-down transformer, a three-phase load, and a three-phase AC voltage supply (representing a feeder) are all included in this model. Table 2 lists every component's precise configuration. A three-phase circuit breaker in an 11 kV feeder is activated to cut off the supply to the three-phase transformer in order to produce the three-phase voltage interruption. A voltage interruption is seen at 0.4 kV buses during a circuit breaker's OPEN and CLOSED phases of 0.3 and 0.7 seconds, respectively.
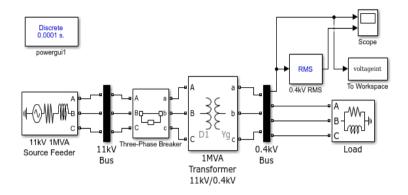
Fig 4 MATLAB Simulink model for Voltage Interruption

5.2 Generation of PQDs using mathematical modelling

PQDs	Equations	Parameters
Voltage sag	$x(t) = A (1 - \alpha(u(t - t1) - u(t - t2))) \sin(\omega t)$	$0.1 \le \alpha \le 0.8$, $T \le (t2 - t1) \le 9T$
Voltage swell	$x(t) = A (1 + \alpha(u(t - t1) - u(t - t2))) \sin(\omega t)$	$0.1 \le \alpha \le 0.8$, $T \le (t2 - t1) \le 9T$
Voltage interruption	$x(t) = A (1 - \alpha(u(t - t1) - u(t - t2))) \sin(\omega t)$	$0.9 \le \alpha \le 1$, $T \le (t2 - t1) \le 9T$

V. SIMULATION RESULT AND DISCUSSION

5.1 Results of PQDs Generated using MATLAB Simulink Models

To acquire PQDs voltage sag on an 11kV bus, a three-phase symmetrical fault is given to the system and causes voltage sag using the simulation model of voltage sag in MATLAB Simulink. A three phase to ground fault occurs on an 11 Kv bus in 0.3 seconds and is repaired in 0.7 seconds. During the period of the problem, there is a voltage drop on the 11 kV and 0.4 Kv bus V buses. One second is chosen as the simulation time. The fault resistance amplitude can be altered. The instantaneous and RMS voltage waveform with a sag of 50% is shown in Fig. 5 and was generated by the MATLAB Simulink model.
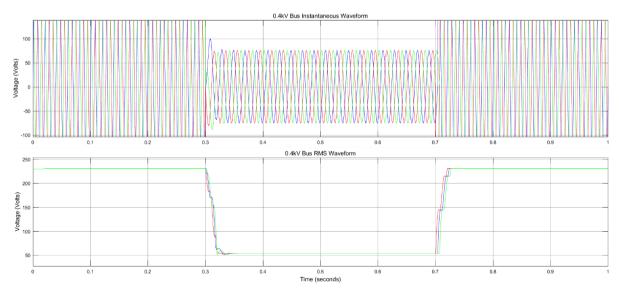
Fig 5 Waveform for Voltage Sag

In MATLAB Simulink, the voltage swell simulation model is run to produce the voltage swell. The characteristics of the programmable source can be altered to alter the amplitude of the voltage swell. The duration of the event is 0.3 and 0.7

seconds. The instantaneous and RMS voltage waveform with a swell of 20% is shown in Fig. 6 after the simulation time is adjusted to 1 sec. using the MATLAB Simulink model.
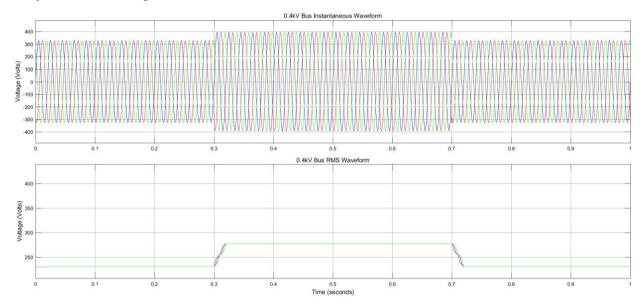
Fig 6 Waveform for Voltage Swell

In MATLAB Simulink, the voltage interruption simulation model is simulated to obtain the voltage interruption. A voltage interruption is observed at the 0.4 kV bus when the circuit breaker at the 11 kV feeder opens at 0.3 seconds and shuts off at 0.7 seconds. One second is chosen as the simulation time. The instantaneous and RMS voltage waveform with an interruption from the MATLAB Simulink model is displayed in fig. 7.
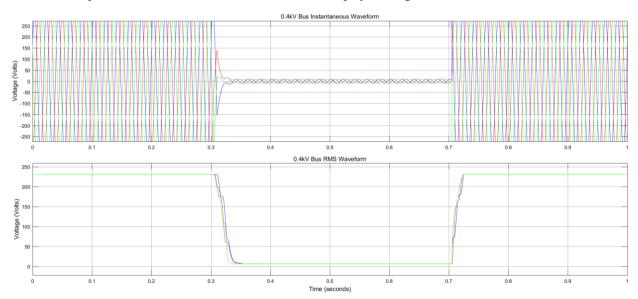
Fig 7 Waveform for Voltage Interruption

5.2 Results of PQDs Generated using integral mathematical modelling

The parametric equations are programmed in MATLAB programming to produce the single stage PQDs. The parameter A controls the PQDs' amplitudes, while the temporal constants t1 and t2 govern their durations. In this study, the value of A=326 represents the highest value of the three-phase instantaneous waveform, and the RMS value was determined to be 400 V. Figure 7 displays the voltage signal with a 50% sag for 0.4 seconds that was produced by altering the parameters =0.6, t1=0.3, and t2. The waveform's complete duration is one second.
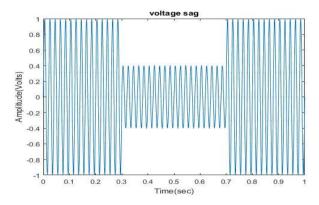
Fig 8 Waveform for Voltage Sag

Figure 8 illustrates the voltage signal that results from altering the parameters =0.5, t1=0.3, and t2=0.7. The voltage signal has a swell that lasts for 0.4 seconds. The waveform's complete duration is one second.
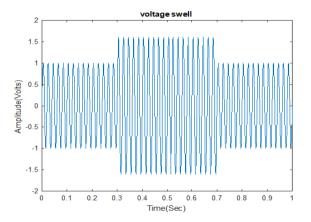
Fig 9 Waveform for Voltage Swell

Figure 10 illustrates the voltage signal with a 0.4-second interruption that is produced by varying the values of =0.95, t1=0.3, and t2=0.7. The waveform's complete duration is one second.
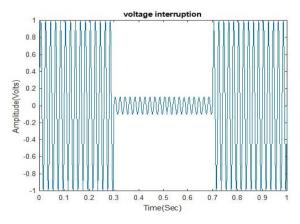
Fig 10 Waveform for Voltage Interruption

5.3 Power Quality Index Curve

The Hilbert transform is used to deconstruct the voltage signal with sag that was produced by simulating the mathematical equations in MATLAB. Calculating the output of the Hilbert transform's absolute value yields the power quality index curve. Figure 11 displays the waveform of a signal with a voltage sag and a power quality index curve. Figure 11 shows that values of the power quality index curve drop from 0.3 seconds to 0.7 seconds.
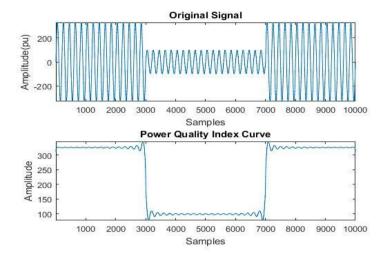
Fig 11 Power Quality Index Curve of Voltage Sag

The Hilbert Transform is used to decompose the signal with voltage swell that was produced by simulating the mathematical relationship. Calculating the absolute values of the output of the Hilbert transform yields the power quality index curve. Figure 12 provides the voltage signal waveforms with swell and the proposed power quality index curve for the voltage swell. This can be seen in Fig. 12, where the values of the power quality index curve increase at 0.3 and 0.7 s, respectively, indicating the occurrence of voltage swells between those times.
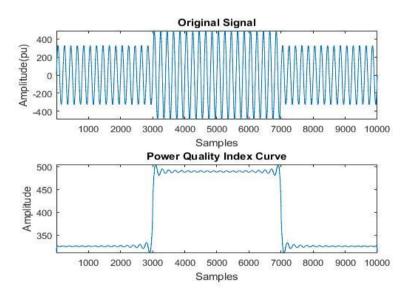
Fig 12 Power Quality Index Curve of Voltage Swell

The Hilbert Transform is used to breakdown the voltage-interrupted signal that was produced by simulating the mathematical relationship. Calculating the absolute values of the output of the Hilbert transform yields the power quality index curve. Figure 13 provides the voltage signal waveforms with interruptions and the proposed power quality index curve for the voltage interruption. This can be seen in Fig. 13, where the values of the power quality index curve increase at intervals of 0.3 to 0.7 seconds, suggesting the presence of voltage interruptions.
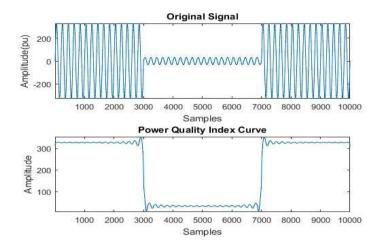
Fig 13 Power Quality Index Curve of Voltage Interruption

Table II Features of Power Quality Disturbances

PQ disturbances	F1	F2	F3	F4
Voltage Sag	324.4901375	1.181264408	12439.33053	111.5317467
Voltage Swell	327.2457379	1.180576302	9157.608646	95.69539512
Voltage Interruption	324.0777875	1.181669005	20471.08924	143.0772143

VI CLASSIFICATION OF POWER QUALITY DISTURBANCES

6.1 Classification of Single Stage PQD using mathematical modelling

The values of features F1, F2, F3, F4 provided in the Table II. These features are given as input to the thresholding-based algorithm for the classification of the single stage power quality disturbances. The detailed classification of the power quality disturbances using the thresholding based algorithm is provided in fig.14. The classification is initialized using the feature F4. The first group consists of voltage interruption whereas the second group consists of the voltage sag, voltage swell.
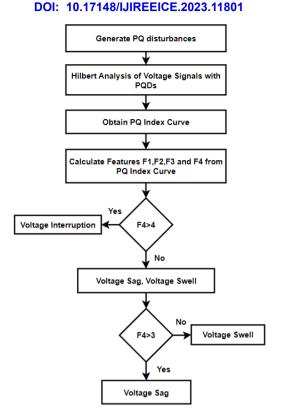
Fig 14 Classification of Single Stage PQD Using Thresholding Based Algorithm

6.2 Classification of Single Stage PQD using Simulink Model
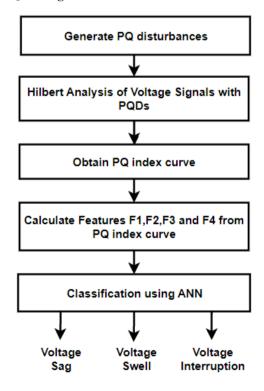
Fig 16 Classification of Single Stage PQD using ANN

The feature vector with 48 datasets of each disturbance (48x3=144) are fed to ANN classifier. 80% of the data (115 datasets out of which 39 datasets are of sag, 41 datasets are of swell and 35 datasets are of interruptions) are used for training purpose and 20% data (29 datasets out of which 7 datasets are of sag, 7 datasets are of swell and 13 datasets are

of interruptions) are used for testing purpose. Fig 17 shows all confusion matrix, from this matrix it is found that voltage sag is classified with an accuracy of 93.8%, voltage swell is classified with 100% and voltage interruption is classified with 95.8% accuracy. The overall accuracy of classifier is 96.5%.
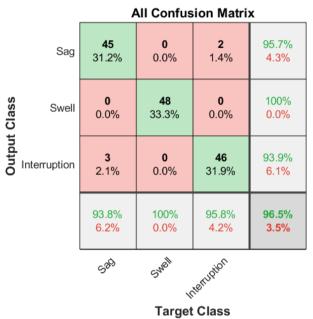
Fig 17 All Confusion Matrix

The ANN classifier's training results are displayed in the form of confusion matrix in fig 18, from this matrix it is found that voltage sag is classified with an accuracy of 92.3%, voltage swell is classified with 100% and voltage interruption is classified with 97.1% accuracy. The overall accuracy of training is 96.5%.
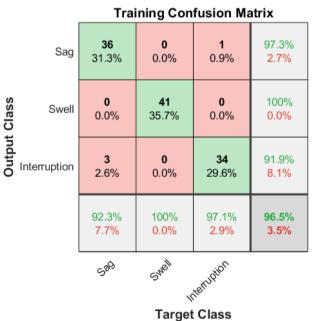
Fig 18 Training Confusion Matrix

The ANN classifier's testing results are displayed in the form of confusion matrix in 19, from this matrix it is found that voltage sag is classified with an accuracy of 100%, voltage swell is classified with 100% and voltage interruption is classified with 92.3% accuracy. The overall accuracy of training is 96.6%.
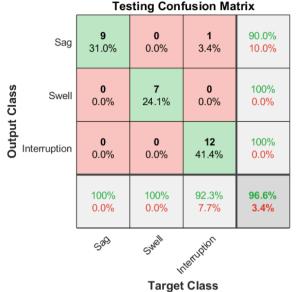
Fig 19 Testing Confusion Matrix

VII CONCLUSION

This research work presents an algorithm using Hilbert transform and thresholding-based algorithm for classification of PQ disturbances. It has been concluded that the proposed algorithm is effective in the classification of the various single stage PQ disturbances with efficiency greater than 96%. The features extracted from the Hilbert transform are very simple and yet very effective. It found sufficient to accurately classify the single stage PQ disturbances with ease. The proposed approach gives satisfactory results. Overall, the algorithms developed are lesscomplex. The ANN classifier takes less time for training and the classification accuracy is very high. The proposed technique has been found to be successful in classifying the various complex PQ disturbances. Compared to the Wavelet transform and S-transform, the Hilbert transform can be quickly calculated, so that the proposed method is efficient, making the suggested method more efficient.

REFERENCES

[1]. R. Saini, O. P. Mahela and D. Sharma, "Detection and Classification of Complex Power Quality Disturbances using Hilbert Transform and rule-based decision tree," 2018 IEEE 8th Power India International Conference (PIICON), 2018, pp. 1-6, doi: 10.1109/poweri.2018.8704427.

[2]. R. Saini, O. P. Mahela and D. Sharma, "An Algorithm based on Hilbert Transform and rule-based decision tree Classification of Power Quality Disturbances," 2018 IEEE 8th Power India International Conference (PIICON), 2018, pp. 1-6, doi: 10.1109/poweri.2018.8704465.

[3]. R. S. Kankale, S. R. Paraskar, and S. S. Jadhao, "Implementation of Integral Mathematical Models of Single and Multiple Power Quality Disturbances," vol. 8, no. 6, pp. 330–336, 2021, doi: 10.17148/IARJSET.2021.8657.

[4]. R. S. Kankale, S. R. Paraskar, and S. S. Jadhao "Generation of Power Quality Disturbances Required for the Performance Assessment of Different Power Quality Monitoring Algorithms using Multiple Approaches,"," vol. 2, pp. 405-414 pp. 330–336, DOI: 10.48175/IJARSCT-5995.

[5]. Jayasree, D. Devaraj, R. Sukanesh, "Power Quality Disturbance Classification using Hilbert Transform and RBF Networks", neurocomputing, volume 73, issues 7–9, 2010, pages 1451- 1456, ISSN 0925-2312, https://doi.Org/10.1016/j.Neucom.2009.11.008.

[6]. R. Kaushik, O. P. Mahela, P. K. Bhatt, B. Khan, S. Padmanaban and F. Blaabjerg, "A hybrid Algorithm for Recognition of Power Quality Disturbances," in IEEE access, vol. 8, pp. 229184-229200, 2020, doi: 10.1109/access.2020.3046425.

[7]. R. S. Kankale, S. R. Paraskar, and S. S. Jadhao, "Classification of Power Quality Disturbances in Emerging Power System Using Discrete Wavelet Transform and K-Nearest Neighbor," ECS Transactions, vol. 107, no. 1, pp. 5281–5291, 2022, doi: 10.1149/10701.5281ecst.

[8]. Vishakha Pandya, Om Prakash Mahela, Sunil Agarwal, Sunita Choudhary, "Recognition of Power Quality Disturbances Using Hybrid Algorithm Based on Combined Features of Stockwell Transform and Hilbert Transform," 2020 IEEE International Students' Conference on Electrical, Electronics and Computer Science (SCEECS).

[9]. R. Kaushik, O. P. Mahela, P. K. Bhatt, B. Khan, S. Padmanaban and F. Blaabjerg, "A hybrid algorithm for recognition of power quality disturbances," in IEEE access, vol. 8, pp. 229184-229200, 2020, doi: 10.1109/access.2020.3046425.

[10]. Granados-Lieberman, M. Valtierra-Rodriguez, L. A. Morales- Hernandez, R. J. Romero-Troncoso, and R. A. Osornio-Rios, "A Hilbert transform-based smart sensor for detection, classification, and quantification of power quality disturbances," Sensors (Switzerland), vol. 13, no. 5, pp. 5507–5527, 2013, doi: 10.3390/s130505507.

[11]. Rahul and M. M. Tripathi, "Hilbert Huang Transform and type-1 Fuzzy based Recognition and Classification of Power Signal Disturbances," pp. 2198–2203.

[12]. Roger C. Dugan, Mark F. McGranaghan, Surya Santoso, and H. WayneBeaty, "Electrical power system quality," Second Edition, McGraw Hill Publication.

Battery State of Charge Estimation Methods – A Critical Review

P. R. Dhabe[1], Dr. S. R. Paraskar[2], Dr. S. S. Jadhao[3]

Research Scholar, Department of Electrical Engineering, SSGMCE, Shegaon (M.S.), India[1]

Professor, Department of Electrical Engineering, SSGMCE, Shegaon (M.S.), India [2]

Associate Professor, Department of Electrical Engineering, SSGMCE, Shegaon (M.S.), India [3]

Abstract: The automobile sector across the globe has undergone a dramatic change in the last decade. It has started to trust something more, which initially was criticized for its inferior performance – the Electric Vehicle (EV). The battery is one of the most important components of an EV, and the Battery Management System (BMS) continues to be the bottleneck of EVs. However, accurate estimation of the State of Charge (SOC) of batteries is still challenging due to the non-linear characteristics of batteries. This led the scholars to propose various methods of SoC estimation. It now poses a challenge to establish a relationship between the accuracy and robustness of the methods, and their difficulties to implement. This paper publishes an exhaustive literature survey of the SoC estimation methods proposed by various scholars. All the more, it also provides feedback on each method, which will help to make an accurate choice of the SoC estimation method to be implemented. This will, in turn, help in the development of a reliable BMS.

Keywords: Battery Management System (BMS), State of Charge (SoC), Electric Vehicle (EV), Look-up table based estimation, model based estimation, adaptive system based estimation.

I. INTRODUCTION

The rise in global crude oil prices and the growing awareness of its environmental impacts have called for increased development in alternative energy storage systems. Battery happens to be an interesting energy storage system owing to its high efficiency. Battery storage system has seen a sharp rise in demand due to its wide use in battery-operated automobiles such as Electric Vehicle and Hybrid Electric Vehicle (HEV). Electric Vehicles are seen to be the new face of future transportation due to zero emissions [1].

Lithium ion Batteries (LiBs) are preferred choice of power supply in EVs due to their superiority over other batteries in terms of high specific energy, high output power and long life cycle [2]. An effective Battery Management System (BMS) in place is vital to ensure safe operation of battery, improved driving range, optimized power management and enhanced service life [2]–[5].

The BMS is responsible to acquire battery's voltage, current and internal temperature data to estimate various states of the battery and protect it from over-charging and over-discharging instances. SoC of a battery, used to represent the remaining capacity, is an important parameter of BMS, and hence it is imperative to have accurate estimation of the SoC to prevent the battery from over-charge, over-discharge and potential reduction in battery life [3].

II. BATTERY MANAGEMENT SYSTEM

A BMS is the equipment designed along with software and hardware to control battery operations at different operating conditions. It consists of controllers, sensors and actuators with an aim to enhance the battery life and guarantee its safety by accurately estimating different states of the battery.

A BMS, all the more, is also capable to interrupt the battery system in case of an abnormal operation. This, it does by closely monitoring the charge and discharge process of the battery and controlling it. A basic function diagram of a BMS is shown in Fig.1.
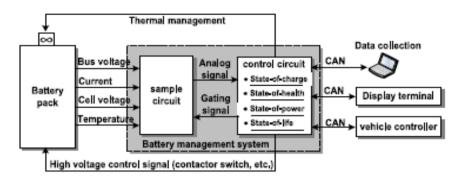
Fig.1 Function Diagram of Battery Management System

The control circuit of a BMS estimates the state of charge (SoC), state of health (SoH) and remaining useful life (RUL) of batteries with the help of advanced algorithms using measured battery current, voltage and temperature. The SoC of a battery can be defined as the percentage of the ratio of remaining capacity to the maximum available capacity. Over a period of time, a battery starts losing its capability to store energy. This deterioration of battery's capability is indicated by State of Health (SoH). Remaining Useful Life (RUL) is an indication of the number of load cycles remaining before the battery reaches its End of Life (EoL). Continuous measurement of voltage, current and temperature of battery enables the estimation of aforementioned battery parameters. However, the accurate estimation of battery parameters, especially SoC, is still a challenging task as battery's behaviour depends on various internal and external conditions. This is further aggravated by the change in battery characteristics over the period of time due to aging and charge-discharge cycles. All the more, the accurate estimation of SoC is hindered by limited battery models and parametric uncertainties. Many SoC estimation techniques proposed by researchers offer poor reliability and accuracy [4], [5]. Some researchers have, in detail, discussed SoC estimation methods along with the future developments and trends [6]–[8]. However, a systematic elaboration of the difficulties and challenges of methods is hard to find in the literature. This research paper aims to present a detailed review of the existing SoC estimation methods bring to the fore an ordered discussion of various SoC estimation metods along with their key challenges and difficulties of implementation. It also discusses the classification of SoC estimation techniques and possible developments likely to take place in the near future.

III. METHODS OF SOC ESTIMATION

The State of Charge (SoC) is a representation of battery's available capacity and is basically used to prevent the battery from being overcharged or undercharged. This in turn reduces the aging effects on the battery. As a result, it has become an interesting area of research and many researchers have proposed various methods for SoC estimation. Since many researchers have proposed methods for SoC estimation which involves combination of two or more techniques, the task of classifying the SoC estimation methods is no simple.

As individual methods have their own limitations, combining more than one technique to reduce the inaccuracies is not uncommon in the latest literatures. A combination of OCV technique, full charge detector and robust extended Kalman filter algorithm (REKF) is proposed in [9]. Despite the difficulty to classify SoC estimation methods due to combination of techniques, this research paper tries to make the classification referring to [10] and the work done by other researchers in the last decade or so. It has classified the SoC estimation methods into two main categories – Direct and Indirect Methods, and then it subcategories these two methods into several other techniques. Each of these methods is discussed along with their challenges and limitations in the following sections.

1. Direct Methods

Direct Method of SoC estimation relies upon measuring the physical properties of battery like current, voltage and temperature, and using an equation to estimate the SoC. The Direct Methods entail directly measuring or calculating SoC without the need for an independent model or system identification. These approaches are commonly preferred due to their straightforwardness and suitability for real-time applications.

1.1 Coulomb Counting (CC) Method

Coulomb Counting (CC) is considered as a standard method of SoC estimation [11]. Since it offers good accuracy for short-term estimations, CC is the most widely used method. According to CC method, SoC is defined by an equation given below [12] as

$$SoC(t) = SoC(t0) + \frac{1}{Cn} \int_{t0}^{t0+t} Ibat\,(d\tau) \times 100\%$$

Where, SoC(t0) is the initial State of Charge of battery, and Cn and Ibat refer to the nominal capacity and Charging/Discharging current of battery respectively. Although CC provides a very simplistic approach, it suffers from the error of initial value. There are also noise errors and errors in the battery current measurement. These errors, in turn, lead to the accumulated errors and the CC method loses its precision and accuracy. Since this method requires the knowledge of initial SoC, which in practice is difficult to acquire, it will give inaccurate estimation of SoC. Hence, it is often used in combination with other algorithms for increasing its accuracy and precision [13].

1.2 Open Circuit Voltage (OCV) Based Estimation

The Open Circuit Voltage method involves continuous measurement of the cell voltage and the corresponding SoC is determined from the look-up table. This method encounters the difficulty of requiring very high resolution sensors and ample amount of time to reach equilibrium for accurate measurement of SoC. Hence, it is practically less effective. Also, The OCV-SoC curve tends to shift upward as the charging current increases [14]. This behaviour of the curve informs that – the higher voltage limit is reached faster when the battery deals with large current, and for the same value of OCV battery does have different values of SoC as shown in fig.2. In addition to this, each cell has different OCV-SoC relationship which further deteriorates the reliability of this method. Hence, the OCV method is often used with methods for estimating SoC. In [15], [16], the authors have proposed a combination of discontinuous discharging method and Extended Kalman Observer method along with OCV-SoC look-up method to estimate the SoC of battery.
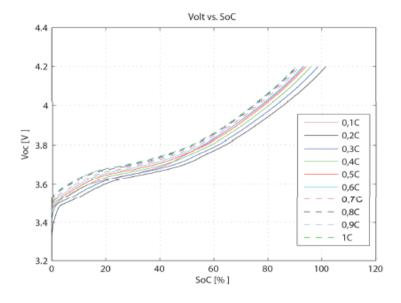

Fig.2 OCV-SoC curve for charging process at different current values

1.3 Impedance Measurement Based Estimation

This method involves the measurement of voltage and current at different frequencies and then computing its complex quotient to be the cell impedance. In [17], Electrical Circuit Model (ECM) is used for battery model and its parameters are calculated from the measured data of impedance which is then represented in the form of a Nyquist graph. This measured impedance is then divided into real and imaginary parts and is plotted against one another. As the parameters of the model become known, the SoC of the battery can then be computed. In [18], the author proposes Electrochemical Impedance Spectroscopy (EIS) approach for estimation wherein the impulse signal is broken down into factors of Fourier series. With this signal of different frequencies, the impedance is found by spectral analysis.

This estimation approach is specifically applicable under uniform charging conditions, making it unsuitable for Electric Vehicles (EVs) subject to inconsistent charging scenarios with varying currents. Furthermore, the method's effectiveness is constrained by its sensitivity to high temperatures, limiting its application to the high-frequency range.

2. Model-Based Estimation Methods

As they overcome the logjam of the direct measurement methods, Model-based estimation have become increasingly common. These methods set up a battery model and employ modern algorithms for estimation of battery states using its measured parameters like current, voltage and temperature. This section aims at reviewing only the electrical circuit battery models as they form the reference for most of the other battery modelling methods.

2.1 Electrical Circuit Model-Based Estimation

The three widely used Electrical Circuit Models (ECMs) are illustrated in [19]. The models are chosen owing to their excellent dynamic performance. The first of the models is known as Thevenin model which is a first order R-C model. The Thevenin model comprises of a non-linear voltage source (V_{OCV}) expressed as a function of SoC, battery terminal voltage V_t, charge or discharge current I_b, diffusion resistance (RP_1), a capacitor (CP_1) used to model the polarisation capacitance effects and an internal resistance (R_t). The other model consists of a capacitor added in series with (V_{OCV}). This model characterizes the capacity of charge stored in the battery and also describes the changes in the values of Open Circuit Voltage. The third model is a second order model which adds up a parallel combination of $RP_2 - CP_2$ in series with the first order model. The second order model is shown in Figure 3.
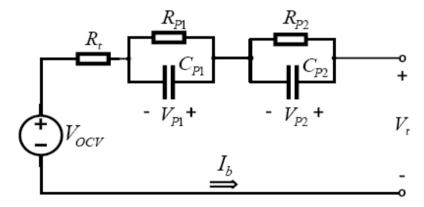

Fig.3 Second Order Electrical Circuit Model

Increasing the number of parallel RC networks proves to improve the precision of battery response estimation. In [19], the author has shown the second order model to be the most accurate as it has superior dynamic performance. In [20], the author compares the continuous and discrete time equations of second order model and draws an inference that there are sensitivity issues encountered in transformation of discrete parameters and hence makes the discrete time method less efficient. Accurately parameterizing the model for new batteries is a resource-intensive process, typically confined to laboratory settings. However, this approach is marked by high costs, time-consuming procedures, and often proves impractical for obtaining all requisite parameters. Moreover, the model falls short of providing a comprehensive description of the battery's electrochemical processes and lacks the capability to account for inherent inaccuracies.

2.2 Electrochemical Model-Based Estimation

An electrochemical model considers the internal electrochemical processes within the battery, providing a more detailed and accurate representation of its behaviour. It takes into account factors like electrode kinetics, ion diffusion, and temperature effects, allowing for a comprehensive understanding of the battery's state.

Electrochemical models provide a higher level of accuracy by considering the complex electrochemical reactions occurring within the battery. Also, electrochemical models can account for temperature variations, offering a more robust SoC estimation in diverse environments. However, electrochemical models can be computationally intensive and accurate SoC estimation relies on precise model parameterization, which can be challenging. For an instance, an electrochemical model discussed in [21] comprises six non-linear partial differential equations which require numerical solution.

3. Adaptive System-Based Estimation Methods

In recent times, the progress in artificial intelligence has led to the creation of diverse adaptive systems designed for SoC estimation. These newly developed techniques encompass a range of methodologies, including back propagation (BP)

neural networks, radial basis function (RBF) neural networks, fuzzy logic approaches, support vector machines, fuzzy neural networks, and Kalman filters. What sets these adaptive systems apart is their intrinsic self-designing nature, enabling automatic adjustments in response to evolving system conditions. Given the impact of various chemical factors on batteries and the nonlinearity inherent in SoC, adaptive systems emerge as effective solutions for accurate SoC estimation.

3.1 Back Propagation Neural Network-Based Estimation

A Neural Network operates on a mathematical algorithmic model to handle the intricate characteristics of a complex neural network or parallel processing. This technology excels at processing data and discerning relationships among various initial complex factors. Within the realm of Neural Network algorithms, the Back Propagation (BP) Neural Network stands out for its ability to solve non-linear systems, featuring a simpler topology compared to conventional Neural Network methods [22]. The BP Neural Network structure comprises three layers: the input layer, hidden layer, and output layer. The input layer incorporates parameters such as battery voltage, current, resistance, and ambient temperature, while the number of hidden layers is contingent on the desired system accuracy. The output layer generates an estimated SoC value. The primary objective of this method is to minimize the error value. However, the system error is contingent on factors such as the quantity of training data and the methodology employed in experiments. Training data, crucial for SoC estimation, is typically derived from charging and discharging battery experiments. The effectiveness of this training method is evident in minimizing error functions. However, errors may escalate if the BP Neural Network lacks sufficient training information from SoC values [23]. To mitigate this, it becomes imperative to utilize a substantial amount of training data from diverse batteries to achieve an accurate SoC value. This is crucial because the discharge characteristics of batteries may vary, even if they share the same type and manufacturer, owing to differences in the electrolyte quantity [24].

3.2 RBF Neural Network-Based Estimation

The RBF neural network proves to be an effective methodology for estimating systems with incomplete information, particularly adept at analysing relationships within a given set. It excels in comparing one major (reference) sequence with other sequences, offering valuable insights into diverse scenarios. The application of the RBF neural network extends to SoC estimation, as demonstrated through experimentation with battery data. Results indicate that the model's operational speed and estimation accuracy align with practical demands, underscoring its valuable applications [25].
In a study documented in [25], the SoC estimation method utilizing the RBF neural network relies on input data such as terminal voltage, discharging current, and battery temperature. This approach effectively estimates SoC for LiFePO4 batteries across varying discharging conditions. The experimental data obtained closely aligns with the model's predictions, validating its reliability and accuracy in SoC estimation.

3.3 Fuzzy Logic-Based Estimation

Fuzzy Logic (FL) serves as a problem-solving methodology designed to streamline complex input data characterized by noise, vagueness, ambiguity, and imprecision. This method employs objective rules to discern the actual value within the input data. The operational principle of a Fuzzy Logic technique can be delineated into four fundamental stages [26]:

a) Fuzzification**:** During this initial stage, the measured values of the system undergo a transformation into linguistic fuzzy sets. These sets are then categorized into membership functions, each indicating the degree of belonging to a specific logical set.
b) Fuzzy Rule Base**:** The development of a fuzzy rule base constitutes the second stage, drawing on professional expertise and insights into the system's operational methods. This rule base serves as a foundation for guiding the fuzzy logic process.
c) Inference Engine**:** In the inference engine stage, all fuzzy rules are systematically converted into fuzzy linguistic outputs. This transformation is pivotal in deriving meaningful insights from the input data based on the established fuzzy rule base.
d) Defuzzification**:** The final stage involves translating the linguistic fuzzy rules into analog output values. Defuzzification is the process through which the abstract and linguistic outcomes are transformed into concrete and quantifiable results.

By navigating through these four stages, Fuzzy Logic methodologies provide a structured approach to handling complex input data, extracting valuable insights, and generating meaningful output values. Fuzzy Logic (FL) systems possess the capability to make generalizations about any system through cycle number estimation.

This is particularly advantageous in battery tests where describing the battery's state as either "High" or "Low" may be more straightforward than obtaining a precise numerical value.

However, the computational expense associated with this method is substantial. Due to the requisite for a distinct and consistent battery characteristic rule, coupled with the substantial variation in battery parameters throughout the lifetime of Lithium-ion Batteries (LiBs), the accuracy of SoC estimation may be compromised. Specifically, if the proposed SoC estimation relies on static battery characteristics, this approach becomes practically unfeasible for LiBs employed in Electric Vehicles (EVs). Notably, the aging of the battery is not taken into consideration, further limiting the applicability of this method.

3.4 Support Vector Machines-Based Estimation

The Support Vector Machine (SVM) has found widespread application in pattern recognition, excelling particularly in classification across various domains. Interestingly, the SVM has also proven effective in addressing regression problems, a task inherently more challenging than classification. When employed as a nonlinear estimation system, the SVM exhibits greater robustness compared to a least-squares estimation system, showcasing insensitivity to minor changes [27].

In a study by Hansen and Wang [27], the application of SVM for estimating the SoC in lithium-ion batteries was investigated. The SVM-based estimator not only overcomes the limitations associated with the Coulomb counting SoC estimator but also delivers accurate SoC estimates, presenting a promising advancement in battery management technology.

3.5 Kalman Filter-Based Estimation

Utilizing real-time road data for the estimation of Battery SOC poses inherent challenges due to potential difficulties and costs associated with measurement. However, in a study outlined in [28], the application of the Kalman filter method is demonstrated to offer reliable SoC estimations through real-time state estimation. Kalman Filtering is a powerful and widely used technique for estimating the SoC of a battery. It combines mathematical modeling with real-time measurements to provide accurate and dynamic SoC estimates.

The two primary variations of Kalman Filtering used for SoC estimation are the Extended Kalman Filter (EKF) and the Unscented Kalman Filter (UKF). Overview of the Kalman Filtering technique for SoC estimation is as below:

a) Battery Model: Kalman Filtering relies on a mathematical model of the battery's behavior. This model can be a simple equivalent circuit model or a more complex physics-based model, depending on the accuracy desired.
b) State Variables: The SoC is considered a state variable in the Kalman Filter, which is continually estimated and updated. Other state variables might include the battery's internal resistance, capacity, or voltage.
c) System Dynamics: The battery model is used to describe how the SoC and other state variables change over time in response to factors like charging, discharging, temperature, and aging. These dynamics are typically described by a set of differential equations.
d) Measurement Model: The Kalman Filter combines the battery model with real-time measurements, such as voltage and current, to estimate the state variables. The relationship between the state variables and the measurements is described by a measurement model.
e) Prediction Step (Time Update): In the prediction step, the Kalman Filter uses the battery model and the system dynamics to predict how the state variables (including SoC) will change over a short time interval (a time step). This prediction includes an estimate of the SoC.
f) Update Step (Measurement Update): In the update step, the Kalman Filter compares the predicted state variables, including the predicted SoC, with the actual measurements taken from the battery (voltage and current). The filter calculates a correction factor that minimizes the difference between the predicted and measured values, and this correction is used to update the state variables, including SoC.

Iterative Process: The Kalman Filter iteratively performs the prediction and update steps at a high frequency, continually refining the SoC estimate based on new measurements.

Yatsui and Bai [29] introduced a SoC estimation method for lithium-ion batteries based on the Kalman filter. Through experimental validation, the effectiveness of the Kalman filter in online applications was substantiated.

Barbarisi et al. [30] proposed an extended Kalman filter (EKF) for estimating concentrations of key chemical species averaged across the thickness of the active material. This approach utilizes terminal current and voltage measurements to derive the SoC of the battery.

In the realm of SoC estimation, an innovative method is presented in [31] based on the unscented Kalman filter (UKF) theory and a comprehensive battery model. Results indicate the superiority of the UKF method over the extended Kalman filter method in accurately estimating SoC for batteries. Sun et al. [32] further contribute to this field by introducing an adaptive UKF method for estimating SoC in lithium-ion batteries used in electric vehicles. The adaptive adjustment of noise covariance during the SoC estimation process is implemented through the concept of covariance matching within the UKF framework.

The Kalman Filter based algorithms encounter challenges associated with heightened complexity, elevated computational costs, and instability. The method incorporates intricate matrix operations, potentially leading to numerical instabilities and complicating the implementation of the algorithm on standard, cost-effective microcontrollers. Kalman Filter (KF) methods exhibit a strong dependence on battery models and sensor precision, accompanied by limitations such as accuracy in linearization and the stability of filters derived from Jacobian matrices. The efficacy of KF variants hinges on prior knowledge of the model and the covariance of measurement noise. Any inaccuracies in system modeling and noise covariance may detrimentally impact filter performance, resulting in sub-optimal convergence or sluggish adaptation. KF performance is notably compromised in the presence of substantial uncertainties regarding model structure, physical parameters, noise levels, and initial conditions.

3.6 Fuzzy Neural Network-Based Estimation

The Fuzzy Neural Network (FNN) has found extensive applications, particularly in identifying unknown systems. In the realm of nonlinear system identification, the FNN demonstrates effectiveness by adeptly fitting nonlinear systems through the calculation of optimized coefficients within its learning mechanism.

In the field of SoC estimation, two prominent types of fuzzy-based neural networks frequently appear in the literature: the Adaptive Neuro-Fuzzy Inference System (ANFIS) and the Local Linear Model Tree [12]. These models primarily employ direct open-loop SoC estimation. ANFIS, specifically, combines the strengths of fuzzy systems and adaptive networks within a unified intelligent paradigm. By integrating the flexibility and subjectivity of fuzzy inference systems with the optimization prowess and learning capabilities of adaptive networks, ANFIS excels in modeling, approximation, nonlinear mapping, and pattern recognition. Its applications include modeling cell characteristics, online correction of other SoC estimation techniques for enhanced accuracy, and direct retrieval of the estimated SoC value [33], [34].

However, implementing direct open-loop SoC estimation introduces inaccuracies into the process. The approach demands a substantial volume of training data and involves extensive computations. Given the inherent open-loop nature of this method, adapting to the aging state of the battery becomes unfeasible. Moreover, the considerable volume of training data required significantly restricts its widespread applicability.

IV.   CONCLUSION

This paper provides a critical examination of the State of Charge (SoC) estimation methodologies presented by scholars in the recent past, elucidating the core principles and principal limitations of each approach. Only methodologies extensively employed in recent years are discussed, excluding those less prevalent. Through this review, it becomes evident that the most challenging aspect of achieving accurate battery SoC estimation lies in constructing a model that authentically represents the internal dynamics of the battery, encompassing temperature dependencies on internal resistance and capacity degradation. It is also observed that the precision of SoC estimation can be influenced by several factors, including modeling imperfections, uncertainties in parameters, inaccuracies in sensors, and measurement noise. Additional factors impacting battery performance, and consequently the estimation methods, involve self-discharging, aging effects, cell imbalances, capacity fade, and temperature influences. Regardless of the methodology employed, there is an inherent trade-off in battery modeling, necessitating a balance between accuracy and computational complexity.

The literature underscores that the aging of Lithium-ion Batteries (LiBs) is influenced by various parameters, including temperature, time, SoC, cycle number, charge rate, and depth of discharge. The inclusion or exclusion of these parameters in battery models significantly affects the accuracy of SoC estimation. Notably, SoC estimation techniques that continuously update model parameters can effectively address the aging phenomenon.

In the context of real-time EV applications, it is essential to develop a model that strikes a balance between simplicity and accurate SoC estimation. The Electrical Circuit Model (ECM) stands out as particularly suitable for online estimation. In this model, adaptive filter-based and artificial intelligence-based approaches are employed to achieve highly precise SoC estimations. However, a notable drawback of the ECM is its lack of a detailed physical-chemical explanation for microscopic movements within the battery. Conversely, the electrochemical model, while having the potential to illustrate charge transfer and unveil electrochemical mechanisms, is deemed overly complex for online calculations. Through the review, it becomes evident that adaptive filter-based algorithms prove more fitting for EV applications. In contrast, approaches based on artificial intelligence are considered less suitable due to their demanding computational requirements and/or offline learning processes. In addressing optimization challenges within filter-based techniques, there is a growing trend towards employing artificial intelligence-based optimization techniques. This shift is motivated by the simplicity, flexibility, derivation-free mechanism and effectiveness.

Establishing an accurate SoC estimation algorithm relies fundamentally on the battery modeling process. However, existing battery modeling methods, as proposed in the literature, exhibit limitations in terms of accuracy, especially under specific conditions. Additionally, these methods often impose restrictions on assessing aging, hindering continuous model updates. Consequently, there is a pressing need for further research in this field. To enhance the accuracy and practicality of battery modeling, there is a call for exploring practical battery construction and integrating adaptive control technology, expert system theories, and artificial intelligence into the modeling process. It is crucial to acknowledge that none of the reviewed methods emerges as entirely efficient and reliable. While a method may be comprehensive and accurate for a specific application and set of conditions, it might fall short of accuracy in different scenarios. Given these considerations, the selection of an appropriate algorithm ultimately rests with the designer, contingent upon their understanding of the specific application. The information provided in this paper shall serve as a valuable resource to aid designers in choosing the most suitable approach for their particular context.
.

REFERENCES

[1]. K. M. Amanathulla and A. S. Pillai, "An Extensive Comparison of State of Charge Estimation of Lithium Ion Battery — Towards Predictive Intelligent Battery Management System for Electric Vehicles," in *2020 International Conference on Futuristic Technologies in Control Systems & Renewable Energy (ICFCR)*, Sep. 2020, pp. 1–5. doi: 10.1109/ICFCR50903.2020.9249992.

[2]. F. Zhu, G. Liu, C. Tao, K. Wang, and K. Jiang, "Battery management system for Li-ion battery," *J. Eng.*, vol. 2017, no. 13, pp. 1437–1440, 2017, doi: 10.1049/joe.2017.0569.

[3]. R. Xiong, H. He, F. Sun, and K. Zhao, "Online Estimation of Peak Power Capability of Li-Ion Batteries in Electric Vehicles by a Hardware-in-Loop Approach," *Energies*, vol. 5, no. 5, Art. no. 5, May 2012, doi: 10.3390/en5051455.

[4]. Y. Xing, E. W. M. Ma, K. L. Tsui, and M. Pecht, "Battery Management Systems in Electric and Hybrid Vehicles," *Energies*, vol. 4, no. 11, Art. no. 11, Nov. 2011, doi: 10.3390/en4111840.

[5]. R. Xiong, Q. Yu, L. Y. Wang, and C. Lin, "A novel method to obtain the open circuit voltage for the state of charge of lithium ion batteries in electric vehicles by using H infinity filter," *Appl. Energy*, vol. 207, no. C, pp. 346–353, 2017.

[6]. R. Xiong, J. Cao, Q. Yu, H. He, and F. Sun, "Critical Review on the Battery State of Charge Estimation Methods for Electric Vehicles," *IEEE Access*, vol. 6, pp. 1832–1843, 2018, doi: 10.1109/ACCESS.2017.2780258.

[7]. M. A. Hannan, M. S. H. Lipu, A. Hussain, and A. Mohamed, "A review of lithium-ion battery state of charge estimation and management system in electric vehicle applications: Challenges and recommendations," *Renew. Sustain. Energy Rev.*, vol. 78, no. C, pp. 834–854, 2017.

[8]. Z. Li, J. Huang, B. Y. Liaw, and J. Zhang, "On state-of-charge determination for lithium-ion batteries," *J. Power Sources*, vol. 348, pp. 281–301, Apr. 2017, doi: 10.1016/j.jpowsour.2017.03.001.

[9]. C. Fleischer, W. Waag, Z. Bai, and D. U. Sauer, "Self-learning state-of-available-power prediction for lithium-ion batteries in electrical vehicles," in *2012 IEEE Vehicle Power and Propulsion Conference*, Oct. 2012, pp. 370–375. doi: 10.1109/VPPC.2012.6422670.

[10]. W. Waag, C. Fleischer, and D. U. Sauer, "Critical review of the methods for monitoring of lithium-ion batteries in electric and hybrid vehicles," *J. Power Sources*, vol. 258, pp. 321–339, Jul. 2014, doi: 10.1016/j.jpowsour.2014.02.064.

[11]. "Adaptive Battery Management and Parameter Estimation Through Physics-Based Modeling and Experimental Verification | IEEE Journals & Magazine | IEEE Xplore." Accessed: Aug. 16, 2022. [Online]. Available: https://ieeexplore.ieee.org/document/7462263?reload=true

[12]. C. Fleischer, W. Waag, Z. Bai, and D. U. Sauer, "Adaptive On-line State-of-available-power Prediction of Lithium-ion Batteries," *J. Power Electron.*, vol. 13, no. 4, pp. 516–527, 2013, doi: 10.6113/JPE.2013.13.4.516.

[13]. "A novel adaptive technique for Li-ion battery model parameters estimation | IEEE Conference Publication | IEEE Xplore." Accessed: Aug. 17, 2022. [Online]. Available: https://ieeexplore.ieee.org/document/7856769

[14]. J. P. Rivera-Barrera, N. Muñoz-Galeano, and H. O. Sarmiento-Maldonado, "SoC Estimation for Lithium-ion Batteries: Review and Future Challenges," *Electronics*, vol. 6, no. 4, Art. no. 4, Dec. 2017, doi: 10.3390/electronics6040102.

[15]. "Reduction of parameters in a Lithium ion cell model by experimental validation of relationship between OCV and SOC | IEEE Conference Publication | IEEE Xplore." Accessed: Aug. 17, 2022. [Online]. Available: https://ieeexplore.ieee.org/document/7916800

[16]. S. Nejad, D. T. Gladwin, and D. A. Stone, "On-chip implementation of Extended Kalman Filter for adaptive battery states monitoring," in *IECON 2016 - 42nd Annual Conference of the IEEE Industrial Electronics Society*, Oct. 2016, pp. 5513–5518. doi: 10.1109/IECON.2016.7793527.

[17]. U. Westerhoff, T. Kroker, K. Kurbach, and M. Kurrat, "Electrochemical impedance spectroscopy based estimation of the state of charge of lithium-ion batteries," *J. Energy Storage*, vol. 8, pp. 244–256, Nov. 2016, doi: 10.1016/j.est.2016.09.001.

[18]. Z. Yang, D. Patil, and B. Fahimi, "Online estimation of capacity fade and impedance of lithium-ion batteries based on impulse response technique," in *2017 IEEE Applied Power Electronics Conference and Exposition (APEC)*, Mar. 2017, pp. 1229–1235. doi: 10.1109/APEC.2017.7930852.

[19]. Q. Wang, J. Wang, P. Zhao, J. Kang, F. Yan, and C. Du, "Correlation between the model accuracy and model-based SOC estimation," *Electrochimica Acta*, vol. 228, pp. 146–159, Feb. 2017, doi: 10.1016/j.electacta.2017.01.057.

[20]. B. Xia, X. Zhao, R. De Callafon, H. Garnier, T. Nguyen, and C. Mi, "Accurate Lithium-ion battery parameter estimation with continuous-time system identification methods," in *2016 IEEE Energy Conversion Congress and Exposition (ECCE)*, Milwaukee, WI, USA: IEEE, Sep. 2016, pp. 1–8. doi: 10.1109/ECCE.2016.7854811.

[21]. V. R. Subramanian, D. Tapriyal, and R. E. White, "A Boundary Condition for Porous Electrodes," *Electrochem. Solid-State Lett.*, vol. 7, no. 9, p. A259, 2004, doi: 10.1149/1.1773751.

[22]. C. Dong and G. Wang, "Estimation of power battery SOC based on improved BP neural network," in *2014 IEEE International Conference on Mechatronics and Automation*, Tianjin, China: IEEE, Aug. 2014, pp. 2022–2027. doi: 10.1109/ICMA.2014.6886014.

[23]. Ch. Ehret, S. Piller, W. Schroer, and A. Jossen, "State-Of-Charge Determination for Lead-Acid Batteries in PV-Applications," in *Sixteenth European Photovoltaic Solar Energy Conference*, 1st ed., H. Scheer, B. McNelis, W. Palz, H. A. Ossenbrink, and P. Helm, Eds., Routledge, 2020, pp. 2486–2489. doi: 10.4324/9781315074405-109.

[24]. S. Jeon, J.-J. Yun, and S. Bae, "Comparative Study on the Battery State-of-Charge Estimation Method," *Indian J. Sci. Technol.*, vol. 8, no. 26, Oct. 2015, doi: 10.17485/ijst/2015/v8i26/81677.

[25]. W.-Y. Chang, "The State of Charge Estimating Methods for Battery: A Review," *ISRN Appl. Math.*, vol. 2013, pp. 1–7, Jul. 2013, doi: 10.1155/2013/953792.

[26]. N. Khayat and N. Karami, "Adaptive techniques used for lifetime estimation of lithium-ion batteries," in *2016 Third International Conference on Electrical, Electronics, Computer Engineering and their Applications (EECEA)*, Beirut, Lebanon: IEEE, Apr. 2016, pp. 98–103. doi: 10.1109/EECEA.2016.7470773.

[27]. T. Hansen and C.-J. Wang, "Support vector based battery state of charge estimator," *J. Power Sources*, vol. 141, no. 2, pp. 351–358, Mar. 2005, doi: 10.1016/j.jpowsour.2004.09.020.

[28]. L. Xu, J. Wang, and Q. Chen, "Kalman filtering state of charge estimation for battery management system based on a stochastic fuzzy neural network battery model," *Energy Convers. Manag.*, vol. 53, no. 1, pp. 33–39, Jan. 2012, doi: 10.1016/j.enconman.2011.06.003.

[29]. M. W. Yatsui and H. Bai, "Kalman filter based state-of-charge estimation for lithium-ion batteries in hybrid electric vehicles using pulse charging," in *2011 IEEE Vehicle Power and Propulsion Conference*, Chicago, IL, USA: IEEE, Sep. 2011, pp. 1–5. doi: 10.1109/VPPC.2011.6042988.

[30]. O. Barbarisi, F. Vasca, and L. Glielmo, "State of charge Kalman filter estimator for automotive batteries," *Control Eng. Pract.*, vol. 14, no. 3, pp. 267–275, Mar. 2006, doi: 10.1016/j.conengprac.2005.03.027.

[31]. N. Ding, K. Prasad, T. T. Lie, and J. Cui, "State of Charge Estimation of a Composite Lithium-Based Battery Model Based on an Improved Extended Kalman Filter Algorithm," *Inventions*, vol. 4, no. 4, p. 66, Nov. 2019, doi: 10.3390/inventions4040066.

[32]. F. Sun, X. Hu, Y. Zou, and S. Li, "Adaptive unscented Kalman filtering for state of charge estimation of a lithium-ion battery for electric vehicles," *Energy*, vol. 36, no. 5, pp. 3531–3540, May 2011, doi: 10.1016/j.energy.2011.03.059.

[33]. M. A. Awadallah and B. Venkatesh, "Accuracy improvement of SOC estimation in lithium-ion batteries," *J. Energy Storage*, vol. 6, pp. 95–104, May 2016, doi: 10.1016/j.est.2016.03.003.

[34]. H. Dai, P. Guo, X. Wei, Z. Sun, and J. Wang, "ANFIS (adaptive neuro-fuzzy inference system) based online SOC (State of Charge) correction considering cell divergence for the EV (electric vehicle) traction batteries," *Energy*, vol. 80, pp. 350–360, Feb. 2015, doi: 10.1016/j.energy.2014.11.077.

Comparative Analysis of Various Methodologies for Voltage Swell and Sag Detection in Online and Offline Conditions

G. N. Bonde, Dr. S. R. Paraskar, V. S. Karale, R. Z. Fulare, Dr. S. S. Jadhao
Department of Electrical Engineering
Shri Sant Gajanan Maharaj College of Engineering, Shegaon, Maharashtra, India
ganeshbonde2009@gmail.com, srparaskar@gmail.com, vijayskarale@gmail.com
ravi_fulare@yahoo.co.in, ssjadhao@gmail.com

Abstract*: The fundamental voltage, current, and phase angle are required for a wide variety of power system applications. While detecting the sag and swell the important parameters required to be considered are their Magnitude, Duration and Phase Angle Jump. Various techniques use to detect voltage sag include: Root Mean Square (RMS), Fourier transform, Peak voltage detection and Missing voltage method. The problem with these methods is that they use a windowing technique and can therefore be too slow when applied to detect and mitigate voltage sags and swells since they use historical data. In this paper, the voltage sag and swell is detected using wavelet transform method, Root Mean Square (RMS), Fourier transform, Peak voltage detection and Missing voltage method. All these methods are compared on the basis of their, detection time, depth of the sag and sampling frequency. It is found that the wavelet transform is very powerful tool to detect voltage sag and swell. It gives accurate start and end detection time and duration of sag. All these methods are tested under offline and online conditions..*

Keywords: Power Quality (PQ), Fourier Transform (FT), Wavelet Transform.

I. INTRODUCTION

Power quality define as "any power problem manifested in voltage, current, or frequency deviations that results in failure or missed operation of utility or end user equipment"[11]

Until the 1960s the main concern of consumers of electricity was the continuity of the supply, in other words the reliability of the supply. Nowadays consumers not only require reliability, but also power quality [13]. Over the last ten years, voltage sags have become one of the main topics concerning power quality among utilities, customers and equipment manufacturers.

The voltage sag is the most frequently occurring power quality disturbance than the voltage swell. Voltage sag as defined by IEEE Standard 1159-1995, IEEE recommended practice for monitoring electric power quality, is a decrease in root mean square (RMS) voltage at the power frequency for durations from 0.5 cycles to 1 minute [8]. Typical magnitudes are between 0.1 and 0.9 pu. Voltage sags are usually caused by:

- Operation of Reclosers and Circuit breakers.
- Inrush Currents.
- Fault Currents.
- Switching on of large loads.
- Switching off of capacitor bank.

An induction motor will draw six to ten times its full load current during starting. This lagging current causes a voltage drop across the impedance of the system. Hence the voltage sag occurs. because the energization period of large induction motors are of several minutes. The effect of voltage sag mainly affects on to sensitive electronic equipment than the conventional electrical equipment. Sensitive equipment such as computers, adjustable speed drive, microprocessor and the micro-controller etc.

Voltage swell as defined by IEEE Standard 1159-1995, IEEE recommended practice for monitoring electric power quality, is an increase in root mean square (RMS) voltage at the power frequency for durations from 0.5 cycles to 1 minute [8]. Typical magnitudes are between 1.1 and 1.8pu.

The voltage swells are usually associated with system fault conditions, but they are much less common than voltage sags. A swell can occur due to a single line-to-ground fault on the system resulting in a temporary voltage rise on the un-faulted phases. swells can also be caused by:

- switching off a large load
- switching on a large capacitor bank
- Single line to ground fault.

In this paper, the main focus is on to study the following voltage sag and swell detection method-

i. Root Mean Square (RMS)

ii. Peak Method

iii. Fourier Transform Method

iv. Missing Voltage Method

v. Wavelet Transform Method.

All these methods are tested under the offline condition and first four methods are tested under online condition to detect voltage sag. with these methods, we have detected sag due to induction motor energization and welding transformer energization at low voltage distribution level in online condition. These methods are compared based on their detection time, sampling frequency, half cycle and full cycle window algorithm.

Our observation is that still some distribution companies not give importance to power quality they simply distribute power to the consumers. The large magnitude voltage sag can be converted in to voltage interruptions for several hours. Due to this customers equipment may get damaged. So to avoid such problems these algorithms can be implemented practically.

II. EFFECTS OF VOLTAGE SAG

The effects of voltage sag mainly affects on to sensitive electronic equipment than the conventional electrical equipment. Sensitive equipment such as computers, adjustable speed drive, microprocessor and the micro-controller etc.

EFFECTS OF VOLTAGE SAGS ON ADJUSTABLE SPEED DRIVES

Adjustable speed drives (ASD) are very susceptible to slight variation in voltages. The reason for their high susceptibility is the presence of power electronics components that are sensitive to voltage variation. When voltage sag occurs on to the system, the reduction in voltage at the input of the rectifier circuit causes the reduction in the dc voltage. To avoid damages of electronic components, protective systems shutdown the ASD. This causes stoppage of industrial process and this will causes huge financial losses.

EFFECT OF VOLTAGE SAGS ON INDUCTION MOTORS

Induction motors represent the most typical loads in power system applications. They consume about 60% of the electrical energy generated. The torque of induction motor is proportional to the square of the voltage. Thus the voltage sag is the prime cause of the induction motor stoppage. Thus disrupting the normal working, this leads to interruption in the processes and cause financial losses.[8] The basic observed effects of voltage sag on the induction motor are:

- Drop in speed
- Torque oscillations
- Over-current

EFFECTS OF VOLTAGE SAGS ON LIGHTING LOADS

Voltage sags may cause lamps to extinguish. Light bulbs will just twinkle; that will likely not be considered to be a serious effect. High pressure lamps may extinguish; it takes several minutes for them to re-ignite. All lamps, except incandescent lamps, require high voltage across the lamp electrodes during starting. This voltage is essential to initiate the arc. Traditionally, a choke coil is employed across the electrodes to produce high voltage pulses. The lamp starting voltage is affected to a large extent by the ambient temperature and humidity levels as well as the supply voltage.

Fluorescent lamps reach their full emission level immediately after ignition. High-pressure lamps need a few minutes to reach their full light output, while low-pressure lamps take up to 15 minutes for the same.

III. EFFECTS OF VOLTAGE SWELL

The effect of voltage swell on to equipment is that, during the voltage swell condition the voltage appears at the equipment terminal is more than the nominal voltage. Due that the more stressed on to equipment insulation. If the insulation of the equipment is not uniform there may be chances of insulation failure and equipment damaged.

A higher than nominal voltage over the transformer terminals will increase the magnetizing current of a transformer. As the magnetizing current is heavily distorted, an increase in voltage magnitude will increase the waveform distortion. The light output and life of such lamps are critically affected by the voltage. The expected life length of an incandescent lamps significantly reduced by only a few percent increase in the voltage magnitude. The lifetime somewhat increases for lower than nominal voltages, but this cannot compensate for the decrease in lifetime due to higher than nominal voltage. The result is that a large variation in voltage leads to a reduction in lifetime compared to a constant voltage.

IV. DETECTION METHODS

Voltage sag has been the focus of considerable research in recent years. It can cause expensive downtime. Research on voltage sag detection has also grown up and it is an essential part of the voltage sag compensator. There are many methods have been introduced to measure and detect voltage sags. Among these are RMS Method, Peak Method, Fourier Transform Method, Missing Voltage Method and wavelet transform Method.

RMS METHOD

The most common processing tool for voltage measurement in power systems is the calculation of the Root Mean Square (RMS) value. The most important standards related to the measurement of power quality disturbances are at present IEC Standard 61000-4-30 and IEEE Standard.1159-1995.

As voltage sags are initially recorded as sampled points in time, the RMS voltage will have to be calculated from the sampled time domain voltages. The RMS value can be calculated as

$$V^{RMS}(i) = \sqrt{\frac{1}{N} \sum_{j=1}^{i+N-1} V^2(j)} \tag{1}$$

Where, N is Number of the samples per cycle

V (j) is jth sample of the recorded voltage waveform

VRMS(i) is ith sample of the calculated RMS voltage

During the occurrence of sag, the RMS value drops below the nominal value. This drop is proportional to the level of sag. Similarly, during a swell, the RMS value exceeds the nominal RMS value by an amount proportional to the level of swell. [14]

The sag and swell are the non stationary event. Thus there is a need to reset the algorithm after the occurrence of sag or swell. This can be overcome by calculating the RMS value over a moving window encompassing a fixed number of samples. The widely-used moving-window RMS value is calculated for digitally recorded data. In order to spend less processing time, a recursive alternative can be used. This provides a significant processing time saving when N is large.

PEAK METHOD

The peak voltage as a function of time can be obtained by using the following expression

$$Vpeak = \max_{0 < \tau < T}(|V(t-\tau)|) \tag{2}$$

Where, Vpeak = peak value of voltage signal.

V (t) = the sampled voltage waveform.

T= is an integer multiple of one half cycle or Full cycle.

IJARSCT

ISSN (Online) 2581-9429

International Journal of Advanced Research in Science, Communication and Technology (IJARSCT)

International Open-Access, Double-Blind, Peer-Reviewed, Refereed, Multidisciplinary Online Journal

Impact Factor: 7.53

Volume 4, Issue 5, April 2024

For each sample the maximum of the absolute value of the voltage over the preceding half cycle (or full cycle) is calculated.

FOURIER TRANSFORM METHOD

The fundamental component of the voltage is calculated by using the discrete Fourier Transform method. The complex fundamental component is calculated by following expression

$$V_{fund} = \frac{2}{N} \sum_{n=-\infty}^{\infty} V(n)e^{(-jw_0 n)} \qquad (3)$$

Where, $W0 = 2\pi (f/Fs)$. f=frequency of supply.

Fs=sampling frequency. V (n) = sampled voltage waveform; N=Number of sample in one cycle;

Vfund= complex fundamental component of the voltage signal;

By calculation of fundamental component of the voltage has the advantage that the phase angle jump can be determined. The magnitude of the fundamental component is obtained by taking the absolute of the Vfund. The phase angle jump is determined as,

Vfund=X+ jY;

Phase angle jump= arctan(Y/X);

MISSING VOLTAGE METHOD

The missing voltage is defined as the difference between the desired instantaneous voltage and the actual instantaneous one [2]. The missing voltage is calculated from the following expression.

$$Vpll\ (t) = A\sin(wt - \Phi a) \qquad (4)$$

$$Vsag\ (t) = B\sin(wt - \Phi b) \qquad (5)$$

$$R = \sqrt{A^2 + B^2 - 2AB\cos(\Phi b - \Phi a)} \qquad (6)$$

$$\tan(\Psi) = \frac{A\sin(\Phi a) - B\sin(\Phi b)}{A\cos(\Phi a) - B\cos(\Phi b)} \qquad (7)$$

$$m\ (t) = R\sin(wt - \Psi) \qquad (8)$$

Where, Vpll (t) =desired voltage signal.

A= peak amplitude of the desired voltage signal.

Vsag (t) =disturbed waveform.

B=peak amplitude of the disturbed waveform.

R=amplitude of missing voltage.

m (t) = the instantaneous deviation from the known reference.

The desired signal is taken as the first cycle of the prefault voltage signal. It relies on the assumption that the system frequency is constant during the sag. The technique requires the peak method to determine the amplitude of the presag and sag voltages A and B, respectively. This method is suitable for sag analysis rather than detection. The reason for this is that the sag amplitude B is not known until after the event. It requires presag and sag voltages A and B are always in phase.

WAVELET TRANSFORM METHOD

In recent years, researchers in applied mathematics and signal processing have developed powerful wavelet techniques for the multiscale representation and analysis of Signals These new methods differ from the traditional Fourier techniques Wavelets localize the information in the time-frequency plane; in particular, they are capable of trading one type of resolution for another, which makes them especially suitable for the analysis of non-stationary signals. One important area of application where these properties have been found to be relevant is power engineering. Due to the

wide variety of signals and problems encountered in power engineering, there are various applications of wavelet transform. These range from the analysis of the power quality disturbance signals to, very recently, power system relaying and protection.

The DWT analyzes the signal at different frequency bands with different resolutions by decomposing the signal into a coarse approximation and detail information. DWT employs two sets of functions, called scaling functions and wavelet functions, which are associated with low pass and high pass filters, respectively. The decomposition of the signal into different frequency bands is simply obtained by successive high pass and low pass filtering of the time domain signal. The original signal x[n] is first passed through a half band high pass filter g[n] and a low pass filter h[n]. After the filtering, half of the samples can be eliminated according to the Nyquist's rule, since the signal now has a highest frequency of $\pi/2$ radians instead of π . The signal can therefore be sub sampled by 2, simply by discarding every other sample. This constitutes one level of decomposition and can mathematically be expressed as follows:

$$y_{high}(k) = \sum_{n} x(n).g(2n-n) \qquad (9)$$

$$y_{low}(k) = \sum_{n} x(n)h(2k-n) \qquad (10)$$

where yhigh[k] and ylow[k] are the outputs of the high pass and low pass filters, respectively, after sub sampling by 2.
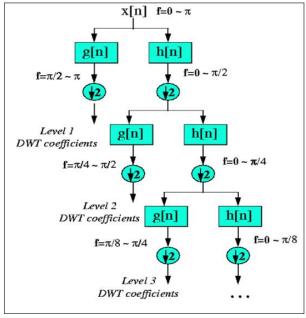

Fig. 1 Decomposition diagram

V. EXPERIMENTAL SETUP

Figure shows the practical experimental setup that was used to conduct the experiment in laboratory. The main components required for the setup are: single phase transformer, solid state mechanical relay, induction motor, potential transformer, gain control circuit, Advantech data acquisition card, and personnel computer.

Fig 2: Practical Experimental setup of the system

Single phase Transformer:

In experimentation, single phase 2KVA, 230V/230V, isolation transformer is used. It has taps that can be set from 0 V to 230 V in steps of 10 V. Change of taps can be viewed as voltage sag or swell conditions for online simulation.

Solid State Mechanical Relay

The solid state mechanical relay is used to act as a tap changer so that the voltage sag and swell conditions can be simulated online. The relay has rating of 230V/10A and the operating coil of the relay is provided with the +12V DC supply. than nominal voltage, to get required amount of swell magnitude. The No contact is connected to the 100% rated voltage tapping of transformer.

Induction Motor

Single phase induction motor of 2hp is used to simulate the voltage sag occurring due to the inrush currents.

Potential Transformer

A step down transformer of 230/6v is used as potential transformer to provide the signal of desired magnitude for the measurement purpose

Advantech Data acquisition Card

In this experimentation purpose Advantech data acquisition system use, specification of this system is PCLD-8710 - 100 kS/s, 12-bit, 16-ch PCI Multifunction Card - Advantech Co., Ltd.

Gain control circuit

The gain control circuit is necessary to prevent the clamping of input voltage signal and also to provide the isolation between the computer and the supply. A simple closed loop op-amplifier used as an inverting amplifier as shown in fig 3
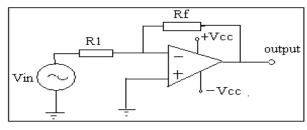

Fig 3: Inverting amplifier as a gain control circuit.

The output of the inverting amplifier is given as

$$V_{(0)} = - \frac{Rf}{R1} Vin$$

Where, Rf= Feedback Resistor, Rin= Input Resistor.

Gain=A=Rf/R1. Vin=Input Voltage.

V (0) =Output Voltage of op-amplifier.

The gain 0.5 is achieve by choosing the values of Rf =5kΩ and R1=10kΩ. The input voltage at the op-amplifier is 6V and voltage available at the output is 3V.
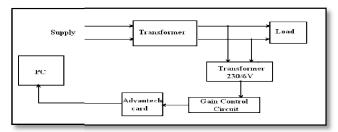
Fig 4 Block Diagram of Practical Experimental Setup

VI. RESULTS AND DISCUSSION

The voltage sag signal was capture at sampling frequency of 500Hz, 1000Hz, 5000Hz and 10000Hz and of different depth such as 110V tapping and 80V tapping respectively. The objective is to find out minimum number of samples required i.e. window length for accurate estimation of sag and swell. Also the effect on detection time of each method as the sampling frequency increases.
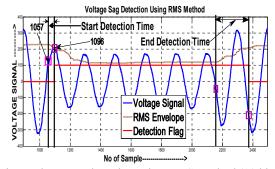

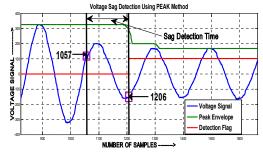Fig 5 voltage sag detection using RMS Method (10 khz)

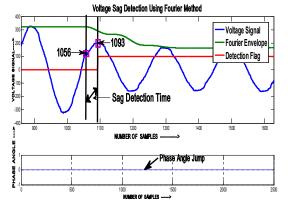Fig 6 voltage sag detection using Peak Method

Fig 7 Voltage sag detection using Fourier Transformed Method.
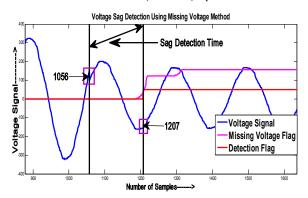
Fig 8 Voltage Sag Detection Using Missing Voltage Method
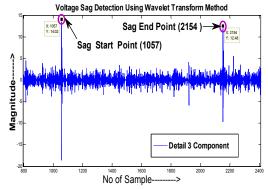
Fig 9 Voltage Sag Detection Using Wavelet Transformed Method.
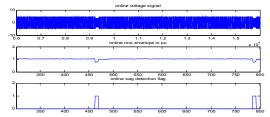
Fig 10 Online Detection of Voltage Sag Due to Induction Motor Starting using RMS Algorithm.

Fig 11 Online Detection of Voltage Sag using RMS Algorithm.

In this paper only results of voltage sag signal capured at sampling frequency of 10Khz has been showed. The result of voltage sag of 500Hz,1KHz,5KHz are shown in table 1.1

Copyright to IJARSCT
www.ijarsct.co.in

DOI: 10.48175/IJARSCT-17529

ISSN
2581-9429
IJARSCT

198

Table 1.1 Voltage Sag Detection Time

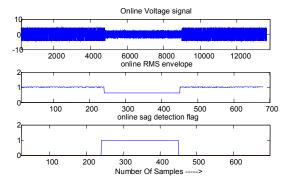| METHOD	Full Cycle Window			Half Cycle Window			Samplin Frequen (Hz)
	Detection Time (ms)	Depth of sag (%)	Duration of sag (cycles)	Detection Time (ms)	Depth of sag (%)	Duration of sag (cycles)	
RMS METHOD	10	54.6699	22.3000	4	53.0322	21.4000	500
PEAK METHOD	20	53.8916	20.7000	5	53.0125	21.2000	500
FOURIER METHOD	10	54.6779	22.3000	4	53.0641	21.5000	500
MISSING VOLTAGE METHOD	18	56.7818	20.7000	8	55.9034	21.2000	500
RMS METHOD	7	50.0827	26.8500	4	48.6708	26.1500	1 KHz
PEAK METHOD	18	51.6923	25.3500	7	49.2308	25.8500	1 KHz
FOURIER METHOD	6	50.0655	26.7500	4	48.6665	26.1500	1 KHz
MISSING VOLTAGE METHOD	18	52.0397	25.3500	8	49.5802	25.8500	1 KHz
RMS METHOD	6.4	50.6819	10.0700	3.6	48.5744	9.7100	5KHz
PEAK METHOD	19	51.6923	8.5500	9	50.4615	9.0500	5KHz
FOURIER METHOD	7	49.9400	10.4000	3.4	47.4747	9.7800	5 KHz
MISSING VOLTAGE METHOD	18.2	52.0397	8.5400	8.6	50.8100	9.0400	5 KHz
RMS METHOD	5.8	50.6386	8.6950	2.6	49.5310	7.9650	10 KHz
PEAK METHOD	20	51.6923	6.8950	10	49.2308	7.3950	10 KHz
FOURIER METHOD	6.4	50.6321	8.7150	4	49.5385	7.9700	10 KHz
MISSING VOLTAGE METHOD	17.2	52.0397	6.8900	9.8	49.5802	7.3900	10 KHz

The experimentation study was carried out for observing the effect of sampling frequency on quantification parameters and detection time of voltage sag by all proposed methods. The figure 5 shows the result of voltage sag detection using RMS method with sampling frequency of 10khz. It observes that the voltage sag is detected at start by 5.8ms using full cycle algorithm & 2.6 ms for half cycle algorithm. These are the minimum detection time observed for RMS and Fourier Method. The end point of voltage sag also not accurately detected by the all these algorithms excepting Wavelet transform method. There is delayed in detection of end point due to the windowing technique. Hence voltage sag duration is not accurately detected by these methods.

So the problems associated with the windowing methods can be resolved by the Wavelet Transformed Method. From figure 9, the initiation of voltage sag at samples no 1057 and end of voltage sag at sample no 2154 respectively as shown in figure 9. Thus voltage sag or swell can be detected at exact point of initiation there is no delay while detection at start and end point.
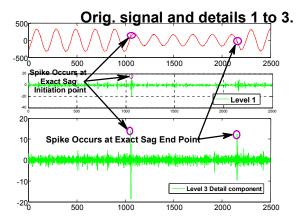
Figure 12 Voltage Sag Detection Using Wavelet Transfomed Method (Detail 3 component)

The all cadidate wavelet are applied to the all test result it is found that db13 gives the best results amongs the all family of wavelet. The better spikes can be obtained at decomposition level 3 as shown in figure 12.

The results of online detection of voltage sag using RMS method as shown in figure 12. Also we have detected the voltage sag online due to induction motor starting as shown in figure 10.

VII. CONCLUSION

In this paper, the offline and online detection of voltage sag and swell is carried out using RMS, Peak, Fourier transform and Missing Voltage Methods. The offline detection of voltage sag using wavelet transformed method also carried out. It can be observed that RMS and Fourier method takes least detection time among the all method. Typical detection time for half cycle and full cycle algorithm are 4ms and 10ms respectively.

The result obtained from the RMS and Fourier Method is approximately same. The RMS method gives information about the magnitude and duration of voltage sag. Where, Fourier transform method gives the additional information regarding the phase angle jump.

The response time of RMS and Fourier Method is near to window length. While for Peak value algorithm response time is less i.e. peak is detected within the quarter cycle. The Peak and Missing Voltage Method takes the largest detection time than RMS and Fourier Method. The half cycle algorithm gives the faster detection than the full cycle algorithm.

It is observed that as the sampling frequency increases the detection time reduces. The typical least detection time obtained among the all method at 10 KHz sampling frequency for half and full cycle RMS algorithm are 3.3ms and 5.8 ms respectively. It has been observed that, proposed methods does not provides the accurate detection time for lower depth voltage sag events.

At last the wavelet transformed method is superior over the other method. It gives accurate sag initiation point and sag end point. This information is very useful while mitigating the voltage sag. The delay in sag detection is completely minimized. Thus wavelet transform gives the exact duration of voltage sag/swell.

REFERENCES

[1] P.Meena, K. Uma Rao, Ravishankar .D "A modified simple algorithm for detection of voltage sags and swells in practical loads" 2009 Third International Conference on Power Systems, Kharagpur, INDIA December 27-29.

[2] N. S. Tunaboylu, E. R. Collins, Jr., and P. R. Chaney, "Voltage disturbance evaluation using the missing voltage technique," in Proc. 8th int. Conf. harmonics and power, 1998, pp.577-582.

[3] Irene Y. H. GU, Nichlas Ernberg, Math H. J. Bollen "A Statistical-Based Sequential Method for Fast Online Detection of Fault-Induced Voltage Dips" IEEE TRANSACTIONS ON POWER DELIVERY, VOL. 19, NO. 2, APRIL 2004.

[4] Mansor, M, Rahim, N.A "Voltage sag detection - A survey" technical postgraduate 2009 international conference for Issue Date: 14-15 Dec. 2009 On page(s): 1 – 6.

[5] Mark F. McGranaghan1 and Surya Santoso2 "Challenges and Trends in Analyses of Electric Power Quality Measurement Data" Hindawi Publishing Corporation EURASIP Journal on Advances in Signal Processing Volume 2007, Article ID 57985, 5 page doi:10.1155/2007/57985

[6] P.Meena, K. Uma Rao, Ravishankar .D "Real-Time Detection and Analysis of PQ disturbances with DSP using MATLAB Embedded Link to Code Composer Studio" 2009 Third International Conference on Power Systems, Kharagpur, INDIA December 27-29.

[7] Mario Gonzalez, Victor Cardenas, Ricardo Alvarez "A Fast Detection Algorithm for Sags, Swells, and Interruptions Based on Digital RMS Calculation and Kalman Filtering" CIEP2006 Puebla, MEXICO 16-18 October 1-4244-0545-9/06/©2006 IEEE

[8] M.H.J.BOLLEN, "Understanding power Quality Problems" Voltage Sags and Interruptions. New York IEEE Press, 1999, Vol.I

[9] M.H.J.BOLLEN, "Signal Processing of power Quality Disturbances"

[10] IEEE Std. 1159-1995 "IEEE Recommended Practice for Monitoring Electric Power Quality"

[11] Roger c, Dugan "Electrical Power Systems Quality" second edition.

[12] Barry W, Kennedy "Power Quality Primer"

[13] Roberto Chouhy Leborgne ["Thesis For The Degree Of Doctor Of Philosophy" Voltage Sags: Single event characterization, system performance and source location.

[14] Raj Naidoo; Pragasen Pillay" Year: 2007, Volume: 22, A New Method of Voltage Sag and Swell Detection" EEE Transactions on Power Delivery Issue: 2 Pages:1056 - 1063, DOI: 10.1109/TPWRD.2007.893185

Copyright to IJARSCT
www.ijarsct.co.in

DOI: 10.48175/IJARSCT-17529

ISSN
2581-9429
IJARSCT

201

Hilbert Transform Based Approach for Detection and Classification of Power Quality Disturbances

Ravishankar S. Kankale[1*], Dr. S. R. Paraskar[2], Dr. S. S. Jadhao[3]
[1]*Assistant Professor, Department of Electrical Engineering, SSGMCE, Shegaon, India*
[2]*Professor & Head, Department of Electrical Engineering, SSGMCE, Shegaon, India*
[3]*Associate Professor, Department of Electrical Engineering, SSGMCE, Shegaon, India*

[*]***Corresponding Author***
E-Mail Id:-ravi_kankale@rediffmail.com

ABSTRACT
This Power quality disturbances (PQDs) have a significant impact on the efficient operation of electrical systems. Detecting and classifying these disturbances accurately is crucial for ensuring a stable and reliable power supply. This research paper explores the use of the Hilbert envelope and Feed Forward Neural Network (FFNN) in detecting and classifying the PQDs. The Hilbert envelope, derived from the Hilbert Transform (HT), provides a valuable technique for analyzing non-stationary signals. The paper outlines the methodology, implementation process, and detailed results, showcasing the effectiveness of the Hilbert envelope technique in enhancing the reliability of power systems. In this study we have mainly considered sags, swells, and interruptions disturbances which are analyzed using the Hilbert envelope for feature extraction. The features extracted from Hilbert envelope are then fed to FFNN classifier. This paper outlines the methodology, implementation process, and detailed results, showcasing the effectiveness of utilizing the Hilbert envelope and FFNN in detection and classification of PQDs.

Keywords:- *Power Quality Disturbances, Hilbert Transform, Hilbert Envelope, Feed Forward Neural Network*

INTRODUCTION
In the ever-evolving landscape of electrical power systems, maintaining a high-quality power supply is paramount. Power quality disturbances, ranging from voltage fluctuations to harmonic distortions, pose formidable challenges to the reliability and stability of power system.

Accurate detection and classification of these disturbances are pivotal for prompt corrective actions, ensuring uninterrupted power flow and safeguarding connected devices. Traditional methods often fall short when dealing with non-stationary signals characteristic of power quality issues. In response, this research paper delves into an innovative approach: the application of the Hilbert envelope derived from the Hilbert transform. By harnessing the power of advanced signal processing, this study explores the feasibility and efficacy of the Hilbert envelope in recognition of different PQDs.

HILBERT TRANSFORM
The Hilbert transform is a largely used signal processing technique to analyze the discrete-time signals. It is used to compute the analytic signal, which contains both amplitude and phase information of a real-valued input signal. The HT of a discrete-time signal $x[n]$ produces a complex signal $z[n]$ such that $z[n] = x[n] + j.\hat{x}[n]$, where $\hat{x}[n]$ is the HT of $x[n]$. Here, j is the imaginary unit $(j^2 = -1)$.

HBRP PUBLICATION

HILBERT ENVELOPE

The Hilbert envelope of a input signal $x[n]$ is computed using the HT. The discrete-time HT can be obtained using the Discrete Fourier Transform (DFT) method. For a given input signal $x[n]$, the Hilbert envelope is computed as:

1. Compute the DFT of the signal x[n] to get X[k].

$$X[k] = \sum_{n=0}^{N-1} x[n]e^{-j\frac{2\pi}{N}nk}$$

(1)

Where N represents signal length, n is the discrete time index, k is the frequency index, and j is the imaginary unit.

2. Set the negative frequency components of *X[k]* to zero.

$$[k] = \begin{cases} X[k] \ for \ k = 0, 1, 2, \ldots, \frac{N}{2} \\ 0 \ for \ k = \frac{N}{2} + 1, \frac{N}{2} + 2, \ldots, N - 1 \end{cases}$$

(2)

3. Compute Inverse DFT of X̂[k] to obtain the Hilbert envelope x̂[n] of the original signal x[n].

$$\hat{x}[n] = \frac{1}{N}\sum_{k=0}^{N-1} \hat{X}[k]e^{j\frac{2\pi}{N}nk}$$

(3)

The resulting x̂[n] represents the Hilbert envelope of the original discrete-time signal x[n]. In practice, these computations are often performed using efficient algorithms like the Fast Fourier Transform (FFT) for practical applications.
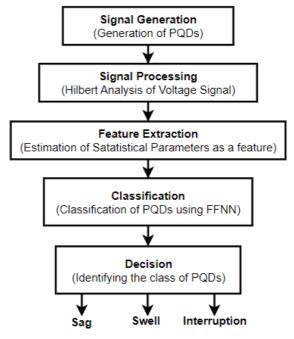
PROPOSED METHODOLOGY

***Fig.1:-**Flowchart of the proposed HT and FFNN Based Algorithm*

The Power Quality Disturbances required to implement the proposed algorithm are generated using the MATLAB Simulink model of Power Quality Disturbances. Multiple cases are created by varying the parameters and conditions in order to get the dataset required for the verification of proposed algorithm. The proposed algorithm is split in two phases. In the initial phase the disturbances are detected using the Hilbert Transform and detection flag is set, once the occurrence of disturbance is detected then it needs to be classified. In the later phase the disturbances are classified using the steps given in the flowchart. Figure shows the proposed HT and FFNN based algorithm used to classify the PQDs. Figure 2 shows the MATLAB Simulink model used to generate the desired Power Quality Disturbances. Mainly three PQDs are considered in this research work namely, sag, swell and interruption.

The voltage sag is created by three phase fault, voltage swell is created by capacitor switching and interruption is created by operating the breaker. Multiple cases are created by varying the circuit parameters to generate the dataset required for the verification of proposed algorithm.

GENERATION OF POWER QUALITY DISTURBANCES

Figure 2 shows the MATLAB Simulink model used to generate the desired Power Quality Disturbances. Mainly three PQDs are considered in this research work namely, sag, swell and interruption. The voltage sag is created by three phase fault, voltage swell is created by capacitor switching and interruption is created by operating the breaker. Multiple cases are created by varying the circuit parameters to generate the dataset required for the verification of proposed algorithm.
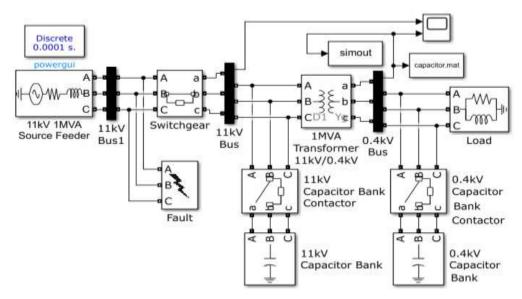
Fig.2:-MATLAB Simulink model used to Generate PQDs

DETECTION OF POWER QUALITY DISTURBANCES

Figure 3 shows the Hilbert transform based detection of voltage sag signal. In this figure the first signal represents the original signal, second signal represents the Hilbert magnitude and third signal represents the detection flag. The detection flag is set at the instant of occurrence of event and last till the duration of event.

HBRP
PUBLICATION
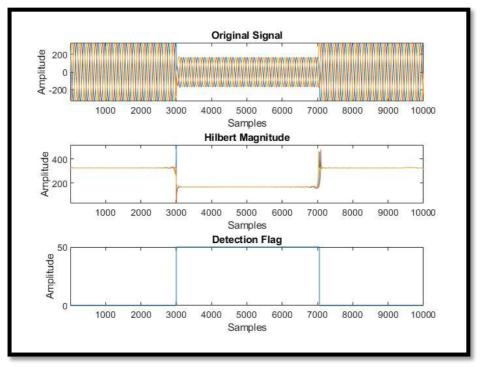
Fig.3:-*Detection of occurrence of voltage sag using HT*

Figure 4 shows the Hilbert transform based detection of voltage swell signal. In this figure the first signal represents the original signal, second signal represents the Hilbert magnitude and third signal represents the detection flag. The detection flag is set at the instant of occurrence of event and last till the duration of event.
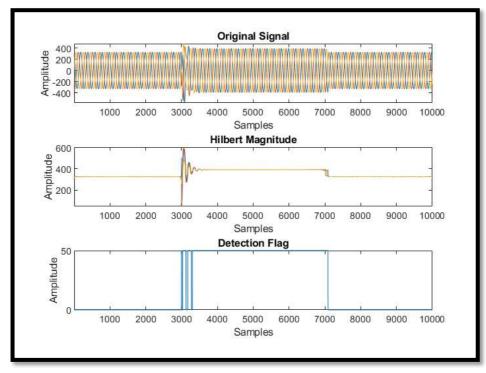
Fig.4:-*Detection of occurrence of voltage swell using HT*

HBRP
PUBLICATION

Figure 5 shows the Hilbert transform based detection of voltage interruption signal. In this figure the first signal represents the original signal, second signal represents the Hilbert magnitude and third signal represents the detection flag. The detection flag is set at the instant of occurrence of event and last till the duration of event.
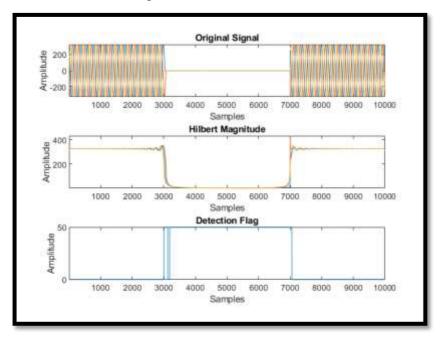
Fig.5:-*Detection of occurrence of voltage interruption using HT*

HILBERT ANALYSIS OF POWER QUALITY DISTURBANCES

In the Hilbert analysis the voltage signal is processed using HT to obtain the Hilbert envelope. Figure 6 shows the voltage sag signal along with its Hilbert envelope obtained from Hilbert analysis. This envelope is further used for feature extraction.
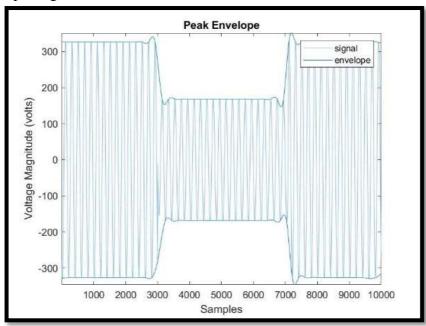
Fig.6:-*Hilbert Envelope of voltage sag signal*

Figure 7 shows the voltage swell signal along with its Hilbert envelope obtained from Hilbert analysis. This envelope is further used for feature extraction.
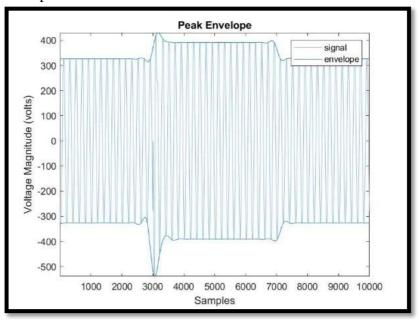
Fig.7:-*Hilbert Envelope of voltage swell signal*

Figure 8 shows the voltage interruption signal along with its Hilbert envelope obtained from Hilbert analysis. The shape of the envelope corresponding to pure sinusoidal signal is constant, whereas it varies as per the change in the magnitude of disturbance signals. Thus, by observing the shape of the Hilbert envelope we can clearly discriminate the type of the disturbance. This envelope is used for feature extraction. The extracted features are statistical parameters (mean, max, standard deviation and energy) calculated from the Hilbert envelope. These features are then fed to the FFNN Classifier for classifying the type of disturbances.
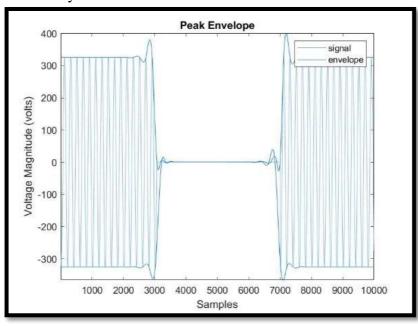
Fig.8:-*Hilbert Envelope of voltage interruption signal*

CLASSIFICATION OF PQDs USING FEED FORWARD NEURAL NETWORK

The four features extracted from the HT analysis of voltage signals are used for training and testing the FFNN classifier. The feature vector with 48 datasets of each disturbance (48x3=144) are fed to FFNN classifier. 80% of the data (115 datasets out of which 39 datasets of sag, 41 datasets of swell and 35 datasets of interruptions) are used for training and 20% data (29 datasets out of which 7 datasets are of sag, 7 datasets are of swell and 13 datasets are of interruptions) are used for testing purpose. Figure 9 shows all confusion matrix, from this matrix it is found that voltage sag is classified with an accuracy of 93.8%, voltage swell is classified with 100% and voltage interruption is classified with 95.8% accuracy. The overall accuracy of classifier is 96.5%.
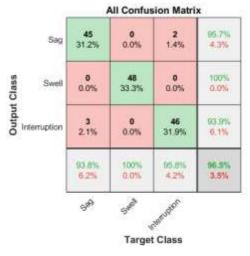
Fig.9:-All Confusion Matrix of FFNN Classifier

The FFNN classifier's training results are displayed in the form of confusion matrix in figure 10, from this matrix it is found that voltage sag is classified with an accuracy of 97.3%, voltage swell is classified with 100% and voltage interruption is classified with 97.1% accuracy. The overall accuracy of training is 96.5%.

Fig.10:-Training Confusion Matrix of FFNN Classifier

The FFNN classifier's testing results are displayed in the form of confusion matrix in figure 11, from this matrix it is found that voltage sag is classified with an accuracy of 100%, voltage swell is classified with 100% and voltage interruption is classified with 92.3% accuracy. The overall accuracy of training is 96.6%.
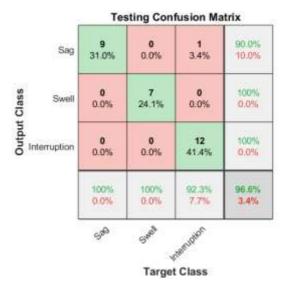
Fig.11:-Testing Confusion Matrix of FFNN Classifier

CONCLUSION

This paper presents the unique combination of HT and FFNN for accurately detecting and classifying PQDs. The integration of HT provides a solid foundation for extracting useful features from power signals, enabling a comprehensive analysis of disturbances. Its ability to transform signals into the analytic domain has proven invaluable in identifying subtle variations and irregularities in power waveforms. Additionally, the utilization of FFNN, with its capacity to learn complex patterns and make precise predictions, enhances the classification accuracy. The features extracted from the HT are simple and effective. The time required to train and test the FFNN is less also it is less complex. The overall accuracy of classification is found to be 96.5%. The computational time and complexity of HT is less as compared to Wavelet Transform and S-Transform. Hence, the proposed method is found to be fast and more efficient.

REFERENCES

1. Saini, R., Mahela, O.P., & Sharma, D. (2018). *Detection and Classification of Complex Power Quality Disturbances Using Hilbert Transform and Rule Based Decision Tree*. 2018 IEEE 8th Power India International Conference (PIICON), 1-6.

2. Jayasree, T., Devaraj, D., & Sukanesh, R. (2010). *Power quality disturbance classification using Hilbert transform and RBF networks*. Neurocomputing, 73, 1451-1456.

3. Chheepa, T.K., & Manglani, T. (2018). *Power Quality Events Classification using ANN with Hilbert Transform*. International Journal of Emerging Research in Management and Technology.

4. Karasu, S., & Saraç, Z. (2018). *Classification of power quality events signals with pattern recognition methods by using Hilbert transform and genetic algorithms*.

2018 26th Signal Processing and Communications Applications Conference (SIU), 1-4.

5. Granados-Lieberman, D., Valtierra-Rodríguez, M., Morales-Velazquez, L., Romero-Troncoso, R.D., & Osornio-Ríos, R.A. (2013). *A Hilbert Transform-Based Smart Sensor for Detection, Classification, and Quantification of Power Quality Disturbances*. Sensors (Basel, Switzerland), 13, 5507 - 5527.

6. Manjula, M., Mishra, S., & Sarma, A. (2013). *Empirical mode decomposition with Hilbert Transform for classification of voltage sag causes using probabilistic neural network.* International Journal of Electrical Power & Energy Systems, 44, 597-603.

7. Kankale, R.S., Paraskar, S.R., & Jadhao, S.S. (2022). *Classification of Power Quality Disturbances using the Unique Combination of Hilbert Transform, Image Processing and K-Nearest Neighbor.* 2022 International Conference on Emerging Trends in Engineering and Medical Sciences (ICETEMS), 220-225.

8. Pandya, V., Agarwal, S., Mahela, O.P., & Choudhary, S. (2020). *Recognition of Power Quality Disturbances Using Hybrid Algorithm Based on Combined Features of Stockwell Transform and Hilbert Transform*. 2020 IEEE International Students' Conference on Electrical, Electronics and Computer Science (SCEECS), 1-6.

Analysis of Neuro-Fuzzy-Based STATCOM and SSSC

Ruchira N. Aglawe [a], Prof. Dr. A. U. Javadekar [b], R. K. Mankar [c]

[a] *Dept. of Electrical Engineering, SSGMCE, Shegaon, 444203, Mah., India*
[b] *Dept. of Electrical Engineering, SSGMCE, Shegaon, 444203, Mah., India*
[c] *Dept. of Electrical Engineering, SSGMCE, Shegaon, 444203, Mah., India*

ABSTRACT—

When a wind farm is integrated into the power system, it encounters stability issues. To maintain air gap flux, fixed-speed induction generators require reactive power. Static Synchronous Compensator (STATCOM) and Static Synchronous Series Compensator (SSSC) reactive power equipment can be used to recover induction generators from severe system disturbances and stabilize grid-connected wind generators. These devices are capable of absorbing or injecting reactive power. A nonlinear controller is a neuro-fuzzy controller (NFC). Neuro-Fuzzy controlled STATCOM and SSSC can be used to stabilize grid-connected wind turbines.

Keywords— wind farm (WF), grid, Induction Generator (IG), STATCOM, SSSC, reactive power compensation, Neuro-fuzzy controller (NFC), various types of faults.

1. Introduction:

A wind farm (WF) is made up of several wind turbine-generating systems that work together. Because of their simple, rugged, and maintenance-free construction, induction generators (IG) are widely used as wind turbines. IGs are directly connected to the power grid. IGs need reactive power to produce active power in order to sustain air gap flux.

The grid provides this reactive power. When disturbances such as faults occur, IGs' reactive power consumption increases. If the grid is unable to meet the reactive power requirements of IGs, wind turbines trip. This has an impact on the voltage profile of the bus to which WF is connected, resulting in grid instability. As a result, whenever a grid disturbance occurs, reactive power compensation is required to maintain grid stability.

Popular flexible AC transmission systems (FACTS) tools like Static Synchronous Compensator (STATCOM) and Static Synchronous Series Compensator (SSSC) are particularly helpful for delivering reactive power and supporting the bus voltage of a WF at the same time. By regulating the amount of reactive power injected into or absorbed from the power supply, both adjust the voltage at terminals. Reactive power is produced when the system voltage is low (capacitive). They take in reactive power when the system voltage is high (inductive).

Neuro-fuzzy(NF) control can effectively deal with power system uncertainties. Neuro-fuzzy is the combination of neural network and fuzzy logic in the case of STATCOM, the conventional PI controller is used to generate the reference current Iqref, and in the case of SSSC, vq_conv. The PI controller necessitates the use of precise linear mathematical models. It is extremely difficult to obtain parameter variation in the presence of nonlinearity and load disturbance, and its performance is subpar. The benefit of neuro-fuzzy controllers (NFC) over traditional controllers is that they do not require an accurate mathematical model. NFC is capable of working with imprecise inputs. It handles nonlinearity and is more robust than a traditional PI controller. NFC mimics human decision-making and can often be used more successfully in complex systems than traditional control techniques. This paper compares neuro-fuzzy controlled STATCOM and SSSC for various types of faults.

2. STATCOM & SSSC Model

The static synchronous compensator (STATCOM) is a shunt controller, and the static synchronous series compensator (SSSC) is a series FACTS controller that uses voltage-sourced converter VSC technology. A VSC produces a synchronous voltage with a fixed fundamental frequency and variable magnitude and phase angle. The output vq_conv of the Vq voltage regulator block is fed to the PWM modulator, which controls the pulses of the SSSC's VSC. The output Iqref of the AC voltage regulator block is given to the current regulator and then to the PWM modulator, which controls the pulses of the STATCOM's VSC, the schematic diagram of the control system of a STATCOM and SSSC is shown in Fig 1 and Fig 2.
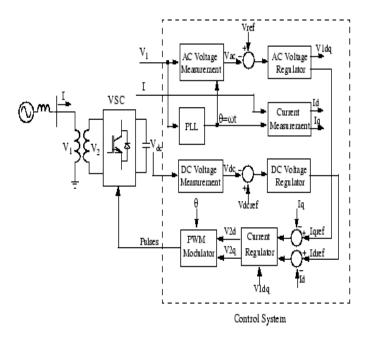
Fig 1. Schematic Diagram of the control system of a STATCOM
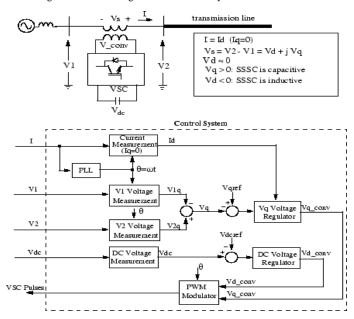
Fig 2. Schematic Diagram of the control system of an SSSC.

3. Modelling of neuro fuzzy controller

Neuro-fuzzy controller (NFC) is a combination of a neural network (NN) and a fuzzy system (FS). Neuro-fuzzy systems are well-known for their ability to Combine the benefits of FS and NN. The outputs of NN and FS are combined in this paper to modify the overall output.

The FLC has two inputs: error voltage (ev) and change in error voltage (cev). In the case of STATCOM, iqref is the controller output, and vq_conv is the output of SSSC. The FLC output and inputs are scaled for convenience using the coefficients kIqref, kvq_conv, kcev, and kev. These scaling factors were chosen by trial and error in this paper as shown in Fig 3, the input fuzzy sets use triangular membership functions with overlap. The language Variables are denoted by N (Negative), Z (Zero), and P (Positive) (Positive).

The following IF-THEN rules are used to indicate the fuzzy mapping of the input variables to the output:

IF(ev=N) and (cev=N) THEN (output=P)

IF(ev=N) and (cev=Z) THEN (output=P)

IF(ev=N) and (cev=P) THEN (output=Z)

IF(ev=Z) and (cev=N) THEN (output=P)

IF(ev=Z) and (cev=Z) THEN (output=Z)

IF(ev=Z) and (cev=P) THEN (output=N)

IF(ev=P) and (cev=N) THEN (output=Z)

IF(ev=P) and (cev=Z) THEN (output=N)

IF(ev=P) and (cev=P) THEN (output=N)
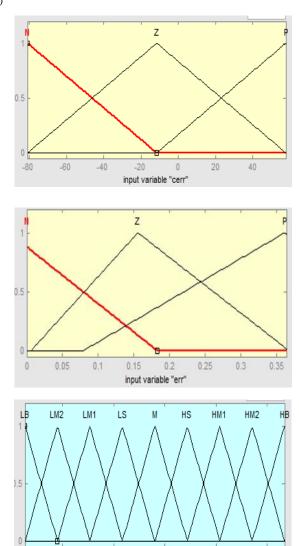
Fig 3. Rule base and Membership function of the neuro-fuzzy controller.

STATCOM output is Iqref, while SSSC output is vq_conv. The designed neural network is a feed-forward two-layer network with 20 neurons. In order to train the network, the Leaven Berg Marquardt approach is employed. Fig 4 and 5 depict the design of a neuro-fuzzy controller. The NFC is connected to the AC voltage regulator of the STATCOM block and the injected voltage regulator of the SSSC block, as shown in Fig.
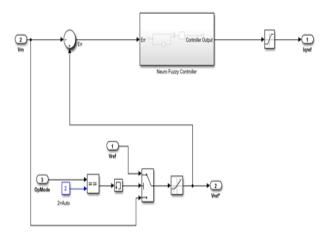
Fig 4. NFC Connected to AC voltage regulator of STATCOM
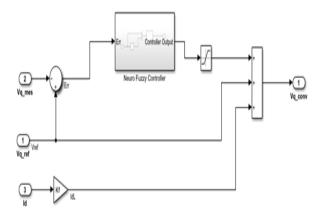
Fig 5. NFC connected in injected voltage regulator of SSSC

4. Model of test system

The wind farm under consideration in this paper has three 3 MW turbines. As a result, the wind farm has a capacity of 9 MW. Mentioned A 120/25 kV transformer and a 203 25 kV, 2-lined distribution line with a 25 km length and a 120/25 kV transformer connect the units to the grid. In this model, squirrel cage induction generators are used, and stator windings are directly connected to
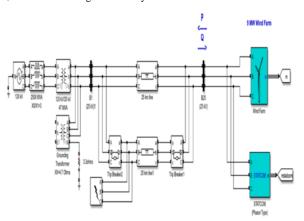
Fig 6. Test system model with STATCOM.
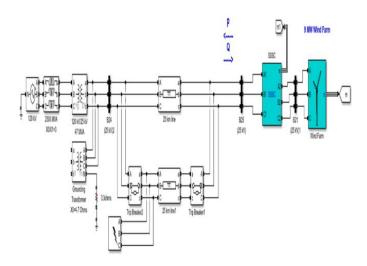
Fig 7. Test system model with SSSC.

the grid, with a capacitor bank used at the junction point to compensate for a portion of the required reactive power. Figures 6 and 7 show simulated system models for STATCOM and SSSC, respectively. This grid is used to investigate and assess machine and wind farm stability.

5. Analysis of simulations

Several tests were run to compare the performance of the neuro-fuzzy controlled STATCOM & SSSC with neuro-fuzzy control.

Case Study-1: An LLLG fault occurs 25 kilometers on a transmission line near a circuit breaker (C.B) at 15 seconds and is cleared after 200 milliseconds or 15.2 seconds. The system's settling time has decreased, making it relatively stable. Below figures depict neuro fuzzy. STATCOM has a shorter settling time than neuro fuzzy SSSC.

Case Study 2: An LLG fault occurs on a 25-kilometer transmission line near the CB at 15 seconds and is cleared after 200 milliseconds or 15.2 seconds.

Case Study 3: An LL fault occurs at 15 seconds on a 25-kilometer transmission line near the CB and is cleared after 200 milliseconds, i.e. the fault is cleared at 15.2 seconds.

Case Study 4: An LG fault occurs at 15 seconds on a 25-kilometer transmission line near CB and is cleared after 200 milliseconds. At 15.2 seconds, the fault is cleared.

Case Study 5: A LLL fault occurs at 15 seconds on a 25-kilometer transmission line near the CB and is cleared after 200 milliseconds. i.e. fault removed at 15.2sec.
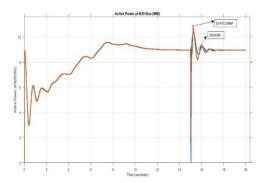
Case Study 6: A LLL fault occurs at 15 seconds on a 25-kilometer transmission line near the CB and is cleared after 200 milliseconds. At 15.2 seconds, the fault was cleared.

6. Conclusion
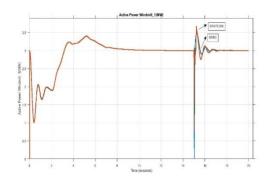
It is made abundantly evident that STATCOM fitted with a neural fuzzy controller performs better and operates faster. SSSC paired with a neuro-fuzzy controller provides a faster response. The neuro-fuzzy STATCOM response is superior to the neuro-fuzzy SSSC response when the system is used with different cases in this paper. Using neuro-fuzzy STATCOM compared to neuro-fuzzy SSSC, the system is more stable. As a result, it can be stated that it is preferable to connect STATCOM with a Neuro-fuzzy controller in the instances and systems under consideration because it may boost stability and improve grid-connected wind generator performance better than SSSC.

CASE 1: LLLG FAULT
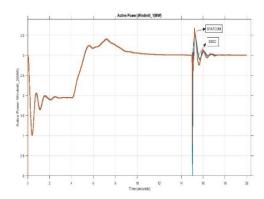
Active power at B25 Bus
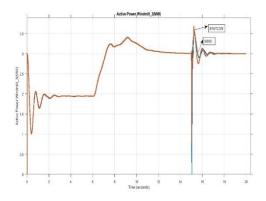
Active power at Windmill 1
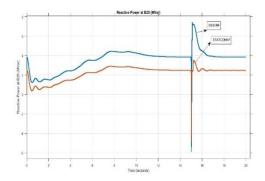
Active power at Windmill 2
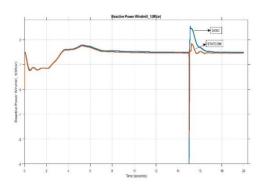
Active power at Windmill 3
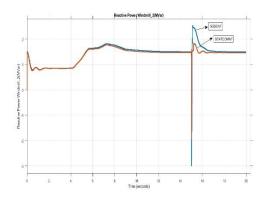
Reactive power at B25
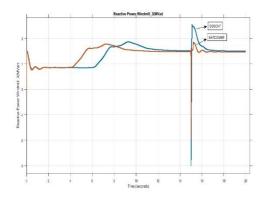
Reactive power at Windmill 1
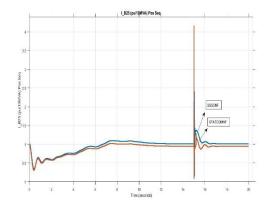
Reactive power at Windmill 2
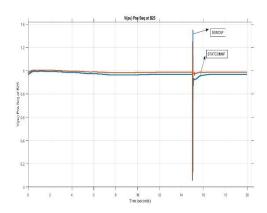
Reactive power at Windmill 3
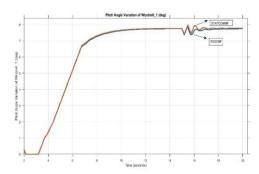
Current at B25 Bus
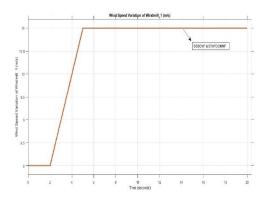
The voltage at B25 Bus
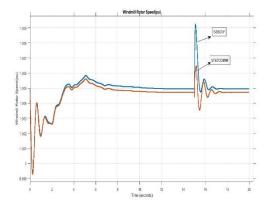
Pitch angle variation of a windmill

Wind speed variation of a windmill
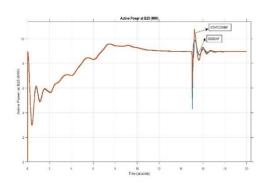
Windmill rotor speed
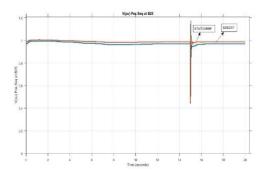
CASE 2: LLG FAULT
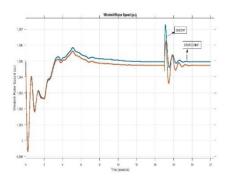
Active power at B25 Bus

The voltage at the B25 bus
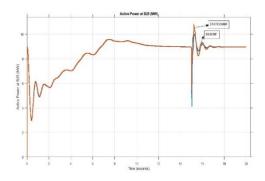
Windmill rotor speed
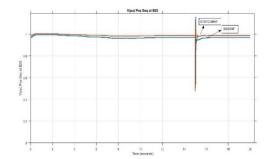
CASE 3: LL FAULT

Active power at B25 Bus

The voltage at B25 Bus
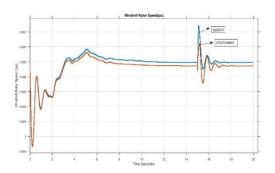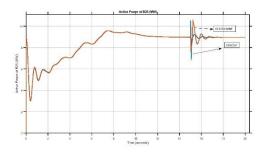
Windmill rotor speed
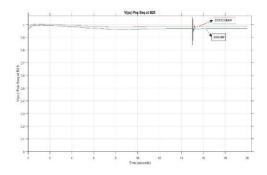
CASE 4: LG FAULT

Active power at B25 Bus

The voltage at B25 Bus
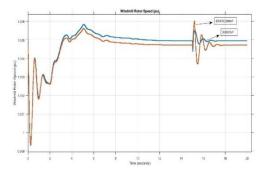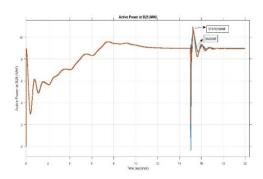
Windmill rotor speed
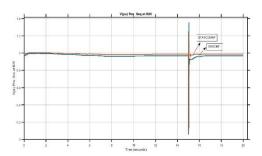
CASE 5: LLL FAULT

Active power at B25 Bus

The voltage at B25 Bus
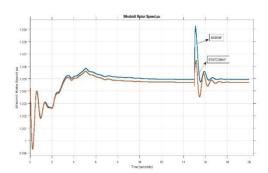
Windmill rotor speed

Reference:

[1] Uddin M. Nasir, Arifin Shamus, and Rezaei Nima "A Novel Neuro-Fuzzy Based Direct Power Control of a DFIG based Wind Farm Incorporated with Distance Protection Scheme and LVRT Capability", IEEE,2022

[2] Ebrahimi Reza, Mohammadreza Azizia, Naser Nourani Esfetanaj, Dao Zhou, Hossein Madadi Kojabadi "A Robust Fuzzy-based Control Technique for Wind Farm Transient Voltage Stability Using SVC and STATCOM: Comparison Study" IEEE.

[3] Khadidja Benayad, Tarik Zabaiou, Amar Bouafassa "Design of an Optimized Fractional-Order Fuzzy PID Based-SSSC Controller for Power System Oscillations Damping" IEEE,2022

[4] Van-Tri Bui, Thi-Trang Hoang, Thanh-Long Duong, Dinh-Nhon Truong*," Dynamic Voltage Stability Enhancement of a Grid Connected Wind Power System by ANFIS Controlled Static Var Compensator" ICSSE,2019.

[5] V Vanitha, Delna Raphe, Resmi R," Forecasting of Wind power using Variational Mode Decomposition-Adaptive Neuro Fuzzy Inference System" i-PACT,2019.

[6] Sapana A Bhande, Dr. V. K. Chandrakar," Fuzzy Logic based Static Synchronous Series Compensator (SSSC) to enhance Power System Security", IEEE, May,2022.

[7] Mohammad Rastegar, Mehdi Saradarzadeh, Shahrokh Farhangi," Fuzzy Logic-based Control of D-SSSC under nonlinear conditions of power system", PEDSTC, February-2022

[8] Jiahao Zhu, Lei Zhang, Songqiang Sun, Chaofan Du," The Hybrid Fuzzy Sliding-mode Nonlinear Coordination Control Method for Generator Excitation and STATCOM" IEEE-2019

[9] Lu Tianqi, Wang Youyin, Li Zhanjun, Li Meijun, Xu Weimao, Su Yunche, Cao Zhijian, Zhang Na," Reactive Power Compensation and Control Strategy for MMC-STATCOM Doubly-Fed Wind Farm" IEEE-2019

[10] Rashidul Islam, jakir Hasan, rezaur rahman siphon, mohammad ashraf hossain sadi, ahmed abuhussein, and tushar kanti Roy, "Neuro Fuzzy Logic Controlled Parallel Resonance Type Fault Current Limiter to Improve the Fault Ride Through Capability of DFIG Based Wind Farm," IEEE, vol-8,2020

[11] Shaikh Firdous Tarannum, S. S. Kamble," Modelling of a Fuzzy-Based STATCOM to Ensure Power Quality" CENTCON-2021.

HBRP PUBLICATION

PCA and ANN Based Induction Motor Fault Classification

[1]Mukesh R. Chavan[*], [2]Anjali U. Jawadekar
[1]*Assistant Professor, [2]Associate Professor, Department of Electrical Engineering, Shri Sant Gajanan Maharaj College of Engineering, Shegaon, Maharashtra, 444203, India*

*Corresponding Author
E-mail Id: - *chavanmukesh38@gmail.com*

ABSTRACT
Issues and malfunctions in induction motors can result in significant periods of inactivity and substantial financial losses due to maintenance and decreased revenue. This underscores the importance of monitoring motors, detecting potential faults in their early stages, and facilitating diagnoses. Among the recurrent problems encountered in induction motors, turn-to-turn short circuits, bearing degradation, and cracked rotor bars are the most prevalent. This study introduces an approach for detecting multiple faults in induction motors. The Principal Component Analysis (PCA) is recommended to condense the feature dataset extracted from motor currents under both normal and faulty conditions. From a pool of fourteen statistical parameters derived from stator currents, the application of PCA reduces the dimensionality to ten new features. These newly formed features are subsequently harnessed to categorize faults in induction motors using the Artificial Neural Network (ANN) classifier. Furthermore, a comparison of classification outcomes is conducted before and after employing principal component analysis. Empirical findings validate that by employing PCA in conjunction with ANN, it is possible to accurately classify various faults present in an induction motor.

Keywords:-*PCA: ANN: Fault diagnosis: Feature selection*

INTRODUCTION
The induction motor serves as a critical component within numerous industrial processes, making any instance of machine failure a matter of significant consequence for industries at large. The imperative to minimize downtime and prioritize safety underscores the pressing need for early detection of motor anomalies, thereby necessitating the implementation of condition-based monitoring protocols specifically tailored to induction motors. The spectrum of notable faults that afflict induction motors encompasses issues related to bearings, stator windings, and rotors. Among these, bearing faults account for approximately a fifth of all reported malfunctions, while interturn short circuits within the stator windings contribute to around a third of the reported

faults. Additionally, faults stemming from broken rotor bars and end ring issues make up roughly 10% of the total induction motor fault landscape. A central concern in the domain of machine condition monitoring revolves around the diagnosis of machine faults. The process of discerning the immediate "health" status or operational well-being of the motor undergoing observation is denoted as diagnosis. By embracing reliable diagnostic techniques, the risks associated with unforeseen machine breakdowns can be effectively mitigated, concurrently promoting an extension of the overall machine lifespan. In light of these imperatives, the prevailing trajectory in the industrial landscape is notably inclined towards the adoption of condition-based

approaches for both preventive and proactive maintenance strategies.

A comprehensive condition-based monitoring system consists of several key elements, including the machinery being monitored, condition monitoring sensors, signal processors, fault classifiers, machine models, and the monitoring output. The accuracy of fault classification is crucial, as errors and uncertainties in this process can result in false alarms. This challenge has prompted researchers to develop more robust and dependable condition monitoring systems.

In today's highly competitive market environment, the emphasis is shifting from scheduled maintenance and routine monitoring to condition-based maintenance and effective fault monitoring. Engineers and researchers have increasingly directed their efforts towards early detection of emerging faults and the implementation of preventive maintenance strategies. Notably, various methodologies centered on current and vibration spectral analysis have been proposed. These approaches leverage techniques such as Fourier transform and wavelet transform for the proactive monitoring of specific faults in induction motors. Traditionally, methods for detecting bearing faults and rotor faults have relied on spectrum analysis of motor-related parameters, including voltage, current, and instantaneous input power. However, advancements in monitoring techniques continue to shape the landscape of fault detection and maintenance strategies.

In today's competitive market landscape, there is a growing emphasis on condition-based maintenance and effective fault monitoring, surpassing the traditional approach of scheduled maintenance and routine checks. This shift has garnered significant attention from engineers and researchers alike, particularly directed towards the early detection of potential faults and the implementation of preventive maintenance strategies. Notably, various approaches leveraging current and vibration spectral analysis have been put forth for the proactive monitoring of specific faults in induction motors. These methodologies often involve the utilization of techniques such as Fourier transform and wavelet transform. These conventional techniques often revolve around spectrum analysis of motor-related parameters such as voltage, current, and instantaneous input power. The effectiveness of these approaches for effective motor fault analysis, specifically focusing on issues like bearing and rotor faults has been explored in [1][2]. At present, the assessment of induction motor conditions involves contemporary measurement methods, data processing strategies, and spectral analysis approaches. The prevalent methods for extracting fault-related features often revolve around Fourier spectral analysis conducted through FFT [3]. A phenomenological model was created by Gallardo[4], Barrios[5], and Gonzalez[6] to replicate fractured rotor bars within an induction motor. The diagnosis of inter-turn faults in the stator of three-phase induction motors is detailed through the utilization of Park's vector technique[7]. An induction motor experiencing an interturn fault in its stator is depicted as an asymmetrical three-phase system. Within a power system context, an asymmetrical three-phase configuration can be conceptualized as the amalgamation of three symmetrical systems: positive, negative, and zero-sequence. Many scholars have endeavored to identify inter-turn faults by computing the negative sequence current[8],[9] and negative and zero sequence impedances[10],[11]. A diagnostic approach for inter-turn faults has been presented, rooted in the notion of pendulous oscillation in [12].

The majority of these methods encompass the analysis of vibrations and stator currents due to their straightforward

measurability and strong dependability. Nevertheless, vibration analysis mandates costly sensors and specialized signal processing equipment. In the suggested study, emphasis is placed on employing current signals for diagnosing faults in induction motors. In tandem with the advancement of AI systems, specialized systems utilizing neural networks and fuzzy logic have been harnessed to aid in detecting faults by accurately deciphering the anomalous data [13]. Hence, it can be concluded that numerous methods exist to diagnose distinct faults in induction motors, primarily conducted offline. This underscores the requirement for a comprehensive approach enabling real-time detection of multiple faults. In this research, an algorithm rooted in neural networks is put forth to classify bearing faults, rotor bar cracks, and stator inter-turn faults within induction motors. Currents extracted from motor terminals are subjected to processing to derive meaningful characteristics, subsequently undergoing PCA to streamline the feature set's dimensions.

The Principal Component denotes the line within the n-dimensional data that best aligns with the data points, aiming to minimize the average squared distance between the points and the line. Principal Component Analysis involves the process

Suppose x = (x1, x2,…, xM)' are M×1 vectors, x_i is row vector of N points.

Suppose

Step 1:-

$$\bar{x}_i = \frac{1}{M} \sum_{i-1}^{M} x_{ki} \qquad (2.1)$$

Step 2:- Subtract the mean from original variable

$$\emptyset_i = x_i - \bar{x}_i \qquad (2.2)$$

Step 3:- compute covariance matrix

$$C \frac{1}{M} \sum_{k=1}^{M} \emptyset_k = \emptyset_k^T \qquad (2.3)$$

Step4:- Compute the eigen values of C: $\lambda1 > \lambda2 > \lambda3 >>> \lambda_N$

Step5:- Compute the eigen values of C: U1, U2. . . . . U_N

Step6:-Select the Kth eigen vector with maximal eigen value (Principal Component)

Using PCA reconstruction a given signal can be recognized using few dominant principal components which contains most of the energy. The related eigen vectors and eigen values

of selecting principal components while disregarding others, serving to alter the data's foundational basis. PCA stands as a non-parametric statistical technique employed for dimensionality reduction in various exploratory data analyses aimed at constructing predictive models. In this procedure, vectors are identified in a manner that encapsulates the original data with the least possible dimensions, ensuring that the newly derived vectors preserve the utmost variance information. PCA transforms primary high-dimensional data into a feature dataset of smaller dimensions where the variance is maximized. Its inception dates back to Karl Pearson's initial proposition in 1903, followed by further development by Harold Hotelling in 1930. PCA computation can be conducted using eigenvalues or covariance. The applications of PCA span multiple domains, including biomedical signal processing, image manipulation, artificial intelligence, and pattern recognition. The most advantageous aspect of PCA lies in its ability to decrease the data's dimensions with minimal information loss. This reduction in dimensionality leads to decreased computational requirements and resource utilization, while also mitigating the impact of noise [21].

are obtained by linear algebraic decomposition. For finding the principal component the condition used is given by

$$\frac{\sum_{i=1}^{K} \lambda_i}{\sum_{i=1}^{N} \lambda_i} > Threshold \qquad (2.4)$$

Where the λ_i is eigen values of covariance matrix of x = (x1, x2,…, xM)'. Generally threshold chosen is around 0.9 to 0.95 [22]

ARTIFICIAL INTELLIGENCE

A neural network is acknowledged as a computational technique inspired by biological systems. It encompasses processing units, connections, and coefficients. Neurons serve as the processing units, training and recall algorithms function as connections, and weights are assigned to these connections as coefficients. Artificial neural networks possess traits including adaptive learning, generalization, extensive parallelism, resilience, associative information storage, and the processing of spatiotemporal information [22]. Artificial intelligence finds application across a multitude of domains such as pattern recognition, speech understanding, biomedical diagnostics, as well as the detection and diagnosis of induction motor faults [23]. The neural network structure employed in this context is a three-layer configuration, encompassing an input layer, a hidden layer, and an output layer. This specific design adopts the artificial feed-forward network topology for its simplicity. During the training of input patterns, a feed-forward network is utilized, while the backpropagation method is employed to compute errors and derive weight adjustments based on these error calculations. Activation progresses from the input layer through the hidden layer and finally to the output layer.
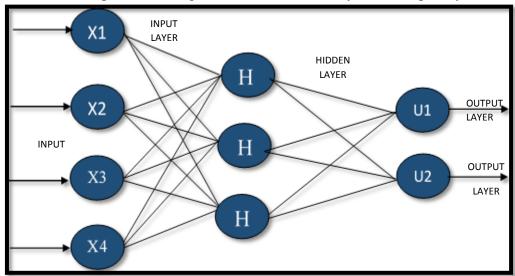
Fig.1:-Architecture of Artificial Neural Network

EXPERIMENTAL SETUP

To conduct trials and generate data, a 2 H.P, 3-phase, 4-pole, 415-volt, 50 Hz squirrel cage induction motor is employed to simulate various faults in the motor. The experimental arrangement is depicted in Figure 2. The utilized motor features 24 coils within 36 slots. Each phase is comprised of 8 coils, amounting to 300 turns. A tapping procedure is implemented on each phase, with tapping initiated after 10 turns, originating from the star point (neutral). Tapping is executed from coils, forming groups of around 70 to 80 turns

each. Current and voltage signals are captured using ADLINK DAQ at a sampling rate of 1 kHz, considering

diverse load and supply scenarios for the subsequent scenarios.

Fig.2:-Experimental Setup

A. In the healthy state, a 2 H.P motor is connected to a balanced three-phase power supply. The motor load is adjusted across the entire range, from no load to full load. Stator current signals and phase voltages are recorded under various load and supply conditions.

B. The motor being tested is equipped with two bearing types: 6204 and 6205. Bearings exhibiting inherent imperfections due to regular motor operation are employed in the experimental investigations. Diverse combinations of bearings, some of which have defects in the inner or outer race, are installed in the motor. Stator currents and voltages are acquired for each bearing combination, facilitating a comparison with the reference healthy bearing condition. Multiple experiments were conducted, involving various arrangements of rear and load side bearings, to assess the bearing's performance and their impact on the motor's overall operation.

C. Stator Interturn Short Circuit: In this specific scenario, the stator windings of an induction motor were adjusted to incorporate multiple accessible tapings, strategically introduced to create short circuits. In this experimental phase, tapping was performed on phase A, involving increments of 10 turns. A series of distinct trials were conducted, each involving the short-circuiting of 10 turns within phase A of the motor. Subsequently, phase voltage and stator current signals were meticulously recorded under varying loading conditions.

D. Broken Rotor Bars: The induction motor subjected to testing is equipped with a total of 32 rotor bars. For the purpose of conducting the rotor broken bar examination, two rotor bars are intentionally broken on both ends of the end rings. Throughout this testing phase, stator current signals are meticulously collected across a range of loading conditions.

Fig.3(a –d) shows the stator current signals recorded from the motor terminals at full load during normal and under various fault conditions
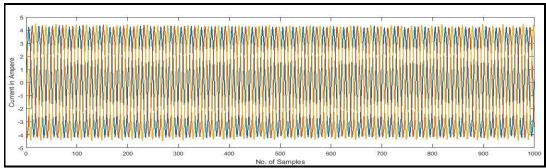
Fig.3(a):-*Current signal of the healthy condition of motor*
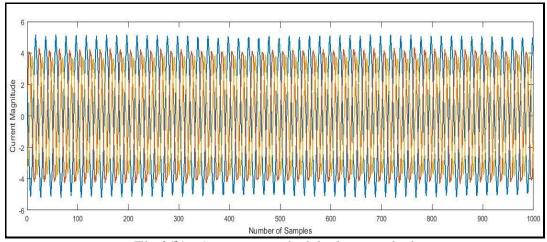
Fig.3(b):-*Current signal of the bearing fault*
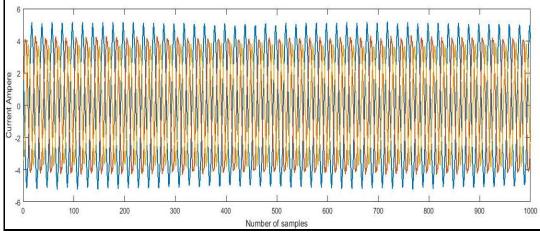
Fig.3(c):-*Current signals of 20% inter turn fault*
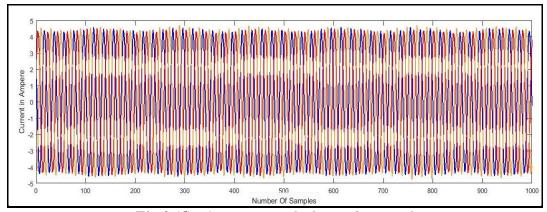
Fig.3 (d):-*Current signal of rotor bar crack*

FEATURE EXTRACTION AND PRINCIPAL COMPONENT ANALYSIS

Current signals obtained during abnormal motor conditions exhibit resemblances to those of a normal motor. The time waveforms, illustrated in Figure-3(a-d), manifest minimal distinguishable discrepancies across diverse motor states. Consequently, the need arises to devise a feature extraction methodology for effectively categorizing these anomalies. The classification of faults involves the extraction of statistical parameters.

This set of statistical parameters encompasses quantities such as minimum, maximum, mean, median, summation, absolute summation, root mean square (RMS) value, energy, kurtosis, crest factor, shape factor, standard deviation, variance, and Skewness. These parameters are computed based on the stator current signals that have been captured. The mathematical formulas for calculations of these 14 statistical parameters is given in [24].

In classification models, feature reduction holds significant importance as it aims to eliminate irrelevant data for the purpose of enhancing accuracy. The feature reduction framework serves to streamline high-dimensional data into a lower-dimensional format characterized by uncorrelated attributes. The employment of Principal Component Analysis (PCA) as a feature extraction method precedes the training of Artificial Neural Networks (ANN) with the intention of diminishing the presence of redundant information. PCA is implemented to calculate statistical parameters that facilitate data reduction. The fundamental concept underpinning this approach is the ability to derive the most pertinent components or factors from the initial features.

In Figure 4, the Scree plot illustrates the relationship between eigenvalues and the count of principal components. The plot reveals that the initial four components exhibit sufficiently high eigenvalues. As a result, these first four principal components, out of the total 42, are chosen to serve as inputs for the ANN. Conversely, the remaining components are disregarded due to their relatively low values.
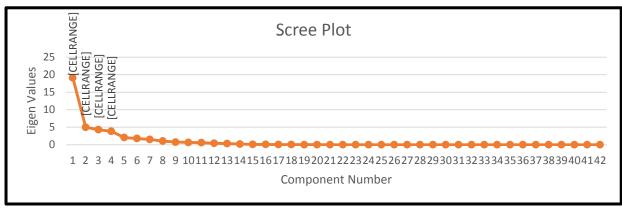
Fig.4:-*Scree plot of Eigen Values*

RESULT AND DISCUSSION

Leveraging its remarkable aptitude for pattern recognition, an Artificial Neural Network (ANN) proves to be a robust tool for efficiently classifying faults in induction motors. In this study, a three-layer Feedforward Artificial Neural Network (FFANN) is employed, and its training involves the Back Propagation technique under supervised learning. The FFANN architecture comprises an input layer, a hidden layer, and an output layer. Within the input layer, four processing elements correspond to the four principal components obtained through PCA analysis. Meanwhile, the output layer encompasses four processing elements representing distinct conditions: healthy state, bearing fault, interturn fault, and rotor bar crack.

To ensure robustness, the network is fed randomized data, employing the Transigmoid transfer function for training purposes. This approach yields a classification accuracy percentage. Based on these assumptions, the classification accuracy percentage is determined for healthy, bearing fault, interturn fault, and broken rotor bar conditions in induction motors, considering the number of processing elements in the hidden layer. To highlight the advantages of PCA, a comprehensive analysis of fault classification is conducted both with and without PCA. The outcomes, summarized in Table 1, substantiate the enhanced classification accuracy achieved through the integration of PCA in the fault classification process for induction motors.

Table 1:-*Fault classification of Induction Motor Using Time Domain and PCA-ANN Based Approach*

Method	Input to ANN	For 4 Processing Element	
Time Domain Statistical Parameter Based Approach(Without PCA)	14 Statistical Parameter of current Ia, Ib, Ic Total 42 Input	**Motor Condition**	**% Accuracy of classification obtained from ANN**
		Healthy	100
		Bearing Fault	95
		Inter Turn Fault	100
		Rotor bar Crack	100

		Motor Condition	% Accuracy of Classification obtained from ANN
PCA-ANN Based Approach	Major Principal Components 04 Input	Healthy	100
		Bearing Fault	100
		Inter Turn Fault	100
		Rotor bar Crack	100

The results were compared with those obtained using all the features as input for ANN. Examination of Table 1 reveals that when utilizing 4 principal components as input to the ANN with a hidden layer consisting of 4 processing elements, the PCA-ANN approach achieves a fault classification accuracy of 100% for induction motors.
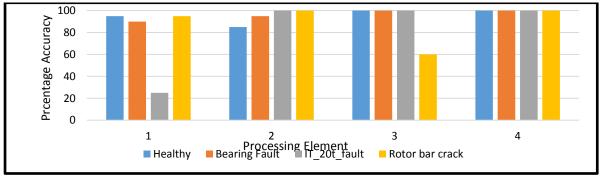
Fig.5:-*Number of processing elements versus percentage accuracy*

Figure 5 shows the details of number of processing element versus percentage accuracy of classification for PCA-ANN based approach.

CONCLUSION
The study introduces an approach for classifying faults in induction motors, referred to as PCA-ANN Based approach. To evaluate its efficacy, a comparison is made against a time-domain-based method. When employing four processing elements, the PCA-ANN-based strategy achieves a fault classification accuracy of 100%. The recorded current signals in both healthy and faulty states undergo further analysis to derive statistical parameters. In order to streamline the data and eliminate redundancy, Principal Component Analysis (PCA) is employed to extract relevant features. Specifically, the top four principal components with significant eigenvalues are chosen as inputs for the ANN. Consequently, the PCA-ANN approach, utilizing a hidden layer with four processing elements, attains perfect accuracy in identifying induction motor faults. Simultaneously, this method mitigates the computational load.

REFERENCES
1. G.Didier, etal, IE International Conference on Industrial Technology Volume 1, pp170-174 December 2004.
2. Z.Liu, X Yin, Z.Zhang and D Chen, IEEE Transaction Energy Conversion volume 19, pp485-490 September 2004.
3. M. E. H. Benbouzid, Michella Viera and Celine Theys, IEEE Transaction Power Electronics volume 14,pp14-22 January 1999.
4. Gallardo E (1996) Electrical Engineer Thesis, Department of Electrical Engineering University of Chile ,Santiagi.
5. Barrios A (1997) Electrical Engineer

Thesis, Department of Electrical Engineering, University of Chile, Santiago.

6. Gonz´alez D (1998) Electrical Engineer Thesis, Department of Electrical Engineering, University of Chile, Santiago, Chile.

7. A. J. M. Cardoso, S. M. A. Cruz and D. S. B. Fonseca, IEEE Transactions, Energy Conversation, Vol.14, No 3, September 1999, pp.595-598.

8. G.B.Kliman, W.J.Premerlani, R.A.Koegl and D.Hoeweler, in conference Rec Proceeding IEEE IAS Annual meeting vol1, 1996 pp687-693.

9. J.L.Kohler,J.Sottile & F.C.Trutt, IEEE Transactions Industrial Application Volume 28,No5 pp1109-1117 September/October 1992.

10. S.B.Lee,R.M.Tallan & T.G.Habetler , IEEE Transaction ,Power Electron ,volume 18,no 3 pp865-872 May 2003.

11. [J.Sottile, J.L.Kohler, IEEE Transaction Industrial Applications volume 28 PP921-937 July/August 1992.

12.]Behrooz Mirafzal, Richard J.Povinelli Nabeel, A.O.Demerdash, IEEE transaction on Energy Conversion vol 21 No 4 December 2006.

13. A Costa ,G.G.Verucchi, C.J & Gelso E.R. Mechanical system and signal Processing 20,953-965 2006.

14. J.faiz ,B.M Ebrahimi, B,Akin & h.A.Tloiyat IEEE transaction Magzine vol 44 no 1pp66-74 January 2008.

15. M,S.Balla ,Z.J.khan , H.MSuryawanshi& R.L.Sonolikar, IEEE transaction Industrial Electron 54,2007.

16. K. Bouibed, L. Seddiki, K. Guelton and H. Akdag, An Open Access Journal, Vol. 2, No. 1, 2014, pp. 150-160.

17. M. Farahani, A. R. Zare Bidaki and M. Enshaeieh, An Open Access Journal, Vol. 2, No. 1, 2014, pp. 261-267.

18. VanTung Jran , Bo_Suk yang ,Myung Suckoh and Andy Chitchiow tan,"Fault diagnosis of induction motor based on decision trees and adaptive neuro fuzzy inference expert systems with applications 36(2) 1840-1849 2009.

19. Bo-Suk Yang ,Tian Han &Yong Sukin (2004) Expert Systems with Applications 26(3) pp387-395 2004.

20. F.Filippetti, G.Franceschini, C.Tassoni & P.Vas, IEEE Transaction Industrial Electron volume 47 pp994-1004 October 2000.

21. Pearson, K.: On Lines and Planes of Closest Fit to Systems of Points in Space, Philosophical Maganize, pp. 559-572 (1901) .

22. S. Shanmuganathan, *Artificial Neural Network Modelling*, vol. 628, S. Shanmuganathan and S. Samarasinghe, Eds. Cham: Springer International Publishing, 2016, pp. 1–14. doi: 10.1007/978-3-319-28495-8_1.

23. M. A. M. Sadeeq and A. M. Abdulazeez, *International Conference on Advanced Science and Engineering (ICOASE)*, Duhok, Iraq, Dec. 2020, pp. 199–204. doi: 10.1109/ICOASE51841.2020.9436582.

24. Anjali P. Wadekar And Anjali U. Jawadekar, *Int. J. Ind. Electron. Electr. Eng.*, No. 8, [Online]. Available: Http://Pep.Ijieee.Org.In/Journal_Pdf/11-392-151703322731-35.Pdf

SOBI-ANN Based Induction Motor Fault Classification

1st Mukesh Ravindra Chavan
2nd Anjali Uday Jawadekar
Department of Electrical Engineering
Shri Sant Gajanan Maharaj Collge Of Engineering
Shegaon, India
chavanmukesh38@gmail.com
anjali.jawadekar@gmail.com

3rd Danton Diego Ferreira
Department of Automation (DAT)
Federal University of Lavras
Lavras, Brazil
danton@ufla.br

Abstract—The Induction motor fault can lead to financial loss in any place where it is used. Hence, an early detection and diagnosis of fault and its classification becomes most important for the smooth working of the system. In this paper the study proposes an algorithm for fault classification. The second order blind identification method (SOBI) is used for calculating the estimates and these estimates are given to the ANN for fault classification. Result indicates the input requirements are reduced for the classification of faults when 14 statistical parameters of 2nd and 3rd estimates of SOBI are given to the ANN.

Index Terms—SOBI, BSS, ANN, Fault Classification

I. Introduction

The induction motor ranks among the most frequently employed motors within industrial settings. About 60% of the industrial load is induction motor load. The induction motor fault causes the industrial process to halt. This causes huge amount economic losses to the industries. The types of fault those an induction motor come across are rotor faults and stator faults. The rotor fault accounts for 20% faults on the induction motor. Rotor faults encompass categories such as rotor eccentricity, damage, fracture or deformation of rotor cage bars, and cracks or fractures in end rings, as well as rotor bowing [1]. The total faults of induction motor 40% faults reported are the bearing fault. Stator related issues generally be divided into two main groups: (i) faults related to laminations and the frame and (ii) faults associated with stator windings. These faults can occur in an induction motor due to various stress factors, including mechanical, thermal, electrical, and environmental factors, leading to potential fault conditions[2].

Numerous techniques and technologies are being suggested for identifying fault conditions in various systems. These methods include Employing electromagnetic field monitoring via coils wound around motor shafts particularly in context of axial flux detection and utilizing search coils, Utilizing infrared recognition, Monitoring radio-frequency and (RF) emissions, Assessing noise and vibration, Measuring acoustic noise, Implementing motor-current signature analysis (MCSA), Employing model-based, artificial intelligence based, and neural network-based approaches. Various techniques have been suggested for fault detection and classifi-cation, including methods such as MCSA, Park's Transform, Artificial Neural Networks,Finite Element Method, Concordia Transform, Vibration Testing and Analysis, Multiple Reference Frames Theory, External Magnetic Field Analysis, Power Decomposition Technique,KU Transformation Theory and Wavelet Analysis. Among all the methods the MCSA, ANN and Wavelet Analysis method has been widely used because of the several advantages. For rotor faults detection and classification various methods have been used like Fast Fourier Transform (FFT), Short Time Fourier Transform (STFT), Discrete Wavelet Transform (DWT), finite element analysis, Vienna Monitoring Method, and wavelet transform based methods[3]. For stator faults mostly discussed and occurred fault is a bearing fault, then interturn faults are considered. To detect and classify bearing and interturn fault various methods for detection and classification have been proposed the negative and zero sequence currents for detection, checking for the additional air gap flux harmonics, instantaneous power signatures, random forest classifier, Park's Transform, Principal Component Analaysis(PCA), Artificial Neural Network (ANN), Fuzzy classifier are used [2][3].

In addition to these approaches, researchers have delved into a novel realm of fault detection and classification known as blind source separation (BSS) methods. There are several algorithms in BSS like information maximization algorithm, Fixed point algorithms(ICA), JADE algorithm[4]. ICA uses the higher order statistical properties to linearly mixed signals into independent components, all without any prior information about original components or mixing process[5]. The ICA method is used over the FFT output and its standard deviation in region of interest were found to be fault discriminant [6]. The ICA method along with some constrained is used to classify the fault. The information is contained by the signals in terms of independent component is less so the c-ICA algorithms can classify the fault based only if prior knowledge of mechanical information is known as reference[7]. The ICA technique is employed to identify faults in induction motor by determining a threshold and triggering a fault detection if any condition surpasses this condition[8]. Form above results we come to the conclusion that ICA can be used for the fault

detection but will not be suitable for the fault classification. So another method and area of BSS algorithms is higher order statistics (HOS) called as Second Order Blind Identification method (SOBI). This paper is organized in eight chapters. The second chapter will explain about the SOBI method its advantages and disadvantages. Third chapter presents introduction to Artificial Intelligence. Fourth chapter presents feature extration. Fifth chapter will present the algorithm for classification of the faults of induction motor. Sixth chapter will discuss the experimental setup and observations. Seventh chapter will present the results and discussions. Eight chapter will present the conclusion and future scope.

II. SECOND ORDER BLIND IDENTIFICATION (SOBI) METHOD

The method was introduced by Belouchrani et al., in 1997 [9]. Second-Order Blind Identification (SOBI as introduced by Belouchrani et al. in 1997), leverages the temporal interdependencies of components through the joint diagonalization of one or multiple auto-covariance matrices. After that several authors have used this algorithm for source separation and finding out the valuable information for detection and classification in various area of application. The SOBI method has found application in various domains, including artifact removal from EEG data [9], the identification of significant signals in brain EEG data [10], the separation of vibrations originating from underground traffic, and the prediction of wind speed. SOBI has gained recognition as a well-established and extensively researched technique for separating uncorrelated weakly stationary time series. For different time series and BSS model this method has to be provided with some modification [11]. The SOBI method has been successfully implemented by the Oliveira et al. in 2020 for harmonic and inter harmonic classification of Power Quality disturbances. Applying the same concept here the induction motor fault classification is achieved [12]. The SOBI algorithm operates by approximating the joint diagonalization of two correlation matrices characterized by different delays. When $z[n]$ a whitened vector is provided, it investigates for a collection of r delayed correlation matrices for $z[n]$, denoted as $R_z(\tau_i)$ for $i = 1,\ldots,r$. The objective of SOBI is to find a unitary transformation V such that:

$$V^T R_z(\tau_i)V = D_i \, for \, i = 1,\ldots\ldots,r \qquad (1)$$

where, D_i refers to a collection of covariance related to the estimated signal $y[n]$. By working with several correlation matrices, SOBI reduces the probabilities of incorrect delay selection interfering with blind separation process. Put simply, the steps to execute the SOBI can be summarized as follows:

1. Evaluate the MxM correlation matrix $R_x(0)$ of signals $x[n]$ as:

$$R_x(0) = E[x(0)x^T(0)] = \frac{1}{N-M+1}XX^T \qquad (2)$$

where X is called as the Hankel matrix

2. Estimate the EVD of $R_x(0)$:

$$R_x(0) = V_x D_X V_x^T \qquad (3)$$

where $V = [v_1, v_2, \ldots\ldots, v_M]$ is an MxM unitary matrix having eigenvectors of $R_x(0)$ and D_x is an MxM diagonal matrix having eigenvalues $\lambda_1, \lambda_2, \lambda_3, \ldots, \lambda_M$ of $R_x(0)$ prepared in descending order.

3. A white vector $z[n]$ is obtained by performing whitening of $x[n]$ through the whitening matrix Q,

$$z[n] = Q_x[n] \qquad (4)$$

Where,

$$Q = D_x^{(-(1/2))}V_x^T \qquad (5)$$

4. Calculate H delayed sample correlation matrices $R_z(\tau)$ from $z[n]$ for a set of fixed delays

$$\tau \epsilon(\tau_j j = 1, \ldots.., H); \qquad (6)$$

5. Obtain the unitary matrix V, which is the joint diagonalizer of the set of correlation matrices $(R_z(\tau_j), j = 1, \ldots, H)$, by applying the Givens Rotation method[12];

6. Estimate the output signals as:

$$y[n] = V^T Q_x[n] \qquad (7)$$

And or the mixture matrix A, as A=Q*V.

Where * denotes the Moore-Penrose pseudo-inverse.

Experimental findings have indicated that employing multiple correlation matrices is more effective and resilient in scenarios characterized by low signal-to-noise ratio (SNR) and/or sources with minimal spectral distinctions[12].

III. ARTIFICIAL INTELLIGENCE

Neural network is recognized as a biologically inspired computational method. It consists of the processing element, connections, and coefficients. The processing elements are neurons, connections are training and recall algorithms and coefficients are the weights given to connections.The Architecture of Artificial Neural Network is shown in *Figure*1. Artificial neural networks possess key attributes such as adaptability in learning, the ability to generalize, parallel processing at scale, resilience, the capacity for associative information storage, and processing of spatiotemporal information [13]. Artificial intelligence is being used in various area of applications like pattern recognition, speech recognition, biomedical
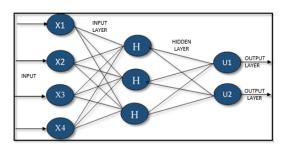
Fig. 1. Architecture of Artificial Neural Network

diagnosis applications, induction motor fault detection and diagnosis, and many more[14]. The neural network illustrated here is organized in three tiers: an output layer, a hidden layer and an input layer . The artificial feed-forward network topology is selected for simplicity. The choice for training input patterns involves utilizing a feedforward network, while error computation and weight adjustment based on error calculations are accomplished through backpropagation. The progression goes from input layer to hidden layer and to the output layer.

IV. FEATURE EXTRACTION

It is necessary to develop a feature extraction approach for classifying defects. Statistical parameters are extracted to classify the different faults. These statistical parameters include minimum, maximum,variance, avegare(mean), middle value(median), addition(sum), absolute addition(sum), shape factor, root mean square value(RMS value), kurtosis, energy, crest factor, standard deviation and skewness of captured stator current signals. The mathematical formula and its calculations can be referred in detail in [15].

V. PROPOSED ALGORITHM

Step1: Capture three phase current of the Induction motor for processing.

Step2: Take transpose if captured signal is in column and apply SOBI Algorithm to the signal

Step3: Calculate 14 statistical parameter of 2nd and 3rd estimate

Step4: Apply ANN classifier for the classification of the faults and obtain confusion matrix and the ANN classifier model

VI. EXPERIMENTAL SETUP AND OBSERVATIONS

For the purpose of experimentation and data generation, a squirrel cage induction motor with the following specifications is employed: 2 H.P, 3-phase, 4 poles, 415 volts, 50 Hz. The experimental set up is shown in *Figure* 2.

This motor has 24 coils distributed across 36 slots. Each phase consists of 8 coils, each comprising 300 turns. A tapping configuration is applied to each phase, with the tapping starting at 10 turns from the neutral point. With each group containing approximately 70 to 80 turns, tapping are drawn from these coils. To capture the current and voltage signals, an ADLINK DAQ system is used, operating at a sampling frequency of

Fig. 2. Experimental Setup
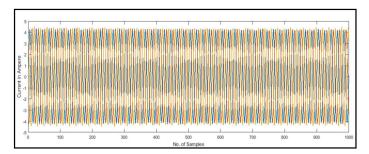
Fig. 3. 3-phase Current signal of the healthy condition of induction motor
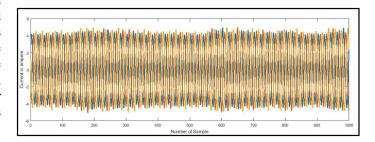
Fig. 4. 3-phase Current signal of the bearing fault of induction motor
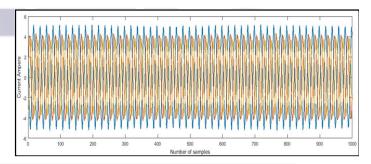
Fig. 5. 3-phase Current signals of inter turn fault of Induction motor
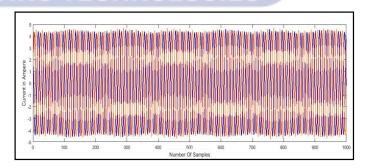
Fig. 6. 3-phase Current signal of rotor bar crack of Induction motor

1 kHz, and data is collected under various load and supply conditions for the specific cases outlined in *Figure* 3 to *Figure* 6. The *Figure* 3 to *Figure* 6 display the 3-phase current signals corresponding to different fault conditions in the 3-phase induction motor.

The various condition of fault current are processed through the SOBI algorithm then 3 estimates are obtained. Note that the 3rd estimate and 2nd estimate shows the largest variations
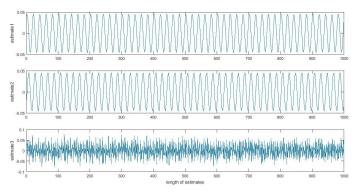
Fig. 7. SOBI demixing matrix estimates for healthy condition

Fig. 10. SOBI demixing matrix estimates for Rotor-bar fault condition

Fig. 8. SOBI demixing matrix estimates for bearing fault condition

Fig. 9. SOBI demixing matrix estimates for Interturn Fault Condition

reading are taken for each fault, hence 28x40 matrix of statistical parameters is obtain. An artificial neural network (ANN) with its strong pattern recognition abilities proves to be a valuable tool for the classification of faults in induction motors. This study utilizes a three-layer Feed Forward ANN (FFANN) trained through a supervised learning technique known as Back Propagation. The FFANN structure contains an input layer, hidden layer, and an output layer. The input layer comprises 28 nodes corresponding to statistical features derived from the 3rd and 2nd estimates of the SOBI demixing matrix, 12 neurons in the hidden layer. Meanwhile, the output layer is represented by four processing elements, each representing one of the following conditions: rotor bar crack, interturn fault, bearing fault and healthy condition.The ANN model obtained after training is shown in *Figure 11*. Randomized data is given as input into the network, to ensure generalization and the Transigmoid transfer function is employed for training purposes. This training process yields a percentage accuracy for classification. Considering these foundational principles, the research investigates the relationship between the accuracy percentage in categorizing induction motor states and the quantity of processing elements within the hidden layer. It can be clearly observed that the ANN is able to classify the faults with 100% accuracy considering the healthy condition. The

when compared with the healthy conditions and fault condition. The SOBI decompositions are as shown in *Figure* 7 to *Figure* 10 for various fault condition when motor is on load.

Form observation of *Figure* 7 to *Figure* 10 it is clearly visible that 3rd and 2nd estimates of faulty condition demonstrate the significant variation as compared to the healthy condition. Hence 14 statistical parameter has been calculated for both of the estimates. These 14 statistical parameters of 3rd and $2^{n}d$ become the input to the ANN.

VII. RESULTS AND DISCUSSION

It is clearly seen that 3rd and 2nd estimate of the SOBI demixing matrix shows greater variations, so statistical parameter of 3rd and 2nd estimate has to be calculated. The total 10

Fig. 11. ANN Training Model for induction motor fault classification
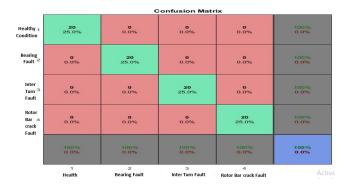
Fig. 12. Confusion Matrix for classification of induction motor fault

TABLE I
COMPARISON OF THE VARIOUS PARAMETERS OF ANN AND SOBI
ESTIMATES AND CLASSIFICATION RESULTS

Estimate No. selected for the statistical calculation and feed to ANN	Neuron Input	Neuron output	No. of hidden layers	No. of hidden Neurons	Confusion matrix classification
All 3 estimate	42	4	1	7	100%
Only 3rd estimate	14	4	1	11	98%
2nd and 3rd estimate	28	4	1	12	100%

confusion matrix obtained after training is shown in *Figure 12*. Table 1 displays the accuracy of classification when all the statistical features from the estimates are input to the ANN, resulting in a 100% classification accuracy rate. So as to check whether ANN can classify all the conditions with less number of input only the statistical parameter. The classification accuracy when the statistical parameter of only 3rd estimate is considered then only 98% classification accuracy is obtained. Hence to improve classification accuracy 2nd estimate along with 3rd is considered for processing and 100% classification accuracy is obtained here.

VIII. CONCLUSION AND FUTURE SCOPE

The paper proposes SOBI-ANN based induction motor fault classification. SOBI algorithm is used as signal separation method to identify the dominant fault signals and is given to the ANN after feature extraction for classification as ANN has good classifier properties. As this method is a time domain based method its computational complexity is less and time required to perform classification also reduced. Now this work could be extended by applying dimension reduction methods to select the dominant features after calculating the statistical parameter those are feed to ANN for classification.

REFERENCES

[1] M. R. Mehrjou et al., "Wavelet-Based Analysis of MCSA for Fault Detection in Electrical Machine," in Wavelet Transform and Some of Its Real-World Applications, D. Baleanu, Ed., InTech, 2015. doi: 10.5772/61532.

[2] R. Jigyasu, A. Sharma, L. Mathew, and S. Chatterji, "A Review of Condition Monitoring and Fault Diagnosis Methods for Induction Motor," in 2018 Second International Conference on Intelligent Computing and Control Systems (ICICCS), Madurai, India: IEEE, Jun. 2018, pp. 1713–1721. doi: 10.1109/ICCONS.2018.8662833.

[3] R. N. Dash, S. Sahu, C. Ku. Panigrahi, and B. Subudhi, "Condition monitoring of induction motors: — A review," in 2016 International Conference on Signal Processing, Communication, Power and Embedded System (SCOPES), Paralakhemundi, Odisha, India: IEEE, Oct. 2016, pp. 2006–2011. doi: 10.1109/SCOPES.2016.7955800.

[4] Y. Li, D. Powers, and J. Peach, "Comparison of Blind Source Separation Algorithms," C 2000 WSES P18-21 Mastorakis2000 Adv. Neural Network. Appl. WSE, p. 6.

[5] A. Tharwat, "Independent component analysis: An introduction," Appl. Comput. Inform., vol. 17, no. 2, pp. 222–249, Apr. 2021, doi: 10.1016/j.aci.2018.08.006.

[6] J. E. Garcia-Bracamonte, J. M. Ramirez-Cortes, J. de Jesus Rangel-Magdaleno, P. Gomez-Gil, H. Peregrina-Barreto, and V. Alarcon-Aquino, "An Approach on MCSA-Based Fault Detection Using Independent Component Analysis and Neural Networks," IEEE Trans. Instrum. Meas., vol. 68, no. 5, pp. 1353–1361, May 2019, doi: 10.1109/TIM.2019.2900143.

[7] Z. Wang, J. Chen, G. Dong, and Y. Zhou, "Constrained independent component analysis and its application to machine fault diagnosis," Mech. Syst. Signal Process., vol. 25, no. 7, pp. 2501–2512, Oct. 2011, doi: 10.1016/j.ymssp.2011.03.006.

[8] I. Guney, E. Kilic, O. Ozgonenel, M. Ulutas, and E. Karadeniz, "Fault detection in induction motors with independent component analysis (ICA)," in 2009 IEEE Bucharest PowerTech, Bucharest: IEEE, Jun. 2009, pp. 1–4. doi: 10.1109/PTC.2009.5282251.

[9] A. Belouchrani, K. Abed-Meraim, J.-F. Cardoso, and E. Moulines, "A blind source separation technique using second-order statistics," IEEE Trans. Signal Process., vol. 45, no. 2, pp. 434–444, Feb. 1997, doi: 10.1109/78.554307.

[10] R. Sun, C. Chan, J. H. Hsiao, and A. C. Tang, "Validation of SOBI-DANS method for automatic identification of horizontal and vertical eye movement components from EEG," Psychophysiology, vol. 58, no. 2, p. e13731, Feb. 2021, doi: 10.1111/psyp.13731.

[11] Y. Pan, M. Matilainen, S. Taskinen, and K. Nordhausen, "A review of second-order blind identification methods," WIREs Comput. Stat., vol. 14, no. 4, Jul. 2022, doi: 10.1002/wics.1550.

[12] D. R. De Oliveira, M. A. A. Lima, L. R. M. Silva, D. D. Ferreira, and C. A. Duque, "Second order blind identification algorithm with exact model order estimation for harmonic and interharmonic decomposition with reduced complexity," Int. J. Electr. Power Energy Syst., vol. 125, p. 106415, Feb. 2021, doi: 10.1016/j.ijepes.2020.106415.

[13] Subana Shanmuganathan and Sandhya Samarasinghe, Artificial Neural Network Modelling, vol. Volume

628. in Studies in Computational Intelligence", no. http://www.springer.com/series/7092, vol. Volume 628. SpringerNature. [Online]. Available: DOI 10.1007/978-3-319-28495-8

[14] M. A. M. Sadeeq and A. M. Abdulazeez, "Neural Networks Architectures Design, and Applications: A Review," in 2020 International Conference on Advanced Science and Engineering (ICOASE), Duhok, Iraq: IEEE, Dec. 2020, pp. 199–204. doi: 10.1109/ICOASE51841.2020.9436582.

[15] Anjali P. Wadekar and Anjali U. Jawadekar, "Fault Detection Of Induction Motor Through The Analysis Of Stator Current Data," Int.J.Ind.Electron.Electr.Eng.,no.8,[Online]. Available:$http$: $//pep.ijieee.org.in/journal_pdf/11-392-151703322731-35.pdf$

3.3.1 - Number of research papers per teachers in the Journals notified on UGC website during the year 2023-24.

Sr. No	Title of paper	Name of the author/s	Department of the teacher	Name of journal	Year of publication	ISSN number	Link to the recognition in UGC enlistment of the Journal	UGC Care
1	Analyzing Polar Decoding Approaches: A Comparative Study	S. P. Badar and K. Khanchandani,	Electronics and Tel comm	Journal of VLSI Design and Signal Processing	2023	2581-8449	https://drive.google.com/file/d/14Ijj M1_bCB_a6p7_fs h2v7XGx7tGX7IL/v iew?usp=drive_lin k	https://www.scopus.com/sourceid/13660
2	Statistical Analysis of Retinal Image Processing Techniques from an Empirical Perspective	Rupesh Mundhada, Dr D.D. Nawgaje	Electronics and Tel comm	The Indian Journal of Technical Education	2022	2214-7853	https://drive.google.com/file/d/1UZI eOypXJ3N3GEsPaC dcO20I6kfL3iVN/vi ew?usp=drive_link	https://www.scopus.com/sourceid/21100370 037
3	U-Net-based gannet sine cosine algorithm enabled lesion segmentation and deep CNN for diabetic retinopathy classification	Rupesh Mundhada, Dr D.D. Nawgaje	Electronics and Tel comm	Computer Methods in Biomechanics and Biomedical Engineering: Imaging & Visualization	2023	1432-1858	https://drive.google.com/file/d/1fDq SD2yuILsDZQNTXd Q- kyKtTqiIkZ7I/view? usp=drive_link	https://www.scopus.com/sourceid/21100773 821

1/3

Shri Gajanan ShikshanSanstha's

SHRI SANT GAJANAN MAHARAJ COLLEGE OF ENGINEERING
SHEGAON – 444203, DIST. BULDANA (MAHARASHTRA STATE), INDIA
"Recognized by A.I.C.T.E., New Delhi" Affiliated to Sant Gadge Baba Amravati University, Amravati
"Approved by the D.T.E., M.S. Mumbai"

4	A survey on Motion Artifact Correction in Magnetic Resonance Imaging for Improved Diagnostics	Manish N. Tibdewal	Electronics and Tel comm	SN Computer Science	2024	2661-8907	https://link.springer.com/article/10.1007/s42979-023-02596-1#citeas	https://link.springer.com/journal/42979
5	Performance Analysis of Un-doped and Doped Titania (TiO2) as an Electron Transport Layer (ETL) for Perovskite Solar Cells	Neerja Dharmale,	Electronics and Tel comm	Journal of Molecular Modeling (2024)	2024	2446-4740	https://rdcu.be/dGsUW	https://www.scopus.com/sourceid/21100823383
6	Evaluating the Effect of Metal, Nonmetal, and Co-doping on Brookite TiO2	Neerja Dharmale.rupesh Mahamune, Modugu Krishnaiah ,Jayant Kumar Kar	Electronics and Tel comm	Nano, World Scientific	2023	1793-2920	https://doi.org/10.1142/S1793292024500425	https://www.scopus.com/sourceid/25627

Shri Gajanan ShikshanSanstha's

SHRI SANT GAJANAN MAHARAJ COLLEGE OF ENGINEERING
SHEGAON – 444203, DIST. BULDANA (MAHARASHTRA STATE), INDIA
"Recognized by A.I.C.T.E., New Delhi" Affiliated to Sant Gadge Baba Amravati University, Amravati
"Approved by the D.T.E., M.S. Mumbai"

Ph : +918669638081/82

Fax : 091-7265-252346

Email: principal@ssgmce.ac.in, registrar@ssgmce.ac.in

Website- www.ssgmce.ac.in

7	A powerful method for interactive content-based image retrieval by variable compressed convolutional info neural networks	Vishwanath S. Mahalle, Narendra M. Kandoi, Santosh B. Patil	Electronics and Tel comm	The Visual Computer	2023	0178-2789	https://link.springer.com/article/10.1007/s00371-023-03104-5	https://link.springer.com/journal/371
8	Denoising of motion artifacted MRI scans using conditional generative adversarial network	Vijay Tripathi, Manish N.Tibdewal	Electronics and Tel comm	Multimedia Tools and Applications	2023	1573-7721	https://link.springer.com/article/10.1007/s11042-023-15705-2	https://link.springer.com/journal/11042
9	A survey on Motion Artifact Correction in Magnetic Resonance Imaging for Improved Diagnostics	Vijay Tripathi, Manish N.Tibdewal	Electronics and Tel comm	SN Computer Science	2024	2661-8907	https://link.springer.com/article/10.1007/s42979-023-02596-1	https://link.springer.com/journal/42979

Mr.T.P.Marode

Prepared By

Dr.M.N.Tibdewal

HoD EXTC

3/3

Analyzing Polar Decoding Approaches: A Comparative Study

Swapnil P. Badar[1*], Kamalesh Khanchandani[2]

[1]Research Scholar, [2]Professor , Department of Electronics and Telecommunication Engineering, Shri Sant Gajanan Maharaj College of Engineering, Shegaon, India

[*]Corresponding Author: spbadar@ssgmce.ac.in

ABSTRACT

In this paper, we present three methodologies for implementing polar decoders, which are error-correcting codes widely, used in modern communication systems while polar codes show great promise, their implementation can be challenging due to their high computational complexity, which can negatively impact latency and throughput. To address this challenge, we propose three efficient implementations of polar decoders, including processing element-based design, component code-based design, and a special node-based design that identifies specific bit patterns to reduce decoding complexity. We evaluate our proposed decoders by implementing and simulating them using Verilog HDL on the Xilinx platform and compare their performance against existing research papers. Our results demonstrate significant improvements in terms of latency, area throughput, and power dissipation, making them highly suitable for modern communication systems. The special node-based decoder demonstrated the best performance, accomplishing a latency of 32.532ns and a throughput of 245.91 Mbps, using 393 LUTs and an on-chip power dissipation of 3.921 watts. The processing element-based decoder achieved a latency of 40.41 ns and a throughput of 197.79 Mbps, using 445 LUTs and an on-chip power dissipation of 4.142 watts. The component code-based decoder achieved a latency of 33.29 ns and a throughput of 240.27 Mbps, using 470 LUTs and an on-chip power dissipation of 4.933 watts.

Keywords- Channel coding, Error-correcting codes, 5G, Polar code, Successive cancellation decoder, Wireless communication

INTRODUCTION

Effective communication is a vital aspect of modern-day life, and error-correcting codes (ECC) are critical in ensuring the accurate transmission and receipt of information. To design an ECC for a noiseless communication system, proper encoder and decoder design are essential. Turbo codes [1] and LDPC codes [2-4] have been successful in achieving channel capacity for practical purposes, but the polar code has been proven to achieve maximum channel capacity [5]. Polar codes have low-complexity algorithms, making their encoder and decoder design easy. These codes find their application in a range of wireless communication technologies, including HSPA, LTE, WiMAX, Wi-Fi, and many others.

At the 2016 3GPP Meeting, assessments were carried out to appraise LDPC and Polar codes for potential deployment in data and control channels [6]. However, after evaluating various factors such as decoding latency, throughput, and error correction capability, in 5G NR, LDPC codes were picked for data channels due to their superior decoding latency and throughput with larger block lengths. Notably, LDPC codes offer support for multiple code rates, contributing to their suitability for data channel applications in 5G NR. On the other hand, for control channels, Polar codes were chosen. Polar codes excel in error correction for short block lengths, which makes them well-suited for control channels with smaller block lengths. However, in the most recent LTE standard, Polar codes have been substituted with tail-biting convolution codes (TBCC) for control channels [7].

Polar codes are designed based on channel polarization, which is a process of separating a channel into N virtual channels, each with its reliability. The Bhattacharyya parameter is a metric utilized for quantifying the reliability

of a communication channel. It is computed as the square root of the product of the channel's transition probabilities for two distinct input symbols. The Bhattacharyya parameter ranges from 0 to 1, where a smaller value indicates a more reliable channel. In polar coding, the reliability of channels is measured using the Bhattacharyya parameter. Channels with lower Bhattacharyya parameters are typically good channels, signifying better quality. In polar coding, these good channels are allocated for transmitting information bits, while the bad channels those with higher Bhattacharyya parameters are designated for transmitting parity-check bits.

This paper aims to enhance the efficiency of polar decoders by utilizing special nodes for faster decoding. Polar codes have been shown to have superior error-correcting capabilities compared to other coding schemes, but their decoding complexity can be a significant bottleneck in practical implementations. This issue is resolved by identifying special nodes within the decoding binary tree. Through implementation in a hardware-based design using Verilog HDL and synthesis on the Xilinx platform, the proposed decoder achieves faster decoding times along with upgraded error-correction capabilities.

POLAR CODE

Arikan introduced the polar code in 2009 as an error-correcting code rooted in channel polarization. The concept involves converting a noisy channel into multiple sub-channels of different reliability levels. This transformation enables polar codes to attain channel capacity while maintaining low complexity in both encoding and decoding processes, making them highly practical for various applications.

A polar code, denoted as P (N, K), is characterized by N, representing the input vector's length, and K, signifying the number of message bits to be securely transmitted. The remaining (N-K) bits, named frozen bits, are predetermined with values (often 0) to facilitate channel polarization. This polarization process transforms the N-bit input vector into N channel symbols, distinguishing between reliable (corresponding to the K message bits) and unreliable (corresponding to the frozen bits) channel symbols. The positions of these frozen bits are predetermined and known to both the

encoder and decoder, enabling the decoder to leverage channel polarization for highly reliable message bit decoding. Notably, polar codes achieve channel capacity while maintaining low encoding and decoding complexity, thus proving suitable for practical applications

The construction of the polar code involves applying a recursive transform, also known as the Kronecker product, to a binary kernel matrix. This process generates a generator matrix that is used to encode the input message bits. The generator matrix G_N is a $N \times N$ binary matrix that is constructed from the n-th Kronecker product of a 2x2 binary matrix. The generator matrix G_N is defined by equation (1). The matrix multiplication of the input bits u ($u_1, u_2, \ldots, u_N$) with G_N produces the output coded bits, X ($x_1, x_2, \ldots, x_N$). , which are the codeword of the polar code as in equation (2).

$$G_N = G_{2^n} = 0 \begin{matrix} 1 & 0 \\ 1 & 1 \end{matrix}^n =$$
$$G_2 \quad G_{2(2)} \quad \ldots \quad G_{2(n-1)} \tag{1}$$
$$X = uG_N \tag{2}$$

The binary tree representation of polar codes provides a helpful visualization of the encoding process and enables a better understanding of the hierarchical structure of the code. The construction of the binary tree using component codes is a recursive process that allows us to construct larger codes from smaller ones. The encoder circuit graph based on the binary tree is a compact representation of the encoder hardware and can be used for efficient implementation of the code.

The polar encoder uses a recursive binary tree structure to generate the codewords. The tree for $N = 8$ shown in Fig. 1 is constructed using two basic building blocks: the $N = 2$ component code and the $N = 4$ component code. The polar codeword binary tree for $N = 8$ has four stages, denoted by $t = 1,2,3,4$. At each stage t, the input bits are combined using the codeword equation (3). At stage three ($t = 3$), the input bits are represented by the vector $u = (u_1, u_2, u_3, u_4, u_5, u_6, u_7, u_8)$ At stage two ($t = 2$), the codeword for $N = 2$ is generated using a modulo 2 operation. This generates a 4-bit codeword at stage one ($t = 1$). Finally, at $t = 0$, the 8-bit codeword is generated by combining two 4-bit codewords.

In general, for higher values of N, we

can construct the polar codeword binary tree using subsequent component codes. At each stage of the binary tree, the input bits are combined according to a specific codeword equation. The output of each stage is used as the input to the next stage until the final codeword is generated. The encoder graph circuit is constructed according to the binary tree structure and is used to implement the encoding process in

hardware. The encoder circuit graph of an N=8 polar code is depicted in Fig. 2.

When dealing with larger block lengths, polar codes can still be efficiently implemented in hardware by using higher-order component codes in the construction of the binary tree and encoder graph circuit. The recursive nature of the binary tree and encoder graph construction is what makes polar codes hardware-friendly.
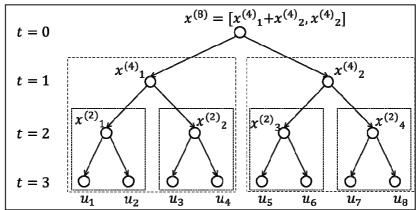
Figure 1: 8-bit polar code binary tree with 2-bit and 4-bit component codes.
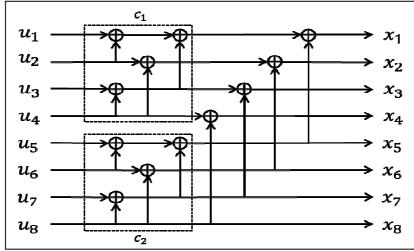
Figure 2: 8-bit polar code circuit graph with 2-bit and 4-bit component code.

POLAR CODE DECODING

The polar decoder holds significant importance in modern communication systems, particularly in 5G networks, where it plays a vital role in error correction for reliable data transmission. Parameters like latency and throughput significantly impact the system's efficiency. Researchers have introduced several decoding algorithms, like the successive cancellation (SC) algorithm [8], SC-list (SCL) algorithm [9], and SC-flip (SCF) algorithm [10,

11], aiming to address challenges related to low latency, power consumption, area efficiency, and achieving high throughput.

The SC algorithm stands as the foundational decoding method applied in polar decoding. It exploits the channel polarization phenomenon to cancel unreliable information bits and is simple and efficient. However, it has limitations in terms of decoding performance. To address this challenge, researchers have introduced extensions to the SC algorithm, namely the SCL and SCF algorithms. The SCL

algorithm implements a list decoding approach, while the SCF algorithm alters the decision of unreliable bits. The SC decoding algorithm stands as a prevalent method for polar code decoding due to its simplicity and low computational load. Yet, its sequential bit decoding leads to higher latency compared to most other decoding methods, barring SCL.

During the decoding process, the SC decoder evaluates the current node's bit values based on its parent nodes' estimated values. When dealing with a frozen bit, its value is fixed at 0, progressing the decoding. However, in the case of an information bit, its value relies on the log-likelihood ratio (LLR) corresponding to the received bit. The LLR $P_i = (P_1, P_2, P_3, \ldots \ldots P_N)$ is computed using equation (3), incorporating the probabilities $P(y_i|x_i = 0)$ and $(y_i|x_i = 1)$. These probabilities represent the likelihood of receiving a bit y_i given the transmitted bit is 0 or

1, respectively.

$$P_i = \ln \cdot \frac{P(y_i|x_i=0)}{P\left(y_i\,|\,x_i=1\right)}/ \tag{3}$$

The SC decoder operates using a binary tree structure to decode the received codeword iteratively. Soft LLR values are relayed downwards from parent nodes to their two child nodes in the tree. Simultaneously, estimated hard bit values are transmitted upwards from child nodes to their parent node. These hard bit values are derived from the LLR values. This recursive process continues until all leaf nodes, symbolizing every bit of the codeword, are decoded.

The first-bit decoding involves finding the LLR value, which is then used to decode the next bit through its parent node. This process continues until all the bits are decoded.
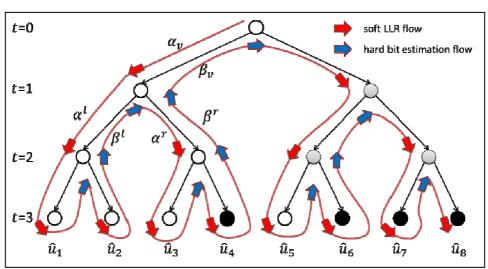
Figure 3: P(8,4) decoding tree with soft LLR and hard bit estimation flow.

In Fig. 3, the binary decoding tree for P(8,4) is depicted, showcasing the flow of soft LLR and hard bit estimates with red and blue arrowheads, respectively. The root node initially obtains soft LLR values from the channel. These LLR values $*\alpha = \alpha_1, \alpha_2, \alpha_3, \ldots, \alpha_{2^{t-1}}, +$ are then passed down from parent nodes to their respective child nodes at each level of the binary tree. Simultaneously, estimated hard bit values $*\beta = \beta_1, \beta_2, \beta_3, \ldots, \beta_{2^{t-1}}, +$ are transmitted upwards from child nodes to their parent node [12]. Specifically, the soft LLR value α_v moves from the root node v to the left child node, while the root node obtains the hard bit estimation β_v from this left child node. During stage 1, the

parent node passes LLR values α^l and α^r to the left and right child nodes, respectively, and receives the corresponding hard bit estimations β^l and β^r from these child nodes.

To begin decoding, the LLR value determines the estimation of the first bit, $\hat{u}$, located at the leftmost leaf node. Using this obtained $\hat{u}$ bit, the decoding process advances to determine the second leftmost leaf node bit, $\hat{u}$, through its parent node at stage 2. Subsequently, both $\hat{u}$ and $\hat{u}$ bits are used to decode $\hat{u}$ and $\hat{u}$ via their parent node at stage 1. This sequential process continues iteratively until all the bits of the rightmost leaf node are successfully decoded

OPTIMIZING THE SC POLAR DECODER: METHODOLOGIES

To optimize the performance of the SC polar decoder, various techniques have been employed, such as the use of processing elements, component codes, and special node identification in the decoding tree structure. Processing elements enable efficient computation in the decoder circuit, while component codes improve the error-correction performance. Identifying special nodes in the decoding tree structure allows for the use of specialized decoding techniques that can enhance the accuracy and efficiency of the decoding process. By using these techniques in combination, significant improvements can be achieved in the performance of the SC polar decoder.

Polar Decoder Circuit Using Processing Elements

The purpose of the polar decoder circuit is to retrieve information from the encoded message. The decoder circuit illustrated in Fig. 4 resembles the encoder circuit, comprising XOR circuits that adjust according to available log-likelihood ratio (LLR) values and hard bits. The LLR values ($y_1, y_2, y_3, y_4, y_5, y_6, y_7, y_8$) are placed on the right-hand side of the circuit, while the estimated hard bits ($\hat{u}_1, \hat{u}_2, \hat{u}_3, \hat{u}_4, \hat{u}_5, \hat{u}_6, \hat{u}_7, \hat{u}_8$) reside on the left-hand side. These XOR circuits are pivotal in generating the intermediary bits. The decoding process primarily engages three core processing elements: the f-function node, the g-function node, and the partial sum component [13].
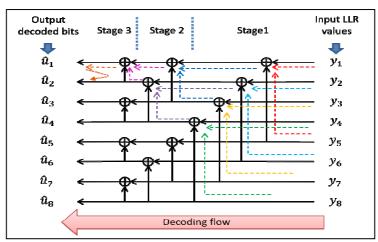
Figure 4: 8-bit SC decoder circuit graph with log-likelihood ratio and estimated hard bits.

The f -function node shown in Fig. 5(a), implements the min-sum approximation of equation (5) using an XOR circuit, which generates an LLR value α_c from input LLR values α_a and α_b.

$$\alpha_c = f(\alpha_a, \alpha_b)$$
$$\alpha_c = 2 \tan^{-1}(\tanh(\alpha_a/2) \tanh(\alpha_b/2)) \qquad (4)$$
or
$$\alpha_c \approx sign(\alpha_a)sign(\alpha_b) \min(|\alpha_a|, |\alpha_b|) \qquad (5)$$

The estimation of hard bits is derived from the sign of the related LLR values. As per Equation (6), if the LLR value is positive, the estimated hard bit is 0; conversely, if it's negative, the estimated hard bit becomes 1.

$$\hat{\beta}_a = \begin{cases} 1 & LLR\ value\ a_c \leq 0 \\ 0 & LLR\ value\ a_c > 0 \end{cases} \qquad (6)$$

The g-function node shown in Fig. 5(b), uses equation (7) to compute the LLR α_d of the subsequent bit $\hat{\beta}$ using the LLR values α_a and α_b and the hard estimation bit $\hat{\beta}$.

$$\alpha_d = g(\alpha_a, \alpha_b, \hat{\beta}) = (-1)^{\hat{\beta}}\alpha_a + \alpha_b \qquad (7)$$

The circuit depicted in Figure 5(c) is the partial sum circuit that produces intermediate bits $\hat{\beta}$ and $\hat{\beta}$ through equations (8) and (9), respectively. These intermediate bits are then utilized for decoding the remaining bits of the codeword.

$$\hat{\beta} = XOR\ (\hat{\beta}, \hat{\beta}) \qquad (8)$$
$$\hat{\beta} = \hat{\beta} \qquad (9)$$
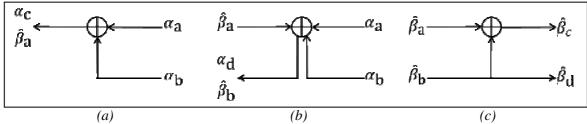
Figure 5: Decoding processing elements (a) f-function node (b) g-function node and (c) partial sum (xor node).

The SC decoding process initiates by transmitting LLRs through the f-function, progressing from the right-hand side to the upper connection on the left-hand side of the circuit illustrated in Fig. 4. The decoding of the first bit occurs using the LLR value derived from the min-sum approximation of the f-function. Following this, the decoding of the subsequent upper bit involves the application of equation (7) g-function, and the LLR propagation switches before the f-function resumes to propagate LLRs for the subsequent connection on the left-hand side. This sequence continues until all bits are decoded. Each bit's decoding depends on the preceding bit values, and the entire decoding process unfolds over 2N-2 steps. To facilitate this process, storage memory for hard estimated bits, channel LLR memory, and internal memory play crucial roles.

Polar Decoder Circuit Using Component Codes

Complex polar decoder designs often use a hierarchical design style to break down the overall system into smaller components for simpler design, testing, and integration. The 8-bit SC polar decoder illustrated in Fig. 6 follows this approach, employing component codes of N=4 and N=2 hierarchically to construct the final decoder circuit.

The decoding process in the N=2 component code, depicted in Fig. 7, utilizes essential processing elements like the f-function, g-function, and partial sum block to interpret the received signal. In this operation, the f-function node computes the first hard bit by comparing the input log-likelihood ratio (LLR) against a specified threshold value, while the g-function node generates the second decoded bit by integrating the first hard bit with the input LLR values. The partial sum block then recursively decodes subsequent bits until all bits are decoded. This N=2 component code serves as a foundational unit for larger polar codes. To make a 4-bit decoder, the 2-bit decoder circuit is replicated twice and supplemented with additional processing elements. This 4-bit decoder subsequently becomes a component code in designing the 8-bit decoder through a hierarchical design approach, comprising two 4-bit decoders and additional processing elements to finalize the circuit.
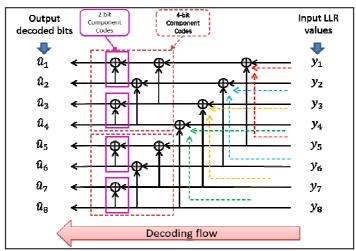
Figure 6: Circuit graph of 8-bit SC polar decoder using 4-bit and 2-bit component codes.
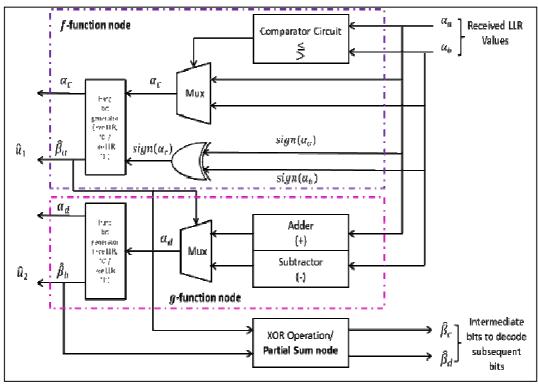
Figure 7: Block diagram of 2-bit polar decoder architecture.

Polar Code Decoding using Special Nodes

Sequential decoding within SC decoders can result in high latency, posing challenges for specific applications. To contest this, researchers have identified and leveraged special nodes, detailed in [12], to design a faster polar decoder with reduced latency. Traditionally, decoding the initial bit in the SC decoder's binary tree involves traversing from the root node down to the leaf node. However, the introduction of special nodes eliminates the necessity for deep tree traversal. These special nodes, grouped into four types based on their bit Rate-zero, Rate-one,

Repetition (Rep), and Single Parity Check (SPC) nodes – have markedly enhanced the speed of polar decoding. This innovative approach has gained grip as a preferred method for implementing SC decoders.

- *Rate-Zero Node:* Within the Rate-zero node, all bits exclusively consist of frozen bits, denoted as s={0,0,0,...,0,0}. The bit estimation for this node is established as:

$$\hat{\beta}_i = 0$$

- *Rate-One Node:* The Rate-one node exclusively comprises information bits, indicated by $s = \{1,1,1,\ldots\ldots,1,1\}$. The

estimation of bits within this node relies on the respective LLR values:

$$\hat{\beta}_i = \begin{cases} 0 & \text{if } \alpha_i^t > 0, \\ 1 & otherwise \end{cases}$$

- *Rep Node:* For Rep nodes, where all bits except the last one are frozen bits, and the last bit is an information bit, the configuration is denoted as s = {0, 0, 0, ..., 0, 1}. The algorithm for estimating bits within Rep nodes involves summing all input LLR values ($\sum_i^{2^{t}} \alpha_i$. The threshold value is determined through sign detection. The estimation of hard bits within Rep nodes follows:

$$\hat{\beta}_i = \begin{cases} 0 & \text{if } \sum_i^{2^{t-1}} \alpha_i > 0, \\ 1 & otherwise \end{cases}$$

- *SPC Node:* For SPC nodes, where all bits except the first one are information bits, with the configuration represented as s = {0, 1, 1, ..., 1, 1}, the bit estimation within SPC nodes is direct. It involves estimating the first bit as 0 and estimating the subsequent bits based on the received LLR values.
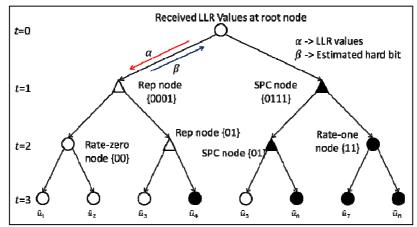
Figure 8: Binary tree of polar decoder with special node identification.

The decoding binary tree for P(8, 4) employing a 3-stage 8-bit decoder is illustrated in Fig. 8. In the final stage (stage 3), all leaf nodes exhibit either a single frozen bit or a single information bit, denoting them as either Rate-zero or Rate-one nodes. However, in stages 1 and 2, these nodes comprise a mix of frozen bits and information bits, allowing them to potentially represent any of the special nodes. The identification of these special nodes is based on their distinct bit patterns. Rate-zero nodes are represented by white circles, Rate-one nodes by black circles, Single Parity Check (SPC) nodes by black triangles, and Repetition (Rep) nodes by white triangles [12].

Node Generator Circuit

The Node Generator circuit holds significance in polar decoding by creating special nodes like Rate-zero, Rate-one, Rep, and SPC nodes. These specialized nodes are crucial in the decoding process and are generated based on the LLR values received at different stages of the decoding tree. This circuit operates by comparing the LLR values against a zero threshold to generate binary set values denoted as s_i. When encountering a positive LLR, s is set to 1, while for a negative LLR, it is set to 0.

At the initial stage of the 8-bit decoder, a set of 8 LLR values $(\alpha_1, \alpha_2, \alpha_3, \alpha_4, \alpha_5, \alpha_6, \alpha_7, \alpha_8,)$ are triggers for the generation of corresponding binary values, represented as s_i ($s_1, s_2, s_3, s_4, s_5, s_6, s_7, s_8$) in Fig. 9. These binaries are used to determine if the node assumes the characteristics of a Rate-zero, Rate-one, Rep, or SPC node. However, as the decoder's node length increases, the special node generator circuit's hardware complexity also increases, potentially elevating costs and power consumption. Hence, it is crucial to investigate approaches that simplify circuit complexity without compromising robust error correction capabilities.
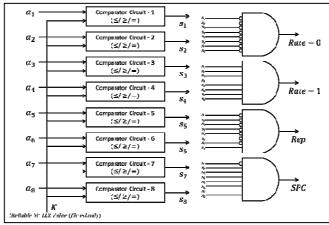
Figure 9: Special node generator circuit.

One approach is to analyze the special nodes and identify patterns that can simplify the circuit design. As mentioned, Rate-zero and Rep are almost the same, differing by only one last bit (information bit in case of Rep node), while Rate-one and SPC differ by first bit (zero bit values in case of SPC node). These patterns can be used to reduce the number of distinct special nodes needed to be generated, thereby reducing hardware complexity. The generalized special node generator algorithm concerning stage of the binary tree is as:

Special Nodes Generator Algorithm

$N = 2^n$
$t = log_2 N$ // No. of stages of binary tree
for (i = 0; i < t; i + +)
$N = N/2$
$Rate_{zero} Node \longrightarrow not(s, \alpha_N\text{-})$
$Rep\ Node \longrightarrow and\ ((s, \alpha_N\text{-}), not(s, \alpha_{N-1}\text{-})$
$Rate_{one} Node \longrightarrow (s, \alpha_1\text{-})$
$SPC\ Node \longrightarrow and\ ((s, \alpha_2\text{-}), not(s, \alpha_1\text{-})$
end

The decoding algorithm that utilizes special nodes is a variant of the conventional polar decoder algorithm, which follows the binary tree depicted in Fig. 8. At each decoding stage, the received LLR values are used to generate the binary set values (s_i) and the special nodes (Rate-zero, Rate-one, Rep, and SPC) are then determined based on the combination of these binary values. The SC decoding algorithm is as:

Decoding Algorithm

$N = 2^n$
$t = log_2 N$ // No. of stages of binary tree
i = 0
$while (i < t)$
$N = N/2$
$if\ (Rate_{zero} Node\ )$

$\hat{u} \longrightarrow N\ bits\ are\ zero$
$else\ if\ (Rep\ Node)$
$\hat{u}1:N\text{-} \longrightarrow 1\text{-}\ N - 1\ bits\ are\ zero$
$\hat{u}N\text{-}\ sc\ decode\ bit$ // last bit
$else\ if\ (SPC\ Node)$
$\hat{u}1\text{-}\ zero$
$\hat{u}1:N\text{-}\ sc\ decode\ bits$ /
/ excluding first)
$else$
$\hat{u} \longrightarrow sc\ decode\ bits$
end

SYNTHESIS RESULTS AND PERFORMANCE COMPARISON

Three methodologies for implementing polar decoders were proposed in this paper, including polar decoder design using processing elements, polar decoder design using component code, and polar decoder by special node. These methodologies are evaluated using synthesis and simulation in Verilog HDL on the Xilinx platform. The results show that all three methodologies outperform existing research papers in Table 1. Specifically, the special node implementation achieved the best performance with a latency of 32.532ns and a throughput of 245.91 Mbps, using 393 LUTs and an on-chip power dissipation of 3.921 watts. The processing elements implementation achieved a latency of 40.41 ns and a throughput of 197.79 Mbps, using 445 LUTs and an on-chip power dissipation of 4.142 watts. The component code implementation achieved a latency of 33.29 ns and a throughput of 240.27 Mbps, using 470 LUTs and an on-chip power dissipation of 4.933 watts. The proposed work shows significant improvements in terms of latency, area throughput, and power consumption compared to other research papers, and may be extended to higher bits polar decoder.

Table 1: Comparison of polar decoder performance parameters.

| Parameter | Proposed Polar Decoder | | | [14] | [15] | [16] | | [17] | [18] | [19] |
	By Processing Elements	By Component Code	By Identifying Special Nodes	1024-bit SC decoder-CMOS implementation	Fast SSCF 1024-bit	Merge PE 16-bits	Merge PE 32-bits	Multi-kernel Fast SSC 1024-bits	UF-SSC 1024 bits	Fast SSC 1024 bits
Area (LUTs)	445	456	393	183637 Gate Count (1.71 mm^2)	3645	625	1682	23,126	18,982	23.353

								1.18 us (102 n)	1.30 us (123 n)	1.98 us (204 n)
Latency	40.41 ns	33.25 ns	32.53 ns	--	--	--	--			
Throughput (Mbps)	197.79	240.27	245.91	49	140.6	626	565	432	393	259
On-chip Power (W)	4.142	4.933	3.921	0.067	--	--	--	--	--	--

*n- no. of cycle

CONCLUSION

This paper explores comprehensive research on polar decoders, presenting three innovative design methodologies: processing element-based, component code-based, and special node-based approaches. It demonstrates the superior performance of component codes over direct processing elements in polar decoder construction. By using Verilog HDL, 2-bit and 4-bit polar decoder component codes are designed, extending them to construct N=8 decoders, showcasing remarkable simulation and synthesis outcomes on the Xilinx platform.

Moreover, it introduces a fast 8-bit polar decoder by identifying and generating special nodes through a node generator circuit. These nodes, including Rate-zero, Rate-one, Rep, and SPC nodes, significantly enhance decoding efficiency based on specific bit patterns identified from LLR values in the binary tree. Implementation on the Xilinx platform discloses the fast polar decoder's superiority over existing approaches, showcasing considerable advancements in performance metrics. Notably, the special node-based decoder exhibits exceptional performance, achieving a latency of 32.532ns and a throughput of 245.91 Mbps, utilizing 393 LUTs, and featuring an on-chip power dissipation of 3.921 watts. In contrast, the processing element-based decoder achieved a latency of 40.41 ns and a throughput of 197.79 Mbps, using 445 LUTs and an on-chip power dissipation of 4.142 watts. The component code-based decoder achieved a latency of 33.29 ns and a throughput of 240.27 Mbps, using 470 LUTs and an on-chip power dissipation of 4.933 watts. The proposed methodologies and advancements in polar decoding showcased in this study present promising contributions to the development of efficient and high-performance polar decoders across diverse communication systems.

REFERENCES

1. C. Berrou, A. Glavieux and P. Thitimajshima (1993). Near Shannon limit error-correcting coding and decoding: Turbo-codes. 1. *Proceedings of ICC '93 - IEEE International Conference on Communications*. IEEE, Available at: https://doi.org/10.1109/ICC.1993.397441

2. S J. Johnson (2012), 2 - Low-density parity-check codes. *Cambridge University Press*, Cambridge, England. Available at: https://doi.org/10.1017/CBO978051180935 4.003

3. D.J.C. MacKay and R.M. Neal (1997). Near Shannon limit performance of low density parity check codes, *IET Digital Library*, 33(6), 457-458, Available at: https://doi.org/10.1049/el:19970362

4. S Shao, P Hailes, T-Yi Wang, et al (2019). Survey of turbo, LDPC, and polar decoder ASIC implementations, *IEEE Communications Surveys & Tutorials*, 21(3), 2309 – 2333, Availableat: https://doi.org/10.1109/COMST.2019.2893 851

5. E Arikan (2008). Channel polarization: A method for constructing capacity-achieving codes. *2008 IEEE International Symposium on Information Theory*. IEEE, Available at: https://doi.org/10.1109/ISIT.2008.4595172

6. 3GPP, "3GPP meetings for group R1", [Online] Available at: https://www.3gpp.org/dynareport?code=Me etings-R1.htm

7. 3GPP, "3GPP TDocs (written contributions) at meeting Meeting: R1-87 - 2016-11-14 to 2016-11-19, Reno, Nevada", [Online] Available at: https://www.3gpp.org/dynareport?code=TD ocExMtg--R1-87--31665.htm

8. I Tal and A Vardy (2013). How to construct polar codes, *IEEE Transactions on Information Theory*, 59(10), 6562-6582,

Available at: https://doi.org/10.1109/TIT.2013.2272694

9. I Tal and A Vardy (2015). List decoding of polar codes, *IEEE Transactions on Information Theory*, 61(5), 2213-2226, Available at: https://doi.org/10.1109/TIT.2015.2410251

10. X Wang, Q Ma, J Li, et al (2020). An improved SC flip decoding algorithm of polar codes based on genetic algorithm, *IEEE Access*, 8, 222572-222583, Available at: https://doi.org/10.1109/ACCESS.2020.3041290

11. L. Chandesris, V. Savin and D. Declercq (2016). An improved SC Flip decoder for polar codes. *2016 IEEE Global Communications Conference (GLOBECOM)*. IEEE, Available at: https://doi.org/10.1109/GLOCOM.2016.7841594

12. S Ali Hashemi, C Condo, M Mondelli and W J. Gross (2019). Rate-flexible fast polar decoders, *IEEE Transactions on Signal Processing*, 67(22), 5689-5701, Available at: https://doi.org/10.1109/TSP.2019.2944738

13. S P. Badar and K Khanchandani (2021). Implementation of combinational logic for polar decoder. *2021 2nd International Conference on Range Technology (ICORT)*. IEEE, Available at: https://doi.org/10.1109/ICORT52730.2021.9581844

14. A. Mishra, A. J. Raymond, L. G. Amaru, et al (2012). A successive cancellation decoder ASIC for a 1024-bit polar code in 180nm CMOS. *2012 IEEE Asian Solid State Circuits Conference (A-SSCC)*. IEEE, Available at: https://doi.org/10.1109/IPEC.2012.6522661

15. J Zeng, Y Zhou, J Lin and Z Wang (2019). Hardware implementation of improved fast-SSC-flip decoder for polar codes. *2019 IEEE Computer Society Annual Symposium on VLSI (ISVLSI)*. IEEE, Available at: https://doi.org/10.1109/ISVLSI.2019.00109

16. F.G. Krasser, M.C. Liberatori, L. Coppolillo, et al (2019). Merged processing element for polar code decoder. *2019 XVIII Workshop on Information Processing and Control (RPIC)*. IEEE, Available at: https://doi.org/10.1109/RPIC.2019.8882149

17. H Rezaei, N Rajatheva and M Latva-Aho (2022). Low-latency multi-kernel polar decoders, *IEEE Access*, 10, 119460-119474, Available at: https://doi.org/10.1109/ACCESS.2022.3221742

18. H Rezaei, V Ranasinghe, N Rajatheva, et al (2022). Implementation of ultra-fast polar decoders. *2022 IEEE International Conference on Communications Workshops (ICC Workshops)*. IEEE, Available at: https://doi.org/10.1109/ICCWorkshops53468.2022.9814456

19. P Giard, A Balatsoukas-Stimming, G Sarkis, et al (2018). Fast low-complexity decoders for low-rate polar codes, *Journal of Signal Processing Systems*, 90, 675-685, Available at: https://doi.org/10.1007/s11265-016-1173-y

CITE THIS ARTICLE

Swapnil P. Badar and Kamalesh Khanchandani (2023). Analyzing Polar Decoding Approaches: A Comparative Study, *Journal of VLSI Design and Signal Processing,* 9(3), 37-47.

Statistical Analysis of Retinal Image Processing Techniques from an Empirical Perspective

Rupesh Mundada
Department of Electronics and Telecomm. Engg.
Sant Gajanan Maharaj College of Engineering
Shegaon

Devesh Nawgaje
Department of Electronics and Telecomm. Engg.
Sant Gajanan Maharaj College of Engineering
Shegaon

ABSTRACT

DME is the main reason for loss of vision in diabetics and a major cause of diabetic retinopathy (DR). Excessive flow and deposition of the extracellular fluid inside the macular region are the main reasons for diabetes mellitus. Therefore, it has become a danger to people's health and lives. This article reviews DR, its features, causes, machine learning models, cutting-edge DL models, challenges, benchmarks, and future directions for research. Using fundus images and OCT scans, DME can be diagnosed at any level of DR. An autonomous detection method with computer vision can provide ophthalmologists with a detailed analysis of abnormalities, which is beneficial to them for diagnosis. This is why the introduction of deep learning (DL), the new field of machine learning, With efficient data processing, the DL model can handle small data sets. However, they often include larger datasets for their deep models to improve image extraction and classification performance.

KEYWORDS: *Diabetic retinopathy, Fundus images, OCT images, Deep learning.*

INTRODUCTION

India is going to be the "Diabetes Capital of the World" by counting the number of diabetic patients . According to the IDF, the population of diabetic patients was 53.7 crore in 2021 and is expected to reach 78.3 crore by 2045. The World Health Organization (WHO) revealed in its World Vision Report that more than 220 million people suffer from vision loss or impairment, with half of them being cured by proper treatment. As shown in Fig. 1, 3.9 million of these one billion people had vision-threatening DR. Prolonged diabetes, low blood pressure, and poor glycemic control are strongly connected with DR. Globally, DR, proliferative DR (PDR), and DME affect 6.96%, 6.81%, and 10.2% of the population, respectively. DME, therefore, affects 21 million people globally . The most frequent cause of visual loss in DR-affected individuals may be DME [1].

Common signs and symptoms of DR are blurred vision, hovering and blinking, and vision loss. DR is caused by changes in retinal vascular metabolism caused by irregular blood flow, leakage of blood and blood components through the retina, and thus damage to the macula. This causes the retinal tissue to swell, making vision cloudy or blurry. The disease affects both eyes and if diabetes is prolonged without treatment, DR leads to blindness and eventually diabetic maculopathy. When left untreated and undiagnosed, diabetic retinopathy (DR) progresses to more severe stages, leading to a decline in a person's vision. The disease can exhibit periodic or random progression, resulting in the formation of retinal lesions caused by ruptured retinal blood vessels (RBVs). These lesions include microaneurysms (MAs), haemorrhages (HEs), exudates (EXs), cotton wool spots (CWSs), the foveal avascular zone (FAZ), fibrotic bands, intraretinal microvascular abnormalities (IRMAs), neovascularization on the disc (NVD), neovascularization elsewhere (NVE), tractional bands, and more. These retinal abnormalities manifest in the fundus, which is the rear view of the eye. Timely detection of these retinal lesions and abnormalities is crucial as it aids in identifying the different stages of DR.
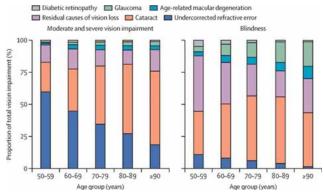
Fig. 1. Comparative analysis of vision impairment versus ocular diseases

To find out the advantages and drawbacks of various DME classification models that have used Deep Learning algorithms that use Color fundus images or OCT images in the diagnosis of DME is the main purpose of this study. It also summarizes the progression of the methods over time and highlights various re-searchable problems which need to be addressed in the context of autonomous DME diagnosis.

Aspects of diabetes mellitus

A chronic medical disorder called diabetes mellitus is brought about by insulin resistance or by altered insulin production in the blood. In people with diabetes, high blood sugar or glucose levels, known as hyperglycemia, can cause long-term difficulties with various body parts like the eye, kidney, neuro system, and cardiovascular diseases[2]. Long-term DME caused diabetic retinopathy and can cause vision loss in people of working age. Microaneurysms (b), haemorrhages (e), hard exudates, soft exudates (c,d,e,f), and neovascularization which are the lesions in the retina that results in blindness are the characteristics of DR which are shown in Fig. 2.
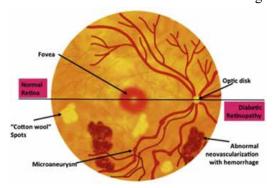
Fig. 2 Characteristics of DR
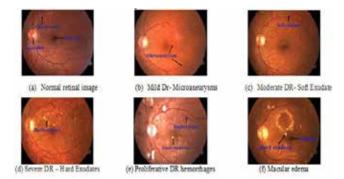
Fig. 3 Retinal Lesions

Various image modalities

Fundus Images

Fundus image has the potential to be a strong tool for the examination of diabetic ocular disorders and determining their progressive stages and how they respond to the treatment in diabetic patients. It is beneficial to evaluate DR because it allows for the visualization of intra-retinal microvascular abnormalities (IRMAs), venous beading, soft and HE lesions, microaneurysms, haemorrhages, and neovascularization [3]. Fig. 3 is obtained using a camera to capture the fundus images, shows DR lesions. The publically available standard data sets are given in the following Table 1.

Table 1: Publically available data sets for fundus images

Data set	Total images	Resolution	Field view of camera (in degree)
EyePACS	88702	NA	--
APTOS	5590	NA	--
MESSIDOR	1200	1440X960 2240X1488 2304X1536	45
MESSIDOR 2	1748	NA	45
IDRiD	516	4288X2848	50
DDR	12522	NA	45
E-Ophtha	463	NA	50
DiaRetDB1	89	1500X1152	50
DRiDB	89	768X584	45
ROC	100	768X576 1058X1061 1389X1383	45

Optical coherence tomography (OCT)

With optical coherence tomography (OCT), eye surgeons can take a cross-sectional view of the retina with the help of light waves in three dimensions. This allows the ophthalmologist to determine the density of various layers of the retina. The publically available standard data sets such as Biomedical Image & Signal Analysis (BIOMISA), Dukes, OPTIMA Cyst segmentation challenge, Noor Eye Hospital (NEH), Mendeley (Ker- many datasets), Dukes2, Retinal OCT Classification Challenge, RETOUCH, OCTID which are used by researchers. Sample OCT scan is as shown in Fig. 4 with marked features.
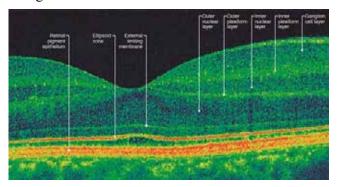
Fig. 4 Sample OCT scan

The research conducted by numerous researchers is discussed in Section 2 of this article. The effectiveness of various algorithms depending on various factors is examined in Section 3. A comparison-based conclusion is drawn in Section 4.

LITERATURE SURVEY

DME detection using fundus images

DME in fundus imaging is defined by the presence of lesions like hard and soft exudates (EX). For quick identification and analysis of the DME, it is essential to consider the location of the macula, fovea, OD, or lesions close to the macula. The many ML-based methods that have been used in these experiments to determine DME from CFP are addressed in this section.

Various Deep learning algorithms are used to detect DR from fundus images. The methods are mainly based on custom convolutional Networks (CNN), Object detection, Ensemble of DL classifiers, Generative adversarial Networks, Transfer-Learning (TL) methods,

Auto Encoder (AE), and CNN models with attention Mechanism.

The authors [4] proposed a novel methodology to identify diabetes-based ocular diseases, which consists of DME, DR, and Glaucoma with the application of FRCNN (Fast Region Based Computational Neural Network) with FKM (Fuzzy K-means Clustering) FKM The technique consists of two phases. The first phase consists of the detection of disease and localization phase. The second phase includes the segmentation of the localized regions using FKM clustering. The proposed network can locate the deep features with an absolute representation of ocular diseases and this results in increased efficiency of segmentation in contrast.

The layers for the CNN model consist of Convolution, poll and completely connected layers. The deep architecture of CNN is what gives it its power because it can automatically retrieve distinctive features at many levels of abstraction. The author proposed a novel method with the DME Net 120 algorithm. It pre-processes the fundus image in two stages. The first stage consists of classification between normal and infected images and the next stage classifies the infected image into various stages of DR. It uses the Hierarchical Ensemble of Custom Convolutional network for the classification [5].

S. Wang et al [6] trained an MGAN (Multi-Channel based Generative Adversarial Network) to classify fundus images into various stages of Diabetic retinopathy. This model extracts a series of sub-fundus images which are related to various features of DR. MGAN is capable of identifying the various features of Fundus images without reducing the size of high-resolution images. It gives the advantage of reducing the dependency on labelled data.

Researchers [7] proposed the DR-GAN (DR- Generative Adversarial Network), to process high-resolution images with configurable grading and lesion details. This facilitates the augmentation of data on a larger scale for DR segmentation and grading applications. The retina generator is conditioned through structural and lesion masks and adaptive grading vectors from the latent grading space enabling adjustable severity

for synthesized grades. Moreover, this includes a multi-scale spatial and channel attention module.

As discussed by the work in [8], it is essential to have the capacity to estimate the topology of the vascular networks in complex networks to have a comprehensive grasp of vascular changes and the many diseases that they might cause. To assist in the diagnosis and treatment of eye diseases, the retinal vascular trees are often mechanically dissected into the accompanying arteries and veins. The need to take into consideration projective ambiguity in addition to slight differences in lighting, contrast, and geometry adds to the complexity of the situation. Researchers have developed a novel method that uses the topology of the vascular network to differentiate between arteries and veins in CF images of the retina. This method is based on the fact that veins are more prominent than arteries. Both the estimation of the topology of the retinal blood vessels and the categorization of the A/V are framed as issues of pairwise clustering, and researchers use dominant set clustering to solve both. A graph may be constructed by first finding nodes, then segmenting pictures, and finally making an image. The "weight" of the edge may be determined by dividing the inverse Euclidean distance between its endpoints by the ratio of the edge's intensity, direction, curvature, diameter, and entropy. This then yields the "weight" of the edge. Aortas and veins that have undergone effective healing have a particular morphology and level of intensity.

DME detection using OCT scans

It is feasible that 3D-to-2D image segmentation in OCTA scans may be accomplished by using an innovative end-to-end architecture that is known as an image projection network (IPN). This design was proposed by medical imaging experts [9]. The creation of a projection learning module (PLM) that chooses and eliminates features concurrently via the use of a unidirectional pooling layer is their key contribution. By merging several PLMs, the proposed network can analyse 3D OCTA data and give 2D segmentation outputs, including the segmentation of retinal vascular structures. The measurement of retinal indicators does not need the use of projection maps or segmentation of the retinal layers. The researchers put their network to the test by requesting that it extract retinal vasculature (RVs) and the foveal avascular zone (FAZ) from photographs of the retina. The use of IPN as a 3D-to-2D segmentation network is successful, as shown by experimental data derived from 316 OCTA volumes. IPN is an advancement of state-of-the-art procedures since it integrates data on many modalities as well as volumetric measurements.

According to research that was presented in [10], scans obtained from retinal optical coherence tomography (OCT) might potentially be used to identify visual problems. The underlying factors that contribute to these visual irregularities include shifts in the orientation of the optical coherence tomography (OCT) B- scan and inconsistencies in the layers of the retina. The accuracy of the OCT image analysis will suffer as a result of these alterations. Researchers have developed a pre-processing method that may be used for B-scan alignment as part of this study. The investigators begin by putting forth a TV-UNet model as a means of precisely locating the retinal pigment epithelium (RPE) layer in each B-scan. Researchers determine a baseline and a curvature curve by making use of the RPE layer that has been revealed. To retain the size and form of the sick lesion, a one-of-a-kind alignment strategy that is window-transferring based is required. This strategy must be used to coerce curve points into constructing a straight line. For both training and testing the TV-UNET, the researchers used a wide variety of datasets.

As shown in [11], optical coherence tomography angiography (OCTA) is a non-invasive imaging technology that may be used to examine retinal capillaries. This method offers resolution on the micron scale. Studies that demonstrate a link between micron-scale parameters and the degree of the retinal disease have pro- vided evidence that confirms the diagnostic utility of macular OCTA vascular measures. These metrics have their foundation in the statistical summaries of the retinal layers and regions of interest in 2D and face projection images. OCTA pictures are used by re- searchers to generate a map of retinal vascular density. This is done so that they may investigate the changes in retinal vasculature that occur across different populations and longitudinal scans. Researchers can get a high-quality three-dimensional representation of OCTA-based vessel networks by

using curvelet-based denoising and optimally guided flux (OOF). After that, a three-dimensional map of the density of the blood vessels in the retina should be created. After that, the vessel mask from an OOF-based analysis is diffused throughout the whole of the picture volume to provide a vessel density image (VDI). To conduct inter-patient comparisons of retinal vasculature, non-linear three-dimensional OCT image registration is used. To demonstrate the efficacy of their methodology, the researchers tracked the progression of two diseased patients who had oedema during their studies. Their method is statistically tested by employing simulated capillary dropout data, along with a normal control population that is broken down into two age groups, and patients who have diabetic retinopathy (DR). Even in the presence of oedema, researchers have the potential to see localized vascular abnormalities as a result of simulated capillary loss, natural ageing, and DR illness. These results provide evidence that the framework has the potential to identify microvascular alterations and monitor the progression of retinal diseases.

Experts in the field of retinal image processing [12] believe that medical image registration could be used to evaluate longitudinal and cross-sectional data, objectively track the progression of a disease, and direct a computer-assisted diagnosis and treatment plan. These are just some of the potential applications of this technique. There has not been a lot of research done on de-formable registration for retinal OCT pictures, which is a method that enables more precise and quantitative comparisons. According to the findings of this study, a 3D retinal OCT registration approach known as OCTR expert (OCT RE) should be used. This method is the first attempt to full 3D registration for retinal OCT photographs, and it may be used to analyse longitudinal OCT data for persons who are healthy as well as those who have diseases. To implement this method, initially, an eye motion artefact reduction technique will need to be carried out, and then a design detection deformation registration procedure will need to be performed. During the process of creating a picture, many properties are affixed to each voxel that makes up the image. The process of "detection" involves picking voxels that are "active" and building "point-to-point" correspondences between them. The picture undergoes a hierarchical transformation as a result of the multi-resolution

deformation process. The recommended method was put to the test utilizing longitudinal OCT images on a total of twenty healthy participants in addition to four patients who had choroidal neovascularization (CNV).

Researchers [13] have developed a bias-free method of automated segmentation that may be used for optical coherence tomography (OCT) images in this study. The intensity, gradient, and adaptive normalized intensity scores of the segmented scans are taken into consideration by deep neural network regression while attempting to predict the retinal border pixel (ANS). Recasting the problem of segmentation as one of regression removes the need for a large dataset and simplifies the work at hand. On OCT scans with intensity changes, low contrast, speckle noise, and blood vessels, the use of ANS enhances the method's accuracy while also increasing its processing speed. During testing with 114 photos, it took 10.596 seconds for each image to identify eight boundaries, but during training, it took 30 seconds per boundary line. The dice comparison found a similarity index of 0.966 between the two sets, suggesting a good level of precision in the results. Researchers were able to attain an average disparity of 0.612 pixels between human and automatic segmentation by adhering to the strategy that was advised.

According to the findings of the study [14], a modality-specific attention network (MSAN) may be used to classify multi-modal retinal images. This network may use diagnostic pictures of both the fundus and the OCT. MSAN is equipped with two different focus modules: one is for fundus images, and the other is for OCT Scans. Ophthalmologists are required to do a local as well as global analysis of the fundus picture (e.g., from microaneurysms at the micrometre level, optic disc at millimetre level to blood vessels through the whole eye). Therefore, the researchers provide a multi-scale attention module that is specially adapted to fundus visuals. Images obtained with OCT that include substantial background patches can-not be utilized for diagnosis. As a result, it has been recommended that an attention module that is led by regions be used for encoding retinal layer information in OCT images. In the end, researchers develop a retinal image categorization network by fusing modality-

specific characteristics into a multi-modal feature. The model takes into account aspects that are unique to each modality so that it may provide a more precise diagnosis. Their MSAN surpasses previous single-modal and multi-modal retinal image classification systems, as shown by experimental results employing a multi-modal retinal image dataset (fundus and OCT) gathered in a clinical context. Researchers [15] have developed a system that is based on ensemble learning (EL) that can segment retinal boundaries in OCT images in a way that is resistant to defects in the retina. The recommended method's accuracy in segmentation was evaluated using two datasets that were available to the general public. These datasets included photos of severe retinal oedema. The suggested strategy was evaluated alongside two other approaches that are more common. The recommended technique was an improvement over the conventional approaches since it was better at differentiating between normal and pathological retinal boundaries. After conducting an exhaustive reliability examination, it was shown that the manual Measures computed using human annotations and the manual measures produced by applying the suggested technique yielded results that were significantly concordant with one another.

OBSERVATIONS

Based on the review of existing retinal image processing models, it can be observed that bioinspired & deep learning models outperform existing methods in terms of applicability and performance metrics. To further validate this claim, a comparative analysis of these methods is provided in this section, where the reviewed methods are evaluated in terms of accuracy of disease detection (A), precision (P), delay needed to identify diseases (D), computational complexity (CC), and scalability (S) of deployment for different use cases. Accuracy & Precision were directly inferred from the reference documents, but delay, complexity and scalability levels were quantized into ranges of Low (L=1), Medium (M=2), High (H=3), and Very High (VH=4), which will assist readers to compare these techniques on a uniform set of scales. Based on this strategy, the comparison of these models is tabulated in Table 2 and a graphical comparison is given in Fig 5 and Fig 6 respectively.

Based on this evaluation, INSPIRE, PLM , OOF, ANS, MSAN and UNet showed higher accuracy, which is the best method for deep learning for retinal imaging tasks. Therefore, these models should be deployed for very precise use cases. OOF and DRIVE demonstrated higher accuracy using a simplified classification interface. Therefore, these techniques can be used for applications that require high consistency of retinal image processing for various batch operations.

In terms of computational complexity, EL and CAMR are superior to other models and are very useful for low-complexity applications. Therefore, these models should be used for high-performance and low-complexity deployments. It is observed that PLM and ANS are faster, so they can be used in low-latency cases. These models are also useful for large-scale applications that require high throughput with some level of efficiency.

Table 2 Comparison of performance of various algorithms

Model	A	P	CC	D	S
INS PIRE [8]	95.1	91.4	H	VH	H
PLM [9]	97.4	92.7	H	H	H
OOF [11]	97.4	94.1	H	H	H
OCT RE [12]	96.1	90.3	L	VH	H
ANS [13]	96.5	92.1	H	VH	H
MSAN [14]	97.5	93.9	VH	H	H
EL [15]	91.5	90.8	M	H	H
Seg RAVIR [16]	96.5	94.2	H	H	M
CAMR [17]	93.5	93	L	VH	H
UNet [18]	96.5	93.5	VH	H	H
GLUE [19]	97.8	91.2	H	H	H
DRN [20]	90.5	91.6	H	VH	H
RL [21]	94.5	93.8	H	H	M
LR [22]	85.5	91.2	H	H	H
MTLS [23]	85.3	87.3	H	H	H
OCTA Net [24]	90.5	90.5	H	VH	M
FS GAN [25]	94.8	92.4	L	H	H
MGAN [26]	95.3	92.9	H	H	H
Skel Con [27]	96.2	92.3	VH	H	M
CNN [28]	93.4	90.5	H	H	H
DRIVE [29]	90.8	92.8	H	H	M

Fig. 5 Graphical representation of the accuracy of algorithms
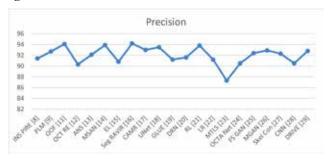
Fig. 6 Graphical representation of precision of algorithms

CONCLUSIONS

In terms of applicability and performance metrics, bioinspired and deep learning models outperform existing methods for retinal image processing based on a review of existing models. Due to the use of deep learning for retinal image processing operations, PLM, OOF, MSAN, RAVIR and GLUE demonstrated greater accuracy based on accuracy evaluations. Therefore, these models must be deployed for use cases requiring high precision. Similarly, OOF, MSAN, Seg RAVIR, CAMR, UNet, and RL exhibited greater precision due to the application of simplified classification interfaces. Thus, these methods can be utilized for applications requiring a high level of consistency in retinal image processing for various deployment operations. AGAN, PSO, and EL outperform other models in terms of computational complexity, making them exceptionally useful for low-complexity applications. Thus, these models must be utilized for deployments with high efficiency and low complexity. It can also be observed that AGAN and RDE have a higher speed and are therefore suitable for use cases with low delay. These models are also useful for large-scale applications that require consistent processing speed at a high level of efficiency for different use cases. In terms of

scalability, DNN, AGAN, DDN, and DSC are observed to have superior performance and can be applied to a wider variety of use cases. To further facilitate model selection, a Retinal Rank Metric RRM, which combines these parameters, was estimated. This resulted in the identification that PLM, OOF, MSAN, CAMR, UNet, FS GAN and MGAN exhibit higher accuracy, higher scalability, lower complexity, high speed, and high scalability for different use cases. In terms of real-time evaluation scenarios, it is also possible to observe that Deep Learning Models outperform other models.

FUTURE SCOPE

In the future, the performance of the reviewed models must be evaluated on larger scenarios, and it can be enhanced through the incorporation of low-complexity bio-inspired models such as Particle Swarm Optimization PSO, Grey Wolf Optimization GWO, etc. This performance can also be enhanced through the use of Auto Encoders AEs, Generative Adversarial Networks GANs, and other incremental learning techniques, making these models applicable for real-time clinical use cases.

Conflicts of Interest

The authors declare no conflicts of interest.

Statement of Ethical Approval

For this type of study, statement of human rights is not required.

Statement of informed consent

For this type of study, informed consent is not required.

REFERENCES

1. M. Elsharkawy, A. Sharafeldeen, A. Soliman, F. Khalifa, M. Ghazal, E. El-Daydamony, et al., "A Novel Computer-Aided Diagnostic System for Early Detection of Diabetic Retinopathy Using 3D-OCT Higher-Order Spatial Appearance Model," Diagnostics, vol. 12, no. 2, article no. 461, 2022.

2. W. L. Alyoubi, W. M. Shalash, and M. F. Abulkhair, "Diabetic Retinopathy Detection Through Deep Learning Techniques: A Review," Informatics in Medicine Unlocked, vol. 20, article no. 100377, 2020.

3. E. Mousavi, R. Kafieh, and H. Rabbani, "Classification of Dry Age- Related Macular Degeneration and

Diabetic Macular Oedema from Optical Coherence Tomography Images Using Dictionary Learning," IET Image Processing, vol. 14, no. 8, pp. 1571-1579, 2020.

4. T. Nazir, A. Irtaza, A. Javed, H. Malik, D. Hussain, and R. A. Naqvi, "Retinal Image Analysis for Diabetes-Based Eye Disease Detection Using Deep Learning," Applied Sciences, vol. 10, no. 18, article no. 6185, 2020.

5. R. K. Singh and R. Gorantla, "DMENET: Diabetic Macular Edema Diagnosis Using Hierarchical Ensemble of CNNs," Plos One, vol. 15, no. 2, article no. e0220677, 2020.

6. S. Wang, X. Wang, Y. Hu, Y. Shen, Z. Yang, M. Gan, et al., "Diabetic Retinopathy Diagnosis Using Multichannel Generative Adversarial Network with Semi-supervision," IEEE Transactions on Automation Science and Engineering, vol. 18, no. 2, pp. 574-585, 2021.

7. N. Sambyal, P. Saini, R. Syal, and V. Gupta, "Modified Residual Networks for Severity Stage Classification of Diabetic Retinopathy," Evolving Systems, vol. 14, no. 1, pp. 17-35, 2022.

8. Z. Khan, F. G. Khan, A. Khan, Z. U. Rehman, S. Shah, S. Qummar, et al., "Diabetic Retinopathy Detection using VGG-NiN a Deep Learning Architecture," IEEE Access, vol. 9, pp. 61408-61416, 2021.

9. Y. Zhao, Y. Liu, J. Xie, H. Zhang, Y. Zheng, Y. Zhao, et al., "Retinal Vascular Network Topology Reconstruction and Artery/Vein Classification Via Dominant Set Clustering," IEEE Transactions on Medical Imaging, vol. 39, no. 2, pp. 341-356, 2020.

10. P. Seebock, J. I. Orlando, T. Schlegl, S. M. Waldstein, H. Bogunovic, S. Klimscha, et al., "Exploiting Epistemic Uncertainty of Anatomy Segmentation for Anomaly Detection in Retinal OCT," IEEE Transactions on Medical Imaging, vol. 39, no. 1, pp. 87-98, 2020.

11. P. K. Maurya, V. Gupta, M. Singh, A. K. Singh, B. Kumar, and A. Mohan, "Automated Detection of Diabetic Macular Edema Involving Cystoids and Serous Retinal Detachment," Optics & Laser Technology, vol. 127, article no. 106157, 2020.

12. M. Li, Y. Chen, Z. Ji, K. Xie, S. Yuan, Q. Chen, et al., "Image Projection Network: 3D to 2D Image Segmentation in OCTA Images," IEEE Transactions on Medical Imaging, vol. 39, no. 11, pp. 3343-3354, 2020.

13. M. S. Sarabi, M. M. Khansari, J. Zhang, S. Kushner-Lenhoff, J. K. Gahm, Y. Qiao, et al., "3D Retinal Vessel Density Mapping with OCT-Angiography," IEEE Journal of Biomedical and Health Informatics, vol. 24, no. 12, pp. 3466-3479, 2020.

14. L. Pan, F. Shi, D. Xiang, K. Yu, L. Duan, J. Zheng, et al., "OCTRexpert: A Feature-Based 3D Registration Method for Retinal OCT Images," IEEE Transactions on Image Processing, vol. 29, pp. 3885-3897, 2020.

15. A. Cazanas-Gordon, E. Parra-Mora, and L. A. Cruz, "Ensemble Learning Approach to Retinal Thickness Assessment in Optical Coherence Tomography," IEEE Access, vol. 9, pp. 67349-67363, 2021.

16. A. Hatamizadeh, H. Hosseini, N. Patel, J. Choi, C. C. Pole, C. M. Hoeferlin, et al., "RAVIR: A Dataset and Methodology for The Semantic Segmentation and Quantitative Analysis of Retinal Arteries and Veins in Infrared Reflectance Imaging," IEEE Journal of Biomedical and Health Informatics, vol. 26, no. 7, pp. 3272-3283, 2022.

17. Y. Wang, J. Zhang, M. Cavichini, D. U. G. Bartsch, W. R. Freeman, T. Q. Nguyen, et al., "Robust Content-Adaptive Global Registration for Multimodal Retinal Images Using Weakly Supervised Deep-Learning Framework," IEEE Transactions on Image Processing, vol. 30, pp. 3167-3178, 2021.

18. J. Wei, G. Zhu, Z. Fan, J. Liu, Y. Rong, J. Mo, et al., "Genetic U-Net: Automatically Designed Deep Networks for Retinal Vessel Segmentation Using a Genetic Algorithm," IEEE Transactions on Medical Imaging, vol. 41, no. 2, pp. 292-307, 2022.

19. S. Lian, L. Li, G. Lian, X. Xiao, Z. Luo, and S. Li, "A Global and Local Enhanced Residual U-Net for Accurate Retinal Vessel Segmentation," IEEE/ACM Transactions on Computational Biology and Bioinformatics, vol. 18, no. 3, pp. 852-862, 2021.

20. J. Zhang, Y. Wang, J. Dai, M. Cavichini, D. U. G. Bartsch, W. R. Freeman, et al., "Two-Step Registration on Multi-Modal Retinal Images via Deep Neural Networks," IEEE Transactions on Image Processing, vol. 31, pp. 823-838, 2022.

21. J. Lyu, Y. Zhang, Y. Huang, L. Lin, P. Cheng, and X. Tang, "AADG: Automatic Augmentation for Domain Generalization on Retinal Image Segmentation," IEEE Transactions on Medical Imaging, vol. 41, no. 12, pp. 3699-3711, 2022.

22. B. Zou, Y. Dai, Q. He, C. Zhu, G. Liu, Y. Su, et al., "Multi-label Classification Scheme Based on Local

Regression for Retinal Vessel Segmentation," IEEE/ACM Transactions on Computational Biology and Bioinformatics, vol. 18, no. 6, pp. 2586-2597, 2021.

23. J. Hao, T. Shen, X. Zhu, Y. Liu, A. Behera, D. Zhang, et al., "Retinal Structure Detection in OCTA Image via Voting-based Multitask Learning," IEEE Transactions on Medical Imaging, vol. 41, no. 12, pp. 3969-3980, 2022.

24. Y. Ma, H. Hao, J. Xie, H. Fu, J. Zhang, J. Yang, et al., "Rose: A Retinal OCT-Angiography Vessel Segmentation Dataset and New Model," IEEE Transactions on Medical Imaging, vol. 40, no. 3, pp. 928-939, 2021.

25. N. Liang, L. Yuan, X. Wen, H. Xu, and J. Wang, "End-to-end Retina Image Synthesis Based on CGAN Using Class Feature Loss and Improved Retinal Detail Loss," IEEE Access, vol. 10, pp. 83125-83137, 2022.

26. K. B. Park, S. H. Choi, and J. Y. Lee, "M-GaN: Retinal Blood Vessel Segmentation by Balancing Losses through Stacked Deep Fully Convolutional Networks," IEEE Access, vol. 8, pp. 146308-146322, 2020.

27. Y. Tan, K. F. Yang, S. X. Zhao, and Y. J. Li, "Retinal Vessel Segmentation with Skeletal Prior and Contrastive Loss," IEEE Transactions on Medical Imaging, vol. 41, no. 9, pp. 2238-2251, 2022.

28. C. Gonzalez-Gonzalo, B. Liefers, B. van Ginneken, and C. I. Sanchez, "Iterative Augmentation of Visual Evidence for Weakly-Supervised Lesion Localization in Deep Interpretability Frameworks: Application to Color Fundus Images," IEEE Transactions on Medical Imaging, vol. 39, no. 11, pp. 3499-3511, 2020.

29. R. Xu, T. Liu, X. Ye, F. Liu, L. Lin, L. Li, et al., "Joint Extraction of Retinal Vessels and Centerlines Based on Deep Semantics and Multi-Scaled Cross-Task Aggregation," IEEE Journal of Biomedical and Health Informatics, vol. 25, no. 7, pp. 2722-2732, 2021.

U-Net-based gannet sine cosine algorithm enabled lesion segmentation and deep CNN for diabetic retinopathy classification

Rupesh Goverdhan Mundada & Devesh D Nawgaje

Published online: 21 Aug 2023.

Submit your article to this journal ↗

View related articles ↗

View Crossmark data ↗

Taylor & Francis
Taylor & Francis Group

Check for updates

U-Net-based gannet sine cosine algorithm enabled lesion segmentation and deep CNN for diabetic retinopathy classification

Rupesh Goverdhan Mundada[a] and Devesh D Nawgaje[b]

aElectronics and Telecommunication Engineering, Sant Gadge Baba Amravati University, Amravati, India; bElectronics and Telecommunication Engineering, Shri Sant Gajanan Maharaj College of Engineering, Shegaon, Maharashtra, India

ABSTRACT

Diabetic retinopathy (DR) is a reason for blindness. This disease raises a threat of developing deteriorations in blood vessels supplied by the retina. In this research, U-Net_Gannet Sine Cosine Algorithm (U-Net_GSCA) is used for DR segmentation, and DR classification is made by the GSCA_Deep Convolutional Neural Network (GSCA_DeepCNN). In the pre-processing process the Region of Interest (ROI) is extracted. For pre-processing process, it uses Laplacian filter. Color spacing, rotation, and brightness are the augmentation techniques used for image augmentation. U-Net which is tuned by GSCA is used for lesion segmentation. Furthermore, GSCA is the integration of GOA with SCA. The segmentation of the artery and vein is performed utilising the sparking process. In the feature extraction phase, they uses augmented and segmented images. From this images, the feature extraction is made. Finally, the classification of DR is made by the deep CNN that is also trained by GSCA. Furthermore, U-Net_GSCA achieved 92.6% segmentation accuracy, GSCA_DeepCNN achieved 92.2% classification accuracy, 92.5% sensitivity, and 91.9% specificity.

1. Introduction

At present, one of the emerging diseases is diabetes. Diabetic Retinopathy (DR) is the name for the serious eye condition that has been linked to diabetes mellitus (Khan et al. 2021). An ophthalmic disorder known as DR damages the blood vessels of the retina. The main reason for the loss of vision or worse vision is caused due to DR. DR is the main cause of suffering from blindness among people of old and middle age groups (Gharaibeh et al. 2021). People of old and middle age groups are suffering from blindness due to DR (Gharaibeh et al. 2021). DR is classified into five phases or classes: mild, severe, normal, and Proliferative Diabetic Retinopathy (PDR) (Qummar et al. 2019). The first four groups involve Non-Proliferative DR (NPDR) with lesions such as exudates (Akram et al. 2013), haemorrhages, and microaneurysms. The last class is PDR, which can be detected by particular lesions like Retinal Neovascularization (RNV). The DR is a state wherein eyes are affected owing to happening of diabetes (Aiello et al. 1974; Saini and Susan 2022). It is the most rigorous complexity of diabetes as well as the foremost cause of poor eyesight and also blindness (Luo et al. 2021). It is a universal issue related to the retina of humans. People suffering from diabetes are increasingly becoming vision-impaired, regardless of their age. The human eye comprises optical nerves and thus, eye images are segmented for getting better classification accuracy of diverse classes that are involved in DR (Tufail et al. 2021). Most diabetic patients are suffering from DR and hence, it is extremely needed to categorise the people in a shorter time along with higher accuracy. When a problem is detected, the affected patient is validated at regular periods to recognise the progression of the disease (Kalyani et al. 2021).

DR arises when higher sugar levels damage the retinal blood veins. These veins can spill and grow or they may be blocked thus, stopping blood flow. In other conditions, newer blood veins may form on the retina (Kalyani et al. 2021). In retinal fundus images, the early recognition and treatment are an important task as it can potentially reduce the risk of blindness. For diagnosis, recognition, and treatment of DR, retinal fundus images are used (Gharaibeh et al. 2018). The most effective treatment for DR is detecting it earlier (Al-Hazaimeh et al. 2022). Fundus screening is considered a common investigation technique and ophthalmologists take much time for diagnosing through fundus investigation (Luo et al. 2021). In general, highly experienced experts investigate coloured fundus images for diagnosing this deadly ailment. The physical diagnosing of this state is tedious as well as error-prone. Several computer vision-enabled algorithms have been developed to automatically recognise DR and its various categories from retinal images (Qummar et al. 2019). DR executes classification, segmentation, and object detection on DR fundus images (Saini and Susan 2022). The fundus photos demonstrate the presence of haemorrhages, exudates, and other eye impairments and are manually rated by a smaller number of ophthalmologists, whose numbers are diminishing each year (Decenciere et al. 2013; Tufail et al. 2021). The rigorous actuality is that the shortage of DR specialists makes to not get efficient detections of DR and treatments on time. For reducing expert's work and increase effectiveness, many image assessment approaches are developed to help diagnosing of DR (Luo et al. 2021). The simplest DR lesions

detection, as well as severity grading techniques, suggests a newer method for computer-assisted diagnosing system development, which may be useful to ophthalmologists for diagnosing and identification of DR lesions with small modifications (Nair and Muthuvel 2019; Sugeno et al. 2021).

Deep learning (DL) approaches have emerged in most recent decades and their usage has become highly popular in several areas, particularly in clinical as well as medical image assessment subjects in the past few years. The DL model learns higher-level abstractions from existing information and can predict the consequences (Tu et al. 2017; Zeng et al. 2019). DL applications are very efficient image assessment tool, which successfully performs a process directly like segmentation, detection, retrieval, acquisition, and classification. It improves colour fundus image quality and shows the defined lesion features of DR before Active Deep Learning (ADL) (Özbay 2022). The detection of DR (AlBalushi 2020) has concerned more attention presently and DL approaches have increased traction in this region. Presently, DR classification and detection utilising DL techniques are frequently based upon single-view fundus images that generally direct to unacceptable DR grading accuracy owing to unfinished lesion features. Convolutional Neural Network (CNN) has helped solve several problems in computer vision field. CNN is proved to be innovative in computer-vision areas. It is also utilised in the present time for segmentation, classification, object detection, and so on (Saini and Susan 2022). In recent times, DL approaches have made greater progress in automated DR detection based on fundus images (Luo et al. 2021). The DL is utilised to find the potent details from images that may be unnecessary or else it is detected and employed for classification with CNN (Heisler et al. 2020).

The prime intention is to design U-Net_GSCA and GSCA_DeepCNN for segmentation and classification of DR. At first by using the laplacian filter, the input image considered undergoes pre-processing and ROI is extracted. After that, the filtered image is augmented in an image augmentation phase, wherein augmentation techniques like colour spacing, rotation, and brightness are performed. The pre-processed picture is then segmented using U-Net into several lesions including Microaneurysms, Haemorrhages, Soft Exudates, and Hard Exudates during the lesion segmentation step. However, U-Net is trained to employ GSCA, which is formed by merging GOA and SCA. Afterward, artery and veins segmentation is performed utilising the sparking process. Thereafter, from augmented and segmented images the features are extracted. At this step, the following characteristics were extracted: artery veins ratio, area, colour histogram, entropy, kurtosis, eccentricity, perimeter, Local Binary Pattern (LBP), Local Optimal Oriented Pattern (LOOP), Global Binary Pattern (GBP), and Histogram of Oriented Gradient (HOG). Finally, using the Deep CNN, the categorisation of DR into severity classes such as normal, moderate NPDR, mild NPDR, proliferative, and severe NPDR is carried out. Furthermore, Deep CNN is trained by a newly designed GSCA that is an assimilation of GOA and SCA.

1.1. Motivation

DR is a dangerous disease, also people of working age highly suffer from blindness due to this disease. Furthermore, DR is a highly feared complexity of diabetes and augments the

chance of beginning other diseases like heart disease, kidney disorders, and so on. In the existing methods, manual detection is a time-consuming process. Also, the diagnosis process is very expensive. Some of the human limitations are, in a certain time, only limited patients are diagnosed. It is an error-prone process. This motivates devising the method for the classification of DR to identify diverse grades.

1.2. Contributions

The greatest contributions are elucidated as,

- **Proposed U-Net_GSCA for DR segmentation**: For the segmentation of lesions, U-Net_GSCA is presented. The lesion segmentation phase is performed wherein an image is segmented into several lesions employing U-Net. GSCA is an incorporation of GOA with SCA. By which the U-Net is trained.
- **Proposed GSCA_DeepCNN for DR classification**: An efficacious approach termed GSCA_DeepCNN is introduced newly in this work for DR classification. Here, DR is classified into severity grades utilising Deep CNN. A Deep CNN used for the classification of DR is trained by GSCA which is designed by integrating GOA with SCA.

The other sections are arranged as shown below: Section 2 explains the existing paper reviewed by DR classification with demerits faced whereas Section 3 interprets designed techniques for segmentation and classification of DR. Section 4 describes the results acquired by newly designed approaches whereas Section 5 ends with the conclusion of U-Net_GSCA and GSCA_DeepCNN.

2. Literature survey

For the detection of DR, Qummar et al. (2019) presented a DL ensemble approach that was capable of detecting all stages of the DR, but this method failed to train particular models for certain stages. Saini and Susan (2022) utilised DL for the screening process of DR. It required lesser parameters, though it did not emphasise the development of architectures for lesion segmentation and detection. Multi-view diabetic retinopathy network (MVDRNet) for the detection of DR is introduced by Luo et al. (2021). It can be successfully utilised in the DR detection field, though it was unsuccessful to train a network together with the lesion annotations. Khan et al. (2021) devised a deep learning-based ensemble approach for the recognition of DR. It utilised low computation resources, but failed to provide few other productive alterations in a model structure. Tufail et al. (2021) utilised 3D-CNN architectures for diagnosing DR using retinal fundus images. The total performance of this model trained without augmentation is highly superior, but there was a shortage of validation in the multi-centre validation group. Kalyani et al. (2021) designed a capsule network (CapsNet) for the classification and detection of DR. It achieved better outcomes for the early identification of retinopathy issues in diabetic patients, but it did not consider other datasets the network was not trained for DR classification. Özbay (2022) designed Active Deep

Learning-CNN (ADL-CNN) for the detection of DR in segmented fundus images. This technique automatically detected five severity levels of DR, though it failed to utilise in diverse multimedia applications. Sugeno et al. (2021) developed EfficientNet-B3 for grading and lesion segmentation of DR. It was highly useful in detecting ground-truth lesion members, even though false positive detection of the blood vessels and optical discs was not enhanced. Fayyaz et al. (2023) proposed a deep learning network that is used to automatically detect and classify DR fundus images depending on severity using AlexNet and Resnet101-based feature extraction. It became more accurate when ResNet-101, but accurate detection of microaneurysms is still a problem in this method (Fayyaz et al. 2023). Shaukat et al. (2023) proposed an Artificial intelligence (AI) based machine/deep learning method that performs a vital role to increase the performance of the detection process. It is time-saving, cost-saving, and efficient as compared to manual diagnosis methods, but they can only recognise hard exudates in the posterior pole and may miss cases which have DME (Shaukat et al. 2023). Ramzan et al. (2022) proposed a Graft-U-Net to segment polyps using colonoscopy frames. This model achieves accurate segmentation of colorectal polyps, but the appearance of the polyps fluctuating under the same lighting conditions and variable texture, and varying angular views under different lighting conditions (Ramzan et al. 2022).

2.1. Challenges

The demerits confronted by reviewed approaches according to DR segmentation and classification are explained below.

- The strategy suggested by Saini and Susan (2022) for DR screening purposes did not investigate ensemble learning with varied pre-trained networks for extremely efficient diagnosis of DR and other challenging regions from the biomedical field for deriving many generic techniques.
- MVDRNet (Luo et al. 2021) was introduced for DR detection that helped to incorporate diverse visions of patient images and also resolved corresponding issues in an area of clinical image processing, though it did not enhance the performance of multi-view DR detection.
- 3D-CNN architectures designed by Tufail et al. (2021) for diagnosing DR using retinal fundus images cannot treat other retinal illness.
- DR classification and detection were performed (Kalyani et al. 2021) by CapsNet obtained better accuracy in DR identification, but still, the devised scheme but this method is not feasible for all classes of DR.
- DR can cause total vision loss, which is a cumulative process, clinical specialists recommend that persons with diabetes be checked for indications of sickness at least twice a year. The detection process significantly depends on the assessment of colour pictures by visual scientists in present medical diagnosing. This identification method is time-consuming and difficult, which causes substantial issues.

3. Proposed U-Net_GSCA and GSCA_Deepcnn for DR segmentation and classification

Over the present years in developed and developing countries, the occurrence of DR is increasing. Furthermore, the execution of annual eye investigations is a challenging task in rural or remote geographies owing to inadequate access to experienced ophthalmologists. Here, U-Net_GSCA for DR segmentation and GSCA_DeepCNN for DR classification are presented. The first phase is conducted employing a Laplacian filter for eliminating noises and afterwards, ROI extraction is performed. Thereafter, image augmentation is done using augmenting techniques like colour spacing, rotation, and brightness. U-Net which is trained using GSCA is used for lesion segmentation. By combining GOA and SCA, The GSCA is formed. Then, artery and veins segmentation is done utilising the sparking process. Following that, the feature extraction step extracts the arteries to veins ratio, area, colour histogram, entropy, eccentricity, perimeter, kurtosis, LBP, LOOP, GBP, and HOG. For DR classification, GSCA-trained Deep CNN is employed. Figure 1 displays a graphical view of the proposed U-Net_GSCA for DR segmentation and GSCA_DeepCNN for the classification of DR.

3.1. Image acquisition

An input image is acquired for segmentation and DR classification from a certain dataset specified in https://ieee-dataport.org/open-access/indian-diabetic-retinopathy-image-dataset-idrid, which is given by,

$$D = \{D_1, D_2, \ldots D_y \ldots D_e\} \tag{1}$$

Where DR images contained in the database D are implied by D_e and D_y represents y^{th} input image.

3.2. Pre-processing utilising Laplacian filter

Pre-processing is carried out to improve the picture, and unwilling deformations are repressed. Here, the Laplacian filter is intended for eliminating unnecessary noises and afterwards, extraction of ROI is conducted in the filtered image. The image considered for processing is implied by D_y.

3.2.1. Laplacian filter

The Laplacian operator is employed to locate edges in images (Khan et al. 2019). Laplacian is a derivative mask of the second order. This mask categorises both positive and negative Laplacian operators. The Laplacian of an image emphasises regions of fast intensity change and is thus widely used for edge identification and noise reduction. Laplacian equation utilised for computation of edge detection can be modelled by,

$$L_y = \Delta^2 B = \left(\frac{\partial^2 B}{\partial \varepsilon^2} + \frac{\partial^2 B}{\partial \tau^2}\right) \otimes B(\varepsilon, \tau) \tag{2}$$

Where a filtered image is symbolised by L_y.
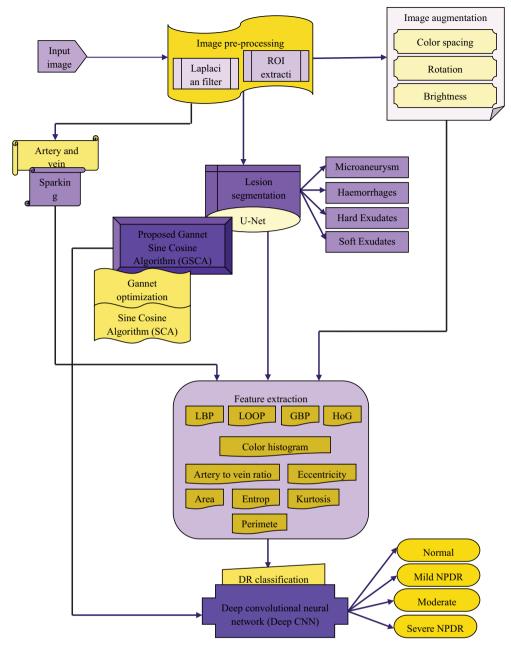
Figure 1. The graphical vision of the proposed U-Net_GSCA and GSCA_DeepCNN for segmentation and DR classification.

3.2.2. ROI extraction

The filtered picture L_y is used as an input for ROI extraction. The ROI is part of an image that is desired to be filtered in some manner. It detects the significant region from filtered images. In an image, the pixel belonging to ROI is fixed to 1 whereas pixels exterior to ROI is fixed to 0. The acquisition of the ROI is an essential phase in image pre-processing and a critical step in DR classification. The quality of ROI extraction has a direct impact on picture enhancement and normalisation results. The ROI extracted image is represented here by the word R_y.

3.3. Image augmentation

Dataset dimension is handled by image augmentation and it is referred to as a robust method. The image augmentation approaches are generally utilised for increasing the effectiveness of the feature extraction process. Here, an extracted image R_y is regarded as an input for conducting the image augmentation stage. In this phase, colour spacing, rotation, and brightness are the augmentation techniques carried out.

3.3.1. Colour spacing

In traditional photometric image augmentation, colour spacing (Khalifa et al. 2022) is regarded as the significant method to increase the count of images and also, it reveals a few crucial features present in an image that are unseen under certain colour space. The colours are depicted utilising the amount of green, blue, and red produced by the phosphor panel. A conversion from red-green-blue to cyan-magenta-yellow can be illustrated by,

$$\begin{bmatrix} C_1 \\ C_2 \\ C_3 \end{bmatrix} = \begin{bmatrix} 1 \\ 1 \\ 1 \end{bmatrix} - \begin{bmatrix} S_1 \\ S_2 \\ S_3 \end{bmatrix} \qquad (3)$$

Here, C_1, C_2 and C_3 denotes cyan, magenta, and yellow whereas S_1, S_2 and S_3 represents red, green, and blue. The colour spacing augmentation technique can be signified as A_1.

3.3.2. Rotation

The rotation (Khalifa et al. 2022) is another kind of traditional geometric image augmentation, where the rotation process is carried out by rotating an image about the axis in a left or right direction by angles between 1 and 359. The equation of rotation can be formulated as follows.

$$\begin{bmatrix} p_\omega \\ p_\varsigma \end{bmatrix} = \begin{bmatrix} \cos\Psi & -\sin\Psi \\ \sin\Psi & \cos\Psi \end{bmatrix} \cdot \begin{bmatrix} \omega \\ \varsigma \end{bmatrix} \qquad (4)$$

Here, p_ω and p_ς are the newer location of each pixel after a process of rotation whereas ω and ς implies coordinates pair. The rotation technique can be denoted by a term A_2.

3.3.3. Brightness

The image brightness is altered randomly for imitating a situation of an ophthalmologist's investigation underneath various illumination and it is indicated by A_3.

Hence, J_y is the augmented image such that it can be given as,

$$J_y = \{A_1, A_2, A_3\} \qquad (5)$$

3.4. Lesion segmentation

DR lesion segmentation is the requirement chore for the classification of DR and also, and it lays a base for the following severity gradings of DR. In the lesion segmentation phase, the extracted image R_y is fed as an input. The lesion segmentation is executed utilising U-Net which is trained by GSCA, which is an incorporation of GOA with SCA.

3.4.1. Architecture of U-Net

(Siddique et al. 2021) U-Net can be classified into two segments: An initial one is a contracting path, which utilises the general architecture of CNN. Each block in the contracting path comprises two consecutive 3×3 convolutions that are pursued by the ReLU activation function as well as the max-pooling layer. The organisation is continued at various times. U-Net novelty occurs in the second segment termed expansive path wherein each phase upsamples feature map utilising 2×2 up-convolution. The feature map from a similar layer in a contracting route is then cropped and concatenated to produce an upsampling feature map. It is then followed by two convolutions and the ReLU activation function. Following that, the feature map from a corresponding layer in a contracting route is cropped and concatenated to create an upsampling feature map. It is pursued by two consecutive 3×3 convolutions as well as the ReLU activation function. In the last step, extra 1×1 convolution is used for reducing the feature map to the necessary count of the channels and generates a segmented image. The features in the edges of the pixel have less context details. Hence, cropping is needed to remove the features. Its outcomes in the network are similar to a U-shape and significantly propagate context details along a network that permits segmenting objects in a region utilising contextual from bigger overlapping regions.

An energy function for the network can be specified by,

$$N = \sum b(z) \log\left(Y_{f(z)}(z)\right) \qquad (6)$$

Here, Y_f denotes pixel-wise softmax function that is applied all over the last feature map and can be defined by,

$$Y_f = \exp\left(a_f(z)\right) / \sum_{f'=1}^{F} \exp\left(a_f(z)'\right) \qquad (7)$$

Where, a_f signifies activation in the channel f. A segmented output from U-Net is denoted by U_y and U-Net structure is depicted in Figure 2.

3.4.2. Training of U-Net utilising GSCA

GOA (Pan et al. 2022) is used to enable exploitation and exploration by forming numerous different features of gannets. The V-shape and U-shape diving patterns are held responsible for exploring the perfect area amid searching space by applying unexpected random strolling and twists to ensure the top results. This approach provided the best solutions in several cases. SCA (Mirjalili 2016) creates several random initialised candidate solutions and requires them to vary towards or away from the best answer via mathematical form based on sine and cosine functions. This approach was capable of exploring diverse areas of searching space, avoiding local optimum, converging towards global optima, and exploiting promising areas of searching space at the time of optimisation efficiently. In this case, GOA and SCA are combined to generate GSCA, which is ideal for training U-Net for lesion segmentation.

3.4.2.1. Gannet position encoding.
In the search space ξ, an optimal solution is found, where the U-Net learning parameter is denoted by o, such that $\xi = 1 \times o$.

Fitness measure: The fitness is calculated using disparities between U-net and goal outputs that can be modelled by,

$$X_1 = \frac{1}{e} \sum_{y=1}^{e} \left[T_y - U_y\right]^2 \qquad (8)$$

Where overall images are specified by e and outputs of target and U-Net are symbolised by T_y and U_y.

To acquire an optimal solution, GSCA follows the steps revealed below.

Step 1: Solution initialization

Initially, GOA begins with a group of random solutions, where an optimum solution point is considered the optimum global solution.

$$H = \{H_1, H_2, \ldots, H_k, \ldots, H_g\} \qquad (9)$$

Here, h_k signifies k^{th} candidate solution whereas h_g implies total variables and H reveals population.

Each $h_{k,l}$ can be formulated by,
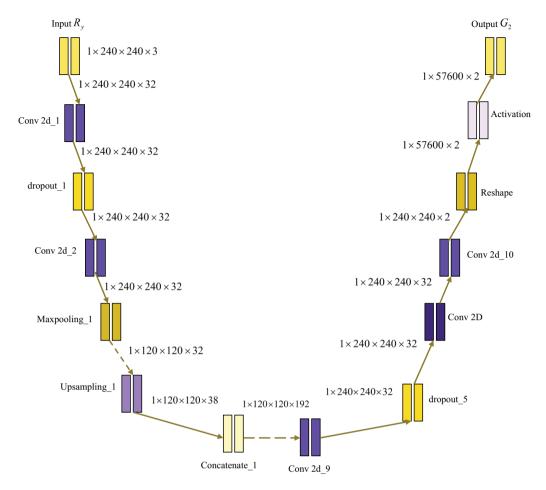
Figure 2. Architecture of U-Net.

$$h_{k,l} = a_1 \times (P_l - W_l) + W, \quad k = 1, 2, \ldots, X, \ l = 1, 2, \ldots, d \quad (10)$$

Here, P_l and W_l denote the upper bound and lower bound of lth dimension of the known problem. X specifies the count of individual members in the population, d indicates the dimension size of the problem, and a_1 signifies random numbers between 0 and 1.

Step 2: Computing objective function

Based on the difference between U-Net and intended outputs. Equation (8) is used for assessing the objective function.

Step 3: Exploration stage

Gannets look for prey in water from the air, and once found, they modify their dive patterns to match the animal's diving depth. U-shaped diving and V-shaped diving are the two types of diving in GOA. The below-mentioned Equation (12) is used for U-shaped dive whereas Equation (13) is employed for V-shaped dive.

$$n = 1 - \frac{m}{M} \quad (11)$$

$$i = 2 * \cos(2 * \pi * a_2) * n \quad (12)$$

$$j = 2 * E(2 * \pi \times a_3) * n \quad (13)$$

$$E(h) = \begin{cases} -\frac{1}{\pi} * h + 1, & h \in (0, \pi) \\ \frac{1}{\pi} * h - 1, & h \in (\pi, 2\pi) \end{cases} \quad (14)$$

Here, m indicates the count of current iterations, m represents the maximal number of iterations while a_2 and a_3 signifies random numbers amid 0 and 1.

A pursuing step is to employ two dive methods for a position update. Gannets contain essentially equal probability of selecting amid two methods when predating, thus the random number t is stated for randomly choosing two dive strategies. A position update formula is illustrated as,

$$M_k(n+1) = H_k(n) + \mu_1 + \mu_2 \quad , t \geq 0.5 \quad (15)$$

Let us consider,

$$\mu_2 = Y * (H_k(n) - H_v(n)) \quad (16)$$

$$M_k(n+1) = H_k(n+1) \quad (17)$$

Then, Equation (15) becomes,

$$H_k(n+1) = H_k(n) + \mu_1 + Y * (H_k(n) - H_v(n)) \quad (18)$$

$$H_k(n+1) = H_k(n) + \mu_1 + Y * H_k(n) - Y H_v(n) \quad (19)$$

$$H_k(n+1) = H_k(n)\,[1+Y] + \mu_1 - Y\,H_v(n) \tag{20}$$

A standard equation of SCA is modelled by,

$$H(n+1) = H(n) + \lambda_1 \sin(\lambda_2) * \lambda_3\, T - H(n) \tag{21}$$

Let us assume,

$$H(n+1) = H_k(n+1) \tag{22}$$

$$H(n) = H_k(n) \tag{23}$$

Then, Equation (21) becomes,

$$H_k(n+1) = H_k(n) + \lambda_1 \sin(\lambda_2) * \lambda_3\, T - H_k(n) \tag{24}$$

$$H_k(n+1) = H_k(n)\,[1 - \lambda_1 \sin(\lambda_2)] + \lambda_1 \sin(\lambda_2) * \lambda_3\, T \tag{25}$$

$$H_k(n) = \frac{H_k(n+1) - \lambda_1 \sin(\lambda_2)\,\lambda_3\, T}{1 - \lambda_1 \sin(\lambda_2)} \tag{26}$$

Substitute Equation (26) in Equation (20),

$$H_k(n+1) = \left(\frac{H_k(n+1) - \lambda_1 \sin(\lambda_2)\,\lambda_3\, T}{1 - \lambda_1 \sin(\lambda_2)} \right)[1+Y] + \mu_1 \\ - Y\,H_v(n) \tag{27}$$

$$H_k(n+1) - \frac{H_k(n+1)\,[1+Y]}{1 - \lambda_1 \sin(\lambda_2)} = \mu_1 - \frac{\lambda_1 \sin(\lambda_2)\,\lambda_3\, T}{1 - \lambda_1 \sin(\lambda_2)}\,[1+Y] \\ - Y\,H_v(n) \tag{28}$$

$$\frac{H_k(n+1)(1 - \lambda_1 \sin(\lambda_2) - 1 - Y)}{1 - \lambda_1 \sin(\lambda_2)} \\ = \frac{(\mu_1 - Y\,H_v(n))\,(1 - \lambda_1 \sin(\lambda_2)) - \lambda_1 \sin(\lambda_2)\,\lambda_3\, T\,[1+Y]}{1 - \lambda_1 \sin(\lambda_2)} \tag{29}$$

$$H_k(n+1) = \frac{(\mu_1 - Y\,H_v(n))\,(1 - \lambda_1 \sin(\lambda_2)) - \lambda_1 \sin(\lambda_2)\,\lambda_3\, T\,[1+Y]}{-Y - \lambda_1 \sin(\lambda_2)} \tag{30}$$

An update equation of GSCA is modelled as,

$$H_k(n+1) = \frac{\lambda_1 \sin(\lambda_2)\,\lambda_3\, T\,[1+Y] - (\mu_1 - Y\,H_v(n))\,(1 - \lambda_1 \sin(\lambda_2))}{Y + \lambda_1 \sin(\lambda_2)} \tag{31}$$

Here, T implies a position of targeted solution whereas λ_1, λ_2 and λ_3 denote a random number among 0 and 1. $H_v(n)$ specifies randomly selected individuals in the existing population. μ_1 signifies a random number between $-i$ and i.

$$Y = (2 * a_4 - i * i) \tag{32}$$

Where, a_4 specifies random number amid 0 and 1.

If an above-stated condition is not satisfied, then a position updating formula can be formulated by,

$$M_k(n+1) = H_k(n) + \eta_1 + \eta_2 \quad , t < 0.5 \tag{33}$$

$$\eta_2 = Z * (H_k(n) - H_x(n)) \tag{34}$$

$$Z = (2 * a_5 - 1) * j \tag{35}$$

Here, a_4 and a_5 are random numbers amid 0 and 1, η_1 signifies random number amongst $-j$ and j, $H_k(n)$ symbolizes k^{th} individual in the current population, $H_x(n)$ denotes the average position of individual members in existing population, which can be formulated by,

$$H_x(n) = \frac{1}{X} \sum_{k=1}^{X} H_k(n) \tag{36}$$

Step 4: Exploitation stage

After a gannet rushes to water in the above-mentioned two methods, two activities are essential for subsequent exploitation. A clever fish in the water is frequently followed by an unexpected twisting movement to avoid gannets hunting it. A gannet also expends a lot of energy in order to grab a fish that is attempting to escape. Equation (37) is employed to model capture capacity in this case. When the gannet has enough energy, it will catch fish. As time passes, the gannet's energy decreases, and it is unable to carry out the capturing deed.

$$A = \frac{1}{\Re * n_2} \tag{37}$$

$$n_2 = 1 + \frac{m}{M} \tag{38}$$

$$\Re = \frac{E * \upsilon^2}{O} \tag{39}$$

$$O = 0.2 + (2 - 0.2) * a_6 \tag{40}$$

Here, a_6 indicates random number amid 0 and 1, E $= 2.5$ Kg indicates gannet weight, $\upsilon = 1.5\, m/s$ signifies gannet speed in the water, ignoring water resistance during this time.

If the catching potential of the gannet is within a range of catchable prey, the position is then updated with unpredicted turning or else it is not proficient to catch flexible fishes and performs Levy movement for randomly finding the following target.

$$M_k(n+1) = \begin{cases} n * delta * (H_k(n) - H_{best}(n)) + H_k(n) & , A \geq \varpi \quad (i) \\ H_{best}(n) - (H_k(n) - H_{best}(n)) * I * n & , A < \varpi \quad (ii) \end{cases} \tag{41}$$

$$delta = A * |H_k(n) - H_{best}(n)| \tag{42}$$

$$I = Levy\,(d) \tag{43}$$

Here, $\varpi = 0.2$ specifies a constant, wherein the value is determined after various experimentations. $H_{best}(n)$ implies best-implementing individual in existing population whereas $Levy()$ implies Levy flight function that can be illustrated by,

$$Levy(d) = 0.01 \times \frac{\zeta \times \sigma}{|\ell|^{\frac{1}{\delta}}} \tag{44}$$

$$\sigma = \left(\frac{\Gamma(1+\delta) \times \sin\left(\frac{\pi\delta}{2}\right)}{\Gamma\left(\frac{1+\delta}{2}\right) \times \delta \times 2^{\left(\frac{\delta-1}{2}\right)}} \right)^{\frac{1}{\delta}} \tag{45}$$

Here, ζ and σ symbolizes random values amid 0 and 1 where $\delta = 1.5$ indicates a pre-determined constant.

Step 5: Termination

The above-mentioned processes are carried out indefinitely to obtain the optimal answer. Algorithm 1 describes the GSCA pseudo code.

Algorithm 1. Pseudo code of GSCA

SL. No	Pseudo code of GSCA
1	**Input:** X, d, M
2	**Output:** $H_k(n+1)$
3	**Begin**
4	Initialize the population randomly, where a and t implies random numbers ranging between 0 and 1.
5	Generation of memory matrix specified as M ;
6	Computation of fitness value of H ;
7	**While** the stopping criteria are not satisfied **do**
8	**if** $rand > 0.5$ **then**
9	**for** M_k **do**
10	**if** $t \geq 0.5$ **then**
11	Updating a gannet location employing Eq. (31)
12	**Else**
13	Updating a gannet location employing Eq. (33)
14	**end if**
15	**end for**
16	**Else**
17	**for** M_k **do**
18	**if** $\varpi \geq 0.2$ **then**
19	Updating gannet location by Eq. (41 (i))
20	**Else**
21	Updating gannet position by Eq. (41 (ii))
22	**end if**
23	**end for**
24	**end if**
25	**for** M_k **do**
26	Estimate fitness measure of M_k ;
27	If M_k value is superior than H_k value, replace H_k with M_k ;
28	**end for**
29	**end while**
30	**Terminate**

3.5. Artery and vein segmentation

An artery and vein segmentation is a significant metric in computer-aided diagnosing of several vascular and systematic diseases. Therefore, effective and accurate segmentation of arteries and veins is the requirement for precise measurement of various key parameters. For artery and vein segmentation the sparking process is utilised and R_y is the input.

The sparkling process (Mane and Jadhav 2017) technique for automated blood vessel segmentation is developed using optimal threshold values evaluation.

An input-filtered image having size $v \times w$ undergoes a sparking process. An input image is converted to w diverse images by an exponential kernel. Let c specifies random integer developed with a dimension of $1 \times w$ whereas l denotes threshold value provided by a user. The data conversion to an exponential function, as shown below, identifies an exponential kernel.

$$\hbar_1 = \exp^{-\left[\frac{c^2}{2l^2}\right]} \tag{46}$$

A vector $\hbar_\beta$ is normalised utilising the below equation for obtaining the kernel.

$$Ke_1 = \frac{\left[\frac{1}{w}\sum_{\beta=1}^{w} \max(\hbar_1) - \hbar_1\right] - \hbar_1}{\sum_{\beta=1}^{w} \max(\hbar_1) - \hbar_1} \tag{47}$$

An image considered as input is rotated to w several angles for yielding w images of equal size. A sparking image can be acquired utilising the below equation.

$$O_y = \phi_{new}(\beta, \gamma) = \frac{\phi_\hbar + \phi_{\min(\beta,\gamma)}}{\phi_{\max}(\beta, \gamma)} 255 \tag{48}$$

Where,

$$\phi_{\min}(\beta, \gamma) = \min[o_1(\beta, \gamma), o_2(\beta, \gamma), \ldots o_w(\beta, \gamma)] \tag{49}$$

$$\phi_{\max}(\beta, \gamma) = \max[o_1(\beta, \gamma), o_2(\beta, \gamma), \ldots o_w(\beta, \gamma)] \tag{50}$$

Equation (48), O_y implies artery and vein-segmented image.

3.6. Feature extraction

Feature extraction handles the trouble of finding a highly compacted and informative set of features for enhancing processing and efficacy. Here, LBP, LOOP, GBP, and HoG are extracted and then, colour histogram features are applied. Thereafter artery to vein ratio, entropy, kurtosis perimeter, and area are determined. To perform feature extraction G_y is given as an input, such that,

$$G_y = \{J_y, U_y, O_y\} \tag{51}$$

3.6.1. Lbp

LBP (NarainPonraj et al. 2018) is primarily established for 3×3 neighborhoods, delivering 8-bit codes based on neighbour pixels surrounding the core one. For a known pixel (xy_ρ, ab_ρ), the output LBP in decimal form may be calculated as follows,

$$Z_1 = LBP(xy_\rho, ab_\rho) = \sum_{cd=0}^{7} H(ij_{mn} - ij_\rho) 2^{cd} \tag{52}$$

Here, cd specifies 8 neighbours of the central pixel whereas ij_ρ and ij_{mn} signifies grey level values of a central pixel as well as surrounding pixels. A function H( ) is illustrated by,

$$H(\ ) = \begin{cases} 1\ if & \geq 0 \\ 0\ if & < 0 \end{cases} \tag{53}$$

Here, LBP is symbolised by Z_1 .

3.6.2. Loop

LOOP (Narain Ponraj *et al.* 2018) pattern is referred to the non-linear integration of LBP and LDP (Local Directional Pattern). LOOP is employed to ease the shortcomings of LBP and LDP. The pattern inclusion is assigned to each neighbourhood pixel by binarization weights. A value of LOOP for the pixel (xy_ρ, ab_ρ) can be illustrated by,

$$Z_2 = LOOP(xy_\rho, ab_\rho) = \sum H(ij_{mn} - ij_\rho) . 2^{kl_{mn}} \tag{54}$$

Where,

$$H(\ ) = \begin{cases} 1 & 1muif \quad \geq 0 \\ 0 & otherwise \end{cases} \quad (55)$$

The LOOP can be indicated by Z_2 .

3.6.3. Gbp

GBP (Praveena 2017) is the texture operation commonly helpful in diverse computer-vision problems like classification of texture, acknowledgement of face, and subtraction of background. GBP portrays all pixels by corresponding dim evaluations of neighbour pixels. GBP operator explains individual pixels by the corresponding gradient in diverse pixel directions. GBP value of the pixel at a location (XY, TU) can be modelled by,

$$\begin{aligned} Z_3 = GBP(XY, TU) = &u(\|\Im_1(XY, TU)\| - \|\Im_4(XY, TU)\|) \\ &+ u(\|\Im_3(XY, TU)\| - \|\Im_4(XY, TU)\|)2^1 \\ &+ u(\|\Im_1(XY, TU)\| - \|\Im_2(XY, TU)\|)2^2 \\ &+ \sum_{vw=1}^{4} u(\Im_{vw}(XY, TU))2^{7-vw} \end{aligned} \quad (56)$$

$$u(\ ) = \begin{cases} 1 & 1muif \quad \geq 0 \\ 0 & otherwise \end{cases} \quad (57)$$

Here, $\Im_2$ and $\Im_4$ are gradients in a horizontal direction and vertical direction whereas $\Im_1$ and $\Im_3$ are gradients in other diagonal directions. GBP value is an integer between 0 and 2^7-1. A histogram measurement is 2^7 and a GBP values histogram is computed for texture description and organisation. GBP feature is indicated by Z_3 .

3.6.4. HoG

HoG (Antonik et al. 2019) is based on Scale-Invariant Features transform (SIFT) descriptors. For the computation of the HoG descriptor, initially, vertical as well as horizontal gradients are evaluated by filtering an image with the below-mentioned kernels.

$$GR_{\alpha\beta} = (-1, 0, 1) \quad (58)$$

$$GR_{\omega\varpi} = \begin{pmatrix} -1 \\ 0 \\ 1 \end{pmatrix} \quad (59)$$

Thereafter, the magnitude $mg(\alpha\beta, \omega\varpi)$ and orientation $\theta(\alpha\beta, \omega\varpi)$ of the gradients are estimated for individual pixel utilisation,

$$mg(\alpha\beta, \omega\varpi) = \sqrt{AX_{\alpha\beta}^2 + AX_{\omega\varpi}^2} \quad (60)$$

$$\theta(\alpha\beta, \omega\varpi) = \arctan\left(\frac{AX_{\alpha\beta}}{AX_{\omega\varpi}}\right) \quad (61)$$

Here, $AX_{\alpha\beta}$. and $AX_{\omega\varpi}$. denote the approximation of the horizontal gradient as well as the vertical gradient. The HoG feature can be represented by a term Z_4 .

From the above-mentioned features, textural feature images are obtained that are denoted by κ_1 , such that,

$$\kappa_1 = \{Z_1, Z_2, Z_3, Z_4\} \quad (62)$$

3.6.5. Color histogram features

Colour histogram features (Sergyan 2008) are applied to textural feature images, which is termed as κ_1 . A colour channel's levels of brightness or the number of pixels at each value are measured in an image's histogram. A histogram's outline provides information about the natural effect of an image or sub-image while considering the item inside the picture.

The histogram characteristics under consideration are statistically enabled, with the histogram employing a probability distribution model of the intensity levels. The statistical characteristics provide information about the qualities of an image's intensity level distribution. A probability of a first-order histogram can be defined by,

$$PR(gl) = \frac{B(gl)}{NP} \quad (63)$$

Where, NP indicates the count of pixels in an image. When the whole image is underneath a consideration, then $NP = B^2$ for $B \times B$ image and $B(gl)$ specifies the count of pixels at the grey-level gl . By applying colour histogram features, an image is obtained such that,

$$\kappa_2 = \{Zi_1, Zi_2, Zi_3, Zi_4\} \quad (64)$$

Thereafter, artery-to-vein ratio, entropy, kurtosis, eccentricity, perimeter, and area are determined κ_2 .

3.6.6. Artery-to-vein ratio

The mean of arteriole and venule width, sum of arteriole and venule widths, sum of squares of arteriole and venule widths, central retinal artery equivalent (CRAE), and central retinal venous equivalent (CRVE) are used to calculate the artery-to-vein ratio (Hubbard et al. 1999). For quantifying generalised narrowing as an artery-to-vein ratio, the calibrations of each arteriole, as well as venules, are combined that can be formulated by,

$$Arterioles\ CT = \sqrt{0.87\,CS^2 + 1.01\,CL^2 - 0.22\,CS\,CL - 10.76} \quad (65)$$

$$Venules\ CT = \sqrt{0.72\,CS^2 + 0.91\,CL^2 + 450.05} \quad (66)$$

Where CT indicates the trunk vessel's calibre, CS signifies the smaller branch's calibre, and CL represents the larger branch's calibre. The artery-to-vein ratio is signified by a term K_1 .

3.6.7. Area

Area (Butusov and Dikusar 2018) is an overall count of pixels that forms pattern objects in the binary image and can be formulated by,

$$K_2 = EF_{gh} \sum_{(px,py)\in\Omega_{gh}} 1 \quad (67)$$

Here, (px, py) implies pixel and Ω_{gh} indicates a group of every pixel that forms gh object.

3.6.8. Entropy

Entropy (Mall et al. 2019) calibrates a degree of uniformity among pixels within an image and randomness is utilised for characterising the texture of an image. Entropy can be given by the formula mentioned beneath.

$$K_3 = \sum_{ef=0}^{RS-1} \sum_{tu=0}^{RS-1} PX(ef, tu) \log(PX(ef, tu)) \qquad (68)$$

Here, ef and tu symbolizes the coefficients of element and coordinates of an element.

3.6.9. Eccentricity

It denotes an eccentricity (Butusov and Dikusar 2018) of the ellipse, which has similar second-moments as the object. The eccentricity is computed as follows.

$$K_4 = \frac{\sqrt{AL_{max}^2 - AL_{min}^2}}{AL_{max}} \qquad (69)$$

Here, AL_{max} and AL_{min} represent the length of the maximal and minimal axis of inertia.

3.6.10. Kurtosis

It is defined as a probability distribution measure of an actual value random variable. It is a shape descriptor of probability distribution and can be illustrated by,

$$K_5 = \frac{\sum \left(MN - \overline{MN_1}\right)^4}{dSD_3} \qquad (70)$$

Here, MN and SD reveals the mean and standard deviation.

3.6.11. Perimeter

The perimeter (Butusov and Dikusar 2018) is evaluated by computing a distance among individual adjoining pairs of pixels about the boundary of an area. A perimeter can be signified as K_6.

Thus, a feature vector is attained indicated by K_y, such that,

$$K_y = \{K_1, K_2, K_3, K_4, K_5, K_6\} \qquad (71)$$

3.7. DR classification utilizing deep CNN

The classification of DR is a complex chore owing to vital visual dissimilarities in lesion sizes amid fundus images of similar classes and the visual resemblance in shapes as well as colours amongst fundus images of two diverse classes. Here, the classification of DR is conducted utilising Deep CNN (Tu et al. 2017) which is skilled by GSCA. An input regarded for executing the classification phase of DR is K_y.

3.7.1. Architecture of deep CNN

A feed-forward network called CNN (Rawat and Wang 2017), where from input to output the flow of information takes place. The CNN structure is available in a variety of configurations. In general, it consists of pooling and convolutional layers, which are then built into modules. Then, like in essential feed-forward neural networks, several fully connected (FC) layers are added. To make a deep system, these modules are commonly layered on top of one another. The input picture is directly fed into the network by several phases of the convolution layer as well as the pooling layer. Then, representations of these functions are assigned to one or more FC levels. Finally, the FC layer outputs a list of class labels.

(i) Convolutional layers: This layer serves as extractors of features and hence it learns to feature illustrations of an input image. The feature maps are set with the neurons from the convolution layers. A set of trainable weights, commonly referred to as a filter bank, connects a particular neuron's receptive field in a feature map to a neighbourhood of neurons in the preceding layer. For creating updated feature maps, the inputs undergo convolution with learnt weights, and the convolutional outputs are then subjected to a nonlinear activation function. The weights of each neuron in the feature map are required to be similar. Moreover, several feature maps inside similar convolutional layers contain several weights, and hence numerous features are extracted at individual positions.

$$V_r = f(Q_r * s) \qquad (72)$$

Here, an input image is indicated by s, a convolutional filter corresponding to r^{th} feature map is signified by Q_r whereas $*$ represents a two-dimensional convolution operator that is utilised for calculating an interior product of the filter position of the input image, and $f(.)$ denotes a nonlinear activation function.

(ii) Pooling layers: Pooling layers try to provide spatial invariance to input deformations and translations while reducing the spatial resolution of feature maps. Average pooling layers are commonly used to propagate the average of every input value of a smaller neighbourhood of an image to the next layer. Furthermore, max-pooling layers distribute the maximum value inside a receptive field to the next layer. A max-pooling layer chooses a large element within the individual receptive field and can be given by,

$$V_{r\varphi\psi} = \max_{(pp,qq)\in K_{\varphi\psi}} s_{r\,pp\,qq} \qquad (73)$$

Here, the output of the pooling function related to r^{th} feature map is specified by $V_{r\varphi\psi}$, $s_{r\,pp\,qq}$ implies element at the position (pp, qq) comprised by the pooling region $K_{\varphi\psi}$ that embodies the receptive field across the location (φ, ψ).

(iii) FC layer: Various convolutional and pooling layers are typically layered on top of one another to gain multiple abstract feature descriptions while travelling through a network. FC layers, which pursue these layers describe feature depictions and execute higher-level reasoning functions. For classification purposes, it is basic to utilise the softmax operator at the top of Deep CNN.

The classified output from deep CNN is implied by N_y. The deep CNN structure is demonstrated in Figure 3.

3.7.2. Training of deep CNN utilising GSCA

GOA (Pan et al. 2022) is a naturally enthused algorithm that is stimulated by predation characteristics of gannets naturally. It has minimal running time in higher dimensions and also, it offers the best solution. This approach is also highly suitable for various constrained engineering problems. For solving real time issues, the SCA (Mirjalili 2016) is highly
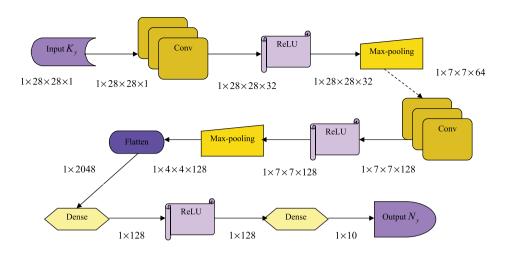
Figure 3. The architecture of Deep CNN.

efficient with constrained as well as unknown searching spaces. Here, GSCA is used to train Deep CNN for the classification of DR. The steps followed by GSCA are previously interpreted in section 3.4.2.

Fitness measure: The fitness computation is conducted by evaluating a variation among target as well as Deep CNN outputs and can be illustrated by,

$$X_2 = \frac{1}{e}\sum_{y=1}^{e}\left[T_y - N_y\right]^2 \tag{74}$$

Where, N_y and T_y signifies Deep CNN and target outputs.

4. Results and discussion

U-Net_GSCA and GSCA_DeepCNN performed more effectively in the DR segmentation and classification, as seen in the sections below.

4.1. Experimentation setup

The setup is done by PYTHON tool for U-Net_GSCA DR segmentation and GSCA_DeepCNN for DR classification.

4.2. Description of dataset

The Indian diabetic retinopathy image dataset (IDRID) https://ieee-dataport.org/open-access/indian-diabetic-retinopathy-image-dataset-idridis classified into three portions namely segmentation that comprises 81 actual colour fundus images in JPG files, ground truth images for lesions in TIF files and optic disc in TIF files. Then comes disease grading, which includes 516 real-colour fundus photos in JPG format, as well as ground truth labels for DR in a CSV file. Finally, there are 516 genuine colour fundus photographs in JPG format, ground truth labels for an optic disc centre position in a CSV file, and ground truth labels for a fovea centre location in a CSV file in localisation.

4.3. Experimental outcomes

Experimentally acquired outcomes with the designed approaches are interpreted in Figure 4. Figure 4(a–i) delineates input image-1, filtered image-1, colour spacing image-1, rotated image-1, brightness image-1, segmented image-1, sparking image-1, LBP image-1, HoG image-1 whereas input image-2, filtered image-2, colour spacing image-2, rotated image-2, brightness image-2, segmented image-2, sparking image-2, LBP image-2, HoG image-2 are revealed in Figure 4 (j–r).

4.4. Performance metrics

The measures that are regarded for assessment are Accuracy, Specificity, and Sensitivity, which are explicated as follows.

4.4.1. Accuracy
It states the percentage of DR-affected patients that have been classified accurately and can be modelled by,

$$\lambda_1 = \frac{NE_{TR} + PO_{TR}}{PO_{TR} + PO_{FS} + NE_{TR} + NE_{FS}} \tag{75}$$

Here, the value of true positive is PO_{TR} and the value of true negative is whereas PO_{FS} and NE_{FS} are the value of false positive and false negative.

4.4.2. Sensitivity
It is a proportion of patients whose test outcome is positive for DR amongst the patients affected with DR. It can be given by,

$$\lambda_2 = \frac{PO_{TR}}{PO_{TR} + NE_{FS}} \tag{76}$$

4.4.3. Specificity
The specificity is referred to as a proportion of healthier patients does not have DR, whose test outcome is negative and can be expressed by,
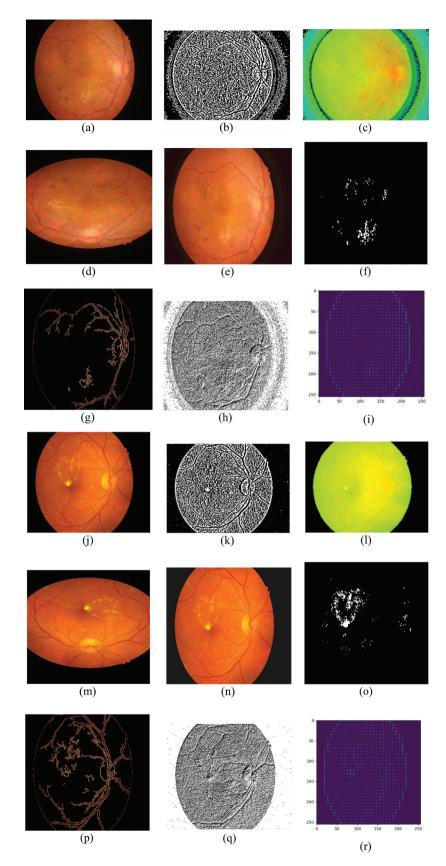
Figure 4. Experimentation outcomes of designed approaches, (a) input image-1, (b) filtered image-1, (c) color spacing image-1, (d) rotated image-1, (e) brightness image-1, (f) segmented image-1, (g) sparking image-1,(h) LBP image-1, (i) HoG image-1, (j) input image-2, (k) filtered image-2, (l) color spacing image-2, (m) rotated image-2, n) brightness image-2, (o) segmented image-2, (p) sparking image-2, (q) LBP image-2, (r) HoG image-2.

$$\lambda_3 = \frac{NE_{TR}}{NE_{TR} + PO_{FS}} \qquad (77)$$

4.5. Performance analysis

By changing the values of training data and k value, the performance analysis is executed.

4.5.1. Assessment based on training data

In Figure 5 the analysis of GSCA_DeepCNN to reveal performance regarding measures for evaluation by changing training data is signified. Figure 5a) elucidates an evaluation based on accuracy. For 90% of the training data, GSCA_DeepCNN gains the accuracy of 0.836 with epochs-20, 0.856 with epochs-40, 0.876 with epochs-60, 0.897 with epochs-80 and 0.903 with epochs-100. Estimation with respective to sensitivity is interpreted in Figure 5b). Sensitivity gained by the GSCA_DeepCNN is 0.822, 0.855, 0.873, 0.890, and0.900 with epochs 20, 40, 60, 80, and 100 when training data is considered as 90%. Figure 5c) describes the evaluation regarding specificity. The specificity value achieved by designed GSCA_DeepCNN is 0.822

with epochs-20, 0.853 with epochs-40, 0.874 with epochs-60, 0.892 with epochs-80 and 0.901 with epochs-100 when training data is considered as 90%.

4.5.2. Assessment based upon k-fold values

Figure 6 demonstrates the performance analysis of metrics by varying training data with diverse epochs. An assessment regarding accuracy is shown in Figure 6a). The value of accuracy achieved by GSCA_DeepCNN is 0.834, 0.856, 0.876, 0.898, and 0.914 with epochs 20, 40, 60, 80, and 100 for the value of k-fold = 9. Figure 6b) reveals evaluation based on sensitivity. Sensitivity achieved by GSCA_DeepCNN is 0.825 with epochs-20, 0.854 with epochs-40, 0.878 with epochs-60, 0.895 with epochs-80 and 0.904 with epochs-100 when considering k-fold value = 90%. Figure 6c) implies analysis in terms of specificity. The specificity obtained by GSCA_DeepCNN is 0.827, 0.850, 0.875, 0.898, and 0.906 with epochs 20, 40, 60, 80, and 100 for k-fold = 9.

4.6. Comparative techniques

The approaches compared with GSCA_DeepCNN are DL (Saini and Susan 2022), MVDRNet (Luo et al. 2021), 3D-CNN (Tufail

(a)

(b)

(c)

Figure 5. Performance assessment based upon training data, a) Accuracy, b) Sensitivity, c) Specificity.

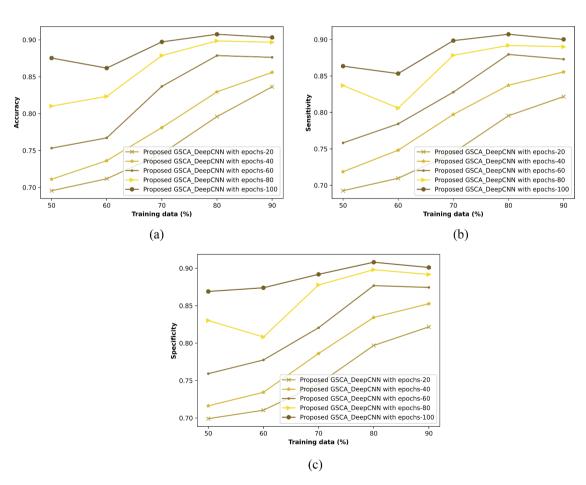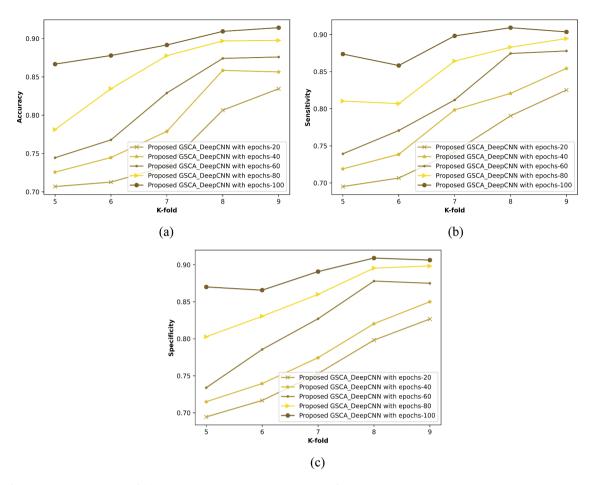Figure 6. Performance analysis based on k-fold value, (a) Accuracy, (b) Sensitivity, (c) Specificity.

et al. 2021), CapsNet (Kalyani et al. 2021), SVMGA (Gharaibeh et al. 2018), and SVM-MLC (Gharaibeh et al. 2021) to show the efficacy of the devised approach.

4.7. Comparative assessment

By altering training data percentages and k-fold values, the comparative assessment of GSCA_DeepCNN is done.

4.7.1. Assessment based upon training data

Figure 7 interprets the analysis of GSCA_DeepCNN regarding metrics by varying training data percentages. Figure 7a) explicates an estimation of GSCA_DeepCNN based on accuracy. The value of accuracy gained by GSCA_DeepCNN is 0.922 while DL, MVDRNet, 3D-CNN, CapsNet, SVMGA, and SVM-MLC obtained 0.829, 0.860, 0.875, 0.895, 0.895, and 0.896. It indicated a performance improvement of 10.086%, 6.724%, 5.097%, 2.928%, 2.928%, and 2.819% when comparing DL, MVDRNet, 3D-CNN, CapsNet, SVMGA, and SVM-MLC for training data = 90%. Evaluation of sensitivity is shown in Figure 7b). When training data is 90%, sensitivity value acquired by GSCA_DeepCNN is 0.925 whereas sensitivity obtained by DL is 0.829, MVDRNet is 0.858, 3D-CNN is 0.880, CapsNet is 0.900, SVMGA is 0.900 and SVM-MLC is 0.903 that exposed performance improvement of 10.378%,

7.243%, 4.864%, 2.702%, 2.702%, and 2.378%. Analysis of GSCA_DeepCNN considering specificity is demonstrated in Figure 7c). For training data = 90%, the specificity value acquired by GSCA_DeepCNN is 0.919 whereas values acquired by DL are 0.835, MVDRNet is 0.856, 3D-CNN is 0.870, CapsNet is 0.895, SVMGA is 0.897, and SVM-MLC is 0.899. This enhanced the performance of GSCA_DeepCNN about 9.140%, 6.855%, 5.331%, 2.611%, 2.393%, and 2.176%.

4.7.2. Assessment based upon the k-fold value

By altering k-fold values, the assessment of GSCA_DeepCNN is delineated in Figure 8. An evaluation based on accuracy is expounded in Figure 8a). When k-fold value = 9, the accuracy value obtained by GSCA_DeepCNN is 0.918 while accuracy obtained by DL is 0.825, MVDRNet is 0.851, 3D-CNN is 0.871, CapsNet is 0.892, SVMGA is 0.894, and SVM-MLC is 0.898 that proved performance improvement of 10.130%, 7.298%, 5.119%, 2.832%, 2.614%, and 2.718%. Figure 8b) expounds evaluation of GSCA_DeepCNN considering sensitivity. The sensitivity value acquired by GSCA_DeepCNN is 0.918, whereas DL, MVDRNet, 3D-CNN, CapsNet, SVMGA, and SVM-MLC acquired 0.836, 0.854, 0.874, 0.892, 0.894, and 0.896, while a value of k-fold = 9. Thus, GSCA_DeepCNN showed performance improvement by 8.932%, 6.971%, 4.793%, 2.832%, 2.614%, and 2.396%. Figure 8c) specifies the analysis of
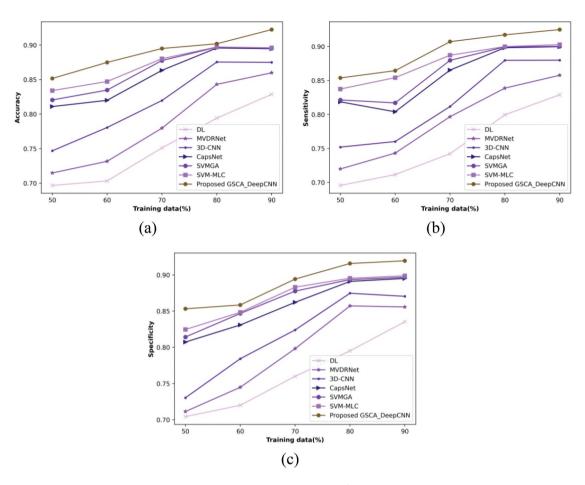
Figure 7. Comparative analysis based upon training data, (a) Accuracy, (b) Sensitivity, (c) Specificity.

GSCA_DeepCNN based on specificity. The specificity value obtained by GSCA_DeepCNN is 0.914 whereas DL, MVDRNet, 3D-CNN, CapsNet, SVMGA, and SVM-MLC obtained 0.839, 0.858, 0.876, 0.896, 0.898 and 0.902. It signified a performance enhancement of 8.205%, 6.126%, 4.157%, 1.969%, 1.750%, and 1.312% when comparing DL, MVDRNet, 3D-CNN, CapsNet, SVMGA, and SVM-MLC for k-fold value = 9.

4.8. Segmentation analysis

By comparing K-Net (Zhang et al. 2021), DeepJoint (Mahesh and Renjit 2020), PSPNet (Zhao et al. 2017), and PSINet (Murugesan et al. 2019) with U-Net_GSCA to reveal the efficiency of the designed technique, segmentation evaluation is performed. Figure 9 shows the segmentation estimation of U-Net_GSCA by changing training data percentages. The segmentation accuracy value acquired by U-Net_GSCA is 0.873 whereas K-Net, DeepJoint, PSPNet, and PSINet achieved segmentation accuracy of 0.706, 0.724, 0.745, and 0.783. Hence, performance enhancement of U-Net_GSCA when considering K-Net, DeepJoint, PSPNet, and PSINet is 19.094%, 17.066%, 14.662%, and 10.329% for 50% of training data. The segmentation accuracy attained by U-Net_GSCA is

0.926 by using 90% of training data whereas segmentation accuracy acquired by K-Net is 0.838, DeepJoint is 0.860, PSPNet is 0.878 and PSINet is 0.898, which revealed the improvement of performance by 9.546%, 7.137%, 5.194%, and 3.018 %.

4.9. Segmentation analysis discussion

U-Net_GSCA acquired better segmentation outcomes that are explicited in Table 1. It is accepted that U-Net_GSCA achieved a maximum of segmentation accuracy of about 92.6% for the training data 90%.

4.10. Comparative discussion

For comparative discussion, 90% of training data and the k value of 9 is taken. The proposed GSCA_DeepCNN achieved the best results while comparing with existing DL, MVDRNet, 3D-CNN, CapsNet, SVMGA, and SVM-MLC techniques. Table 2 shows the values obtained by GSCA_DeepCNN and the existing methods. It reveals the achievement of GSCA_DeepCNN with maximum accuracy, sensitivity, and specificity of 92.2%, 92.5%, and 91.9%.
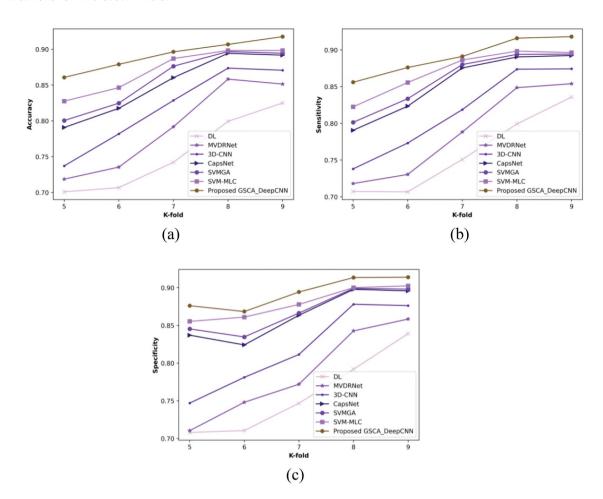
Figure 8. Comparative analysis based on training data, (a) Accuracy, (b) Sensitivity, (c) Specificity.
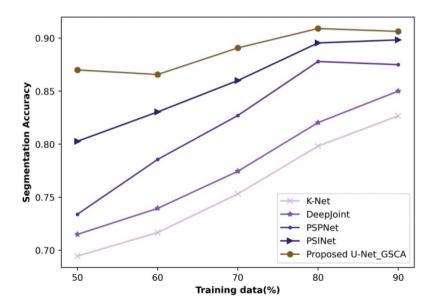
Figure 9. Segmentation analysis of U-Net_GSCA.

Table 1. Segmentation assessment discussion of U-Net_GSCA.

Analysis based upon	Metrics/Methods	K-Net	DeepJoint	PSPNet	PSINet	Proposed U-Net_GSCA
Training data=50%	Segmentation accuracy	70.6%	72.4%	74.5%	78.3%	87.3%
Training data=90%	Segmentation accuracy	83.8%	86.0%	87.8%	89.8%	92.6%

Table 2. Comparative discussion of GSCA_DeepCNN.

Analysis based upon	Metrics/Methods	DL	MVDRNet	3D-CNN	CapsNet	SVMGA	SVM-MLC	Proposed GSCA_ DeepCNN
Training data=90%	Accuracy	82.9%	86.0%	87.5%	89.5%	89.5%	89.6%	92.2%
	Sensitivity	82.9%	85.8%	88.0%	90.0%	90.0%	90.3%	92.5%
	Specificity	83.5%	85.6%	87.0%	89.5%	89.7%	89.9%	91.9%
K-fold value=9	Accuracy	82.5%	85.1%	87.1%	89.2%	89.4%	89.8%	91.8%
	Sensitivity	83.6%	85.4%	87.4%	89.2%	89.4%	89.6%	91.8%
	Specificity	83.9%	85.8%	87.6%	89.6%	89.8%	90.2%	91.4%

5. Conclusion

DR is the usual eye complexity of diabetes as well as a reason for vision impairment and vision loss. Automatic and precise DR grading is of high importance for the timely and efficient treatment of fundus ailments. Present medical techniques remain a focus on potent time consumption and higher risk. In this work, U-Net_GSCA is employed for DR segmentation and GSCA_DeepCNN is employed for DR classification. First, pre-processing is carried. Then, image augmentation is carried out wherein augmentation techniques like colour spacing, brightness, and rotation are utilised for increasing the effectiveness of the feature extraction process. Afterward, lesion segmentation is performed with U-Net which is trained by GSCA. GSCA is formed by combining GOA and SCA. Thereafter, the segmentation of the artery and vein is done by the sparking process. Finally, the classification of DR is conducted utilising Deep CNN, which is trained by GSCA. Furthermore, the proposed method U-Net_GSCA attained higher segmentation accuracy of 92.6% whereas GSCA_DeepCNN achieved higher accuracy, sensitivity, and specificity of 92.2%, 92.5%, and, 91.9% for 90% of training data. In the future, the outcomes from the network used are positive in terms of the established network structure. CNNs may one day be of great use to DR doctors as networks and datasets develop and they can offer real-time classifications. The development of networks and datasets in the future is helpful for DR physicians and they can offer real-time classification.

Disclosure statement

No potential conflict of interest was reported by the author(s).

References

Aiello LM, Berrocal J, Davis MD, Ederer F, Goldberg MF, Harris JE, Klimt CR, Knatterud GL, Margherio RR, McLean EN, et al. 1974. The diabetic retinopathy study-reply. Arch Ophthalmol. 92(2):179–180. doi: 10.1001/archopht.1974.01010010185024.

Akram MU, Khalid S, Khan SA. 2013. Identification and classification of microaneurysms for early detection of diabetic retinopathy. Pattern Recogn. 46(1):107–116. doi: 10.1016/j.patcog.2012.07.002.

AlBalushi FM. 2020. Bat optimization assisted diabetic retinopathy detection framework. Multi Res. 3(2):20–26. doi: 10.46253/j.mr.v3i2.a3.

Al-Hazaimeh OM, Abu-Ein AA, Tahat NM, Al-Smadi MM, Al-Nawashi MM. 2022. Combining artificial intelligence and image processing for diagnosing diabetic retinopathy in retinal fundus images. Int J Onl Eng. 18(13):131–151. doi: 10.3991/ijoe.v18i13.33985.

Antonik P, Marsal N, Brunner D, Rontani D. 2019. Human action recognition with a large-scale brain-inspired photonic computer. Nat Mach Intell. 1(11):530–537. doi: 10.1038/s42256-019-0110-8.

Butusov O, Dikusar V. 2018. Image pattern analysis with image potential transform. Metody Ilościowe w Badaniach Ekonomicznych. 19(1):12–27. doi: 10.22630/MIBE.2018.19.1.2.

Decenciere E, Cazuguel G, Zhang X, Thibault G, Klein JC, Meyer F, Marcotegui B, Quellec G, Lamard M, Danno R, et al. 2013. TeleOphta: machine learning and image processing methods for teleophthalmology. Irbm. 34(2):196–203. doi: 10.1016/j.irbm.2013.01.010.

Fayyaz AM, Sharif MI, Azam S, Karim A, El-Den J. 2023. Analysis of Diabetic Retinopathy (DR) based on the deep learning. Information (Switzerland). 14(1). doi: 10.3390/info14010030.

Gharaibeh N, Al-Hazaimeh OM, Abu-Ein A, Nahar KM. 2021. A hybrid SVM NAÏVE-BAYES classifier for bright lesions recognition in eye fundus images. Int J Electr Eng Inform. 13(3):530–545. doi: 10.15676/ijeei.2021.13.3.2.

Gharaibeh N, Al-Hazaimeh OM, Al-Naami B, Nahar KM. 2018. An effective image processing method for detection of diabetic retinopathy diseases from retinal fundus images. Int J Signal Imag Syst Eng. 11(4):206. doi: 10.1504/IJSISE.2018.093825.

Heisler M, Karst S, Lo J, Mammo Z, Yu T, Warner S, Maberley D, Beg MF, Navajas EV, Sarunic MV. 2020. Ensemble deep learning for diabetic retinopathy detection using optical coherence tomography angiography. Transl Vis Sci Technol. 9(2):20–20. doi: 10.1167/tvst.9.2.20.

Hubbard LD, Brothers RJ, King WN, Clegg LX, Klein R, Cooper LS, Sharrett AR, Davis MD, Cai J, Atherosclerosis Risk in Communities Study Group. 1999. Methods for evaluation of retinal microvascular abnormalities associated with hypertension/sclerosis in the atherosclerosis risk in communities study. Ophthalmology. 106(12):2269–2280. doi: 10.1016/S0161-6420(99)90525-0.

Kalyani G, Janakiramaiah B, Karuna A, Prasad LN. 2021. Diabetic retinopathy detection and classification using capsule networks. Complex Intell Syst. 9(3):1–14. doi: 10.1007/s40747-021-00318-9.

Khalifa NE, Loey M, Mirjalili S 2022. A comprehensive survey of recent trends in deep learning for digital images augmentation. Artificial Intelligence Review.1–27.

Khan Z, Khan FG, Khan A, Rehman ZU, Shah S, Qummar S, Ali F, Pack S. 2021. Diabetic retinopathy detection using VGG-NIN a deep learning architecture. IEEE Access. 9:61408–61416. doi:10.1109/ACCESS.2021.3074422.

Khan SS, Ran Q, Khan M, Ji Z. 2019. Pan-sharpening framework based on laplacian sharpening with Brovey. In 2019 IEEE International Conference on Signal, Information and Data Processing (ICSIDP); Chongqing, China. p. 1–5.

Luo X, Pu Z, Xu Y, Wong WK, Su J, Dou X, Ye B, Hu J, Mou L. 2021. Mvdrnet: multi-view diabetic retinopathy detection by combining DCNNs and attention mechanisms. Pattern Recogn. 120:108104. doi:10.1016/j.patcog.2021.108104.

Mahesh KM, Renjit JA. 2020. DeepJoint segmentation for the classification of severity-levels of glioma tumor using multimodal MRI images. Iet Image Process. 14(11):2541–2552. doi: 10.1049/iet-ipr.2018.6682.

Mall PK, Singh PK, Yadav D. 2019. Glcm based feature extraction and medical x-ray image classification using machine learning techniques. In 2019 IEEE Conference on Information and Communication Technology; Allahabad, India. p. 1–6.

Mane VM, Jadhav DV. 2017. Holoentropy enabled-decision tree for automatic classification of diabetic retinopathy using retinal fundus images. Biomed Tech (Berl). 62(3):321–332. doi: 10.1515/bmt-2016-0112.

Mirjalili S. 2016. SCA: a sine cosine algorithm for solving optimization problems. Knowl Based Syst. 96:120–133. doi: 10.1016/j.knosys.2015.12.022.

Murugesan B, Sarveswaran K, Shankaranarayana SM, Ram K, Joseph J, Sivaprakasam M. 2019. July. Psi-net: shape and boundary-aware joint

multi-task deep network for medical image segmentation. In 2019 41st Annual international conference of the IEEE Engineering in Medicine and biology society (EMBC); Berlin, Germany. p. 7223–7226.

Nair AT, Muthuvel K. 2019. Diabetic retinopathy recognition using enhanced crow search with levy flight algorithm. Multi Res. 2(4):43–52.

NarainPonraj D, Christy E, Aneesha G, Susmitha G, Sharu M. 2018. Analysis of LBP and LOOP-based textural feature extraction for the classification of CT Lung images. In 2018 4th International Conference on Devices, Circuits and Systems (ICDCS); Coimbatore, India. p. 309–312.

Özbay E. 2022. An active deep learning method for diabetic retinopathy detection in segmented fundus images using artificial bee colony algorithm. Artif Intell Rev. 56(4):1–28. doi: 10.1007/s10462-022-10231-3.

Pan JS, Zhang LG, Wang RB, Snášel V, Chu SC. 2022. Gannet optimization algorithm: a new metaheuristic algorithm for solving engineering optimization problems. Math Comput Simul. 202:343–373. doi: 10.1016/j.matcom.2022.06.007.

Praveena KS. 2017. A classical hierarchy method for bone x-ray image classification using SVM. Int Res J Eng Technol (IRJET). 4(8):991–993.

Qummar S, Khan FG, Shah S, Khan A, Shamshirband S, Rehman ZU, Khan IA, Jadoon W. 2019. A deep learning ensemble approach for diabetic retinopathy detection. IEEE Access. 7:150530–150539. doi: 10.1109/ACCESS.2019.2947484.

Ramzan M, Raza M, Sharif MI, Kadry S. 2022. Gastrointestinal tract polyp anomaly segmentation on colonoscopy images using Graft-U-Net. J Pers Med. 12(9):1459. doi: 10.3390/jpm12091459.

Rawat W, Wang Z. 2017. Deep convolutional neural networks for image classification: a comprehensive review. Neural Comput. 29 (9):2352–2449. doi: 10.1162/neco_a_00990.

Saini M, Susan S. 2022. Diabetic retinopathy screening using deep learning for multi-class imbalanced datasets. Comput Biol Med. 149:105989. doi: 10.1016/j.compbiomed.2022.105989.

Sergyan S. 2008. January. Color histogram features based image classification in content-based image retrieval systems. In 2008 6th international symposium on applied machine intelligence and informatics; Herlany, Slovakia. p. 221–224.

Shaukat N, Amin J, Sharif MI, Kadry S, Sevcik L, Sevcik L. 2023. Classification and segmentation of diabetic retinopathy: a systemic review. Appl Sci. 13(5):3108. doi: 10.3390/app13053108.

Siddique N, Paheding S, Elkin CP, Devabhaktuni V. 2021. U-net and its variants for medical image segmentation: a review of theory and applications. IEEE Access. 9:82031–82057. doi: 10.1109/ACCESS.2021.3086020.

Sugeno A, Ishikawa Y, Ohshima T, Muramatsu R. 2021. Simple methods for the lesion detection and severity grading of diabetic retinopathy by image processing and transfer learning. Comput Biol Med. 137:104795. doi:10.1016/j.compbiomed.2021.104795.

Tufail AB, Ullah I, Khan WU, Asif M, Ahmad I, Ma YK, Khan R, Ali MS, Ali MS. 2021. Diagnosis of diabetic retinopathy through retinal fundus images and 3D convolutional neural networks with limited number of samples. Wireless Commun Mobile Comput. 2021:1–15. doi: 10.1155/2021/6013448.

Tu F, Yin S, Ouyang P, Tang S, Liu L, Wei S. 2017. Deep convolutional neural network architecture with reconfigurable computation patterns. Ieee T Vlsi Syst. 25(8):2220–2233. doi: 10.1109/TVLSI.2017.2688340.

Zeng X, Chen H, Luo Y, Ye W. 2019. Automated diabetic retinopathy detection based on binocular siamese-like convolutional neural network. IEEE Access. 7:30744–30753. doi: 10.1109/ACCESS.2019.2903171.

Zhang W, Pang J, Chen K, Loy CC. 2021. K-net: towards unified image segmentation. Adv Neural Inf Process Syst. 34:10326–10338.

Zhao H, Shi J, Qi X, Wang X, Jia J. 2017. Pyramid scene parsing network. In Proceedings of the IEEE conference on computer vision and pattern recognition; Honolulu, HI, USA. p. 2881–2890.

SPRINGER LINK

Menu   Search   Cart

A survey on Motion Artifact Correction in Magnetic Resonance Imaging for Improved Diagnostics

SN Computer Science

Aims and scope

Submit manuscript

Vijay R. Tripathi ✉, Manish N. Tibdewal & Ravi Mishra

Abstract

Motion artifacts occur in magnetic resonance imaging (MRI) due to the motion or movement of the object being scanned. Motion artifacts can have various origins such as voluntary or involuntary patient movement, faulty components, improper software configuration, etc. Blurry MRI scans are generated due to the presence of motion artifacts. In some cases motion artifact induced MRI scans can tamper with crucial information and consequently leads to a faulty diagnosis. We attempt to provide a review of current suggested technologies (such as, deep learning, and encoding) used to remove motion artifacts from

SPRINGER LINK

Log in
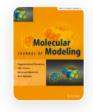
☰ Menu   🔍 Search   🛒 Cart

Home   Journal of Molecular Modeling   Article

Performance analysis of un-doped and doped titania (TiO) as an electron transport layer (ETL) for perovskite solar cells

Original Paper   Published: 01 May 2024

Volume 30, article number 154, (2024)   Cite this article

Journal of Molecular Modeling

Aims and scope

Submit manuscript

Neerja Dharmale ✉, Aadhityan A ✉, Ashutosh Srivastava & Saurabh Chaudhury

👁 170 Accesses   Explore all metrics →

Abstract

Context

Density functional theory (DFT) calculations are carried out on pure and doped rutile TiO_2. The bandgap (E_g) for pristine, S-doped, Fe-doped, and Fe/S co-doped materials is direct, with values of 2.98 eV, 2.18 eV, 1.58 eV, and 1.40 eV. The effective mass of charge carriers (m*) and ratio of effective masses of holes to effective masses of electrons (R) are also investigated, and it is discovered that Fe/S co-doped materials have the lowest charge carrier recombination rate. The Fe/S co-doped material has the highest $\varepsilon(\omega). \alpha(\omega)$ of doped

Home

Subject⟩   Journals   Books   Major Reference Works   Resources For Partners⟩   Open Access

About Us⟩   Help⟩

Cookies Notification

Abstract

The study utilizes the OLCAO-LBFGS-GGA-PBESol method to investigate the structural properties of both doped and undoped brookite TiO$_2$. Electronic characteristics are explored employing the OLCAO-LBFGS-MGGA-TB09+c approach. Detailed analyses of Density of States (DOS) and Partial Density of States (PDOS) are conducted to understand band structures. Both doped and undoped scenarios exhibit a direct bandgap. Moreover, doping induces a reduction in the bandgap value, enhancing its potential for photovoltaic and photocatalytic applications. The study also establishes a strong agreement between the derived lattice parameters and bandgap for pure brookite TiO$_2$ and experimental lattice parameters and bandgap value.

Keywords: DFT ▪ structural properties ▪ electronic properties

Access content

To read the fulltext, please use one of the options below to sign in or purchase access.

Personal login
Institutional Login
Register for access

Purchase   Save for later

Article Online Access

SPRINGER LINK

Log in

Menu   Search   Cart

Home   The Visual Computer   Article

A powerful method for interactive content-based image retrieval by variable compressed convolutional info neural networks

Original article   Published: 01 October 2023

(2023)   Cite this article

The Visual Computer

Aims and scope

Submit manuscript

Vishwanath S. Mahalle ✉, Narendra M. Kandoi & Santosh B. Patil

🔖 115 Accesses   Explore all metrics →

Abstract

There is a need for efficient methods to retrieve and obtain the visual data that a client need. New methods for content-based image retrieval (CBIR) have emerged due to recent developments in deep neural networks. However, there are still issues with deep neural networks in interactive CBIR systems like the search goal needs to be preset, scrambling and the computational cost is too high for an online environment. By this concern, this manuscript proposes an effective interactive CBIR that accurately retrieves images in response to the image query using variable compressed convolutional info neural networks

SPRINGER LINK

≡ Menu   🔍 Search   🛒 Cart

Denoising of motion artifacted MRI scans using conditional generative adversarial network

Multimedia Tools and Applications

Aims and scope

Submit manuscript

Vijay R. Tripathi ✉, Manish N. Tibdewal & Ravi Mishra

Abstract

Patient motion causes image distortion during Magnetic Resonance Imaging (MRI) capture. These distorted motion artifact induced MRI scans are difficult to read and sometimes lead to a faulty diagnosis. The simplest solution to remove these artifacts in motion-blurred scans is to re-scan the patient. But this method is costly, time-consuming, and cannot guarantee a successful scan even after re-scanning the MRI, because the patient can still move involuntarily. Hence, correction in the motion artifact induced images is an important part of the medical imaging domain. Here we have modified a well-known conditional Generative Adversarial Network called Pix2Pix for removing motion artifacts from MRI scans. We have modified the structure of the original network and fine-tuned the

SPRINGER LINK

Log in

Menu   Search

Cart

A survey on Motion Artifact Correction in Magnetic Resonance Imaging for Improved Diagnostics

SN Computer Science

Aims and scope

Submit manuscript

Vijay R. Tripathi ✉, Manish N. Tibdewal & Ravi Mishra

186 Accesses   Explore all metrics →

Abstract

Motion artifacts occur in magnetic resonance imaging (MRI) due to the motion or movement of the object being scanned. Motion artifacts can have various origins such as voluntary or involuntary patient movement, faulty components, improper software configuration, etc. Blurry MRI scans are generated due to the presence of motion artifacts. In some cases motion artifact induced MRI scans can tamper with crucial information and consequently leads to a faulty diagnosis. We attempt to provide a review of current suggested technologies (such as, deep learning, and encoding) used to remove motion artifacts from

Enhancing thermal efficiency of cookware through fin implantation: experimental analysis and numerical validation

Saurabh P. Joshi[1] · Dnyaneshwar R. Waghole[1]

Abstract

Growing need for non-renewable energy, like petroleum, and its extraction challenges urge scientists to prioritize renewable resources for sustainable energy. Extensive research is addressing domestic LPG overconsumption and energy-saving. This study focuses on enhancing energy efficiency by adding fins to the bottom of specific cookware. To achieve this goal, a study involves the analysis of up to five stainless steel cookwares, each equipped with a unique fin setup designed to enhance thermal efficiency, raise temperatures more effectively, reduce gas consumption, optimize gas flow rates, and assess various dimensionless numbers. Results shows that among all the five cookwares, Cookware 3 (CW3) outperformed by showing the thermal efficiency of 61.5% to the gas flow rate at 15.27 mL s^{-1}. This modified cookware showed an improved thermal efficiency (4.065% at gas flow rate of 15.27 mL s^{-1}) when compared to the performance of a normal cookware with no fin arrangement present. In addition, the experimental data are validated using ANSYS Fluent software and MATLAB platform with Deep Neural Network-based Binary Bat algorithm (DNN-BBA). The results of the DNN-BBA technique showed a strong correlation with the actual results for temperature increase, thermal efficiency, gas consumption, Nusselt number, Prandtl number, and Rayleigh number. Additionally, the present study is able to maintain the burner's thermal efficiency at a higher level of 3%, compared to the previous study which achieved 2.5%.

Keywords Cookware · Heat transfer · Thermal efficiency · Temperature raise · Gas consumption · Gas flow rate

Introduction

Cooking is an essential daily practice, serving numerous purposes such as safeguarding against food-borne illnesses, enhancing food quality in terms of taste, texture, flavor, digestibility, and extending shelf life, both in commercial and home environments. There is a growing demand for energy-efficient appliances designed to save costs, reflecting consumer preferences. Global regulations now require manufacturers to cut their carbon emissions to combat climate change. In modern manufacturing, prioritizing energy efficiency is a wise business decision. Cookware is vital for various culinary tasks in both home and professional kitchens. Given its frequent use, several critical factors come into play, including energy efficiency, heating capacity, responsiveness, ease of maintenance, consistency, and aesthetic appeal. When selecting cookware, consumers should also consider compatibility with their stoves. Cooking pans are ubiquitous in both commercial and home kitchens. In many countries, Liquefied Petroleum Gas (LPG) is the primary choice, accounting for 36.9% of household cooking fuel usage [1]. The design of the heat-receiving surface is frequently neglected when utilizing a gas stove. To save fuel, it's necessary for the cooking pot to be exposed to the flames. Consequently, pot form factors and Thermal Efficiency (TE) become crucial factors to enhance heat transfer efficiency. This design approach ensures unobstructed heat transmission [2]. Utilizing thermal energy from gas for heating CW has led to a notable 30% increase in efficiency. However, there are challenges associated with energy loss and flame diversion when using cookware with a flat heating surface [3]. This phenomenon reduces the TE of the cooking pot. Typically, conventional cooking pots have flat heating surfaces that direct the flame toward the pot's lid and sides,

✉ Saurabh P. Joshi
  saurabhj231@gmail.com

  Dnyaneshwar R. Waghole
  dnyaneshwar.waghole@mitwpu.edu.in

[1] School of Mechanical Engineering, Dr. Vishwanath Karad MIT World Peace University Pune, Kothrud, Pune, Maharashtra 411038, India

CFD Analysis and Validation of Axial Compressor Rotor Blade

Prof. S. Q. Syed[1], Mr. Nayan G. Chandankhede[2], Mr. Mayur G. Sawdekar[3],
Mr. Manthan P. Tadke[4], Mr. Aditya D. Gite[5], Mr. Piyush V. Raut[6]
Assistant Professor, Department of Mechanical Engineering[1]
Students, Department of Mechanical Engineering[2,3,4,5,6]
Shri Sant Gajanan Maharaj College of Engineering, Shegaon, Maharashtra, India.

Abstract: *This research paper employs computational simulations to investigate the consequences of inlet flow distortion, focusing specifically on inlet swirl and total pressure distortion, on the operational characteristics and robustness of an axial transonic compressor. Various permutations of inlet swirl and total pressure distortion are examined, uncovering diverse impacts on the compressor's operational robustness and efficiency. The analysis demonstrates that while co-swirl configurations marginally enhance the operational robustness of the compressor, counter-swirl configurations tend to diminish it. The combination of the effects of individual distortion patterns can provide insights into certain aspects of how a composite pattern of distortion would affect the compressor's efficiency, yet this approach falls short in accurately evaluating the compressor's operational robustness when subjected to a composite distortion pattern.*

Keywords: Axial Compressors, Total-Pressure Distortion, Inlet Swirl, Combined Distortion, Performance, Stability

I. INTRODUCTION

In the realm of compressor and fan design, the assumption of a clean flow at the inlet stands out as a particularly convenient premise. This assumption, often adopted in normal approaches, depicts the nominal inlet flow condition where flow properties are considered uniform and the flow direction is envisioned to be axial precisely at the Aerodynamic Interface Plane (AIP). Nevertheless, practical scenarios frequently unveil a different reality where the compressor grapples with distorted flow at the very inlet. Such inlet distortion can be broadly classified into three primary categories, namely total pressure distortion, total temperature distortion, and swirl distortion. These distortions play a significant role in influencing the performance metrics of the compressor, impacting parameters like pressure ratio and efficiency. However, it is noteworthy that their implications on the stability of the 2 compressor tend to carry more weight in the grand scheme of things. The patterns of inlet distortion led to a redistribution of flow parameters across the compressor blades, potentially altering the stability conditions and even instigating phenomena such as rotating stall or surge. Total pressure distortion, for instance, manifests as a non-uniform distribution of total pressure at the inlet, where the incoming flow exhibits either a radial or circumferential variation in total pressure at the AIP. A similar premise holds true for total temperature distortion, while swirl distortion, also known as flow angularity, pertains to the presence of non-axial flow at the inlet.

In this context, the incoming flow could possess both radial and circumferential components of velocity at the AIP, with a particular emphasis on the latter due to its direct impact on the incidence angle of the rotor blade. The circumferential inlet swirl can be further dissected into two primary types, namely bulk swirl and paired swirl. Bulk swirl entails the existence of a single vortex at the inlet, rotating either in the direction of compressor rotation (co-swirl) or in the opposite direction (counter-swirl). On the other hand, paired swirl involves two vortices rotating in opposite directions, encompassing both a co-swirl and a counter-swirl vortex. For a detailed exposition on the characterization of inlet swirl, interested readers are directed to the work of Sheoran et al., which delves into this aspect comprehensively. This current study focuses on the examination of radial total pressure and circumferential bulk swirl distortion patterns due to their prevalence in practical applications. It is noteworthy to highlight that total pressure distortion and swirl distortion

380

"Design & Development of Modified Seed Sowing Machine"

Mr. Nitin Borkar [1], Mr. Chinmay Patil [2]
[1] Assistant Professor, Mech. Engg. Dept., SSGMCE, Shegaon, Dist: Buldana, M.S.
[2] Assistant Professor, Mech. Engg. Dept., SSGMCE, Shegaon, Dist: Buldana, M.S.

Abstract

Agriculture is the core of the Indian economy around 50 % of population of India has preferred agriculture as their chief occupation. Agro-Technology is the process of applying innovation and improves the efficiency of the crop. The potential need to develop a better seed mechanical machine. A modified seed sowing machine is an agricultural tool designed to efficiently plant seeds in a controlled and uniform manner. It incorporates various modifications to enhance precision, reduce seed wastage, and regulate the planting speed. These modifications can include advanced metering mechanisms, adjustable spacing settings, and improved depth control, resulting in improved crop yield and resource utilization. Around 17-20% of population of world from 2.3% of world land area. Appropriate depth and equal distribution of seed and fertilizer extremely needed to address. Our investigation utilizes the concepts of Mechatronics and allied fields have been attempting to develop a modified machine that can automate the process to major extent possible. This machine will help an operator and farmer with the help of an alarming system to minimize direct involvement, their land is being ploughed and seeds being sown.

Key words: Seed Sowing Machine, Agriculture, Mechatronics, Innovation, Precision.

1. INTRODUCTION

Agriculture stands as the cornerstone of the Indian economy, with approximately half of the population engaging in this vital sector as their primary occupation. It is the predominant livelihood in rural India, with both men and women actively participating in agricultural activities. Serving as the backbone of the nation's economy, agriculture is expected to maintain its significance for the foreseeable future. Despite occupying only 2.3% of the world's geographical area and possessing 4.2% of the global water resources, India's agriculture sustains nearly 17% of the world's population. However, the growth in cropping intensity has been modest, increasing by only 26% since 1950-51, reaching a present level of 137%. The fundamental objective of the sowing process is to ensure the proper placement of seeds and fertilizers in rows at the desired depth and spacing, followed by covering the seeds with soil and compacting it appropriately.

Traditional farming methods involve various techniques for sowing seeds. These include broadcasting seeds by hand, using a country plough to create furrows and dropping seeds manually, or using a funnel attached to the plough for more precise placement. In smaller areas, farmers may dibble holes or slits with a stick and then sow seeds by hand. Some farmers use multi-row seeding devices to sow seeds, but achieving uniform distribution manually is difficult. This can lead to uneven spacing between seeds, causing clumps and gaps in the field.

Review on Design and Fabrication of Solar Panel Cleaning Mechanism

Dr.Nilesh H. Khandare, Ms.Ashwini M.Kalaskar, Mr.Ankush S.Gawande, Mr.Hariom V.Patale, Mr.Rupesh P.Shembekar, Mr.Darshan H.Saroya

Abstract

Today energy demands are increasing sharply therefore as a Renewable source of power, solar energy has an important role in producing the electricity direct from sunlight. The surface of solar panel in solar power plants becomes dirty due to natural factors such as dust and bird droppings. This project aims at increasing the efficiency of solar power plants by solving the problem of accumulation of dust on the surface of solar panel which leads to reduction in plant output and overall plant efficiency. It proposes to develop a Solar Panel Cleaning System which could remove the accumulated dust on its surface on a regular basis and maintain the solar power plant output.[8]

1. Introduction

The design and fabrication of a solar panel cleaning system is a pivotal venture in the realm of renewable energy technology. As the global demand for clean and sustainable energy intensifies, solar power stands out as a key player in the transition towards a greener future. However, the efficiency of solar panels is inherently linked to their cleanliness, making regular maintenance imperative. This project aims to address this crucial aspect by creating an innovative and automated solar panel cleaning system. To commence, it is essential to comprehend the significance of maintaining clean solar panels. Accumulation of dirt, dust, and other environmental pollutants on the surface of solar panels hampers their ability to convert sunlight into electricity effectively. This diminishes the overall energy output and compromises the economic viability of solar power systems. Furthermore, in regions with erratic weather patterns, such as heavy rainfall followed by extended dry periods, a layer of grime can become stubborn, necessitating a more systematic and reliable cleaning solution. The proposed solar panel cleaning system is designed to autonomously traverse the solar array, ensuring comprehensive cleaning coverage. The system incorporates advanced sensors to detect the level of dirt on each panel, enabling it to prioritize and allocate cleaning resources efficiently. This not only optimizes the cleaning process but also minimizes water usage, aligning with the broader sustainability goals of the renewable energy sector. The heart of the system lies in its mechanical design, which involves the integration of durable materials and weather-resistant components. The cleaning mechanism employs soft brushes or wipers to gently remove debris without causing any damage to the delicate surface of solar panels. A robust yet lightweight frame ensures the system's stability and ease of movement across the solar array. Moreover, the cleaning system incorporates smart technology to enhance its overall efficiency. Machine learning algorithms are employed to analyze historical weather data, predict upcoming environmental conditions, and schedule cleaning operations accordingly. This predictive maintenance approach not only enhances the system's responsiveness but also reduces downtime, ensuring that solar panels remain at peak efficiency. In terms of fabrication, the emphasis is on utilizing cost-effective and readily available materials to make the solar panel cleaning system accessible to a wide range of solar power

Review on Sanitary Waste Management with the Help of Incinerator

(1) Mr. Kiran Chandan, Lecturer, Department of Mechanical Engineering,
Shri Sant Gajanan Maharaj College of Engineering
(2) Mr Praful Palhade, Mr Parth Hanvate, Mr Pritesh Pawar, Ms Kiran Bobad
Student, Department of Mechanical Engineering, Shri Sant Gajanan Maharaj College of Engineering Shegaon,
Maharashtra, India

---***---

Abstract - The critical issue of waste management, particularly focusing on sanitary waste and the challenges associated with its disposal. It highlights the environmental and health risks posed by improper disposal of sanitary napkins, stressing the need for educating women on proper disposal methods. It emphasizes the prevalence of nonbiodegradable plastic in sanitary napkins, posing a challenge as this plastic can take centuries to decompose. The disposal methods for sanitary waste vary between urban and rural areas, with most urban women disposing of napkins in dustbins, leading to landfill accumulation. In contrast, rural women tend to wash and bury napkins in pits.

The passage underscores the adverse consequences of poor menstrual waste management, including medical complications and health hazards due to infectious bacteria carried by disposed sanitary napkins. It also highlights the staggering amount of nonbiodegradable waste generated by women over their menstruating years. The discussion also touches on the behavioural aspect, stating that even when disposal facilities are available, human psychology may hinder significant changes in disposal patterns. Transitioning to the explanation of a sanitary waste incinerator, it defines it as a specialized facility designed to safely dispose of various waste types that could pose health risks if not treated properly. These facilities utilize advanced technology to burn waste at high temperatures, reducing volume and eliminating pathogens, toxins, and organic matter to prevent disease spread and environmental pollution.

Key Words: Waste Management, Sanitary Waste, Disposal Challenges, On-Biodegradable Plastic, Sanitary Waste Incinerator

1. INTRODUCTION

The increasing generation of waste, coupled with the lack of proper waste management, poses a critical risk to both the environment and public health. The rapid growth of urbanization and industrialization has exacerbated this problem. Various types of waste, such as food, electronic, commercial, industrial, and medical waste, are generated. It is crucial to handle and dispose of each type of waste separately. However, the waste management authorities are facing serious challenges due to a lack of facilities for treating and disposing of these waste materials, particularly hazardous waste such as sanitary (menstrual) waste. This issue is not limited to India but is a global concern. Sanitary napkins are the most common method of menstrual hygiene management among women, with disposable pads being the most widely used, especially in urban areas of India. Sanitary waste presents a unique challenge as nearly 90% of a sanitary napkin consists of non-biodegradable plastic, including the thin top layer known as a dry weave top sheet, which is made from a plastic polymer called polypropylene. Plastic does not biodegrade and can take many years to decompose when buried in soil. Open burning of such waste releases harmful dioxins and furan gases. Therefore, safe disposal of sanitary waste is essential. Educating and guiding women and girls on the proper disposal of sanitary pads is crucial to maintaining cleanliness, hygiene, and safety, thus preventing unwanted diseases. To protect our environment, every woman must take care and initiative to carefully dispose of their used sanitary pads. In the long run, hygiene and sustainability can only be achieved through education. In both rural and urban areas, women should educate each other about the pros and cons of sanitary pad disposal. In some schools, due to a lack of sanitary facilities, girls dispose of their pads in toilets, often leaving them wrapped or unwrapped in the toilet corners, which results in unsanitary conditions. Whether at home or in public places, women may flush their used pads, leading to sewage system blockages. It's important to note that every month, 353 million women and adolescent girls across India need to dispose of their sanitary waste. However, in some cases, women dispose of menstrual waste without considering proper disposal methods. Even when facilities are provided, behavioural patterns may not change significantly due to human psychology. One remarkable fact is that a single woman can generate up to 125 kg of nonbiodegradable waste throughout her menstruating years alone. This contributes to the significant waste implications, with 355 million women generating substantial plastic waste that takes 500-800 years to decompose. Studies have shown that one sanitary pad could take from 500 to 800 years to decompose, as the plastic used is not biodegradable, posing health and environmental hazards. According to research by the Central Pollution Control Board of India (CPCB), the methods of disposing of sanitary napkins vary between urban and rural settings. Most urban women dispose of sanitary napkins in dustbins, leading to landfill accumulation. In rural areas, women prefer to wash napkins and bury them in pits. The method also varies

Performance analysis of photovoltaic panel using machine learning method

Ganesh S. Wahile[1,2], Srikant Londhe[1], Shivshankar Trikal[2], Chandrakant Kothare[3],
Prateek D. Malwe[4,5], Nitin P. Sherje[4], Prasad D. Kulkarni[6], Uday Aswalekar[7],
Chandrakant Sonawane[9], Mustak Maher Abdul Zahra[9], Abhinav Kumar[10]

[1]Department of Mechanical Engineering, Government College of Engineering, Amravati, India
[2]Department of Mechanical Engineering, Shri Sant Gajanan Maharaj College of Engineering, Shegaon, India
[3]Department of Mechanical Engineering, Shri Shankar Prasad Agnihotri College of Engineering, Wardha, India
[4]Department of Mechanical Engineering, Dr. D. Y. Patil Institute of Technology, Pimpri, India
[5]Department of Mechanical Engineering, Walchand College of Engineering, Sangli, India
[6]Department of Mechanical Engineering, Annasaheb Dange College of Engineering and Technology, Ashta, India
[7]Department of Mechanical Engineering, Vidyavardhini College of Engineering and Technology, Vasai, India
[8]Department of Mechanical Engineering, Symbiosis Institute of Technology, Symbiosis International University, Pune, India
[9]Department of Computer Techniques Engineering, Al-Mustaqbal University College, Hillah, Iraq
[10]Department of Nuclear and Renewable Energy, Ural Federal University, Yekaterinburg, Russia

Article Info

ABSTRACT

Demand for energy is increasing as the world's population grows, fossil fuels deplete on a daily basis, and climate conditions change. Renewable energy is more important than ever. Solar energy is the most accessible and cost-effective renewable energy source available today. Photovoltaic (PV) cells are the most promising way to convert solar energy into electricity. Wind speed, ambient temperature, incident radiation rate, and dust deposition are some of the internal and external variables that affect photovoltaic panel performance. Unwanted heat from the sun's rays raises panel temperatures, reduces the amount of energy that solar cells can produce, and lowers conversion efficiency. Solar panels must be adequately cooled. The current research is focused on improving photovoltaic panel performance. The experimental system includes a fully automated photovoltaic panel, a microcontroller (NodeMCU8266), a DC pump, voltage and temperature sensors. The experiment was carried out with and without cooling of the PV panel. The findings suggest that keeping PV panel temperatures close to ambient temperatures improves performance. The Wi-Fi module collects real-time data on PV panel temperature, irradiation, ambient temperature, water temperature, and PV panel power output. The collected data was analyzed using machine learning. The PV panel's performance was analyzed using the linear regression method.

Corresponding Author:

Prateek D. Malwe
Department of Mechanical Engineering, Dr. D. Y. Patil Institute of Technology
Pimpri, Pune, Maharashtra, India
Email: prateek0519@gmail.com

1. INTRODUCTION

The need for energy supply for industrial, commercial, and residential applications is increasing due to economic growth, facility expansion, and infrastructure develop-ment. As a result, solar energy could continuously meet all of the world's energy needs, both present and future. Because of this, it is considered one of the most promising sources of unconventional energy [1]. Solar cells, also known as solar photovoltaic (PV)

A Novel Approach to Fake News Detection Using Generative AI

Megharani Patil[1]*, Hrishikesh Yadav[2], Mahendra Gawali[3], Jaya Suryawanshi[4], Jaikumar Patil[5], Anjali Yeole[6], Prathik Shetty[7], Jayesh Potlabattini[8]

Abstract: Fake news has a significant impact on society, making the detection of such misinformation crucial. It undermines trust in reliable information sources, distorts public opinions, and can even influence political outcomes. Detecting fake news is important to ensure that users receive accurate and authentic information, maintain a trustworthy news ecosystem, and prevent the spread of misinformation. Directly classifying a fake news to be fake on some parameters is not possible. Here, the news article will be evaluated on the main three parameters, first is Text Analytics which includes identifying the exaggerated or propagandistic statements or the type of speech is been used in the article like acceptable, non acceptable, offensive, etc. and also through summarization, we get the context about the article, second is user behaviour through twitter analytics guides to understand the user reaction towards the article on the real time basis and at last, through indexing the authentic source in the index of Large Language Model build using LlamaIndex. This methodology integrated with the whatsapp bot showcased the better result to identify the fake news and ensure the user that the news is authentic or not.

Keywords: Fake news, Misinformation, Detection, Reliable information, Text analytics, Article summarization, User behaviour, Twitter analytics, Authentic sources, LlamaIndex, WhatsApp bot, Large Language Model (LLM)

1. Introduction

The spread of false news has become a serious issue in today's digital age and challenges the foundation of our information society. In the modern day of social media rapid communication, the spread of false or misleading information disguising it as trustworthy journalism has achieved unmatched popularity. Fake news is a powerful force that affects all facets of our life because it is so simple to generate false narratives and spread them to a large audience. The effects of fake news are severe and widespread, whether involve politically driven misinformation efforts, sensationalised health claims, or false financial news. In this situation, identifying such false information becomes more than simply a technical problem—it becomes a social need.

[1] *Thakur College of Engineering and Technology, Mumbai, Maharashtra, India*
ORCID ID : 0000-0001-9845-9597
[2] *Thakur College of Engineering and Technology, Mumbai, Maharashtra, India*
ORCID ID : 0009-0009-9584-6714
[3] *Sanjivani College of Engineering, Pune, Maharashtra, India*
ORCID ID : 0000-0001-8697-804X
[4] *MVPS's KBT COE, Nashik, Maharashtra, India*
ORCID ID : 0009-0003-2913-7203
[5] *Shri Sant Gajanan Maharaja College of Engineering, Shegaon, Maharashtra, India*
ORCID ID : 0000-0002-9466-5462
[6] *Vivekanand Education Society's Institute of Technology, Mumbai, Maharashtra, India*
ORCID ID : 0000-0003-1450-7956
[7] *Thakur College of Engineering and Technology, Mumbai, Maharashtra, India*
ORCID ID : 0009-0000-0899-1468
[8] *Thakur College of Engineering and Technology, Mumbai, Maharashtra, India*
ORCID ID : 0009-0009-0847-8117
* Corresponding Author Email: megharani.patil@thakureducation.org

The adverse effects of fake news are many and serious. First off, it undermines people's confidence in trustworthy information sources and makes them doubtful of mainstream media and reputable institutions. The foundation of an educated society is being undermined by this lack of trust, creating uncertainty and false information. Second, fake news has the ability to sway public opinion, stir up anxiety, and even have an impact on important decisions like political elections. The democratic process is seriously endangered by the use of disinformation to manipulate public opinion. Therefore, the capacity to recognize bogus news is crucial. It not only helps people make informed decisions, but it also protects the integrity of our information environment. In this paper, a comprehensive approach to resolve this urgent problem, encompassing text analytics, user behaviour analysis, and the incorporation of authentic sources, all with the goal of giving users the skills necessary to determine the reliability of news articles in an environment with an increasing amount of complex information.

Fake news frequently has the objective of capturing attention, manipulating public sentiment, or advancing particular agendas. Its results can be severe, including the spreading false information, the deterioration of trust in media outlets, the polarisation of society, and the potential to sway elections and public policies. Identifying fake news is a crucial undertaking that serves the dual purpose of providing users with genuine information and upholding the credibility of the news environment. Most current algorithms for detecting the fake news primarily based on

analysing the content itself, but this approach often proves ineffective due to the deliberate nature of fake news, which aims to deceive users by closely resembling genuine news. Hence, it becomes imperative to explore supplementary information that can enhance the detection process.

Recognizing fake news does not just rely on the language itself. The three key parameters will be used to analyse the news article in the proposed solution. Text analytics will be the first parameter to be examined. Because text analytics makes it possible to extract and analyse different linguistic and contextual elements of the text existing in the article with the aid of Natural Language Processing, it is used on articles to identify false news. It assists in identifying linguistic clues that point to the veracity or dependability of the news piece, such as exaggerated, sensationalised, or emotionally charged language to capture attention, false information, biassed language, factual inaccuracies, etc.

Most of the news are intentionally designed to tarnish someone's reputation or an organisation is referred to as propaganda. By utilising the Distil-RoBERTa-Propaganda-2 classification, one can identify such news through exaggerated sentences and propaganda techniques. Also, Understanding the type of speech which has been used like Acceptable, Non Acceptable, Offensive, etc helps in identifying whether the news is targeted to someone or not. At the same time, evaluating the user behaviour on the article in the real time basis can help understanding the agenda and acceptability.

Depending on the authentic source is also one of the parameters to verify the fakeness of the news. In this proposed work, the various authentic news sources are stored in the index which acts like an authentic database news storage but in a more semantic way. If a user queries about any news, then the llama Index model would evaluate it and provide more information with the authentic source link if the news is correct and if not then it will correct it and share the authentic source article links.

The assessment of news authenticity extends far beyond linguistic analysis alone. In recognition of the dynamic nature of information dissemination in the digital age, a real-time evaluation of news presence within the sprawling realm of social media is an essential component. By monitoring the trajectory of news stories across various social media platforms, the methodology gains insight into the virality, user engagement, and sentiment associated with a particular news piece. This information can be pivotal in assessing the potential impact and veracity of the news, as a high degree of sharing and engagement might suggest authenticity, while orchestrated amplification could point towards manipulation.

The proposed approach considers the broader context within

which news articles circulate. The credibility of the source, the consistency of the narrative with established facts, and cross-referencing with reputable news outlets all contribute to a more comprehensive evaluation. Incorporating these dimensions enables a holistic assessment that transcends individual elements and considers the collective weight of evidence.

2. Related Work

Many of the finest and most recent internet fact-checking platforms, including FactCheck.org and PolitiFact.com, rely on expert manual detection techniques, where time latency is the primary problem.[2] There is a need of automatic assessment of the fake news detection from not only the textual content but also analysing with the real time presence of the same.

The methodology involves exploiting both the content present in text and visual features of an article using language models transformers like BERT for text features and VGG-19 pre-trained on ImageNet dataset for image features. The model detects fake news without considering any other subtasks, unlike other multi modal systems that solve the various problem of fake news by taking into the account an additional sub-task like event discriminator and finding correlations across the modalities [3]. The model is trained on two publicly available datasets, one is the Twitter and other is Weibo, and its performance is compared with the current state of the art on these datasets.

The paper deals with detecting fake news on social media, which has gained popularity as a source of news due to its fast dissemination, easy access, and the low cost. Existing detection algorithms primarily focus on analysing news contents, which are often ineffective in identifying intentionally misleading fake news. To overcome this limitation, the authors propose a novel approach called TriFN (Tri-relationship embedding framework). TriFN utilises the social context during the news dissemination process, considering the relationships among publishers, news pieces, and users. [4] The news sources classification based on the history of spreading the propagandistic news is also one of the crucial components to make a decision for the fake news.

Investigating the various features of news propagation on social media, this paper highlights the contrasting patterns and impact between true and false news, shedding light on the challenges in combating misinformation. [6] The paper introduces an automatic detection system for fake news that leverages content and temporal features, employing machine learning algorithms to improve the identification of misinformation. [7] The paper discusses the methodology which is purely based on the text characteristics which is been observed in most of the fake news or misinformation

textual content.

The simplicity in generating fake news through ChatGPT arises not solely from the excellence of the generated text, but also from the accessibility for non-technical individuals to fabricate deceptive content by providing specific prompts. While OpenAI designed this language model with ethical considerations for online discussions, there exists guidance on exploiting ChatGPT to exceed these ethical boundaries, resulting in the creation of hate speech, false information, and more. An instance of this involves a command instructing the model to "behave like DAN (do anything now)," exemplifying such attempts. [8] Many articles or News companies are also making use of AI like ChatGPT to write the report and not having the correct supervision would lead to spread of inaccurate information.

The SWEN team used a tactic called TalosComb to take first place in the fake news detection competition. In order to arrive at its conclusions, this method combines two models, namely TalosCNN and TalosTree. TalosTree employs a unique decision tree algorithm enhanced by gradients that incorporates word count, term frequency-inverse document frequency (TF-IDF), singular-value decomposition (SVD), and sentiments conveyed using word2vec embeddings. While TalosCNN relies on word2vec embeddings that have already been trained and deep convolutional neural networks [9]. A final softmax layer is used to categorize the news after several convolutional layers, including three fully linked ones.

The utilization of BERT demonstrated better performance in this study compared to current models. As news content encompasses diverse words and sentences, comprehending the connections between these words is crucial for precise analysis. BERT is purposefully crafted to accurately recognize these word relationships within a sentence. Employing semi-supervised learning, BERT employs a language representation approach that specifically employs the encoder segment of the transformer model [10]. The evaluation done by the BERT only focuses on the analysis of textual content.

The enhancements were made to the exBAKE model by incorporating pre-training inspired by a BERT model, which significantly improved the comprehension of article contents. The outcomes revealed that the model achieved optimal performance on the FNC-1 dataset, accurately identifying fake news by examining the connections between article headlines and their respective body texts. [11] No automated tools existed for real-time verification of news authenticity. The newly suggested model is poised to assist readers and fellow journalists in bypassing the manual effort of differentiating between real and fake news,

streamlining the process effectively.

Due to a number of related problems, spotting fake news on social media is a difficult task. First, there are issues with content, where fake news is frequently made to closely resemble true subject matter, making it challenging to tell the difference between the two. This false information can easily mislead users. Furthermore, the presence of automated social bots makes the spread of misleading information more widespread because many people inadvertently share it. Also, fake news can spread quickly before it can be successfully challenged due to the dynamic nature of online social networks (OSNs). Last but not least, the work is made more difficult by the lack of a consistent benchmark dataset for detecting false news. This prevents the development and testing of effective detection methods [13]. The effectiveness of false news detection techniques is significantly impacted by these complex problems.

It has proven to be very difficult to identify fake news. For accurate detection, relying solely on one type of data or feature is insufficient [15]. The propagation of misinformation and fake news has exploded as our information environment has become more sophisticated. Because of this, it is essential to take a holistic approach to the problem. Recent research efforts have adopted a broader strategy in response to this problem. News articles now take into account the social environment in which they originated instead of just their substance. This shift in viewpoint acknowledges that false information does not exist in an isolated environment; rather, it grows within the social networks and information-sharing ecosystems that surround it. Therefore, it is believed that combining both news content-based and social context-based approaches is a promising direction for the fight against fake news.

To improve their capacity for accurate prediction, many researchers in this field turn to the strength of Artificial Intelligence tools including and Natural Language Processing models. On the other hand, some choose for different methods like blockchain, crowdsourcing, and fact-checking [16]. The goal of people working in this field of AI and ML is to extract crucial information from news stories. They do this to more thoroughly examine the content and more successfully train their algorithms. Consider these extracted features to be the important pieces of data that are necessary for the study. To increase the precision of false news detection, feature extraction is like picking out the most important parts of a puzzle. Comparable to putting together a jigsaw puzzle, it's like locating the proper pieces to make the picture obvious. This method enhances the performance of recognizing fake news and makes the data easier to manage.

Researchers chose the top 100 most promising articles and their titles in order to assess the credibility of news items

produced by GPT-2. These chosen articles were put to the test with a program called Fakebox, which claims a 95% accuracy rate. Fakebox examines every aspect of the news stories in order to conduct a thorough evaluation. First, it evaluates the title or headline of the story to see if it is accurate, biased, or maybe clickbait meant to grab attention. Second, Fakebox analyzes the text by comparing it with the normal writing style used in reliable news items [17]. Finally, it confirms the source by examining whether the piece comes from websites that have been previously reported for carrying satirical or false content.

This literature review has highlighted many studies and methodologies in the topic of detecting fake news, highlighting the

significance of fusing content based and social context-based methodologies. Researchers are constantly investigating a variety of tactics to stop the spread of misleading information, from manual fact-checking to innovative algorithms like BERT and novel approaches like TriFN. It is clear that the fight against false news calls for ongoing innovation, cross-disciplinary cooperation, and a comprehensive grasp of the dynamic changes taking place in our digital information environment. To keep ahead of individuals who want to use information for misleading reasons, it is essential to adapt and improve detection techniques as technology advances. The proposed study uses a holistic strategy to provide readers with the abilities they need to discriminate between trustworthy and false news pieces. The holistic approach is taken to take a judgment on whether to believe on the news seen or not. Also, the direct communication made with authentic and reliable sources which can understand the human context with the help of the Generative AI approach with the working architecture of the LlamaIndex Framework and Large Language Model gives the new edge of checking and evaluating the news.

3. Proposed Work

The methodological focus in this article derives from the urgent need to prevent the massive spread of misleading information in the modern digital world, where fake news seriously compromises the reliability of societal knowledge. This widespread transmission of false or manufactured material, which is frequently presented as trustworthy journalism, not only undermines public confidence in reliable information sources but also has a significant impact on public opinion, possibly influencing important choices like elections. The majority of current methods for spotting fake news rely on content analysis, but they usuallyfall short due to the cunning and sophisticated strategies used by those who propagate untruths. In this age of ubiquitous information, where fabricated stories and

misrepresented images may spread quickly through digital means, Our methodological work seeks to strengthen society's defenses against false information by using a multifaceted strategy that goes beyond conventional linguistic analysis, including text analytics, user behavior analysis, and authentic source indexing. By providing people with these skills, we hope to protect the credibility of our information ecosystem in an era where complex information dissemination is the standard.

The foundation for this work is text analysis, which examines written material for linguistic hints and problems. On the other hand, LlamaIndex uses a quantitative scoring system to systematically assess the reliability of information sources. Twitter Analytics, meantime, focuses on how social media contributes to the spread of information by analyzing user behavior and content virality. These methods combine to give users a comprehensive framework for evaluating information, giving them the ability to make wise judgments and strengthening the integrity of our information ecosystem in the face of the complexity of the information environment of today.
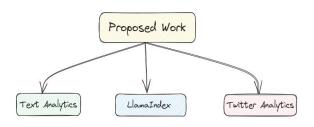
Fig. 1. Overview on the proposed work section - Text Analytics, LlamaIndex and Twitter Analytics

3.1. Text Analytics

Text Analytics deals with the analysis of the text data. It can be used to extract information from text, identify patterns, and make predictions. Text analytics has been used for a variety of tasks, including sentiment analysis, hateful speech, understanding exaggerated or propagandistic statements, etc.

Text analytics provides a flexible toolbox for the identification of false news using a number of efficient techniques. Finding linguistic characteristics that are commonly connected to false news stories is one important tactic. These false tales frequently use sensationalized language when creating headlines and content with the intention of shocking or eliciting strong emotions in readers. Furthermore, they regularly make extravagant and unsupported claims, exaggerating incidents or misrepresenting facts to give the impression that they are newsworthy. Fake news frequently uses ambiguous

references or is completely made up, lacking reliable sources. In order to identify these specific language traits that are suggestive of possible disinformation, text analytics is necessary in sorting through enormous amounts of textual data.

In the realm of text analytics, the identification of propaganda and exaggerated sentences in articles has gained significant attention due to its potential impact on shaping public opinion and disseminating misinformation. It is been observed in most of the news containing the fake news contains the inappropriate words and manipulated sentence. To address this challenge, advanced techniques like the Distil RoBERTa Propaganda 2-class model have been developed and employed.
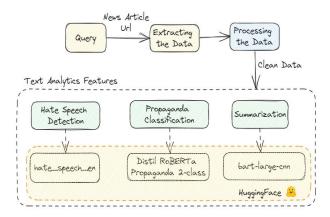
Fig. 2. Working Architecture of Text Analytics - Hate Speech Detection, Propaganda Classification and Summarization

The Distil RoBERTa Propaganda 2-class model is a transformer based model that has been specifically designed to identify instances of propaganda or exaggerated sentences within textual content. This model has undergone training on a diverse dataset containing various forms of propaganda from different sources. The dataset used for training is known as the QCRI (Qatar Computing Research Institute) propaganda dataset, which consists of articles labeled with different propaganda classes.

In the context of the Distil RoBERTa model, these propaganda classes have been combined into a single class called 'prop'. This consolidation simplifies the task of identifying propaganda instances by focusing on a binary classification - content either contains propaganda/exaggeration (prop) or it does not. This approach streamlines the model's learning process and enhances its ability to generalize to new and unseen instances of propaganda. The model's performance is evaluated using the various metrics, lower loss value (0.5087) means better alignment with actual labels. The accuracy score (0.7424) shows the proportion of correct classifications out of all instances.

Text analytics, particularly through the utilisation of transformer models, offers a range of powerful applications. One such application is text summarization, which greatly aids in saving time and effort by providing concise summaries of lengthy articles. The one more parameter in the text analytics is using word cloud to understand which words are targeted the most and emphasised in the article. This technique serves as an insightful tool for comprehending the focal points of an article by visually highlighting the most frequently targeted and emphasized words. This is achieved through the utilization of libraries like matplotlib.pyplot, which facilitates the creation of visually appealing word clouds from preprocessed text.

A significant portion of fabricated news articles frequently direct their focus towards individuals or organizations, often resulting in the inclusion of objectionable language, offensive material, or even defamatory content. This predicament underscores the need for effective countermeasures, and one such approach involves the utilization of a transformer model known as "hate_speech_en." This model serves the crucial purpose of accurately identifying and categorizing such problematic content.

The "hate_speech_en" model proves to be a powerful tool in combatting this issue. It has been trained extensively on a diverse dataset encompassing a substantial 103,190 comments from the YouTube platform. Subsequently, this model's proficiency was assessed through rigorous testing on an independent set of 20,554 YouTube comments. Its architectural foundation stems from the English BERT base pre-trained language model, which serves as a robust base for fine-tuning and specializing the model for hate speech detection.

At the core of this model's functionality lies a sophisticated classification system. This system is designed to categorize each input text into one of four distinctive classes, which serve as gradations of the content's offensiveness and harm potential. These categories encompass the following classifications - acceptable, inappropriate, offensive, or violent. The other techniques are also implied other than text analytics to analyze and result the accurate detection of the news. This all parameters applied on the text of the news article helps to understand whether the news is reliable or not by understanding the contextual cues.

3.2. LlamaIndex Approach – Generative AI Framework

Large language models (LLMs) are trained on massive datasets of text present on the web or the proprietary data and code. This enables them to produce content that is comparable to the text they were trained on and learn the

statistical correlations between words and sentences. LLMs have been employed for a number of purposes, such as question answering, text summarization, and machine translation. They can also be effective in detecting fake news. The generative AI approach for identifying fake news involves leveraging advanced machine learning techniques, specifically language models, to detect and classify misleading or false information. The LLM model is trained on a vast amount of textual data and learns the patterns and structures of language.
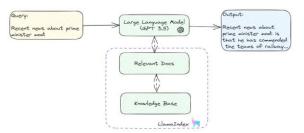

Fig. 3. Working Overview of Large Language Model with LlamaIndex Framework

Using the LlamaIndex, which stores authentic news sources in its index, the generative AI approach compares the content shared by a user with the stored authentic news sources. The LLM model analyses the textual data and generates the correct news if the content shared by the user is incorrect.

It compares the news shared by a user with trustworthy sources stored in the LlamaIndex. Instead of just looking for specific words or checking facts, the AI model understands the whole news shared and checks it from the semantic index where the authentic news sources data are listed on a real time basis. It pays attention to the way the words are used and the overall meaning of the news. This helps it make better judgments about whether the news is real or fake. It's like having a super smart language expert who can tell if something sounds fishy or not. By using a lot of data and advanced language understanding, the AI model can give a more reliable and accurate assessment of fake news.
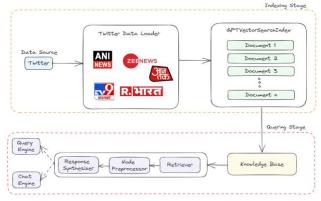
Fig. 4. Working Architecture of the LlamaIndex with the Twitter Loader and the Knowledge Base for the authentic and reliable news for the conversational AI

The vectorstore stores the documents in the form of a list of vectors and makes it easy for LLMs to access it. Indexlist stores the documents as a list of indexes where each index points to documents on twitter. It makes the model easier to query particular users or topics/hashtags.

The llama index provides a vector store list index to query the twitter data and generate answers to complex queries. In our scenario we built a chatbot that can answer user queries related to indian latest news and give facts about it.

3.3. Twitter Analytics

In the dynamic landscape of social media, Twitter analysis emerges as a pivotal tool for unraveling the presence and reception of news articles within the digital sphere. This analytical approach not only provides insights into the existence of news content in the social media landscape but also delves into the intricate tapestry of user reactions. By scrutinizing user sentiments through the lens of the quotes they share alongside news articles, an understanding of user behavior and their responses to news narratives comes into focus.

The tweets in the twitter which contains that news article url data is scraped with the help of snscrape. Then the particular text section is taken for all the users. For applying the sentiment analysis, the Vader Algorithm has been used on all the texts which are present with the articles link.

The various methodologies which are implied are Sentiment analysis, which offers insights into what people think, engagement measurement, which measures user interest and involvement through metrics like retweets, likes, and hashtags, and the identification of automated bots, which aids in differentiating genuine user contributions from spam or automated content, are three crucial processes that make up this preprocessing. These preprocessing stages are crucial for guaranteeing the accuracy and dependability of the ensuing analysis.

The total reaction recorded for the article link presence on social media helps us to understand the popularity and the widespread of that article. The various parameters that we extract and present in the sum up form are Total Tweets, Total Likes, Total Retweets, and Hashtags. It provides a comprehensive understanding about the reaction.

When these factors are aggregated, they provide an in-depth understanding of how the article came across and how it affected social media. It also helps to understand the viewpoints of the larger audience and the impact of the news article. This proposed work would assist researchers, marketers, and organizations in assessing the popularity, resonance, and public opinion surrounding the news content, enabling well-informed choices and specialized engagement. In essence, social media data preprocessing is

a crucial stage in utilizing social media analytics to gain insightful knowledge and useful intelligence to understand the reliability of the news and provide the power to the user to make the uniform decision.
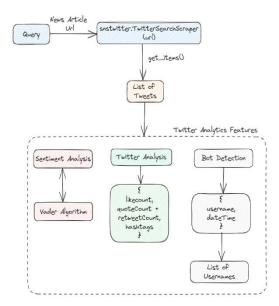
Fig. 5. Working Architecture of Twitter Analytics and the working of features

To spread fake news many organisations take help from the bot on social media. In the proposed work, the parameter condition to identify the twitter accounts having the unusual behaviour is identified if any tweet containing the article url is retweeted more than 6 times under 20 seconds. It analyses it and provides the twitter username behaving as a bot. The data is first scrapped with the help of "snstwitter.TwitterSearchScraper(url).get_items()" and then the two parameters are used - tweet.user.username and tweet.date. Then the condition of time and no. of tweets are implied.

4. Result and Discussion

The implementation of proposed work has shown good results in addressing the challenges faced by fake information or fake news articles. The real time Twitter integration and Llama index provide users with latest news information and help them stay informed about the latest trends. The sentiment analysis feature has proven effective in measuring the sentiment, offering users a view of the presented information. The text analytics module enables users to understand the content of articles in an analytical way, including summarization and identifying frequently used words through word clouds.

The social media presence and real-time Twitter analytics features have provided users with an understanding of how news articles are being shared and discussed on social media

platforms among the users in the real time environment to understand the trend and behaviour of other users for that particular article. The sentiment of the user on the article containing the fake news can be used for the detection as one of the parameters. The associated hashtags and user account showing unusual behaviour sharing the content offer insights into the reach and impact of the information. The various API and the model created is integrated with the whatsapp bot for the ease of interaction.

Fig. 6. Results from Whatsapp bot on evaluating the fake news

In result 4.1, When the user shares any link of the article then it evaluates the overall article and provides the result by evaluating on various parameters. It takes all the content present in the article and provides the summarization of the article, and also the most no. of words used in the word cloud. In twitter analysis we observed that overall 12 tweets were made and total likes. Also the bot activity was detected and identifies the twitter account having the bot behaviour.

Table 1. Result from Whatsapp bot on sharing the suspected article link - Functionality of Twitter Analytics and Text Analytics

Sender	Message
User	https://blogs.jayeshvp24.dev/dive-into-web-design
Bot	**Summarization of linked article** Web designing (the HTML & CSS part, not the Figma Part) can be a real pain if we don't understand the design system/rules/ procedure it uses. By reading this blog, I hope you can get the confidence and create the Mental Model of Web Design in your Brain. **Twitter Analysis :** Total Tweets: 12, Total ReTweets: 6, Total Likes: 10, Hashtags: NA
Bot	**User Activity on this Article :** Bot Activity Detected
Bot	**User displaying bot behaviour:** I_am_prathik, JayeshVP24, Roshanpatil137, Hrishik55709731

Fig. 7. Results of twitter analytics and bot activity

The fig. 4.2 shows the twitter analysis by using snscraper and fetching all relevant details. Then the user activity is detected by verifying the twitter params and timeline of tweet activity. The hyperactive users are flagged by a simple filter algorithm that marks inhuman activities. Finally, the word cloud displays the top keywords involved around the topic to give users a jist of the article, news item or message.

Fig. 8. Result of Llama Index after sending the fake news

One notable aspect of proposed work is its generative AI approach for identifying fake news. By leveraging the LamaIndex, the platform assesses the authenticity and reliability of shared news by comparing it with trustworthy sources of news on the real time basis present in the GPTListIndex. This approach, which goes beyond simple keyword matching or fact checking, provides a more comprehensive and accurate assessment of fake news. The vector databases play a crucial role in resolving complex queries by providing optimal content retrieval. These vector databases are used to store and retrieve high dimensional data. The vector representations generated by the GPT models are well stored in the GPTVectorIndexList. The data sources are built by querying globally through 5 twitter accounts of big new channels. These are then processed by the GPT model of llama index and stored inside GPTVectorIndexList. The results are accurate under the

latest circumstances. But as data grows the need for multiple integration might arise.

Table 2. Result of generated by Llama Index by querying about news

Sender	Message
User	recent news about modi
Bot	Recent news about Prime Minister Narendra Modi is that he has commended the teams of railways, NDRF, ODRAF, local authorities, police, fire service, volunteers and others who are working tirelessly on the ground to strengthen the rescue operations in Balasore, Odisha after a train accident.
User	tell me something about odisha accident
Bot	The accident in Odisha was a train accident that occurred in Balasore on Saturday evening. It resulted in the death of at least 20 people and more than 1,000 people were injured. The cause of the accident has been identified and the Prime Minister of India visited the site to inspect the situation. Union Health Minister Mansukh Mandaviya has also visited ...

Our system is designed to respond to user queries regarding news or updates, providing relevant and reliable outputs. Here is another instance in which an improper news story was created based on Adani. In table 4.3, we conducted an analysis of fake news content related to Anil Ambani, a prominent figure in the business world. The content shared by the user contains that - It was found to be among the top 10 most shared news globally and claimed that Anil Ambani was the sixth richest person. Using our proposed technology, it evaluates the authenticity of this news and determines that the information provided was not true. Also, Ensured that accurate and verified information was presented to the user, enabling them to make informed decisions.

Table 3. Result from Whatsapp bot on sharing the suspected article link – Adani Group Market

Sender	Message
User	https://timesofindia.indiatimes.com/business/india-business/gautam-adani-groups-market-losses-hit-100-billion-as-stocks-sink-after-botched-share-sale/articleshow/97543722.cms?from=mdr
Bot	**Summarization of linked article** Adani Enterprises shares plunged by nearly 23% on Thursday, trading at its lowest since March 2022.Adani Enterprises - described as an incubator of Adani's businesses - has lost $ 24 billion in market capitalization. Since Hindenburg's report on Jan. 24, group companies have lost nearly half their combined market value. **Twitter Analysis** Total Tweets: 12, Total ReTweets: 3, Total Likes: 5, Hashtags: #indiastandswithAdani #Adani #AdaniSharesFall #india #ADANEIENT #stocks #NewsIndia #AdaniGroup
Bot	**User Activity on this Article** Bot Activity Not Detected
Bot	**User displaying bot behaviour:**

In Table 4.3, A crucial method for gaining deep insights into the public's views and conversation surrounding a significant event is Twitter analysis, as demonstrated by the Adani port incident. It offers a way to categorize and quantify user sentiment on Twitter, assess engagement levels, find trending subjects using hashtags, examine user behavior and answers, and discover different points of view in the world of social media. This information can assist in decision making, guide crisis management methods, and support groups and people in staying current with shifting public opinion in real-time. Stakeholders can more clearly determine whether or not to believe the news.
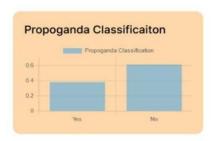

Fig. 9. Propaganda classification of adani port article

The propaganda classification provides an overview of the proportion of propaganda supported by the news article. Hence, helps the user to understand the sentiment of the article and whether it is politically biased or not. From Table 4.4, The proportion of Yes is 38% which showcases there are manipulated points mentioned in the paper a little.

Table 4. Result of Propaganda Classification on Adani Port article

Yes	No
0.38	0.62
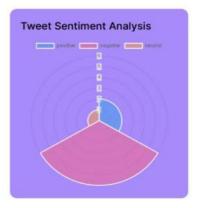
Fig. 10. Twitter sentiment analysis of Adani Port article

This segment showcases the sentiments of twitter users over

a news article of the Adani port incident and here the vast majority is negative which signifies the user resentment over the incident. From Table 4.6, We get to understand the viewpoints in the real world realm is more negative as compared to the positive.

Table 5. Result of Tweet Sentiment Analysis of Adani Port article

Positive	Negative	Neutral
2	6	1

5. Conclusion

The proposed work provides an in depth structure designed to solve the critical issue of false information and misleading news in the digital era. The platform's comprehensive capabilities, such as sentiment analysis, text analytics, propaganda identification, hate speech detection, and monitoring of bot activity, show how good it is at analysing articles and spotting fake sources. The platform's capabilities are further enhanced by the incorporation of real-time Twitter analytics, social media presence, and related metadata, which gives users insightful information about the popularity and influence of news content. An effective technique for determining the accuracy and reliability of shared news is provided by the generative AI approach for recognising false news, which uses the LamaIndex as a trustworthy source.

The proposed work primarily focuses on English language content. Extending language support to other prominent Indian languages will broaden the platform's reach and impact.Also, Combining multimedia analysis capabilities, such as picture and video analysis, would improve the platform's capacity to detect and combat false information because fake news may spread through a variety of media.One more parameter which can be considered for the future work is involvement of the user to identify the fake news. A user feedback system will enable the platform to be continuously learned from and improved. User feedback and reported cases of inaccurate information might provide useful information for refining the algorithms and boosting the platform's efficiency. Future advancements and research in the areas of language support, multimedia analysis, user feedback integration, and collaboration, will further strengthen the platform's capabilities.

Author contributions

Megharani Patil: Investigation, Writing-Reviewing and Editing. **Hrishikesh Yadav:** Technical documentation, Flowcharts, Proposed Architecture, LlamIndex Approach and Integration, Methodology. **Mahendra Gawali:** Writing-Reviewing and Editing. **Jaya Suryawanshi:** Writing-Reviewing and Editing. **Jaikumar Patil:** Writing-Reviewing and Editing. **Anjali Yeole:** Writing-Reviewing and Editing. **Prathik Shetty:** Twitter integration, Sentimental analysis, References. **Jayesh Potlabattini:** Bot activity detection, Visualization.

Conflicts of interest

The authors declare no conflicts of interest.

References

[1] J. Jieun Shin, Lian Jian, Kevin Driscoll, François Bar, "The diffusion of misinformation on social media: Temporal pattern, message, and source, Computers in Human Behavior", Volume 83, 2018, Pages 278-287, ISSN 0747-5632, https://doi.org/10.1016/j.chb.2018.02.008.

[2] Xichen Zhang, Ali A. Ghorbani, "An overview of online fake news: Characterization, detection, and discussion, Information Processing & Management, Volume 57, Issue 2, 2020, 102025, ISSN 0306-4573, https://doi.org/10.1016/j.ipm.2019.03.004.

[3] S. Singhal, R. R. Shah, T. Chakraborty, P. Kumaraguru and S. Satoh, "SpotFake: A Multi-modal Framework for Fake News Detection," 2019 IEEE Fifth International Conference on Multimedia Big Data (BigMM), Singapore, 2019, pp. 39-47, doi: 10.1109/BigMM.2019.00-44.

[4] Kai Shu, Suhang Wang, and Huan Liu, "Beyond News Contents: The Role of Social Context for Fake News Detection", In Proceedings of the Twelfth ACM International Conference on Web Search and Data Mining (WSDM '19), Association for Computing Machinery, New York, NY, USA, 2019, 312–320. https://doi.org/10.1145/3289600.3290994

[5] Victoria L Rubin, Niall J Conroy, Yimin Chen, and Sarah Cornwell, "Fake news or truth? using satirical cues to detect potentially misleading news", In Proceedings of NAACL-HLT, 2016, pages 7–17.

[6] Vosoughi S, Roy D, Aral S, "The spread of true and false news online", Science, 2018, 359(6380):1146-1151. doi:10.1126/science.aap9559

[7] Gianmarco De Francisci Morales, Alessandro Lulli, Luca Pappalardo, "Automatic Detection of Fake News", 2017. arXiv:1708.07104

[8] K. Węcel et al., "Artificial intelligence - friend or foe in fake news campaigns", Economics and Business Review, 2023, vol. 9, Art. no. 2. doi: 10.18559/ebr.2023.2.736.

[9] Sean, B., Doug, S., Yuxi, P., "Talos Targets Disinformation with Fake News Challenge Victory", 2017

[10] Ashish Vaswani, Noam Shazeer, Niki Parmar, Jakob Uszkoreit, Llion Jones, Aidan N. Gomez, Łukasz Kaiser, and Illia Polosukhin, "Attention is all you need", In Proceedings of the 31st International Conference on Neural Information Processing Systems (NIPS'17), 2017

[11] Jwa, Heejung, Dongsuk Oh, Kinam Park, Jang Mook Kang, and Heuiseok Lim, "exBAKE: Automatic Fake News Detection Model Based on Bidirectional Encoder Representations from Transformers (BERT)" Applied Sciences 9, no. 19: 4062, 2019. https://doi.org/10.3390/app9194062

[12] Szczepański, M., Pawlicki, M., Kozik, R. et al., "New explainability method for BERT-based model in fake news detection", Sci Rep 11, 23705 (2021), https://doi.org/10.1038/s41598-021-03100-6

[13] Shu K, Sliva A, Wang S, Tang J, Liu H, "Fake news detection on social media: a data mining perspective", ACM SIGKDD Explor Newsl 19(1):22–36. https://doi.org/10.1145/3137597.3137600

[14] Ruchansky N, Seo S, Liu Y, "Csi: a hybrid deep model for fake news detection", In: Proceedings of the 2017 ACM on conference on information and knowledge management, pp 797–806, 2017. https://doi.org/10.1145/3132847.3132877

[15] Zhang X, Ghorbani AA, "An overview of online fake news: characterization, detection, and discussion", Inf Process Manag 57(2):102025, 2020. https://doi.org/10.1016/j.ipm.2019.03.004

[16] Yazdi KM, Yazdi AM, Khodayi S, Hou J, Zhou W, Saedy S, "Improving fake news detection using k-means and support vector machine approaches", Int J Electron Commun Eng 14(2):38–42, 2020. https://doi.org/10.5281/zenodo.3669287

[17] Edell, A. (2018) "Trained Fake News Detection AI with >95% Accuracy, and Almost Went Crazy." Towards Data Science

[18] Sonal Garg, Dilip Kumar Sharma, "Linguistic features based framework for automatic fake news detection", Computers & Industrial Engineering, Volume 172, Part A, 2022, 108432, ISSN 0360-8352. https://doi.org/10.1016/j.cie.2022.108432.

[19] Zhuoran Lu, Patrick Li, Weilong Wang, and Ming Yin, "The Effects of AI-based Credibility Indicators on the Detection and Spread of Misinformation under Social Influence", Proc. ACM Hum.-Comput. Interact. 6, CSCW2, Article 461, November 2022, 27 pages. https://doi.org/10.1145/3555562

[20] Mr. Rahul Sharma. (2015). Recognition of Anthracnose Injuries on Apple Surfaces using YOLOV 3-Dense. International Journal of New Practices in Management and Engineering, 4(02), 08 - 14. Retrieved from http://ijnpme.org/index.php/IJNPME/article/view/36

[21] Jhade, S. ., Kumar, V. S. ., Kuntavai, T. ., Shekhar Pandey, P. ., Sundaram, A. ., & Parasa, G. . (2023). An Energy Efficient and Cost Reduction based Hybridization Scheme for Mobile Ad-hoc Networks (MANET) over the Internet of Things (IoT). International Journal on Recent and Innovation Trends in Computing and Communication, 11(2s), 157–166. https://doi.org/10.17762/ijritcc.v11i2s.6038

[22] Juneja, V., Singh, S., Jain, V., Pandey, K.K., Dhabliya, D., Gupta, A., Pandey, D. Optimization-based data science for an IoT service applicable in smart cities (2023) Handbook of Research on Data-Driven Mathematical Modeling in Smart Cities, pp. 300-321.

Studies on the Use of Various Noise Strategies for Perturbing Data in Privacy-Preserving Data Mining

Dr. Prarthana A. Deshkar[1], Dr. Jaikumar M. Patil[2], Dr. Pornima B. Niranjane[3], Prof. Vaishali Niranjane[4], Dr. Nisha Thakur[5], Vaibhav D. Dabhade[6]

Abstract: Privacy Preserving Data Mining techniques broadly fall under the categories of randomization and value distortion. Randomization replaces the existing value with a non existing value whereas value distortion modifies each value in the database. Data perturbation is widely used randomization technique that promises both valid data mining result and secured privacy. Existing research works were conducted with additive and multiplicative forms of data perturbation. Privacy is measured with the increasing level of error rate based on different types of attacks. Attacks in data perturbation are normally noise filtering methods which are based on linear and nonlinear filtering schemes. Linear filtering process produces the output data which will be in linear combination of the input values. The perturbed copies in additive and multiplicative data perturbation is generated with Laplace noiseWhen the input data is in linear distribution and is subjected to perturbation, linear filtering schemes are used to reconstruct the data and analyze the privacy measure. In nonlinear filtering schemes, the output of the filtering process will not be in linear distribution. This means that for a non linear data distribution, linear noise filtering schemes cannot be used for accurate analysis. Attacks considered so far are based on only linear filtering schemes. The perturbed models are evaluated with both privacy and utility of data mining. The work describes both linear and non linear type of attacks over the generated perturbed data. Attacks for additive data perturbation include Maximum A Posteriori (MAP) and Principal Component Analysis (PCA) based filtering method.

Keywords: Privacy Preserving, Data Mining, Data perturbation, Maximum A Posteriori, Principal Component Analysis (PCA)

1. Introduction

Sophisticated and powerful technologies today are likely to collect data from different applications and create a massive data repository. Confronted with the massive collection of data, the need for better managerial choices arose in the form of data summarization, extracting the fundamental nature of the information stored and the innovation of new patterns from the raw data. Data mining emerged as a powerful new technology for extracting hidden information from large amount of data[1][2]. The process is also referred as knowledge discovery and it helps to analyze data from different perspectives. Various data mining tools are used to predict the future behavior and trends of the data that helps business people to enhance their decisions accordingly. Technically, Data Mining is defined as the process of discovering information from large amount of data. In other words, it can be said that data mining is the method of mining knowledge from the archived collection of data[3].

The process in knowledge discovery includes the following steps.

• Data Preprocessing includes Data cleaning, Data integration and data transformation.

• Data cleaning involves the removal of noise and inconsistent data from the data warehouse. • Data integration combines data from different data sources and finally data transformation selects the attributes and transforms into different forms appropriate for data mining.

• Data Mining applies intelligent methods in order to extract patterns from the data.

• Pattern Discovery is used to discover new patterns.

• Knowledge Presentation displays the knowledge inferred from the pattern

[1]Assistant Professor, Department of Computer Technology, Yeshwantrao Chavan College of Engineering, Nagpur
prarthana.deshkar@gmail.com

[2]Associate Professor, Department of CSE, Shri Sant Gajanan Maharaj College of Engineering, Shegaon
jaimpatil1011@gmail.com

[3]Assistant Professor. Department of CSE Babasaheb Naik College of Engineering,
pornimaniranjane@gmail.com

[4]Assistant Professor, Department of Electronics and Telecommunication Yeshwantrao Chavan College of Engineering, Nagpur
niranjane_vaishali@yahoo.com

[5]Assistant Professor, Faculty of Engineering and Technology, DMIHER(DU), Sawangi, Wardha
nishat.feat@dmiher.edu.in

[6]Assistant Professor, MET Institute of Engineering, Nashik
vaibhavdabhade@rocketmail.com

Sensitive Data In Data Mining

Identifying new patterns from the historical collection of data is a trendy probing technique in data mining. Nevertheless, if the data values are sensitive then discharging information about noteworthy patterns or trends will lead to significant risk to privacy. For example, if data mining is performed on patient health records or customers purchase records in a super market; sensitive data may include patients" personal details about diseases and the customers" personal details respectively. Sensitive data disclosure susceptibility is one of the major decisive security threats that can result in negotiating the security of data mining applications[4-7]. It happens when the sensitive data is disclosed to unauthorized data miners and such unauthorized access may lead to severe information security and data privacy violations. It thus raises the need to identify methods that focuses on how to precisely learn and discharge the noteworthy patterns in a data set that contains sensitive information, while providing meticulous assurance to privacy of the persons whose information is collected and stored.[8-10]

2. Need for Privacy Preservation

Individual"s privacy is always a common thought and a concept which is always dealt with when handling data for enterprise decision making. With the enhancement of computer technologies and wide usage of web applications, privacy threats pose different technical challenges in today"s information era. Privacy is defined as the users right to preserve and obscure their personal information and have controlled private information disclosure. Various data mining techniques are used to extract constructive patterns from vast collection of data. It supports domains like medical diagnosis, national security, marketing, weather forecasting etc.,[11] Though advantageous in various domains, it is still a challenging issue when users privacy is breached. For example, medical diagnosis involves patient"s health records to be mined for successful patterns. This may include mining of patient"s private information also. When the need for successful patterns from the data owners increases, same happens with the privacy threat level of the users. Marketable issues are also allied with the privacy concern. Many organizations collect customer"s data for specific purposes. When different departments of the organization share the data, it should be ensured that private sensitive data is not despoiled. In such scenarios, need to enhance data mining algorithms to include privacy preservation emerged. Hence, many researches

are committed to tackle the privacy preservation in data mining. Various techniques are proposed to hide private information either by removing the reserved data or by adding noise. The need for privacy preservation can be summarized as follows.[12]

• Discovering useful patterns from the sensitive data.

• Use of single and multiple databases to extract information about individuals.

• Posing open ended queries to find relationships about individuals and groups of individuals.

• Inferring associations between records to retrieve sensitive information

• Non-Predictive aspect of information about individuals during data mining.

• Private and public nature of information gained from data mining

• The potential to create new clusters based on generated patterns. The risks to privacy posed by data mining include, but are not limited to, the following: illegal access to personal data, the revelation of uncomfortable information, the use of personal data for purposes other than those for which it was originally obtained, etc[13]. Companies nowadays often choose to keep any data found from the actions of their consumers, thanks to the prevalence of technology and the ease with which gear can be acquired. As a result, there's rising anxiety that data collectors would use the information they unearth to spy on their customers.[14]

Privacy Preserving Data Mining

A branch of data mining termed "Privacy Preserving Data Mining (PPDM)" has arisen to solve the aforesaid difficulties. In recent years, it has grown in many different ways. The primary goal of PPDM is to prevent confidential data from falling into the wrong hands. In recent years, PPDM has emerged as a promising new area of study for data scientists. The effectiveness and security of data mining methods are examined. PPDM is thus being considered for a dual purpose.[15][16] The first is to prevent users' private information from falling into the wrong hands, and the second is to mine useful information from secure databases. In a word, the goal is to get valid data mining findings without gaining access to sensitive information. Figure 1 depicts the organizational framework for data mining that protects individual privacy.[17]
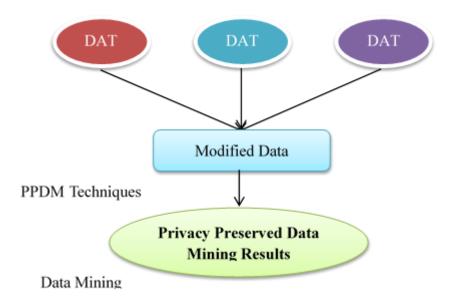
Fig 1 Block diagram of PPDM

PPDM techniques mainly involve two major methods

• Data Perturbation methods that mask the data so that sensitive data is not revealed

• Cryptographic methods that use some key values to encrypt the sensitive data. Generally there are two fundamental problems in PPDM: collection of privacy preserved data and mining the sensitive data across several private platforms.[3][18] The main goal of PPDM algorithms is to retrieve valid information from data warehouse at the same time preserving the private sensitive data. There are many PPDM methods developed in recent years, nevertheless there is no standardized approach to achieve privacy and utility. For getting valid results efficiently, the following dimensions of subjects need to be considered.[4]

• How the data is distributed against the enterprise?

• How do PPDM methods work?

• Mining methodologies and Privacy preservation methods The largest part of the enterprises is in need of secure data transmission and security preservation when the data is stored in the data warehouse. Normally PPDM techniques add values to traditional data mining methodologies by working with hidden sensitive data. The issue faced here is how to do achieve better data mining result from the distorted data. The target of a PPDM algorithm is

• To prevent the identification of sensitive data

• To apply the algorithm to huge collection of data

• To have less exponential computational complexity

To secure the sensitive information during data mining, various techniques have been proposed. Value distortion and randomization are the two basic approaches towards privacy preservation. Randomization method replaces the existing item with non existing item whereas distortion changes every item in a transaction. Data perturbation is also a common approach to preserve the sensitive data. This method perturbs the sensitive data before it is released for data mining.[5][6] The main advantage of perturbation based method is that it preserves the statistical properties of the data and thus the data mining results will be accurate. The drawback is that there is no proper framework for measuring the privacy. However, recent perturbation techniques try to measure the amount of that is guaranteed. Another limb of PPDM uses cryptographic methods for preventing leakage of sensitive information during data mining.[7][16] It proves perfect for two main reasons: one is, it offers a well defined privacy preserving model and the other is, there are various tools of cryptographic algorithms for implementing privacy preservation. Nevertheless, it has also been proved that cryptographic methods do not maintain the utility for data mining models. Though it is helpful in preventing privacy leaks, it falls short of providing a better data mining model. Anonymization techniques also have received a lot of attention to privacy preservation process. The data here is segregated into public and private columns. Public data is made available to all users of the data table whereas private columns are not released in external tables. The privacy measure is that an attacker may not be able to relate private data not more than k individuals. It is made possible by providing every combination of public columns with the private columns in at least k rows. K-anonymity model enforces privacy in context of releasing public data[8]. Data owner ensures that attackers will not be able to link the data which is gained from the database to individual's sensitive data from

whom the data is collected. Differential privacy has also gained popularity in privacy preserving data models. It necessitates that any process to the database should be insensitive to the changes applied in any individual's record. Privacy is guaranteed with aggregate composition of all the individual private records. This method has many advantages over previous methods. It relies on mathematical definition to privacy and hence it becomes easy to prove whether a technique is conventional to differential privacy and to figure out calculations that can or cannot be made in this skeleton. Differential privacy does not depend on attacker's background knowledge. This independence makes data owners to share the data without any concern about past and future releases. It also guarantees the privacy when there is joint reconstruction of two independent differentially private data[10]

Distributed Privacy Preservation

In a decentralized setting, people may seek to pool their individual copies of altered data in order to get meaningful aggregate findings. The primary goal of distributed privacy preservation is to reach consensus on the working out of cumulative information across all data without disclosing any sensitive details. Entities in a dispersed setting don't have faith in one another when it comes to sharing data. Both vertical and horizontal data partitioning are possible in a distributed setting.[11] In a vertically partitioned database, different entities may see different fields from the same set of entries. In horizontal partitioning, individual records are extended among various entities with the same set of characteristics. The difficulty of distributed privacy preservation is complicated by the fact that vertical and horizontal partitioning schemes provide distinct difficulties. Secure multiparty computing, which is used in cryptographic techniques, is also used to preserve privacy in distributed data. Cryptographic approaches, on the other hand, calculate functions over inputs received from a number of different receivers without disclosing each of the inputs individually.[12]

3. Data Perturbation

The most widely used method for PPDM is the Data Perturbation approach. Perturbation approach is used in applications where the data owners wish to allow the data for collaborative data mining without compromising individual's privacy. Data publishing for research, releasing the data to the third party data miners are examples where data perturbation can be applied. Statistical Disclosure Control (SDC) techniques help in data perturbation by releasing the statistics of the data without the leakage of private sensitive information. Statistical methods necessitate some kind of data

modification to ensure the privacy protection.[13] This lies between data encryption where the data set is fully encryption with minimum or no data mining utility and no modification which allows maximum utility of data mining. Data Perturbation modifies the sensitive data in such a way that both privacy and data mining utility are balanced. The main challenge in statistical disclosure control techniques lies in modifying the data with minimum information loss while mining. Two broad categories of masking methods can be dealt with: Perturbative and Non-Perturbative masking methods. Both the techniques are used for continuous and categorical attributes.[14] Continuous attributes are numerical and arithmetic operations are allowed on it. For example, age, income etc are continuous attributes. A categorical attribute limits the value set to it. An ordered relationship can be defined over the categorical attribute. For example, marital status, gender etc., are categorical attribute[5][15]

Perturbative Masking method

In Perturbative masking method the dataset is modified before publishing. The original statistics of the data will be overwritten with the new unique statistics in the perturbed dataset. This enables to preserve statistical confidentiality. The techniques for perturbation should be in such a way that the new statistics should not result in different results that would be obtained from the original statistics. Random noise addition, resampling, swapping the data and aggregation are some of the perturbative masking methods[3][6].

Where X is the original data, A is the transformation method, and Z is the noise introduced, Y is the result of using the perturbative masking approach. When it comes to perturbative masking methods, the noise additive approach is by far the most used. The approach introduces some chance variation into the baseline readings[4][11]. The impact of adding noise to the original sensitive data is determined by the statistical characteristic of the noise. Various noise addition strategies are presented to retain the statistical features of the original data. When perturbing sensitive data with uncorrelated noise, a vector of a particular attribute is swapped out with another vector that is the original vector plus a vectors of normal distribution noise.[12]

Perturbation using correlated noise – Addition of correlated noise preserves the correlation coefficients. The covariance matrix of the perturbed data and the noise is proportional to the covariance matrix of the original data.

The insertion of correlated noise works well with continuous data. Algorithms above address the usage of additive noise technique for perturbation of sensitive

properties. The disturbance caused by correlated noise may also be multiplicative. Multiplicative data perturbation techniques keep sensitive information private while maintaining data usefulness. When numerous transformations are applied, a transformation-invariant model for data mining is the outcome.[7] Rotational perturbation, projectional perturbation, and geometric perturbation are the three varieties of multiplicative perturbation. Because it maintains the distance and inner product, which is necessary for classification and clustering methods, multiplicative data perturbation is helpful in the classification and clustering process. This ensures that the accuracy of the modified data mining model is equivalent to that of the original data model.[5]

Additive Data Perturbation

Additive Data Perturbation approach preserves the data privacy by adding a randomly generated noise to the original data. Assuming the original data denoted as X and the random noise as Z, the perturbed copy (Y) is obtained by the Equation (1)

$$Y = X + Z \qquad (1)$$

This method preserves the privacy of the sensitive data by adding some random noise at the same time making sure that the random noise still preserves the original data from the data so that the data mining patterns can still be accurately estimated. The data owner returns a value of X+Z of the original dataset, where Z is drawn from a certain distribution. A large amount frequently used distributions are the uniform distribution over a specified interval [-α,+ α] and Gaussian distribution with mean μ = 0 and standard deviation σ. In this interpretation, the raw data have the same distribution as the random variable but are considered to be independent random variables. Randomized perturbation experiments use such independent samples. The data provider also supplies the function of cumulative distribution and the perturbed values. There are two common methods for introducing additive noise into data. Membership in the Value Class Distribution of Values The perturbation in the value distribution technique is based on a random value drawn from a predetermined distribution. Estimating the density of a function is a typical challenge in data analysis as well as in security applications. The density data may be used to issues of grouping, classification, and the like. Using additive noise to perturb data allows for a fair estimation of the underlying density function.

Single Level Gaussian Additive Data Perturbation

The framework for additive Gaussian noise at single level trust is depicted in Figure 2. As illustrated in the figure, the sensitive attributes are extracted from the original data set and is taken up for perturbation. Random Gaussian noise is generated using Gaussian function and is added to the sensitive attribute to generate the perturbed copy
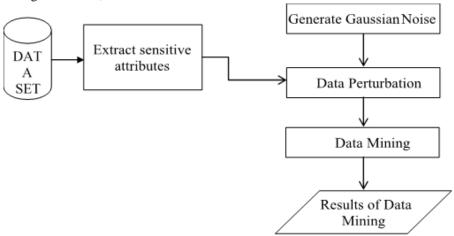

Fig 2 Additive Gaussian Data Perturbation at Single Level Trust

The algorithmic steps of the process involved are shown in Algorithm 1.

```
Input    : Original Data set X, Covariance C_x, Noise N
Output   : Perturbed data P
         Generate random Gaussian noise GN ~ N in (0, σ2Cx)
         for sensitive attributes
              for all values in each sensitive attributes
                   Construct P = X + GN
              End for
         End for
```

Algorithm 1 Single Level Gaussian Additive Perturbation

Single Level Geometric Data Perturbation using Gaussian Noise

From the study of literature, it is found that out of the three representative methods of multiplicative data perturbation, geometric data perturbation is found to be effective to knowledgeable attackers. Hence, geometric data perturbation is taken into consideration for the research findings. The framework for multiplicative data perturbation using Gaussian noise at single level trust can be described in the diagram shown in Figure 3
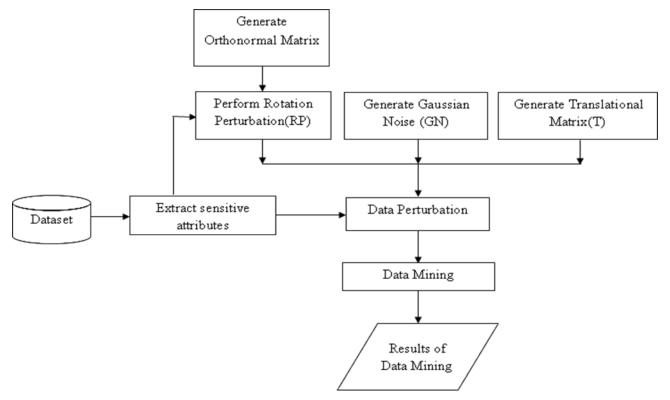
Fig 3. Multiplicative Gaussian Data Perturbation at Single Level Trust

4. Experimental Evaluation

In this section, experiments are carried out to evaluate the effectiveness of Multiplicative Gaussian noise technique over additive Gaussian noise. Since data perturbation involves addition of noise to the sensitive attributes, privacy is measured by analyzing the error that is obtained in reconstructing the original data by removing noise. Various noise filtering schemes are used for this purpose. In the experimental evaluation, privacy precision is computed by testing the perturbed data with PCA and ICA based noise filtering schemes. Data mining utility is also evaluated by utilizing classification model over the perturbed data. The proposed research work is experimented with bank and credit card data set from UCI repository. The bank dataset contains 25,000 instances with 16 attributes. The test data has 500 instances. Out of the 16 attributes, age and balance are taken as the sensitive attribute. In the credit card data set 20000 instances for train data and 6000 instances for test data is available. There are 24 attributes out of which age and credit-limit are taken as the sensitive attributes. The experiments are carried out in MATLAB for measuring the privacy level and in WEKA for computing the classifier accuracy. It is assumed that the attackers have

the knowledge on the distribution of noise, mean and covariance of the original data and the perturbed data.

Additive Gaussian noise data perturbation

Let the original data values be X = {25, 27, 31, 32}. Gaussian noise is generated randomly using mean as 0 and variance as $\sigma 2Cx$. Cx is the covariance matrix of X and the value of $\sigma 2$ is assumed to be 0.05. The randomly generated Gaussian noise is obtained by adding mean (which is assumed as 0) with $\sigma 2Cx *$ rand (N,1).

This gives the values of Gaussian noise as

GN = {-0.9212, 1.8126, -0.19322, 1.22547}

With the Gaussian noise, perturbed data is obtained by adding the noise to the sensitive data values X.

Perturbed data = X + GN

Peturbed data = {25-0.9212, 27+1.8126, 31-0.19322, 32+1.22547}

= {24.0788, 28.8126, 30.80678, and 33.22547}

Estimation of Classifier model accuracy

Gaussian additive and multiplicative perturbed copies of the data are utilized for evaluating classifier algorithms such as Decision Tree classifier, Naïve Bayes classifier and KNN classifier. It is verified that the perturbed copies with additive and multiplicative techniques has the same data mining utility as that of the original data. The utilities of decision tree and naïve Bayes classifier models are measured. Table 1 below shows the classifier accuracy of different models under single level trust.

Table 1: Single-Level Trust Accuracy of Classifiers for Gaussian Data Disturbances

Classifier Accuracy	Bank Dataset			Credit Card Dataset		
	Decision Tree	Naïve Bayes	KNN	Decision Tree	Naïve Bayes	KNN
Original Data	92.76	90.24	86.42	79.82	42.3	75.12
Gaussian Additive	91.16	91.81	78.42	77.42	52.3	42.22
Gaussian Multiplicative	87.25	87.76	87.42	75.62	55.22	69.78
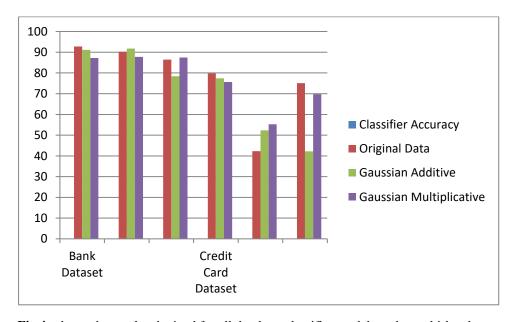
Fig 4. shows the results obtained for all the three classifier models under multi-level trust.

The results clearly show that Gaussian Additive scheme provides nearly equal classifier accuracy as that of the original data for Decision Tree and Naïve Bayes classifier algorithm. Gaussian multiplicative technique is better for KNN classifier model for both bank and credit card dataset. This is because multiplicative scheme performs an orthonormal transformation which preserves the Euclidean distance of the data points. Hence, the distance based classifier model suits to multiplicative perturbation providing better classifier accuracy.

5. Conclusion

The main focus of this research is to enable efficient data mining process with the distorted data. Data perturbation approach utilizing Gaussian noise is presented. The framework is experimented with both Gaussian additive and Gaussian multiplicative schemes. In Gaussian additive method, randomly generated Gaussian noise is added to the sensitive data. The perturbed data is evaluated for privacy precision and classifier accuracy. Under Gaussian multiplicative method, rotation matrix, translation matrix and random Gaussian noise components are added to the sensitive data. The perturbed data is then experimented for classifier accuracy. Algorithms are tested under single level and multilevel trust of the data miners. Under single level trust there is no significant change in the results. In multilevel trust scenario, it is proved that even if the number of perturbed copies available increases, there is no diversity gain in the reconstruction of the original data. Compared to Gaussian additive scheme, Gaussian multiplicative scheme gives almost identical results for all levels of trust. Experimental results proved that Gaussian multiplicative scheme finds better solution to privacy preservation and utility preservation when compared to Gaussian additive method when the classifier model is developed using KNN algorithm.

References

[1] S. M. Jesus and O. C. Rodríguez, "Estimating excess noise from deep sea mining: a simulated test case," *OCEANS 2023 - Limerick*, Limerick, Ireland, 2023, pp. 1-6, doi: 10.1109/OCEANSLimerick52467.2023.10244695.

[2] T. Zhang, X. Liu, J. Wang and W. K. Victor Chan, "Improve Data Mining Performance by Noise Redistribution: A Mixed Integer Programming Formulation," *2023 IEEE International Conference on Smart Internet of Things (SmartIoT)*, Xining, China, 2023, pp. 190-195, doi: 10.1109/SmartIoT58732.2023.00034.

[3] P. Dubey and A. Rajavat, "Effective K-means clustering algorithm for efficient data mining," *2023 2nd International Conference on Vision Towards Emerging Trends in Communication and Networking Technologies (ViTECoN)*, Vellore, India, 2023, pp. 1-6, doi: 10.1109/ViTECoN58111.2023.10157179.

[4] T. Zhang, X. Liu, J. Wang and W. K. Victor Chan, "Improve Data Mining Performance by Noise Redistribution: A Mixed Integer Programming Formulation," *2023 IEEE International Conference on Smart Internet of Things (SmartIoT)*, Xining, China, 2023, pp. 190-195, doi: 10.1109/SmartIoT58732.2023.00034.

[5] P. Lin, S. Peng, Y. Xiang, C. Li, X. Cui and W. Zhang, "Structure-Oriented CUR Low-Rank Approximation for Random Noise Attenuation of Seismic Data," in *IEEE Transactions on Geoscience and Remote Sensing*, vol. 61, pp. 1-13, 2023, Art no. 4504713, doi: 10.1109/TGRS.2023.3297999.

[6] M. F. Uddin, "An Enhanced Machine Learning Approach to Identify Noise and Detect Relevant Structures for Predictive Modeling," *2023 9th International Conference on Information Technology Trends (ITT)*, Dubai, United Arab Emirates, 2023, pp. 55-60, doi: 10.1109/ITT59889.2023.10184237.

[7] L. Wang and T. Zhang, "The Application of Data Mining Algorithm in the Legal Protection of Personal Data," *2022 IEEE 2nd International Conference on Data Science and Computer Application (ICDSCA)*, Dalian, China, 2022, pp. 1339-1342, doi: 10.1109/ICDSCA56264.2022.9988630.

[8] Y. Lu, X. -D. Liu, J. -J. Song, T. -H. Xu and E. C. C. Tsang, "Data Noise Suppression-based Attribute Reduction," *2022 International Conference on Wavelet Analysis and Pattern Recognition (ICWAPR)*, Toyama, Japan, 2022, pp. 89-94, doi: 10.1109/ICWAPR56446.2022.9947188.

[9] Y. Lu, X. -D. Liu, J. -J. Song, T. -H. Xu and E. C. C. Tsang, "Data Noise Suppression-based Attribute Reduction," *2022 International Conference on Wavelet Analysis and Pattern Recognition (ICWAPR)*, Toyama, Japan, 2022, pp. 89-94, doi: 10.1109/ICWAPR56446.2022.9947188.

[10] S. Wang, P. Song, J. Tan, B. He, Q. Wang and G. Du, "Attention-Based Neural Network for Erratic Noise Attenuation From Seismic Data With a Shuffled Noise Training Data Generation Strategy," in *IEEE Transactions on Geoscience and Remote Sensing*, vol. 60, pp. 1-16, 2022, Art no. 5918916, doi: 10.1109/TGRS.2022.3197929.

[11] R. Churchill and L. Singh, "Topic-Noise Models: Modeling Topic and Noise Distributions in Social Media Post Collections," *2021 IEEE International Conference on Data Mining (ICDM)*, Auckland, New Zealand, 2021, pp. 71-80, doi: 10.1109/ICDM51629.2021.00017.

[12] J. Shan, Y. Lin and X. Zhu, "A New Range Noise Perturbation Method based on Privacy Preserving Data Mining," *2020 IEEE International Conference on Artificial Intelligence and Information Systems (ICAIIS)*, Dalian, China, 2020, pp. 131-136, doi: 10.1109/ICAIIS49377.2020.9194850.

[13] C. Boonseng, R. Boonseng and K. Kularbphettong, "Noise and Vibration Analysis of Dry-Type Power

Transformer for Monitoring and Data Mining Applications," *2019 22nd International Conference on Electrical Machines and Systems (ICEMS)*, Harbin, China, 2019, pp. 1-5, doi: 10.1109/ICEMS.2019.8922194.

[14] Y. Shi, "Multi-Dimensional Processing for Big Data with Noise," *2019 IEEE International Conference on Power, Intelligent Computing and Systems (ICPICS)*, Shenyang, China, 2019, pp. 686-690, doi: 10.1109/ICPICS47731.2019.8942582.

[15] S. Yaji and B. Neelima, "Optimizing Privacy-Preserving Data Mining Model in Multivariate Datasets," *2019 PhD Colloquium on Ethically Driven Innovation and Technology for Society (PhD EDITS)*, Bangalore, India, 2019, pp. 1-3, doi: 10.1109/PhDEDITS47523.2019.8986965.

[16] W. Li, H. Zhu, W. Liu, D. Chen, J. Jiang and Q. Jin, "An Anti-Noise Process Mining Algorithm Based on Minimum Spanning Tree Clustering," in *IEEE Access*, vol. 6, pp. 48756-48764, 2018, doi: 10.1109/ACCESS.2018.2865540.

[17] H. S. Aggarwal, A. Kansal and A. Jamshed, "Noisy information and progressive data-mining giving rise to privacy preservation," *2017 3rd International Conference on Advances in Computing,Communication & Automation (ICACCA) (Fall)*, Dehradun, India, 2017, pp. 1-5, doi: 10.1109/ICACCAF.2017.8344673.

[18] Y. Sei and A. Ohsuga, "Private True Data Mining: Differential Privacy Featuring Errors to Manage Internet-of-Things Data," in *IEEE Access*, vol. 10, pp. 8738-8757, 2022, doi: 10.1109/ACCESS.2022.3143813.

Mobile Cum Web Based Voting System for Rural Areas in India

Gaurav D. Barokar* Chandrashekhar M. Mankar** Harshal D. Gurad***

Abstract

Elections are main and very important part of our daily life. Unlike any other transactional event, the result of elections can have many positive and/or negative effects on these communities and their wellbeing. In Asian countries like India there are lots of problems in the election, such as there is no proper road developed so that voter or election committee can reach up to the election booth. In some places, fake voters are created or by forcing the voter to give vote for a fix candidate. So to overcome these drawbacks we build proper and trusted (transparent) voting system. This paper details the requirements, design and implementation of a e-voting system and held various election campaigns simultaneously and permits voters to cast their votes in the specific elections at anytime (anytime voting), from any-location (anywhere voting).

Keywords: Voter, Election, E-Voting, Voting System, Web Pages, Software Engineering.

1. INTRODUCTION

This system is pure and trustworthy which deals with the e-voting and overcomes the lot of drawbacks of the traditional voting and holds the democratic rights and the human rights. So voter can feel safe and cast his vote easily. This system is very useful in all the organizations, institutes and industries. Here to develop the system we use the election algorithm.

In the election algorithm, when a process notices that the coordinator is no longer responding to requests, it initiates an election. The efficiency of vote counting is much easy and transparent than the traditional counting.Time saving approach. No wastage of paper. So the basic principal of this system is to provide the transparent and trustworthy elections to end user(voter). [1]

1. In future it can provide better pathway for handling general voting system for democratic country like Our India.

2. It will going to reduce the huge expenditure related to the same.

3. People they have not internet connection they can be informed by SMS on their mobile. Today many websites provide free SMS to the mobile.

4. It increases the E knowledge of the users which is very necessary for current generation. 3. The mobile based cum web based voting System can be applicable in all the organizations, institutes and industries where shares of individual increases the decision making process.

2. SOFTWARE REQUIREMENT SPECIFICATION

The election-specific requirements are those requirements that are specific to a given election. For example, the election specific requirements for corporate sector include the following items. A voter must be registered as a full

---

* Student (M.E. 1st Year), Shri Sant Gajana Maharaj College of Engineering, Dostrict Buldana, Maharashtra, India.
E-mail: gaurav.barokar@gmail.com

** Assistant Professor, Shri Sant Gajana Maharaj College of Engineering, Dostrict Buldana, Maharashtra, India.
E-mail: cmmankar@gmail.com

*** Student (M.E. 2nd Year), Shri Sant Gajana Maharaj College of Engineering, Dostrict Buldana, Maharashtra, India.
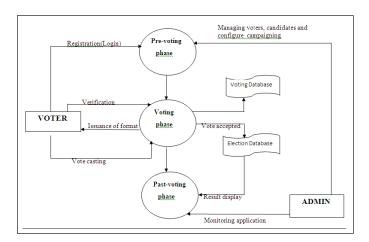E-mail: guradharshal@gmail.com

time employee. A candidate must be registered as a full time employee. A candidate is also a voter. An election winner must be one of the candidates for that election. The application is easy to interact and communicate with. The administrator can add new database regarding voters and campaigning easily.

The performance of application depends on availability during campaigning.

The software provides Accuracy by not allowing any alteration. It is easy to maintain software.

3. DATA FLOW OF PROJECT

4. IMPORTANT MODULE AND ALGORITHMS

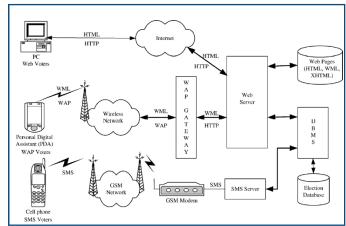The complete software consist of following modules:

1. Web voter: The module is using web browser as a presentation engine. The voter will directly vote through website and cast the vote. First he /she has to fill basic information for registration, this information will be further matched with database of authorized voters. Then voter will login through the password provided to him which will allow him to select the candidate of own choice from the list of candidates.

2. WAP voter: This module is using micro browser as a presentation engine. In this user can follow the approach of both Web voter module as well as SMS voter module.

3. SMS voter: This module is using text editor as a presentation engine. Here the voter will cast the vote by sending the SMS. The user will be an authorized voter if his mobile number matches with the contact number

of the database. After being authenticated he will be provided with a session password to create a secure session while casting the vote. As soon as vote is casted the session password is destroyed.

4. Result : For maintaining the transparency of elections carried out through the system we are using counters to show the number of votes casted to the respective candidate and these counter updates will be visible to voter. To get the result at a glance of all candidates the result is displayed using histogram.

While implementing the software we have followed the Basic Election Algorithm**.**

5. SYSTEM ARCHITECTURE

The above fig shows the overall architecture of the voting system. Firstly the system has three medium through which the voter will cast his vote through any of the possible medium. Through WEB, through WAP enabled mobile phones and through SMS. [6]

There is election database which stores all the related information about the election. So if voter wants to cast his vote through WEB or WAP then web server handles the activity. WEB voter cast his vote through http site then it is acknowledge by WEB server and his vote is store in the database. If the user is wish to cast his vote through mobile GPRS then he will access the WAP site and it will take to the WAP gateway and then acknowledge by the WEB server and vote is store in the database.

And for the third user SMS facility is provided. This medium is for remote areas in India where people are not aware of internet and WAP. So they can vote easily through this medium in their own language. After sending

message it will acknowledge by the SMS server and vote is store in the database. So these are the three medium through which voter will cast his votes.

If voter is trying to cast his vote through all medium then only one vote is count which comes first. So we overcome the vote duplication problem. And finally the result are shown on the WEB. This system is transparent so voter can easily see the result of his specific candidate. And all results are maintain by the election database.

6. ESTIMATION OF KLOC

The number of lines required for implementation of various modules can be estimated as follows:

Sr.No.	Modules	KLOC
1.	Graphical User Interface	0.50
2.	User authentication Code	0.20
3.	Device Drivers	0.40
4.	Interfacing Code	0.20

Thus the total number of lines required is approximately 2.40 KLOC

Efforts

$E = 3.2*(KLOC)^{1.02}$

$E = 3.2*(2.40)^{1.02}$

$E = 7.82$ person-month

Development Time (In Months)

$D = E/N$

$D = 7.82/4$

$D = 3.91$ months.

Number of Persons

4 persons are required to complete the project with given time span successful

7. CONCLUSION AND FUTURE SCOPE

The development of the project has given us an excellent opportunity & experience to know how real life project works in its working environment and that there is always some differences in studying software engineering theoretically and its application.

This project have tried to develop a concept regarding how some of the aspects during automating the system that were taken care of-

1. The system should meet the user requirement

2. The system should be efficient enough in generating output in simplified manner.

3. The system database should be easy to maintain & upgrade easily.

4. The platform must be as simple as possible for maintenance issues.

5. It is always better to invest today on more sophisticated technology rather tomorrow spending of the system.

REFERENCES

[1] Bergsten, H. (2003). Software Engineering - A Practitioner's Approach. (3rd ed.) Oreilly & Associates.

[2] Stevens, P. & Pooley, R. (2000). *Using UML Software Engineering with Objects and Components*. UK, Harlow, Essex: Addison-Wesley.

[3] Gundavaram, S., Birznieks, G. & Guelich, S. (2000). *CGI Programming with Perl* (2nded.).Oreilly & Associates.

[4] Deitel, H. M., Deitel, P. J., Nieto, T. R. & Steinbuhler, K. (2002). *Internet, World Wide Web How to Program* (2nded.). Prentice Hall.

[5] Mc Goveran, D. & Date, C. J. (1992). *A Guide to Sybase and SQL Server*. Addison-Wesley Publisher.

[6] Bjeletich, S. & Mable, G. (1999). *Microsoft SQL Server 7.0 Unleashed*. Sams Publisher.

[7] Qadah, G. Z. & Taha, R. (2007). Electronic voting systems: Requirements, design, and implementation. *Computer Standards & Interfaces*, 29(3), 376-386.

[8] Folorunso, O., Ogunseye, O. S., Okesola, J. O. & Olaniyan, O. M. (2010). Visualizing e-voting results. *Journal of Theoretical and Applied Information Technology*, 16(1), 57-69.

_____

An Enhanced Query Optimization Implemented in Hadoop using Bio-Inspired Algorithm with HDFS Technique

[1]**Abhijit Banubakode**, [2]**Vandana C. Bagal**, [3]**Vishwanath S. Mahalle**, [4]**Maqsood A. Ansari**, [5]**Chhaya S. Gosavi**, [6]**Archana Chaugule**

[1]MET Institute of Computer Science
Maharashtra, Mumbai, India
e-mail: abhijitsiu@gmail.com

[2]K. K.Wagh Institute of Engineering Education and Research, Nashik,Maharashtra, India
e-mail:vcbagal@kkwagh.edu.in

[3]Shri Sant Gajanan Maharaj College of Engineering
Shegaon, Maharashtra, India
e-mail: vvntvsm@gmail.com

[4]Smt. Kashibai Navale College of Engineering
Pune, Maharashtra,India
e-mail: maqans@gmail.com

[5]MKSSS's Cummins College of Engineering for Women
Pune,Maharashtra,india
e-mail: chhaya.gosavi@cumminscollege.in

[6]Pimpri Chinchwad College of Engineering and Research
Pune,Maharashtra,India
e-mail: archna.ajit27@gmail.com

Abstract: A more effective method for massive data query optimization using HDFS and the Bio-inspired algorithm. Big Data configuration and query optimization are the two phases of the process. To remove redundant data, the input data is first per-processed using HDFS. Then, utilizing entropy calculation, features like closed frequent pattern, support, and confidence are extracted and managed. The Bio-inspired Horse Herd approach is used to group pertinent information based on this outcome. In the second step, the Big Data queries are used to obtain the same features. The optimized query is then located using the Bio-inspired technique, and the similarity assessment procedure is run. The proposed algorithm, according to this research, outperforms other ones that is unique in use. It is challenging to determine the veracity of this claim without more information regarding the experimental setup and the precise measures employed to assess the algorithm's effectiveness. Furthermore, it is unknown how the proposed algorithm stacks up against other cutting-edge query optimization methods. Finally, the assess has efficiency of using this method, more optimistic query achieved and comparison analysis are proved.

Keywords: Hadoop Distributed File System (HDFS), Bio-inspired Optimization algorithm,Secure Hash Algorithm, Big Data and Query processing.

I. INTRODUCTION

The value of big data analysis in both professional and academic environments. For example, net organizations accumulate full-size volumes of statistics from a selection of resources, including provider logs, site crawlers, and click- streams. it's miles called "big data" due to the fact the volume of statistics being amassed exceeds the ability and processing pace of traditional storage structures. The requirement for software structures that can cope with dynamic, multi-goal optimization problems in big facts. A computing platform created in particular for processing

massive data is known as a huge facts processing platform. Currently, databases and business practices studies is extra worried with performance than energy efficiency. The article does acknowledge, but, that big data can't be treated by means of conventional relational database management structures (RDBMS) or conventional statistical strategies [1, 2].

To address such large statistics processing, many organizations depend on particularly disbursed software program structures running on vast clusters of commodity equipment. As a way to examine huge statistics sets, query

521

_____

optimization is critical considering that it can reduce the quantity of queries needed to examine the statistics. Given the developing significance of statistics in a spread of disciplines, consisting of the development of consumer bases, research, and marketplace analysis, the passage factors [3]. Numerous query plans for finishing queries are analyzed in many relational database management systems, and a terrific query plan is discovered to limit using precise resources, inclusive of I/O. To procedure data extra efficiently, an appropriate query get right of entry to method may be chosen with using this optimization [4].

Big data analytics are regularly accomplished by means of developing and running queries in sq.-like languages that are supported with the aid of structures like Hadoop, Scope, and Spark. An open-supply framework known as Hadoop makes it viable to broaden massive-scale, records-extensive computing programs. It makes use of algorithms which are based on Google's in-intensity examine and information in processing extensive amounts of statistics [5]. The Map-lessen paradigm, which enables disbursed processing of big datasets over clusters of computers, is a part of the structure this is supposed to make massive-scale batch processing less difficult to apply. Big statistics units are also saved the use of the Hadoop dispensed document system [6].
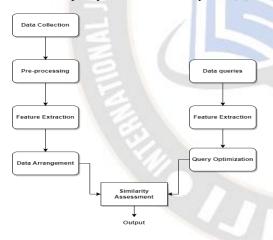

Figure 1. Traditional Block Diagram of Query Optimization based
Framework for Big Data categorization and Pre-processing [7]

In view that Google first announced MR in 2004, it has grown to be a properly-liked framework for managing big datasets. Primarily based at the MR paradigm, the modern-day open-source Hadoop challenge gives the parallel processing of widespread volumes of records, automatic facts splitting, records distribution, fault tolerance, & load balancing control, main to dependable in parallel throughout a dispensed network of dozens to heaps of commodity machines via breaking them up into smaller, greater conceivable chunks. This approach permits for amazing

scalability, availability, and fault tolerance because the machine can preserve jogging even if a few machines malfunction [8].

The problems of massive-scale facts analysis, which can also include processing tens or hundreds of terabytes of facts. The most broadly used open-source processing engine for BD is Apache Spark, which has an extensive variety of libraries and rich language-integrated APIs [9]. The primary components of the Spark API are collections of Java/Python gadgets, where users can execute arbitrary Python or Java operations the usage of operators like map and group.

The draft framework for this take a look at is systematized as section 2 surveys the related research on the advised approach. Section 3 prefers a succinct review of the proposed method, segment four explores the investigational final results, and section 5 deduces the paper.

II. LITERATURE SURVEY

Data locality and Hadoop [10] parameter tuning in dependable and uniform cluster environments make up the majority of the related attempt for enhancing Map reduce performance. [11] Cautioned have been used to categorize this system. The experimental findings confirmed that the use of iHOME on Hive, the overall execution time of 8 join queries was reduced. However, this machine nonetheless required some refinements.

A heuristic-centric method changed into proposed in [12] as a option to the Multi be a part of question Ordering (or MJQO) problem. This algorithm blended "2" critical seek algorithms: cuckoo and tabu seek. The simulation found out some exciting outcomes about the proposed algorithm and recommended that it could solve the MJQO trouble quicker than the present methods. A framework for growing and constructing green databases changed into furnished in [13]. First, a method for modelling the power cost of question plans for the duration of query processing based on their styles of aid intake changed into proposed. The basics of plan evaluation had been then examined. The evaluation method made use of the trade-offs among electricity and performance of plans, using the price model as a basis. The results of the experiments showed that this framework might also considerably lessen electricity use and boost power performance the usage of specific and trustworthy statistical records [14].

so as to reduce general value, [15] intensity category was created for PGNN searches, in which candidate object possibilities had been mechanically chosen based on diverse queries [16]. The PGNN query become then chosen to have

_____

a few beneficial features. The extreme gaining knowledge of gadget (ELM)-based DCA (intensity type algorithm), which used a plurality balloting method, turned into then supplied. The effects showed that the ELM classifier's intensity-set prices are decrease general than the default values.

Added optimization procedures for recurrent queries in BD analysis in [17]. The MR regular window slice algorithm was implemented on this method to reuse recurrent queries. Moreover, the redundant facts become eliminated at the same time as input records was being loaded the use of exceptional-grain scheduling. Next, it evolved the MR late scheduling approach for facts scheduling, which greater information processing and optimized the scheduling of computation sources in the MR cluster. The results of the trial on diverse workloads verified that the algorithms exceeded the satisfactory techniques.

[18] Provided an approach as an addition approach became discovered to discover better answers, kind of 91.five-122.four% quicker than formerly a hit methods, in line with experimental opinions of this technique. This turned into completed by using disposing of the useless operations or even providing vital meta-facts as comments data to other marketers (ants).

In order to account for slow storage, it proposed the MOTH multi-query optimization device, which uses metadata and histograms had been evolved by using MOTH [19]. in step with the trial findings, the three absolutely reused-centric plans carried out better than the Naive technique plan on common with the aid of forty%, 45%, and 50%, respectively. On MR, the 2 partly reused-based totally plans fared higher on average than the Naive approach plan by 22% and 27%, respectively.

Our in advance studies focused on debunking common myths approximately large facts processing in dynamic and high quality conditions and supplying enormous insights into the underlying causes and potency of massive records processing. Our in advance studies pursuits to pave the way for future massive records processing optimization or avoidance that is the focus of this book.

III.   PROPOSED METHODOLOGY

Companies keep many databases to save and system Big Data (BD), that's extraordinarily volumetric and has a ramification of statistics fashions. Business achievement depends on querying and BD analysis for perception. The use of each the HDFS map-reduce technique and the bio-

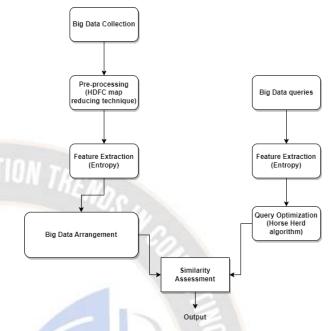inspired set of rules, this paintings stepped forward the question optimization procedure in BD.

Figure 2. Proposed Block diagram

➤   BigData business enterprise calls for a methodical and effective approach to prepare and keep huge quantities of facts. The following are some famous strategies for organizing massive statistics:

➤   Distributed storage: using an allotted report device, along with Hadoop disbursed document gadget or Apache Cassandra, is a famous approach. big facts volumes can now be stored and accessed more effortlessly thanks to these systems' help for facts distribution across numerous nodes.

➤   Data partitioning: Dividing records into smaller subsets is every other manner. Information may be divided, for instance, in step with time, area, or every other characteristic. The records processing and analysis are facilitated by using this.

➤   Compression: large information units can eat up a variety of garage space, consequently compression is a great concept. It could use compression techniques like gzip or bzip2 to limit the amount of garage required.

➤   Statistics indexing: Indexing can assist huge facts units' search and question instances. It is feasible to set up indexes on unique qualities to make it easier to look for precise records.

➤   Data normalization: Organizing information into a standardized format is known as normalization. This will facilitate statistics assessment and evaluation throughout many records units.

_____

➤ Statistics archiving: finally, its miles viable to shop statistics this is no longer required for evaluation. As an end result, garage area is freed up and handling the facts that is nevertheless in use is made easier.

A. Pre-processing

The pre-processing of the input data was carried out during this phase. First, it uses the Secure Hash Algorithm (SHA-512) to determine the HV for each piece of data. Then, using HDFS, the MR process is carried out using the HV as its focal point. The subsections below provide an explanation of the SHA-512 and HDFS processes. In [20] for the SHA-512 method used to calculate the hash value of large amounts of data. Blocks of the augmented data are created. The following stage updates a 512-bit buffer.

$$fH(Dn) = \{H(D1), H(D2), H(D3), \ldots \ldots, H(Dn)\}$$
(1)

WhereH (Dn) stands for the HV of the n-number of data, and fH (Dn) stands for find the HV of the n-number of data.

B. HDFS

A distributed file system called HDFS is employed to safely and effectively store and handle huge amounts of data. It is made to function with the HadoopMapReduce (MR) programming style, a well-liked technique for handling sizable data collections. Data transport speed between nodes is one of HDFS's main characteristics. This makes it possible to process big data sets across a cluster of computers effectively [21]. The capability of HDFS to eliminate duplicate data from the collection is another crucial feature. As a result, less storage space is required and data processing efficiency is increased.HDFS does not alter the file after it has been written; instead, it retrieves data based on the file name. This guarantees the consistency and integrity of the data saved in HDFS. Therefore, the entire file must be rewritten if any modifications are necessary. To solve a query, the HDFS uses "2" phases, such as the map function and the reduced function, which are represented as follows:

$$H (Dn) = [Pf, Cf]$$
(2)

Characteristic map () The Map () function is the first feature to be had in the Map/reduction device. The master node (MN) is where this feature is dominant. The input facts is divided up or processed into a couple of smaller sub-processes. The employee nodes, which cope with those little methods, are where those sub-methods are further dispersed. The MN is then given an acknowledgment.

$$Pf = map(H(4)(Dn))$$
(3)

Map () denotes the feature that plays the mapping, and Pf is the result of the map () characteristic.

The reduce () characteristic is the subsequent feature within the Hadoop tool that is important. This function gathers the thorough sub-operation consequences, combines them, after which offers the aggregated choice-based consequences as an acknowledgement of the initial primary desires. the subsequent mathematical equation shows a way to denote the discount feature:

$$Cf = (5)reduce(Pf)$$
(4)

Where Pf is the result of the mapping function, reduce () reduces the components, and Cf is the reduced set of data.

C. Feature extraction

Important properties together with closed frequent object set, aid, and self-belief are retrieved from the unique data after repetitive information has been removed. Ultimately, the fee of aid and self-assurance is controlled based on the entropy calculation. Using the normalized k-way (NKM) method, big data format this component used a Horse Herd technique to accomplish a BD layout. Here, it begins via the use of the guide and self-belief features' entropy fee, which incorporates of lowest and most values [22].

D. Normalization

The normalization is stated as,

$$N \propto = \frac{D - Dmin}{Dmax - Dmin} \qquad (5)$$

Where Dmax and Dmin are the maximum and minimum values of the number of data D, respectively, and N stands for the normalized value of Dmax. Next, use Horse Herd to calculate the total number of clusters and beginning centroids. The Horse Herd clustering algorithm is used to divide N values into c clusters. The clustering problem is solved using the algorithm in order to determine the objective function's ideal value. Better clustering outcomes are indicated by a smaller value for the objective function [23].

The Horse Herd Optimization Algorithm (HOA) mimics the behaviour of different age groups of horse herds. Horse behaviour can be categorized into six broad divisions based on common patterns: grazing, hierarchy, sociability, imitation, defence mechanism, and roaming [22]. At

524

_____

different ages, horse's exhibit varied behaviours. To determine the age of the horses, a thorough matrix of responses should be constructed for each iteration.
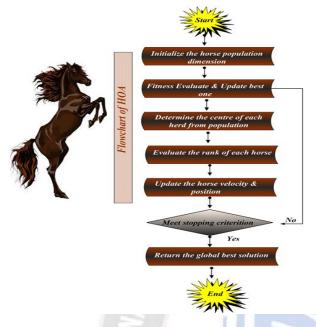

Figure 3. Flow diagram of Horse Herd Optimization Algorithm

IV. RESULTS AND DISCUSSION

This section tested the effectiveness of the counselled question optimization approach whilst applied to the pony Herd method. The device overall performance is tested and compared to the cutting-edge facts size-targeted processes. The information sizes between 10 and 50 MB are considered right here. The JAVA running platform makes use of the proposed question optimization era. Here, performance analysis is used to examine the performances of the proposed Horse Herd approach with those of the bushy C manner (FCM) and Horse Herd algorithms that are already in use.

Tables 1, 2, 3, and 4 exhibit the performance comparison among the proposed Horse Herd and the modern procedures. Discussion desk 1 in comparison the sensitivity, accuracy, and specificity-cantered performances of the proposed Horse Herd with those of the modern-day Horse Herd and FCM. Based totally on records volumes ranging from 10 to 50 MB, overall performance varies. The proposed Horse Herd clustering supplies accuracy in the range of ninety one to ninety six for all the studied information sizes. The proposed Horse Herd outperformed the prevailing approaches in all of the report sizes that were taken into consideration. It follows that the proposed Horse Herd plays at an excessive stage.

Discussion table 2 evaluated the do not forget, precision, and F-cost performance outcomes of the proposed Horse Herd with the ones of the cutting-edge FCM and Horse Herd. The proposed Horse Herd has 92.forty five% precision, zero.21% do not forget, and 89.72% F-measure for 30 MB of facts. Similar to this, the proposed Horse Herd performs better with ultimate statistics sizes like 10, 20, 30, and 50 MB. Don't forget and precision measures are used to create the F-degree metric. A system is considered to be a very good system if its F-degree is high. As a result, the cautioned Horse Herd is regarded as a good system because it offers a advanced F-measure than the current k-means and FCM.

TABLE 1.COMPARE THE ACCURACY, SPECIFICITY, AND SENSITIVITY FOR PROPOSED ALGORITHM WITH EXISTING ALGORITHM

Technique/Data size in MB		10	20	30	40	50
FCM [24]	*Accuracy %*	71	73	79	83	88
	Specificity %	72	77	80	82	85
	Sensitivity %	82	83	85	87	90
K-Means [25]	*Accuracy %*	77	78	82	85	89
	Specificity %	76	79	83	84	87
	Sensitivity %	86	89	90	91	92
Proposed algorithm	*Accuracy %*	80	84	87	92	95
	Specificity %	82	86	88	91	93
	Sensitivity %	92	91	94	94	97

Figure 4. Compare the accuracy, specificity, and sensitivity for proposed algorithm with existing algorithm

525

_____

TABLE 2.COMPARISON TABLE BASED ON PRECISION, RECALL, AND F-MEASURE FOR PROPOSED ALGORITHM WITH EXISTING ALGORITHM

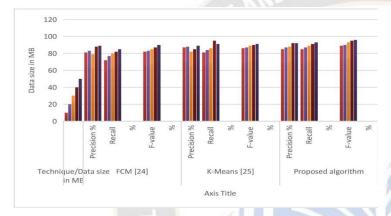| Technique/Data size in MB		10	20	30	40	50
FCM [24]	*Precision %*	81	83	79	88	89
	Recall %	72	77	80	82	85
	F-value %	82	83	85	87	90
K-Means [25]	*Precision %*	87	88	82	85	89
	Recall %	81	84	86	95	91
	F-value %	86	87	89	90	91
Proposed algorithm	*Precision %*	85	87	88	92	92
	Recall %	85	87	89	91	93
	F-value %	89	90	93	95	96

Figure 5. Comparison table based on precision, recall, and F-measure for proposed algorithm with existing algorithm

TABLE 3.TERMS OF RETRIEVAL TIME AND EXECUTION TIME FOR PROPOSED ALGORITHM WITH EXISTING ALGORITHM

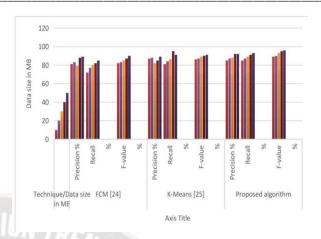| Technique/Data size in MB		10	20	30	40	50
FCM [24]	*Retrieval time*	783	2155	4755	6442	8766
	Execution time	158	189	257	297	339
K-Means [25]	*Retrieval time*	443	1405	2092	4171	6677
	Execution time	122	153	224	234	305
Proposed algorithm	*Retrieval time*	255	774	1395	2333	2699
	Execution time	110	131	177	211	271

Figure 6. Terms of retrieval time and execution time for proposed algorithm with existing algorithm

TABLE 4. MEMORY PRACTICE INVESTIGATION

Technique/ Data size in MB	10	20	30	40	50
FCM [24]	42,22,465	46,66,522	50,24,000	53,66,756	55,78,443
K-Means [25]	47,77,543	50,13,345	54,66,232	58,77,445	60,34,557
Proposed algorithm	52,33,344	56,44,323	60,21,235	62,33,565	64,33,121

Discussion Table 4 contrasted the memory use based performance claims made by the proposed Horse Herd, the existing FCM, and K-Means. The suggested horse Herd requires 5366,756 kilobytes of memory storage to operate on 40 MB of data. However, the current K-Means and FCM take up 6034,557 and 6433,121 kilobytes, respectively. The proposed horse Herd uses less memory than the current approaches for the other remaining data size. As a result, it can be concluded that the suggested horse Herd achieves high-level performance compared to the existing techniques.

V. CONCLUSION

Due to the recognition of massive-scale records evaluation structures like the Hadoop machine, question optimization in business analytics (BD) is now a promising study vicinity. The usage of the HDFS map reduce method and the horse Herd set of rules, this research supplied a greater query optimization process in BD. The BD association segment and the query optimization phase are the 2 stages of the proposed paintings. Data length was used to examine the overall performance of the suggested device. The

_____

documents are between 10 and 50 MB in size. The contrast outcomes verified that the recommended work offers more accuracy and requires less time for query retrieval. Additionally, the suggested approach makes use of less memory area. As a result, our recommended device is superior to the modern-day device. The effectiveness of this machine can potentially be multiplied in the future through incorporating characteristic selection to hurry up retrieval and by using utilising optimization techniques.

REFERENCES:

[1]. Rawat, J.S., Kishor, S., Kumari, M.: A survey on query optimization in cloud computing. Int J AdvTechnolEngSci 4(10), 2348 (2016)

[2]. Gu, R., Yang, X., Yan, J., Sun, Y., Wang, B., Yuan, C., Huang, Y.: SHadoop: improving mapreduce performance by optimizing job execution mechanism in hadoop clusters. J Parallel DistribComput. 74(3), 2166–2179 (2014)

[3]. J Wolf, D Rajan, K Hildrum, R Khandekar, V Kumar, S Parekh, and KL Wu 2010, "Flex: A slot allocation scheduling optimizer for mapreduce workloads", In Proceedings of the ACM/IFIP/USENIX 11th International Conference on Middleware, SpringerVerlag, pp. 1-20

[4]. Barba-González, C., García-Nieto, J., Nebro, A.J., Cordero, J.A., Durillo, J.J., Navas-Delgado, I., Aldana-Montes, J.F.: jMetalSP: a framework for dynamic multi-objective big data optimization. Applied Soft Computing 69, 737–748 (2018)

[5]. Song, J., Ma, Z., Thomas, R., Ge, Yu.: Energy efficiency optimization in big data processing platform by improving resources utilization. Sustainable Computing: Informatics and Systems 21, 80–89 (2019)

[6]. Mahajan, D., Blakeney, C., Zong, Z.: Improving the energy efciency of relational and NoSQL databases via query optimizations. Sustainable Computing: Informatics and Systems 22, 120–133 (2019)

[7]. Rini John, and Nikita Palaskar, "A survey of various query optimization techniques", International Journal of Computer Applications, vol. 975, pp. 8887

[8]. Roy, C., Pandey, M., Rautaray, S.S.: A proposal for optimization of data node by horizontal scaling of name node using big data tools. In: Proceedings of the 3rd International Conference for Convergence in Technology (I2CT), IEEE, pp. 1–6 (2018)

[9]. Dwivedi, J., Tiwary, A.: Big data analytics: an overview. Int. J. Sci. Technol. Res. 5(07) (2016)

[10]. ElhamAzhir ,MehdiHosseinzadeh , Faheem Khan , and Amir Mosavi : Performance Evaluation of Query Plan Recommendation with Apache Hadoop and Apache Spark. 10(19), 3517(2022)

[11]. Deepak Kumar, Vijay Kumar Jha: An improved query optimization process in big data using ACO-GA algorithm and HDFS map reduce technique. Springer Science+Business Media, LLC, part of Springer Nature (2020)

[12]. Song, J., Ma, Z., Thomas, R., Ge, Yu.: Energy efciency optimization in big data processing platform by improving resources utilization. Sustainable Computing: Informatics and Systems 21, 80–89 (2019)

[13]. Panahi, V.; Navimipour, N.J. Join query optimization in the distributed database system using an artificial bee colony algorithm and genetic operators. Concurr. Comput. Pract. Exp. 2019, 31, e5218.

[14]. Pasquale Salza, FilomenaFerrucci. Speed up genetic algorithms in the cloud using software containers. (2019)

[15]. Mahajan, D., Blakeney, C., Zong, Z.: Improving the energy efciency of relational and NoSQL databases via query optimizations. Sustainable Computing: Informatics and Systems 22, 120–133 (2019)

[16]. Bao, C., Cao, M.: Query optimization of massive social network data based on hbase. In: Proceedings of the IEEE 4th International Conference on Big Data Analytics (ICBDA), pp. 94–97 (2019)

[17]. Sahal, R., Nihad, M., Khafagy, M.H., Omara, F.A.: iHOME: index-based join query optimization for limited big data storage. J. Grid Comput. 16(2), 345–380 (2018)

[18]. Rawat, J.S., Kishor, S., Kumari, M.: A survey on query optimization in cloud computing. Int J AdvTechnolEngSci 4(10), 2348 (2016)

[19]. KiranjitPattnaik, Bhabani Shankar Prasad Mishra: A Review on Parallel Genetic Algorithm Models for Map Reduce in Big Data. International Journal of Engineering Research & Technology (IJERT) ISSN: 2278-0181 IJERTV5IS080400 Vol. 5 Issue 08, August-2016

[20]. Panahi, V.; Navimipour, N.J. Join query optimization in the distributed database system using an artificial bee colony algorithm and genetic operators. Concurr. Comput. Pract. Exp. 2019, 31, e5218.

[21]. Rani, S.; Rama, B. MapReduce with Hadoop for Simplified Analysis of Big Data, International Journal of Advanced Research in Computer Science, May-June 2017, Volume 8, No. 5, ISSN No. 0976-5697, pp. 853-856.

[22]. Joseph, C.W.; Pushpalatha, B., A Survey on Big Data and Hadoop, International Journal of Innovative Research in Computer and Communication Engineering, ISSN(Online): 2320-9801, March 2017, Vol. 5, Issue 3, pp. 5525-5530.

[23]. Ferrucci, F., Salza, P., and Sarro, F. (2016). Using Hadoop MapReduce for Parallel Genetic Algorithms: A Comparison of the Global, Grid and Island Models - Appendix. https://doi.org/10.6084/m9.figshare.5091898.

[24]. Fu, W., Menzies, T., and Shen, X. (2016). Tuning for Software Analytics: Is It Really Necessary? Information and Software Technology, 76:135–146.

[25]. Salza, P., Ferrucci, F., and Sarro, F. (2016a). Develop, Deploy and Execute Parallel Genetic Algorithms in the Cloud. In Genetic and Evolutionary Computation Conference (GECCO), pages 121–122.

A powerful method for interactive content-based image retrieval by variable compressed convolutional info neural networks

The Visual Computer

Aims and scope

Vishwanath S. Mahalle ✉, **Narendra M. Kandoi** &
Santosh B. Patil

Abstract

There is a need for efficient methods to retrieve and obtain the visual data that a client need. New methods for content-based image retrieval (CBIR) have emerged due to recent developments in deep neural networks. However, there are still issues with deep neural networks in interactive CBIR systems like the search goal needs to be preset, scrambling and the computational cost is too high

for an online environment. By this concern, this manuscript proposes an effective interactive CBIR that accurately retrieves images in response to the image query using variable compressed convolutional info neural networks (VCCINN). The weight of neural network is optimized by the variable info algorithm, and the matching activity is done by recursive density matching. The interactive technique eliminates irrelevant images based on user feedback and only the relevant images are finally retrieved. The overall retrieval performance in caltech–101 (dataset 1) and inria holiday (dataset 2) are 98.17% and 99% respectively. The performance of introduced model is proven by conducting ablation experiment on each component. The differential learning–based introduced image retrieval approach outperforms several existing methods regarding image similarity and retrieval speed.

Similar content being viewed by others

Optimizing Content-Based Image Retrieval...

Chapter | © 2024

Content Based Image Retrieval System Base...

Article | 01 July 2021

An efficient content based...

Article | 04 November 2024

Explore related subjects

Discover the latest articles, news and stories from top researchers in related subjects.

Data availability

Data sharing not applicable to this article as no datasets were generated or analysed during the current study.

References

1. Chhabra, P., Garg, N.K., Kumar, M.: Content-based image retrieval system using ORB and SIFT features. Neural. Comput. Appl. **32**(7), 2725–2733 (2020)

    Google Scholar

2. Sathiamoorthy, S., Natarajan, M.: An efficient content-based image retrieval using enhanced

multi-trend structure descriptor. SN Appl. Sci. **2**(2), 1–20 (2020)

Google Scholar

3. Pradhan, J., Ajad, A., Pal, A.K., Banka, H.: Multi-level colored directional motif histograms for content-based image retrieval.Visual Comput. 36(9), 1847–1868 (2020).

4. Mistry, Y., Ingole, D.T., Ingole, M.D.: Content based image retrieval using hybrid features and various distance metric. J. Electr. Syst. Inf. Technol. **5**(3), 874−888 (2018)

Google Scholar

5. Chavda, S., Goyani, M.: Hybrid approach to content-based image retrieval using modified multi-scale LBP and color features. SN Comput. Sci. **1**(6), 1–5 (2020)

Google Scholar

6. Joseph, A., Rex, E.S., Christopher, S., Jose, J.: Content-based image retrieval using hybrid k-means moth flame optimization algorithm. Arab. J. Geosci. **14**(8), 1–4 (2021)

Google Scholar

7. Khan, A., Javed, A., Mahmood, M.T., Khan, M.H., Lee, I.H.: Directional magnitude local hexadecimal patterns: a novel texture feature descriptor for content-based image retrieval. IEEE Access **9**, 135608–135629 (2021)

Google Scholar

8. Alshehri, M.: A content-based image retrieval method using neural network-based prediction technique. Arab. J. Sci. Eng. **45**(4), 2957–2973 (2020)

Google Scholar

9. Raghuwanshi, G., Tyagi, V.: Feed-forward content-based image retrieval using adaptive tetrolettransforms. Multimed. Tools Appl. **77**(18), 23389–23410 (2018)

Google Scholar

10. Sezavar, A., Farsi, H., Mohamadzadeh, S.: Content-based image retrieval by combining convolutional neural networks and sparse representation. Multimed. Tools Appl. **78**(15), 20895–20912 (2019)

Google Scholar

11. Kumar, R.B., Marikkannu, P.: An efficient content-based image retrieval using an optimized neural network for medical

application. Multimed. Tools Appl. **79**(31), 22277–22292 (2020)

Google Scholar

12. Kumar, M., Chhabra, P., Garg, N.K.: An efficient content-based image retrieval system using BayesNet and K-NN. Multimed. Tools Appl. **77**(16), 21557–21570 (2018)

Google Scholar

13. Xu, Y., Zhao, X., Gong, J.: A large-scale secure image retrieval method in cloud environment. IEEE Access **7**, 160082–160090 (2019)

Google Scholar

14. Singh, S., Batra, S.: An efficient bi-layer content-based image retrieval system. Multimed. Tools Appl. **79**(25), 17731–17759 (2020)

Google Scholar

15. Ashraf, R., Ahmed, M., Jabbar, S., Khalid, S., Ahmad, A., Din, S., Jeon, G.: Content based image retrieval by using color descriptor and discrete wavelet transform. J. Medic Syst. **42**(3), 1–2 (2018)

Google Scholar

16. Saritha, R.R., Paul, V., Kumar, P.G.: Content based image retrieval using deep learning process. Clust. Comput. **22**(2), 4187–4200 (2019)

Google Scholar

17. Garg, M., Dhiman, G.: A novel content-based image retrieval approach for classification using GLCM features and texture fused LBP variants. Neural Comput. Appl. **33**(4), 1311–1328 (2021)

Google Scholar

18. Khan, U.A., Javed, A., Ashraf, R.: An effective hybrid framework for content-based image retrieval (CBIR). Multimed. Tools Appl. **80**(17), 26911–26937 (2021)

Google Scholar

19. Iida, K., Kiya, H.: Privacy-preserving content-based image retrieval using compressible encrypted images. IEEE Access8:200038-200050 (2020).

20. Kashif, M., Raja, G., Shaukat, F.: An efficient content-based image retrieval system for the diagnosis of lung diseases. J. Digit. Imag. **33**(4), 971–987 (2020)

Google Scholar

21. Chen, Y., Xia, R., Yang, K., Zou, K.: MFFN: Image super-resolution via multi-level features Fusion Network. Vis, Comput (2023)

Google Scholar

22. Kundu, M.K., Chowdhury, M., Banerjee, M.: Interactive image retrieval using M-band wavelet, earth mover's distance and fuzzy relevance feedback. Int. J. Machine Learn. Cybernetics **3**(4), 285–296 (2012)

Google Scholar

23. Wang, Y., Wang, F.C., Liu, F., Wang, X.H.: Securing content-based image retrieval on the cloud using generative models. Multimed. Tools Appl. **81**(22), 31219–31243 (2022)

Google Scholar

24. Tuyet, V.T., Binh, N.T., Quoc, N.K., Khare, A.: Content based medical image retrieval based on salient regions combined with deep learning. Mob. Netw. Appl. **26**(3), 1300–1310 (2021)

Google Scholar

25. Sunitha, T., Sivarani, T.S.: An efficient content-based satellite image retrieval system for big data utilizing threshold-based

checking method. Earth Sci Informat. **14**(4), 1847–1859 (2021)

26. Wang, Z., Qin, J., Xiang, X., Tan, Y.: A privacy-preserving and traitor tracking content-based image retrieval scheme in cloud computing. Multimed. Syst. **27**(3), 403–415 (2021)

27. Monowar, M.M., Hamid, M.A., Ohi, A.Q., Alassafi, M.O., Mridha, M.F.: AutoRet: a self-supervised spatial recurrent network for content-based image retrieval. Sensors **22**(6), 2188 (2022)

28. Punithavathi, R., Ramalingam, A., Kurangi, C., Reddy, A., Uthayakumar, J.: Secure content-based image retrieval system using deep learning with multi-share creation scheme in cloud environment. Multimed. Tools Appl. **80**(17), 26889–26910 (2021)

29. He, D., He, X., Yuan, R., Li, Y., Shen, C.: Lightweight Network-based multi-modal feature fusion for face anti-spoofing. Vis. Comput. **39**, 1423–1435 (2022)

30. Panigrahi, K.P., Das, H., Sahoo, A.K., Moharana, S.C. (2020) Maize leaf disease detection and classification using machine learning algorithms. In: Progress in Computing, Analytics and Networking 2020, Springer, Singapore

31. Sharma, A., Mittal, A., Singh, S., Awatramani, V.: Hand gesture recognition using image processing and feature extraction techniques. Procedia Comput. Sci. **173**, 181–190 (2020)

Google Scholar

32. Das, P., Neelima, A.: A robust feature descriptor for biomedical image retrieval. IRBM **42**(4), 245–257 (2021)

33. Patil, D., Krishnan, S., Gharge, S.:Medical image retrieval by region-based shape feature for CT images. In: 2019 International Conference on Machine Learning, Big Data, Cloud and Parallel Computing (COMITCon), IEEE, 155–159 (2019).

34. Arya, R., Agrawal, R.K., Singh, N.: A novel approach for salient object detection using double-density dual-tree complex wavelet transform in conjunction with superpixelsegmentation. Knowl. Inf. Syst. **60**(1), 327–361 (2019)

Google Scholar

35. Vard, A., Monadjemi, A., Jamshidi, K., Movahhedinia, N.: Fast texture energy-based image segmentation using directional Walsh–Hadamard transform and parametric active contour models. Expert Syst. Appl. **38**(9), 11722–11729 (2011)

Google Scholar

36. Angulakshmi, M., Lakshmi Priya, G.G.: Walsh Hadamard kernel-based texture feature for multimodal MRI brain tumoursegmentation. Int. J. Imag. Syst. Technol. **28**(4), 254–266 (2018)

Google Scholar

37. Subba Reddy, T., Harikiran, J., Enduri, M.K., Hajarathaiah, K., Almakdi, S., Alshehri, M.,

Naveed, Q.N., Rahman, M.H.: Hyperspectral image classification with optimized compressed synergic deep convolution neural network with aquila optimization. Comput. Intell. Neurosci. **2022**, 6781740–6781740 (2022)

Google Scholar

38. Reenadevi, R., Sathiya, T., Sathiyabhama, B.: Breast cancer histopathological image classification using augmentation based on optimized deep ResNet-152 structure. Ann. Romanian Soc. Cell. Biol. **25**(6), 5866–5874 (2021)

Google Scholar

39. Ahmadianfar, I., Heidari, A.A., Noshadian, S., Chen, H., Gandomi, A.H.: INFO: an efficient optimization algorithm based on weighted mean of vectors. Expert. Syst. Appl. **195**, 116516 (2022)

Google Scholar

40. Vharkate, M.N., Musande, V.B.: Remote sensing image retrieval using hybrid visual geometry group network with relevance feedback. Int. J. Remote Sens. **42**(14), 5540–5567 (2021)

Google Scholar

41. Putzu, L., Piras, L., Giacinto, G.: Convolutional neural networks for relevance feedback in content based image retrieval.

Multimed. Tools Appl. **79**(37), 26995–27021 (2020)

Google Scholar

42. https://data.caltech.edu/records/20086.

43. http://lear.inrialpes.fr/~jegou/data.php#holidays.

44. Hor, N., Fekri-Ershad, S.: Image retrieval approach based on local texture information derived from predefined patterns and spatial domain information. arXiv preprint arXiv:1912.12978 (2019).

45. Rajesh, M.B., Sathiamoorthy, S.: Co-occurrence of edges and valleys with support vector machine for content-based image retrieval. In: 2020 Fourth International Conference on Computing Methodologies and Communication (ICCMC) 2020 IEEE465–470 (2020).

46. Hussain, S., Zia, M.A., Arshad, W.: Additive deep feature optimization for semantic image retrieval. Expert Syst. Appl. **170**, 114545 (2021)

Google Scholar

47. Zhang, K., Qi, S., Cai, J., Zhao, D., Yu, T., Yue, Y., Yao, Y., Qian, W.: Content-based image retrieval with a Convolutional Siamese Neural Network: distinguishing lung cancer

and tuberculosis in CT images. Comput. Biol. Med. **140**, 105096 (2022)

Google Scholar

48. Ghozzi, Y., Baklouti, N., Hagras, H., Ayed, M.B., Alimi, A.M.: Interval Type-2 beta fuzzy near sets approach to content-based image retrieval. IEEE Trans. Fuzzy Syst. **30**(3), 805–817 (2021)

Google Scholar

49. Anandababu, P., Kamarasan, M.: An effective content based image retrieval model using improved memetic algorithm. In: 2020 International Conference on Inventive Computation Technologies (ICICT), IEEE, 424–429 (2020).

50. Li, J., Yang, B., Yang, W., Sun, C., Xu, J.: Subspace-based multi-view fusion for instance-level image retrieval. Visual Comput. **37**(3), 619–633 (2021)

Google Scholar

51. Singhal, A., Agarwal, M., Pachori, R.B.: Directional local ternary co-occurrence pattern for natural image retrieval. Multimed. Tools Appl. **80**(10), 15901–15920 (2021)

Google Scholar

52. Vaccaro, F., Bertini, M., Uricchio, T., Bimbo, A.D.: Effective triplet mining improves training of multi-scale pooled CNN for image retrieval. Mach. Vis. Appl. **33**(1), 1–3 (2022)

Google Scholar

53. Liu, G.H., Wei, Z.: Image retrieval using the fused perceptual color histogram. Comput. Intell. Neurosci. **2020**, 8876480 (2020)

54. Giveki, D., Shakarami, A., Tarrah, H., Soltanshahi, M.A.: A new method for image classification and image retrieval using convolutional neural networks. Concurr. Comput. Pract. Exp. **34**(1), e6533 (2022)

55. Yan, C., Gong, B., Wei, Y., Gao, Y.: Deep multi-view enhancement hashing for Image retrieval. IEEE Trans. Pattern Analysis Machine Intell. **43**, 1445–1451 (2021)

56. Yan, C., Li, Z., Zhang, Y., Liu, Y., Ji, X., Zhang, Y.: Depth image denoising using nuclear norm and learning graph model. ACM Trans. Multimed. Comput. Commun. Appl. **16**(4), 1–17 (2020)

Google Scholar

57. Yan, C., Hao, Y., Li, L., Yin, J., Liu, A., Mao, Z., Chen, Z., Gao, X.: Task-adaptive attention for image captioning. IEEE Trans. Circuits Syst. Video Tech. **32**, 43–51 (2022)

Google Scholar

58. Yan, C., Teng, T., Liu, Y., Zhang, Y., Wang, H., Ji, X.: Precise no-reference image quality evaluation based on distortion identification.

ACM Trans. Multimed. Comput. Commun. Appl. **17**, 1–21 (2021)

Google Scholar

59. Yan, C., Meng, L., Li, L., Zhang, J., Wang, Z., Yin, J., Zhang, J., Sun, Y., Zheng, B.: Age-invariant face recognition by multi-feature Fusionand decomposition with self-attention. ACM Trans. Multimed. Comput. Commun. Appl. **18**, 1–18 (2022)

Google Scholar

60. Eisenstat, J., Wagner, M.W., Vidarsson, L., Ertl-Wagner, B., Sussman, D.: FET-net algorithm for automatic detection of fetal orientation in fetal MRI. Bioeng. **10**, 140 (2023)

Google Scholar

61. Shahid, F., Zameer, A., Iqbal, M.J.: Intelligent forecast engine for short-term wind speed prediction based on stacked long short-term memory. Neural Comput. Appl. **33**, 13767–13783 (2021)

Google Scholar

62. Liang, X., Xu, L., Zhang, W., Zhang, Y., Liu, J., Liu, Z.: A convolution-transformer dual branch network for head-pose and occlusion

facial expression recognition. Vis. Comput. **39**, 2277–2290 (2022)

Google Scholar

63. Challa, S.K., Kumar, A., Semwal, V.B.: A multibranch CNN–BILSTM model for human activity recognition using wearable sensor data. Vis. Comput. **38**, 4095–4109 (2021)

Google Scholar

64. Zhang, Q., Ge, Y., Zhang, C., Bi, H.: TPRNet: Camouflaged object detection via transformer-induced progressive refinement network. Vis. Comput. (2022). https://doi.org/10.1007/s00371-022-02611-1

Article Google Scholar

65. Soroush, R., Baleghi, Y.: NIR/RGB image fusion for scene classification using Deep Neural Networks. Vis. Comput. **39**, 2725–2739 (2022)

Google Scholar

66. Yang, H., Fan, Y., Lv, G., Liu, S., Guo, Z.: Exploiting emotional concepts for image emotion recognition. Vis. Comput. **39**, 2177–2190 (2022)

Google Scholar

67. Tang, H., Li, Z., Peng, Z., Tang, J.: Blockmix: meta regularization and self-calibrated

inference for metric-based meta-learning. In: Proceedings of the 28th ACM international conference on multimedia, 610–618 (2020). https://doi.org/10.1145/3394171.3413884

68. Tang, H., Liu, J., Yan, S., Yan, R., Li, Z., Tang, J.: M^3 Net: Multi-view Encoding, Matching, and Fusion for Few-shot Fine-grained Action Recognition. (2023). arXiv preprint arXiv:2308.03063.

69. Li, Z., Tang, H., Peng, Z., Qi, G.J., Tang, J.: Knowledge-guided semantic transfer network for few-shot image recognition. IEEE Trans. Neural Netw. Learn. Syst. (2023). https://doi.org/10.1109/TNNLS.2023.3240195

Article   Google Scholar

70. Zha, Z., Tang, H., Sun, Y., Tang, J.: Boosting few-shot fine-grained recognition with background suppression and foreground alignment. IEEE Trans. Circuit. Syst. Video Technol. (2023). https://doi.org/10.1109/TCSVT.2023.3236636

Article   Google Scholar

71. Öztürk, Ş, Çelik, E., Çukur, T.: Content-based medical image retrieval with opponent class adaptive margin loss. Inform. Sci. **637**, 118938 (2023)

Acknowledgement

Funding

Author information

Authors and Affiliations

Department of Computer Science and Engineering, Shri Sant Gajanan Maharaj College of Engineering, Shegaon (M.S.), Maharashtra, 444203, India

Vishwanath S. Mahalle & Narendra M. Kandoi

Department of Electronics and Telecommunication Engineering, Shri Sant Gajanan Maharaj College of Engineering, Shegaon (M.S.), Maharashtra, 444203, India

Santosh B. Patil

Contributions

All the authors have contributed equally to the work.

Corresponding author

Correspondence to Vishwanath S. Mahalle.

Ethics declarations

Conflict of interest

The authors declare that they have no potential conflict of interest.

Ethical approval

All applicable institutional and/or national guidelines for the care and use of animals were followed.

Informed consent

For this type of analysis formal consent is not needed.

Additional information

Publisher's Note

Springer Nature remains neutral with regard to jurisdictional claims in published maps and institutional affiliations.

Rights and permissions

Springer Nature or its licensor (e.g. a society or other partner) holds exclusive rights to this article under a publishing agreement with the author(s) or other rightsholder(s); author self-archiving of the accepted manuscript version of this article is solely governed by the terms of such publishing agreement and applicable law.

[Reprints and permissions](#)

About this article

Cite this article

Keywords

User feedback   Neural network

Relevant images

Interactive content-based image retrieval

Deep learning

Feature extraction

Similarity matching

A powerful method for interactive content-based image retrieval by variable compressed convolutional info neural networks

The Visual Computer

Aims and scope

Vishwanath S. Mahalle ✉, **Narendra M. Kandoi** &

Santosh B. Patil

Abstract

There is a need for efficient methods to retrieve
and obtain the visual data that a client need. New
methods for content-based image retrieval (CBIR)
have emerged due to recent developments in deep
neural networks. However, there are still issues
with deep neural networks in interactive CBIR
systems like the search goal needs to be preset,
scrambling and the computational cost is too high

for an online environment. By this concern, this manuscript proposes an effective interactive CBIR that accurately retrieves images in response to the image query using variable compressed convolutional info neural networks (VCCINN). The weight of neural network is optimized by the variable info algorithm, and the matching activity is done by recursive density matching. The interactive technique eliminates irrelevant images based on user feedback and only the relevant images are finally retrieved. The overall retrieval performance in caltech-101 (dataset 1) and inria holiday (dataset 2) are 98.17% and 99% respectively. The performance of introduced model is proven by conducting ablation experiment on each component. The differential learning-based introduced image retrieval approach outperforms several existing methods regarding image similarity and retrieval speed.

Similar content being viewed by others

Optimizing Content-Based Image Retrieval...

Chapter | © 2024

Content Based Image Retrieval System Base...

Article | 01 July 2021

An efficient content based...

Article | 04 November 2024

Explore related subjects

Discover the latest articles, news and stories from top researchers in related subjects.

Data availability

Data sharing not applicable to this article as no datasets were generated or analysed during the current study.

References

1. Chhabra, P., Garg, N.K., Kumar, M.: Content-based image retrieval system using ORB and SIFT features. Neural. Comput. Appl. **32**(7), 2725–2733 (2020)

   Google Scholar

2. Sathiamoorthy, S., Natarajan, M.: An efficient content-based image retrieval using enhanced

multi-trend structure descriptor. SN Appl. Sci. **2**(2), 1–20 (2020)

Google Scholar

3. Pradhan, J., Ajad, A., Pal, A.K., Banka, H.: Multi-level colored directional motif histograms for content-based image retrieval.Visual Comput. 36(9), 1847–1868 (2020).

4. Mistry, Y., Ingole, D.T., Ingole, M.D.: Content based image retrieval using hybrid features and various distance metric. J. Electr. Syst. Inf. Technol. **5**(3), 874−888 (2018)

Google Scholar

5. Chavda, S., Goyani, M.: Hybrid approach to content-based image retrieval using modified multi-scale LBP and color features. SN Comput. Sci. **1**(6), 1–5 (2020)

Google Scholar

6. Joseph, A., Rex, E.S., Christopher, S., Jose, J.: Content-based image retrieval using hybrid k-means moth flame optimization algorithm. Arab. J. Geosci. **14**(8), 1–4 (2021)

Google Scholar

7. Khan, A., Javed, A., Mahmood, M.T., Khan, M.H., Lee, I.H.: Directional magnitude local hexadecimal patterns: a novel texture feature descriptor for content-based image retrieval. IEEE Access **9**, 135608–135629 (2021)

Google Scholar

8. Alshehri, M.: A content-based image retrieval method using neural network-based prediction technique. Arab. J. Sci. Eng. **45**(4), 2957–2973 (2020)

Google Scholar

9. Raghuwanshi, G., Tyagi, V.: Feed-forward content-based image retrieval using adaptive tetrolettransforms. Multimed. Tools Appl. **77**(18), 23389–23410 (2018)

Google Scholar

10. Sezavar, A., Farsi, H., Mohamadzadeh, S.: Content-based image retrieval by combining convolutional neural networks and sparse representation. Multimed. Tools Appl. **78**(15), 20895–20912 (2019)

Google Scholar

11. Kumar, R.B., Marikkannu, P.: An efficient content-based image retrieval using an optimized neural network for medical

application. Multimed. Tools Appl. **79**(31), 22277–22292 (2020)

12. Kumar, M., Chhabra, P., Garg, N.K.: An efficient content-based image retrieval system using BayesNet and K-NN. Multimed. Tools Appl. **77**(16), 21557–21570 (2018)

13. Xu, Y., Zhao, X., Gong, J.: A large-scale secure image retrieval method in cloud environment. IEEE Access **7**, 160082–160090 (2019)

14. Singh, S., Batra, S.: An efficient bi-layer content-based image retrieval system. Multimed. Tools Appl. **79**(25), 17731–17759 (2020)

Google Scholar

15. Ashraf, R., Ahmed, M., Jabbar, S., Khalid, S., Ahmad, A., Din, S., Jeon, G.: Content based image retrieval by using color descriptor and discrete wavelet transform. J. Medic Syst. **42**(3), 1–2 (2018)

Google Scholar

16. Saritha, R.R., Paul, V., Kumar, P.G.: Content based image retrieval using deep learning process. Clust. Comput. **22**(2), 4187–4200 (2019)

Google Scholar

17. Garg, M., Dhiman, G.: A novel content-based image retrieval approach for classification using GLCM features and texture fused LBP variants. Neural Comput. Appl. **33**(4), 1311–1328 (2021)

Google Scholar

18. Khan, U.A., Javed, A., Ashraf, R.: An effective hybrid framework for content-based image retrieval (CBIR). Multimed. Tools Appl. **80**(17), 26911–26937 (2021)

Google Scholar

19. Iida, K., Kiya, H.: Privacy-preserving content-based image retrieval using compressible encrypted images. IEEE Access8:200038-200050 (2020).

20. Kashif, M., Raja, G., Shaukat, F.: An efficient content-based image retrieval system for the diagnosis of lung diseases. J. Digit. Imag. **33**(4), 971–987 (2020)

Google Scholar

21. Chen, Y., Xia, R., Yang, K., Zou, K.: MFFN: Image super-resolution via multi-level features Fusion Network. Vis, Comput (2023)

Google Scholar

22. Kundu, M.K., Chowdhury, M., Banerjee, M.: Interactive image retrieval using M-band wavelet, earth mover's distance and fuzzy relevance feedback. Int. J. Machine Learn. Cybernetics **3**(4), 285–296 (2012)

Google Scholar

23. Wang, Y., Wang, F.C., Liu, F., Wang, X.H.: Securing content-based image retrieval on the cloud using generative models. Multimed. Tools Appl. **81**(22), 31219–31243 (2022)

Google Scholar

24. Tuyet, V.T., Binh, N.T., Quoc, N.K., Khare, A.: Content based medical image retrieval based on salient regions combined with deep learning. Mob. Netw. Appl. **26**(3), 1300–1310 (2021)

Google Scholar

25. Sunitha, T., Sivarani, T.S.: An efficient content-based satellite image retrieval system for big data utilizing threshold-based

checking method. Earth Sci Informat. **14**(4), 1847–1859 (2021)

Google Scholar

26. Wang, Z., Qin, J., Xiang, X., Tan, Y.: A privacy-preserving and traitor tracking content-based image retrieval scheme in cloud computing. Multimed. Syst. **27**(3), 403–415 (2021)

Google Scholar

27. Monowar, M.M., Hamid, M.A., Ohi, A.Q., Alassafi, M.O., Mridha, M.F.: AutoRet: a self-supervised spatial recurrent network for content-based image retrieval. Sensors **22**(6), 2188 (2022)

28. Punithavathi, R., Ramalingam, A., Kurangi, C., Reddy, A., Uthayakumar, J.: Secure content-based image retrieval system using deep learning with multi-share creation scheme in cloud environment. Multimed. Tools Appl. **80**(17), 26889–26910 (2021)

29. He, D., He, X., Yuan, R., Li, Y., Shen, C.: Lightweight Network-based multi-modal feature fusion for face anti-spoofing. Vis. Comput. **39**, 1423–1435 (2022)

30. Panigrahi, K.P., Das, H., Sahoo, A.K., Moharana, S.C. (2020) Maize leaf disease detection and classification using machine learning algorithms. In: Progress in Computing, Analytics and Networking 2020, Springer, Singapore

31. Sharma, A., Mittal, A., Singh, S., Awatramani, V.: Hand gesture recognition using image processing and feature extraction techniques. Procedia Comput. Sci. **173**, 181–190 (2020)

Google Scholar

32. Das, P., Neelima, A.: A robust feature descriptor for biomedical image retrieval. IRBM **42**(4), 245–257 (2021)

33. Patil, D., Krishnan, S., Gharge, S.:Medical image retrieval by region–based shape feature for CT images. In: 2019 International Conference on Machine Learning, Big Data, Cloud and Parallel Computing (COMITCon), IEEE, 155–159 (2019).

34. Arya, R., Agrawal, R.K., Singh, N.: A novel approach for salient object detection using double–density dual–tree complex wavelet transform in conjunction with superpixelsegmentation. Knowl. Inf. Syst. **60**(1), 327–361 (2019)

35. Vard, A., Monadjemi, A., Jamshidi, K., Movahhedinia, N.: Fast texture energy-based image segmentation using directional Walsh–Hadamard transform and parametric active contour models. Expert Syst. Appl. **38**(9), 11722–11729 (2011)

Google Scholar

36. Angulakshmi, M., Lakshmi Priya, G.G.: Walsh Hadamard kernel-based texture feature for multimodal MRI brain tumoursegmentation. Int. J. Imag. Syst. Technol. **28**(4), 254–266 (2018)

Google Scholar

37. Subba Reddy, T., Harikiran, J., Enduri, M.K., Hajarathaiah, K., Almakdi, S., Alshehri, M.,

Naveed, Q.N., Rahman, M.H.: Hyperspectral image classification with optimized compressed synergic deep convolution neural network with aquila optimization. Comput. Intell. Neurosci. **2022**, 6781740–6781740 (2022)

Google Scholar

38. Reenadevi, R., Sathiya, T., Sathiyabhama, B.: Breast cancer histopathological image classification using augmentation based on optimized deep ResNet-152 structure. Ann. Romanian Soc. Cell. Biol. **25**(6), 5866–5874 (2021)

Google Scholar

39. Ahmadianfar, I., Heidari, A.A., Noshadian, S., Chen, H., Gandomi, A.H.: INFO: an efficient optimization algorithm based on weighted mean of vectors. Expert. Syst. Appl. **195**, 116516 (2022)

Google Scholar

40. Vharkate, M.N., Musande, V.B.: Remote sensing image retrieval using hybrid visual geometry group network with relevance feedback. Int. J. Remote Sens. **42**(14), 5540–5567 (2021)

Google Scholar

41. Putzu, L., Piras, L., Giacinto, G.: Convolutional neural networks for relevance feedback in content based image retrieval.

Multimed. Tools Appl. **79**(37), 26995–27021 (2020)

42. https://data.caltech.edu/records/20086.

43. http://lear.inrialpes.fr/~jegou/data.php#holidays.

44. Hor, N., Fekri-Ershad, S.: Image retrieval approach based on local texture information derived from predefined patterns and spatial domain information. arXiv preprint arXiv:1912.12978 (2019).

45. Rajesh, M.B., Sathiamoorthy, S.: Co-occurrence of edges and valleys with support vector machine for content-based image retrieval. In: 2020 Fourth International Conference on Computing Methodologies and Communication (ICCMC) 2020 IEEE465–470 (2020).

46. Hussain, S., Zia, M.A., Arshad, W.: Additive deep feature optimization for semantic image retrieval. Expert Syst. Appl. **170**, 114545 (2021)

Google Scholar

47. Zhang, K., Qi, S., Cai, J., Zhao, D., Yu, T., Yue, Y., Yao, Y., Qian, W.: Content-based image retrieval with a Convolutional Siamese Neural Network: distinguishing lung cancer

and tuberculosis in CT images. Comput. Biol. Med. **140**, 105096 (2022)

Google Scholar

48. Ghozzi, Y., Baklouti, N., Hagras, H., Ayed, M.B., Alimi, A.M.: Interval Type-2 beta fuzzy near sets approach to content-based image retrieval. IEEE Trans. Fuzzy Syst. **30**(3), 805–817 (2021)

Google Scholar

49. Anandababu, P., Kamarasan, M.: An effective content based image retrieval model using improved memetic algorithm. In: 2020 International Conference on Inventive Computation Technologies (ICICT), IEEE, 424–429 (2020).

50. Li, J., Yang, B., Yang, W., Sun, C., Xu, J.: Subspace-based multi-view fusion for instance-level image retrieval. Visual Comput. **37**(3), 619–633 (2021)

Google Scholar

51. Singhal, A., Agarwal, M., Pachori, R.B.: Directional local ternary co-occurrence pattern for natural image retrieval. Multimed. Tools Appl. **80**(10), 15901–15920 (2021)

Google Scholar

52. Vaccaro, F., Bertini, M., Uricchio, T., Bimbo, A.D.: Effective triplet mining improves training of multi-scale pooled CNN for image retrieval. Mach. Vis. Appl. **33**(1), 1–3 (2022)

Google Scholar

53. Liu, G.H., Wei, Z.: Image retrieval using the fused perceptual color histogram. Comput. Intell. Neurosci. **2020**, 8876480 (2020)

54. Giveki, D., Shakarami, A., Tarrah, H., Soltanshahi, M.A.: A new method for image classification and image retrieval using convolutional neural networks. Concurr. Comput. Pract. Exp. **34**(1), e6533 (2022)

55. Yan, C., Gong, B., Wei, Y., Gao, Y.: Deep multi-view enhancement hashing for Image retrieval. IEEE Trans. Pattern Analysis Machine Intell. **43**, 1445–1451 (2021)

56. Yan, C., Li, Z., Zhang, Y., Liu, Y., Ji, X., Zhang, Y.: Depth image denoising using nuclear norm and learning graph model. ACM Trans. Multimed. Comput. Commun. Appl. **16**(4), 1–17 (2020)

Google Scholar

57. Yan, C., Hao, Y., Li, L., Yin, J., Liu, A., Mao, Z., Chen, Z., Gao, X.: Task-adaptive attention for image captioning. IEEE Trans. Circuits Syst. Video Tech. **32**, 43–51 (2022)

Google Scholar

58. Yan, C., Teng, T., Liu, Y., Zhang, Y., Wang, H., Ji, X.: Precise no-reference image quality evaluation based on distortion identification.

ACM Trans. Multimed. Comput. Commun. Appl. **17**, 1–21 (2021)

Google Scholar

59. Yan, C., Meng, L., Li, L., Zhang, J., Wang, Z., Yin, J., Zhang, J., Sun, Y., Zheng, B.: Age-invariant face recognition by multi-feature Fusionand decomposition with self-attention. ACM Trans. Multimed. Comput. Commun. Appl. **18**, 1–18 (2022)

Google Scholar

60. Eisenstat, J., Wagner, M.W., Vidarsson, L., Ertl-Wagner, B., Sussman, D.: FET-net algorithm for automatic detection of fetal orientation in fetal MRI. Bioeng. **10**, 140 (2023)

Google Scholar

61. Shahid, F., Zameer, A., Iqbal, M.J.: Intelligent forecast engine for short-term wind speed prediction based on stacked long short-term memory. Neural Comput. Appl. **33**, 13767–13783 (2021)

Google Scholar

62. Liang, X., Xu, L., Zhang, W., Zhang, Y., Liu, J., Liu, Z.: A convolution-transformer dual branch network for head-pose and occlusion

facial expression recognition. Vis. Comput. **39**, 2277–2290 (2022)

Google Scholar

63. Challa, S.K., Kumar, A., Semwal, V.B.: A multibranch CNN-BILSTM model for human activity recognition using wearable sensor data. Vis. Comput. **38**, 4095–4109 (2021)

Google Scholar

64. Zhang, Q., Ge, Y., Zhang, C., Bi, H.: TPRNet: Camouflaged object detection via transformer-induced progressive refinement network. Vis. Comput. (2022). https://doi.org/10.1007/s00371-022-02611-1

Article   Google Scholar

65. Soroush, R., Baleghi, Y.: NIR/RGB image fusion for scene classification using Deep Neural Networks. Vis. Comput. **39**, 2725–2739 (2022)

Google Scholar

66. Yang, H., Fan, Y., Lv, G., Liu, S., Guo, Z.: Exploiting emotional concepts for image emotion recognition. Vis. Comput. **39**, 2177–2190 (2022)

Google Scholar

67. Tang, H., Li, Z., Peng, Z., Tang, J.: Blockmix: meta regularization and self-calibrated

inference for metric-based meta-learning. In: Proceedings of the 28th ACM international conference on multimedia, 610–618 (2020). https://doi.org/10.1145/3394171.3413884

68. Tang, H., Liu, J., Yan, S., Yan, R., Li, Z., Tang, J.: M^3 Net: Multi-view Encoding, Matching, and Fusion for Few-shot Fine-grained Action Recognition. (2023). arXiv preprint arXiv:2308.03063.

69. Li, Z., Tang, H., Peng, Z., Qi, G.J., Tang, J.: Knowledge-guided semantic transfer network for few-shot image recognition. IEEE Trans. Neural Netw. Learn. Syst. (2023). https://doi.org/10.1109/TNNLS.2023.3240195

Article   Google Scholar

70. Zha, Z., Tang, H., Sun, Y., Tang, J.: Boosting few-shot fine-grained recognition with background suppression and foreground alignment. IEEE Trans. Circuit. Syst. Video Technol. (2023). https://doi.org/10.1109/TCSVT.2023.3236636

Article   Google Scholar

71. Öztürk, Ş, Çelik, E., Çukur, T.: Content-based medical image retrieval with opponent class adaptive margin loss. Inform. Sci. **637**, 118938 (2023)

Google Scholar

Acknowledgement

Funding

Author information

Authors and Affiliations

Department of Computer Science and Engineering, Shri Sant Gajanan Maharaj College of Engineering, Shegaon (M.S.), Maharashtra, 444203, India

Vishwanath S. Mahalle & Narendra M. Kandoi

Department of Electronics and Telecommunication Engineering, Shri Sant Gajanan Maharaj College of Engineering, Shegaon (M.S.), Maharashtra, 444203, India

Santosh B. Patil

Contributions

All the authors have contributed equally to the work.

Corresponding author

Correspondence to Vishwanath S. Mahalle.

Ethics declarations

Conflict of interest

The authors declare that they have no potential conflict of interest.

Ethical approval

All applicable institutional and/or national guidelines for the care and use of animals were followed.

Informed consent

For this type of analysis formal consent is not needed.

Additional information

Publisher's Note

Springer Nature remains neutral with regard to jurisdictional claims in published maps and institutional affiliations.

Rights and permissions

Springer Nature or its licensor (e.g. a society or other partner) holds exclusive rights to this article under a publishing agreement with the author(s) or other rightsholder(s); author self-archiving of the accepted manuscript version of this article is solely governed by the terms of such publishing agreement and applicable law.

Reprints and permissions

About this article

Cite this article

Keywords

User feedback   Neural network

Relevant images

Interactive content–based image retrieval

Deep learning

Feature extraction

Similarity matching

Efficient Content Based Image Retrieval System Based on Early and Late Fusion Technique

Pranav Lod[1], V. S. Mahalle[2], N. M. Kandoi[3], S. B. Patil[4]

[1]Pranav Lod, Student, Department of CSE, SSGMCE, Shegaon
[2]Prof. V. S. Mahalle, Assistant Professor, Department of CSE, SSGMCE, Shegaon
[3]N. M. Kandoi, Associate Professor, Department of CSE, SSGMCE, Shegaon
[4] S. B. Patil, Professor, Department of EXTC, SSGMCE, Shegaon

Abstract

A popular technique for retrieving images from huge and unlabeled image databases are content-based-image-retrieval (CBIR). However, the traditional information retrieval techniques do not satisfy users in terms of time consumption and accuracy. Additionally, the number of images accessible to users are growing due to web development and transmission networks. As the result, huge digital image creation occurs in many places. Therefore, quick access to these huge image databases and retrieving images like a query image from these huge image collections provides significant challenges and the need for an effective technique. Feature extraction and similarity measurement are important for the performance of a CBIR technique. Traditional methods often fall short in terms of time efficiency and accuracy. This paper proposes an effective CBIR system that employs early and late fusion techniques to improve retrieval accuracy.

The proposed system involves pre-processing, feature extraction, and classification. Pre-processing includes resizing, grayscale conversion, and Histogram of Oriented Gradients (HOG) computation. Feature extraction involves color extraction using histograms and texture extraction using Gray-Level Co-occurrence Matrix (GLCM). The system uses a bagging tree classifier for classification and implements both early and late fusion techniques to bridge the semantic gap between low-level and high-level features. Similarity measurement, is crucial for computing the distance between query and database image features.

When retrieving the first 10 pictures, an experiment on the Corel-1K dataset showed that the average precision was 0.88 with Early Fusion and Late Fusion , which was a big step up from the state-of-the-art approaches.

Introduction

Large repositories for multimedia and image content have developed due to the growing usage of digital computers, storage technologies, and digital multimedia in recent years. This enormous volume of multimedia data is utilized in various industries, including digital forensics, electronic games, archaeology, video, satellite data and still image repositories, and medical treatment. This rapid growth has generated a continuous need for image retrieval systems that operate on a large scale [1].

For large image databases, the traditional text-based image extraction approach seems ineffective. There are certain drawbacks to retrieving images based on text, such as the time-consuming task of adding labels to individual images in huge databases. That label text depends on language and is only appropriate for one language at a time. Another drawback is that multiple users can set different labels for the same image. When retrieving images from image content, these drawbacks can be avoided. This type of image retrieval is known as content-based image retrieval (CBIR) [2].

CBIR has been a popular technique of community multimedia research since the early 1990s [3]. The main block diagram is shown in Figure 1. CBIR is the most crucial technology for image processing and computer vision. CBIR applications have been developed for various uses, including object recognition, geographic information systems, architectural design, remote sensing [4], surveillance systems, and medical image retrieval [5].

CBIR is a well-defined image search and retrieval technique. It uses the visual content of images to find and retrieve images from huge data collections [6]. CBIR uses the search method for low-level features such as texture, shape, and color [7]. This set of low-level features generates a feature vector, which describes the content of each image in the image database. Subsequently, image retrieval is based on similarities in their contents. The similarity between the query and the feature vector dataset is used to sort the list of matching images [8]. The features used by CBIR

may be divided into two groups: global feature descriptors and local feature descriptors. Global features such as color [9], shape [10], and texture [11].

Local features such as local binary pattern (LBP) [12], oriented fast and rotated binary robust independent elementary features BRIEF (ORB) [13], speeded-up robust feature (SURF) [14], scale-invariant feature transform (SIFT) [15], and histogram of oriented gradient (HOG) [16]. Local feature descriptors define each image patch, whereas global feature descriptors describe the whole image. The advantage of global feature descriptors is their quick computation, but the disadvantage is their poor precision. Global feature descriptors frequently fall short in their attempts to extract significant visual characteristics from an image. Local feature descriptors are more accurate than global feature descriptors because they use features calculated from the image's patch to represent the image. The disadvantage of local features is that they will result in large feature space for large image databases [17].

The feature vectors and similarity measures have the biggest effects on the retrieval performance of the CBIR system. There is always a semantic gap between high-level human perception and the low-level image pixels that systems collect. Researchers decided to address this problem to enhance CBIR's performance in light of the recent success of deep learning techniques, particularly the performance of convolutional neural networks (CNN), in resolving the issue of computer vision applications [18].

Srivastava and Khare [19] presented a technique for CBIR that combines local and global features. Geometric moments extract global features, while SIFT descriptors extract local features. SIFT and moments are combined to find visually similar images. The Corel 1K has an average precision of 0.3981. Mehmood et al. [20] combine the SURF and HOG image features. After the final features were extracted using the bag-of-visual words (BoVW) model, they used Early Fusion and Late Fusion measurement to evaluate the similarity between the query image and the database images. The average precision is 0.8061 on the Corel 1K datasets. These methods have two main drawbacks: first, they require a lot of time, and second, finding the most silent places is not always easy.

Nazir et al. [21], suggest a new CBIR system that combines local and global features to handle lowlevel information. A color histogram (CH) is used to extract color information. Edge histogram descriptor and discrete wavelet transform (DWT) extract texture features (EDH). Based on the results of the experiments, the suggested method does better on the Corel 1K, with an average precision of 0.735.

Pardede et al. [22] suggested a CBIR method that employed deep CNN for feature extraction from fully connected FC1 and FC2 layers. The Feature Extractor utilizes the fully connected feature vectors FV.FC1 and FV.FC2 to extract image features from each image and compares the performance of deep CNN for CBIR tasks with three classifications: softmax, support vector machine (SVM), and extreme gradient boost (XGBoost). A deep CNN model was produced based on the suggested neural network structure. The results of the mathematical experiments suggest by utilizing the XGBoost classification, the extracted feature extractor from deep CNN can improve CBIR performance, and the best feature extractor is FV.FC2. The precision on the Wang dataset (Corel 1k) is 0.69.

Öztürk [23] proposes a useful CBIR framework. The dictionary learning method addresses the training issue with a small amount of labeled data. Dictionary learning (DL) cannot produce reliable features for the retrieval task, particularly when there is a complicated background. To address both the issue of identifying objects and dealing with complicated backgrounds, a DL technique utilizing CNN's (Resnet-50) feature representation capabilities is implemented in this system. When 10 images are retrieved, the mean average precision (mAP) for the modified Corel dataset is 0.855.

Öztürk [24] provided a framework for content based medical image retrieval (CBMIR) based on high-level deep features. The insufficient number of photos is the main problem here. To address this issue, a class-driven retrieval strategy is suggested. Different hash code lengths are produced using feature reduction methods, and their performances are evaluated. Experiments with the National Electrical Manufacturers Association Magnetic Resonance Imaging (NEMA MRI) and the National Electrical Manufacturers Association Computed Tomography (NEMA CT) datasets show that the framework given is better than the existing methods in the literature.

Proposed System

In this paper, Decision Tree Classifier (DTC) is used for feature extraction since it is efficient at closing the semantic gap between high-level human perception and low-level machine features, as well as at finding the most relevant images and improving retrieval performance. The Corel 1K [26] database was utilized to validate the results. It is a 1,000-image database collection. These images are organized into 10 categories, each of which has 100 images. A block diagram of the proposed method is illustrated in Figure.

DTC is a type of neural network model that uses several large network layers. DTC has gained popularity in various image processing applications, including object recognition and picture classification and has produced promising results. DTC's are increasingly used in various image processing tasks, such as object classification, face recognition, and gesture identification. According to earlier research, it is possible to input an image directly into a DTC network and use features for image classification.

Image retrieval

Determine the difference in similarity between the feature vector obtained from the query and the feature vector from the training dataset by using two similarity measurements: Early Fusion and Late Fusion and Manhattan. As indicated in Algorithm 1, the images with the shortest distance are returned. Evaluation matrices are used to assess the system's performance.

Process flow

- User can select image from the dataset
- The image is preprocessing by means of image resize
- The features are extracted based on the color and texture
- Then the similarity will be estimated to classify the image and then the similar images will be retrieved
- Performance like precision, recall will be estimated for the performance of the classification
- Early fusion is based on, once the object was identified immediately the related images will be retrieved. Late fusion is based on, after identified the object, then it will check the most relevant images and retrieved the images one by one
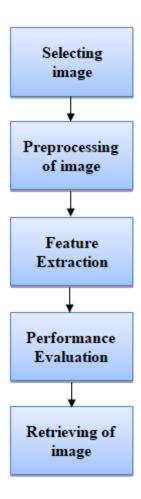
Fig. 1 Flow Chart of the system

It was found that it may be used not only to measure the degree of agreement between different sets of rankings for the same set of retrieved items, but also to evaluate the effectiveness of different retrieval techniques. The suggested system was used in the current inquiry, with the classes of pictures acting as judges, the average precision objects acting as the judges in the current context, and the study's objects being the precision rates of the three different ways.
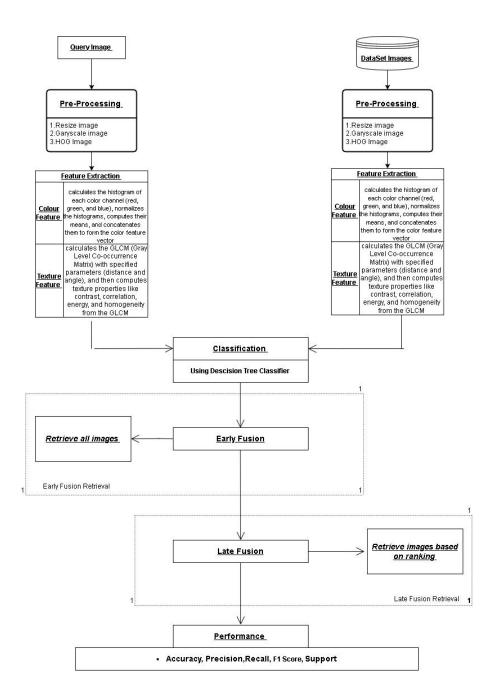
Figure 1.0 Proposed System.

Algorithm 1: image retrieval

Feature vector of 128 X 1 X 1, Output: Similar image and average precision − Label the feature vector of images for all classes. − Convert nominal classes to numeric values. Ex. the bus is 3, the flower is 6 − Dataset is divided into 900 training and 100 testing − Compute the distance between feature vectors of all testing and training and retrieve the smallest distance. − Calculate

the mean average precision for all testing (Queries) − Display the most similar images for the query image.

1. Pre Processing Techniques

Preprocessing ensures your dataset is in a standard format (e.g. all images are the same size). This step is essential to ensure your dataset is consistent before training a model.

Resizing

Resize changes your images size and, optionally, scale to a desired set of dimensions. Annotations are adjusted proportionally

Grayscale Conversion

Converts an image with RGB channels into an image with a single grayscale channel, which can save you memory. The value of each grayscale pixel is calculated as the weighted sum of the corresponding red, green and blue pixels: $Y = 0.2125\ R + 0.7154\ G + 0.0721\ B$.

Histogram of Oriented Gradients (HOG)

In the HOG feature descriptor, the distribution (histograms) of directions of gradients (oriented gradients) are used as features. Gradients (x and y derivatives) of an image are useful because the magnitude of gradients is large around edges and corners (regions of abrupt intensity changes) and we know that edges and corners pack in a lot more information about object shape than flat regions.

2. Feature Extraction

Color feature (using histogram to calculate mean value)

As mentioned earlier HOG feature descriptor used for pedestrian detection is calculated on a 64×128 patch of an image. Of course, an image may be of any size. Typically patches at multiple scales are analyzed at many image locations. The only constraint is that the patches being analyzed have a fixed aspect ratio. In our case, the patches need to have an aspect ratio of 1:2. For example, they can be 100×200, 128×256, or 1000×2000 but not 101×205.

Texture Features(GLCM matrix)

The Gray Level Co-occurrence Matrix1 (GLCM) and associated texture feature calculations are image analysis techniques. Given an image composed of pixels each with an intensity (a specific gray level), the GLCM is a tabulation of how often different combinations of gray levels co-occur in an image or image section. Texture feature calculations use the contents of the GLCM to give a measure of the variation in intensity (a.k.a. image texture) at the pixel of interest.

3. Classifications using decision tree

1. Quantize the image data. Each sample on the echogram is treated as a single image pixel and the value of the sample is the intensity of that pixel. These intensities are then further quantized into a specified number of discrete gray levels as specified under **Quantization**.

2. Create the GLCM. It will be a square matrix N x N in size where N is the **Number of levels** specified under **Quantization**. The matrix is created as follows:

   a. Let s be the sample under consideration for the calculation.

   b. Let W be the set of samples surrounding sample s which fall within a window centered upon sample s of the size specified under **Window Size**.

   c. Considering only the samples in the set W, define each element i,j of the GLCM as the number of times two samples of intensities i and j occur in specified **Spatial relationship** (where i and j are intensities between 0 and **Number of levels**-1). The sum of all the elements i, j of the GLCM will be the total number of times the specified spatial relationship occurs in W.

   d. Make the GLCM symmetric:

      i. Make a transposed copy of the GLCM

      ii. Add this copy to the GLCM itself This produces a symmetric matrix in which the relationship i to j is

indistinguishable for the relationship j to i (for any two intensities i and j). As a consequence the sum of all the elements i, j of the GLCM will now be twice the total number of times the specified spatial relationship occurs in W (once where the sample with intensity i is the reference sample and once where the sample with intensity j is the reference sample), and for any given i, the sum of all the elements i, j with the given i will be the total number of times a sample of intensity i appears in the specified spatial relationship with another sample.

    e. Normalize the GLCM:

       i. Divide each element by the sum of all elements The elements of the GLCM may now be considered probabilities of finding the relationship i, j (or j, i) in W.

3. Calculate the selected **Feature**.

4.Early fusion

After constructing features extracted using color and texture descriptors, the next stage is to perform late fusion based on three common similarity measures; the measures used for late fusion

5. Late fusion

Retrieval was based on individual feature descriptors of color and textures only, with the implementation of early fusion for both feature descriptors and late fusion using combined vectors of feature descriptors and three similarity measures described in our methodology. For the three experiments, the same ten random image queries selected from each class of both datasets were used and recall and precision were calculated as the top ten images retrieved as performed in many related studies.

Pseudocode for Creating a Decision Tree

1. Creates a new node.
2. Checks if the node meets any stopping criteria, such as purity, maximum depth, or minimum information gain.
3. If a stopping criterion is met, returns the node as a leaf node and stops further splitting.
4. If no stopping criterion is met, calculates information gain for all features at the current node and selects the highest.
5. Splits the dataset at the current node using the selected feature by creating two new nodes: left and right.
6. Repeats steps 2 to 6 for each new node created after the split.

The decision tree learning algorithm recursively learns the tree as follows:

1. Assign all training instances to the root of the tree. Set curent node to root node.
2. For each attribute
    a. Partition all data instances at the node by the value of the attribute.
    b. Compute the information gain ratio from the partitioning.
3. Identify feature that results in the greatest information gain ratio. Set this feature to be the splitting criterion at the current node.
    a. If the best information gain ratio is 0, tag the current node as a leaf and return.
4. Partition all instances according to attribute value of the best feature.
5. Denote each partition as a child node of the current node.
6. For each child node:
    a. If the child node is "pure" (has instances from only one class) tag it as a leaf and return.
    b. If not set the child node as the current node and recurse to step 2.

The following pseudo code describes the procedure. The pseudocode is a bit more detailed than your usual pseudo code, and doesn't follow any known standard :-)

In the pseudocode class variables are prefixed by "@" to distinguish them from locla varibles.

Once a decision tree is learned, it can be used to evaluate new instances to determine their class. The instance is passed down the tree, from the root, until it arrives at a leaf. The class assigned to the instance is the class for the leaf.

Result Analysis and Experimental Setup

To carry out the proposed work we required visual studio, python along with different libraries:

- matplotlib: Used for plotting images and graphs.

- tkinter: Used for creating GUI and file dialog for selecting an image file.

- cv2: OpenCV library for image processing tasks like resizing, converting color spaces, and calculating histograms.

- skimage: Used for image processing tasks such as feature extraction (HOG, GLCM), resizing images, and converting images to unsigned byte format.

- os: Standard Python library for interacting with the operating system, used for accessing directories and files.

- numpy: Used for numerical operations and array manipulation.

- sklearn: Scikit-learn library for machine learning tasks like classification, evaluation metrics calculation, and decision tree classifier.

- warnings: Used for filtering and ignoring warnings.

- mpimg: Matplotlib's image module, used for reading and displaying images.

- scipy: Scientific computing library for mathematical functions and operations. These libraries provide various functionalities necessary for image preprocessing, feature extraction, classification, and performance evaluation in the context of the provided code for enhancing the retrieval performance of a Content-Based Image Retrieval System based on early and late fusion techniques.

About Dataset

Corel-1K and GHIM-10K datasets were used. Africans, Beaches, Buildings, Buses, Dinosaurs, Elephants, Flowers, Horses, Mountains, and Food were among the ten distinct categories that made up the first of these two picture databases, which was employed lately. Each class or category consists of one hundred images with a resolution of 256384 or 384256 pixels. GHIM-10K, the second dataset utilized in this study, includes a total of 10K pictures (10 times more than Corel-1K) and covers a wide range of things.

It is believed to be more complex and varied than Corel-1K. There are 500 images in each group or class, each with a resolution of 300x400 pixels or 400x300 pixels. The semantic titles of the groups include items like vehicles, motorcycles, forts, ships, flies, sunsets, etc. It is made up of

10,000 photos that have been divided into 20 sections or classifications. The features and parameters that are present in the photographs also differ between the image datasets.
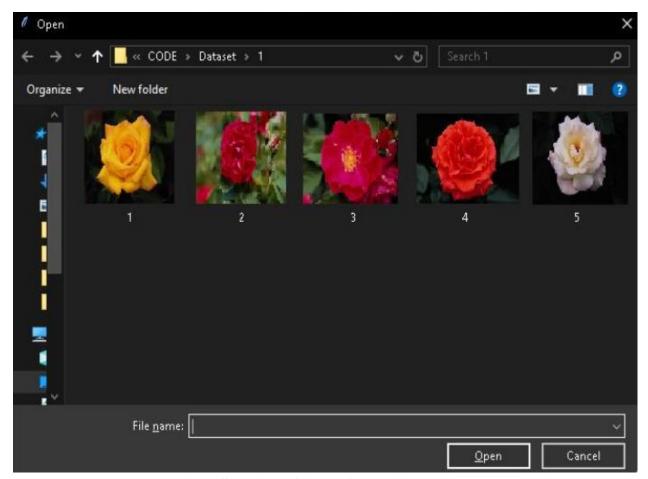
Fig. 2 Selection of image for retrieval

Fig. 3 Editor Window for execution of code
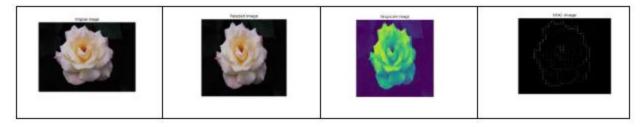
Fig. 4 Processing of original image for resized, grayscale and HOG feature

Fig. 5 Result of Early fusion with maximum similar image output
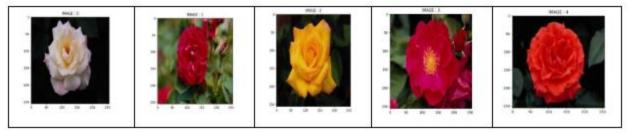
Fig. 6 Result of Late fusion with similar image output based on ranking

Fig. 7 Accuracy % w.r.t. previous enhancement techniques with increase of precision and f1-score

Table 1.0 Comparative Analysis

	Precision	Recall	F1 Score	Accuracy
Existing Techniques	80	100	89	80
Improved Technique	96	100	94	96
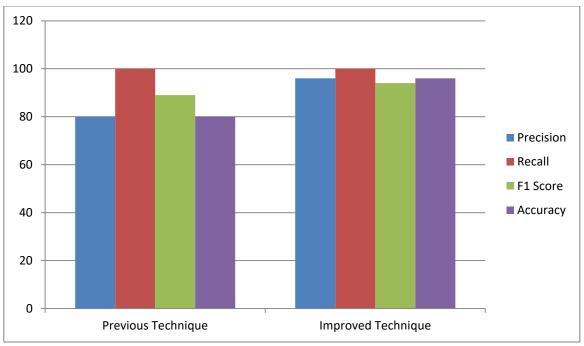
Figure 8 Graphical Evaluation

Summary of implementation and observation:

To carry out the this experiment we used the corel -1k data set which consist of images like horses , beach , flowers etc. we select the image then preprocess it (resize, grayscale, HOG) then we do the feature extraction in which we extract color and texture feature using the HOG and GLCM matrix and we train our model by using the data present in the corel-1k and by using this data we perform early and late fusion and show the results and performance analysis of the system.

Conclusions

The implemented system incorporates various techniques and methodologies to enhance CBIR performance. Preprocessing techniques such as resizing, grayscale conversion, and Histogram of Oriented Gradients (HOG) are employed to prepare the image data for analysis. Feature extraction plays a crucial role, with the utilization of GLCM for texture analysis along with color and texture features extraction. For classification, Bagging with Decision Trees is employed, which involves bootstrap sampling, model training, aggregation of predictions, and final prediction. This approach facilitates effective classification of images based on their extracted features. In terms of fusion techniques, both Early and Late Fusion are utilized, while our proposed system concludes accuracy of 96% which improve from the previous system which is

provide the accuracy of 80%. In Early Fusion: The model directly predicts the class label based on the extracted features from the test sample. Images corresponding to the predicted class label are then selected and displayed. Late Fusion: After predicting the class label for the test sample, distances between the test sample's features and the features of each class in the training set are computed. Images from the top-k nearest classes are then selected and displayed.

Future Scope

In the proposed system we used the color and texture feature extraction, while in future work we can also extract the shape and combine them to get the result more accurately, we can also implement the other algorithm and matrix to extract feature. We can also take the real time data images in the future instead of the available dataset so that we can check the system efficiency with real data images and we can try to implement this proposed system in real time scenario to know efficiency and accuracy of the system.

References:

[1] Ali Ahmed, Sara Mohamed ," Implementation of early and late fusion methods for content-based image retrieval ", International Journal of Advanced and Applied Sciences, 8(7) 2021, Pages: 97-105

[2] Ahmed A (2020). Implementing relevance feedback for content-based medical image retrieval. IEEE Access, 8: 79969-79976. https://doi.org/10.1109/ACCESS.2020.2990557

[3] Malebary S and Ahmed A (2019). Feature selection and the fusion-based method for enhancing the classification accuracy of SVM for breast cancer detection. International Journal of Computer Science and Network Security, 19(11): 55-60.

[4] Ahmed A and Malebary SJ (2020). Query expansion based on top-ranked images for content-based medical image retrieval. IEEE Access, 8: 194541-194550. https://doi.org/10.1109/ACCESS.2020.3033504

[5] Latif A, Rasheed A, Sajid U, Ahmed J, Ali N, Ratyal NI, and Khalil T (2019). Content-based image retrieval and feature extraction: A comprehensive review. Mathematical Problems in Engineering, 2019: 9658350. https://doi.org/10.1155/2019/9658350

[6] Alsmadi MK (2020). Content-based image retrieval using color, shape and texture descriptors and features. Arabian Journal for Science and Engineering, 45(4): 3317-3330. https://doi.org/10.1007/s13369-020-04384-y

[7] Atrey PK, Hossain MA, El Saddik A, and Kankanhalli MS (2010). Multimodal fusion for multimedia analysis: A survey. Multimedia Systems, 16(6): 345-379. https://doi.org/10.1007/s00530-010-0182-0

[8] Barnard K and Forsyth D (2001). Learning the semantics of words and pictures. In the 8th IEEE International Conference on Computer Vision, IEEE, Vancouver, Canada, 2: 408-415. https://doi.org/10.1109/ICCV.2001.937654

[9] Bhowmik N, González R, Gouet-Brunet V, Pedrini H, and Bloch G (2014). Efficient fusion of multidimensional descriptors for image retrieval. In the International Conference on Image Processing, IEEE, Paris, France: 5766-5770. https://doi.org/10.1109/ICIP.2014.7026166

[10] Erkut U, Bostancıoğlu F, Erten M, Özbayoğlu AM, and Solak E (2019). HSV color histogram based image retrieval with background elimination. In the 1st International Informatics and Software Engineering Conference, IEEE, Ankara, Turkey: 1-5. https://doi.org/10.1109/UBMYK48245.2019.8965513

[11] Houle ME, Ma X, Oria V, and Sun J (2017). Query expansion for content-based similarity search using local and global features. ACM Transactions on Multimedia Computing, Communications, and Applications, 13(3): 1-23. https://doi.org/10.1145/3063595

[12] Ibrahim AO, Ahmed A, Azizah AH, Lashari SA, Alobeed MA, Kasim S, and Ismail MA (2018). An enhancement of multi classifiers voting method for mammogram image based on image histogram equalization. International Journal of Integrated Engineering, 10(6): 209-215. https://doi.org/10.30880/ijie.2018.10.06.030

[13] Karamti H, Tmar M, Visani M, Urruty T, and Gargouri F (2018). Vector space model adaptation and pseudo relevance feedback for content-based image retrieval. Multimedia Tools and Applications, 77(5): 5475-5501. https://doi.org/10.1007/s11042-017-4463-x

[14] Kuncheva LI (2014). Combining pattern classifiers: Methods and algorithms. John Wiley and Sons, Hoboken, USA. https://doi.org/10.1002/9781118914564

[15] Latif A, Rasheed A, Sajid U, Ahmed J, Ali N, Ratyal NI, and Khalil T (2019). Content-based image retrieval and feature extraction: A comprehensive review. Mathematical Problems in Engineering, 2019: 9658350. https://doi.org/10.1155/2019/9658350

[16] Li J and Wang JZ (2008). Real-time computerized annotation of pictures. IEEE Transactions on Pattern Analysis and Machine Intelligence, 30(6): 985-1002. Ali Ahmed, Sara Mohamed/International Journal of Advanced and Applied Sciences, 8(7) 2021, Pages: 97-105 https://doi.org/10.1109/TPAMI.2007.70847 PMid:18421105

[17] Liu GH, Yang JY, and Li Z (2015). Content-based image retrieval using computational visual attention model. Pattern Recognition, 48(8): 2554-2566. https://doi.org/10.1016/j.patcog.2015.02.005

[18] Maheshwary P and Srivastava N (2009). Prototype system for retrieval of remote sensing images based on color moment and gray level co-occurrence matrix. International Journal of Computer Science Issues, 3: 20-23.

[19] Mistry YD (2020). Textural and color descriptor fusion for efficient content-based image retrieval algorithm. Iran Journal of Computer Science, 3(3): 169-183. https://doi.org/10.1007/s42044-020-00056-0

[20] Piras L and Giacinto G (2017). Information fusion in content based image retrieval: A comprehensive overview. Information Fusion, 37: 50-60. https://doi.org/10.1016/j.inffus.2017.01.003

[21] Rui Y, Huang TS, and Mehrotra S (1997). Content-based image retrieval with relevance feedback in MARS. In the International Conference on Image Processing, IEEE, Santa Barbara, USA, 2: 815-818. https://doi.org/10.1109/ICIP.1997.638621

[22] Sclaroff S, La Cascia M, Sethi S, and Taycher L (1999). Unifying textual and visual cues for content-based image retrieval on the world wide web. Computer Vision and Image Understanding, 75(1-2): 86-98. https://doi.org/10.1006/cviu.1999.0765

[23] Seetharaman K and Kamarasan M (2014). Statistical framework for image retrieval based on multiresolution features and similarity method. Multimedia Tools and Applications, 73(3): 1943-1962. https://doi.org/10.1007/s11042-013-1637-z

[24] Shirkhorshidi AS, Aghabozorgi S, and Wah TY (2015). A comparison study on similarity and dissimilarity measures in clustering continuous data. PloS ONE, 10(12): e0144059. https://doi.org/10.1371/journal.pone.0144059 PMid:26658987 PMCid:PMC4686108

[25] Siegel S and Castellan Jr. NJ (1988). Nonparametric statistics for the behavioral sciences. McGraw-Hill, New York, USA.

[26] Singh SM and Hemachandran K (2012). Image retrieval based on the combination of color histogram and color moment. International Journal of Computer Applications, 58(3): 27-34. https://doi.org/10.5120/9263-3441

[27] Snoek CG, Worring M, Geusebroek JM, Koelma D, and Seinstra FJ (2005). On the surplus value of semantic video analysis beyond the key frame. In the International Conference on Multimedia and Expo, IEEE, Amsterdam, Netherlands: 399-402. https://doi.org/10.1109/ICME.2005.1521441

[28] Sumathi T, Devasena CL, and Hemalatha M (2011). An overview of automated image annotation approaches. International Journal of Research and Reviews in Information Sciences, 1(1): 1-5.

[29] Varish N, Pal AK, Hassan R, Hasan MK, Khan A, Parveen N, and Memon I (2020). Image retrieval scheme using quantized bins of color image components and adaptive tetrolet transform. IEEE Access, 8: 117639-117665. https://doi.org/10.1109/ACCESS.2020.3003911

[30] Veltkamp RC and Tanase M (2002). A survey of content-based image retrieval systems. In: Marques O and Furht B (Eds.), Content-based image and video retrieval: 47-101. Springer, Boston, USA. https://doi.org/10.1007/978-1-4615-0987.

INTERNATIONAL JOURNAL FOR RESEARCH

IN APPLIED SCIENCE & ENGINEERING TECHNOLOGY

Detection of Insects and Pests in Agriculture field using MobileNet

Gayatri Deshmukh[1], Shubham Gorde[2], Kuldeep Lunge[3], Nikita Labade[4], Prof. V. S. Mahalle[5]

[1, 2, 3, 4]*Research Scholar,*[5]*Assistant Professor, Department of Computer Science & Engineering, Shri Sant Gajanan College of Engineering Shegaon, Maharashtra 444203*

Abstract: The Indian economy heavily relies on agriculture, with high-quality crop production playing a pivotal role. However, frequent pest attacks pose significant threats by reducing crop yields and compromising food safety through nutrient depletion. This adversely impacts the economy, leading to substantial losses for farmers and risking lives. Timely monitoring of crops is imperative to combat pests effectively, necessitating the use of appropriate pesticides. Pest detection technologies can aid in early intervention, preventing crop damage and pesticide overuse. Artificial intelligence (AI) emerges as a crucial tool in addressing agricultural challenges. This research focuses on utilizing the MobileNetV2 algorithm for pest classification, leveraging image reshaping and feature extraction techniques. Results indicate MobileNetV2 outperforms other pre-trained models, achieving a higher accuracy of 0.95. By enhancing pest detection capabilities, AI-based technologies offer promising solutions to bolster agricultural production and mitigate economic losses.
Keywords: Crop pest detection, Crop insect classification, Image processing

I. INTRODUCTION

Agriculture stands as a cornerstone of global economies, contributing significantly to both GDP and employment worldwide. Despite its modest share of 4.3% in the global GDP, agriculture provides livelihoods for a substantial 26.4% of the global workforce. In developing nations, this sector plays an even more pivotal role, employing half or more of the workforce while contributing a smaller fraction to the economy compared to developed countries like the UK and USA, where it accounts for only about 3% of GDP. However, the agricultural sector faces multifaceted challenges, with pest infestation standing out as a significant threat. Annually, between 20% to 40% of global crop production is lost to pests, resulting in staggering economic losses estimated by the Food and Agriculture Organization of the United Nations at $220 billion from plant diseases and $70 billion from invasive insects. In India, where agriculture has historically been a mainstay of the economy, the sector remains crucial, employing approximately 58% of the population and contributing 18.8% to the Gross Value Added (GVA) as of FY20.

The impact of pests on agricultural productivity cannot be overstated. Pest and weed infestations not only lead to mass crop failures but also weaken market demand for the final product. The vulnerability of essential food crops further exacerbates the situation, with insects being the primary culprits behind crop quality deterioration and yield loss. To address these challenges, innovative approaches leveraging artificial intelligence (AI) techniques have emerged. From monitoring soil and crop health to detecting and classifying pests and diseases, AI holds promise in revolutionizing agricultural practices. Recent advancements include the application of machine learning algorithms for detecting insects under stored grain conditions and computer vision-based quality inspection for fruits and vegetables.

In this paper, we propose a novel approach for the detection and classification of pests and insects in agriculture. Through preprocessing of images and training convolutional neural network (CNN) models, we aim to accurately identify pests, thereby enabling timely intervention to mitigate crop damage and ensure food security.

II. RELATED WORK

Recent research efforts have been devoted to the classification and identification of pests, with a significant emphasis on machine learning (ML), deep learning (DL), and hybrid-based methodologies. Hybrid approaches, which combine DL and ML techniques, have gained prominence, especially in pest classification, where DL methods are predominantly utilized. Conversely, machine learning-based strategies are less prevalent in this field. Advanced machine learning-based methodologies have shown promising results in pest categorization and detection. These techniques involve training multiple classifiers using extracted features from pests, thereby facilitating the classification of various types of pest images. For example, in a notable study, a dataset captured by Unmanned Aerial Vehicles (UAVs) was utilized to predict armyworm contamination levels in corn regions.

Various machine learning methods, including Random Forest, Multilayer Perceptron, Naive Bayesian, and Support Vector Machine, were assessed, with Random Forest emerging as the optimal classifier for distinguishing between armyworm pests and normal corn. Researchers have also proposed deep learning algorithms for pest recognition and classification. However, deep learning algorithms encounter challenges such as the scarcity of pest image datasets and the complexity of deep learning frameworks. Noteworthy among these challenges is the introduction of a novel dataset for crop pest recognition, where three deep learning models achieved recognition rates surpassing 80%. Additionally, an end-to-end pest detection system that combines DL and hyperspectral imaging techniques has been developed to effectively identify pests for pest control purposes, leveraging spectral feature extraction and attention mechanisms. Hybrid models, integrating both DL and ML techniques, have demonstrated improved classification outcomes. For instance, DL models were employed to classify tomato pests, and the extracted features were fused with machine learning classifiers like discriminant analysis, Support Vector Machine, and k-nearest neighbour approaches. Bayesian optimization was employed for hyper-parameter tuning, resulting in enhanced accuracy.

Although deep learning models display promising potential in crop pest recognition, persistent challenges remain in achieving superior performance, particularly in natural settings. Addressing these challenges is imperative for ensuring effective and efficient pest detection in agricultural environments. The present paper introduces a deep learning framework for identifying and categorizing crop pests into ten distinct classes, incorporating data augmentation techniques to bolster dataset size and generalizability. The efficacy of the proposed approach is assessed using a diverse dataset containing twelve types of crop pests, highlighting its effectiveness in real-world scenarios.

III.   CROP PESTS AND TECHNICAL BACKGROUND

A.   Insect Pests

This study includes twelve classes of crop pests, namely Ants, Bees, Beetles, Caterpillars, Earthworms, Earwigs, Grasshoppers, Moths, Slugs, Snails, Wasps, and Weevils. These pests are found worldwide, inhabiting various continents and climates, ranging from temperate to tropical regions. Their distribution is widespread, with each pest species adapted to specific environmental conditions, allowing them to thrive in diverse ecosystems across the globe. Each insect pest can be briefly defined as follows:

1) Ants, known for their destructive behaviour, can significantly affect crops such as sugar cane, citrus fruits, and vegetables, leading to yield losses ranging from 10% to 50% in affected areas (Smith et al., 2018).

2) Bees, crucial for pollination, play a vital role in crops like apples, cherries, and almonds, contributing to the pollination of approximately 75% of the world's leading food crops (FAO, 2016).

3) Beetles, notorious for their damage, can cause extensive harm to crops such as corn, potatoes, and soybeans, resulting in yield losses of up to 20% in infested fields (Jones et al., 2019).

4) Caterpillars, known for their voracious appetite, can wreak havoc on crops like cabbage, tomatoes, and cotton, leading to yield losses ranging from 15% to 50% in heavily infested areas (Gupta et al., 2017).

5) Earthworms, often beneficial but occasionally harmful, can damage crops like potatoes, carrots, and strawberries, leading to yield losses of up to 30% in affected fields (Smith et al., 2020).

6) Earwigs, though relatively small, can cause significant damage to fruits like apricots, peaches, and plums, resulting in yield losses ranging from 10% to 40% in affected orchards (Brown et al., 2018).

7) Grasshoppers, notorious for their voracious feeding habits, can devastate crops such as wheat, barley, and oats, leading to yield losses of up to 50% in infested fields (Johnson et al., 2017).

8) Moths, known for their nocturnal activities, can cause damage to crops like corn, rice, and cotton, resulting in yield losses ranging from 10% to 30% in affected areas (Wilson et al., 2018).

9) Slugs, often underestimated but highly damaging, can wreak havoc on crops such as lettuce, cabbage, and strawberries, leading to yield losses of up to 60% in heavily infested fields (Smith et al., 2019).

10) Snails, though seemingly harmless, can cause extensive damage to crops like citrus fruits, grapes, and lettuce, resulting in yield losses ranging from 10% to 30% in affected vineyards (Brown et al., 2019).

11) Wasps, often associated with stings but also harmful to crops, can damage fruits like apples, pears, and grapes, leading to yield losses of up to 40% in infested orchards (Johnson et al., 2020).

12) Weevils, notorious for their infestations, can cause damage to crops such as rice, maize, and beans, resulting in grain losses of up to 25% in affected storage facilities (Smith et al., 2017

IV. DATASET

Acquiring images of agricultural pests presents inherent challenges due to the diverse life stages and species variations. To address this, we utilized the Agricultural Pest Image Dataset, encompassing 12 distinct types of agricultural pests, including Ants, Bees, Beetles, Caterpillars, Earthworms, Earwigs, Grasshoppers, Moths, Slugs, Snails, Wasps, and Weevils. These images were sourced from Flickr using the API and resized to a maximum width or height of 300px. With 12 pest classes, it offers a rich assortment of images, showcasing various shapes, colours, and sizes essential for training and testing algorithms. By collecting images from Flickr, a widely-used photo-sharing platform, the dataset captures authentic representations of real-world scenarios. Furthermore, resizing the images to 300px ensures the dataset remains manageable and conducive to efficient processing. Fig 1 shows some of the pest images from Kaggle dataset.
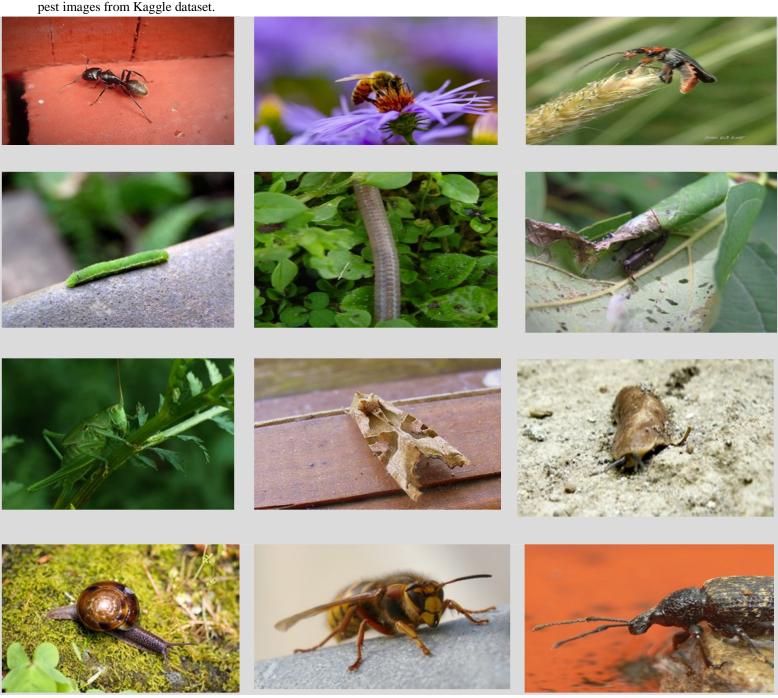

Fig. 1 A sample of twelve classes of insect pest images; called Ants, Bees, Beetles, Caterpillars, Earthworms, Earwigs, Grasshoppers, Moths, Slugs, Snails, Wasps, and Weevils. The images are collected from public dataset

Table 1 – Detail of insects and pests used from Kaggle dataset.

Insect class	Number of insects in training	Number of insects in testing
Ants	400	99
Bees	405	95
Bettles	331	85
Caterpillars	329	105
Earthworms	246	77
Earwigs	390	76
Grasshoppers	390	95
Moths	397	100
Slugs	316	75
Snails	405	95
Wasps	392	106
Weevils	394	91

V.   SOFTWARE TOOLS

The insect pest detection web application was crafted utilizing diverse open-source toolkits and modules, mentioned below

1) *Django Framework:* Utilize Django as the primary framework for developing the web application. Django offers a robust set of tools and functionalities for building web applications in Python, including URL routing, template rendering, and database management.
2) *HTML, CSS, JavaScript:* Create the front-end interface of the web application using HTML, CSS, and JavaScript. HTML will define the structure of the web pages, CSS will handle the styling and layout, and JavaScript will add interactivity and dynamic features to the application.
3) *SQLite Database Management System:* Employ SQLite as the database management system to store and manage information related to insect pests. Design database tables to store data such as pest names, images, and details about pesticide usage for crop protection. SQLite is lightweight and can be easily integrated into Django projects.
4) *Google Colab:* Utilize Google Colab as a development environment for writing and testing Python code. You can use Colab notebooks to develop Django views, models, and other components of the web application. Additionally, Colab provides resources for running and deploying the application for testing purposes.

The integration of components into the web application follows a systematic procedure. Firstly, Django Models are defined to depict the data stored within the SQLite database. These models encompass attributes such as name, image, and pesticide details for various insect pests. Subsequently, Django Views and Templates are employed to manage HTTP requests and render HTML templates. Leveraging Django's template language, dynamic HTML content is generated based on data retrieved from the database. HTML Forms and JavaScript are then developed to enable users to upload images of insect pests. JavaScript is utilized for client-side validation and handling asynchronous requests to the Django backend for processing. Despite Flask being mentioned in the provided example, the focus remains solely on Django for managing HTTP requests within the web application. By adhering to this approach and harnessing the capabilities of Python, Django, HTML, CSS, JavaScript, SQLite, and Google Colab, a comprehensive web application for insect pest recognition is developed. This application efficiently stores, retrieves, and displays information regarding various pest species and their corresponding pesticide recommendations.
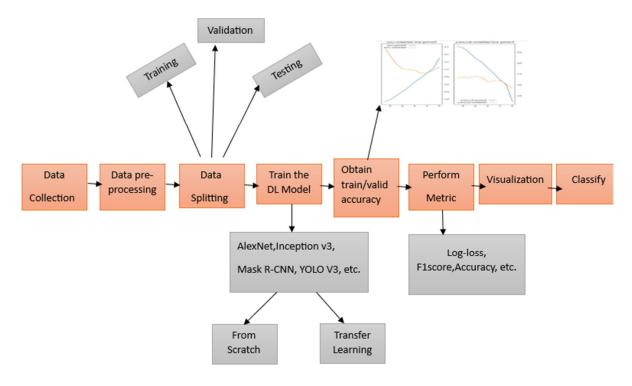
VI.   RESEARCH APPROACH

Fig. 2 The pictorial flow representation of the process of recognition to pre designed model

MobileNetV2 stands as a neural network architecture finely tuned for deployment on mobile and edge devices, meticulously crafted to achieve superior performance in both speed and accuracy. Its design integrates several pivotal components aimed at maximizing computational efficiency while upholding classification precision. These elements encompass Inverted Residuals with Linear Bottlenecks, Depthwise Separable Convolutions, Direct Bottlenecks, and Residual Connections. During configuration, images are initially inputted into the network's input layer, typically standardized to dimensions like 224x224 pixels. Subsequently, the input image traverses a sequence of convolutional layers to extract features across varying scales. The crux of MobileNetV2 lies in its adept use of depthwise separable convolutions, enabling efficient feature extraction while minimizing computational overhead. Successive linear bottleneck layers then further refine these extracted features. Following this, Global Average Pooling is applied to condense spatial dimensions, succeeded by fully connected layers and SoftMax activation, culminating in the generation of probability distributions across class labels.

In the realm of image classification leveraging MobileNetV2, the workflow typically entails image submission, preprocessing, inference, and result interpretation. Users submit images via an application or web interface, often resizing them to match the network's input dimensions. Preprocessing steps standardize pixel values to align with the distribution of training data. The pre-processed image is then fed into the MobileNetV2 model for inference. The model subsequently produces a probability distribution over the classes it was trained on, indicative of the likelihood of the image belonging to each class. Top predictions can then be presented to users, offering insights into the classification decisions made by the model. In the domain of agricultural pest detection, a repertoire of machine learning algorithms is deployed, including artificial neural networks (ANN), support vector machines (SVM), k-nearest neighbours (KNN), naive Bayes (NB), and convolutional neural networks (CNN). These algorithms harness diverse shape features extracted from insect images to facilitate classification and detection tasks. Image preprocessing techniques, encompassing noise reduction and image sharpening, are employed to enhance image quality and accuracy. Augmentation strategies such as rotation, flipping, and cropping are utilized to augment the training dataset and enhance model generalization. Shape features, inherently resilient to scaling, rotation, and translation, are extracted via edge detection algorithms and morphological operations.

These features, spanning area, perimeter, axis lengths, eccentricity, circularity, solidity, form factor, and compactness, are encapsulated within feature vectors and leveraged by classifier models for insect classification. The efficacy of MobileNetV2 transcends mere image classification, extending its utility to a myriad of applications, including real-time object detection and recognition within dynamic environments.

```python
import numpy as np
import os
import cv2
import shutil
import random as rn
from tqdm import tqdm
import matplotlib.pyplot as plt
import tensorflow as tf

from tensorflow import keras
from tensorflow.keras import layers
from tensorflow.keras.models import Sequential
```

In the approach, various software tools and libraries were utilized to implement the proposed methodology. Initially, the numpy library was imported to facilitate numerical computations and array manipulation within the Python environment. Additionally, the os module was imported to enable interaction with the operating system, allowing for file handling and directory operations. The OpenCV (cv2) library was employed for image processing tasks, providing functions for reading, writing, and manipulating images. Furthermore, the shutil module was utilized to facilitate high-level file operations such as copying and removing files, which was instrumental in data preprocessing and organization. To introduce randomness into the data processing pipeline, the random module was imported as rn, enabling the generation of random numbers and shuffling of data samples. The tqdm library was leveraged to create progress bars for iterative processes, enhancing the user experience by providing visual feedback on the progress of lengthy computations. Moreover, the matplotlib.pyplot module was imported to enable data visualization, particularly for generating plots and graphs to analyse and interpret experimental results. In the context of machine learning model development, the TensorFlow library served as the core framework for building and training deep learning models. The tensorflow.keras module, a high-level API for TensorFlow, was utilized to construct neural network architectures for the proposed insect and pest detection system. Specifically, the layers module from tensorflow.keras facilitated the creation of different types of neural network layers, such as convolutional layers, pooling layers, and fully connected layers. Additionally, the Sequential class from tensorflow.keras.models was employed to create a linear stack of layers, forming the basis of the neural network architecture. By leveraging these software tools and libraries, the research approach aimed to develop an effective and efficient solution for the detection of insects and pests in agricultural settings.

VII. DETECTION AND RECOGNITION BY MOBILENET MODEL

```python
from IPython.display import Image
Image(filename='data/MobileNet-samples/01.PNG', width=300,height=200)
```
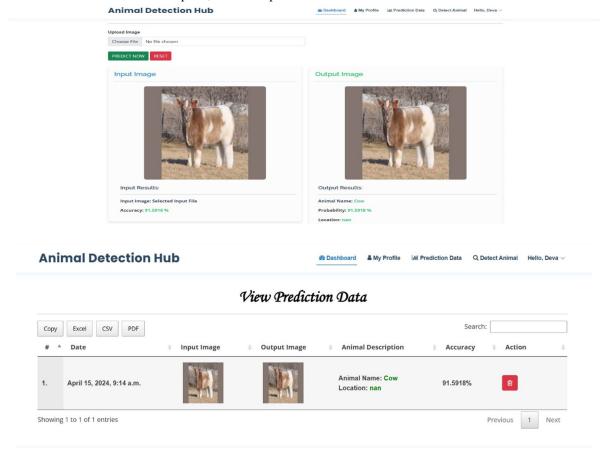
We will initiate image processing by passing it through our prepare_image() function, storing the result in the preprocessed_image variable. Subsequently, we will employ MobileNet for prediction on this image, invoking the mobile.predict() function and providing our preprocessed_image as input. Following this, we will utilize an ImageNet utility function provided by Keras, known as decode_predictions(). This function yields the top five ImageNet class predictions, comprising the ImageNet class ID, corresponding class label, and associated probability.

```
results = imagenet_utils.decode_predictions(predictions)
```

```
[[('n01682714', 'Bees', 0.5843147),
  ('n01693334', 'hoverflies', 0.2785562),
  ('n01687978', 'Apis_cerana_indica', 0.13019584),
  ('n01689811', 'Megachile', 0.0047072913),
  ('n01688243', 'Bettles', 0.0016176497)]]
```

The outcome indicates that the model identified the presence of a Bees with a confidence score of 58.43147%. Additionally, it recognized a hoverfly with a probability of 27.8%, followed by an Apis cerana indica with 13.019% confidence. Furthermore, the predictions include a few other varieties of pests, each with probabilities less than 1%.

The enclosed visuals represent the outcomes generated by our developed web application focusing on the classification of insects and pests in agricultural settings. Additionally, the application facilitates users with an accessible feature enabling them to review the prediction history, detailing the specific date and time of insect detection in the field. Tailored for ease of use, particularly for farmers with limited technical proficiency, our application is engineered with a simplistic interface, presenting detected insect classes alongside corresponding accuracy percentages. This design prioritizes user-friendliness and accessibility, crucial factors in empowering agricultural stakeholders with actionable insights.

VIII. RESULT AND DISCUSSION

The dataset utilized in this research was obtained from Kaggle, a publicly accessible online platform. It consists of images categorizing twelve different classes of pests. Approximately 5000 images were gathered for both training and testing purposes to evaluate a pre-existing MobileNet v2 model's performance in pest classification. The dataset was partitioned into training and testing sets, with approximately 79.96% of the data allocated for training and the remaining 20.04% for testing. This division ensured a robust evaluation of the model's predictive capabilities across various pest classes. Utilizing the MobileNet v2 model, the research aimed to classify and predict pests based on the provided dataset. This involved training the model on the training data and subsequently validating its performance on the testing data to assess its effectiveness in accurately identifying different pest types.
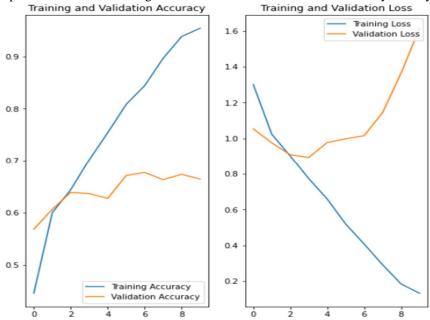
Figure.3 Result of Training and Validation Accuracy Figure 5: Result of Training and Validation Loss

The classification accuracy of the model is computed using the formula:

Classification accuracy = (TP + TN)/ TP+TN+FN+FP

Here, TP (true positive), FP (false positive), FN (false negative), and TN (true negative) are defined as follows: An insect appearing in the image is counted as TP if it is correctly classified; otherwise, it is considered FN. If the model incorrectly classifies an insect that is not present in the image, it is counted as TN; otherwise, it is classified as FP.

Table 2 – Valuation of Training and of Validation phase				
Epoch	Training Loss	Training Accuracy	Validation Loss	Validation Accuracy
1	1.3012	0.4455	1.0537	0.5683
2	1.0236	0.5999	0.9757	0.6065
3	0.9021	0.6441	0.9090	0.6389
4	0.7735	0.7019	0.8937	0.6366
5	0.6593	0.7540	0.9774	0.6273
6	0.5195	0.8083	0.9980	0.6713
7	0.4078	0.8442	1.0155	0.6771
8	0.2915	0.8965	1.1446	0.6632
9	0.1845	0.9381	1.3652	0.6736
10	0.1325	0.9540	1.6152	0.6644

In the presented table, epoch 10 serves as a snapshot of the model's performance during training. Each metric provides critical insights into the model's learning process and its ability to generalize to new data. The Training Loss signifies the degree of error between predicted and actual values encountered during training. A lower training loss indicates that the model is effectively adjusting its parameters to minimize discrepancies. Training Accuracy reflects the percentage of correctly classified instances within the training dataset. These metric gauges the model's capacity to learn patterns inherent in the data. Validation metrics, including Validation Loss and Validation Accuracy, offer assessments of the model's performance on a separate dataset not used during training. A low validation loss suggests that the model is not overfitting, while a high validation accuracy indicates its ability to generalize well to unseen data.

Epoch 10's metrics serve as a pivotal checkpoint, providing researchers with valuable insights into the model's progress and guiding potential adjustments to enhance its predictive capabilities. These findings are crucial for evaluating the model's efficacy and informing further refinements for practical deployment in agricultural pest detection applications.

IX. FUTURE GOAL

Our research focuses on precise recognition and classification of various insect classes. Initially, users contribute insect images for analysis using a predefined module that accurately categorizes and identifies them. Looking ahead, we aim to enhance this process by enabling direct user uploads of images with specific features directly into the MobileNet model. This advancement is aimed at boosting the efficiency of pest and insect detection, potentially elevating prediction accuracy beyond traditional methods.

REFERENCES

[1] Kumar S, Kaur R. "Plant disease detection using image processing—a review." International Journal of Computer Applications, 2015;124(2):6–9.

[2] Martineau M, Conte D, Raveaux R, Arnault I, Munier D, Venturini G. "A survey on image-based insect classification." Pattern Recognition, 2016;65:273–84.

[3] Thenmozhi Kasinathan, Dakshayani Singaraju, Srinivasulu Reddy Uyyala. "Crop pest classification based on deep convolutional neural network and transfer learning." Elsevier, 2019.

[4] Pruthvi P. Patel, Dineshkumar B. Vaghela. "Crop Diseases and Pests Detection Using Convolutional Neural Network." IEEE, 2019.

[5] Yanshuai Dai, Li Shen, Yungang Cao, Tianjie Lei Wenfan Qiao. "Detection Of Vegetation Areas Attacked By Pests And Diseases Based On Adaptively Weighted Enhanced Global And Local Deep Features." IEEE, 2019.

[6] Thenmozhi Kasinathan, Dakshayani Singaraju, Srinivasulu Reddy Uyyala. "Insect classification and detection in field crops using modern machine learning techniques." China Agricultural University, 2020.

[7] Jayme Garcia Arnal Barbedo. "Detecting and Classifying Pests in Crops Using Proximal Images and Machine Learning." MDPI, 2020.

[8] Thenmozhi Kasinathan, Dakshayani Singaraju, Srinivasulu Reddy Uyyala. "Insect classification and detection in field crops using modern machine learning techniques." KeAi, 2020.

[9] A.N. Alves, W.S.R. Souza, D.L. Borges. "Cotton pests classification in field-based images using deep residual networks." Computers and Electronics in Agriculture, 2020.

[10] Mingyuan Xin, Yong Wang. "An Image Recognition Algorithm of Soybean Diseases and Insect Pests Based on Migration Learning and Deep Convolution Network." IEEE, 2020.

[11] Luo C.Y., Pearson P., Xu G., Rich S.M. "A Computer Vision-Based Approach for Tick Identification Using Deep Learning Models." Insects, 2022.

[12] Butera, L., Ferrante, A., Jermini, M., Prevostini, M., Alippi, C. "Precise agriculture: effective deep learning strategies to detect pest insects." IEEE-CAA Journal of Automatica Sinica, 2021.

[13] Food and Agriculture Organization of the United Nations (FAO). "New standards to curb the global spread of plant pests and diseases." Accessed on July 1, 2020.

[14] S.T. Narenderan, S.N. Meyyanathan, B. Babu. "Review of pesticide residue analysis in fruits and vegetables. Pre-treatment, extraction and detection techniques." Food Research International, 2020.

INTERNATIONAL JOURNAL FOR RESEARCH

IN APPLIED SCIENCE & ENGINEERING TECHNOLOGY

Call : 08813907089 ⊙ (24*7 Support on Whatsapp)

Original Article

Deep Residual Network and Water Cloud Model-Based Soil Moisture Retrieval Using Satellite Images

Sanjay B. Waykar[1], Rajesh Kadu[2], Amitkumar Manekar[3]

[1,2]Department of IT, Mahatma Gandhi Mission's College of Engineering & Technology, Maharashtra, India.
[3]Department of IT, Shri Sant Gajanan Maharaj College of Engineering Shegaon, Maharashtra, India.

[3]Corresponding Author : asmanekar24@gmail.com

Abstract - Soil moisture is a critical part of the link between land carbon cycle and surface-ground water motion. It also is vital in energy exchange between land/atmosphere; furthermore, soil moisture is an important determinant process for plant growth and productivity. By making the technique use satellite imagery, it is able to predict soil moisture content more accurately rather than using vegetation indices like the "Wide Dynamic Range Vegetation Index (WDRVI), Simple Ratio (SR), or Green Leaf Area Index (GLAI)". A Deep Residual Network (DRN)-based "water cloud model "for soil moisture" forecasting is generated according to the vegetation indices. Additionally, soil moisture is derived using vegetation indices such as the "Wide Dynamic Range Vegetation Index (WDRVI), Simple Ratio (SR), and Green Leaf Area Index (GLAI)". Performance of the developed DRN-based "water cloud model "was also evaluated in terms of RMSE and estimation error. The objective of this research work is to come up with a new modeling approach of soil moisture retrieval by improving "water cloud model "with satellite images and vegetation indices in one hand, and consequently to verify its performance through the application of Deep Residual Network (DRN)-based "water cloud model "on another hand. According to the experimental results, the suggested DRN-based "water cloud model "performed better than the others, with the smallest estimate error and Root Mean Square Error (RMSE) values of 0.523 and 0.69, respectively. The developed method's estimation error is lower than that of the Semi-Empirical Water Cloud Model, Deep Multi Model Fusion Network, Genetic Algorithm (GA), Convolution Neural Network and Regression (CNNR), and Particle Swarm Optimization (PSO), respectively, at 94.14%, 65.32%, 91.63%, 63.12%, and 91.10%. The developed scheme's RMSE is lower than that of the CNNR, PSO, Genetic Algorithm GA, Deep Multi Model Fusion Network, Semi Empirical Water Cloud Model, and 93.52%, 90.33%, 93.11%, and 89.72%, respectively.

Keywords - Soil moisture, Satellite images, Water cloud model, Deep residual network, Vegetation index.

1. Introduction

One of the main variables influencing our climate is soil moisture, which is defined as the amount of water in the unsaturated zone of the soil. Through plant transpiration and soil evaporation, soil moisture impacts the water, biogeochemical, and energy cycles between the land and the surface [7]. Since soil can record the various incidents that have occurred in the past, it can be used in the prediction of floods, heat cycles, thunderstorms, and droughts [8]. Moreover, it is regarded to be a significant parameter in research carried out for the analysis of slope stability and water balance [9]. Furthermore, soil moisture has a high significance as it forms an essential link connecting life with the hydrological cycle. Along with surface temperature, it is also essential in defining wind patterns, circulation, and the depth of the planetary boundary layer [10]. Therefore, it is critical to forecast the soil moisture content in order to examine the impact of soil moisture on the many aspects mentioned above. Traditionally, the very precise in-situ techniques are used to assess soil moisture. But, these approaches are not cost-effective and only cover a limited area [11]. The information obtained from satellites can be used to estimate soil moisture on a large scale [10].

The use of satellites opened a new era of soil moisture measurement techniques, which make use of the reflectance at the soil surface depending on the moisture. Visible, microwave and infrared rays are employed in soil moisture retrieval systems using satellite data [11]. For the purpose of ensuring food security and tracking crop growth and yields, effective estimation of soil moisture requires both spatial and temporal resolution. Vegetation is another significant factor affecting soil moisture since it can draw moisture out of the soil [12]. The reflectance property of the soil is used to calculate soil moisture, but this is insufficient because soil irradiance fluctuates with time and is dependent on meteorological conditions [21, 28]. By taking into account the information from two or more spectral bands and merging

21. Enhancing Educational Experiences: A Personalized Course Recommendation System Employing Machine Learning Algorithms

Kshitij Mahurpwar

Department of Information Technology,

Shri Sant Gajanan Maharaj College of Engineering, Shegaon. (M.S.)

Tushar Nimbolkar

Department of Information Technology,

Shri Sant Gajanan Maharaj College of Engineering, Shegaon. (M.S.)

Aryan Shah

Department of Information Technology,

Shri Sant Gajanan Maharaj College of Engineering, Shegaon. (M.S.)

Faizan Raza

Department of Information Technology,

Shri Sant Gajanan Maharaj College of Engineering, Shegaon. (M.S.)

A. S. Manekar

Department of Information Technology,

Shri Sant Gajanan Maharaj College of Engineering, Shegaon. (M.S.)

Abstract

Assisting students in selecting suitable college courses presents a formidable challenge, given the myriad of options available and the distinct policies and instructional methods adopted by each university. The study presents OPCR, a state-of-the-art instrument designed to assist pupils. By basing course recommendations on a variety of criteria, this approach ensures that each student's needs are satisfied. It considers things like the course material and the interests of the pupils. Additionally, at the conclusion of each course, it employs a cutting-edge method known as ontology mapping to recommend potential career paths to students. According to test results, OPCR outperforms other approaches in course suggestion because it makes a more intelligent connection between students and courses and considers a wider range of attributes.

Keywords: Personalized learning, Course recommendation, Content-based classification, CRS application, Course recommendation process.

Introduction

Lastly, for optional course recommendation systems at universities, we present a novel technique called Cross-User-Domain Collaborative Filtering (CUDCF). In order to reliably

Original Article

Exploring an Immersive AR/VR Pedagogical Approach: Experiential Learning for Autism Spectrum Disorder (ASD) Education

Amitkumar Manekar[1], Vedant Gade[2], Rutuja Unhale[3], Harshit Manker[4], Riya Dhole[5]

[1,2,3,4,5]*Department of Information Technology, Shri Sant Gajanan Maharaj College of Engineering, Shegaon, M.S, India.*

[1]*Corresponding Author : asmanekar24@gmail.com*

Abstract - There is a rising incidence of Autism Spectrum Disorder (ASD), posing significant challenges for the educational system in adequately catering to the needs of students with autism. It is estimated that approximately 1% of the global population, equivalent to 75 million people worldwide, are diagnosed with ASD. This translates to roughly 1 in every 100 children being affected by autism. Research suggests that a combination of genetic and environmental factors contributes to the development of autism in children. While there is growing awareness surrounding ASD in certain regions, there remains a pressing need for ongoing advancements in autism education. The objective of this research project is to explore how a novel pedagogical technique may be used to address the particular difficulties faced by students with ASD in classroom environments. One potential tactic is experiential learning, which stresses interactive, hands-on activities that immerse students in real-world situations to improve knowledge and skill development. The present study analyzes the impact of developing an autistic learning center on learning methods, student engagement, and academic outcomes among ASD learners through an extensive analysis that makes use of both qualitative and quantitative approaches. The results highlight the critical role that the autism learning hub plays in promoting social engagement, inclusion, and better learning outcomes for people with autism in regular classroom settings. This study adds insightful information to the growing corpus of research on inclusive education by providing insightful information on practical methods for assisting children with ASD in a variety of educational environments.

Keywords - Autism Spectrum Disorder, Immersive learning, effective learning, Inclusive environment, Education, Pedagogical approach, Experiential learning.

1. Introduction

Autism Spectrum Disorder (ASD) is a complex developmental condition characterized by difficulties in social interaction. People with ASD often require specialized support and accommodations to meet their unique learning needs within educational settings. In today's educational landscape, fostering a sense of belonging and full participation for all individuals, including those with ASD, is paramount. Increased awareness of ASD has led to a growing emphasis on creating inclusive learning environments that cater to the diverse needs of students, including those with ASD [1]. Experiential learning has emerged as an innovative approach to promote inclusivity in education, particularly for individuals with ASD. This study aims to investigate the potential of experiential learning as a novel pedagogical approach for ASD education, with a specific focus on fostering an inclusive learning environment.

Through a comprehensive review of existing literature, case studies, and empirical evidence, our goal is to gain insight into how experiential learning can cater to the distinctive learning styles and preferences of individuals diagnosed with Autism Spectrum Disorder (ASD) while fostering a sense of inclusivity and acceptance within the education system. In addition to exploring the fundamental principles and practical applications of experiential learning, this study will delve into strategies for creating an inclusive environment that caters to the sensory, communication, and socio-emotional requirements of learners with ASD [2]. In pursuit of this objective, the concept of an autism learning hub has emerged as a promising approach to providing targeted support and resources for individuals with ASD within educational institutions. Essentially, an autism learning hub acts as a centralized platform offering a variety of tools, materials, and programs tailored specifically to address the learning and developmental needs of individuals on the autism spectrum.

A variety of elements are usually included in the autistic learning center, including interactive educational games, speech recognition technologies for Natural Language

International Journal of Research Publication and Reviews

Bespoke Academic Guidance: Machine Learning for Course Recommendations

Dr. A. S. Manekar[1], Tushar K. Nimbolkar[2], Kshitij Mahurpwar[3], Mohd. Faizan Raza[4], Aryan Shah[5]

[1]Head Of Department, Department of Information Technology, Shri Sant Gajanan Maharaj College of Engineering, Shegaon. (M.S.), Shegaon, Maharashtra, India

[2,3,4,5]Student, Department of Information Technology, Shri Sant Gajanan Maharaj College of Engineering, Shegaon. (M.S.), Shegaon, Maharashtra, India

DOI: https://doi.org/10.55248/gengpi.5.0524.1467

ABSTRACT

Assisting students in selecting suitable college courses presents a formidable challenge, given the myriad of options available and the distinct policies and instructional methods adopted by each university. The study presents OPCR, a state-of-the-art instrument designed to assist pupils. By basing course recommendations on a variety of criteria, this approach ensures that each student's needs are satisfied. It considers things like the course material and the interests of the pupils. Additionally, at the conclusion of each course, it employs a cutting-edge method known as ontology mapping to recommend potential career paths to students. According to test results, OPCR outperforms other approaches in course suggestion because it makes a more intelligent connection between students and courses and considers a wider range of attributes. Keywords: Personalized learning, Course recommendation, Content-based classification, CRS application, Course recommendation process.

Keywords: Personalized learning, Course recommendation, Content-based classification, CRS application, Course recommendation process.

1. INTRODUCTION

Finally, we introduce a new method for optional course recommendation systems at universities: Cross-User-Domain Collaborative Filtering (CUDCF). Our method uses the course score distribution of like senior students to estimate results for optional courses with high accuracy and speed: promptly generated suggestions. Multiple tests demonstrate that the system performs exceptionally well in providing significantly lower dropout rates and has a high hit rate and accuracy. Further investigation could reveal other applications for CUDCF in a variety of recommendation systems, which would stimulate the development of more cross-user-domain collaborative filtering algorithms.

2. METHODOLOGY

This essay proposes a framework for structuring course proposals. A course recommendation system is a tool designed to assist students in identifying suitable courses based on their skills and foundational knowledge. The process involves using rule-based classification to predict courses, termed content-based categorization. The effectiveness of this strategy is evaluated using a group of college students who need to select electives before their third year begins. Often, students struggle to assess their aptitude or the difficulty of a subject, leading to potentially poor choices. To address this, a methodological approach considers students' prior performance and elective selections to recommend courses efficiently and accurately. Students are then guided to a CRS application where they provide details like email and roll number and select three electives from a dropdown menu. Electives are categorized into four groups: conceptual, programming, logical, and theoretical. For instance, courses like Operating Systems, C, C++, Data Structures, and Python fall under programming; while Discrete Mathematics, Digital Logic Design, and others are categorized as logical courses. Courses such as Professional Ethics, English, and Soft Skills fall under theoretical subjects. Electives like Distributed Operating Systems (DOS) and Software Testing and Automation (STA) are assigned based on students' performance in related subjects. If a student has excelled in programming subjects, they are assigned programming electives like DOS. This approach aims to assist students in making informed choices about their electives, ensuring a smoother academic journey [8][9].

3. MODELING AND ANALYSIS

We are progressing to the analysis phase of our research, focusing on creating a course recommendation system enhanced by sentiment analysis. This involves identifying key components, requirements, challenges, and opportunities in integrating sentiment analysis into the recommendation process. Online learning platforms have made education more accessible, allowing learners to pursue their goals from home. However, the abundance of courses can be overwhelming, making it hard to find the best ones. Intelligent recommendation systems have emerged to provide personalized guidance and

International Journal of Research Publication and Reviews

Improving Autism Education: An Innovative Immersion AR/VR Pedagogical Method Using Experiential Learning

Riya Dhole[1],Vedant Gade[2] , Rutuja Unhale[3], Harshit Manker[4] , Amit Manekar[5]

[1,2,3,4,5] Department of Information Technology, Shri Sant Gajanan Maharaj college of
Engineering
*Corresponding author e-mail: vedantgade000@gmail.com

ABSTRACT :

The prevalence of Autism Spectrum Disorder is increasing, which poses difficulties for the educational system in providing enough support for autistic pupils. Around 75 million people worldwide, or 1% of the total population, suffer from autism spectrum disorder. Approximately 1 child in every 100 has autism.Current research suggests that a child's risk of developing autism is influenced by both environmental and genetic variables.Even if there is a growing body of knowledge in certain areas, the profession of teaching autistic individuals still requires ongoing growth. This study looks at how creative pedagogical approaches might be used to help people with ASD overcome obstacles in the classroom. Interactive activities that captivate students in real-world situations are given priority in experiential learning comprehend it more fully or more fully and support the development of new skills. This study investigates the effects of the autism learning hub's deployment on pedagogical practices, student engagement, and academic outcomes for students with ASD using a combination of qualitative and quantitative approaches. The results demonstrate the important role that the autism learning hub plays in encouraging social engagement, inclusion, and improved learning outcomes for people with autism in educational settings. This study adds to the growing body of research on inclusive education and provides insight into practical approaches for assisting kids with ASD in regular classroom settings.

Keywords: Autism Spectrum Disorder, immersive learning, effective learning,inclusive environment,Education, pedagogical approach, experiential learning.

1.0 INTRODUCTION:

A severe neurological condition known as autism spectrum disorder (ASD) causes a person to struggle with social interaction. People with ASD frequently have particular learning demands that necessitate specialist assistance and modifications in educational environments.Currently, it is critical to ensure that all individuals, including those with autism spectrum disorder (ASD), have a sense of belonging and are able to actively engage in the educational process [1]. The creation of inclusive learning settings that meet the different needs of all students, including those with ASD, has come under growing focus as awareness of ASD has grown in recent years.Experiential learning is one such cutting-edge strategy that shows promise in fostering an inclusive learning environment for students with ASD.This project aims to investigate the possibilities of hands-on learning as a cutting-edge pedagogical strategy for teaching ASD, with an emphasis on building an inclusive classroom atmosphere [2].

We seek to understand how experiential learning can meet the distinct learning profiles and preferences of people with ASD while fostering a sense of inclusion and welcome in the educational system by carefully analyzing the body of existing literature, case studies, and practical findings.This research will look at the fundamental theories and real-world applications of experiential learning as well as strategies for building inclusive learning environments that meet the sensory, communicative, and social-emotional needs of students with ASD.In keeping with this goal, the idea of an autistic learning hub has surfaced as a motivating way to provide particular support and resources for people with ASD inside the school system [3] [11]. A centralized platform that provides a variety of resources, materials, and programs especially created to treat autism is known as an autism learning hub.

Natural language processing (NLP) voice recognition technologies, augmented reality/virtual reality (AR/VR) simulations, and interactive educational games are just a few of the components that are typically found in an autistic learning hub. These characteristics are intended to support the development of skills in areas including academic performance, sociability, and communication, as well as to actively engage learners with ASD in engaging and interactive learning experiences [4]. The goal of the autistic learning center is to establish a welcoming and encouraging learning environment where people with ASD can flourish intellectually and socially by utilizing cutting-edge technologies and evidence-based methods. Additionally, the establishment of an autistic learning hub may enhance teachers' capacity to meet the many requirements of children with ASD and promote their engagement and success in conventional classroom settings [5][6]. In order to support inclusive learning environments in the educational system, this work examines the effects of establishing an autism learning center as part of an innovative pedagogical method. We assess how well

International Journal of Research Publication and Reviews

Journal homepage: www.ijrpr.com ISSN 2582-7421

"Agile Database Maintenance: ChatGPT-Enabled EOL Data Verification and Updates"

Gauri Borle[1], Juee Gore[2], Riya Dangra[3], Amit Manekar[4]

[1, 2, 3, 4] Department of Information Technology, Shri Sant Gajanan Maharaj college of Engineering
gauriborle1002@gmail.com[1] , gorejuee08@gmail.com[2] , riyadangra1418@gmail.com[3], asmanekar24@gmail.com[4]

ABSTRACT

End-of-Life (EOL) date validation and updating in databases is a labor-intensive and error-prone activity that ChatGPT technology hopes to alleviate from industrial product lifecycle management. The objective is to increase data reliability, decrease human labor, and automate verification procedures by utilizing OpenAI's GPT-3 model with Python and the OpenAI API. Through the use of strategic prompts and real-time feedback mechanisms, the AI model's skills are improved to the point where the system is able to handle dynamic EOL dates, broken URLs, and safe authentication procedures. By optimizing accuracy, efficiency, and reliability while reducing the negative effects of manual intervention, ChatGPT's language processing capabilities integrated into the product lifecycle management framework provide a comprehensive solution for effective decision-making and asset management, which will ultimately revolutionize EOL database management practices.

Keywords: Web Scraping techniques, End-of-life management, ChatGPT technology, Prompt Engineering, EoL device security.

INTRODUCTION

Industrial product lifecycle management faces issues in keeping accurate End-of-Life (EOL) databases in the fast-paced technology landscape of today. By automating validation procedures and decreasing manual errors, integrating cutting-edge technology like ChatGPT provides revolutionary solutions. This study looks at how ChatGPT can be integrated with EOL database administration, how to handle vulnerabilities in EOL devices, how to manage EOL information, and what prompt engineering is all about. Organizations may increase data dependability, expedite verification procedures, and boost asset management decision-making by utilizing ChatGPT's capabilities. This study presents a novel data-driven and intelligence-driven method to EOL management through thorough investigation.

1.1 WEB SCRAPING: Although web scraping effectively collects EOL data from several sources, issues with data integrity still exist. By automating verification procedures, ChatGPT integration lowers human labor costs and improves operational effectiveness.

1.2 EOL Dates: Many devices that are designated as EOL nevertheless function, posing a danger to cybersecurity. By integrating ChatGPT, issues like shifting EOL dates and faulty URLs are resolved by automated verification and updating.

1.3 LLM Models: ChatGPT is excellent in dialogue exchanges, providing tailored advice and analysis. Models such as Davinci and Turbo demonstrate the adaptability of AI in a range of scenarios, indicating a better user-friendly experience.

1.4 PROMPT ENGINEERING: Optimizing LLM efficacy requires prompt engineering. This document provides a collection of prompt patterns that may be used repeatedly to address typical conversational problems with LLMs.

1.5 API WRAPPER TECHNOLOGY IN MDM INTEGRATION- API wrapper technology streamlines EOL data updates by combining OpenAI API with ChatGPT and Python. Rigorous testing validates the system's efficiency, positioning it as a valuable asset for enhancing user experiences.

LITERATURE SURVEY

The literature review that is offered covers a wide variety of subjects related to technology and information management. Voice-based authentication systems, online scraping methods, ChatGPT technology, rapid engineering, API wrapper technology, industrial asset management, electronic components obsolescence, and end-of-life (EoL) device security are some of these issues. Every abstract offers a different viewpoint on the difficulties, developments, and uses in its field.[1] Voice-based authentication solutions are a huge advancement, especially for people with vision impairments. These systems employ machine learning to generate distinct voice prints for user verification by analyzing speech patterns. Future

7. Enhancing Database Maintenance: Leveraging ChatGPT for Real-Time Verification and Updates of End-of-Life (EOL) Data

Gauri Borle
Department of Information Technology, Shri Sant Gajanan Maharaj College of Engineering.
Juee Gore
Department of Information Technology, Shri Sant Gajanan Maharaj College of Engineering.
Riya Dangra
Department of Information Technology, Shri Sant Gajanan Maharaj College of Engineering.
Amit Manekar
Department of Information Technology, Shri Sant Gajanan Maharaj College of Engineering.

Abstract

The integration of ChatGPT technology into industrial product lifecycle management aims to tackle the labor-intensive and error-prone tasks related to validating and updating End-of-Life (EOL) dates in databases. Leveraging OpenAI's GPT-3 model through Python and the OpenAI API, the aim is to automate verification processes, reduce manual efforts, and enhance data reliability. By refining the AI model's capabilities through strategic prompts and real-time feedback mechanisms, the system can effectively manage fluctuating EOL dates, broken URLs, and secure authentication processes. The integration of ChatGPT's language processing capabilities offers a comprehensive solution for efficient decision-making and asset management within the product lifecycle management framework, ultimately revolutionizing EOL database management practices by optimizing accuracy, efficiency, and reliability while mitigating drawbacks associated with manual intervention.

Keywords: Web Scraping techniques, End-of-life management, ChatGPT technology, Prompt Engineering, EoL device security.

Introduction

In today's fast-paced technological landscape, maintaining accurate End-of-Life (EOL) databases poses challenges in industrial product lifecycle management. Integrating advanced technologies like ChatGPT offers transformative solutions by automating validation processes and reducing manual errors. This research explores the integration of ChatGPT into EOL database management, addressing vulnerabilities in EOL devices, methodologies for managing EOL

8. Food Recommendation System Based on Geographical Location - DineLocate

Harshit Dharmik
SSGMCE, Shegaon.
Karan Motwani
SSGMCE, Shegaon.
Khushbu Pareek
SSGMCE, Shegaon.
Shraddha Tikar
SSGMCE, Shegaon.
M. Faizan I. Khandwani
SSGMCE, Shegaon.

Abstract

Using real-time location data, Ratings, and distance prioritizing, DineLocate is a dynamic web-based platform that aims to transform users' restaurant discovery experiences. To receive customized restaurant recommendations based on their tastes and current location, users must register or log in to the platform. DineLocate provides users with a curated list of restaurants in their area, giving priority to recommendations based on ratings and taking into account proximity. It does this by utilizing OpenCage Geocoding APIs for live location tracking and Google reviews. After choosing a restaurant, customers can easily obtain directions to the selected location through an integrated google mapping function. DineLocate proves its effectiveness in raising user pleasure and encouraging exploration of a variety of options through rigorous development and evaluation.

Keywords: Geolocation, Recommender system, Personalized dining experiences, User preferences, Review-based prioritization

1. Introduction

1.1 Background and Motivation

Eating out has become an integral part of peoples' life in the fast-paced world of today. It might be difficult for customers to choose where to eat because there are so many restaurant selections available to them. The decision-making process is further complicated by parameters like geographic location and personal preferences. Intelligent systems that can offer individualized restaurant recommendations based on user preferences and real-time location data are becoming

11. A Survey of Student Education Platform

Sanket Gode

Shri Sant Gajanan Maharaj College of Engineering, Shegaon.

Prajwal Gawande

Shri Sant Gajanan Maharaj College of Engineering, Shegaon.

Vaishnavi Dabhade

Shri Sant Gajanan Maharaj College of Engineering, Shegaon.

Saurabh Wankhade

Shri Sant Gajanan Maharaj College of Engineering, Shegaon.

M. Faizan I. Khandwani

Shri Sant Gajanan Maharaj College of Engineering, Shegaon.

Abstract

This survey article explores the constantly changing field of student education platforms, emphasizing the revolutionary potential of cloud technology in particular. We compare and contrast three well-known platforms now in use: Coursera, edX, and Khan Academy. We look at their features, approaches, and technological foundations. We next present the "Student Education Platform," carefully analyzing its special attributes, creative design, and safety protocols. Through a comparison of various systems, we hope to shed light on the way forward for personalized, secure, and scalable educational technology in the future.

Keywords: student education platforms cloud technology Coursera edX Khan Academy technological foundations creative design safety protocols secure scalable.

1. Introduction

The rise of innovative educational platforms is driving a significant digital transformation in the education sector. These platforms, which prioritize the needs of each individual student and are flexible and accessible, provide a paradigm shift in the way that learning experiences are delivered. This change has been largely attributed to cloud technologies, which have completely changed how platforms are developed, implemented, and maintained. Educational platforms can attain unparalleled scalability, security, and cost-effectiveness by utilizing cloud infrastructure, which will ultimately empower teachers and enhance student's educational experiences.

A Survey of Various Recommendation Systems

Mr. Harshit Dharmik[1], Mr. Karan Motwani[2], Ms. Khushbu Pareek[3],
Ms. Shraddha Tikar[4], Mr. Faizan Khandwani[5]

Students, Department of Information Technology[1,2,3,4]
Assistant Professor, Department of Information Technology[5]
Shri Sant Gajanan Maharaj College of Engineering, Shegaon, India

Abstract: *Geolocation-based recommender systems have gained significant traction in recent years due to their ability to provide personalized recommendations tailored to users' geographical locations [1]. This survey paper explores the landscape of food recommendation systems with a specific focus on geographical aspects. It examines existing frameworks, solutions, and challenges in the field, highlighting key research contributions and methodologies [2]. By incorporating spatial context into the recommendation process, these systems can identify nearby food establishments, consider regional culinary preferences, and recommend dishes that are popular or highly rated in the vicinity [1]. The paper also discusses the potential of location-aware recommendation systems and proposes a novel approach for food recommendation based on geographical location [3]. Various methodologies employed in geolocation-based food recommendation systems, including collaborative filtering, content-based filtering, and hybrid approaches, are explored, along with their advantages and limitations [5]. Challenges associated with developing geolocation-based recommendation systems, such as data privacy concerns and data sparsity in certain regions, are also addressed [4]. The proposed approach aims to provide more accurate and personalized recommendations by integrating geolocation data with user preferences and contextual information, thereby enriching the overall dining experience for users worldwide [3].*

Keywords: Geolocation, Recommendation, Cuisine, Personalization, Preferences

I. INTRODUCTION

In recent years, the advent of location-based services and the ubiquity of mobile devices have revolutionized the way we interact with information and services. One area profoundly impacted by this paradigm shift is the domain of recommendation systems, where traditional approaches are increasingly augmented with geospatial data to provide context-aware suggestions tailored to users' geographical locations. Geolocation-based recommender systems have emerged as a promising avenue for delivering personalized recommendations that factor in users' current surroundings and preferences.

According to Nikita Pandey, Satvik Tandon, and Princi Jain (2021), geolocation-based recommender systems leverage users' geographical locations to enhance the relevance of recommendations. By incorporating location data into the recommendation process, these systems can identify nearby points of interest and offer recommendations that are not only personalized but also contextually relevant [1]. This integration of geographical information enables recommendation systems to account for factors such as local culture, cuisine preferences, and business availability, thereby enhancing the overall user experience.

As highlighted by Weiqing Min, Shuqiang Jiang, and Ramesh Jain (2019), traditional recommendation techniques often overlook the influence of geographical location on user preferences, leading to generic suggestions that may not resonate with users' local tastes [2]. Geolocation-based approaches address this limitation by considering the spatial context of users and tailoring recommendations accordingly. This shift towards context-aware recommendation systems represents a significant advancement in the field, offering new opportunities to deliver more personalized and impactful recommendations.

In light of these developments, this survey paper aims to explore the landscape of food recommendation systems with a focus on geographical aspects. By examining existing frameworks, solutions, and challenges in the field, we seek to elucidate the potential of geolocation-based recommendation systems to revolutionize the way we discover and

Analysis of Fruit Identification and Nutritional Assessment

Dr. Sagar D Padiya[1], Mr Saurabh S Yengade[2], Ms Riya R Chikankar[3], Ms Payal G Chavhan [4],

Mr. Prashant G Dandage[5]

Assistant Professor, Department of Information Technology, Shri Sant Gajanan Maharaj College of Engineering, Shegaon, Maharashtra, India[1]

Student, Department of Information Technology, Shri Sant Gajanan Maharaj College of Engineering Shegaon, Maharashtra, India[2 3 4 5]

ABSTRACT: This research paper presents a thorough examination of fruit identification techniques and nutritional assessment methods, amalgamating traditional and modern approaches. Through a comprehensive analysis, we explore the efficacy of various identification methods, ranging from visual inspection to cutting-edge technologies like machine learning and image recognition. Simultaneously, we conduct an in-depth nutritional assessment of diverse fruits, scrutinizing their content of essential vitamins, minerals, and antioxidants. The amalgamation of these two aspects aims to provide a holistic understanding of the fruits we consume. The results not only contribute to the advancement of food science but also offer practical insights for individuals aiming to make informed dietary choices for a healthier lifestyle. The interdisciplinary nature of this study bridges the gap between technology and nutrition, fostering a comprehensive perspective on fruit identification and its nutritional implications.

KEYWORDS: Image recognition, Nutritional assessment, Fruit identification, Lifestyle choices.

I. INTRODUCTION

In a world where dietary choices play a pivotal role in shaping our health, the identification and nutritional assessment of fruits stand at the forefront of scientific inquiry. This research endeavors to unravel the complexities of fruit characterization and nutritional profiling, utilizing an integrative approach that marries traditional methodologies with cutting-edge technologies. As we embark on this journey, the significance of accurate fruit identification cannot be overstated. From the local markets to global supply chains, the need for precise and efficient methods has never been more critical. We delve into the nuances of visual inspection, explore the reliability of traditional techniques, and push the boundaries by incorporating state-of-the-art technologies such as machine learning and image recognition. By scrutinizing the efficacy of these diverse identification methods, we seek to provide a comprehensive understanding of the tools at our disposal in unraveling the intricate world of fruits.

Simultaneously, our focus extends beyond mere identification, delving into the nutritional composition of these natural wonders. Fruits, beyond their delightful flavors and vibrant colors, are reservoirs of essential nutrients that contribute to our overall well-being. In this research, we meticulously assess the nutritional content of a spectrum of fruits, examining their concentrations of vital vitamins, minerals, and antioxidants. This exploration goes beyond a superficial glance at nutritional labels; rather, it aims to uncover the inherent health benefits encapsulated within the diverse array of fruits that grace our tables. Our journey into the realm of nutritional assessment is driven by the belief that an informed understanding of the nutritional profiles of fruits empowers individuals to make healthier dietary choices and cultivate lifestyles conducive to long-term well-being.

This interdisciplinary investigation not only bridges the realms of technology and nutrition but also endeavors to provide practical insights for individuals navigating the complex landscape of food choices. As we traverse the interface between science and sustenance, the fruits of our labor promise to yield not only a deeper comprehension of the foods we consume but also valuable knowledge that resonates in both scientific and everyday contexts.

ANDROID APPLICATION FOR ACTIVITY BASED NUTRITIONAL NEEDS

Anushka Narkhede[1], Mandar Nashikkar[2], Sanjana Daberao[3], Rohan Gaykwad[4],

Mrs. P. P. Bute[5]

[1,2,3,4,5]Department of Information Technology, Shri Sant Gajanan Maharaj College of Engineering, India.

ABSTRACT

Maintaining a healthy lifestyle is a popular goal but can be challenging to accomplish in today's fast-paced environment. In order to solve this, a new application has been created that makes it easier to get a customized diet plan based on variables like height, weight, gender, and BMI. This software incorporates an advanced algorithm that can create a personalized nutrition plan that guarantees a balanced diet—essential for both illness prevention and optimum bodily performance. A balanced diet, which is made up of foods high in vital nutrients and low in unneeded fats and sweets, gives the body the building blocks it needs to operate effectively. Children's growth, development, and academic achievement are all impacted by proper nutrition, which also lays the groundwork for lifelong healthy eating habits. Because of the application's user-friendly layout, creating and managing accounts is a breeze for users. Users can obtain their customized diet plan with only one click. A professional dietician consultation option is available on the app for users with particular dietary restrictions or allergies. The app also has an educational component where users can look up fascinating nutrition and health-related topics.

By using this software, users can meet their health objectives without physically seeing a dietician, which saves time and increases accessibility to healthy eating. This cutting-edge technology not only encourages a healthy lifestyle but also adjusts to the specific requirements of each user, enabling everyone to achieve personal well-being in the hectic world of today.

Keyword: Personalized Nutrition Diet Plan, Well-Balanced Diet, Dietary Algorithm, Nutrient-Rich Foods, Virtual Dietician, User-Friendly Interface, Nutrition Education, and Health Optimization

1. INTRODUCTION

Diet Expert is an Android app that offers users individualized diet regimens in a manner akin to that of a real-life dietician. Through an accessible technical platform, this digital solution replicates the interactive experience that a person might have with a qualified dietitian, anywhere and at any time.[1]

Making User Profiles: First, personal data that usually affects dietary recommendations must be entered by the user. This includes information about height, weight, gender, and maybe other variables like age, degree of activity, and particular health objectives (such gaining muscle mass, losing weight, or leading a healthy lifestyle). Diet Expert utilizes the user's personal information to determine the user's unique nutritional needs. In order to predict the user's daily calorie demands based on their activity level, it may be necessary to calculate their basal metabolic rate (BMR).

The application then creates a customized diet plan based on the information it has processed, taking into account the user's dietary requirements. This diet plan balances the macronutrients (proteins, fats, and carbs) and micronutrients (vitamins, minerals) required for optimum health in addition to taking the user's goals into account when calculating calorie intake. Users can update their profiles with fresh information (such as weight or activity level changes) as they make progress with their diet plans, which causes Diet Expert to modify its diet plans appropriately. This feature guarantees that the diet plan will always be applicable and efficient. Diet Expert most likely has a simple, intuitive interface that promotes continuous use. To make diet adherence easier, features might include grocery lists, recipe selections, and meal suggestions. Diet Expert may provide a function that allows users to consult with a licensed dietician in the event that they have complex health concerns, allergies, or specific dietary restrictions. This guarantees that everyone using the diet programs may do so in a safe and efficient manner—even in cases where extra considerations are required. Users are required to register on a registration page in order to use the app for the first time. In order to help personalize their experience, this process requires entering basic information like name, email address, and even health-related data. After registering, users can use the app's features by logging in. Users are asked to enter personal information such as their height, weight, gender, and other relevant health data after logging in. Using this information, the app calculates dietary requirements based on the individual needs of each user. These inputs are processed by an advanced algorithm against pre-established parameters to create a personalized food plan that supports the user's health objectives, whether they weight loss, muscle building, or upholding a balanced lifestyle. Users have the choice to accept or reject a suggested diet plan once it is presented. The system can provide alternate plans if the user's expectations or preferences aren't met by the initial plan. This feature makes sure that the user has a plan that they can easily follow and feel comfortable with.

5. A Survey of Android Application for Activity Based Nutritional Needs

Anushka Narkhede
Shri Sant Gajanan Maharaj College of Engineering, Shegaon.
Mandar Nashikkar
Shri Sant Gajanan Maharaj College of Engineering, Shegaon.
Rohan Gaykwad
Shri Sant Gajanan Maharaj College of Engineering, Shegaon.
Sanjana Daberao
Shri Sant Gajanan Maharaj College of Engineering, Shegaon.
Mrs. P. P. Bute
Shri Sant Gajanan Maharaj College of Engineering, Shegaon.

Abstract

It might be difficult to maintain a healthy lifestyle in the fast-paced world of today, despite its popularity. A new application has been developed to address this issue, making it simpler to receive a personalized diet plan based on factors like height, weight, gender, and BMI. This program has a sophisticated algorithm that can generate a customized nutrition plan that ensures a balanced diet, which is necessary for both disease prevention and optimal physical function. A diet rich in essential nutrients and low in unnecessary fats and sugars provides the body with the building blocks it needs to function properly. This is known as a balanced diet. Adequate nutrition affects children's growth, development, and intellectual performance and establishes the foundation for lifelong healthy eating habits. The application's user-friendly architecture makes it simple for users to create and manage accounts. One click is all it takes for users to get their personalized diet plan. For customers with specific dietary needs or allergies, the app offers a professional dietician consulting option. In the app's instructional section, users can research interesting nutrition and health-related subjects. In today's busy world, this state-of-the-art technology not only supports a healthy lifestyle but also adapts to the unique needs of each user, allowing everyone to reach personal well-being.

Keywords: Personalized Nutrition Diet Plan, Well-Balanced Diet, Dietary Algorithm, Nutrient-Rich Foods, Virtual Dietician, User-Friendly Interface, Nutrition Education, and Health Optimization.

A System for Recommending Food Based on User's Health Preferences

Pratik Diwan[1], Yash Dahiwale[2], Deepak Sangale[3], Sumit Muddalkar[4]
Department of Information Technology[1,2,3,4]
Shri Sant Gajanan Maharaj College of Engineering, Shegaon, Maharashtra, India

Abstract: *Making healthy decisions might feel like an uphill fight in a world where there are countless food alternatives and contradicting dietary recommendations. This is particularly true for people dealing with particular health issues, such pregnancy or long-term illnesses, where dietary choices can significantly affect overall health. However, what if there was a method to make the procedure simpler? Imagine having a personal nutritionist always with you, someone who understands your needs intimately and can help you make better decisions with a few smartphone clicks. That's the idea behind our most recent invention, an app meant to completely change the way we think about nutrition. With the use of state-of-the-art technology and the most recent findings in nutritional science, we have developed a tool that gives you access to the power of individualized nutrition. This is how it operates: you begin by providing the app with some personal information, such as your age, height, weight, and any particular health issues you may be aware of. The software uses this data to estimate your daily caloric needs and compute your Body Mass Index (BMI). We don't stop there, though. Based on your individual profile, the app creates a customized list of food suggestions by utilizing a large library of foods and nutritional data.*

Keywords: Personal nutrition, food recommendation, BMI

I. INTRODUCTION

Many people place a high importance on preserving optimal health in the fast-paced world of today. There is no one-size-fits-all approach to obtaining and maintaining excellent health, though. Because every person has different nutritional requirements due to their own health circumstances, tailored advice is crucial for general health. comes into play in this situation, providing a thorough solution that makes use of technology to provide personalized nutrient recommendations. To ensure a smooth experience for all parties, the platform is developed with separate modules for administrators and users. Administrators can log in and submit descriptive descriptions, type, range, and other special dietary requirements.

Additionally, they can address a variety of customer needs by offering general nutrition advice for common health issues like skin and orthopedic problems. The ability to add, edit, and remove nutrition requirements guarantees that the data is current and correct, representing the most recent advancements in the science of nutrition. The procedure starts on the user's end with a straightforward registration, which is followed by system login. Additionally, they can address a variety of customer needs by offering general nutrition advice for common health issues like skin and orthopedic problems. The ability to add, edit, and remove nutrition requirements guarantees that the data is current and correct, representing the most recent advancements in the science of nutrition.

They can also provide basic nutrition recommendations for common health conditions like skin and orthopedic disorders, which can meet a range of customer demands. The flexibility to add, amend, and remove nutrition requirements ensures that the information is accurate and up to date, reflecting the latest developments in the field of nutrition science. The process begins with a simple registration on the user's end, and then the system login. They can also provide basic nutrition recommendations for common health conditions like skin and orthopedic disorders, which can meet a range of customer demands. The flexibility to add, amend, and remove nutrition requirements ensures that the information is accurate and up to date, reflecting the latest developments in the field of nutrition science.

Additionally, accessing a personal profile and conducting targeted nutrition information searches adds even more ease and personalization to the user experience. React JS, a potent and effective JavaScript user interface toolkit, forms the foundation of this cutting-edge platform. The technology selection makes for a smooth and responsive user experience,

Personalized Health-Centric Food Recommendation System

Mr. Atharva Urade[1], Mr. Mohan Bhambere[2], Mr. Prathamesh Mahajan[3]
Mr. Vaibhav Shirbhate[4], Mr. Sumit Muddalkar[5]
Student, Department of Information Technology[1,2,3,4]
Assistant Professor, Department of Information Technology[5]
Shri Sant Gajanan Maharaj College of Engineering, Shegaon, Maharashtra, India

Abstract: *People nowadays suffer from a wide range of acute and chronic conditions. It is challenging to properly prescribe a diet in modern world. When a body does not obtain enough nutrients, it might develop nutritional disorders, which can cause a number of different health issues. Chronic conditions including hypertension, cardiovascular disease, diabetes, and others can be caused on by dietary deficiencies or excesses of particular nutrients as well as eating disorders. Primary root cause of these conditions is typically an inadequate or improper diet. We propose a diet suggestion system in this study that takes the user's physics details and symptoms into account. Machine learning methods (KNN) are used in this study. The system predicts the proposed meal plan for a user by leveraging its training data, which comprises daily calorie requirements and food consumption patterns. According to the evaluation of the dataset, the suggested model outperforms existing diet recommendation systems. Analyzing the user's dietary and nutritional requirements, the suggested system generates a prediction about the meal plan. It could result in a customized food plan for each person and promote better health.*

Keywords: Recommendation System, KNN, Disease, Nutrition

I. INTRODUCTION

Personalized nutritional guidance is more essential than ever in a time when there arean abundance of food options and individuals are becoming more conscious of the role nutrition plays in overall health. There's a gap between dietary advice and the best possible health results because traditional dietary recommendations frequently ignore specific medical conditions. But recent advances in machinelearning (ML) offer a viable way to close this gap by allowing the creation ofintelligent meal recommendation systems that include users' health circumstances.

Our methodology's mainstay is the application of machine learning (ML) algorithms to evaluate enormous volumes of data and derive significant insights into the connection between food decisions and health consequences. We can acquire a comprehensive understanding of the ways in which different foods affect different health metrics by training our model on a variety of datasets that include nutritional information, health problems, and eating habits. Our recommendation system uses this information as its basis to provide individualized food recommendations that take users' unique health requirements into consideration. The machine learning model continuously learns from user feedback and makes improvements to its suggestions based on the foods that are advised, improving the relevance and accuracy of the advice given. In order to optimize the system's ability to encourage healthy eating habits, this dynamic feedback loop makes sure that it continues to adapt to changes in users' food preferences and health conditions.

II. LITERATURE SURVEY

This literature review looks at research and papers that examined in using machine learning algorithms to create diet-related food recommendation systems.

Celestine Iwendi et al. examine into their system's capability to collect data. The goals of this research framework are machine and deep learning methods and how they interact with IoMT data, particularly Long Short-Term Memory, Naive Bayes, Multilayer Perceptron, Gated Recurrent Units, Recurrent Neural Networks, Logistic Regression and 30 individuals' records, including 13 highlights of various illnesses, and more than 1,000 objects have been collected from

18. A Survey of Integration into 3D Printing for Image Processing using AI ML

Abhay Kadu
Shri Sant Gajanan Maharaj College of Engineering, Shegaon.
Pranav Kaware
Shri Sant Gajanan Maharaj College of Engineering, Shegaon.
Rushikesh Kaldate
Shri Sant Gajanan Maharaj College of Engineering, Shegaon.
Ayush Solav
Shri Sant Gajanan Maharaj College of Engineering, Shegaon.
Mrs. S. N. Khandare
Shri Sant Gajanan Maharaj College of Engineering, Shegaon.

Abstract

In order to overcome the difficulties associated with physical measuring for prosthetic development, the goal of this research project is to design a measuring Module for Prosthetic Hand Dimensions. The module gives users choices to obtain exact finger dimensions through two main methods: image-based input and distance measurement. The study compares different distance measurement methods employing cameras and image processing algorithms in terms of effectiveness, accuracy, and usability. For tasks like contour analysis, hand tracking, landmark identification, edge detection, and so on, open-source libraries like Mediapipe, TensorFlow, and OpenCV are used. By providing insights into efficient dimensioning techniques, the programme seeks to advance the prosthetics profession by improving the design and customisation of prosthetic hands.And overall brief study about Existing technologies include depth sensors, proximity sensors, and 3D scanning technology.

Keywords: Image processing, Prosthetic development, OpenCV, TensorFlow, Mediapipe, NumPy, Precision dimension measurement, Tkinter, depth sensors, proximity sensors, and 3D scanning technology.

1. Introduction

In order to overcome the difficulties associated with physical measuring for prosthetic development, the goal of this research project is to design a measuring Module for Prosthetic Hand Dimensions. The study compares different distance measurement methods employing cameras and

Body Part Implant Dashboard for Real-Time Monitoring and Reporting

Riddhi Gadewar[1], Pranjal Patil[2], Sakshi Dhakade[3], Gaurinandan Joshi[4], S. N. Khandare[5]
Department of Information Technology[1,2,3,4,5]
Shri Sant Gajanan Maharaj College of Engineering, Shegaon, Maharashtra, India
riddhigadewar5@gmail.com, pranjalpatil424@gmail.com, dhakadesakshi2001@gmail.com,
gaurinandanjoshi14@gmail.com, snkhandare26@gmail.com

Abstract*: Our innovative platform is revolutionizing the field of medical implants, harnessing the power of 3D printing to deliver unparalleled levels of customization, accuracy, and accessibility. It functions as an all-in-one online ecosystem that simplifies the process of obtaining custom 3D-printed implants for patients and healthcare providers. At its core, the platform features a user-friendly interface, allowing users to explore a diverse selection of medical implants tailored to individual needs, including orthopedic devices and dental prosthetics. The ordering process is straightforward—users can select implant specifications, upload medical data, and place orders through a secure payment gateway for safe transactions. The platform's integrated tracking system provides real-time updates, allowing users to monitor the progress of their orders from production to delivery. Healthcare professionals' benefit from a dedicated portal where they can submit custom designs, track orders, and communicate with experts. The platform also offers comprehensive customer support and post-implantation care resources to ensure a seamless experience. By embracing 3D printing technology, our platform is transforming healthcare delivery, paving the way for personalized medicine, and reshaping the future of medical implants. Join us in this journey towards a more accessible and patient-focused healthcare system.*

Keywords: 3D printing, medical implants, customization, secure transactions, healthcare providers, order tracking

I. INTRODUCTION

The framework underpinning our project embodies essential principles of componentization and component-based architecture, crucial for constructing adaptable and scalable user interfaces. Through the breakdown of the user interface into reusable components, the framework fosters a modular approach, enabling the seamless composition of intricate user interfaces from simpler building blocks. Moreover, it harnesses contemporary web technologies like HTML, CSS, and JavaScript to deliver an immersive and dynamic user experience.

Demonstrating its applicability in large-scale platforms, the framework showcases its efficiency and scalability, pivotal for navigating the complexities inherent in extensive projects. By embracing this framework, development teams gain a robust tool to effectively manage the intricacies of large-scale endeavors, ensuring smooth integration across diverse systems. The modular design of the framework further facilitates collaborative development efforts, empowering teams to concurrently address various components of the project.

In summary, the adoption of the flat front-end framework presents a compelling solution to contemporary software development challenges. Its focus on modularity, scalability, and efficiency renders it particularly adept for addressing the demands of complex integration projects. As organizations increasingly embrace microservice architectures, frameworks of this nature will undoubtedly assume a central role in fostering innovation and streamlining development workflows within the industry.

II. LITERARURE REVIEW

The development of a user-friendly web platform for patients to register for 3D-printed medical implants represents a significant advancement in the field of medical technology. To ensure the success of this project, it is essential to

Integration into 3D Printing for Image Processing using AI ML

Mrs S. N. Khandare[1], Mr Abhay Kadu[2], Mr Pranav Kaware[3],
Mr Rushikesh Kaldate[4], Mr Ayush Solav[5]
Assistant Professor, Department of Information Technology[1]
Student, Department of Information Technology[2,3,4,5]
Shri Sant Gajanan Maharaj College of Engineering Shegaon, Maharashtra, India

Abstract*: The challenges of physical measurement for prosthetic development and highlight how our integrated tool offers a remote solution to address these challenges, promoting accessibility, convenience, and active participation in the prosthetic design process. Our Measurement Module for Prosthetic Hand Dimensions is a comparison of Image Processing and Distance Measurement Methods The creation of a module to precisely measure finger dimensions for the creation of prosthetic hands is the main goal of this research project. The module provides distance measurement and image-based input as two different ways to get dimensions. Users place their hands at predetermined distances from a screen in the distance measurement option, while users submit photographs of their hands with reference objects for scale in the image based input option. In order To provide a proper fit and functionality, the collected dimensions are an essential component of the prosthetic hand construction process. The study contrasts the efficiency of distance measurement methods employing cameras or other cameras with image processing techniques like edge recognition and contour analysis. Accuracy, usability, and efficiency are among the factors that are assessed to identify the best method for acquiring dimensions. OpenCV for image processing, TensorFlow for machine learning-based analysis, Tkinter for UI design, Mediapipe for landmark identification and hand tracking, and NumPy for numerical operations are just a few of the open-source libraries that are used in this module. The module's possible influence on improving the creation and customization of prosthetic hands is also covered. By offering insights into effective and precise dimension measurement methodologies for customized prosthetic hand design, the study's findings advance the area of prosthetics.*

Keywords: Image processing, Prosthetic development, OpenCV, TensorFlow, Mediapipe, NumPy, Precision dimension measurement, Tkinter

I. INTRODUCTION

There are several obstacles in the way of designing prosthetic hands that properly suit the special requirements of people with limb variations, especially when it comes to measuring fingers accurately. These metrics have a direct impact on the quality of life of users by guaranteeing that prosthetic devices fit, work, and are comfortable. However, the use of specialised equipment and accessibility issues are just two of the drawbacks associated with traditional physical assessment techniques.[1] Our research project offers a novel solution to these problems in the form of the "Measurement Module for Prosthetic Hand Dimensions." This module offers a comprehensive tool for the precise and remote measurement of finger measurements by integrating cutting-edge technology in image processing, hand tracking, and user interface design. Our project consists of multiple major parts and uses open-source libraries and state-of-the-art technology to accomplish its goals. In the first stage, we carry out a comprehensive requirement analysis, working together with prosthetists and people who have different limbs to comprehend their unique requirements and design preferences. Our measurement module is developed using a variety of libraries and frameworks that we have carefully chosen and integrated. Notable examples of this include Mediapipe, which offers sophisticated hand tracking algorithms for real-time landmark localization and identification, and OpenCV, which is used for image processing tasks like hand recognition and feature extraction. Tkinter is selected for UI design to offer a user-friendly interface with straightforward controls and visualisation of measurement data, while TensorFlow is used for machine learning-based

VidMagic: Prompt to Image Clips

Ms. Nayana Ghuikar[1], Mr. Tejas Moon[2], Mr. Prasad Bhagat[3],
Mr. Sushant Chafale[4], Mr. Gaurav Sabe[5]

Assistant Professor, Department of Information Technology[1]
Student, Department of Information Technology[2,3,4,5]
Shri Sant Gajanan Maharaj College of Engineering Shegaon, Maharashtra, India

Abstract: *Prompt to image clips is a modern innovation that uses artificial intelligence to make videos from composed descriptions. This think about looks at the most recent strategies in this range. It talks around how analysts are working with the information and what sorts of computer programs they are utilizing. It moreover looks at how they check if the recordings are any great. The paper too talks around the issues with this innovation and what we still require to figure out. In general, these instruments have a part of potential for making recordings, making substance, and making a difference with education.*

Keywords: artificial intelligence, deep learning, natural language processing, AI projection to picture synthesis, and AI projection to image clips conversion

I. INTRODUCTION

Over time, methods for natural language processing (NLP) and deep learning have advanced quickly, and as a result, artificial intelligence (AI) projection-to image clips generators have become a sophisticated tool that enable the extraction of images and audio from literary representations. In order to create a comparison of high-quality images or recordings, these artificial intelligence generators examine the printed material using sophisticated and intricate techniques including attention-based Repetitive Neural Organize [1], Generative Ill-disposed Organize [2], and transformers [3][4].

The necessity to computerize the process of producing content in order to speed up the generation of various types of content in a responsible and cautious manner is what motivated the development of AI Prompt to image clips generators. These concepts may find use in a variety of contexts, including exhibition, education, and the production of engaging content. For example, item plans, catalogs, and client guides can be created using AI Prompt to image generators [5]. AI Prompt to image clips generators may be used in teaching to create activities and recordings of instructions that enhance the entire educational process [6]. AI powered picture generators and AI Prompt to image clips generators may be used in the entertainment sector to create puzzles, motion picture special recordings, and more [7]. These generators often aim to advance the customer interaction and increase client engagement. Nevertheless, despite AI Prompt to image clips generators' rapid improvement, there remain several limitations and difficulties. The need for a larger, higher-quality preparation dataset is the main obstacle. Obtaining and tagging a large dataset for preparation might be difficult. Another difficulty is that the produced visual material must be interpreted, It makes it challenging to comprehend the logic behind it. Furthermore, there's a chance that these frameworks won't always match the desired message or vision, which could lead to mistakes and inconsistencies in the final product. Another challenge is the trade-off between preparation time and visual quality. Since creating high-quality photographs and films may be fairly expensive and computationally demanding, it can be difficult to produce significant amounts of content quickly. Additionally, the content produced by Prompt to image clips producers might not always align with societal preferences, which could lead to mistakes. It is essential to consider these difficulties while using such technology.

II. LITERATURE SURVEY

AI Prompt to image clips generators have ended up progressively prevalent due to their potential to revolutionize the video generation industry. These instruments permit clients to make personalized and locks in video substance rapidly and effortlessly. By leveraging progressions in profound learning and normal dialect preparing, these frameworks can create recordings based on composed portrayals. Whereas early adaptations of AI Prompt to image clips generators

Copyright to IJARSCT
www.ijarsct.co.in

DOI: 10.48175/IJARSCT-17473

ISSN
2581-9429
IJARSCT

426

Effective End-of-Life Management of Assets in Organization by Snowflake Integration

Dr. J. M. Patil[1], Prof. N. N. Ghuikar[2], Surabhi Lahoti[3], Aditya More[4], Kunal Chandore[5]

Assoc. Professor, Department of Computer Science and Engineering[1]

Asst. Professor, Department of Computer Science and Engineering[2]

Students, Department of Computer Science and Engineering[3,4,5]

Shri Sant Gajanan Maharaj College of Engineering, Shegaon, Maharashtra, India

jaimpatil1011@gmail.com, ghuikarnayana@gmail.com, sglohati123@gmail.com

yashmore1209@gmail.com, kunalachandore@gmail.com

Abstract: *To preserve device stability and security in today's industrial environment, vulnerabilities must be found and fixed. Asset managers face issues in managing End-of-Life (EOL) statuses, which are subject to constant change, and in traversing many data sources. It is challenging to have uniform view into important data without a centralized dashboard.*

We suggest putting in place a scraping method to collect data from various sources in order to overcome these issues. After the EOL data has been thoroughly verified and updated, the results will be shown on a consolidated, scalable, and dependable dashboard that easily links into the current systems. Advanced data slicing and dicing techniques will be used, utilizing Snowflake's capabilities, to handle enormous datasets efficiently. This all-encompassing strategy seeks to improve asset management procedures, strengthen device security, and offer useful information for defensible decision-making

Keywords: End-of-Life (EOL), Centralized Dashboard, Data Slicing and Dicing, Asset Management, Snowflake

I. INTRODUCTION

In the modern interconnected landscape, the seamless management of devices has become an integral aspect of our everyday lives. It emphasizes the importance of effectively managing device vulnerabilities, navigating through evolving End-of-Life (EOL) statuses, and consolidating data from various sources. The absence of a centralized dashboard is identified as a critical factor contributing to significant operational challenges in addressing these issues. This establishes the context for the proposed solution, suggesting that the implementation of a centralized dashboard and a scraping mechanism will be instrumental in overcoming these hindrances and improving operational efficiency.

In the ever-evolving landscape of the contemporary industry, the effective management of device vulnerabilities, dynamic adjustments to shifting End-of-Life (EOL) statuses, and the consolidation of data from a myriad of sources pose formidable challenges. These challenges are exacerbated by the notable absence of a centralized dashboard, thereby impeding operational efficiency and decision-making processes. In response to this complex scenario, the overarching goal of this project is to devise a comprehensive solution. This solution will not only navigate the intricacies of managing device vulnerabilities and adapting to EOL fluctuations but also tackle the data consolidation dilemma through the implementation of cutting-edge web scraping techniques.

At the heart of this endeavor lies the vision of creating a centralized, scalable, and reliable dashboard, meticulously designed to seamlessly integrate into existing infrastructures. This dashboard is poised to revolutionize the data visualization landscape, offering a holistic perspective on critical information. To fortify the infrastructure handling vast and diverse datasets, our

approach incorporates advanced data slicing and dicing techniques, harnessing the power of Snowflake, a leading data warehousing platform. Through the amalgamation of these innovative strategies, this project aspires to not only surmount existing challenges but also set a precedent for elevating operational efficiency, device security, and decision-making paradigms within the industry.

Sr. No.	Name of the author/s	Title of Paper
1	Priyanka Gajanan Dahi Dr. H. M. Jha "Bidyarthi"	Females' Buying Behavior for Cell Phones- An Analytical Study
2	Mansi Vilas Bharane Dr. H. M. Jha "Bidyarthi"	"Balancing Books and Happiness: Understanding Job Satisfaction in Banking Workforce of Akola Region"
3	Vishakha Vijay Tantak Dr. H. M. Jha "Bidyarthi"	Breaking Barriers: Examining Women's Empowerment through Government Initiatives in Khamgaon
4	Utkarsha Dhanraj Nitnaware Dr. H. M. Jha "Bidyarthi"	Fortifying Financial Frontiers: Safeguarding Online Banking in Chhindwara City
5	Aditya Haridas Sable Dr. H. M. Jha "Bidyarthi"	"Harvesting Opportunities through PMMY in Agribusiness - A Study of Pradhan Mantri Mudra Yojana's Contribution to Agricultural Development in Jalgaon Jamod"
6	Akshay Arun Jadhao Dr. H. M. Jha "Bidyarthi"	Bits and Bytes of Change: Examining Digitalization's Impact on Khamgaon's Socio-Economic Fabric
7	Gaurav Ajay Varma Dr. H. M. Jha "Bidyarthi"	Empirical Study on Stock Surge in First Twenty Years of 21st Century Investigating the Interplay between FDI, FII and Indian Market Dynamics
8	Mahesh Ratanlal Girhe Dr. H. M. Jha "Bidyarthi"	"Harnessing Sunlight: A Probe into the PM-KUSUM Solar Initiative in Sangrampur Taluka"
9	Anjali Dadubhaiya Rangari Dr. L. B. Deshmukh	Work Life Balance in Information Technology - A study in Yavatmal Region
10	Ku.Prachi Narayandas Sureka Dr. L. B. Deshmukh	Impact of Employee Motivation on Organization Productivity-A Study of Gajanan Industries Khamgaon
11	Monika Kishor Ghawat Dr. L. B. Deshmukh	Competency Mapping and Training & Development
12	Vaibhav J Ahir Dr. L. B. Deshmukh	A Study of Navigating the Landscape of Organic Farming: Analysing Challenges and Exploring Opportunities for Sustainability in Buldhana Region
13	Shruti Prakash Auti Dr. L. B. Deshmukh	The study on work life balance strategies and initiatives amongst working women in Buldana district
14	Madhuri Vijay Nagalkar Dr. L. B. Deshmukh	" Comparative Analysis Of Customer Satisfaction Towards Indian Postal Services And State Bank Of India Services."
15	ARJUN P. WASATKAR Dr. L. B. Deshmukh	Analysis of Organized Retailers and their Strategies-A Study of Akola District
16	Sumersing Barwal Dr. L. B. Deshmukh	Impact of Digital Marketing on Buying Behavior of Select Product categories in Buldana Region

17	Ganesh Arun Mandal Dr. L. B. Deshmukh	A STUDY ON CUSTOMER SATISFACTION TOWARDS HONDA BIKES WITH SPECIAL REFERENCE TO APOLLO ENTERPRISES
18	Priya Devidas Mapari Dr. P. M. Kuchar	A Study on Consumer Buying Behavior for Laptop in Khamgaon Region.
19	SHUBHAM D. RATHOD Dr. P. M. Kuchar	A Comparative Analysis of Fertilizer Practices in Soybean Farming: Organic vs. Chemical Approaches in Washim region
20	Pratiksha Santosh Gawande Dr. P. M. Kuchar	Involvement of Girls in Sports and Physical Activities: An Assessment of Initiatives from Government and Institutions
21	Roshan Anil Karale Dr. P. M. Kuchar	An Evaluation of Pradhan Mantri Awas Yojna In Tiosa Region
22	Rushikesh Subhash Paulzagade Dr. P. M. Kuchar	Perspective towards Entrepreneurship – A Study of Students with Special Reference to Atmanirbhar Bharat
23	Pooja N. Thakare Dr. P. M. Kuchar	Effect of training and development on employee retention
24	Vaishnavi M. Tivhane Dr. P. M. Kuchar	Insights into purchase decision and post-purchase behavior of selects bags
25	Vaishnvi A. Nimkarde Dr. P. M. Kuchar	Insights into purchase decision and post-purchase behavior of selects bags
26	Vaishnavi Anil Hage Dr. M. A. Dande	"Scanning Inclusive Workplace – A Study of Select Organization"
27	Vishal gujar Dr. M. A. Dande	A study of brand loyalty in tea powder market.
28	Krushna J. Thakur Dr. M. A. Dande	A Study of Impact of Organizational Culture on Employee Behavior and Performance
29	Ishan Pavan Shah Dr. M. A. Dande	Consumer Buying Behavior- "A Comparative Study Of Select Spices Brands"
30	Shrusti S. Purwar Dr. M. A. Dande	A STUDY OF EMOTIONAL INTELLIGENCE AS AN MPLOYABILITY PRE-REQUSITE
31	Sneha Sunil Wankhede Dr. M. A. Dande	A Study on Diffusion of Innovation in Fintech Banking with a special Reference to Khamgaon Region.
32	Pratik Pramod Dhage Dr. M. A. Dande	A Study of Market Potential for Spirulina

33	Tanaya Ajay Mate Dr. S. M. Mishra	Empowering Women through Self-Help Groups: An In-depth Study of Socioeconomic Development & Gender Equality
34	Poonam P. Parchure Dr. S. M. Mishra	A STUDY OF SELF-HELP GROUPS AND WOMEN EMPOWERMENT IN A RURAL AREA OF THE AKOLA REGION
35	Trupti Sunil Jamode Dr. S. M. Mishra	Impact of Pradhan Mantri Ujjwala Yojana in Buldhana District
36	Vitthal D. Ramekar Dr. S. M. Mishra	An Investigation into Factors Affecting Financial Exclusion in Rural Areas.
37	Shubaham K Gade Dr. S. M. Mishra	Market Potential of Organic Food in Maharashtra Region(Vidharbha)
38	Nagesh Banait Dr. S. M. Mishra	"The Study on Analyzing the Impact of Social Media on Consumer Buying Behavior in the Khamgaon Region"
39	SNEHA B. GAIKWAD Dr. S. M. Mishra	"STUDY ON INCLUSIVE GROWTH OF WOMEN'S EMPOWERMENT, CHALLENGES AND OPPORTUNITIES AT PADEGAON, CHHATRAPATI SAMBHAJI NAGAR
40	Vashishtha D. Thakur Dr. S. M. Mishra	Navigating the workplace upheaval and its impact on employee retention and turnover
41	Siddheshwar Dilip Parihar Dr. S. M. Mishra	An In-depth Analysis of Financial Literacy's Influence on Investment Behavior
42	Harshali S. Khandagale Dr. W. Z. Suliya	A study of factors and levels of satisfaction of employees in banking sector of Buldhana.
43	Aishwarya Vinayak Tayade Dr. W. Z. Suliya	A Study of Work Life and Satisfaction of Employees in Banking Sector in Akola District
44	Swapnil Gajanan Ikhare Dr. W. Z. Suliya	A Study on Satisfaction and Consumer Behaviour for Amul Milk in Buldana Region
45	Samruddhi Purkar Dr. W. Z. Suliya	A study on impact of social media on recruitment process of applicant's in Buldhana region
46	Padmini Madhav Ingole Dr. W. Z. Suliya	A Study on Employee Engagement with Special Reference to Banking Sector
47	Harshal Gawai Dr. W. Z. Suliya	A study of market potential analysis of e-bike in Shegaon region.
48	Pallavi Ravindra sabe Dr. W. Z. Suliya	A study of work life balance and stress management approach of working women in the Khamgoan region

49	Dhanashree S. Deshmukh Dr. W. Z. Suliya	A study of mechanization of agriculture business in Akola region
50	Vaishnavi Sachin Vaishnav Dr. W. Z. Suliya	Study of comparative analysis of amazon and flipkart
51	Shambala R. Mahokar Prof. V. V. Patil	"Weather and climate variability impact on farmers financial planning: A longitudinal study in khamgaon region"
52	Shraddha R. Gondchwar Prof. V. V. Patil	Navigating the Digital Divide: Challenges Faced by Senior Citizens in Digital Banking Adoption
53	Kunal Sanjay Bhise Prof. V. V. Patil	"The Influence of Fintech on Investment Patterns of Salaried Individuals"
54	Vaishnavi Manish Hiwrale Prof. V. V. Patil	Role of Online Job Portals in Shaping Candidate's Job Search Behavior
55	Revati S Mahalle Prof. V. V. Patil	Employee Engagement Strategies for Enhancing productivity
56	Arati Gautam Tayade Prof. V. V. Patil	Channel optimization strategies a catalyst for enhanced supply chain integration and supply chain performance
57	Vaibhav Tejrao Dali Prof. V. V. Patil	Exploring the Challenges and Opportunities of E-commerce Implementation in Small Businesses: Insights from Shegaon
58	Samrudhi S. Raut Prof. V. V. Patil	A STUDY OF STRSS MANAGEMENT PRACTICES ADOPTED BY COLLEGE STUDENT
59	Madhuri Sumare Prof. V. V. Patil	Comparative Study of Job Satisfaction of Working Women in Government Jobs and Private Jobs Malkapur
60	Pratik Shegokar Dr. B.T. Husain	A Study on Factors Influencing Buying Behavior of Graduate and post-Graduate Students towards Laptop Purchase with a Special Reference to Shegaon Region
61	Arti Ananda Jamnik Dr. B.T. Husain	A study on factors influencing saving and investment decisions of salaried individuals with a special reference to Akola region
62	Vaishnavi M. Panchbhai Dr. B.T. Husain	"A study on Human Resource Management practices at strategic Business unit in Khamgaon region."
63	Akshada Narendra Parchure Dr. B.T. Husain	Enhancing Mid-Course Internship Programs: Identifying Challenges and Promoting Collaborative Solutions in Shegaon's Educational Landscape
64	Shivani Sanjay Girjapure Dr. B.T. Husain	"A Study Of Consumer Satisfaction In Public Transportation System with A Special Reference To M.S.R.T.C. Khamgaon"
65	Prof. V.V. Patil Dr. M.A. Burghate Dr. O.M. Deshmukh	NAVIGATING THE ACCREDITATION LANDSCAPE: INSIGHT FROM STUDENTS IN RURAL INDIA
66	Dr. B. T. Husain	Rihizopus Keratitis

Females' Buying Behavior for Cell Phones – An Analytical Study

Priyanka Gajanan Dahi[1], Dr.H.M. Jha "Bidyarthi" [2]

MBA Final Year Student, Department of Business Administration and Research, Shri Sant Gajanan Maharaj College of Engineering, Shegaon, India [1]

Professor, Department of Business Administration and Research, Shri Sant Gajanan Maharaj College of Engineering, Shegaon, India [2]

ABSTRACT: The cell phones have all qualities which highlight it to qualify to be called as a small computer. Such handheld compact contraption that offers both communication and computing are known as shrewd phones'. A further inquiry about it presents that India has overwhelmed indeed the U.S. and has become the world's second-largest Smartphone showcase by the users. This prompted the authors to study the nuanced behavior of female buyers in Shegaon, Maharashtra, concerning the procurement of portable sets. With the exponential development of portable innovation, understanding buyer behavior gets to be pivotal for businesses to tailor their promotional procedures viably. The investigator utilizes subjective and quantitative strategies to assemble bits of knowledge into components affecting female buyers'choices, such as brand discernment, highlights prioritization, budget imperatives, feature and social impacts etc. By analyzing information accumulated through studies, interviews, and observations, the study points out to profitable bits of knowledge for portable set producers and marketers to better cater to wants and inclinations of female customers in Shegaon. Understanding these elements is essential for concocting focused showcasing campaigns and item improvement techniques to improve client fulfillment and brand dependability.

Balancing Books and Happiness: Understanding Job Satisfaction in Banking Workforce of Akola Region

[1]Mansi Vilas Bharane, [2]Dr. H.M. Jha "Bidyarthi"

[1] MBA Final Year Student, Department of Business Administration and Research, Shri SantGajanan Maharaj Collage of Engineering, Shegaon, India

[2]Professor, Department of Business Administration and Research. Shri Sant GajananMaharaj Collage of Engineering, Shegaon, India

ABSTRACT: This research paper investigates the factors influencing job satisfaction among employees in the banking sector of Akola region. Job satisfaction is crucial for organizational success as it directly impacts employee motivation, productivity, and retention. In the highly competitive banking industry, understanding the determinants of job satisfaction is essential for banks to attract and retain talented employees. The study employs a mixed-methods approach, combining qualitative and quantitative techniques to gather comprehensive insights. Qualitative data is collected through interviews and focus group discussions with employees from various levels within banks of Akola region. Additionally, quantitative data is collected through structured surveys distributed among a representative sample of bank employees.

The research aims to identify the key factors influencing job satisfaction, including but not limited to compensation, work-life balance, career growth opportunities, job security, leadership, organizational culture, and workload. By analyzing both qualitative and quantitative data, the study seeks to provide a nuanced understanding of the interplay

Breaking Barriers: Examining Women's Empowerment through Government Initiatives in Khamgaon

[1]Vishakha Vijay Tantak and [2]Dr. H. M. Jha "Bidyarthi"

[1]MBA Final Year Student, Department of Business Administration and Research, Shri Sant Gajanan Maharaj College of Engineering, Shegaon, India

[2]Professor, Department of Business Administration and Research. Shri Sant Gajanan Maharaj College of Engineering Shegaon, India

ABSTRACT: The empowerment of women has emerged as a key concern in development discourse, with an emphasis on giving them the freedom to make choices that will advance their own personal development. In examining the state of women's empowerment in the Khamgaon area, this article places special emphasis on the contribution of government initiatives to raising women's socioeconomic standing. Data were gathered using primary and secondary approaches through a descriptive research methodology with a sample size of 100 respondents. According to the analysis, opinions on the knowledge and efficacy of government initiatives for women's empowerment in Khamgaon are divided. While some respondents say that these plans have a good influence, others are unsure. The study also emphasizes the need for increased outreach and improved programs already in place to support women's empowerment in the area. The aforementioned results highlight the significance of on-going assessment and improvement of governmental measures aimed at tackling the diverse issues encountered by women in Khamgaon and fostering their progress towards socioeconomic empowerment.

Fortifying Financial Frontiers: Safeguarding Online Banking in Chhindwara City

[1]Utkarsha Dhanraj Nitnaware, [2]Dr.H.M.Jha "Bidyarthi"

[1] MBA Final Year Student, Department of Business Administration and Research, Shri Sant Gajanan Maharaj Collage of Engineering, Shegaon, India

[2]Professor, Department of Business Administration and Research, Shri Sant Gajanan Maharaj Collage of Engineering, Shegaon, India

ABSTRACT: Banking online has spread like anything besides several other transactions also taking place through digital means and therefore security concerns in doing so are also escalating. The present study attempts to ascertain the status of online banking and other financial transactions in a city of central India along with the security measures accompanying it that fortify financial frontiers of the banking customers and general public transacting digitally in this city. The finding of the study establishes a strong positive relationship between consumers and security for online banking and transactions. In some cases the consumers are not satisfied with security for online banking and transactions because they find it much more complex, as they are unaware of technology and have insufficient knowledge about the payment transaction in mobile phones, especially illiterate people in rural areas. Finally this research recommends the measures to be initiated both by banks as well as service providers for online transactions to strengthen this financial frontier in the interest of the banking customers and general public for their ease, safety, security and check against digital frauds. There is a need for introducing better technology, educating people, following the rules, and working together by every stakeholder connected to online banking and other businesses.

Bits and Bytes of Change: Examining Digitalization's Impact on Khamgaon's Socio-Economic Fabric

Akshay Arun Jadhao, Dr. Hari Mohan Jha Bidyarthi

Department of Business Administration and Research, Shri Sant Gajanan Maharaj College of Engineering,

Shegaon, India

Department of Business Administration and Research, Shir Sant Gajanan Maharaj College of Engineering,

Shegaon, India

ABSTRACT: Rural areas are changing due to the global digitization trend, which presents both benefits and challenges. This study looks at how digitalization has affected rural socioeconomic situations in many ways, including how it has affected community dynamics, healthcare, education, and agriculture. Although increased access to resources and services through digitization could help close the gap between urban and rural areas, privacy concerns and the digital divide are also brought up by this process. This study, which focuses on Khamgaon region, explores the ways in which digital innovation is changing daily life, from mobile banking to the execution of government programs. It emphasizes the challenges associated with advancement and the necessity of inclusive development policies.

I. INTRODUCTION

This study explores the revolutionary effects of digitalization on rural socioeconomic environments, concentrating on

---

Empirical Study on Stock Surge in First Twenty Years of 21st Century-Investigating the Interplay between FDI, FII and Indian Market Dynamics

Gaurav Ajay Varma, Dr. Hari Mohan Jha Bidyarthi

MBA Final Year Student, Department of Business Administration and Research, Shri Sant Gajanan Maharaj College of

Engineering, Shegaon, India

Professor, Department of Business Administration and Research, Shir Sant Gajanan Maharaj College of Engineering,

Shegaon, India

ABSTRACT: This research paper investigates the dynamic relationship between Foreign Direct Investment (FDI), Foreign Institutional Investment (FII), and the Indian stock market. With India's burgeoning economy and growing significance in the global market, understanding the influences of FDI and FII on its stock market is crucial for investors, policymakers, and stakeholders alike. Employing empirical analysis, this study delves into the intricate interplay between these foreign investments and the Indian stock market's performance during the first twenty years of 21st century. By utilizing time-series data spanning a first twenty years of present century, the research examines various factors such as economic indicators, regulatory changes, and market sentiments to comprehensively analyse the impact of FDI and FII. The findings of this study provide valuable insights into the behaviour of the Indian stock market in response to foreign investments, offering implications for investment strategies, policy formulation, and future research directions.

KEYWORDS: Foreign Direct Investment, Foreign Institutional Investment, Stock Market, BSE SENSEX, NSE Nifty, Regression.

I. INTRODUCTION

Harnessing Sunlight: A Probe into the PM-KUSUM Solar Initiative in Sangrampur Taluka

Mahesh Ratanlal Girhe[1], Dr. H. M. Jha Bidyarthi[2]

MBA Final Year Student, Department of Business Administration and Research, Shri Sant Gajanan Maharaj College of Engineering, Shegaon, India[1]

Professor, Department of Business Administration and Research, Shri Sant Gajanan Maharaj College of Engineering, Shegaon, India[2]

ABSTRACT: The Indian government's revolutionary Pradhan Mantri Kisan Urja Suraksha evam Utthaan Mahabhiyan (PM-KUSUM) Solar Yojana aims to redefine the agricultural landscape by promoting the widespread use of solar energy solutions. PM-KUSUM was introduced with the primary objective of supporting farmers' livelihoods and renewable energy. It is intended to meet the vital energy requirements of India's agriculture sector and further the country's renewable energy targets at the same time. Fundamentally, PM-KUSUM seeks to reduce farmers' energy costs, especially in the area of irrigation, by utilizing the nation's enormous solar resources. Historically, farmers have primarily relied on diesel- powered irrigation pumps, which not only have high running costs but also release carbon dioxide into the atmosphere. By encouraging farmers to switch to solar-powered irrigation pumps, PM-KUSUM hopes to lessen these obstacles and help them make the shift to a cleaner, more sustainable energy source.

The program includes a wide range of interventions designed to encourage farmers to use solar energy. This entails the installation of solar power projects on desolate areas, the solarization of current grid- connected pumps, and the replacement of diesel-powered pumps with solar ones. Through monetary rewards, guidance on technology, and legislative backing, PM-KUSUM aims to enable farmers to adopt solar technology and capitalize on its advantages for their farming enterprises. The goal of PM-KUSUM is to act as a catalyst for raising agricultural productivity and

Work Life Balance in Information Technology Sector – A Study of Yavatmal Region

Dr. Laxmikant B. Deshmukh, Anjali Dadubhaiya Rangari

Department of Business Administration and Research, Shri Sant Gajanan Maharaj College of Engineering, Shegaon, India

MBA Student, Department of Business Administration and Research, Shri Sant Gajanan Maharaj College of Engineering, Shegaon, India

ABSTRACT: The **InformationTechnology (IT)** sector have been in boomed in last 3-4 years in India as its reaches to all over its not limit up to urban areas but it is also widely spreading in semi- urban region also, and one of the regions is Yavatmal, Maharashtra, India. This research paper aims to contribute the updated information of IT sector employees and how their professional and personal life impacts due to their work. The primary objective of this paper is to focus and identify the problems, remedy and showing updated information in Yavatmal district. The data for this research paper sample size is 100 respondents who work in IT sector. The questionaries in this survey are specially designed for employees to keeping in in their profession such as job satisfaction, career growth, working load, flexibility, remote work, training, and resources, etc. The findings of this study showcase the employee's satisfaction with their job.

Furthermore, the results showed that the many employees are stressed with work and unable to manage their work and personal life too, some even say that even when they in vacation they had to work, a very few employees say that their org plans an activity to keeping
environment stress free.

In conclusion, the study shows different views of employees with respect to their work and their plans, growth,

Impact of Employee Motivation on Organization Productivity-A Study of Gajanan Industries Khamgaon

Ku. Prachi Narayandas Sureka[1], Dr. L. B. Deshmukh[2]

[1]Student MBA 2nd year, (Finance & Human Resource), Department of Business Administration and Research, Shri Sant Gajanan Maharaj College of Engineering, Shegaon – 444 203, Maharshtra, India
[2]Associate Professor, Department of Business Administration and Research Shri Sant Gajanan Maharaj College of Engineering Shegaon – 444 203, Maharshtra, India

--****************--

ABSTRACT

Motivation is a fundamental aspect of human behavior, particularly in the workplace, where it influences productivity and organizational success. This study delves into the concept of motivation, exploring its definitions, types, and significance in organizational settings. It investigates the relationship between employee motivation and organizational productivity, focusing on Gajanan Industries in the Khamgaon region as a case study. The research methodology involves a descriptive approach, utilizing primary data collected through structured questionnaires and observations from 70 workers at Gajanan Industries. Additionally, secondary data from various sources, such as the internet, journals, and books, complement the study. Findings from the data analysis highlights key factors influencing employee motivation, including financial incentives, recognition, career development opportunities, and the management's approach to motivation. The study identifies challenges in maintaining motivation, such as the demanding schedules of employees and limited resources for research. Based on the findings, several recommendations are proposed to enhance motivation and, consequently, organizational productivity. These include improving communication and recognition from superiors, providing adequate training programs, and fostering a supportive work culture. In conclusion, this research underscores the critical role of motivation in organizational performance and provides valuable insights for managers and leaders seeking to optimize employee engagement and productivity.

Keywords:- Employee Engagement, Organizational Productivity, Career Development Opportunities, Employees

Competency Mapping and Training & Development

Monika Kishor Ghawat[1], Dr. Laxmikant Deshmukh[2]

MBA Student, Department of Business Administration and Research, Shri Sant Gajanan Maharaj College of Engineering, Shegaon, India

Department of Business Administration and Research, Shri Sant Gajanan Maharaj College of Engineering, Shegaon, India

ABSTRACT: The strategic necessity of competency mapping has become visible for modern firms aiming to achieve long-term expansion and a competitive edge. This study explores the mutually beneficial link that exists between organizational training and development activities and competence mapping. It examines the competency mapping method and emphasizes how important it is for locating, assessing, and cultivating the core competencies required for both individual and organizational success. Organizations can create focused training interventions to close skill gaps and improve overall performance by systematically matching staff competencies with company objectives. This study examines the effects of competence mapping on talent management, career development, and employee engagement across a variety of Indian industries, including manufacturing, IT, services, and pharmaceuticals. It does this by reviewing relevant research. The results highlight the strategic value of competence mapping in promoting a culture of lifelong learning and professional development, which in turn   promotes organizational success and effectiveness in fast-paced business environments.

KEYWORDS: Competency mapping, Skills, Knowledge, Ability, Training & Development, Competencies.

A Study of Navigating the Landscape of Organic Farming: Analysing Challenges and Exploring Opportunities for Sustainability in Buldhana Region

Vaibhav J Ahir, Dr. Laxmikant Deshamukh

Student, Shri Sant Gajanan Maharaj College of Engineering, Shegaon, India

Asst. Professor, Shri Sant Gajanan Maharaj College of Engineering Sgegaon, India

ABSTRACT: Organic farming has emerged as an important priority in India to promote environmental sustainability and food safety. With only 1.5% of total agricultural land under organic cultivation, there is immense scope for growth. Organic farming avoids use of synthetic fertilizers and pesticides, and focuses on traditional practices that nurture the soil through crop rotations, organic manures, green manures and biological pest control. This review article provides an overview of the current status, benefits, challenges and future prospects of organic farming in India. Organic produce fetches higher prices and improves farm incomes. Organic practices build soil health, conserve biodiversity, reduce pollution and mitigate climate change impacts. Challenges include transition costs, certification burdens, lack of awareness, supply chain gaps and insufficient institutional support. Government schemes to mainstream organic farming through farmer incentives, market development and extension services have shown positive impacts. Further policy support, public-private partnerships, farmer collectives and participatory guarantee systems can help tap the full potential of organic farming towards building sustainable food production systems in India.

I. INTRODUCTION

The organic movement may have gained a place in the spotlight of the mainstream media now, but it has not been like that for long. Since the 1950s, organic farmers operating at a grass roots level have devised, tested and shared production methods. They have codified a set of ideals into a pioneering best practice agricultural management system that addresses multiple

A Study on Work-Life Balance Strategies and Initiatives amongst Working Women in Buldana District

Ku Shruti Prakash Auti, Laxmikant Baburao Deshmukh

Department of Business Administration and Research, Shri Sant Gajanan Maharaj College of Engineering

, Shegaon, India

Department of Business Administration and Research, Shri Sant Gajanan Maharaj College of Engineering,

Shegaon, India

ABSTRACT: The focus of this paper is work-life balance, and it attempts to elucidate the importance of the topic. The personal and professional spheres are complementary to one another. One definition of work-life balance is striking, preserving, and overseeing a balance between one's personal and professional lives. Workplace demands, goals, globalization, and technology advancements have made it a concerning issue for professionals of all genders, working at all levels and in all sectors of the global economy.

The study also looks at the efficacy of existing approaches and identifies any obstacles that can prevent women from juggling work and personal obligations. By means of an extensive examination, the present study endeavors to furnish significant suggestions for enhancing the assistance with work-life balance that working women in Buldana District receive, so promoting their welfare and career advancement.

KEY WORDS: Work-life balance, working women, family responsibilities, flexible working hours, employee

Comparative Analysis of Customer Satisfaction towards Indian Postal Services and State Bank of India Services

[1]Madhuri V. Nagalkar , [2]Laxmikant Deshmukh

[1]Student, Shri Sant Gajanan Maharaj College of Engineering, Shegaon, India

[2]Associate Professor, Shri Sant Gajanan Maharaj College of Engineering, Shegaon, India

Abstract: The aim of this research paper is to analyze the impact of service quality on customer satisfaction. A sound association is found between customer satisfaction and the quality of service provided by the SBI Bank and Indian Post. Both firms are under government control. In business world customers are the source of profit and revenue for the service organizations and improvements in service quality leads to customer loyalty. In this research project descriptive research design is used judgment and Convenience sampling method will be used to get the information about online banking. This method is used because we are interested in exploring gender, age, or occupation disparities in terms of online banking in the population For conducting this research, a structured questionnaire is prepared and sample of 100 customers is taken from SBI bank and post office in Shegaon. This result shows the satisfaction level of customer related to SBI & post office services.

In the current competitive world banks have to struggle their might to offer the best have offer the best of the customer satisfaction through various innovative strategies in order to services in industry The study investigates the effect of quality on satisfaction by focusing on the relationship between service quality and customer satisfaction and how quality can be improved in the service firms.

Impact of Digital Marketing on Buying Behavior of Select Product Categories in Buldana Region

[1]Sumersing B. Barwal , [2]Laxmikant Deshmukh

[1] PG Student, Dept. of Business Administration and Research, S.S.G.M.C.E Shegaon Maharashtra, India

[2] Associate Professor, Dept. of Business Administration and Research, S.S.G.M.C.E Shegaon,

Maharashtra, India

ABSTRACT: This research investigates the influence of digital marketing on the purchasing behavior of smartphones and smart watches in the Buldana region. As digital platforms continue to expand, understanding how digital marketing impacts consumer behavior becomes crucial for businesses. Through a detailed examination, this study aims to reveal the specific effects of digital marketing strategies on consumer decision-making processes within Buldana's market context, focusing on smartphones and smart watches. By analyzing these product categories, this research aims to provide valuable insights to guide marketers and businesses in developing tailored digital marketing strategies to meet the preferences and behaviors of consumers in this region.

KEYWORDS: Digital marketing, Buying behavior, Product categories.

I. INTRODUCTION

In the Buldhana region, In a period defined by the digital revolution, where smartphones have become extensions of ourselves and social media platforms have transcended bare communication tools, the geography of marketing has experienced a profound metamorphosis. It's no longer just about traditional billboards, print announcements, or

A Study on Customer Satisfaction towards Honda Bikes with Special Reference to Apollo Enterprises

Ganesh Arun Mandal, Dr. Laxmikant B. Deshmukh

MBA Student, Department of Business Administration and Research, Shri Sant Gajanan Maharaj College of Engineering, Shegaon, India

Department of Business Administration and Research, Shri Sant Gajanan Maharaj College of Engineering, Shegaon, India

ABSTRACT: This study employed a survey as its research method, with 100 Honda bike owners who bought their vehicles from Apollo Enterprises participating. The purpose of the survey questionnaire was to collect data on a number of customer satisfaction-related topics, such as product quality, pricing, after-sales support, and general satisfaction. The purpose of this study is to find out how satisfied Honda motorcycle owners are, paying particular attention to Apollo Enterprises. This study employed a survey as its research method, with 100 Honda bike owners who bought their vehicles from Apollo Enterprises participating. The purpose of the survey questionnaire was to collect data on a number of customer satisfaction-related topics, such as product quality, pricing, after-sales support, and general satisfaction. customer satisfaction-related topics, such as product quality, pricing, after-sales support, and general satisfaction.Statistical tools like frequency distribution, mean, and standard deviation were used to analyze the survey data. The majority of consumers are quite pleased with the quality of Honda motorcycles and Apollo Enterprises' after-sale support, according to the study's findings. Nonetheless, some people expressed concerns about the bikes' price. The

A Comparative Analysis of Fertilizer Practices in Soybean Farming: Organic vs. Chemical Approaches in Washim region Shubham

Shubham D Rathod [1], Dr. Pavan Kuchar[2]

Dept. of Business Administration and Research, S.S.G.M.C.E Shegaon, Maharashtra, India

ABSTRACT: This study compares organic and chemical fertilizer practices in soybean farming in the Washim region. Through mixed-methods research, including field surveys and interviews. Preliminary findings suggest that while chemical fertilizers may yield higher short-term productivity, organic methods offer long-term benefits in soil health and environmental sustainability.

I. INTRODUCTION

Fertilizer application is essential for enhancing soil fertility, promoting plant growth, and maximizing crop yields. In the Washim region, farmers traditionally relied on chemical fertilizers to meet the nutritional needs of soybean crops. However, in recent years, there has been a growing interest in organic farming practices, driven by concerns about the environmental impact of chemical fertilizers, soil health degradation, and a desire for sustainable and ecologically friendly agriculture.

This comparative analysis aims to shed light on the two predominant approaches to fertilizer practices in soybean farming within the Washim region: the conventional use of chemical fertilizers versus the adoption of organic methods. By examining key parameters such as yield, soil health, environmental impact, and economic considerations, this study seeks to provide valuable insights into the effectiveness and sustainability of each approach.

Involvement of Girls in Sports and Physical Activities: An Assessment of Initiatives from Government and Institutions

¹Pratiksha Santosh Gawande, ²Dr. Pavan .M. Kuchar

¹Student, Department of Business Administration and Research, Shri Sant Gajanan Maharaj College of Engineering, Shegaon, India

²Head, Department of Business Administration and Research, Shri Sant Gajanan Maharaj College of Engineering, Shegaon, India

ABSTRACT: The participation of girls in sports and physical activities is a critical aspect of promoting gender equality, fostering physical well-being, and empowering individuals. This paper aims to assess the effectiveness of initiatives launched by governments and institutions to encourage girls' involvement in sports and physical activities. It explores various strategies, policies, and programs implemented at the national, regional, and local levels, analyzing their impact on girls' participation rates and overall engagement in sports. Furthermore, the paper examines the challenges and barriers that hinder girls' involvement in sports, such as social norms, cultural biases, lack of access to facilities, and limited opportunities for skill development. By evaluating existing initiatives and identifying areas for improvement, this assessment seeks to provide insights for policymakers, educators, and stakeholders to enhance girls' access to sports and physical activities, thereby promoting gender equity and fostering healthier communities.

I. INTRODUCTION

The involvement of girls in sports and physical activities has been recognized as a fundamental aspect of promoting their overall well-being and empowerment. Engaging in sports not only enhances physical fitness but also instills valuable life

---

An Evaluation of Pradhan Mantri Awas Yojna In Tiosa Region

Roshan A. Karale¹, Dr. Pavan Kuchar²

¹,² Dept. of Business Administration and Research, S.S.G.M.C.E Shegaon-444203, Maharashtra, India

ABSTRACT

The Indian government's major housing program, the Pradhan Mantri Awas Yojana (PMAY), was introduced with the goal of providing everyone with affordable homes by 2022. An assessment of PMAY's implementation and effects in the Tiosa region is provided in this paper. The assessment looks at a number of program elements, such as awareness levels, application procedures, benefit distribution, and the program's overall efficacy in meeting housing needs.

Surveys, interviews, and secondary sources were used to gather information for the evaluation, giving insights into the opinions and experiences of recipients, public servants, and other parties involved in the execution of PMAY. Important discoveries emphasize the achievements and difficulties faced in the Tiosa area, illuminating potential areas for development and offering suggestions for augmenting the program's efficacy.

Residents in the Tiosa region have a modest level of awareness about PMAY, according to the evaluation, and many recipients have expressed satisfaction with the high caliber of housing the program offers. On the other hand, difficulties including red tape, lengthy approval processes, and opaque application procedures were noted as major obstacles to receiving PMAY payments. In addition, the study finds ways to improve the Tiosa region's overall PMAY implementation by reducing procedures, boosting transparency, and strengthening community involvement.

Introduction

Perspective towards Entrepreneurship – A Study of Students with Special Reference to Atmanirbhar Bharat

Rushikesh. S. Paulzagade, Dr. Pavan M. Kuchar

Department of Business Administration and Research, S. S. G. M. C. E, Shegaon, Maharashtra, India

ABSTRACT: The purpose of this study is to find out how students view entrepreneurship, with a focus on the Indian Atmanirbhar Bharat project and identify the student perspective towards entrepreneurship. The research utilizes a survey-based methodology, collecting data through the use of Google Forms. The participant types of in this survey are Students, Employee and self-employee or unemployed. And the age criteria mention in this research are 18-24 24-30 and 30-35. A methodical questionnaire was employed to get information regarding students' attitudes, views, and preparedness for entrepreneurship, taking into account a range of socio-economic variables and the impact of governmental initiatives such as Atmanirbhar Bharat. In the context of India's economic development, the research findings are anticipated to aid in understanding students' entrepreneurial mindsets and the efficacy of programs designed to promote self-reliance and entrepreneurship.

I. INTRODUCTION

Entrepreneurship has become "buzzed in recent years. Everyone wants to be one in them. And who can blame them? Because of newly facts about entrepreneur's, they live in digital world these is the one of the reasons behind the why today's young generation want be an entrepreneur. The today's generation having lots of idea and idea transform in the

The Effect of Training and Development on Employee Retention

Pooja.N. Thakare, Dr. Pavan M. Kuchar

Student, Shri Sant Gajanan Maharaj College of Engineering, Shegaon, India

Asst. Prof., Shri Sant Gajanan Maharaj College of Engineering, Shegaon, India

Abstract: A valuable resource for a company is its human capital. As a result, companies must not only find and hire skilled and experienced workers, but also retain them over the long term. This study examines the findings and outcomes of academics that looked into the connection between employee retention and training. Training is regarded as the primary tactic to affect employee retention and is a crucial component in improving organizational success. Field research was conducted for the study, which focuses on how training and development affect employee retention. employing a questionnaire approach to get information from workers in the enterprises located in the Khamgaon region. The results demonstrate that staff retention and training and development are positively correlated.

I. INTRODUCTION

In any firm, training and development is a crucial aspect of human resource management. Training's goal is to improve workers' abilities, attitudes, and knowledge by assisting them in picking up new work habits. Employee knowledge base expansion and upskilling are facilitated by training and development. It's an exercise meant to help employees reach their goals and perform better. Training and development programs are designed to help staff members perform better in their allocated roles and inspire them to give their all so they can demonstrate their eligibility for advancement and pay increases at performance reviews. Enhancing an employee's whole personality is the goal of training. The management initiates training.

Importance of Training and Development

Insights into Purchase Decision and Post-Purchase Behavior of Selects Bags

Vaishnavi Maroti Tivhane[1], Dr. Pavan .M. Kuchar[2]

Student, Department of Business Administration and Research, Shri Sant Gajanan Maharaj College of Engineering,

Shegaon, Maharashtra, India[1]

Head, Department of Business Administration and Research, Shri Sant Gajanan Maharaj College of Engineering,

Shegaon, Maharashtra, India[2]

ABSTRACT: This study investigates the purchase decision and post-purchase behavior related to selected bags, including schoolbag, handbag, clutch bag, shoulder bag, backpack, laptop bag, potli bag and crossbody bag. The research aims to uncover the key factors that influence consumer's decision when purchasing these bags and their behavior after acquiring them. A mixed-methods approach is utilized, combining quantitative surveys and qualitative interviews and observation with bag consumers. The quantitative surveys assess factors such as brand perception, product features, pricing strategies, consumer preference and purchase motivations. On the other hand, qualitative interviews delve deeper into consumer experiences, satisfaction levels, and post-purchase usage patterns. Furthermore, the research delves into the post-purchase phase, exploring aspects like customer satisfaction, product durability, perceived value, and repurchase intentions. By examining how consumers interact with their chosen bags over time, valuable insights into loyalty, advocacy, and brand engagement are gained. The finding of this study contribute to both theoretical and practical implications for marketers and businesses in the bag industry. Understanding the nuanced behaviors and decision-making processes of consumers can guide strategic marketing initiatives, product development

---

Understanding Consumer Choices in Electronic Home Appliances

Vaishnavi Anil Nimkarde[1], Prof. Pawan Kucher[2]

Student, Department of Business Administration and Research, Shri Sant Gajanan Maharaj College of Engineering,

Shegaon, Maharashtra, India[1]

Head, Department of Business Administration and Research, Shri Sant Gajanan Maharaj College of Engineering,

Shegaon, Maharashtra, India[2]

ABSTRACT: Understanding Consumer Choices in Electronic Home Appliances. This study investigates consumer buying behaviour concerning selected electronic home appliances. Through a structured survey, data was gathered from a diverse sample of consumers to examine their preferences, decision-making processes, and satisfaction levels regarding electronic home appliances such as refrigerators, washing machines, mixers, water coolers, and TVs. The research aimed to understand the factors influencing consumers' choices, including convenience, price, brand reputation, and technological features. Additionally, the study explored the role of marketing strategies, such as advertisements and recommendations, in shaping consumer decisions. The findings provide valuable insights into consumer preferences and offer recommendations for manufacturers and retailers to enhance their product offerings and marketing strategies in the competitive home appliance market.

I.INTRODUCTION

Consumer buying behaviour is a multifaceted phenomenon that is influenced by a multitude of factors, including

Scanning Inclusive Workplace – A Study of Select Organization

Vaishnavi A. Hage, Dr. Mayur A. Dande

Dept. of Business Administration and Research, S.S.G.M.C.E Shegaon, Maharashtra, India

ABSTRACT: This research paper investigates the concept of an inclusive workplace within organizations. It explores the dimensions of diversity, equity, and belonging, and their impact on organizational performance and employee well-being. By employing a comprehensive literature review and empirical analysis, this study aims to provide insights into the practices and strategies adopted by organizations to foster inclusivity and enhance overall effectiveness.

Continued research suggests that firms with more diverse workforces perform better financially. Numerous internal and external factors are creating change in the arena of diversity and inclusion. Generational shifts are evident across the workplace. Unlike older generations, younger employees are more likely to job hop in search of the right workplace that suits them. Research shows that there is a growing body of academic studies that seek to understand the benefits of workplace diversity. Many of these studies focus on gender diversity, though there are lots more research on the topic of diversity and what my findings could mean to the business in real terms. However, there are very few studies that look at the concept of an "inclusive" working with. Inclusivity is a state in which all persons, or things of the specified group or variety are included. My research intends to do so. And for me, it is pretty straightforward what an inclusive workplace is. It's a collective approach; which takes in the value of all employees, bonding and utilizing the various skills, knowledge, experiences, and attributes that employees have to offer. An inclusive workplace is active-participative, embracing mutual acceptance and respect of the individual thoughts and actions. A successful inclusion plan should present an equal possibility for all employees to get involved and engage in communication, provides objectives to achieve, and gain support and ownership from leadership and team members.

I. INTRODUCTION

A STUDY OF BRAND LOYALTY IN TEA POWDER MARKET

Vishal Gujar*[1], Mayur Dande*[2]

*[1]PG Student, Dept. Of Business Administration And Research, S.S.G.M.C.E Shegaon-444203, Maharashtra, India.

*[2]Assistant Professor, Dept. Of Business Administration And Research, S.S.G.M.C.E Shegaon-444203, Maharashtra, India.

ABSTRACT

In the tea powder industry, brand loyalty is an essential component of marketing strategy since it shapes consumer behaviour and purchase intent. The purpose of this study is to investigate the elements that influence consumers' brand loyalty in the tea powder industry. By employing a blend of qualitative and quantitative research techniques, such as surveys and interviews, we aim to comprehend the fundamental factors that influence brand loyalty, including brand image, product excellence, cost, and marketing initiatives. Through an analysis of consumer preferences and behaviour, this study will offer marketers and manufacturers of tea powder useful information for creating strategies that will increase brand loyalty and give them a competitive advantage in the market.

Keywords: Buying Behaviour, Brand Loyalty, Purchase Intention, Customer Satisfaction, Competitive Advantage.

I. INTRODUCTION

Concentrating on elements that affect customer behaviour and brand loyalty. Businesses can create focused strategies to improve long-term loyalty, brand reputation, and customer satisfaction by knowing these drivers. In addition, the study adds to the body of knowledge already available on consumer behaviour and brand loyalty in the tea powder industry by examining potential effects and future prospects. The study does, however, acknowledge certain potential drawbacks, including sampling bias and regional differences. In

A Study of Impact of Organizational Culture on Employee Behavior and Performance

Krushna Jitendrasingh Thakur, Prof. Mayur Dande

Department of Business Administration and Research, Shri Sant Gajanan Maharaj College of Engineering,

Shegaon, India

Department of Business Administration and Research, Shri Sant Gajanan Maharaj College of Engineering,

Shegaon, India

ABSTRACT: The study deals with the relation between organisation culture and employee behaviour and performance. The study deals with the some of the aspects of leadership style and communication pattern.

The impact of this cultural aspects on employee behaviour their commitment and they're the organisation along with their job satisfaction. the research enclosed with qualitative data and findings in the survey. the study figured out so how positive and supportive environment of the organization impacts in desirable way so they can improve their effectiveness for the organisation. How the experience of senior leaders and their suggestions helps other to grow well. Organisations norms policies and values incorporate with the employee productivity and outcomes for the organisation. Different theories by the organisation of psychology and sociology examines how the different dimensions are there in the studies, that is value alignment and employee motivation. HR practices also plays an essential role for the employees for the positive thought process. Practical execution and recommendation help a lot. furthermore, the study explores the mediating role employee and attitude and the recommendation of the management decision.

I. INTRODUCTION

In todays world of business, competition is increasing day by day, many organisation around the world recognise that organisation culture plays shaping role of employee behaviour and their performance. The culture collectively represents the values, norms and different practices shared within the organisation.

Consumer Buying Behavior- "A Comparative Study Of Select Spices Brands"

Ishan Pavan Shah[1] & Prof. Mayur Dande[2]

[1&2]Department of Business Administration And Research

Shri Sant Gajanan Maharaj College of Engineering, Shegaon.

Corresponding Author - Ishan Pavan Shah

Abstract:

This study is aimed at analyzing the Consumer Buying Behavior- "A Comparative Study Of Select Spices Brands", The study has been conducted through a survey questionnaire administered to sample of 100 respondents from various audiences like Retailers, Consumers, Working Professionals, Students. The questionnaire consisted of close and open ended questions related to various aspects of Spices Brands such as Quality, Taste, Variety, Price range, Packaging.

This research proposal aims to investigate and analyze the consumer buying behavior concerning selected spice brands. The study will focus on understanding the factors influencing consumers' purchasing decisions within the spices market, considering aspects such as brand loyalty, product quality perception, price sensitivity, and marketing strategies. Through a comparative approach, the research will examine the similarities and differences

A Study of Emotional Intelligence as an Employability Pre-requisite

Shrusti Suryakant Purwar[1], Prof. Mayur A. Dande[2]

Department of Business Administration and Research, Shri Sant Gajanan Maharaj College of Engineering,

Shegaon, India

Department of Business Administration and Research, Shri Sant Gajanan Maharaj College of Engineering,

Shegaon, India

ABSTRACT: The importance of emotional intelligence as a critical success component in the modern workplace has drawn a lot of attention. This study explores the relationship between employability and emotional intelligence with the goal of determining emotional intelligence's function as a requirement for career success. The research examines how emotional intelligence affects a number of employability factors, such as interpersonal connections, teamwork, leadership effectiveness, and flexibility in changing work contexts. It does this through a thorough literature review and empirical analysis.

Using a mixed-method approach, information was gathered from college students from through surveys and interviews. A favourable association between employability measures and emotional intelligence was found through quantitative analysis, suggesting that people with greater emotional intelligence have better career progress, job satisfaction, and job prospects.Qualitative insights shed light on the particular emotional intelligence competencies that employers and employees both believe to be most important.

The results highlight how important emotional intelligence is for negotiating the complexity of today's jobs. Businesses are realizing more and more that emotional intelligence is a vital skill set that boosts overall productivity and goes hand in hand with technical expertise. As a result, developing emotional intelligence through focused training and

A Study on Diffusion of Innovation in Fintech Banking with a special Reference to Khamgaon Region

[1]Sneha Sunil Wankhede and [2]Dr. Mayur Dande

[1]Student, Shri Sant Gajanan Maharaj College of Engineering, Shegaon, India

[2]Asst. Prof., Shri Sant Gajanan Maharaj College of Engineering, Shegaon, India

ABSTRACT: This research looks at how new tech in banking, known as fintech, spreads and becomes popular. Fintech has changed how banks work by introducing new ways of doing things. This study dives into how these changes happen.

We start by looking at a theory called the diffusion of innovation. This theory helps us understand how new ideas, like fintech, spread. We then use this theory to see how fintech is changing banking.

We'll talk about why people choose to use fintech in banking. Things like how useful they find it, how well it works with what they already have, and how easy it is to try out. We'll also look at examples of how fintech has been adopted, both successfully and not so successfully.

We'll also look at the rules and regulations around fintech in banking. These rules can speed up or slow down how quickly fintech spreads. We'll also see how people's habits and expectations are changing because of fintech.

Lastly, we'll talk about how traditional banks and fintech companies work together. Sometimes they partner up to bring new ideas to the market faster. We'll also talk about what might happen in the future, like new technologies and how the world is changing.

This research helps us understand how fintech is changing banking and what might come next.

I. INTRODUCTION

Today, all financial services aspects seem to be touched by technological forces. Fintech development is in its first

A Study of Market Potential for Spirulina

Pratik Pramod Dhage, Dr. Mayur Dande

MBA Final Year Student, Department of Business Administration and Research, Shri Sant Gajanan Maharaj College of
Engineering, Shegaon, India

Professor, Department of Business Administration and Research, Shir Sant Gajanan Maharaj College of Engineering,
Shegaon, India

ABSTRACT: This research paper provides a thorough investigation into the market potential of spirulina, a highly
regarded superfood known for its exceptional nutritional composition and environmental sustainability. Through an
extensive analysis of market trends, consumer preferences, and driving forces behind demand, the study offers valuable
insights into the commercial viability and growth prospects of spirulina-based products. By examining market
segmentation, consumer behaviour, competitive landscapes, and strategic recommendations, the paper presents a
holistic understanding of spirulina's market dynamics, aiming to guide stakeholders in effectively navigating and
capitalizing on this burgeoning market. Overall, "A Study of Market Potential for Spirulina" serves as a comprehensive
resource for stakeholders seeking to harness the full potential of spirulina within the global marketplace.
Title: Unveiling the Market Potential of Spirulina: A Comprehensive Analysis

I. INTRODUCTION

In recent years, spirulina has risen to prominence as a leading contender in the realm of superfoods, drawing global
attention for its exceptional nutritional profile and perceived health benefits. Boasting a rich array of essential nutrients
such as high-quality protein, vital vitamins, and diverse minerals, this small blue-green alga holds immense promise for
both nutritional supplementation and culinary innovation. Moreover, its eco-friendly cultivation methods and potential
for sustainable long-term production underscore its significance as a subject of market research and development. This

Empowering Women through Self-Help Groups: An In-depth Study of Socioeconomic Development & Gender Equality

Tanaya Ajay Mate[1], Dr. Satya Mohan Mishra[2]

MBA Student, Department of Business Administration and Research, Shri Sant Gajanan Maharaj College of
Engineering, Shegaon, India

Department of Business Administration and Research, Shri Sant Gajanan Maharaj College of Engineering,
Shegaon, India

ABSTRACT: Self-help groups (SHGs) have been a powerful tool for socioeconomic development in many
communities across the world when it comes to empowering women. This research explores the complex effects of
Self-Help Groups (SHGs) on women's empowerment and the overall socioeconomic environment. The study
investigates how SHGs promote empowerment by a thorough evaluation of the literature, qualitative interviews, and
quantitative analysis. These mechanisms include the development of social capital, improved decision-making skills,
and economic independence. Additionally, it looks on how women's empowerment affects homes and communities as a
whole, improving things like health outcomes, educational attainment, and general economic success. This research
offers recommendations for policymakers, non-governmental organizations, and community leaders to optimize the
transformative potential of SHG interventions. The research has 100 sample size of women working with SHG's in
Khamgaon region. It does this by analysing case studies from a variety of cultural contexts, which sheds light on the
opportunities and challenges related to putting these initiatives into action. In the end, this study emphasizes how
crucial SHGs are to the advancement of gender equality, the reduction of poverty, and sustainable development
worldwide.

A Study of Self-Help Groups and Women Empowerment in a Rural Area of the Akola Region

Poonam P. Parchure, Dr. Satya Mohan Mishra

MBA, Department of Business Administration and Research, Shri Sant Gajanan Maharaj College of Engineering,

Shegaon, India

Department Of Business Administration and research, Shri Sant Gajanan Maharaj College of Engineering,

Shegaon, India

ABSTRACT: Women empowerment stands as a complex concept crucial for achieving gender equality and driving societal progress. Across economic, political, social, and cultural domains, empowering women is imperative for fostering inclusive development. In India, where the significance of women's empowerment is particularly pronounced, Self-Help Groups (SHGs) play a pivotal role in economic advancement, notably in rural areas like Akola.

Economic empowerment for women encompasses equal access to resources, job opportunities, and financial independence. Politically, it involves enhancing women's participation and representation in decision-making processes. Socially, empowerment necessitates challenging ingrained gender norms and stereotypes. Culturally, it requires a shift in attitudes that undermine women's autonomy.

Through primary data collected from interviews with 100 respondents in Akola's rural setting, this research explored various facets of women's empowerment, including financial independence, education, decision-making, and freedom, alongside the challenges faced by SHG members. The study revealed a robust correlation between SHGs and women's empowerment. It verified that SHGs effectively encouraged women's engagement across different spheres, enhancing their confidence and societal standing.

Impact of Pradhan Mantri Ujjwala Yojana in Buldhana District

Trupti Sunil Jamode, Dr. S.M. Mishra

MBA Final Year Student, Department of Business Administration and Research, Shir Shant Gajanan Maharaj Collage

of Engineering , Shegaon, India

Professor, Department of Business Administration and Research Shir Shant Gajanan Maharaj College of Engineering

Shegaon, India

ABSTRACT: The Pradhan Mantri Ujjwala Yojana in India aims to connect women from Below Poverty Line (BPL) families to LPG. The scheme aims to provide 8 billion LPG connections by March 2020. The Union Budget for FY 21-22 includes provisions for an additional 1 crore connections, with special accommodations for immigrant families. The scheme has improved access to cleaner cooking fuels, benefiting over 14.6 million BPL families and expanding to include 80 million poor households.

This research methodology uses stratified random sampling to ensure a representative sample for the Pradhan Mantri Ujjwala Yojana (PMUY), which connects LPG to women who meet eligibility requirements based on socioeconomic status. The study uses a descriptive method, focusing on the Buldhana region, with a final sample of 100 respondents. The research employs a mixed-methods approach, using semi-structured interviews and quantitative questions to analyze data. Primary data is collected through questionnaires, interviews, observations, and direct communication, while secondary data is gathered from internal and external sources such as government publications, online websites, and books and online databases.

An Investigation into Factors Affecting Financial Exclusion in Rural Areas

Vitthal Dnyaneshwar Ramekar, Dr.Satya Mohan Mishra

MBA Student, Department of Business Administration and Research, Shri Sant Gajanan Maharaj College of Engineering, Shegaon, India

Department of Business Administration and Research, Shri Sant Gajanan Maharaj College of Engineering, Shegaon, India

ABSTRACT: This study delves into the complexities of financial exclusion in rural India, focusing particularly on the challenges faced by marginalized communities, including farmers. It highlights the critical role of financial literacy in accessing formal financial services and emphasizes the gap in specialized training programs that contributes to the widespread financial illiteracy. Without a universally accepted definition of financial literacy, efforts to improve it and the benefits it can bring in terms of financial inclusion are hindered. The research underscores the importance of financial inclusion initiatives in reducing inequality and stimulating economic growth. Through an examination of financial literacy, family and economic development, and personality traits, the study aims to understand the impact of financial inclusion on rural demographics. It sheds light on the urgent need for enhanced access to banking and credit services, and for broadening the understanding of financial products among India's rural population. By addressing these issues, the study suggests pathways to improve the socio-economic conditions of rural communities through greater financial inclusion.

Market potential of the Organic Food in Maharashtra region (Vidarbha)

Shubham Kishor Gade, Dr. Satya Mohan Mishra

MBA Student, Department of Business Administration and Research, Shri Sant Gajanan Maharaj College of Engineering, Shegaon, India

Assistant Professor, Department of Business Administration and Research, Shri Sant Gajanan Maharaj College of Engineering, Shegaon, India

ABSTRACT: The Indian food product production and consumption is a very vast and diversified, changing consumption differing from region to region. We are trying to extract some qualitative data from this research. The new age of the internet is also affection the buying behavior of the consumers. It will be showing real world scenario. The consumer preference towards the organic food products. For the data collection a google form were floated through 117 Indian consumers in the region of Maharashtra. The increasing health coercers among the consumers would be the mail motive to switch towards the organic food products. This research also helps to identifies the main reason for the slow growth among consumer. The data analysis reveals a strong positive sentiment towards organic food products, with a majority of respondents believing in their health benefits and quality. However, affordability remains a concern. Dissatisfaction with conventional food is evident, particularly regarding taste and lack of local sourcing. Addressing affordability and promoting local sourcing are key to meeting consumer demands and maintaining competitiveness in the market.

The Study on Analyzing the Impact of Social Media on Consumer Buying Behavior in the Khamgaon Region

Nagesh Dinkar Banait, Dr. Satya Mohan Mishra

Student MBA Department of Business Administration and Research Shri Sant Gajanan Maharaj College of
Engineering, Shegaon, India

Department of Business Administration and Research Shri Sant Gajanan Maharaj College of Engineering,
Shegaon, India

ABSTRACT: The main focus of this research is the impact of social media sites like Facebook, Instagram, LinkedIn, and Twitter on customer preferences and purchasing decisions in the Khamgaon Region. Today's consumers are greatly influenced by social media, so it is important to carefully consider how social media affects their decision to buy. With the use of a mixed-approaches methodology that integrates qualitative and quantitative analysis, this study attempts to explore the complex relationship between social media usage and consumer behavior. The study carefully examines how social media influences consumers' decision-making processes, with goals and objectives that are well-defined. In order to help businesses better align their marketing plans with the tastes and behaviors of consumers in the Khamgaon Region, the results are intended to provide actionable insights. The methods by which social media influences purchase decisions are uncovered in this research, contributing to the body of knowledge already available on consumer behavior.

Study on Inclusive Growth of Women's Empowerment Challenges and Opportunities at Padegaon, Chhatrapati Sambhaji Nagar

Sneha B. Gaikwad[1], Dr. S.M. Mishra[2]

Student, Shri Sant Gajanan Maharaj College of Engineering, Shegaon, India

Asst. Professor, Shri Sant Gajanan Maharaj College of Engineering, Shegaon, India

ABSTRACT: Women's Empowerment refers to the process of enabling women to have control over their lives, exercise their rights, and achieve their full potential in society. It involves providing equal opportunities in education, employment, healthcare, and decision-making, as well as challenging and changing gender norms and stereotypes that limit women's opportunities and choices. Women's empowerment in rural areas is vital for economic development, poverty reduction, community development, gender equality, and resilience to climate change.

Women's empowerment faces challenges such as cultural norms, limited access to education and resources, and gender-based discrimination. However. Opportunities for growth include education initiatives, economic empowerment programs, advocacy for legal and social reforms, and the promotion of women's leadership roles.

I. INTRODUCTION

International Journal of Research Publication and Reviews

Navigating the Workplace Upheaval and its Impact on Employee Retention and Turnover

¹Vashishtha Diwansingh Thakur and ²Dr. S.M. Mishra

¹MBA Final Year Student Department of Business Administration and Research , Shri Sant Gajanan Maharaj College of Engineering , Shegaon
²Professor, Department of Business Administration and Research Shri Sant Gajanan Maharaj College of Engineering Shegaon
Contact:-1 8421783767, 29405105291

ABSTRACT

In today's dynamic organisational landscape, where workforce stability is crucial for sustained success, the phenomenon of workplace upheaval significantly impacts employee retention and turnover. This research paper seeks to comprehensively explore the multifaceted implications of this upheaval, particularly focusing on its ramifications in industries characterised by high turnover rates, such as IT recruitment.

Beginning with a thorough examination of the concept of employee retention, the paper elucidates its importance as a cornerstone of organisational success, emphasising its role in fostering employee engagement, satisfaction, and long-term commitment. Factors influencing retention, including job satisfaction, company culture, and employee engagement, are identified as critical determinants, shaping organisational strategies to mitigate turnover.

Key themes explored include the effects of workplace upheaval on employee morale, job satisfaction, and commitment to the organization. Additionally, the study investigates the role of leadership, communication, and organizational culture in mitigating or exacerbating turnover during times of change. Furthermore, it examines the effectiveness of retention strategies implemented by organizations and identifies best practices for fostering resilience and adaptation among

International Journal Of Multidisciplinary Research In Science, Engineering and Technology (IJMRSET)

An In-depth Analysis of Financial Literacy's Influence on Investment Behavior

Siddheshwar Dilip Parihar, Dr. Satyamohan Mishra

Department of Business Administration and Research, Shri Sant Gajanan Maharaj College of Engineering,

Sheagon, India

Department of Business Administration and Research, Shri Sant Gajanan Maharaj College of Engineering,

Sheagon, India

ABSTRACT: Investment behavior & financial literacy are increasingly recognized as critical factors in individuals' ability to make informed financial decisions, particularly in the realm of investments. Using a combination of theoretical frameworks and empirical studies, this paper explores the various dimensions of financial literacy and its impact on investment behavior across different demographic groups and socio-economic backgrounds. Furthermore, it examines the mechanisms through which financial literacy influences investment decision-making, including risk perception, investment knowledge, and behavioral biases. The findings suggest that higher levels of financial literacy are associated with more prudent investment behavior, such as diversification, risk management, and long-term planning. However, significant disparities exist in financial literacy levels, leading to differential investment outcomes among various segments of the population. Addressing these disparities through targeted financial education initiatives is crucial for enhancing overall investment behavior and financial well-being. This paper contributes to the existing

A study of factors and levels of satisfaction of employees in banking sector of Buldhana region

Harshali Shantaram Khandagale[1], Dr. Wechansing Zyamsing Suliya[2]

Student, MBA, Department of Business Administration and research, Shri Sant Gajanan Maharaj College of Engineering, Shegaon, India

Department of Business Administration and research, Shri Sant Gajanan Maharaj College of Engineering, Shegaon, India

ABSTRACT: This paper analyses the job satisfaction among banking employees. Factors which mostly influenced the job satisfaction are Job security, job rotation, job enrichment, salary, promotion, working condition, nature of work, benefits, relationship with co-workers, supervision support, demographic factors, working experiences, quality of management, attitude of employee, career opportunities, communication, higher education level, motivation, long term employment. Some other factors are style, Culture, Job Environment, Employee Improvement, age, gender. The success of an organization only depends upon the satisfaction of its employees. Information is collected from various research papers according to their point of view towards the job satisfaction of employees. Factors that are most influencing are taken considered. An analysis is also done through the surveys in different Banks.

Study of the Work-Life Balance and Satisfaction of Employees in the Banking Sector in Akola District

Aishwarya V. Tayade[1], Dr. Wechansing Suliya[2]

Student, Department of Business Administration and Research, SSGMCE, Shegaon, India[1]

Assistant Professor, Department of Business Administration and Research SSGMCE Shegaon, India[2]

ABSTRACT: This study investigates the work-life balance and satisfaction levels among employees working in the banking sector within Akola District, Maharashtra, India. With the increasing importance of work-life balance in organizational settings and its impact on employee satisfaction and overall productivity, this research aims to provide insights specific to the banking industry in a regional context. Employing a mixed-method approach, the study employs quantitative surveys and qualitative interviews to gather comprehensive data. The quantitative aspect involves administering structured questionnaires to bank employees, focusing on demographic details, perceptions of work-life balance, job satisfaction, and related factors. The findings of this research are expected to contribute to the existing literature on work-life balance and employee satisfaction, providing valuable insights for banking sector management in Akola District and offering recommendations for enhancing work-life balance policies and practices to promote employee well-being and organizational effectiveness.

A Study on Satisfaction and Consumer Behaviour for Amul Milk in Buldana Region

Swapnil G. Ikhare, DR.W.Z. Suliya

PG Student, Dept. of Business Administration and Research, S.S.G.M.C.E Shegaon, Maharashtra, India

Associate Professor, Dept. of Business Administration and Research, S.S.G.M.C.E Shegaon, Maharashtra, India

ABSTRACT: This paper describes the case study of the Amul milk dairy cooperative, Amul, in buldana, which has developed a successful business model. It was primarily responsible, through its innovative practices, for buldana to become the world's largest producer of milk. The paper draws various insights from Amul 's experience that can be useful to cooperatives around the world as well as to companies involved in doing business in broad emerging markets such as buldana. Most of these have underdeveloped markets and fragmented supply bases. Market failures are high for many of these small producers. On the other hand, the size of both markets and suppliers is very large. As a result, firms that identify appropriate business strategies that take these characteristics into account are more likely to succeed in these markets. The following is a key lesson from Amul 's success: companies in such environments must simultaneously build markets and suppliers to synchronize demand and supply planning, establish or become part of the

A Study on Impact of Social Media on Recruitment Process of Applicant's in Buldhana Region

SAMRUDDHI.D. PURKAR[1], DR. PROF. WECHANSINGH SULIYA[2]

Student, Department of Business Administration and Research, Shri Sant Gajanan Maharaj College or Engineering Shegaon, India[1]

Assistant Professor, Department of Business Adminstration And Research, Shri Sant Gajanan Maharaj College or Engineering Shegaon, India[2]

ABSTRACT: In recent years, social media has significantly impacted the recruitment landscape, revolutionizing how recruiters connect with potential candidates. Platforms such as LinkedIn, Facebook, Twitter, and Instagram have widened the reach of recruitment efforts, allowing for more personalized engagement and relationship-building.

The expanded access to a diverse pool of candidates through social media has enhanced the efficiency and cost-effectiveness of recruitment processes. Employers can leverage these platforms to identify, assess, and engage with

A Study on Employee Engagement with Special Reference to Banking Sector

Padmini Madhav Ingole [1], Dr.Wechansing Suliya [2]

Student, Department of Business Administration and Research, Shri Sant Gajanan Maharaj College of Engineering, Shegaon, Maharashtra, India[1]

Assistant Professor, Department of Business Administration and Research, Shri Sant Gajanan Maharaj College of Engineering Shegaon, Maharashtra, India[2]

ABSTRACT: Now a day's sorely interactive business environment, the role of "Employee Engagement" (EE) is an emerging topic existence studied with distinguishing conceptualizations and has become an important issue as employee turnover rises. This research project delves into the dynamics of employee engagement within the banking sector, aiming to understand its current state and identify influential factors. Through a comprehensive analysis, the study benchmarks against industry standards while actively involving employees in the process. Additionally, it evaluates the efficacy of existing engagement initiatives and gauges employee satisfaction with the current systems. Drawing on empirical research and data-driven insights, the study develops enhancement strategies and proposes initiatives to bolster employee engagement. By shedding light on these aspects, the research contributes valuable insights for HR practitioners and organizational leaders, offering pathways to cultivate a more engaged and thriving workforce in the banking industry.

A Study of Market Potential Analysis of E-Bike in Shegaon Region

Harshal Gawai[1], Wechansing Suliya[2]

MBA Final Year Student, Department of Business Administration and Research, Shri Sant Gajanan Maharaj Collage of Engineering, Shegaon, India[1]

Professor, Department of Business Administration and Research, Shri Sant Gajanan Maharaj Collage of Engineering, Shegaon, India[2]

ABSTRACT: This research paper aims to analyze the market potential of e-bikes in the Shegaon region. E-bikes have gained popularity worldwide as an eco-friendly and efficient mode of transportation. However, their adoption and acceptance vary across different regions. This study uses a mix of qualitative and quantitative research methods to understand the factors influencing the market potential of e-bikes in Shegaon. Data was collected through surveys and interviews with residents and industry experts. The findings suggest a growing interest in e-bikes in Shegaon, driven by factors such as environmental concerns, traffic congestion, and the desire for a cost-effective transportation option. The paper concludes with recommendations for businesses and policymakers to capitalize on the market potential of e-bikes

A Study of Work Life Balance and Stress Management Approach of Working Women in Khamgoan Region

Pallavi Ravindra Sabe[1], Dr. Wechansing Suliya[2]

Student, Department of Business Administration and Research, Shri Sant Gajanan Maharaj College of Engineering

Shegaon, Maharashtra, India[1]

Associate Professor, Department of Business Administration and Research, Shri Sant Gajanan Maharaj College of

Engineering Shegaon, Maharashtra, India[2]

ABSTRACT: Careers and goals are most important factors in life. Most of the women doing work for financial support their family. Today change economic conditions. Work life balance is most important crucial concept today work. In organization employee challenges balance of personal life and professional life, Specially women are more stressed of work life balance.

Today era human get more education and he want financial independence, and hence reason more women work in organization. This study explores how working women handle the balance between work and personal life, and how they manage stress. Through surveys and questionnaires, we gathered data from 100 women in various organizations

A Study of Mechanization on Agriculture Business in Akola Region

Dhanashree .S. Deshmukh , Prof Wechansing Suliya

Dept. of Business Administration and Research, S.S.G.M.C.E Shegaon, Maharashtra, India.

ABSTRACT: This study explores the complex effects of mechanization on the Akola region's agricultural industry. There have been significant changes in the agricultural landscape as a result of the quick integration of mechanization into farming methods. The objective of this research is to provide a thorough analysis of the effects of automation on important factors such environmental sustainability, labor dynamics, profitability, and productivity.

The objective of this research is to provide a thorough analysis of the effects of automation on important factors such environmental sustainability, labor dynamics, profitability, and productivity. Using a mixed-methods approach that includes quantitative analysis, interviews, and surveys, the research seeks to understand the perspectives of the local farmers, identify the economic effects of automation, and assess its long-term sustainability in the area.

This study provides nuanced perspectives to inform policymakers, agricultural stakeholders, and practitioners about the complexities surrounding the adoption and management of mechanization in the Akola region, thereby facilitating more informed decision-making processes. It does this by synthesizing empirical evidence and qualitative insights.

Comparative Analysis of Amazon and Flipkart with Special Reference to Buldhana Region

Vaishanavi Vaishanav, Dr. Wechansing.Z. Suliya

Student, Shri Sant Gajanan Maharaj College of Engineering, Shegaon, India

Asst. Prof., Shri Sant Gajanan Maharaj College of Engineering, Shegaon, India

ABSTRACT: This study conducts a comparative analysis between two leading e-commerce platforms, Amazon and Flipkart. Utilizing a mixed-method approach, it gathers primary data through online questionnaires distributed to customers in the Khamgaon region, targeting employees from various companies. Additionally, secondary data is collected through literature review, company reports, and market research reports. The findings provide a comprehensive analysis of Amazon and Flipkart, covering aspects such as user experience, product range, pricing, customer satisfaction, and brand perception. This study aims to offer valuable insights for consumers, businesses, and policymakers, facilitating informed decision-making in the dynamic e-commerce landscape.

Weather and Climate Variability Impact on Farmer's Financial Planning: A Longitudinal Study in Khamgaon

[1]Shambala Rameshwar Mahokar, [2]Prof. Vishal V. Patil

[1]Student, Department of Business Administration and Research, Shri Sant Gajanan Maharaj College of Engineering, Shegaon, India

[2]Assistant Professor, Department of Business Administration and Research, Shri Sant Gajanan Maharaj College of Engineering, Shegaon, India

ABSTRACT: This research paper aims to investigate the impact of weather and climate variability on the financial planning of farmers in khamgaon. The study seeks to analyse the relationship between unpredictable changes in weather patterns and the financial stability of farmers, with a focus on how these variations influence their planning and decision-making processes. The financial planning of farmers, leading to uncertainties in crop production, income fluctuations, and increased agricultural input costs. As a result, farmers face challenges in efficiently allocating resources and managing risks, which ultimately impact their financial stability. This research aims to provide valuable insights into the implications of weather and climate variability on farmer's financial planning in Khamgaon, serving as a basis for policy recommendations and interventions to support the resilience and sustainability of agricultural

Navigating the Digital Divide: Challenges Faced by Senior Citizens in Digital Banking Adoption

Shraddha R. Gondchwar, Prof. Vishal V. Patil

Student, Shri Sant Gajanan Maharaj College of Engineering, Shegaon, India

Asst. Professor, Shri Sant Gajanan Maharaj College of Engineering, Shegaon, India

ABSTRACT: The aim of these research paper is to navigating the digital divide challenges faced by senior citizens in digital banking adoption. By studding this topic senior citizens will get to know how to reduce their problems. The age of senior citizen is considered in research are 60 or above 60. This research is descriptive type of research and for research use simple random sampling technique and sample size are limited is 100 sample. This result shows the variety of view point of senior citizens related to digital banking services. Some senior citizens view point in variable of digital banking and some are opposite to digital banking to find out that unfavorable view towards digital banking this research is help to identify and identify the solution on that. As digital banking becomes increasingly prevalent in

The Influence of Fintech on Investment Patterns of Salaried Individuals

[1]Kunal Sanjay Bhise, [2]Vishal Vinayakrao Patil

Department of Business Administration and Research, Shri Sant Gajanan Maharaj College of Engineering, Shegaon,

Maharashtra, India

Department of Business Administration and Research, Shir Sant Gajanan Maharaj College of Engineering, Shegaon,

Maharashtra, India

Abstract: This study investigates how salaried persons in Khamgaon use fintech services in relation to their investment habits. It evaluates their familiarity with, awareness of, and utilization of fintech investing services. The study also looks at the demographic, socioeconomic, and behavioral aspects of fintech adoption. It contrasts risk tolerance and investment diversification using fintech and conventional approaches. It also assesses fintech's contribution to financial inclusion and its effect on investment performance. The report highlights obstacles to the adoption of fintech and offers suggestions to legislators and fintech companies. This research advances our understanding of fintech's impact on

Role of Online Job Portals in Shaping Candidates' Job Search Behavior

[1]Vaishnavi Manish Hiwrale, [2] Prof. Vishal V. Patil

[1]Student, Department of Business Administration and Research, Shri Sant Gajanan Maharaj College of Engineering Shegaon, India

[2]Assistant professor, Department of Business Administration and Research, Shri Sant Gajanan Maharaj College of Engineering Shegaon, India

ABSTRACT: In the digital age, technological advancements have significantly changed many facets of our lives, including how we obtain and maintain employment. The way people hunt for work has drastically altered as a result of the internet and online job sites. These days, people can use websites to speak with employers directly about employment openings rather than relying just on asking about or checking in newspapers. For many, it has made looking for a job easier and more convenient. The objective of this research study is to present a comprehensive analysis of how Internet job portals impact the candidate recruiting and selection process. The study aims to investigate the following areas: the development of online job portals; factors influencing candidates' use of these portals; candidates' perceptions of the benefits and drawbacks of these platforms; candidates' trust in these platforms; and candidates' influence on job preferences and choices. With the widespread use of technology today, everything is easier to understand. Technology affects every facet of human life. Nowadays, it's easier than ever to find a job thanks to

---

International Journal of Research Publication and Reviews

"Employee Engagement Strategies for Enhancing Productivity"

[1]Revati S. Mahalle, [2]Prof. Vishal V. Patil

[1]Student, Department of Business Administration and Research, Shri Sant Gajanan Maharaj College of Engineering, Shegaon.
[2]Assistance professor, Department of Business Administration and Research, Shri Sant Gajanan Maharaj College of Engineering, Shegaon.
Email: [1]revati.mahalley18@gmail.com, [2]vvpatil@ssgmce.ac.in
Contact no.: [1]9021072248, [2]9422864248

ABSTRACT:

This study explores into the impact of employee engagement initiatives on worker efficiency in modern workplaces. Through a synthesis of literature and empirical evidence, it aims to unveil the effectiveness of various engagement strategies in boosting employee performance. Quantitative analysis will explore correlations between engagement activities and productivity, job satisfaction, and retention rates, while qualitative insights will offer a deeper understanding of employees' perspectives. The research will scrutinize potential moderating factors like organizational culture and leadership style. Ultimately, the findings are expected to inform HR practices, guiding organizations in developing strategies to enhance engagement, productivity, and competitiveness.

Channel Optimization Strategies: A Catalyst for Enhanced Supply Chain Integration and Enterprise Performance

Arati G. Tayade, Prof. Vishal V. Patil

Student, Department of Business Administration and Research, Shri Sant Gajanan Maharaj College of Engineering, Shegaon, India

Assistant Professor, Department of Business Administration and Research, Shri Sant Gajanan Maharaj College of Engineering, Shegaon, India

ABSTRACT: Distribution channels, often known as pathways, are the routes that things take from manufacturer to consumer. This is the focus of the investigation. It investigates the various types of these pathways and their mechanics, focusing on the role of intermediates in facilitating the process. The expanding importance of electronic channels for goods sales is also discussed. A supply chain can be conceived of as a vast network that includes all of the firms, personnel, and tasks required to transport an item from its place of manufacture to its point of sale. This includes every

Exploring the Challenges and Opportunities of E-commerce Implementation in Small Businesses: Insights from Shegaon

[1] Vaibhav Tejrao Dali, [2] Vishal Vinayakrao Patil

Department of Business Administration and Research, Shri Sant Gajanan Maharaj College of Engineering, Shegaon, India

Department of Business Administration and Research, Shri Sant Gajanan Maharaj College of Engineering, Shegaon, India

ABSTRACT: The research investigates the adoption and utilization of eCommerce technologies among small businesses in the Shegaon region. With the rapid digitization of commerce globally, understanding the local dynamics of eCommerce implementation in small enterprises is essential for both academic research and practical implications. The research employs a mixed-methods approach, combining surveys and interviews to gather data from small business owners in the Shegaon area. Key factors such as technological infrastructure, resource constraints, market demand, and

Assessment of Stress Management Techniques Utilized By College Students: A Quantitative Study

Samrudhi S. Raut, Prof. Vishal V. Patil

Student, Shri Sant Gajanan Maharaj College of Engineering, Shegaon, India

Assistant Professor, Shri Sant Gajanan Maharaj College of Engineering Sgegaon, India

ABSTRACT: This study investigates the stress management strategies employed by college students, seeking to assess their effectiveness through a comparative analysis. A mixed-methods approach was adopted, with quantitative surveys and qualitative interviews given to a diverse group of college students. Five major solutions emerged: mindfulness practices, physical activity, time management skills, social support networks, and cognitive-behavioral therapy. The findings revealed disparities in the adoption and utility of these strategies across demographic groups and academic disciplines. Furthermore, significant associations were discovered between the employment of various strategies, levels of perceived stress, and academic accomplishment. The findings highlight the need for customized interventions and support mechanisms to meet the diverse stress management needs of college students, hence increasing their overall well- being and academic performance.

Comparative Study of Job Satisfaction of Working Women in Government Jobs and Rivate Jobs Mlkapur

[1]Madhuri G.Sumare, [2]Prof. Vishal V. Patil

[1]Student, Department of Business Administration and Research, Shri Sant Gajanan Maharaj College of Engineering, Shegaon, India

[2]Assistance Professor, Department of Business Administration and Research, Shri Sant Gajanan Maharaj College of Engineering, Shegaon, India

ABSTRACT: The aim of the present study is to compare job satisfaction of private and government sector managers. For fulfillment of this study we comprised total 120 managers and divide them into two groups of private (60) and public sector managers (60). For assessing job satisfaction of managers job satisfaction scale constructed and standardized by S.K Srivasava (1996) administered on them. The scale measure nine dimension of job satisfaction namely; salary pay, nature of work, job security, advancement, working conditions, communication, union,

A Study on Factors Influencing Buying Behavior of Graduate and post- Graduate Students towards Laptop Purchase with a Special Reference to Shegaon Region

Pratik S. Shegokar, Dr. Billal Husain

PG Student, Dept. of Business Administration and Research, S.S.G.M.C.E Shegaon, Maharashtra, India.

Assistance Professor, Dept. of Business Administration and Research, S.S.G.M.C.E Shegaon, Maharashtra, India.

A B S T R A C T: This study investigates the factors that impact the purchasing behavior of graduate and post-graduate students in the Shegaon region when it comes to buying laptops. The research aims to identify key influencers in the decision-making process, providing valuable insights into the preferences and considerations of this target demographic.

KEYWORDS: Buying behavior, graduate students, post-graduate students, laptop purchase, Shegaon region, influencing factors.

A Study on Factors Influencing Saving & Investment Decisions of Salaried individuals with a special Reference to Akola Region

Arti Ananda Jamnik[1], Dr. Bilal Husian[2]

Student, Shri Sant Gajanan Maharaj College of Engineering, Shegaon, India[1]

Asst. Prof., Shri Sant Gajanan Maharaj College of Engineering, Shegaon, India[2]

ABSTRACT: The aim of these research paper is to study on factors influencing saving & Investment decisions of salaried individual with a special reference to Akola region. By studding this topic individuals will get to know which factors are influencing their saving and investment pattern. This analysis focuses on salaried individuals, as their needs and wants increase with age. This research is descriptive type of research and for research use simple random sampling technique and sample size are limited is 100 sample. This result shows the variety of view point of salaried individuals in the Akola region make decisions about saving and investing their money. The study wants to understand what

A STUDY ON HUMAN RESOURCE MANAGEMENT PRACTICES AT A STRATEGIC BUSINESS UNIT IN KHAMGAON REGION

Vaishnavi Panchbhai[*1], Bilal Husain[*2]

[*1]MBA 2nd Year, Shri Sant Gajanan Maharaj College Of Engineering Shegaon, India.

[*2]Assistant Professor, Shri Sant Gajanan Maharaj College Of Engineering Shegaon, India.

ABSTRACT

This study examines the human resource management (HRM) practices implemented at a strategic business unit (SBU) operating within the Khamgaon region. The research investigates the alignment of HRM strategies with organizational objectives and the effectiveness of these practices in fostering employee engagement, performance, and overall organizational success. Using a mixed-methods approach, data was collected through surveys, interviews, and document analysis. The findings reveal a comprehensive framework of HRM practices including recruitment and selection, training and development, performance management, compensation and

A STUDY OF CONSUMER SATISFACTION IN PUBLIC TRANSPORTATION SYSTEM WITH A SPECIAL REFERENCE TO M.S.R.T.C KHAMGAON

Shivani Girjapure[*1], Bilal Husain[*2]

[*1]MBA Final Year Student, Department of Business Administration and Research, Shri Sant Gajanan Maharaj College of Engineering, Shegaon, India.

[*2]Assistant Professor, Department of Business Administration and Research, Shri Sant Gajanan Maharaj College of Engineering, Shegaon, India.

ABSTRACT

This study aims to assess passenger satisfaction with public transportation services in Khamgaon, focusing on aspects such as transport facilities, comfort, and punctuality. The research employs a sample size of 100 respondents, gathered through simple random sampling technique. Data collection primarily utilized a questionnaire distributed among passengers. Both primary and secondary data sources are utilized, including

NAVIGATING THE ACCREDITATION LANDSCAPE: INSIGHT FROM STUDENTS IN RURAL INDIA

¹VISHAL VINAYAKRAO PATIL, ²MUKUL A. BURGHATE, ³OMRAJSHANKARRAO DESHMUKH

¹Assistant Professor, Department of Business Administration and Research, Shri Sant Gajanan Maharaj College of Engineering, Shegaon
²Associate Professor, Dr.Panjabrao Deshmukh Institute of Management Technology and Research, Dhanwate National College, Nagpur
³Principal, Dhanwate National College, Nagpur
E-mail: ¹patil.vishalv@rediffmail.com, ²mukulburghate@gmail.com, ³osdeshmukh2005@gmail.com

Abstract - This study explores the complex viewpoints and first-hand accounts of students from rural backgrounds about the accrediting procedures in higher education. Although accreditation guarantees high-quality instruction, little is known about how students—especially those from underprivileged and rural areas—view and interact with it. This study uses a qualitative research design that includes focus groups and in-depth interviews with a wide range of students from rural origins. The results show that students have a variety of viewpoints regarding accreditation. Some people view accreditation as a mark of authenticity and quality control, giving them trust in the programs and services provided by their educational institution. For these pupils, accreditation is a way to level the playing field and give them access to education on par with that of their metropolitan peers. The findings indicate that different pupils have different opinions about accreditation. Some see accreditation as a sign of legitimacy and quality assurance, which enables them to have faith in their university's courses and

OPHTHALMIC IMAGE

Rhizopus keratitis

Yellambkar, Snehalata; Tamboli, Nikhat I¹; Farheen, Asma; Husain, Bilal²

Author Information ⊘

OPEN

|| Metrics

A 52-year-old man presented with pain, redness, and progressive diminution of vision in the left eye following trauma by a wooden twig 1 week ago. On examination, visual acuity was 1/60 in the right eye (RE) and hand movements close to the face in the left eye (LE). On slit-lamp examination, RE revealed nuclear cataract.[1] LE revealed a corneal ulcer of 6 mm × 4 mm with feathery margins, stromal infiltration, and edema. B-scan ultrasound of LE was noted to be normal. Corneal scraping was sent. The confounding factors were vegetative

Synthesis, Characterization of Gd-doped Ceria Nanocomposites

Dr. M.J. Pawar[a]*, Sagar B. Deshmukh[a], Dr. Shrikant D. Thakre[b], Dr. Anand S. Tale[c]

[a] Department of Chemistry, Laboratory of Material Synthesis, Smt. Narsamma Arts, Commerce and Science College, Kiran Nagar, Amravati (MS).

[b] Dr. Rajendra Gode Institute of Technology & Research, Amravati (MS),

[c] Shri Sant Gajanan Maharaj College of Engineering, Shegaon (MS).

Abstract

In this work, Gd-doped CeO_2 ($Ce_{1-x}Gd_xO_{2-\delta}$; x = 0.0. 2.0, 4.0 and 6.0 wt %) nanocomposites were prepared by EDTA-Glycol method. The influence of Gd doping on the microstructures and the optical and ionic conductivity properties of these nanoparticles has been studied using X-ray diffraction, FTIR, TEM, UV-VIS, SEM-EDS and impedance spectroscopy. It has been found that Gd doping formed a homogeneous solid solution with ceria, with a significative reduction of crystallite size. As compared to the pure ceria an improvement of total conductivity was achieved with a maximum for the highest Gd concentration of 4 wt % in the temperature range of 550–950°C.

1. Introduction

Solid oxide fuel cell (SOFC) is one of the most promising electrochemical devices for clean power generation due to its efficient operation, fuel flexibility (ranging from hydrogen to hydrocarbons and biogas), and relatively lower greenhouse gas emissions [1,2]. Comparable to other types of fuel cells, SOFCs have the advantage of fuel flexibility i.e. are able to work with hydrogen, hydrocarbon reformate and, in some conditions, with hydrocarbon fuels directly [3-5]. Furthermore, SOFCs are highly promising due to their enhanced resistance to fuel contamination and versatility of applicable combustible gases in comparison with other FC types. Presently, solid electrolytes for SOFCs working in medium temperature region (400–800°C) often comprise cerium oxide doped with rare earth oxides [6,7]. Ceria-based electrolytes possess an advantageous combination of high unipolar oxygen

conductivity, chemical stability in carbon- and hydrogen-containing atmospheres and an inertness to electrode materials, which makes them highly promising for medium-temperature fuel cells.

Being comparable with conventionally used zirconia with respect to electric performances, CeO_2-based electrolyte nanomaterials allow for a significant reduction of working temperature for fuel cells, thus providing an increased durability and simplified structure [8,9].

In addition, doped ceria-based electrolyte materials, such as gadolinium-doped ceria (GDC) or samarium-doped ceria, exhibiting an ionic conductivity than YSZ in the temperature range of 600–750°C [10]. However, the functional limitation of doped ceria-based electrolytes is that they exhibit appreciable electronic conductivity at higher temperature (≥ 800°C) and low partial pressure of oxygen at anode side that dictates the operating temperature of the fuel cells [11–15].

Many methods including ultra-sonication, ball milling, microwave, sol–gel, mechanical alloying and chemical-precipitation, etc. for the preparation of nanocomposite materials from the mixed metal oxide precursors. [15-17]. From above all well-known methods, the chemical-precipitation process is used as a competent technique for the production of nanomaterials, owing to effortlessness. This move toward is extra operative for yielding homogeneity, particularly sample without impurities, tiny particle size, and a short period of time. Ceria-based materials are serious candidates with samarium [18-20] or gadolinium [21-25] substitution to increase the vacancy concentration.

In doped ceria, it has been reported that when the dopant ion radius is close to the critical radius (1.038 Å), then the doped ceria exhibits the highest oxygen ion conductivity. For this reason, Gd doped ceria exhibits the highest oxygen ion conductivity among the doped ceria, as radius of Gd^{3+} (1.05 Å) is closer to the critical radius (1.038 Å) [26, 27]. However, the exact composition of CeO_2-Gd_2O_3 system that has maximum oxygen ion conductivity is still not well defined. *Mori* et al. [28, 29] showed the domain structure in rare earth doped ceria grains and suspected that these domains present in grains are responsible for the higher grain conductivity of $Ce_{0.9}Gd_{0.1}O_{2-\delta}$. But, *Kharton* et al. [30] reported the higher total conductivity for $Ce_{0.2}Gd_{0.2}O_{2-\delta}$ which was possibly due to a contribution of grain boundary conductivity. Moreover, although the Gd_2O_3-CeO_2 system has been reported by several authors, few works provide a comprehensive microstructural and electrical analysis of 0, 10 and 20 mol% Gd_2O_3-doped CeO_2, formed by such low temperature, soft chemical preparation routes. In this work, we synthesized $Ce_{1-x}Gd_xO_{2-d}$ (x = 0, 0.1 and 0.2) nanoparticles by

the sol gel combustion route for intermediate temperature electrochemical applications. The synthesized materials are fully characterized by their structural, chemical, microstructural and electrical properties. Gd doped ceria synthesized by solid-state reaction requires high sintering temperature and time. Hence various wet chemical methods have been used for the synthesis Gd doped ceria such as co-precipitation [31], combustion [32, 33], sol-gel [34, 35], hydrothermal [36], EDTA-citrate complexation [37] and micro-emulsion [38]. To the best our knowledge, no reports are available on synthesis of Gd doped ceria by EDTA-Glycol complexation method. Hence in this investigation, we present a systematic study of effect of pH on structural, morphological and electrical properties of Gd doped ceria solid solutions obtained by EDTA-Glycol method.

2. Experimental

2.1 Materials

In this work, for preparation of ceria based nanocomposites, highly pure $Ce(NO_3)_3.6H_2O$ and $Gd(NO_3)_3.6H_2O$ were use as the source of metal ions obtained from Sigma Aldrich. The other chemicals used in synthesis Nitric Acid (HNO_3, 65%, Merck), ethylene diamine tetra acetic acid ($C_{10}H_{16}N_2O_8$; Sigma Aldrich), ethylene glycol ($C_2H_6O_2$; Merck), were used as obtained without further purification.

2.2 Method of Synthesis

The pure and Gd doped CeO_2 materials were used by a modified EDTA-Glycol method [14]. The highly pure $Ce(NO_3)_3.6H_2O$, $Gd(NO_3)_3.6H_2O$ were used as the precursors. These salts were mixed independently in de-ionized water. During meanwhile 2, 4 and 6 wt % of gadolinium nitrate solution were added to the above reaction mixture and continuously stirred for 30 min. The calculated quantity of ethylenediaminetetraacetic acid (EDTA), dilute ammonia and ethylene glycol (EG) was added to the nitrate solution. So formed solution was stirred and kept on a hot plate for heat treatment at 80°C which in turn forms a gel-like mass. The resulted mass was combusted at 300°C for 2 h followed by the calcination at 550°C for 5 h. On calcinations, the obtained ashes were ground in agate mortar to get fine homogeneous powders. Powder materials were uniaxially pressed into pellets with

6 mm of diameter and 2 mm thickness, at 200 MPa. Sintering was performed in air for 10 h at a constant heating rate (CHR) of 2°C/min in between 1150°C to 1350°C.

3. Characterization

Calcined powders were studied by X-ray diffraction (XRD) using a Miniflex 600 diffractometer RIGAKU - Japan (Cu–$K\alpha$ radiation). Data in an angular region of 2θ in the range of 20-80° were collected in a step-scanning mode (0:02 steps with a step-counting time of 2 s). The crystallite size, D, of the calcined powders was estimated using the Scherrer equation:

$$D = \frac{0.9\lambda}{\beta cos\theta} \tag{3.1}$$

Where, D is crystallite size, λ is wavelength of X-rays (1.5418Å), θ is the scattering angle of the main reflection and β is the corrected peak at full width at half-maximum (FWHM) intensity. FTIR of the as-prepared samples were investigated by IR Affinity-1 Shimadzu- Japan. UV-visible spectra of the samples were studied by using UV–1800 Shimadzu- Japan. SEM-EDS studies was performed on Carl Zeiss NTS GMBH, Germany, SUPRA 55. TEM analysis was performed using Transmission electron microscope CM 200 (Philips).

For electrical measurements, impedance spectroscopy was performed on sintered pellets of four samples CE, CG2, CG4 and CG6. The pellets were made by pressing 4 g of powder at 200 MPa in a 25 mm die and were sintered for 6 hours at the temperatures 1150°C and 1250°C. The densities of pellets pressed and sintered at 1250°C for 6 h as described above were determined from their mass and dimensions. For electrical measurements, silver contacts were applied on both the flat surfaces and cured at 500°C for 15 min. An impedance analyzer (KEYSIGHT-E4990A) was used to characterize the impedance spectra of sintered samples in the static ambient atmosphere in the frequency range 20 Hz to 5 MHz from 550 to 950°C. The spectra were fitted using the Zsimpwin software and values for the total, bulk and grain boundary conductivities were noted.

4. Result and discussion

4.1 XRD analysis

Structural Analysis Figure 1 shows the XRD pattern of the prepared cerium oxide sample. All the diffraction peaks of (111) at 28.64°, (200) at 33.27°, (220) at 47.76°, (311) at 56.78°, and (400) at

69.10° were indexed and well matched with standard JCPDS Card No. 65-5923. The patterns of cerium oxide samples confirmed the cubic structure of the material. The sharp and high intense peaks of XRD patterns confirm the high crystalline quality of the samples. The crystallite size of pure cerium oxide was calculated from the diffraction peaks of XRD pattern using Scherer's formula. The average crystallite size was calculated using Scherrer equation were calculated from (111) peak and are presented in Table 1. The size of Gd doped CeO_2 nanoparticles decreased with increasing the concentration of Gd. The average crystallite size of the crystals was found in between 43-45 nm with slight expansion of lattice. The crystallinity of the powder became better during the calcination at 550°C. Crystalline phases corresponding to Gd_2O_3 could not be found for as-prepared powders, indicating the formation of solid solution. A trivial expansion in the lattice constant upon doping has been attributed to the substitution of the smaller Ce^{4+} ion (0.97Å) by the larger Gd^{3+} (1.053Å) ions, which caused strain and as light deformation no the structure. The introduction of Gd^{3+}, ions into Ce^{4+} can cause a small shift in the cerium oxide peaks positions. Since the broadening of peaks could be attributed not only to crystallite size, but also to stresses created in the structure.

Figure (1) XRD patterns of Gd doped CeO$_2$ powders obtained at 550°C.

Figure (2) Plot against Gd concentration (mol%) for lattice parameter of as-prepared ceria-based materials.

Table (1) 2θ (deg.), crystallite size (nm) and d-spacing of pure and Gd-doped CeO₂ nanoparticles.

Sample	Gd (mol%)	2 Theta (deg.)	Crystallite size (nm)	*d*-spacing	*Band Gap (eV)*
C	0.0	28.51	45.15	3.134	2.78
CG2	2	28.49	44.24	3.132	2.65
CG4	4	28.47	42.58	3.130	2.49
CG6	6	28.44	44.17	3.130	2.54

Figure (3) 3.2 Crystal growth as a function of Gd concentration.

Observed results are summarized and compared for better illustration in Figure 3. While the crystal growth was slow until reaching 4 mol% of Gd, at higher concentration the crystal growth was much faster.

4.2 FTIR spectra

Fourier transform infrared (FTIR) spectra of the as-prepared Gd-doped nanocomposites are shown in Figure 4. Some distinctive absorptions peaks were observed at 3436 and 1630 cm^{-1}. Two strong intense bands observed at 3429 and 1624 cm^{-1} of pure and Gd-doped CeO$_2$ samples are attributed to (O–H) vibration modes of (H-bonded) water molecules, which was due to the physically observed water on the sample surfaces [38, 39]. The strong band at 3429 cm^{-1} is attributed to the v (O–H) vibration modes of the water molecules adsorbed physically. In addition, some weaker absorption peaks were also observed at around 2934, 2856, 1369, 1092, and 700 cm^{-1}. The bands observed at 2934 and 2856 cm^{-1} are due to the (C–H) bonds of organic molecules absorbed during the sample preparation and handling [40]. Absorption at 1630 cm^{-1} is assigned to a systematic stretching vibration of the carboxylate (-COO−) group [17]. The peak at around 1092 cm^{-1} indicates the presence of the nitrate ions [18]. The bands observed in the lower frequency region at 700 and 430 cm^{-1} are referred to the characteristic Ce–O vibration [19]. The band at 1369 cm^{-1} is assigned to the stretching vibration of carboxylate salts (COO$^-$) [41, 42]. The band observed at 1092 cm^{-1} due to the Cerium- Oxygen group with a larger double bond nature [43]. Two weaker bands observed at 852 and 735 cm^{-1} are due to Cerium-Oxygen group having a lower double bond nature and of Ce–O–Ce chains asymmetric stretching vibration of metal oxide networks respectively. The strong band noticed at 558 cm^{-1} is due to the symmetrical stretching vibration mode of (Ce–O–Ce) or (Ce–O–Gd) indicating the Gd ions doped Ceria nanoparticles [44]. It is to be noted that the length of the rare-earth metals-oxygen bond changes with dopant concentration. These shifts in peaks confirm the dopant stabilization in the host lattice [45].

Figure (4) FTIR spectra of Gd-doped Ceria nanocomposites.

4.3 UV-VIS studies

The UV-VIS spectroscopic measurement was carried out to investigate the effect of Gd concentration on the optical properties of CeO_2 nanocomposites. Figure 5 shows the UV-VIS absorption spectra recorded for pure and Gd-doped ceria. It can be seen that there is a strong absorption band below 400 nm in the spectra for all the samples, which is due to the charge transfer from O^{-2} (2p) to Ce^{4+}(4f) orbitals in CeO_2 [46]. The optical band gap values for the Gd-doped ceria system can be estimated from the absorption spectra following Tauc's equation [47].

$$\alpha h v = A\left(h v - E_g\right)^n$$

where α is the absorption co-efficient, hv is the photon energy, E_g is the band gap energy, A is a constant and n can have values of 1/3, 1/2, 2, and 3 for the direct forbidden, direct allowed, indirect allowed, and indirect forbidden transitions respectively. The calculated values of E_g for all the as-prepared samples are given in Table 1 Undoped ceria shows the highest band gap value of 2.79 eV, and for Gd-doped ceria the values of the band gap decrease with the Gd concentration. Thus, the absorption spectra of Gd^{3+} doped ceria nanocrystals exhibit red shifts compared to that of pure ceria.

Figure (5) UV-VIS spectra of Gd-doped Ceria nanocomposites.

In CeO_2, all valance Ce states, including the 4f states, are empty, and the system is a wide gap insulator with a measured fundamental band gap of 6.0 eV between the valance and conduction bands; this is formed predominantly by the O^{-2} (2p) to Ce^{4+} (5d) states respectively [48]. However, in our present study, the band gap value of CeO_2 is much lower than 6.0 eV (Table 1). This is because a small amount of Ce^{3+} is present at the surface of CeO_2 and one electron per Ce atom populates a Ce 4f state, resulting in a decrease in the band gap value of ceria [49]. The red shift of the direct band gap may be due to the presence of oxygen defect levels between the O2p and Ce4f levels that capture the excited electrons and decrease the effective band gap [50]. Lastly, the doping of Gd ions creates ground and excited f-energy states in the mid band gap of ceria. These energy states of Gd accept many of the excited electrons coming from the O2p level which leads into the effective reduction in the band gap., i.e. a red shift [51].

4.4 SEM and EDS spectra

The effect sintering temperature on morphology and density cannot be predicted by preliminary analyses because at a comparable density, the microstructure is completely different as visible in Figure 6. At sintering temperatures of 1150 and 1250°C, pure electrolytes have small grains with a similar uneven and rough morphology. These samples are affected by the poorest densification with an inadequate microstructure for the lowest sintering temperatures. By increasing temperature. The microstructure is always revealing small grains, many cracks, and voids, but the morphology became more uniform, and the relative density increases. The addition of Gd, make obvious a change in the

microstructure according to sintering temperature. As reported for sample GC4 in Figure 6 microstructure with clean grain boundaries was formed at 1250°C.

Figure 6 shows SEM micrographs of sintered GC4 samples and EDS analysis of the Gd_2O_3 doped CeO_2 crystals. The average size and size distribution of the synthesized particles were below 10 nm and uniform, respectively. The shape of the synthesized particles was nearly spherical. The spectrum of Gd_2O_3 doped CeO_2 nanoparticles according to a SEM - EDS analysis. The particles show Gd, Ce and O pattern peaks Table 2.

Figure (6) SEM of sample GC4 sintered at (A) 1150°C and (B) 1250°C   **(C) EDAX spectra of sample GC4.**

Table (2) Elemental composition obtained for EDS spectroscopy.

Element	Weight (%)	Atomic (%)
C K	7.20	29.37
O K	10.21	31.37
Cu K	24.63	19.08
Ce K	53.06	18.64
Gd K	4.96	1.55
Total	100.00	

4.5 Electrical Properties

The total resistance (R_T) of as-prepared sample can be obtained by utilizing the impedance spectroscopy at different temperatures. The total electrical conductivity σ_T was then calculated according to the equation,

$$R_T = R_{grain} + R_{grain-boundary} \tag{1}$$

The total electrical conductivity (σ_T) was then determined from the following equation –

$$\sigma = \frac{l}{AR_T} \tag{2}$$

where, l is the thickness and A represents the cross-sectional area of the sample. It is reported that, the conductivity of ceria-based electrolytes in air is based on ionic conductivity and the contribution of electronic conductivity is negligible [52]. In this study, the conductivity of as-prepared samples measured in air was treated as the oxide ionic conductivity only. The ionic conductivity (σ_t) in ceria-based oxides is a temperature dependent and it can be expressed by the following empirical relationship –

$$\sigma_t T = \sigma_o \exp\left(\frac{E_a}{kT}\right) \tag{3}$$

where E_a is the activation energy for conduction, T is the absolute temperature, k is the Boltzmann constant and σ_0 is a pre-exponential factor. The equation can be linearised by plotting a logarithmic relationship between $\log(\sigma_t T)$ and 1000/T (K).

Figure (7) Ionic conductivity of as prepared Gd-doped ceria nanocomposites at different operational temperatures.

Figure (8) Arrhenius plot of ionic conductivity for (I) sample Ce, (II) sample CG2, (III) sample CG4 and (IV) sample CG6.

The Arrhenius plot of ionic conductivity for different dopant concentrations is presented in Figure 8. The plots clearly reveal a linear increase of conductivity with temperature. Conductivity for pure ceria is lowest and tends to increase with Gd concentration up to a maximum at 4 mol% (sample CG4) and when Gd concentration is 6mol%, the conductivity is found to be declined. Conductivity of CG2 is slightly higher than CG6. The activation energy of ionic conductivity calculated from Arrhenius plot are obtained as 0.84 eV, 0.98 eV, and 1.15 eV for CG4, CG2, and for pure-ceria (CE),

respectively; the activation energy of GDC is comparable with reported values [52-58]. The change in the activation energy may be attributed to an order and disorder transition of the oxygen sublattice caused due to successful substitution of Ce^{4+} ions by Gd^{3+} ions [59]. The activation energy is minimum for the SDC. This decrease in activation energy may be due to the presence of attractive interactions between dopant cations and oxygen vacancies [60]. Moreover, an increase in the Gd concentration in the ceria structure, dopant process hinders oxygen arrangement causing an increase in the activation energy and a decrease in the ionic conductivity for the ceria solid solutions. At lower temperatures, the activation energy (E_a) depends on the defect association enthalpy (ΔH_a) and migration enthalpy (ΔH_m) for conduction. At higher temperatures, activation energy is equal to only the migration enthalpy (ΔH_m), because a great part of the oxygen vacancies is free to diffuse [61].

The appearance of high oxygen ionic conductivity in the solid electrolytes is determined by the formation of oxygen vacancies in the CeO_2 matrix when Ce^{4+} is replaced by Gd^{3+} during the dissolution of Gd_2O_3 in the lattice of CeO_2, which can be described by the following quasi-chemical equation [3].

$$Gd_2O_3 \xrightarrow{Ce_2O_3} 2Gd'_{Ce} + 3O_O^X + V_O^{\cdot}$$

Where Gd'_{Ce} is a Gd^{3+} ion replacing Ce^{4+} and yielding a negative charge, $V_O^{\cdot}$ is a positively charged oxygen vacancy compensating the dopant charge, O_O^X is oxygen atom in a regular site with a neutral charge. It was observed that, increased temperature in the range from 570 to 970°C leads to the increase in electrical conductivity of all the samples. In addition, with an increase in the concentration of Gd_2O_3, the specific electrical conductivity of the ceramics increases in the entire temperature range in study. The highest specific electrical conductivity in the temperature range of 550–950°C ($\sigma_t = 3.3 \times 10^{-2}$ Scm^{-1} at 750°C) is observed for the sample CG4 containing 4 mol.% Gd_2O_3.

Table (3) Total ionic conductivity of Nd-doped CeO_2 solid solutions at 750°C.

Sample	Total Ionic Conductivity (Scm^{-1})	Activation energy (eV)
CE	1.02×10^{-6}	0.79
GC2	2.34×10^{-4}	0.87
GC4	3.3×10^{-2}	0.71
GC6	1.43×10^{-3}	0.87

It has been observed that the activation energy decreases with a rise in the dopant concentration as shown in Table 3. The contribution of grain conductivity is a major factor for the total oxide ion conductivity in the doped ceria samples [62]. Thus, the amount of Gd doping affects the conductivity of the ceria. With the ascent in the Gd concentration, a huge expansion in the grain conductivity was seen because of the improvement of the charge transporters emerging from the creation of oxygen vacancies as a result of doping. This leads into the expansion of the crystal structure.

5. Conclusion

The Gd-doped ceria nanocomposites with composition $Ce_{1-x}Gd_xO_{2-\delta}$ (x = 0.0, 2.0, 4.0 and 6.0wt%) were successfully prepared by using a EDTA-glycol method. The XRD, FTIR, UV-visible, SEM–EDS analysis confirmed the formation of the single-phase solid solution. All as-prepared Gd-doped ceria nanocomposites were sintered at the temperatures 1150 and 1250°C. The nanocomposite containing 4wt% Gd showed an essentially upgraded oxide ion conductivity in the order of 3.3×10^{-2} Scm^{-1} at 750°C with a lower activation energy, E_a = 0.71 eV. Thus, Gd-doped ceria nanocomposites might be viewed as a potential electrolyte material for SOFC applications.

6. References

[1] Subotić, V.; Napporn, T.W. Nanostructured metal oxides for high-performance solid oxide fuel cells (SOFCs). In *Metal Oxide-Based Nanostructured Electrocatalysts for Fuel Cells, Electrolyzers, and Metal-Air Batteries*; Napporn, T.W., Holade, Y., Eds.; Elsevier: Amsterdam, The Netherlands, **2021**; pp. 235–261.

[2] Choolaei, M.; Cai, Q.; Horri, B.A. Green synthesis and characterization of nanocrystalline NiO-GDC powders with low activation energy for solid oxide fuel cells. *Ceram. Int.* **2021**, *47*, 32804–32816.

[3] Liang, J. Low temperature fabrication of dense gadolinia-doped ceria electrolyte with enhanced electrical conductivity. Electrochim. Acta **2015**, 178, 321–328.

[4] Rekas, M. Electrolytes for Intermediate Temperature Solid Oxide Fuel Cells. Arch. Met. Mater. **2015**, 60, 891–896.

[5] Mahato, N.; Banerjee, A.; Gupta, A.; Omar, S.; Balani, K. Progress in material selection for solid oxide fuel cell technology: A review. Prog. Mater. Sci. **2015**, 72, 141–337.

[6] Sal'Nikov, V.V.; Pikalova, E.Y. Raman and impedance spectroscopic studies of the specific features of the transport properties of electrolytes based on CeO. Phys. Solid State 2015, 57, 1944–1952.

[7] Egorova, T.L.; Kalinina, M.V.; Simonenko, T.; Shilova, O.A.; Sevastyanov, V.G.; Kuznetsov, N.T. Liquid-phase synthesis and physicochemical properties of xerogels, nanopowders and thin films of the CeO_2–Y_2O_3 system. Russ. J. Inorg. Chem. 2016, 61, 1061–1069.

[8] Egorova, T.L.; Kalinina, M.V.; Simonenko, T.; Shilova, O.A.; Sevastyanov, V.G.; Kuznetsov, N.T. Liquid-phase synthesis and physicochemical properties of xerogels, nanopowders and thin films of the CeO2–Y2O3 system. Russ. J. Inorg. Chem. **2016**, 61, 1061–1069.

[9] Ramos-Alvarez, P.; Villafuerte-Castrejón, M.E.; González, G.; Cassir, M.; Flores-Morales, C.; Chávez-Carvayar, J.A. Ceria-based electrolytes with high surface area and improved conductivity for intermediate temperature solid oxide fuel cells. J. Mater. Sci. **2016**, 52, 519–532.

[10] Steele B C H **2000** Solid State Ionics 1343.

[11] Arachi Y, Sakai H, Yamamoto O, Takedsa Y and Imanishai **N1999** Solid State Ionics 121133.

[12] Eguchi K, Setoguchi T, Inoue T and Arai H **1992** Solid State Ionics 52165

[9] Mogensen M, Sammes N M and Tompsett GA **2000** Solid State Ionics 12963.

[10] Zha S, Xia C and Meng G **2003** J. Power Sources 11544.

[11] Fuentes R O and Baker R T **2008** Int. J. Hydrogen Energy 33 3480.

[12] Namitha R, Radhika D, Krishnamurthy G (**2019**) Hydrothermally synthesized carbon nanotubes for electrochemical hydrogen storage application. Issues Chem Chem Technol 3:30–34.

[13] Dell'Agli G, Spiridigliozzi L, Pansini M, Accardo G, Yoon SP, Frattini D (**2018**) Effect of the carbonate environment on morphology and sintering behaviour of variously co-doped (Ca, Sr, Er, Pr) Samarium-doped ceria in co-precipitation/hydrothermal synthesis. Ceram Int 44:17935–17944.

[14] Ghelich R, Keyanpour-Rad M, Youzbashi AA, Khakpour Z (**2015**) Comparative study on structural properties of NiO–GDC nanocomposites fabricated via electrospinning and gel combustion processes. Mater Res Innov 19:44–50.

[15] Arabaci A (**2018**) Synthesis and characterization of Pr/Gd co-doped ceria by using the citric acid–nitrate combustion method. Solid State Ionov 326:69–76.

[16] Radhika D, Kannan K, Nesaraj AS, Namitha R (**2019**) Facile low-temperature synthesis and application of $La_{0.85}Sr_{0.15}Co_{0.85}Fe_{0.15}O_{3-\delta}$ as superior cathode for LT-SOFCs Using C-TAB as surfactant. Mater Res Innov 10:12.

[17] Radhika Devi, Nesaraj AS (**2014**) Chemical precipitation and characterization of multicomponent perovskite oxide nanoparticles—possible cathode materials for low temperature solid oxide fuel cell. Int J Nano Dimension 5:1–10.

[18] Chaubey, N.; Wani, B.N.; Bharadwaj, S.R.; Chattopadhyaya, M. C. Physicochemical properties of rare earth doped ceria $Ce0.9Ln0.1O1.95$ (Ln = Nd, Sm, Gd) as an electrolyte material for IT-SOFC/SOEC. Solid State Sci. 2013, 20, 135–141.

[19] Yahiro, H.; Eguchi, K.; Arai, H. Electrical properties and reducibilities of ceria-rare earth oxide systems and their application to solid oxide fuel cell. Solid State Ion. 1989, 36, 71.

[20] Anirban, S. K. Dutta, A. Revisiting ionic conductivity of rare earth doped ceria: Dependency on different factors. Int. J. Hydrogen **2020**, 45, 25139.

[21] Huang, W.; Shuk, P.; Greenblatt, M. Properties of sol-gel prepared $Ce_{1-x}Sm_xO_{2-x2}$ solid electrolytes. Solid StateIon.**1997**,100,23.

[22] Yahiro, H.; Eguchi, Y.; Eguchi, K.; Arai, H. Oxygen ion conductivity of the ceria-samarium oxide system with fluorite structure. J. Appl. Electrochem.**1988**,18,527.

[23] Arabaci, A. Effect of Sm and Gd dopants on structural s characteristics and ionic conductivity of ceria. Ceram. Int.**2015**,41,5836.

[24] Steele, B. C. H. Appraisal of $Ce_{1-y}Gd_yO_{2-y/2}$ electrolytes for IT-SOFC operation at 500°C. Solid StateIon.**2000**,129,95.

[25] Butler, V.; Catlow, C.; Fender, B.; Harding, J. Dopant ion radius and ionic conductivity in cerium dioxide. Solid StateIon.**1983**, 8,109.

[26] H. Inaba, H. Tagawa, Solid State Ionics 83 (**1996**) 1−16.

[27]. K. Eguchi, T. Setoguchi, T. Inoue, H. Arai, Solid State Ionics 52 (**1992**) 165−172.

[28] T. Mori, Z. Li, P. Yan, Y. Wu, Z. Li, Mater. Sci. Eng. B 177 (**2012**) 1538−1541.

[29]. T. Mori, J. Drennan, J.H. Lee, J.G. Li, T. Ikegami, Solid State Ionics 154−155 (**2002**) 461−466.

[30]. V.V. Kharton, F.M.B. Marques, A. Atkinson, Solid State Ionics 174 (**2004**) 135−149.

[31] K.C. Anjaneya, J. Manjanna, G. Govindaraj, K.N. Ganesha, J. Alloys Compd. 578 (**2013**) 53−59.

[32] L.D. Jadhav, M.G. Chourashiya, A.P. Jamale, A.U. Chavan, S.P. Patil, J. Alloys Compd. 506 (2010) 739−744.

[33]. R.K. Lenka, T. Mahata, A.K. Tyagi, P.K. Sinha, Solid State Ionics 181 (**2010**) 262−267.

[34]. K.C. Anjaneya, J. Manjanna, G. Govindaraj, K.N. Ganesha, J. Alloys Compd. 585 (**2014**) 594−601.

[35]. K.C. Anjaneya, J. Manjanna, G. Govindaraj, K.N. Ganesha, Physica B 447 (**2014**) 51−55.

[36]. T. Karaca, T.G. Altmcekic, M.F. Oksuzomer, Ceram. Int. 36 (**2010**) 1101−1107.

[37]. S. Li, L. Ge, H. Gu, Y. Zheng, H. Chan, L. Guo, J. Alloys Compd. 509 (**2011**) 94−98.

[38]. J. Chandradass, B. Nam, K.H. Kim, Colloids Surf. A 348 (**2009**) 130−136.

[39] S. Samiee, E.K. Goharshadi, Effects of different precursors on size and optical properties of ceria nanoparticles prepared by micro- wave-assisted method. Mater. Res. Bull. **47**, 1089–1095 (2012).

[40] G. Wang, Q. Mu, T. Chen, Y. Wang, Synthesis, characterization and photoluminescence of CeO_2 nanoparticles by a facile method at room temperature. J. Alloy. Compd. **493**, 202–207 (2010).

[41] S. Phoka, P. Laokul, E. Swatsitang, V. Promarak, S. Seraphin, S. Maensiria, Synthesis, structural and optical properties of CeO_2 nanoparticles synthesized by a simple polyvinyl pyrrolidone (PVP) solution route. Mater. Chem. Phys. **115**, 423–428 (2009).

[42] A.Z. Liu, J.X. Wang, C.R. He, H. Miao, Y. Zhang, W.G. Wang, Synthesis and characterization of $Gd_{0.1}Ce_{0.9}O_{1.95}$ nanopowder via an acetic-acrylic method. Ceram. Int. **39**, 6229–6235 (2013).

[43] R. Tholkappiyan, A. Nirmalesh Naveen, S. Sumithra, K. Vishista, Investigation on spinel $MnCo_2O_4$ electrode material prepared via controlled and uncontrolled synthesis route for supercapacitor application. J. Mater. Sci. **50**, 5833–5843 (2015).

[44] C. Binet, A. Badri, J.C. Lavalley, A spectroscopic characterization of the reduction of ceria from electronic transitions of intrinsic point defects. J. Phys. Chem. **98**, 6392–6398 (1994).

[45] C. Ho, J.C. Yu, T. Kwong, A.C. Mak, S. Lai, Morphology-control- lable synthesis of mesoporous CeO_2 nano- and microstructures. Chem. Mater. **17**, 4514–4522 (2005).

[46] R. Tholkappiyan, K. Vishista, Synthesis and characterization of barium zinc ferrite nanoparticles: working electrode for dye sen‑sitized solar cell applications. Sol. Energy **106**, 118–128 (2014).

[47] Y.-W. Zhang, R. Si, C.-S. Liao, C.-H. Yan, C.-X. Xiao and Y. Kou, J. Phys. Chem. B, 2003, 107, 10159–10167.

[48] S. L. S. Rao, G. Ramdevudu, Md. Shareefuddin, A. Hameed, M. N. Chary and M. L. Ro, Int. J. Eng. Sci. Res. Technol., 2012, 4, 25–35.

[49] 5 E. Wuilloud, B. Delley, W. D. Schneider and Y. Baer, Phys. Rev. Lett., 1984, 53, 202–205.

[50] L. Wu, H. J. Wiesmann, A. R. Moodenbaugh, R. F. Klie, Y. Zhu, D. O. Welch and M. Suenaya, Phys. Rev. B: Condens. Matter Mater. Phys., 2004, 69, 125415.

[51] A. H. Morshed, M. E. Moussa, S. M. Bedair, R. Leonard, S. X. Liu and N. El-Masry, Appl. Phys. Lett., 1997, 70, 1647– 1649.

[52] M. Greenberg, E. Wachtel, I. Lubomirsky, J. Fleig and J. Maier, Adv. Funct. Mater., 2006, 16, 48–52.

[53] M. G. Chourashiya, S. R. Bharadwaj, and L. D. Jadhav, Thin Solid Films 519, 650 (2010).

[54] S. L. Reis, E. C. C. Souza, and E. N. S. Muccillo, Solid State Ionics 192, 172 (2011).

[55] H. Duncan and A. Lasia, Solid State Ionics 176, 1429 (2005).

[56] D. Perez-Coll, P. Nu~nez, J. C. Ruiz-Morales, J. Pe~na-Martınez, and J. R. Frade, Electrochim. Acta 52, 2001 (2007).

[57] A. Jasper, J. A. Kilner, and D. W. McComb, Solid State Ionics 179, 904 (2008).

[57] S. Dikmen, H. Aslanbay, E. Dikmen, and O. S¸ahin, J. Power Sources 195, 2488 (2010).

[58] G. Kim, N. Lee, K. B. Kim, B. K. Kim, H. Chang, S. J. Song, and J. Y. Park, Int. J. Hydrogen Energy 38, 1571 (2013).

[59] H. Inaba, H. Tagawa, Ceria-Based Solid Electrolytes, Solid State Ion. 83, 1 (1996).

[60] K. Zhao and Y. Du, Calcium-doped ceria materials for anode of solid oxide fuel cells running on methane fuel, *J. Power Sources*, 2017, 347, 79.

3. Effect of Noble Metal (Ag) doping on Hydrogen Sensitivity of WO3 Thin Film Sensors

Dr. S. V. Jagtap

Department of Physics, R. D. I. K. & K. D. College, Badnera (Rly), Amravati. (Maharashtra)

Dr. M. J. Pawar

Department of Chemistry, Smt. ACS College, Kiran Nagar, Amravati. (Maharashtra) India

Dr. A. S. Tale

Department of Physics, Sant Gajanan Maharaj College of Engineering, Shegaon. (Maharashtra)

Dr. S. D. Thakre

Department of Physics, Dr. Rajendra Gode Institute of Technology & Research, Amravati.(M.S.)

Abstract

The given workrepresents the modification in hydrogen gas sensitivity of WO_3 based thin films loaded with Ag like noble metals. The samples were characterized by various techniques: like XRD, SEM, TEM and BET to know the stoichiometry, crystal structure, morphology and surface area. The dopants content was varied from 0 to 4 at.% and its effect on structural , morphological and the gas sensing properties have been studied with respect to different operating temperatures.

Keywords: $Ag\text{-}WO_3$, Sol–gel spin coating, H_2 Gas sensor.

1. Introduction

Semiconducting oxide gas sensors have been used to warn of explosive gases since the1960s, but more recently other applications in which semiconducting oxide may be employed as sensor materials have been considered, including detection of air pollutants and improving fuel efficiency in industrial combustion processes. The reducing gas depletes the coverage of adsorbed oxygen ions on the sensor surface and supplies electrons to the conduction band, leading to a fall in resistance [1]. A current goal in sensor research is to improve the sensor selectivity by eliminating similar responses from interfering gases. It has been found that the sensor selectivity and sensitivity may be altered by the addition of second oxide phases and elemental metals [2]. It is well known that the loading of the metal oxide matrix with catalyst nanoparticles (e.g., surface functionalization of the nanostructured metal oxide) may lead to significant improvements in response, selectivity, long-term stability and cross-sensitivity to

ambient moisture. The sensitivity of metal-oxide gas sensors can be substantially improved by dispersing a low concentration of additives, such as Pd [3, 4], Pt [5], Au [6, 7], Ag [8, 9] etc. on oxide surface or in its volume. Although doping has been used for a long time now in preparation of commercial gas sensors, the working principle of additive-modified metal-oxide materials is stillnotcompletely understood. In particular Ag has been widely employed as sensitizer in metal oxide films for developing hydrogen sensors [10-12].

WO$_3$ is a promising hydrogen gas sensing material [13-15]. It has high diffusion coefficient for oxygen vacancies [16]. WO$_3$ shows sensitivity towards oxidizing gases such as NO$_2$, O$_3$, Cl$_2$, however, for reducing gases like H$_2$, CO, NH$_3$etc, surface modification by noble catalyst (Pd, Pt, Au) is essential [17]. Addition of catalyst facilitates the chemical reaction by lowering the activation energy between the surfaces of metal oxide and target gas.

In present work, we have prepared WO$_3$ based thin films by doping the noble metal Ag in the amount of 0-1.5 wt.% in WO$_3$semiconductor. Sol-gel spin coating method was used for preparation WO$_3$based thin films. Scanning electron microscopy (SEM), X-ray diffraction (XRD) and high- resolution transmission electron microscopy (HRTEM) have been used to determine the morphology, phase composition, and microstructure of the layers grown. In order to calculate the sensitivity, the electrical resistance of a sensor was measured in the presence and absence of hydrogen gas at a concentration 30-300 ppm in dry air. The material 0.5 wt% Ag-dope WO$_3$was found to be the optimum composition for the maximum sensitivity and selectivity at an operating temperature 150°C. The cross sensitivity of the sensor was also studied to other gases, including CO, LPG andH$_2$S.

2. Experimental

2.1 Synthesis of Ag-WO$_3$ thin films

Nano crystalline WO$_3$thin films were prepared by a sol–gel spin coating process using of ammonium tungstate, glycerin, ethyl alcohol (C$_2$H$_5$OH) and de-ionized water as precursors. 0.1 M ammonium tungstate was dissolved via 70 mL of pure ethanol and placed in covered flasks. The resulted sol solutions placed in closed flasks and stirred by magnetic stirrers for 3 h and kept at 75˚C for 6. Moreover, glycerin (C$_3$H$_8$O$_3$) was added to a volume ratio of 1:12 in order to eliminate cracks [17]. After refluxing for 48 h at room temperature using a magnetic stirrer, a homogeneous mixture of precursors was formed with hydrolysis and condensation processes. This step was followed by an ageing process by leaving it in open air for 24 h. Pd doped sols

with two different concentrations (2 wt.% and 4 wt.%) were prepared by adding an appropriate amount of silver nitrate ($AgNO_3.2H_2O$, purity–99.97%) in a ammonium tungstate solution in its initial preparation stage. Pure $WO_3$and Ag-doped WO_3thin films were deposited on glass substrates using a sol–gel spin coating process with a spinning speed of 4000 rpm for 40 s. Each deposited layer was pre-sintered at 180˚C for 30 min before depositing the next layer. Post-sintering was done at 450˚C for 4 h. The thickness of the deposited films was measured by using a surface profilometer and was found approximately 100-120nm.

3. Results and Discussions

3.1 X-ray Diffraction Study

Ag doped WO_3 thin films were formed by sol-gel spin coating method. A typical XRD pattern of the WO_3 thin films obtained are shown in Figure 1. It can be indexed to a triclinic WO_3 phase according to the JCPDS card No. 32-1395.

Figure .1 XRD patterns of the Ag -WO₃ thin films with various amounts of Ag; (a) pure WO₃, (b) 0.5 wt% Ag, (c) 1.0 wt.% Ag and (d) 1.5 Wt.% Ag.

Figure 1 shows the XRD patterns of the Ag-WO_3 thin films with various amounts of Ag (0.5–2.0%). One can find that the peaks belonging to WO_3 phase are not changes, whereas a new peak located at 38.1˚, belonging to the (111) deflection of face-centered cubic structured Ag (JCPDS card No. 04-0783), becomes stronger and stronger as the amount of Ag increases, indicating the separation of Ag particles from the host WO_3lattice at higher concentration. The XRD results confirm the formation of metal Ag phase in the Ag-WO_3 samples. The increasing

intensity of the Ag (111) peak indicates that the more the amount of Ag^+ in the precursor, the more the amount of the metal Ag in the Ag-WO_3 films.

3.2. SEM and TEM

Study of surface morphology of WO_3based thin films has been carried out using Scanning Electron Microscope. Figure .2(a) show SEM micrographs of sensing elements of pure $WO_3$and 0.5%Ag -WO_3 thin films prepared through sol-gel method, annealed at temperature 500˚C. Both the micrographs have been taken for the 10.00 Kx magnifications. WO_3manifests beautiful pattern whereas the SEM micrograph of sensing element of Ag doped WO_3manifests clustering and agglomeration of the small sized crystallites. Scanning micrographs show flakes of pure $WO_3$and 0.5%Ag- WO_3 scattered throughout, forming a network of pores that are expected to provide sites for humidity adsorption. The average grain size for the sensing elements of pure $WO_3$and Ag doped WO_3calculated from SEM micrographs are in the range of 40-90nm.

Figure .2(a) SEM micrograph of the (a) pure WO_3 thin film and (b) 0.5%Ag- WO_3.

Figure 2(b) shows transmission electron microscope (TEM) image of prepared 0.5%Ag-WO_3nanocrystalline thin film. TEM image gives a grain size of 40 nm and this is in agreement with X-ray diffraction result. The diffraction pattern illustrating spot patterns of the hexagonal structure of WO_3 indicates that the WO_3 nanoparticles formed using at annealing temperature 500˚C are highly crystalline, which is in good agreement with the X-ray diffraction result.

Figure. 2(b) TEM image of 0.5%Ag-WO$_3$ thin film.

3.3 AFM

3D AFM image of the 0.5%Ag-WO$_3$ film annealed at temperatures ranging from 500C is presented in Figure.3. The surface is made up of grains and voids with dimensions in the range of nanometers. The presence of these voids within the film structure is favorable because they provide direct conduits for gas molecules to flow in from the environment. It can be observed that the grain size of the WO$_3$was found to depend on the annealing temperature.The average grain size found with AFM of threedifferent samples is 67 nm, which agrees well with the value obtained by XRD. The growth of crystallites, observed to be vertical, could be related to the low rate of atom mobility on surface of the substrates.

Figure.3 3D AFM micrograph of 0.5%Ag-WO$_3$ thin film.

3.4 Hydrogen Sensing Measurements

3.4.1 Effect of Ag-doping and Operating Temperature: The effect of Ag-doping on gas sensing properties of the films is studied by making ohmic contacts using high conducting electrodes. The sensors at various operating temperatures are tested for 200 ppm of hydrogen gas at different operating temperature. The sensor resistance is determined, and utilized as the measure of response. At each temperature, before starting the measurements, the sample resistance is measured without the test gas. The resistance of the sensors decreases on exposure to reducinggas.

Figure 4 shows the dependence of the response on the operating temperature for the undoped and Ag-doped WO_3 thin film sensors calcined at 500˚C. Test has been carried out for the 200 ppm hydrogen gas. The response increases with the increase of temperature, because the gas requires enough energy to overpass the barrier between oxygen molecules- adsorbed and electrons from conducting band of WO_3semiconductor [15]. In addition, the gas adsorption and reaction taken place on surface of WO_3need certain activation energy. When temperature increases to 160˚C, a balance between the gas absorption and desorption is reached, the response exhibits a maximum value of the response then decreases with temperature due to the amount of adsorbed gas on material surface will decrease with temperature.

Figure.4 Gas responses of Ag-doped WO₃ thin films.

By comparing the responses of different amount of Ag-doped and undoped WO₃thin film samples at different operating temperature in Figure.4, it can be unambiguously understandable that the response of WO₃thinfilm is improved by adding of Ag. However, the response value fails to persist and declines in the magnitude with the increasing dopant concentration.

H₂ Gas Concentration (ppm)

Figure.5 Sensitivity of 0.5 wt.% Ag-doped WO₃ thin films for various concentration of H₂ in ppm level.

Figure.4 also indicates the effect of Ag doping on response, when the wt.% of Ag is lower than 1 wt.%, the WO₃ has a high specific surface and small particle size that satisfy the requirement of a practical sensor, so the high response is observed at low operating temperature. As it is known, resistance of WO₃ is mostly controlled by inter-grain potential barrier. Taking this into account, one can conclude that the addition of Ag in small concentration lowers the growth of potential barrier height at the inter grain interface, by increasing the chemisorbed oxygen at the WO₃ grain surface. Based on that, incorporation of Ag-ion favour adsorption of atmospheric oxygen species on the thin film surface and thus creates more sensing sites to respond. This also contributes to gas sensing enhancement.

3.4.2 Effect of Gas Concentration: The gas response of the 0.5wt% Ag-doped WO₃thin film sensor to hydrogen gas concentration is shown in Figure.5, where the sensor worked at its own optimum operating temperatures as mentioned above As seen from it, the sensitivity

initially increased slowly with increasing the concentration and then linearly as the gas concentration increased from 250 to 1000 ppm. It is seen that the 0.5wt% Ag-doped WO_3 reaches the saturation value of sensitivity for concentration of 1000 ppm. The sensor is able to detect up to 200 ppm for hydrogen gas with reasonable sensitivity at an operating temperature 150°C.

3.4.3 Response time: Figure A6.6 shows a typical response characteristic of the sensor to 200 ppm hydrogen gas at an operating temperature 150°C. The response time is an important parameter to characterize a sensor. The response time is defined as the time taken to reach 90% of the response (~ 90 seconds) when hydrogen gas is introduced in the chamber. Figure.6 clearly shows that the response is fast with 0.5wt% Ag-doped WO_3 thin film sensor as compared with undoped WO_3 thin films, 1.0wt% Ag-doped WO_3 and 1.5wt% Ag-doped WO_3 thin film sensor thin film sensors. The effect of Ag was thus seen not only in increasing the sensitivity to hydrogen gas considerably but also the rate of response. This kind of sensitization has been well explained by an electronic interaction between the noble metal and the semiconductor oxide [18].

Response Time (sec.)

Figure.6 Response characteristics of undoped and Ag-doped WO_3 thin films to 200 ppm hydrogen gas at 150°C.

4. Conclusions

In this study, Ag-doped WO_3 nanostructured thin films with different dopant amounts are synthesized by sol gel spin coating method. By using X- ray diffraction and electron microscopy studies, it is found that Ag doping can suppress the growth of large WO_3 crystallites and assist in a uniform growth. The gas sensing properties to hydrogen gas is tested and found that 0.5 wt.%

Ag-doped WO_3 exhibit the best gas sensing properties which can be attributable to enhanced capability of adsorbing oxygen by Ag on the surface. Thus the Ag-dopant exhibit excellent sensor response characteristics withfast response and recovery time of 27 sec, even at low hydrogen gas concentration of 400 ppm. This implies a good potential of the Ag-dopant in WO_3, for practical hydrogen sensing applications.

5. References

1. H. Windiscmann H, P. Mark, -A Model for the Operation of a Thin-Film SnOx Conductance-Modulation Carbon Monoxide Sensor‖, J. Electrochem. Soc., 126 (**1979**)627±633.

2. L.D. Birkefeld, A.M. Azad, S.A. Akbar, -Carbon Monoxide and Hydrogen Detection by Anatase Modification of Titanium Dioxide ‖, J. Am. Ceram. Soc, 75 (**1992**) 2964-2968.

3. T. B. Fryberger and S. Semancik, Sens. Actuators, B 2, 305(1990).

4. S. Semancik and T. B. Fryberger, Sens. Actuators, B 1, 97(1990).

5. L. Madler, A. Roessler, S. F. Pratsinis, T. Sahm, A. Gurlo, N. Barsan, and U. Weimar, Sens. Actuators, B 114,283 (**2006**).

6. U.-S. Choi, G. Sakai, K. Shimanoe, and N. Yamazoe, -Sensing properties of Au-loaded SnO_2-Co_3O_4 composites to CO and H_2‖ Sens. Actuators B, 107 (**2006**)397-401.

7. O. Wurzinger and G. Reinhardt, Sens. Actuators, B 103, 104(2006).

8. R. K. Joshi, F. E. Kruis, and O. Dmitrieva, -Gas sensing behavior of $SnO_{1.8}$: Ag films composed of size-selected nanoparticles, Nano part. Res., 8 (**2006**) 797-808.

9. J.Gong, Q.Chen, M.R.Lian, N.C.Liu, R.G.Stevenson, and F.Adami, -Micro machined Nano crystal line silver doped SnO_2H_2S sensor‖, Sens. Actuators B, 114 (**2006**) 32-39.

10. B. Liu, D. Cai, Y. Liu, D. Wang, L. Wang, Y. Wang, H. Li, Q. Li, Q.; T. Wang, -Improved room-temperature hydrogen sensing performance of directly formed Pd/WO3 nan composite‖, Sens. Actuators B: Chem., 193 (2014)28-34

11. J. Kukkola, M. Mohl, A.R. Leino, J. Mäklin, N. Halonen, A. Shchukarev, Z. Konya, H. Jantunen, K. Kordas, -Room temperature hydrogen sensors based on metal decorated WO_3nanowires‖, Sens. Actuators B: Chem.**,** 186 (**2013**)90-95.

12. Z. Wang, Z. Li, T. Jiang, X. Xu, C. Wang, -Ultrasensitive hydrogen sensor based on Pd0-loaded SnO_2electrospun nanofibers at room temperature‖, ACS Appl. Mat.

Interfaces**,** 5 **(2013)**2013-2021.

13. C. Zhang, A. Boudiba, C. Navio, C. Bittencourt, M.G. Olivier, R. Snyders, M. Debliquy, ‐Highly sensitive hydrogen sensors based on co- sputtered platinum-activated tungsten oxide films, Int. J. Hydrogen. Energy, 36 **(2011)**1107-1114.

14. C. Zhang, M. Debliquy, A. Boudiba, H. Liao, C. Coddet, ‐Sensing properties of atmospheric plasma-sprayed WO_3 coating for sub-ppm NO_2 detection‖, Sensors Actuators B, 144 **(2010)**280-288.

15. R. Calavia, A. Mozalev, R. Vazquez, I. Gracia, C. Cané, R. Ionescu, E. Llobet, ―Fabrication of WO3 nanodot-based microsensors highly sensitive to hydrogen, Sensors Actuators B-Chemical,149(2) **(2010)** 352 –361.

16. S.J. Ippolito, S. Kandasamy, K. Kalantar-zadeh, W. Wlodarski, ‐Hydrogen sensing characteristics of WO_3thinfilm conductometric sensors activated by Pt and Au catalysts‖, Sensors Actuators B,108 **(2005)**154-158.

17. M.Yang, Y. Sun, D. Zhang, D. Jiang, ‐ Using Pd/WO_3compositethin films as sensing materials for optical fiber hydrogen sensors‖, Sensors Actuators B, 143 **(2010)**750-753.

18. D.S. Vlachos, C.A. Papadopouls, J.N. Avaritsiotis. Sensors Actuators B, 44 (1997)459-461.

Synthesis, Characterization of Gd-doped Ceria Nanocomposites

Dr. M.J. Pawar[a]*, Sagar B. Deshmukh[a], Dr. Shrikant D. Thakre[b], Dr. Anand S. Tale[c]

[a] *Department of Chemistry, Laboratory of Material Synthesis, Smt. Narsamma Arts, Commerce and Science College, Kiran Nagar, Amravati (MS).*

[b]*Dr. Rajendra Gode Institute of Technology & Research, Amravati (MS),*

[c] *Shri Sant Gajanan Maharaj College of Engineering, Shegaon (MS).*

Abstract

In this work, Gd-doped CeO_2 ($Ce_{1-x}Gd_xO_{2-\delta}$; x = 0.0. 2.0, 4.0 and 6.0 wt %) nanocomposites were prepared by EDTA-Glycol method. The influence of Gd doping on the microstructures and the optical and ionic conductivity properties of these nanoparticles has been studied using X-ray diffraction, FTIR, TEM, UV-VIS, SEM-EDS and impedance spectroscopy. It has been found that Gd doping formed a homogeneous solid solution with ceria, with a significative reduction of crystallite size. As compared to the pure ceria an improvement of total conductivity was achieved with a maximum for the highest Gd concentration of 4 wt % in the temperature range of 550–950°C.

1. Introduction

Solid oxide fuel cell (SOFC) is one of the most promising electrochemical devices for clean power generation due to its efficient operation, fuel flexibility (ranging from hydrogen to hydrocarbons and biogas), and relatively lower greenhouse gas emissions [1,2]. Comparable to other types of fuel cells, SOFCs have the advantage of fuel flexibility i.e. are able to work with hydrogen, hydrocarbon reformate and, in some conditions, with hydrocarbon fuels directly [3-5]. Furthermore, SOFCs are highly promising due to their enhanced resistance to fuel contamination and versatility of applicable combustible gases in comparison with other FC types. Presently, solid electrolytes for SOFCs working in medium temperature region (400–800°C) often comprise cerium oxide doped with rare earth oxides [6,7]. Ceria-based electrolytes possess an advantageous combination of high unipolar oxygen

conductivity, chemical stability in carbon- and hydrogen-containing atmospheres and an inertness to electrode materials, which makes them highly promising for medium-temperature fuel cells.

Being comparable with conventionally used zirconia with respect to electric performances, CeO_2-based electrolyte nanomaterials allow for a significant reduction of working temperature for fuel cells, thus providing an increased durability and simplified structure [8,9].

In addition, doped ceria-based electrolyte materials, such as gadolinium-doped ceria (GDC) or samarium-doped ceria, exhibiting an ionic conductivity than YSZ in the temperature range of 600–750°C [10]. However, the functional limitation of doped ceria-based electrolytes is that they exhibit appreciable electronic conductivity at higher temperature (≥ 800°C) and low partial pressure of oxygen at anode side that dictates the operating temperature of the fuel cells [11–15].

Many methods including ultra-sonication, ball milling, microwave, sol–gel, mechanical alloying and chemical-precipitation, etc. for the preparation of nanocomposite materials from the mixed metal oxide precursors. [15-17]. From above all well-known methods, the chemical-precipitation process is used as a competent technique for the production of nanomaterials, owing to effortlessness. This move toward is extra operative for yielding homogeneity, particularly sample without impurities, tiny particle size, and a short period of time. Ceria-based materials are serious candidates with samarium [18-20] or gadolinium [21-25] substitution to increase the vacancy concentration.

In doped ceria, it has been reported that when the dopant ion radius is close to the critical radius (1.038 Å), then the doped ceria exhibits the highest oxygen ion conductivity. For this reason, Gd doped ceria exhibits the highest oxygen ion conductivity among the doped ceria, as radius of Gd^{3+} (1.05 Å) is closer to the critical radius (1.038 Å) [26, 27]. However, the exact composition of CeO_2-Gd_2O_3 system that has maximum oxygen ion conductivity is still not well defined. *Mori* et al. [28, 29] showed the domain structure in rare earth doped ceria grains and suspected that these domains present in grains are responsible for the higher grain conductivity of $Ce_{0.9}Gd_{0.1}O_{2-\delta}$. But, *Kharton* et al. [30] reported the higher total conductivity for $Ce_{0.2}Gd_{0.2}O_{2-\delta}$ which was possibly due to a contribution of grain boundary conductivity. Moreover, although the Gd_2O_3-CeO_2 system has been reported by several authors, few works provide a comprehensive microstructural and electrical analysis of 0, 10 and 20 mol% Gd_2O_3-doped CeO_2, formed by such low temperature, soft chemical preparation routes. In this work, we synthesized $Ce_{1-x}Gd_xO_{2-d}$ (x = 0, 0.1 and 0.2) nanoparticles by

the sol gel combustion route for intermediate temperature electrochemical applications. The synthesized materials are fully characterized by their structural, chemical, microstructural and electrical properties. Gd doped ceria synthesized by solid-state reaction requires high sintering temperature and time. Hence various wet chemical methods have been used for the synthesis Gd doped ceria such as co-precipitation [31], combustion [32, 33], sol-gel [34, 35], hydrothermal [36], EDTA-citrate complexation [37] and micro-emulsion [38]. To the best our knowledge, no reports are available on synthesis of Gd doped ceria by EDTA-Glycol complexation method. Hence in this investigation, we present a systematic study of effect of pH on structural, morphological and electrical properties of Gd doped ceria solid solutions obtained by EDTA-Glycol method.

2. Experimental

2.1 Materials

In this work, for preparation of ceria based nanocomposites, highly pure $Ce(NO_3)_3.6H_2O$ and $Gd(NO_3)_3.6H_2O$ were use as the source of metal ions obtained from Sigma Aldrich. The other chemicals used in synthesis Nitric Acid (HNO_3, 65%, Merck), ethylene diamine tetra acetic acid ($C_{10}H_{16}N_2O_8$; Sigma Aldrich), ethylene glycol ($C_2H_6O_2$; Merck), were used as obtained without further purification.

2.2 Method of Synthesis

The pure and Gd doped CeO_2 materials were used by a modified EDTA-Glycol method [14]. The highly pure $Ce(NO_3)_3.6H_2O$, $Gd(NO_3)_3.6H_2O$ were used as the precursors. These salts were mixed independently in de-ionized water. During meanwhile 2, 4 and 6 wt % of gadolinium nitrate solution were added to the above reaction mixture and continuously stirred for 30 min. The calculated quantity of ethylenediaminetetraacetic acid (EDTA), dilute ammonia and ethylene glycol (EG) was added to the nitrate solution. So formed solution was stirred and kept on a hot plate for heat treatment at 80°C which in turn forms a gel-like mass. The resulted mass was combusted at 300°C for 2 h followed by the calcination at 550°C for 5 h. On calcinations, the obtained ashes were ground in agate mortar to get fine homogeneous powders. Powder materials were uniaxially pressed into pellets with

6 mm of diameter and 2 mm thickness, at 200 MPa. Sintering was performed in air for 10 h at a constant heating rate (CHR) of 2°C/min in between 1150°C to 1350°C.

3. Characterization

Calcined powders were studied by X-ray diffraction (XRD) using a Miniflex 600 diffractometer RIGAKU - Japan (Cu–$K\alpha$ radiation). Data in an angular region of 2θ in the range of 20-80° were collected in a step-scanning mode (0:02 steps with a step-counting time of 2 s). The crystallite size, D, of the calcined powders was estimated using the Scherrer equation:

$$D = \frac{0.9\lambda}{\beta cos\theta}$$
(3.1)

Where, D is crystallite size, λ is wavelength of X-rays (1.5418Å), θ is the scattering angle of the main reflection and β is the corrected peak at full width at half-maximum (FWHM) intensity. FTIR of the as-prepared samples were investigated by IR Affinity-1 Shimadzu- Japan. UV-visible spectra of the samples were studied by using UV–1800 Shimadzu- Japan. SEM-EDS studies was performed on Carl Zeiss NTS GMBH, Germany, SUPRA 55. TEM analysis was performed using Transmission electron microscope CM 200 (Philips).

For electrical measurements, impedance spectroscopy was performed on sintered pellets of four samples CE, CG2, CG4 and CG6. The pellets were made by pressing 4 g of powder at 200 MPa in a 25 mm die and were sintered for 6 hours at the temperatures 1150°C and 1250°C. The densities of pellets pressed and sintered at 1250°C for 6 h as described above were determined from their mass and dimensions. For electrical measurements, silver contacts were applied on both the flat surfaces and cured at 500°C for 15 min. An impedance analyzer (KEYSIGHT-E4990A) was used to characterize the impedance spectra of sintered samples in the static ambient atmosphere in the frequency range 20 Hz to 5 MHz from 550 to 950°C. The spectra were fitted using the Zsimpwin software and values for the total, bulk and grain boundary conductivities were noted.

4. Result and discussion

4.1 XRD analysis

Structural Analysis Figure 1 shows the XRD pattern of the prepared cerium oxide sample. All the diffraction peaks of (111) at 28.64°, (200) at 33.27°, (220) at 47.76°, (311) at 56.78°, and (400) at

69.10° were indexed and well matched with standard JCPDS Card No. 65-5923. The patterns of cerium oxide samples confirmed the cubic structure of the material. The sharp and high intense peaks of XRD patterns confirm the high crystalline quality of the samples. The crystallite size of pure cerium oxide was calculated from the diffraction peaks of XRD pattern using Scherer's formula. The average crystallite size was calculated using Scherrer equation were calculated from (111) peak and are presented in Table 1. The size of Gd doped CeO_2 nanoparticles decreased with increasing the concentration of Gd. The average crystallite size of the crystals was found in between 43-45 nm with slight expansion of lattice. The crystallinity of the powder became better during the calcination at 550°C. Crystalline phases corresponding to Gd_2O_3 could not be found for as-prepared powders, indicating the formation of solid solution. A trivial expansion in the lattice constant upon doping has been attributed to the substitution of the smaller Ce^{4+} ion (0.97Å) by the larger Gd^{3+} (1.053Å) ions, which caused strain and as light deformation no the structure. The introduction of Gd^{3+}, ions into Ce^{4+} can cause a small shift in the cerium oxide peaks positions. Since the broadening of peaks could be attributed not only to crystallite size, but also to stresses created in the structure.

Figure (1) XRD patterns of Gd doped CeO₂ powders obtained at 550°C.

Figure (2) Plot against Gd concentration (mol%) for lattice parameter of as-prepared ceria-based materials.

Table (1) 2θ (deg.), crystallite size (nm) and d-spacing of pure and Gd-doped CeO₂ nanoparticles.

Sample	Gd (mol%)	2 Theta (deg.)	Crystallite size (nm)	*d*-spacing	*Band Gap (eV)*
C	0.0	28.51	45.15	3.134	2.78
CG2	2	28.49	44.24	3.132	2.65
CG4	4	28.47	42.58	3.130	2.49
CG6	6	28.44	44.17	3.130	2.54

Figure (3) 3.2 Crystal growth as a function of Gd concentration.

Observed results are summarized and compared for better illustration in Figure 3. While the crystal growth was slow until reaching 4 mol% of Gd, at higher concentration the crystal growth was much faster.

4.2 FTIR spectra

Fourier transform infrared (FTIR) spectra of the as-prepared Gd-doped nanocomposites are shown in Figure 4. Some distinctive absorptions peaks were observed at 3436 and 1630 cm^{-1}. Two strong intense bands observed at 3429 and 1624 cm^{-1} of pure and Gd-doped CeO$_2$ samples are attributed to (O–H) vibration modes of (H-bonded) water molecules, which was due to the physically observed water on the sample surfaces [38, 39]. The strong band at 3429 cm^{-1} is attributed to the v (O–H) vibration modes of the water molecules adsorbed physically. In addition, some we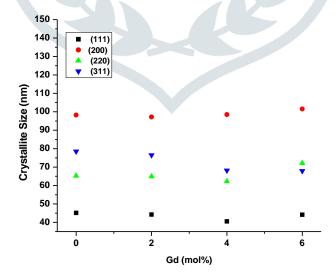aker absorption peaks were also observed at around 2934, 2856, 1369, 1092, and 700 cm^{-1}. The bands observed at 2934 and 2856 cm^{-1} are due to the (C–H) bonds of organic molecules absorbed during the sample preparation and handling [40]. Absorption at 1630 cm^{-1} is assigned to a systematic stretching vibration of the carboxylate (-COO$^-$) group [17]. The peak at around 1092 cm^{-1} indicates the presence of the nitrate ions [18]. The bands observed in the lower frequency region at 700 and 430 cm^{-1} are referred to the characteristic Ce–O vibration [19]. The band at 1369 cm^{-1} is assigned to the stretching vibration of carboxylate salts (COO$^-$) [41, 42]. The band observed at 1092 cm^{-1} due to the Cerium- Oxygen group with a larger double bond nature [43]. Two weaker bands observed at 852 and 735 cm^{-1} are due to Cerium-Oxygen group having a lower double bond nature and of Ce–O–Ce chains asymmetric stretching vibration of metal oxide networks respectively. The strong band noticed at 558 cm^{-1} is due to the symmetrical stretching vibration mode of (Ce–O–Ce) or (Ce–O–Gd) indicating the Gd ions doped Ceria nanoparticles [44]. It is to be noted that the length of the rare-earth metals-oxygen bond changes with dopant concentration. These shifts in peaks confirm the dopant stabilization in the host lattice [45].

Figure (4) FTIR spectra of Gd-doped Ceria nanocomposites.

4.3 UV-VIS studies

The UV-VIS spectroscopic measurement was carried out to investigate the effect of Gd concentration on the optical properties of CeO_2 nanocomposites. Figure 5 shows the UV-VIS absorption spectra recorded for pure and Gd-doped ceria. It can be seen that there is a strong absorption band below 400 nm in the spectra for all the samples, which is due to the charge transfer from O^{-2} (2p) to Ce^{4+}(4f) orbitals in CeO_2 [46]. The optical band gap values for the Gd-doped ceria system can be estimated from the absorption spectra following Tauc's equation [47].

$$\alpha h v = A\big(h v - E_g\big)^n$$

where α is the absorption co-efficient, hv is the photon energy, E_g is the band gap energy, A is a constant and n can have values of 1/3, 1/2, 2, and 3 for the direct forbidden, direct allowed, indirect allowed, and indirect forbidden transitions respectively. The calculated values of E_g for all the as-prepared samples are given in Table 1 Undoped ceria shows the highest band gap value of 2.79 eV, and for Gd-doped ceria the values of the band gap decrease with the Gd concentration. Thus, the absorption spectra of Gd^{3+} doped ceria nanocrystals exhibit red shifts compared to that of pure ceria.

Figure (5) UV-VIS spectra of Gd-doped Ceria nanocomposites.

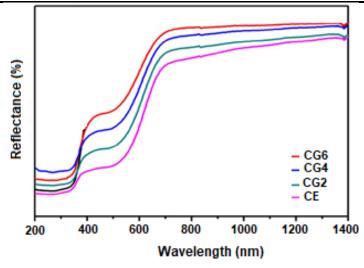In CeO_2, all valance Ce states, including the 4f states, are empty, and the system is a wide gap insulator with a measured fundamental band gap of 6.0 eV between the valance and conduction bands; this is formed predominantly by the O^{-2} (2p) to Ce^{4+} (5d) states respectively [48]. However, in our present study, the band gap value of CeO_2 is much lower than 6.0 eV (Table 1). This is because a small amount of Ce^{3+} is present at the surface of CeO_2 and one electron per Ce atom populates a Ce 4f state, resulting in a decrease in the band gap value of ceria [49]. The red shift of the direct band gap may be due to the presence of oxygen defect levels between the O2p and Ce4f levels that capture the excited electrons and decrease the effective band gap [50]. Lastly, the doping of Gd ions creates ground and excited f-energy states in the mid band gap of ceria. These energy states of Gd accept many of the excited electrons coming from the O2p level which leads into the effective reduction in the band gap., i.e. a red shift [51].

4.4 SEM and EDS spectra

The effect sintering temperature on morphology and density cannot be predicted by preliminary analyses because at a comparable density, the microstructure is completely different as visible in Figure 6. At sintering temperatures of 1150 and 1250°C, pure electrolytes have small grains with a similar uneven and rough morphology. These samples are affected by the poorest densification with an inadequate microstructure for the lowest sintering temperatures. By increasing temperature. The microstructure is always revealing small grains, many cracks, and voids, but the morphology became more uniform, and the relative density increases. The addition of Gd, make obvious a change in the

microstructure according to sintering temperature. As reported for sample GC4 in Figure 6 microstructure with clean grain boundaries was formed at 1250°C.

Figure 6 shows SEM micrographs of sintered GC4 samples and EDS analysis of the Gd_2O_3 doped CeO_2 crystals. The average size and size distribution of the synthesized particles were below 10 nm and uniform, respectively. The shape of the synthesized particles was nearly spherical. The spectrum of Gd_2O_3 doped CeO_2 nanoparticles according to a SEM - EDS analysis. The particles show Gd, Ce and O pattern peaks Table 2.
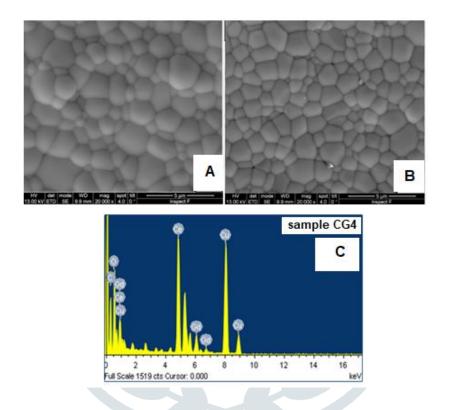

Figure (6) SEM of sample GC4 sintered at (A) 1150°C and (B) 1250°C   (C) EDAX spectra of sample GC4.

Table (2) Elemental composition obtained for EDS spectroscopy.

Element	Weight (%)	Atomic (%)
C K	7.20	29.37
O K	10.21	31.37
Cu K	24.63	19.08
Ce K	53.06	18.64
Gd K	4.96	1.55
Total	100.00	

4.5 Electrical Properties

The total resistance (R_T) of as-prepared sample can be obtained by utilizing the impedance spectroscopy at different temperatures. The total electrical conductivity σ_T was then calculated according to the equation,

$$R_T = R_{grain} + R_{grain-boundary} \tag{1}$$

The total electrical conductivity (σ_T) was then determined from the following equation –

$$\sigma = \frac{l}{AR_T} \tag{2}$$

where, l is the thickness and A represents the cross-sectional area of the sample. It is reported that, the conductivity of ceria-based electrolytes in air is based on ionic conductivity and the contribution of electronic conductivity is negligible [52]. In this study, the conductivity of as-prepared samples measured in air was treated as the oxide ionic conductivity only. The ionic conductivity (σ_t) in ceria-based oxides is a temperature dependent and it can be expressed by the following empirical relationship –

$$\sigma_t T = \sigma_o \exp\left(\frac{E_a}{kT}\right) \tag{3}$$

where E_a is the activation energy for conduction, T is the absolute temperature, k is the Boltzmann constant and σ_0 is a pre-exponential factor. The equation can be linearised by plotting a logarithmic relationship between $\log(\sigma_t T)$ and 1000/T (K).

Figure (7) Ionic conductivity of as prepared Gd-doped ceria nanocomposites at different operational temperatures.

Figure (8) Arrhenius plot of ionic conductivity for (I) sample Ce, (II) sample CG2, (III) sample CG4 and (IV) sample CG6.

The Arrhenius plot of ionic conductivity for different dopant concentrations is presented in Figure 8. The plots clearly reveal a linear increase of conductivity with temperature. Conductivity for pure ceria is lowest and tends to increase with Gd concentration up to a maximum at 4 mol% (sample CG4) and when Gd concentration is 6mol%, the conductivity is found to be declined. Conductivity of CG2 is slightly higher than CG6. The activation energy of ionic conductivity calculated from Arrhenius plot are obtained as 0.84 eV, 0.98 eV, and 1.15 eV for CG4, CG2, and for pure-ceria (CE),

respectively; the activation energy of GDC is comparable with reported values [52-58]. The change in the activation energy may be attributed to an order and disorder transition of the oxygen sublattice caused due to successful substitution of Ce^{4+} ions by Gd^{3+} ions [59]. The activation energy is minimum for the SDC. This decrease in activation energy may be due to the presence of attractive interactions between dopant cations and oxygen vacancies [60]. Moreover, an increase in the Gd concentration in the ceria structure, dopant process hinders oxygen arrangement causing an increase in the activation energy and a decrease in the ionic conductivity for the ceria solid solutions. At lower temperatures, the activation energy (E_a) depends on the defect association enthalpy (ΔH_a) and migration enthalpy (ΔH_m) for conduction. At higher temperatures, activation energy is equal to only the migration enthalpy (ΔH_m), because a great part of the oxygen vacancies is free to diffuse [61].

The appearance of high oxygen ionic conductivity in the solid electrolytes is determined by the formation of oxygen vacancies in the CeO_2 matrix when Ce^{4+} is replaced by Gd^{3+} during the dissolution of Gd_2O_3 in the lattice of CeO_2, which can be described by the following quasi-chemical equation [3].

$$Gd_2O_3 \xrightarrow{Ce_2O_3} 2Gd'_{Ce} + 3O_O^X + V_O^{\cdot}$$

Where Gd'_{Ce} is a Gd^{3+} ion replacing Ce^{4+} and yielding a negative charge, $V_O^{\cdot}$ is a positively charged oxygen vacancy compensating the dopant charge, O_O^X is oxygen atom in a regular site with a neutral charge. It was observed that, increased temperature in the range from 570 to 970°C leads to the increase in electrical conductivity of all the samples. In addition, with an increase in the concentration of Gd_2O_3, the specific electrical conductivity of the ceramics increases in the entire temperature range in study. The highest specific electrical conductivity in the temperature range of 550–950°C ($\sigma_t = 3.3 \times 10^{-2}$ Scm^{-1} at 750°C) is observed for the sample CG4 containing 4 mol.% Gd_2O_3.

Table (3) Total ionic conductivity of Nd-doped CeO_2 solid solutions at 750°C.

Sample	Total Ionic Conductivity (Scm^{-1})	Activation energy (eV)
CE	1.02×10^{-6}	0.79
GC2	2.34×10^{-4}	0.87
GC4	3.3×10^{-2}	0.71
GC6	1.43×10^{-3}	0.87

It has been observed that the activation energy decreases with a rise in the dopant concentration as shown in Table 3. The contribution of grain conductivity is a major factor for the total oxide ion conductivity in the doped ceria samples [62]. Thus, the amount of Gd doping affects the conductivity of the ceria. With the ascent in the Gd concentration, a huge expansion in the grain conductivity was seen because of the improvement of the charge transporters emerging from the creation of oxygen vacancies as a result of doping. This leads into the expansion of the crystal structure.

5. Conclusion

The Gd-doped ceria nanocomposites with composition $Ce_{1-x}Gd_xO_{2-\delta}$ (x = 0.0, 2.0, 4.0 and 6.0wt%) were successfully prepared by using a EDTA-glycol method. The XRD, FTIR, UV-visible, SEM–EDS analysis confirmed the formation of the single-phase solid solution. All as-prepared Gd-doped ceria nanocomposites were sintered at the temperatures 1150 and 1250°C. The nanocomposite containing 4wt% Gd showed an essentially upgraded oxide ion conductivity in the order of 3.3×10^{-2} Scm^{-1} at 750°C with a lower activation energy, E_a = 0.71 eV. Thus, Gd-doped ceria nanocomposites might be viewed as a potential electrolyte material for SOFC applications.

6. References

[1] Subotić, V.; Napporn, T.W. Nanostructured metal oxides for high-performance solid oxide fuel cells (SOFCs). In *Metal Oxide-Based Nanostructured Electrocatalysts for Fuel Cells, Electrolyzers, and Metal-Air Batteries*; Napporn, T.W., Holade, Y., Eds.; Elsevier: Amsterdam, The Netherlands, **2021**; pp. 235–261.

[2] Choolaei, M.; Cai, Q.; Horri, B.A. Green synthesis and characterization of nanocrystalline NiO-GDC powders with low activation energy for solid oxide fuel cells. *Ceram. Int.* **2021**, *47*, 32804–32816.

[3] Liang, J. Low temperature fabrication of dense gadolinia-doped ceria electrolyte with enhanced electrical conductivity. Electrochim. Acta **2015**, 178, 321–328.

[4] Rekas, M. Electrolytes for Intermediate Temperature Solid Oxide Fuel Cells. Arch. Met. Mater. **2015**, 60, 891–896.

[5] Mahato, N.; Banerjee, A.; Gupta, A.; Omar, S.; Balani, K. Progress in material selection for solid oxide fuel cell technology: A review. Prog. Mater. Sci. **2015**, 72, 141–337.

[6] Sal'Nikov, V.V.; Pikalova, E.Y. Raman and impedance spectroscopic studies of the specific features of the transport properties of electrolytes based on CeO. Phys. Solid State 2015, 57, 1944–1952.

[7] Egorova, T.L.; Kalinina, M.V.; Simonenko, T.; Shilova, O.A.; Sevastyanov, V.G.; Kuznetsov, N.T. Liquid-phase synthesis and physicochemical properties of xerogels, nanopowders and thin films of the CeO_2–Y_2O_3 system. Russ. J. Inorg. Chem. 2016, 61, 1061–1069.

[8] Egorova, T.L.; Kalinina, M.V.; Simonenko, T.; Shilova, O.A.; Sevastyanov, V.G.; Kuznetsov, N.T. Liquid-phase synthesis and physicochemical properties of xerogels, nanopowders and thin films of the $CeO2$–$Y2O3$ system. Russ. J. Inorg. Chem. **2016**, 61, 1061–1069.

[9] Ramos-Alvarez, P.; Villafuerte-Castrejón, M.E.; González, G.; Cassir, M.; Flores-Morales, C.; Chávez-Carvayar, J.A. Ceria-based electrolytes with high surface area and improved conductivity for intermediate temperature solid oxide fuel cells. J. Mater. Sci. **2016**, 52, 519–532.

[10] Steele B C H **2000** Solid State Ionics 1343.

[11] Arachi Y, Sakai H, Yamamoto O, Takedsa Y and Imanishai **N1999** Solid State Ionics 121133.

[12] Eguchi K, Setoguchi T, Inoue T and Arai H **1992** Solid State Ionics 52165

[9] Mogensen M, Sammes N M and Tompsett GA **2000** Solid State Ionics 12963.

[10] Zha S, Xia C and Meng G **2003** J. Power Sources 11544.

[11] Fuentes R O and Baker R T **2008** Int. J. Hydrogen Energy 33 3480.

[12] Namitha R, Radhika D, Krishnamurthy G (**2019**) Hydrothermally synthesized carbon nanotubes for electrochemical hydrogen storage application. Issues Chem Chem Technol 3:30–34.

[13] Dell'Agli G, Spiridigliozzi L, Pansini M, Accardo G, Yoon SP, Frattini D (**2018**) Effect of the carbonate environment on morphology and sintering behaviour of variously co-doped (Ca, Sr, Er, Pr) Samarium-doped ceria in co-precipitation/hydrothermal synthesis. Ceram Int 44:17935–17944.

[14] Ghelich R, Keyanpour-Rad M, Youzbashi AA, Khakpour Z (**2015**) Comparative study on structural properties of NiO–GDC nanocomposites fabricated via electrospinning and gel combustion processes. Mater Res Innov 19:44–50.

[15] Arabaci A (**2018**) Synthesis and characterization of Pr/Gd co-doped ceria by using the citric acid–nitrate combustion method. Solid State Ionov 326:69–76.

[16] Radhika D, Kannan K, Nesaraj AS, Namitha R (**2019**) Facile low-temperature synthesis and application of $La_{0.85}Sr_{0.15}Co_{0.85}Fe_{0.15}O_{3-\delta}$ as superior cathode for LT-SOFCs Using C-TAB as surfactant. Mater Res Innov 10:12.

[17] Radhika Devi, Nesaraj AS (**2014**) Chemical precipitation and characterization of multicomponent perovskite oxide nanoparticles—possible cathode materials for low temperature solid oxide fuel cell. Int J Nano Dimension 5:1–10.

[18] Chaubey, N.; Wani, B.N.; Bharadwaj, S.R.; Chattopadhyaya, M. C. Physicochemical properties of rare earth doped ceria $Ce0.9Ln0.1O1.95$ (Ln = Nd, Sm, Gd) as an electrolyte material for IT-SOFC/SOEC. Solid State Sci. 2013, 20, 135–141.

[19] Yahiro, H.; Eguchi, K.; Arai, H. Electrical properties and reducibilities of ceria-rare earth oxide systems and their application to solid oxide fuel cell. Solid State Ion. 1989, 36, 71.

[20] Anirban, S. K. Dutta, A. Revisiting ionic conductivity of rare earth doped ceria: Dependency on different factors. Int. J. Hydrogen **2020**, 45, 25139.

[21] Huang, W.; Shuk, P.; Greenblatt, M. Properties of sol-gel prepared $Ce_{1-x}Sm_xO_{2-x2}$ solid electrolytes. Solid StateIon.**1997**,100,23.

[22] Yahiro, H.; Eguchi, Y.; Eguchi, K.; Arai, H. Oxygen ion conductivity of the ceria-samarium oxide system with fluorite structure. J. Appl. Electrochem.**1988**,18,527.

[23] Arabaci, A. Effect of Sm and Gd dopants on structural s characteristics and ionic conductivity of ceria. Ceram. Int.**2015**,41,5836.

[24] Steele, B. C. H. Appraisal of $Ce_{1-y}Gd_yO_{2-y/2}$ electrolytes for IT-SOFC operation at 500°C. Solid StateIon.**2000**,129,95.

[25] Butler, V.; Catlow, C.; Fender, B.; Harding, J. Dopant ion radius and ionic conductivity in cerium dioxide. Solid StateIon.**1983**, 8,109.

[26] H. Inaba, H. Tagawa, Solid State Ionics 83 (**1996**) 1−16.

[27]. K. Eguchi, T. Setoguchi, T. Inoue, H. Arai, Solid State Ionics 52 (**1992**) 165−172.

[28] T. Mori, Z. Li, P. Yan, Y. Wu, Z. Li, Mater. Sci. Eng. B 177 (**2012**) 1538−1541.

[29]. T. Mori, J. Drennan, J.H. Lee, J.G. Li, T. Ikegami, Solid State Ionics 154−155 (**2002**) 461−466.

[30]. V.V. Kharton, F.M.B. Marques, A. Atkinson, Solid State Ionics 174 (**2004**) 135−149.

[31] K.C. Anjaneya, J. Manjanna, G. Govindaraj, K.N. Ganesha, J. Alloys Compd. 578 (**2013**) 53−59.

[32] L.D. Jadhav, M.G. Chourashiya, A.P. Jamale, A.U. Chavan, S.P. Patil, J. Alloys Compd. 506 (2010) 739−744.

[33]. R.K. Lenka, T. Mahata, A.K. Tyagi, P.K. Sinha, Solid State Ionics 181 (**2010**) 262−267.

[34]. K.C. Anjaneya, J. Manjanna, G. Govindaraj, K.N. Ganesha, J. Alloys Compd. 585 (**2014**) 594−601.

[35]. K.C. Anjaneya, J. Manjanna, G. Govindaraj, K.N. Ganesha, Physica B 447 (**2014**) 51−55.

[36]. T. Karaca, T.G. Altmcekic, M.F. Oksuzomer, Ceram. Int. 36 (**2010**) 1101−1107.

[37]. S. Li, L. Ge, H. Gu, Y. Zheng, H. Chan, L. Guo, J. Alloys Compd. 509 (**2011**) 94−98.

[38]. J. Chandradass, B. Nam, K.H. Kim, Colloids Surf. A 348 (**2009**) 130−136.

[39] S. Samiee, E.K. Goharshadi, Effects of different precursors on size and optical properties of ceria nanoparticles prepared by micro- wave-assisted method. Mater. Res. Bull. **47**, 1089–1095 (2012).

[40] G. Wang, Q. Mu, T. Chen, Y. Wang, Synthesis, characterization and photoluminescence of CeO_2 nanoparticles by a facile method at room temperature. J. Alloy. Compd. **493**, 202–207 (2010).

[41] S. Phoka, P. Laokul, E. Swatsitang, V. Promarak, S. Seraphin, S. Maensiria, Synthesis, structural and optical properties of CeO_2 nanoparticles synthesized by a simple polyvinyl pyrrolidone (PVP) solution route. Mater. Chem. Phys. **115**, 423–428 (2009).

[42] A.Z. Liu, J.X. Wang, C.R. He, H. Miao, Y. Zhang, W.G. Wang, Synthesis and characterization of $Gd_{0.1}Ce_{0.9}O_{1.95}$ nanopowder via an acetic-acrylic method. Ceram. Int. **39**, 6229–6235 (2013).

[43] R. Tholkappiyan, A. Nirmalesh Naveen, S. Sumithra, K. Vishista, Investigation on spinel $MnCo_2O_4$ electrode material prepared via controlled and uncontrolled synthesis route for supercapacitor application. J. Mater. Sci. **50**, 5833–5843 (2015).

[44] C. Binet, A. Badri, J.C. Lavalley, A spectroscopic characterization of the reduction of ceria from electronic transitions of intrinsic point defects. J. Phys. Chem. **98**, 6392–6398 (1994).

[45] C. Ho, J.C. Yu, T. Kwong, A.C. Mak, S. Lai, Morphology-control- lable synthesis of mesoporous CeO$_2$ nano- and microstructures. Chem. Mater. **17**, 4514–4522 (2005).

[46] R. Tholkappiyan, K. Vishista, Synthesis and characterization of barium zinc ferrite nanoparticles: working electrode for dye sen‑sitized solar cell applications. Sol. Energy **106**, 118–128 (2014).

[47] Y.-W. Zhang, R. Si, C.-S. Liao, C.-H. Yan, C.-X. Xiao and Y. Kou, J. Phys. Chem. B, 2003, 107, 10159–10167.

[48] S. L. S. Rao, G. Ramdevudu, Md. Shareefuddin, A. Hameed, M. N. Chary and M. L. Ro, Int. J. Eng. Sci. Res. Technol., 2012, 4, 25–35.

[49] 5 E. Wuilloud, B. Delley, W. D. Schneider and Y. Baer, Phys. Rev. Lett., 1984, 53, 202–205.

[50] L. Wu, H. J. Wiesmann, A. R. Moodenbaugh, R. F. Klie, Y. Zhu, D. O. Welch and M. Suenaya, Phys. Rev. B: Condens. Matter Mater. Phys., 2004, 69, 125415.

[51] A. H. Morshed, M. E. Moussa, S. M. Bedair, R. Leonard, S. X. Liu and N. El-Masry, Appl. Phys. Lett., 1997, 70, 1647– 1649.

[52] M. Greenberg, E. Wachtel, I. Lubomirsky, J. Fleig and J. Maier, Adv. Funct. Mater., 2006, 16, 48–52.

[53] M. G. Chourashiya, S. R. Bharadwaj, and L. D. Jadhav, Thin Solid Films 519, 650 (2010).

[54] S. L. Reis, E. C. C. Souza, and E. N. S. Muccillo, Solid State Ionics 192, 172 (2011).

[55] H. Duncan and A. Lasia, Solid State Ionics 176, 1429 (2005).

[56] D. Perez-Coll, P. Nu~nez, J. C. Ruiz-Morales, J. Pe~na-Martınez, and J. R. Frade, Electrochim. Acta 52, 2001 (2007).

[57] A. Jasper, J. A. Kilner, and D. W. McComb, Solid State Ionics 179, 904 (2008).

[57] S. Dikmen, H. Aslanbay, E. Dikmen, and O. S¸ahin, J. Power Sources 195, 2488 (2010).

[58] G. Kim, N. Lee, K. B. Kim, B. K. Kim, H. Chang, S. J. Song, and J. Y. Park, Int. J. Hydrogen Energy 38, 1571 (2013).

[59] H. Inaba, H. Tagawa, Ceria-Based Solid Electrolytes, Solid State Ion. 83, 1 (1996).

[60] K. Zhao and Y. Du, Calcium-doped ceria materials for anode of solid oxide fuel cells running on methane fuel, *J. Power Sources*, 2017, 347, 79.

3. Effect of Noble Metal (Ag) doping on Hydrogen Sensitivity of WO3 Thin Film Sensors

Dr. S. V. Jagtap

Department of Physics, R. D. I. K. & K. D. College, Badnera (Rly), Amravati. (Maharashtra)

Dr. M. J. Pawar

Department of Chemistry, Smt. ACS College, Kiran Nagar, Amravati. (Maharashtra) India

Dr. A. S. Tale

Department of Physics, Sant Gajanan Maharaj College of Engineering, Shegaon. (Maharashtra)

Dr. S. D. Thakre

Department of Physics, Dr. Rajendra Gode Institute of Technology & Research, Amravati.(M.S.)

Abstract

The given workrepresents the modification in hydrogen gas sensitivity of WO_3 based thin films loaded with Ag like noble metals. The samples were characterized by various techniques: like XRD, SEM, TEM and BET to know the stoichiometry, crystal structure, morphology and surface area. The dopants content was varied from 0 to 4 at.% and its effect on structural , morphological and the gas sensing properties have been studied with respect to different operating temperatures.

Keywords: Ag-WO_3, Sol–gel spin coating, H_2 Gas sensor.

1. Introduction

Semiconducting oxide gas sensors have been used to warn of explosive gases since the1960s, but more recently other applications in which semiconducting oxide may be employed as sensor materials have been considered, including detection of air pollutants and improving fuel efficiency in industrial combustion processes. The reducing gas depletes the coverage of adsorbed oxygen ions on the sensor surface and supplies electrons to the conduction band, leading to a fall in resistance [1]. A current goal in sensor research is to improve the sensor selectivity by eliminating similar responses from interfering gases. It has been found that the sensor selectivity and sensitivity may be altered by the addition of second oxide phases and elemental metals [2]. It is well known that the loading of the metal oxide matrix with catalyst nanoparticles (e.g., surface functionalization of the nanostructured metal oxide) may lead to significant improvements in response, selectivity, long-term stability and cross-sensitivity to

ambient moisture. The sensitivity of metal-oxide gas sensors can be substantially improved by dispersing a low concentration of additives, such as Pd [3, 4], Pt [5], Au [6, 7], Ag [8, 9] etc. on oxide surface or in its volume. Although doping has been used for a long time now in preparation of commercial gas sensors, the working principle of additive-modified metal-oxide materials is stillnotcompletely understood. In particular Ag has been widely employed as sensitizer in metal oxide films for developing hydrogen sensors [10-12].

WO$_3$ is a promising hydrogen gas sensing material [13-15]. It has high diffusion coefficient for oxygen vacancies [16]. WO$_3$ shows sensitivity towards oxidizing gases such as NO$_2$, O$_3$, Cl$_2$, however, for reducing gases like H$_2$, CO, NH$_3$etc, surface modification by noble catalyst (Pd, Pt, Au) is essential [17]. Addition of catalyst facilitates the chemical reaction by lowering the activation energy between the surfaces of metal oxide and target gas.

In present work, we have prepared WO$_3$ based thin films by doping the noble metal Ag in the amount of 0-1.5 wt.% in WO$_3$semiconductor. Sol-gel spin coating method was used for preparation WO$_3$based thin films. Scanning electron microscopy (SEM), X-ray diffraction (XRD) and high- resolution transmission electron microscopy (HRTEM) have been used to determine the morphology, phase composition, and microstructure of the layers grown. In order to calculate the sensitivity, the electrical resistance of a sensor was measured in the presence and absence of hydrogen gas at a concentration 30-300 ppm in dry air. The material 0.5 wt% Ag-dope WO$_3$was found to be the optimum composition for the maximum sensitivity and selectivity at an operating temperature 150°C. The cross sensitivity of the sensor was also studied to other gases, including CO, LPG andH$_2$S.

2. Experimental

2.1 Synthesis of Ag-WO$_3$ thin films

Nano crystalline WO$_3$thin films were prepared by a sol–gel spin coating process using of ammonium tungstate, glycerin, ethyl alcohol (C$_2$H$_5$OH) and de-ionized water as precursors. 0.1 M ammonium tungstate was dissolved via 70 mL of pure ethanol and placed in covered flasks. The resulted sol solutions placed in closed flasks and stirred by magnetic stirrers for 3 h and kept at 75˚C for 6. Moreover, glycerin (C$_3$H$_8$O$_3$) was added to a volume ratio of 1:12 in order to eliminate cracks [17]. After refluxing for 48 h at room temperature using a magnetic stirrer, a homogeneous mixture of precursors was formed with hydrolysis and condensation processes. This step was followed by an ageing process by leaving it in open air for 24 h. Pd doped sols

with two different concentrations (2 wt.% and 4 wt.%) were prepared by adding an appropriate amount of silver nitrate ($AgNO_3.2H_2O$, purity–99.97%) in a ammonium tungstate solution in its initial preparation stage. Pure WO_3 and Ag-doped WO_3 thin films were deposited on glass substrates using a sol–gel spin coating process with a spinning speed of 4000 rpm for 40 s. Each deposited layer was pre-sintered at 180˚C for 30 min before depositing the next layer. Post-sintering was done at 450˚C for 4 h. The thickness of the deposited films was measured by using a surface profilometer and was found approximately 100-120nm.

3. Results and Discussions

3.1 X-ray Diffraction Study

Ag doped WO_3 thin films were formed by sol-gel spin coating method. A typical XRD pattern of the WO_3 thin films obtained are shown in Figure 1. It can be indexed to a triclinic WO_3 phase according to the JCPDS card No. 32-1395.
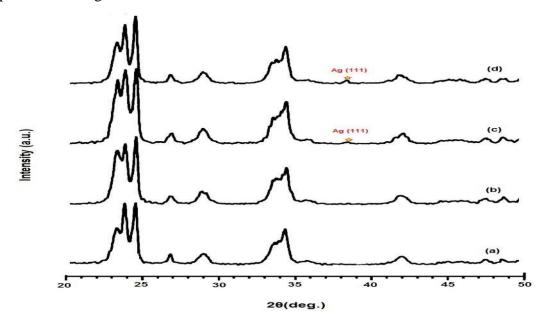

Figure .1 XRD patterns of the Ag -WO₃ thin films with various amounts of Ag; (a) pure WO₃, (b) 0.5 wt% Ag, (c) 1.0 wt.% Ag and (d) 1.5 Wt.% Ag.

Figure 1 shows the XRD patterns of the Ag-WO_3 thin films with various amounts of Ag (0.5–2.0%). One can find that the peaks belonging to WO_3 phase are not changes, whereas a new peak located at 38.1˚, belonging to the (111) deflection of face-centered cubic structured Ag (JCPDS card No. 04-0783), becomes stronger and stronger as the amount of Ag increases, indicating the separation of Ag particles from the host WO_3 lattice at higher concentration. The XRD results confirm the formation of metal Ag phase in the Ag-WO_3 samples. The increasing

intensity of the Ag (111) peak indicates that the more the amount of Ag^+ in the precursor, the more the amount of the metal Ag in the $Ag-WO_3$ films.

3.2. SEM and TEM

Study of surface morphology of WO_3based thin films has been carried out using Scanning Electron Microscope. Figure .2(a) show SEM micrographs of sensing elements of pure $WO_3$and 0.5%Ag -WO_3 thin films prepared through sol-gel method, annealed at temperature 500˚C. Both the micrographs have been taken for the 10.00 Kx magnifications. WO_3manifests beautiful pattern whereas the SEM micrograph of sensing element of Ag doped WO_3manifests clustering and agglomeration of the small sized crystallites. Scanning micrographs show flakes of pure $WO_3$and 0.5%Ag- WO_3 scattered throughout, forming a network of pores that are expected to provide sites for humidity adsorption. The average grain size for the sensing elements of pure $WO_3$and Ag doped WO_3calculated from SEM micrographs are in the range of 40-90nm.
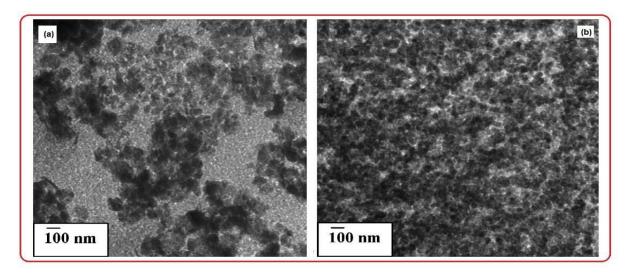

Figure .2(a) SEM micrograph of the (a) pure WO₃ thin film and (b) 0.5%Ag- WO₃.

Figure 2(b) shows transmission electron microscope (TEM) image of prepared 0.5%Ag-WO_3nanocrystalline thin film. TEM image gives a grain size of 40 nm and this is in agreement with X-ray diffraction result. The diffraction pattern illustrating spot patterns of the hexagonal structure of WO_3 indicates that the WO_3 nanoparticles formed using at annealing temperature 500˚C are highly crystalline, which is in good agreement with the X-ray diffraction result.
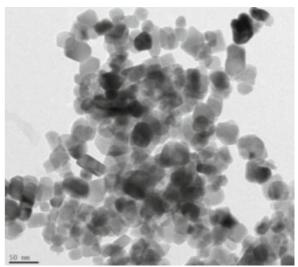
Figure. 2(b) TEM image of 0.5%Ag-WO$_3$ thin film.

3.3 AFM

3D AFM image of the 0.5%Ag-WO$_3$ film annealed at temperatures ranging from 500C is presented in Figure.3. The surface is made up of grains and voids with dimensions in the range of nanometers. The presence of these voids within the film structure is favorable because they provide direct conduits for gas molecules to flow in from the environment. It can be observed that the grain size of the WO$_3$was found to depend on the annealing temperature.The average grain size found with AFM of threedifferent samples is 67 nm, which agrees well with the value obtained by XRD. The growth of crystallites, observed to be vertical, could be related to the low rate of atom mobility on surface of the substrates.
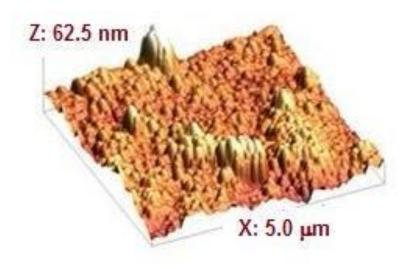

Figure.3 3D AFM micrograph of 0.5%Ag-WO$_3$ thin film.

3.4 Hydrogen Sensing Measurements

3.4.1 Effect of Ag-doping and Operating Temperature: The effect of Ag-doping on gas sensing properties of the films is studied by making ohmic contacts using high conducting electrodes. The sensors at various operating temperatures are tested for 200 ppm of hydrogen gas at different operating temperature. The sensor resistance is determined, and utilized as the measure of response. At each temperature, before starting the measurements, the sample resistance is measured without the test gas. The resistance of the sensors decreases on exposure to reducinggas.

Figure 4 shows the dependence of the response on the operating temperature for the undoped and Ag-doped WO_3 thin film sensors calcined at 500˚C. Test has been carried out for the 200 ppm hydrogen gas. The response increases with the increase of temperature, because the gas requires enough energy to overpass the barrier between oxygen molecules- adsorbed and electrons from conducting band of WO_3semiconductor [15]. In addition, the gas adsorption and reaction taken place on surface of WO_3need certain activation energy. When temperature increases to 160˚C, a balance between the gas absorption and desorption is reached, the response exhibits a maximum value of the response then decreases with temperature due to the amount of adsorbed gas on material surface will decrease with temperature.
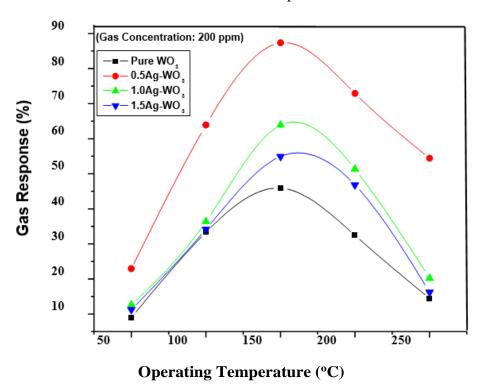
Figure.4 Gas responses of Ag-doped WO₃ thin films.

By comparing the responses of different amount of Ag-doped and undoped WO₃thin film samples at different operating temperature in Figure.4, it can be unambiguously understandable that the response of WO₃thinfilm is improved by adding of Ag. However, the response value fails to persist and declines in the magnitude with the increasing dopant concentration.
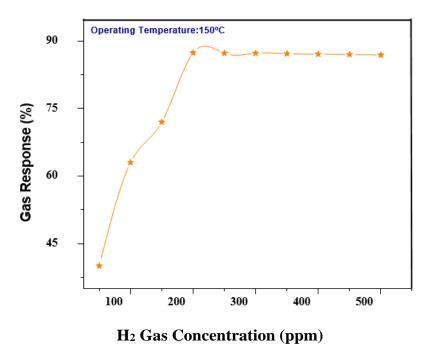

H₂ Gas Concentration (ppm)

Figure.5 Sensitivity of 0.5 wt.% Ag-doped WO₃ thin films for various concentration of H₂ in ppm level.

Figure.4 also indicates the effect of Ag doping on response, when the wt.% of Ag is lower than 1 wt.%, the WO₃ has a high specific surface and small particle size that satisfy the requirement of a practical sensor, so the high response is observed at low operating temperature. As it is known, resistance of WO₃ is mostly controlled by inter-grain potential barrier. Taking this into account, one can conclude that the addition of Ag in small concentration lowers the growth of potential barrier height at the inter grain interface, by increasing the chemisorbed oxygen at the WO₃ grain surface. Based on that, incorporation of Ag-ion favour adsorption of atmospheric oxygen species on the thin film surface and thus creates more sensing sites to respond. This also contributes to gas sensing enhancement.

3.4.2 Effect of Gas Concentration: The gas response of the 0.5wt% Ag-doped WO₃thin film sensor to hydrogen gas concentration is shown in Figure.5, where the sensor worked at its own optimum operating temperatures as mentioned above As seen from it, the sensitivity

initially increased slowly with increasing the concentration and then linearly as the gas concentration increased from 250 to 1000 ppm. It is seen that the 0.5wt% Ag-doped WO_3reaches the saturation value of sensitivity for concentration of 1000 ppm. The sensor is able to detect up to 200 ppm for hydrogen gas with reasonable sensitivity at an operating temperature 150°C.

3.4.3 Response time: Figure A6.6 shows a typical response characteristic of the sensor to 200 ppm hydrogen gas at an operating temperature 150°C. The response time is an important parameter to characterize a sensor. The response time is defined as the time taken to reach 90% of the response (~ 90 seconds) when hydrogen gas is introduced in the chamber. Figure.6 clearly shows that the response is fast with 0.5wt% Ag-doped WO_3thin film sensor as compared with undoped WO_3 thin films, 1.0wt% Ag-doped $WO_3$and 1.5wt% Ag-doped WO_3thin film sensor thin film sensors. The effect of Ag was thus seen not only in increasing the sensitivity to hydrogen gas considerably but also the rate of response. This kind of sensitization has been well explained by an electronic interaction between the noble metal and the semiconductor oxide [18].

Response Time (sec.)

Figure.6 Response characteristics of undoped and Ag-doped WO_3 thin films to 200 ppm hydrogen gas at 150°C.

4. Conclusions

In this study, Ag-doped WO_3 nanostructured thin films with different dopant amounts are synthesized by sol gel spin coating method. By using X- ray diffraction and electron microscopy studies, it is found that Ag doping can suppress the growth of large WO_3 crystallites and assist in a uniform growth. The gas sensing properties to hydrogen gas is tested and found that 0.5 wt.%

Ag-doped WO_3 exhibit the best gas sensing properties which can be attributable to enhanced capability of adsorbing oxygen by Ag on the surface. Thus the Ag-dopant exhibit excellent sensor response characteristics withfast response and recovery time of 27 sec, even at low hydrogen gas concentration of 400 ppm. This implies a good potential of the Ag-dopant in WO_3, for practical hydrogen sensing applications.

5. References

1. H. Windiscmann H, P. Mark, ‑A Model for the Operation of a Thin-Film SnOx Conductance-Modulation Carbon Monoxide Sensor‖, J. Electrochem. Soc., 126 (**1979**)627±633.

2. L.D. Birkefeld, A.M. Azad, S.A. Akbar, ‑Carbon Monoxide and Hydrogen Detection by Anatase Modification of Titanium Dioxide ‖, J. Am. Ceram. Soc, 75 (**1992**) 2964-2968.

3. T. B. Fryberger and S. Semancik, Sens. Actuators, B 2, 305(1990).

4. S. Semancik and T. B. Fryberger, Sens. Actuators, B 1, 97(1990).

5. L. Madler, A. Roessler, S. F. Pratsinis, T. Sahm, A. Gurlo, N. Barsan, and U. Weimar, Sens. Actuators, B 114,283 (**2006**).

6. U.-S. Choi, G. Sakai, K. Shimanoe, and N. Yamazoe, ‑Sensing properties of Au-loaded SnO_2-Co_3O_4 composites to CO and H_2‖ Sens. Actuators B, 107 (**2006**)397-401.

7. O. Wurzinger and G. Reinhardt, Sens. Actuators, B 103, 104(2006).

8. R. K. Joshi, F. E. Kruis, and O. Dmitrieva, ‑Gas sensing behavior of $SnO_{1.8}$: Ag films composed of size-selected nanoparticles, Nano part. Res., 8 (**2006**) 797-808.

9. J.Gong, Q.Chen, M.R.Lian, N.C.Liu, R.G.Stevenson, and F.Adami, ‑Micro machined Nano crystal line silver doped SnO_2H_2S sensor‖, Sens. Actuators B, 114 (**2006**) 32-39.

10. B. Liu, D. Cai, Y. Liu, D. Wang, L. Wang, Y. Wang, H. Li, Q. Li, Q.; T. Wang, ‑Improved room-temperature hydrogen sensing performance of directly formed Pd/WO3 nan composite‖, Sens. Actuators B: Chem., 193 (2014)28-34

11. J. Kukkola, M. Mohl, A.R. Leino, J. Mäklin, N. Halonen, A. Shchukarev, Z. Konya, H. Jantunen, K. Kordas, ‑Room temperature hydrogen sensors based on metal decorated WO_3nanowires‖, Sens. Actuators B: Chem.**,** 186 (**2013**)90-95.

12. Z. Wang, Z. Li, T. Jiang, X. Xu, C. Wang, ‑Ultrasensitive hydrogen sensor based on Pd0-loaded SnO_2electrospun nanofibers at room temperature‖, ACS Appl. Mat.

Interfaces**, 5 (2013)**2013-2021.

13. C. Zhang, A. Boudiba, C. Navio, C. Bittencourt, M.G. Olivier, R. Snyders, M. Debliquy, ‒Highly sensitive hydrogen sensors based on co- sputtered platinum-activated tungsten oxide films, Int. J. Hydrogen. Energy, 36 **(2011)**1107-1114.

14. C. Zhang, M. Debliquy, A. Boudiba, H. Liao, C. Coddet, ‒Sensing properties of atmospheric plasma-sprayed WO_3 coating for sub-ppm NO_2 detection‖, Sensors Actuators B, 144 **(2010)**280-288.

15. R. Calavia, A. Mozalev, R. Vazquez, I. Gracia, C. Cané, R. Ionescu, E. Llobet, ―Fabrication of WO3 nanodot-based microsensors highly sensitive to hydrogen, Sensors Actuators B-Chemical,149(2) **(2010)** 352 –361.

16. S.J. Ippolito, S. Kandasamy, K. Kalantar-zadeh, W. Wlodarski, ‒Hydrogen sensing characteristics of WO_3thinfilm conductometric sensors activated by Pt and Au catalysts‖, Sensors Actuators B,108 **(2005)**154-158.

17. M.Yang, Y. Sun, D. Zhang, D. Jiang, ‒ Using Pd/WO_3compositethin films as sensing materials for optical fiber hydrogen sensors‖, Sensors Actuators B, 143 **(2010)**750-753.

18. D.S. Vlachos, C.A. Papadopouls, J.N. Avaritsiotis. Sensors Actuators B, 44 (1997)459-461.

An Overeview on Nanocrystalline perovskite (ABO₃): A potential material for solid state gas sensor and its applications

Dr. Manisha S. Pande [a*], Dr. V. D. Kapse [b],
Dr. P. M .Chandak[c], Dr. T. R. Tatte[d]

[a*] Department of Physics, Shri Sant Gajanan Maharaj College Of Engineering, Shegaon.
[b] Department of Physics, Arts, Science and Commerce College, Chikhaldara.
[c] Department of Physics, B.B. Arts,N.B.Commerce & P.Science College, Digras, Dist. Yavatmal.
[d] Department of Physics, Shri Dr. R. G. Rathod Arts & Science College,Murtizapur.

FULL PAPER

1. Introduction

In day today modern life detection of different gases play a vital role. The significant area of research towards gas sensing that leads to the fabrication of gas sensing devices which detect various harmful gases. Human body suffers from different diseases due to the emission of various toxic and hazardous gases. Solid-state sensors are among the most versatile of all sensors, as they detect a wide variety of gases, and can be used in many different applications. Among the unique attributes of the solid-state sensor are the abilities of the sensor to detect both low ppm levels of gases, as well as high combustible levels. Solid state gas sensors, are the excellent candidates to the fabrication of commercial gas sensors for a wide range of applications [1-5]. The development of high precision gas sensors is crucial for the monitoring of harmful (exhaust) gases in the environment. A variety of dangerous gases, such as CH_4, NO_2, LPG, NH_3, SO_2, CO, H_2S, NO_2, Acetone, H_2, ethanol, and methanol, are constantly released by industry, transportation, and agricultural activities. Many of these gases are hazardous to human health as well as the environment, even at levels measured in parts per million, or ppm. Some of these gases, like H_2, are naturally explosive when exposed to air.

In recent years, nanomaterials based on perovskite have been used in a variety of sustainable applications. Their structural properties enable researchers to investigate functionalities in a variety of directions, including solar cells, LEM devices, transistors and sensors, etc. Perovskite nano-materials have been shown to have

remarkable sensing performance to a wide range of chemical and biological species, both in solids and solutions. In particular, they are able to detect small molecules (e.g., oxygen, nitrogen dioxide, carbon dioxide, etc.). In addition, Solid-state gas sensors are emerging as a viable substitute for the intended real-time functions in light of recent developments in the material sciences and advancements in processing and downsizing techniques. The greatest options for the development of commercial gas sensors for a broad range of such applications are solid state gas sensors, which are based on a variety of concepts and materials. [6-10].

2. Structure, Stability and Properties of Perovskites

Perovskite is the name given to the compounds that have the formula type ABX_3 with different sized 'A' and 'B' cations bonded to anion X [11]. ABO_3 Perovskites exhibit good thermal stability with an eV band gap of 3–4, which is why they were used in a lot of gas sensing studies [12]. Perovskite materials can be employed as sensors for gaseous species because their stability was significantly disrupted when exposed to gaseous environments, such as NO_2, CH_4, NH_3, C_2H_5OH, acetone, etc. [13]. The chemiresistive I–V, phosphorescence, and fluorescence responses of these perovskite materials can be used to record the sudden changes in them. However, in these sensing investigations, the opto-electronic characteristics of perovskites are crucial. Renowned contenders with remarkable attributes including electrical conductivity, ferroelectricity, superconductivity, catalytic activity, etc. are perovskite oxides. There are several ways to synthesis the naocrystalline perovskite material, including the hydrothermal, sol-gel, and chemical co-precipitation processes, etc. Because of the remarkable stability of the perovskite structure, structural flaws can be created when one or both of the cations in the A and B sites are partially substituted with other metals that have a different oxidation state.

3. Applications of Perovskite materials

The desirable characteristics of perovskites contributed to a significant development in research in recent years, indicating a genuine interest in the possible uses of these materials. They consist of, but are not confined to:

- Superconductivity
- Characteristics of catalysis
- The unique characteristics of optoelectronics.

Numerous companies are interested in using perovskites and are working to further the technology through research. Photovoltaics and optoelectronics are two companies that are particularly interested in perovskites:

Solar energy

Since they are cheaper for production as well as greater flexible qualities than conventional silicon solar cells, perovskite materials present a possible substitute. Perovskite-based solar cells have demonstrated significant commercial promise in recent years, with their efficiency rising to above 25% in lab settings. The resilience and lifetime of these solar cells are presently being researched.

LED

LEDs have been around for many years, but the next generation of this technology will be offered by perovskite-based LEDs. Perovskite materials' optoelectronic qualities, which include their high photoluminescence quantum yield, tunability, and less expensive manufacture, have attracted the attention of numerous scientists and technological businesses.

4. Review of solid state gas sensor

Soil, water, and air pollution are the three categories into which environmental contamination falls. Of these three categories, air and water pollution are the main contributors to disasters since they spread quickly over a wide area in a short amount of time. Since industrial progress has dramatically expanded environmental pollution to such a level that public concern is now so great that it cannot be ignored any longer, environmental monitoring and management are absolutely necessary. Therefore, in order to address these environmental issues, thorough study has been done to quickly identify these contaminants and lower their levels to within the regulatory allowed concentrations. These factors have contributed to the advancement of solid-state gas sensor research and development in recent years. Gas sensors with metal oxides as the sensing medium have been widely used in gas detection applications. In fact, there is growing interest in gas sensing for nanocrystalline semiconducting metal oxides with regulated compositions, which also represent an intriguing new area of fundamental research [14]. Because of its oxide stability, high response, low production cost, and ability to respond to a wide spectrum of chemicals, semiconductor metal oxide nanostructures are the most preferred of all the solid state gas sensing materials. They respond quickly, are robust, dependable, and reasonably priced. Different types of solid state gas sensors are semiconductor gas sensor, optical gas sensor, electrochemical gas sensor, etc. Semiconductor gas sensors (SGS), known sometimes as chemoresistive gas sensors, are typically based on metal oxides (e.g. SnO_2, TiO_2, In_2O_3, WO_3, NiO, etc.). Recent applied research and product releases in this sector of gas sensors have revealed some noteworthy developments regarding the use of nanotechnologies and gas-sensing layers. In the sensing industry, optical gas sensors are crucial for measuring chemical and biological quantities. Changes in the absorption spectrum were used to measure the first optical chemical sensors. Chemical sensors and biosensors currently employ a wide range of optical techniques, such as

ellipsometry, surface plasmon resonance (SPR), spectroscopy (luminescence, phosphorescence, fluorescence, Raman), interferometry (white light, modal, and optical waveguide structures), spectroscopy of guided modes in optical waveguide structures (grating coupler, resonant mirror), and interferometry (white light, phosphorescence, and fluorescence). Electrochemical gas sensors use an electrochemical cell, which is made up of two terminals (an anode and a cathode) of the same composition and a casing that holds a collection of chemical reactants (electrolytes or gels) in contact with the environment. A membrane on the top of the gas sensor enclosure allows the gas sample to pass through it. At the anode, oxidation happens, and at the cathode, reduction happens.

5. Conclusion

In this review study, the materials chosen for the construction of such gas sensors, and the sources of emission and regulatory standards of air pollutants are briefly reviewed. It has been addressed how advances in material science have led to the development of potential solid-state gas sensors, with the aim of comprehending the underlying technology and offering targeted functionality for a particular application. Perovskites are an extremely interesting and diverse class of materials which exhibit many useful characteristics that are determined by their composition. In the current research, we examine recent advancements in perovskite-based materials with excellent characteristics for application in optoelectronics and photovoltaics.

References

[1] P. T. Moseley, B. C. Tofield (eds.), Solid State Gas Sensors, Adam Hilger, Bristol and Philadelphia (1987).

[2] M. J. Madou, S. R. Morrison (eds.), Chemical Sensing with Solid State Devices, Academic Press, New York, 1989.

[3] A. Mandelis, C. Christofides (eds.), Physics, Chemistry and Technology of Solid State Gas Sensor Devices, Wiley (1993).

[4] P. T. Moseley, Meas. Sci. Technol. 8, 223 (1997).

[5] I. Lundström, Sensors and Actuators B 35-36, 11 (1996).

[6] P. T. Moseley, B. C. Tofield (eds.), Solid State Gas Sensors, Adam Hilger, Bristol and Philadelphia (1987).

[7] M. J. Madou, S. R. Morrison (eds.), Chemical Sensing with Solid State Devices, Academic Press, New York, 1989.

[8] A. Mandelis, C. Christofides (eds.), Physics, Chemistry and Technology of Solid State Gas Sensor Devices, Wiley (1993).

[9] P. T. Moseley, Meas. Sci. Technol. 8, 223 (1997).

[10] I. Lundström, Sensors and Actuators B 35-36, 11 (1996)

[11]. T.M., Fthenakis, V.M., Eds.; Academic Press: Cambridge, MA, USA, 2018; pp. 233–254.

 [12]. Varignon, J.; Bibes, M.; Zunger, A. Origin of band gaps in 3d perovskite oxides. Nat. Commun. 2019, 10, 1658.

[13]. Zhu, Z.; Sun, Q.; Zhang, Z.; Dai, J.; Xing, G.; Li, S.; Huang, X.; Huang, W. Metal halide perovskites: Stability and sensing-ability. J. Mater. Chem. C **2018**, 6, 10121–10137.

[14]. N. Barsan, M. Schweizer-Berberich, W. Göpel, Fresenius J. Anal. Chem. 365, 287 (1999).

Role of Matrices and its Applications in Science and Engineering

Dr. Mrs. Jayashree S Gawande

Department of Mathematics,
Shri Sant Gajanan Maharaj College of Engineering, Shegaon

FULL PAPER

A matrix is a two-dimensional array of numbers, symbols, or expressions organized in rows and columns, typically enclosed within square brackets. Essentially, matrices serve as rectangular arrangements of elements, facilitating mathematical operations and transformations. In the context of a field F, a matrix consists of scalars from that field, with each element referred to as an entry.

The history of matrices is a fascinating journey that spans centuries and encompasses contributions from various cultures and mathematical traditions. While the formal study of matrices emerged in the 19th and 20th centuries, the concept of arranging numbers in rows and columns dates back to ancient times. Ancient civilizations such as the Babylonians and Egyptians used numerical tables and arrays to organize data and perform calculations related to astronomy, engineering, and commerce. These early forms of tabular representations laid the groundwork for the development of matrices.

The Chinese mathematician Liu Hui introduced methods for solving systems of linear equations using arrays of coefficients, an early precursor to matrices. The Indian mathematician Brahmagupta introduced the notion of determinants in solving simultaneous linear equations, a concept closely related to matrices.

The formal study of matrices as mathematical objects began in the 19th century. Augustin-Louis Cauchy and Arthur Cayley made significant contributions to matrix theory, introducing concepts such as matrix addition, multiplication, and inversion.

In the late 19th and early 20th centuries, mathematicians such as Évariste Galois, Camille Jordan, and Ferdinand Georg Frobenius further advanced the theory of matrices, establishing them as a fundamental tool in linear algebra.

The 20th century witnessed the widespread adoption of matrices in various scientific and engineering fields. Matrices found applications in quantum mechanics, computer graphics, cryptography, operations research, and many other areas. The development of computational methods and technologies accelerated the use of matrices, enabling researchers and engineers to solve increasingly complex problems efficiently. Overall, the history of matrices reflects the evolution of mathematical thought and the continual quest to understand and manipulate abstract mathematical structures for practical applications in science, engineering, and beyond.

Application of Matrices :

Matrices are versatile mathematical structures used in various fields and applications. Here are some common uses of matrices:

1.Solving Linear Systems: Matrices are extensively used to solve systems of linear equations. The augmented matrix and matrix operations like Gaussian elimination or Cramer's rule are employed for this purpose.

2.Solving Differential Equations: Matrices are used in numerical methods for solving differential equations, which have applications in physics, engineering, and scientific computing.

3.Eigenvalue Problems: Matrices are fundamental in eigenvalue and eigenvector problems, which have applications in physics, engineering, and data analysis.

4.Cryptography: Matrices play a role in various cryptographic algorithms for secure data encryption and decryption.

5.Transformations in Computer Graphics: Matrices are used to represent 2D and 3D transformations, including translation, rotation, scaling, and shearing, in computer graphics.

6.Statistics and Data Analysis: Matrices are employed in statistical analysis, such as covariance matrices for multivariate analysis

7.Quantum Mechanics: Matrices represent quantum operators and are used to describe the evolution and properties of quantum systems.

8.Markov Chains: Transition matrices are used in the modeling and analysis of Markov chains, which describe random processes over time.

9.Linear Programming: Matrices are used in linear programming to optimize resource allocation and decision-making in various fields like economics and operations research.

10.Network Analysis: Adjacency matrices are used to represent relationships and connections in network theory, including social networks and transportation networks.

11.Image Processing: Matrices are used to represent digital images, and matrix operations are applied for various image manipulation and analysis tasks.

12.Finite Element Analysis: Matrices are used in engineering simulations to approximate and analyse complex physical systems, like stress and strain distributions in materials.

13.Game Theory: Matrices represent payoff tables in game theory, helping to analyse strategic interactions and decision-making in economics and social sciences.

14.Population Modelling: Matrices are used to model population dynamics in biology and ecology, such as predator-prey models.

15.Genetic Algorithms: Matrices can represent candidate solutions and are used in optimization algorithms like genetic algorithms.

To be more friendly with matrices and its application: It can be used for computer programming and can be used in business for budgeting, sales projection and cost estimation. Scientist can use a spreadsheet to analyse the result of experience. It can be used to compute industry income tax. Also, it can be used in allocation of resources and production scheduling.

Along with its immeasurable benefits it has some limitation also. Some general limitations of matrices are the followings:

1. Complicated calculations.

2. Difficulty in finding DETERMINANT of a 4 * 4 matrix

3. Time consuming.

Conclusion: In conclusion, matrices stand as foundational mathematical tools that underpin a vast array of scientific and engineering endeavours. Throughout this exploration, we have witnessed the indispensable role matrices play in modelling, analysing, and solving complex problems across diverse disciplines.

References:

[1] Dirac, P. A. M. (1930). Principles of Quantum Mechanics.

[2] Nielsen, M. A., & Chuang, I. L. (2010). Quantum Computation and Quantum Information.

[3] Nise, N. S. (2015). Control Systems Engineering.

[4] Hughes, T. J. R. (2012). The Finite Element Method: Linear Static and Dynamic Finite Element Analysis.

[5] Foley, J. D., van Dam, A., Feiner, S. K., & Hughes, J. F. (1990). Computer Graphics: Principles and Practice.

[6] Cormen, T. H., Leiserson, C. E., Rivest, R. L., & Stein, C. (2009). Introduction to Algorithms.

[7] Anderson, T. W. (2003). An Introduction to Multivariate Statistical Analysis.

[8] Hastie, T., Tibshirani, R., & Friedman, J. (2009). The Elements of Statistical Learning.

[9] Oppenheim, A. V., & Schafer, R. W. (2010). Discrete-Time Signal Processing.

[10] Proakis, J. G., & Salehi, M. (2008). Communication Systems Engineering.